

**DIRECTORIO DE ALUMNOS DEL
IV CURSO INTERNACIONAL DE INGENIERIA GEOLOGICA
APLICADA A OBRAS , MODULO 4
TECNOLOGIA SOBRE EL USO DE EXPLOSIVOS
DEL 22 AL 26 DE JUNIO DE 1992.**

- 1.- ANCHONDO SANCHEZ JORGE ANTONIO
RESIDENTE DE OBRAS
SECRETARIA DE COMUNICACIONES Y TRANSPORTES
EJERCITO NACIONAL No. 700, COL. PROFESORES FEDERALES
MEXICALI BAJA CALIFORNIA, TEL. 4 19 63 DFNA.
- 2.- GALINDO ROMAN VICTOR
- 3.- GUTIERREZ GONZALEZ EMILIO
JEFE DEL DEPTD. DE EXPLOSIVOS
GOBIERNO DEL ESTADO DE MEXICO
RAFAEL M. HIDALGO 1302, DTE, COL. VALLE VERDE, TDLUCA
EDO. DE MEXICO, C.P. 50130, TEL. 17 09 11 DFNA.
17 84 51 DDM.
- 4.- HERNANDEZ ROSAS EDMUNDO
SUPERINTENDENTE DE OBRA EPYCSA S.A.
PROLONG. NOGAL S/N, MAGDALENA ATLIPAC KM 22, CARRETERA
MEXICO, TEXCOCO, LOS REYES LA PAZ, EDO. DE MEXICO
TEL. 856 35 84 DFNA., 839 20 96 DDM.
- 5.- KEER RENDON CUAUHEMOC
JUAN RUIZ ALARCON 24, DRAMATURGOS, SATELITE, NAUCALPAN
D.P. 53100, TEL. 562 76 26 DDM.
- 6.- ROSAS CORTEZ PORFIRIO
- 7.- YANEZ SANTILLAN DAVID
INGENIERO CON MAESTRIA
C.F.E.
AUGUSTO RODIN 265, COL. NOCHEBUENA, DELEG. B. JUAREZ
TEL. 563 37 00 DFNA., 677 40 94 DDM.

Vertical text on the left margin, possibly a page number or reference code.

Main body of text, consisting of several paragraphs of faint, illegible characters. The text appears to be a formal document or report.

CURSOS ABIERTOS

IV CURSO INTERNACIONAL DE INGENIERIA GEOLOGICA APLICADA A OBRAS SUPERFICIALES Y SUBTERRANEAS

TECNOLOGIA SOBRE EL USO DE EXPLOSIVOS

Del 22 al 26 de junio de 1992

FECHA	HORARIO	T E M A	EXPOSITOR
22, 23, 24 y 26	9:00 a 19:00	PROPIEDADES FISICAS Y QUIMICAS DE LOS EXPLOSIVOS PROPIEDADES GEOMETRICAS Y MECANI- CAS DE LAS ROCAS MECANISMOS DE FRAGMENTACION FUNDAMENTOS SOBRE EL DISEÑO DE VOLADURAS EFECTOS ADVERSOS DE LAS VOLADURAS	Ing. Raúl Cuéllar Borja
Jueves 25	15:00 a 19:00	DEMOSTRACION DE INSTRUMENTACION DE MEDICION DE VIBRACIONES Y APLICA- CIONES PRACTICAS	Ing. Jaime Ruiz Reyes Ing. Francisco Torres Rodríguez

EVALUACION DEL PERSONAL DOCENTE

1

CURSO: IV CURSO INTERNACIONAL DE INGENIERIA GEOLOGICA APLICADA A OBRAS SUPERFICIALES Y SUBTERRANEAS TECNOLOGIA SOBRE EL USO DE EXPLOSIVOS

FECHA: Del 22 al 26 de Junio de 1992.

		DOMINIO DEL TEMA	EFICIENCIA EN EL USO DE AYUDAS AUDIO VISUALES	MANTENIMIENTO DEL INTERES. (COMUNICACION CON LOS ASISTENTES, AMENIDAD, FACILIDAD DE EXPRESION).	PUNTUALIDAD	
CONFERENCISTA						
10	ING. RAUL CUELLAR BORJA					
11	ING. JAIME RUIZ REYES					
12	ING. FRANCISCO TORRES RODRIGUEZ					
13						
14						
15						
16						
17						
18						
ESCALA DE EVALUACION: 1 a 10						

EVALUACION DEL CURSO

C O N C E P T O		
1.	APLICACION INMEDIATA DE LOS CONCEPTOS EXPUESTOS	
2.	CLARIDAD CON QUE SE EXPUSIERON LOS TEMAS	
3.	GRADO DE ACTUALIZACION LOGRADO EN EL CURSO	
4.	CUMPLIMIENTO DE LOS OBJETIVOS DEL CURSO	
5.	CONTINUIDAD EN LOS TEMAS DEL CURSO	
6.	CALIDAD DE LAS NOTAS DEL CURSO	
7.	GRADO DE MOTIVACION LOGRADO EN EL CURSO	
EVALUACION TOTAL		

ESCALA DE EVALUACION: 1 A 10

1.- ¿Qué le pareció el ambiente en la División de Educación Continua?

MUY AGRADABLE

AGRADABLE

DESAGRADABLE

2.- Medio de comunicación por el que se enteró del curso:

PERIODICO EXCELSIOR
ANUNCIO TITULADO DI
VISION DE EDUCACION
CONTINUA

PERIODICO NOVEDADES
ANUNCIO TITULADO DI
VISION DE EDUCACION
CONTINUA

FOLLETO DEL CURSO

CARTEL MENSUAL

RADIO UNIVERSIDAD

COMUNICACION CARTA,
TELEFONO, VERBAL,
ETC.

REVISTAS TECNICAS

FOLLETO ANUAL

CARTELERA UNAM "LOS
UNIVERSITARIOS HOY"

GACETA
UNAM

3.- Medio de transporte utilizado para venir al Palacio de Minería:

AUTOMOVIL
PARTICULAR

METRO

OTRO MEDIO

4.- ¿Qué cambios haría en el programa para tratar de perfeccionar el curso?

5.- ¿Recomendaría el curso a otras personas? SI NO

5.a. ¿Qué periódico lee con mayor frecuencia?

6.- ¿Qué cursos le gustaría que ofreciera la División de Educación Continua?

7.- La coordinación académica fué:

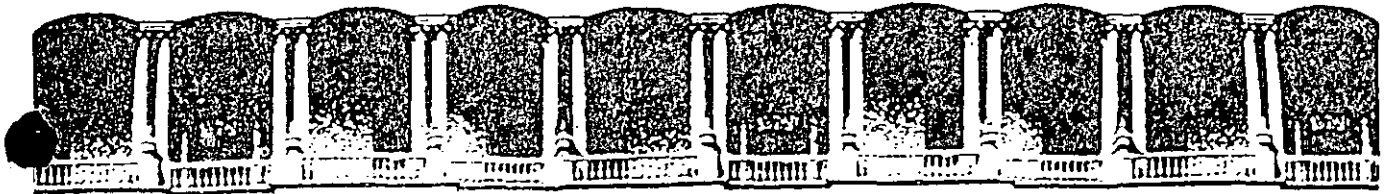
EXCELENTE	BUENA	REGULAR	MALA
<input type="checkbox"/>	<input type="checkbox"/>	<input type="checkbox"/>	<input type="checkbox"/>

8.- Si está interesado en tomar algún curso INTENSIVO ¿Cuál es el horario más conveniente para usted?

LUNES A VIERNES DE 9 a 13 H. Y DE 14 A. 18 H. (CON COMIDAD)	LUNES A VIERNES DE 17 a 21 H.	LUNES A MIERCOLES Y VIERNES DE 18 A 21 H.	MARTES Y JUEVES DE 18 A 21 H.
<input type="checkbox"/>	<input type="checkbox"/>	<input type="checkbox"/>	<input type="checkbox"/>
VIERNES DE 17 A 21 H. SABADOS DE 9 A. 14 H.		VIERNES DE 17 A 21 H. SABADOS DE 9 A 13 H. DE 14 A 18 H.	OTRO
<input type="checkbox"/>		<input type="checkbox"/>	<input type="checkbox"/>

9.- ¿Qué servicios adicionales desearía que tuviese la División de Educación Continua, para los asistentes?

10.- Otras sugerencias:



**FACULTAD DE INGENIERIA U.N.A.M.
DIVISION DE EDUCACION CONTINUA**

CURSOS ABIERTOS

***IV. CURSO INTERNACIONAL DE INGENIERIA GEOLOGICA APLICADA A
OBRAS SUPERFICIALES Y SUBTERRANEAS***

CUARTO MODULO:

TECNOLOGIA SOBRE EL USO DE EXPLOSIVOS

Del 22 al 26 de junio de 1992

USO DE EXPLOSIVOS EN ROCA

ING. RAUL CUELLAR BORJA

JUNIO - 1992

USO DE EXPLOSIVOS EN ROCA

ANTECEDENTES

El uso de los explosivos es más una técnica que un arte. Hasta ahora el método más económico para fragmentar la roca es mediante el uso de explosivos.

La teoría está soportada por la práctica, de tal manera que el diseño de voladuras se realiza más por la relación entre parámetros que mediante fórmulas teóricas, por ejemplo: la relación entre el diámetro y el bordo. Es necesario comprender cómo trabaja el explosivo en la roca, para lo cual se requiere del conocimiento de las propiedades de los dos elementos, *la roca y los explosivos*.

EN RELACION A LA ROCA SE PUEDE DECIR LO SIGUIENTE:

Calidad

Tenemos una gran variedad en la calidad de los macizos rocosos en función de su estructura y resistencia (*caracterización del macizo rocoso*). Este término de calidad involucra muchas propiedades del macizo rocoso, por ejemplo: velocidad de transmisión de ondas de compresión P, resistencia en compresión simple, densidad, dureza, anisotropía, homogeneidad, flujo de agua, temperatura y estado de esfuerzos interno, son algunas de las propiedades más importantes de las rocas para su utilización en el diseño de voladuras.

Mecanismo de fragmentación

En todos los tipos de roca tenemos que la resistencia en compresión simple es mucho mayor que la resistencia en tensión,

cortante o flexión (del orden de 10 veces para tensión y cortante y 4.5 veces para flexión).

De acuerdo con lo anterior, los mecanismos de fragmentación están diseñados para romper la roca por tensión, corte y flexión más que por compresión.

Cuando existe una cara libre se produce el fenómeno de reflexión y refracción de las ondas de choque de compresión o primarias P, creándose vibraciones de alta frecuencia (150 a 200 c.p.s.) que dan lugar a impactos de tensión intermitentes por razón de la fuerza centrífuga hasta que estas fuerzas de inercia vencen la resistencia a la tensión de la roca y entonces se produce el desprendimiento de fragmentos de roca a partir de la periferie hacia el centro.

Por otro lado, las fracturas de tensión en el cilindro de pared gruesa avanzan y los gases penetran en ellas produciendo el desplazamiento de los fragmentos de roca. También se produce un efecto combinado, semejante a una viga con un apoyo empotrado y otro libre bajo la carga de presión producida por el explosivo.

EN RELACION AL EXPLOSIVO SE TIENE LO SIGUIENTE:

Que la generación de la explosión o voladura ocurre por oxidación o reducción de combustible a alta presión. Durante esta reacción se producen temperaturas de 5000°C y gases a presiones muy altas que varían entre 15 000 y 150 000 kg/cm².

Esta presión se produce súbitamente en forma de impacto, propagándose las ondas de choque a velocidades entre 2000 y 7000 m/seg.

El trabajo realizado por 1 kg de TOVEX es de 580 ton-m/seg, o sea, que puede levantar 1 ton a una altura de 580 m en un segundo, equivalente a 5800 KW y 100 kg a 580 000 KW.

INGREDIENTES Y COMPOSICION DE LOS EXPLOSIVOS

La mayor parte de los explosivos comerciales son mezclas de compuestos que contienen 4 elementos básicos: carbón, hidrógeno, nitrógeno y oxígeno.

Otros compuestos con elementos tales como sodio, aluminio y calcio, se incluyen para producir ciertos efectos deseados.

Como regla general estos componentes deben dar un balance de oxígeno correcto.

Esto significa que durante la reacción todo el oxígeno disponible en la mezcla reaccione solamente para formar vapor de agua (H_2O) y que con el carbón reaccione para formar únicamente bióxido de carbono (CO_2) en forma de gas y el nitrógeno quede libre formando sólo gas nitrógeno (N).

Cuando hay otros elementos además de los cuatro básicos, por ejemplo sodio, deberá incluirse suficiente oxígeno adicional para lograr una combinación balanceada.

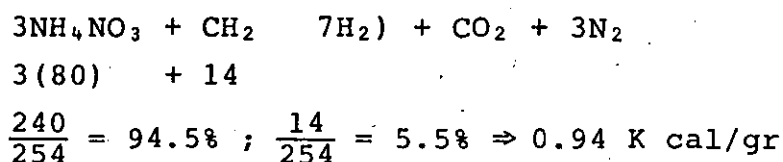
Cuando hay exceso de oxígeno disponible, se producen gases altamente venenosos, como los gases nitrosos NO o NO_2 (óxidos de nitrógeno). Estos gases son fácilmente detectables por su olor y color café-rojizo.

Por otro lado, si estamos en defecto de oxígeno, se forma el mortal gas monóxido de carbono (CO), el cual desafortunadamente no es detectado por olor ni color.

Además de la formación de gases venenosos por exceso o deficiencia de oxígeno, se produce una disminución de temperatura con una consecuente reducción en la presión de los gases producidos.

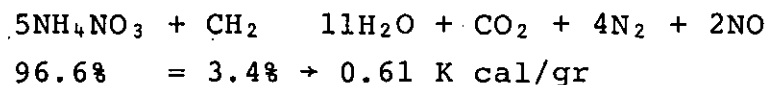
Para ilustrar los efectos del balance de oxígeno en el AN-FO (nitrato de amonio-aceite combustible) como agente explosivo, tenemos:

1. Oxígeno balanceado



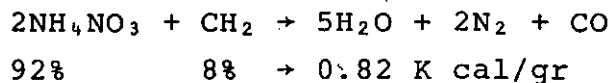
nitrato de amonio + aceite combustible (diesel)

2. Oxígeno en exceso (positivo)



Además de que se produce menor temperatura y presión se produce gas nitroso (NO), que es un gas venenoso.

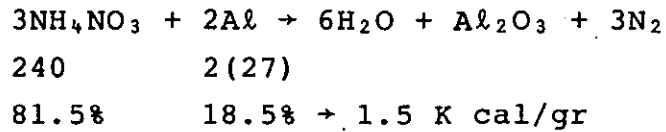
3. Oxígeno deficiente (negativo)



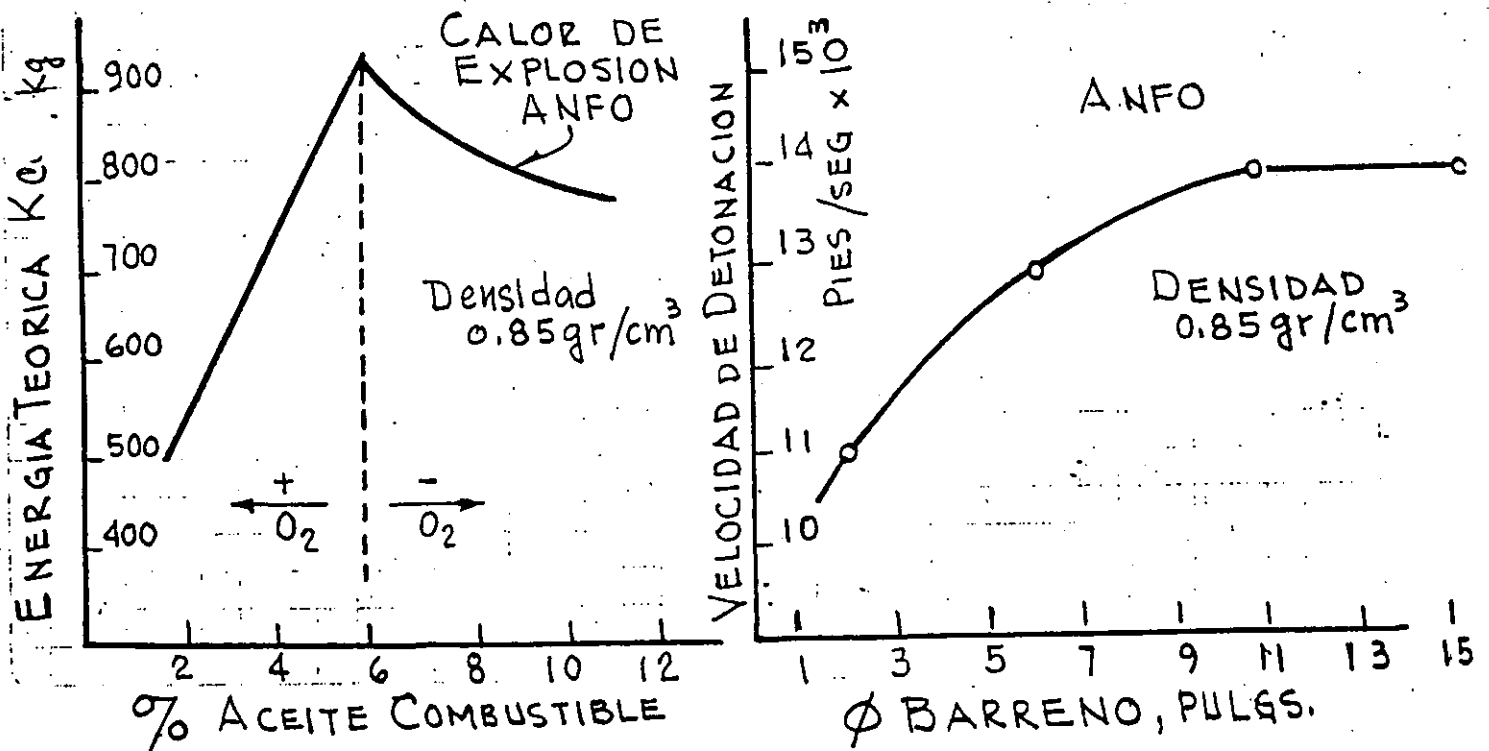
Se tiene menor temperatura y presión y se produce monóxido de carbono (CO) que es mortal.

La reacción química más eficiente para el ANFO es 94% de nitrato de amonio y 6% de aceite combustible diesel.

Se pueden producir otros agentes explosivos más potentes, por ejemplo utilizando aluminio:



La desventaja de este compuesto para uso comercial es su alto costo. Se usa sólo para explosivos militares.





CLASIFICACION DE LOS EXPLOSIVOS

Los ingredientes usados en la fabricación de explosivos se definen como: explosivos bases, oxidantes, antiácidos y absorbentes.

Un explosivo base es un sólido o líquido que bajo la acción de suficiente calor o impacto se transforma en un producto gaseoso con acompañamiento de energía calorífica. Los combustibles y oxidantes se agregan para lograr el balance del oxígeno.

Un antiácido se agrega para incrementar la estabilidad en almacenaje y un absorbente se agrega para absorber o proteger los explosivos bases.

Un agente explosivo es cualquier material o mezcla compuesto por un combustible y un oxidante, de tal modo que ninguno de sus ingredientes sea explosivo base.

En este caso la mezcla ANFO no puede ser detonada por un estopín No. 8, que contiene 2 gr de una mezcla de 80% de fulminato de mercurio y 20% de clorato de potasio.

El ANFO tiene baja resistencia al agua y deflagrante.

La adición de un ingrediente explosivo como el TNT, cambia la clasificación de la mezcla de agente explosivo a explosivo.

Los agentes explosivos pueden ser clasificados como -agentes explosivos secos- o -agentes explosivos "slurry"- . El ANFO (agente explosivo seco) se inició en 1950.

Hidrogeles

Los hidrogeles son los explosivos más recientemente desarrollados y actualmente son los más utilizados. Se fabrican en formulaciones tanto de agentes explosivos como de explosivos.

Contienen alta proporción de nitrato de amonio, parte del cual está en solución acuosa y dependiendo del resto de los ingredientes, puede ser clasificado como agente explosivo o explosivo.

Los agentes explosivos contienen ingredientes no sensibilizadores, como aceite combustible, carbón, azufre o aluminio, y no constituyen cápsulas-sensitivas, mientras que los explosivos hidrogeles sí contienen ingredientes como TNT que los transforma en cápsulas-sensitivas, el TNT sólo es una cápsula-sensitiva. Las mezclas del nitrato de amonio y los aceites o los sensibilizadores se espesan o gelatifican con gomas para proporcionar resistencia al agua.

Los hidrogeles son más seguros y no detonan aún barrenando sobre ellos, lo cual no sucede con las gelatinas.

Dinamita pura

La dinamita pura está compuesta por: nitroglicerina (NG) y sílice (SiO_2) en proporción 50% (NG) y 50% (SiO_2) hasta 25% (NG) y 75% (SiO_2) (Kieselgur o tierra de diatomeas o infusorios). Normalmente se fabrica en 20 a 60% (NG) y 40 a 80% (NS + C, donde NS = Nitrostarch).

TABLA 1 INGREDIENTES USADOS EN LOS EXPLOSIVOS

INGREDIENTE	FORMULA	FUNCION
Nitroglicerina (NG)	$C_3H_3(NO_3)_5$	Explosivo base
Trinitrotolueno (TNT)	$C_6H_2CH_3(NO_2)_3$	Idem
Dinitrotolueno (DNT)	$C_7H_2O_4H_6$	Idem
Glicol de etileno dinitrato (EGDN)	$C_2H_4(NO_3)_2$	Idem, anticongelante
Nitrocelulosa	$C_6H_7(NO_3)_3O_2$	Idem, gelatilizante
Nitrato de amonio (NA)	NH_4NO_3	Idem + oxidante
Clorato de potasio	$KClO_3$	Idem + oxidante
Perclorato de potasio	$KClO_4$	Idem + oxidante
Nitrato de sodio (SN)	$NaNO_3$	Oxidante, reduce congelación
Nitrato de potasio	KNO_3	Oxidante
Pulpa de madera	$C_6H_{10}O_5$	Absorbente, combustible
Aceite combustible	CH_2	Combustible
Parafina	CH_2	Idem
Aceite para lámpara	C	Idem
Gis	$CaCO_3$	Antiácido-estabilizador
Oxido de zinc	ZnO	Idem
Aluminio (metal)	Al	Catalizador
Magnesio (metal)	Mg	Catalizador
Kieselgur	SiO_2	Absorbente anti-cake diatomeas o infusorios
Oxígeno líquido	O_2	Oxidante
Azufre	S	Combustible
Sal	$NaCl$	Anti-inflamante
Compuestos orgánicos nitrosos		Explosivo base, sensibilizadores, anticake

TABLA 2 ENERGIA CALORIFICA (Q) PARA ALGUNOS EXPLOSIVOS

EXPLOSIVO	DENSIDAD	Q. (cal/gr)
Nitroglicerina (NG)	1.6	1420
PETN		
Pentaeritritetetrinitrato	1.6	1400
RDX	1.6	1320
Compuesto B	1.6	1140
Tetрил	1.6	1010
NG, Gelatina 40%	1.5	820
Slurry (TNT-AN-H ₂ O) 20-65-15	1.5	770
NG, Gelatina 100%	1.4	1400
NG, Gelatina 75%	1.4	1150
AN, Gelatina 75%	1.4	990
NG, Dinamita 40%	1.4	930 +
AN, Gelatina 40%	1.4	800
NG, Dinamita 60%	1.3	990
PETN	1.2	1200
Semigelatina	1.2	940
Dinamita extra 60%	1.2	880
Amatol, 50/50	1.1	890
RDX	1.0	1280
DNT	1.0	960
TNT-AN (50-50)	1.0	900
TNT	1.0	870
ANFO (94-6)	0.9	890
AN	0.8	350

Pólvora negra

Es el explosivo comercial más antiguo. Originalmente era una mezcla de nitrato de potasio, carbón vegetal y azufre; ahora se usa nitrato de sodio en lugar del nitrato de potasio.

Composición:	Nitrato de potasio	75%
	Carbón vegetal	15%
	Azufre	10%

Cuando se usa nitrato de sodio se disminuye un poco su porcentaje aumentando el carbón y el azufre.

Tiene propiedades indeseables para su uso, razón por la que ha sido sustituida.

Es extremadamente sensible al deflagarse o quemarse explotando a baja velocidad (1300 pies/seg). Se usa en forma limitada en rocas blandas en canteras.

VELOCIDAD DE DETONACION

La propiedad sola más importante a considerar al evaluar la potencia de un explosivo es su velocidad sónica y puede ser confinada o no confinada.

La velocidad de detonación confinada es una medida de la velocidad con que viaja las ondas de compresión a través de una columna de explosivo dentro de un barreno u otro espacio confinado, mientras que la velocidad no confinada se obtiene cuando se detona el explosivo a cielo abierto.

Como los explosivos se usan con cierto grado de confinamiento, es más significativa la velocidad confinada.

La velocidad de detonación confinada en los explosivos comerciales varía entre 5000 y 25 000 pies/seg.

Las velocidades no confinadas son del orden de 70 a 80% de la velocidad confinada.

PRESION DE DETONACION

La presión de detonación es una función de la velocidad de detonación y de la densidad del explosivo. Usualmente no se menciona como una propiedad, pero es muy importante en la selección del explosivo. Cuando se tiene una cara libre se producen esfuerzos por impulso que son reflejados en la roca y son parte importante del mecanismo de rotura o de fragmentación.

La relación entre la velocidad de detonación, la densidad y la presión de detonación es compleja. La siguiente expresión es una de las aproximaciones obtenidas:

$$P = \frac{4.18 \times 10^{-7} DC^2}{1 + 0.8D}$$

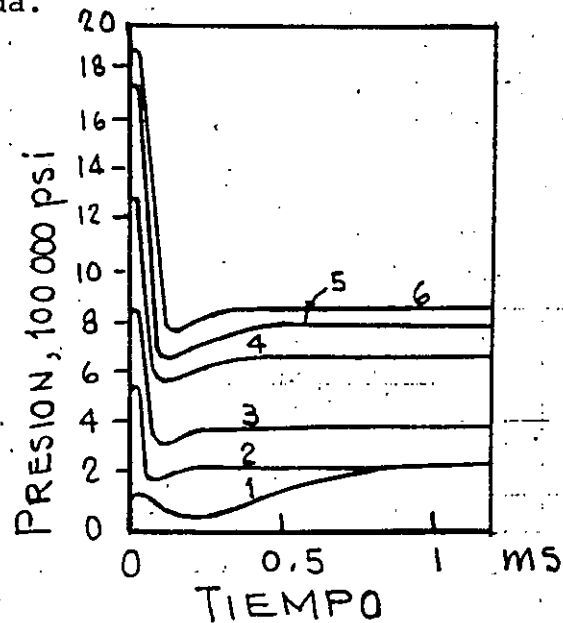
en donde:

- P presión de detonación, en Kbar
1 Kbar = 14 504 lb/pulg²
- D densidad
- C velocidad de detonación, en pies/seg

Hay que distinguir entre presión de detonación y presión de ignición o de explosión.

La presión de ignición o explosión es la que produce el choque o impacto y tiene un valor del doble de la presión de detonación. Esta presión de choque o ignición se caracteriza por una onda muy puntiaguda frente a la cual toda la materia es ionizada y pulverizada.

- 1.- ANFO-94/6 Granulado
- 2.- ANFO-94/6 Fino
- 3.- AN-Dinamita 60%
- 4.- NG-Dinamita 60%
- 5.- TNT-AN-H O-20/65/15
- 6.- AN-GELATINA, 75%



CURVAS DE PRESION CALCULADA BAJO CONFINAMIENTO PERFECTO

CALIDAD DE GASES

La detonación ideal de los explosivos comerciales es que deben producir vapor de agua, bióxido de carbono y nitrógeno. Sin embargo, gases venenosos como el monóxido de carbono y óxidos de nitrógeno (gases nitrosos), se forman muchas veces.

En excavaciones a cielo abierto los gases venenosos no son importantes, por el contrario, en excavaciones subterráneas hay que tener cuidado con ellos.

CRITERIOS PARA SELECCION DE UN EXPLOSIVO

Para cada sitio habrá un explosivo que proporcione los mejores resultados.

La selección del tipo más adecuado está en función de las propiedades geomecánicas de la roca, como son: estructura, dureza, densidad, resistencia, humedad, ventilación, etc., y de la fragmentación obtenida: altura y proyección del banco.

En rocas duras y densas, como la Taconita y los Granitos, un explosivo de alta velocidad tendrá buenos resultados; sin embargo, posiblemente el ANFO también diera buen resultado y es más económico.

En rocas blandas deben usarse explosivos de bajas velocidades, por ejemplo: caliches y basaltos vesiculares.

En general, la velocidad de detonación debe ser igual a la velocidad sónica del macizo rocoso (velocidad de las ondas P de compresión o primarias).

PROPIEDADES DE DINAMITAS PURAS DE NITROGLICERINA

PORCIENTO EN PESO	DENSIDAD	VELOCIDAD CONFINADA pies/seg	RESISTENCIA DEL AGUA	CALIDAD DE GASES
60	1.3	19,000	Buena	Pobre
50	1.4	17,000	Regular	Pobre
40	1.4	14,000	Regular	Pobre
30	1.4	11,000	Pobre	Pobre
20	1.4	9,000	Pobre	Pobre

COMPOSICION DE LAS DINAMITAS PURAS DE NITROGLICERINA

COMPONENTES	PORCENTAJE EN PESO				
	20	30	40	50	60
Nitroglicerina	20.2	29.0	39.0	49.0	56.8
Nitrato de sodio	59.3	53.3	45.5	34.4	22.6
Aceite vegetal	15.4	13.7	13.8	14.6	18.2
Azufre	2.9	2.0	-	-	-
Antiácido	1.3	1.0	0.8	1.1	1.2
Humedad	0.9	1.0	0.9	0.9	1.2

PROPIEDADES DE DINAMITAS DE AMONIO DE ALTA DENSIDAD

PORCIENTO EN PESO	DENSIDAD	VELOCIDAD CONFINADA pies/seg	RESISTENCIA DEL AGUA	CALIDAD DE GASES
60	1.3	12,500	Regular	Buena
50	1.3	11,500	Regular	Buena
40	1.3	10,500	Regular	Buena
30	1.3	9,000	Regular	Buena
20	1.3	8,000	Regular	Buena

COMPOSICION DE LAS DINAMITAS DE AMONIO DE ALTA DENSIDAD

COMPONENTES	PORCENTAJE EN PESO				
	20	30	40	50	60
Nitroglicerina	12.0	12.6	16.5	16.7	22.5
Nitrato de sodio	57.3	46.2	37.5	25.1	15.2
Nitrato de amonio	11.8	25.1	31.4	43.1	50.3
Aceite vegetal	10.2	8.8	9.2	10.0	8.6
Azufre	6.7	5.4	3.6	3.4	1.6
Antiácido	1.2	1.1	1.1	0.8	1.1
Humedad	0.8	0.8	0.7	0.9	0.7



TOVEX 100

(HIDROGEL EN DIÁMETRO PEQUEÑO)

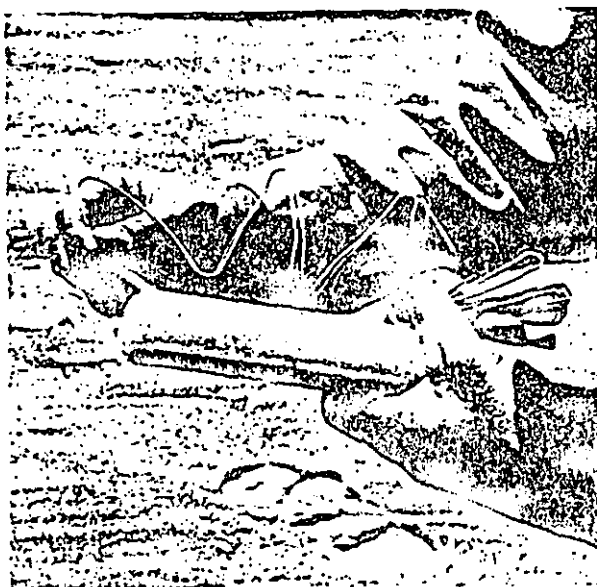
propiedades y especificaciones

TOVEX 100 es un hidrogel (explosivo licuado) de diámetro pequeño, sensible al fulminante, diseñado para usos tanto subterráneo (excepto minas de carbón) como a cielo abierto en barrenos desde 25 mm (1") hasta 50 mm (2") de diámetro. Excelente para plasteos y moneos.

COMPORTAMIENTO: Adecuada densidad, velocidad y alta energía.

CUENTA DE CARTUCHOS:

Los cartuchos son de 203 mm (8") de longitud. Optativamente pueden ordenarse también en 305 y 406 mm (12" y 16"). Se empaican en cajas de cartón de alta resistencia con 25 kgs. netos.



Cebando un cartucho de TOVEX



Cargando en una operación subterránea

NUMERO DE CARTUCHOS POR CAJA DE 25 KGS.

DIAMETRO	LONGITUD DE CARTUCHO		
	203 mm (8")	305 mm (12")*	406 mm (16")*
25 mm. (1")	209	139	105
29 mm. (1 1/8")	165	110	83
32 mm. (1 1/4")	137	90	68

*Longitud optativa

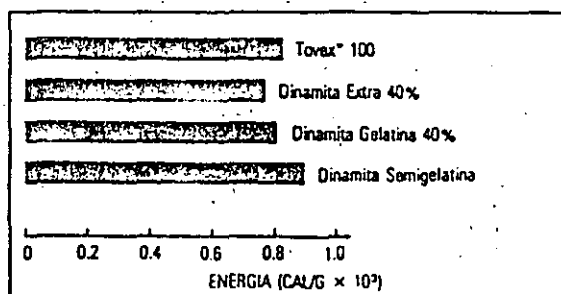
Gases tóxicos: Mínimos, clase I

Requisitos de cebado:

Un fulminante ordinario No. 6. Por las características de ruptura del material de la envoltura, para introducir el detonador dentro del cartucho, se recomienda hacer la perforación en un extremo frontal junto al cierre metálico. No se recomienda perforar lateralmente el cartucho. Es indispensable asegurar que en el manejo del cartucho cebado, el detonador no se salga del cartucho.

Densidad: 1.10 gms/cc.

Energía



Velocidad

DIAMETRO	M/SEG	PIES/SEG
32 mm (1 1/4")	4050	13300

Resistencia al agua: Excelente. Sin envoltura, sumergido en agua, mantiene sus óptimas velocidad y energía.

ventajas:

1. Cargado: TOVEX 100 es sensible a la cápsula. Se ceba y se carga de manera similar a las dinamitas. Su habilidad de compactación proporciona el máximo acoplamiento al barreno y la máxima densidad de carga. Basta un leve empuje del atacador para llenar el barreno.
2. Plasteo y Moneo: Superiormente efectivo para ambas operaciones. Excelentes plasticidad y adherencia.
3. Gases Tóxicos y Humos: Mínimos, clase I.
4. Propagación Entre Barrenos: Los hidrogeles TOVEX están diseñados para minimizar la propagación entre barrenos. Todo sistema de retardo para aumentar la fragmentación y para reducir la vibración funcionará apropiadamente.

Estas informaciones y sugerencias están basadas en la experiencia de Du Pont S.A. de C.V. y se ofrecen como parte del servicio a sus consumidores. Se advierte que los productos explosivos serán usados por personas con el suficiente conocimiento técnico para poder apreciar el riesgo que acompaña su uso. La compañía Du Pont no garantiza resultados favorables ni asume responsabilidad alguna por cuanto a la interpretación de sus sugerencias. Esta información no se ofrece como autorización para usar o violar cualquier patente existente.



TOVEX® 700

(HIDROGEL EN CARTUCHADO)

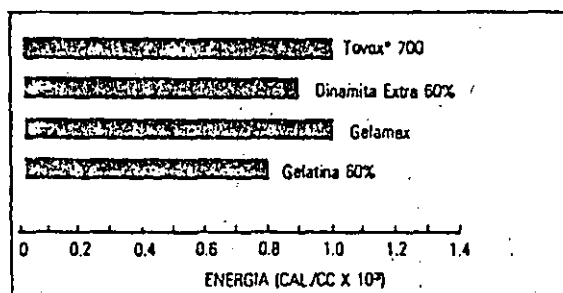
Tovex 700 es un hidrogel (explosivo licuado) sensible al fulminante. Su diseño está particularmente dirigido para los diámetros de barrenación intermedios desde 50 mm (2") hasta 150 mm (6"). De gran versatilidad, tiene las características y propiedades

requeridas para todo tipo de voladuras de roca y mineral de dura a mediana dureza en minas subterráneas, tajos abiertos, canteras y construcción en general. Muy eficaz en plasteos, con superior plasticidad, consistencia y adherencia.

propiedades y especificaciones

Densidad: 1.18 gms./c.c.

Energía:



Velocidad: 4800 m/seg (15750 p/seg)
 Gases Toxicos: Mínimos (Clase 1)
 Resistencia al Agua: Excelente
 Cuenta de Cartuchos:

Diám. del Cartucho mm.	plgs.	Núm de Cartuchos por caja de 25 Kgs.
44	1 3/4	32
50	2	24
64	2 1/2	17
76	3	11

La longitud de los cartuchos es de 406 mm (16 plgs.)

requisitos de cebado:

Un fulminante ordinario No. 6 (Una vuelta y un nudo de Primacord* Reforzado de 50 granos, equivalen para el caso con este producto a un fulminante No. 6)

almacenamiento y transporte:

TOVEX* 700 es compatible con los altos explosivos (dinamitas y agentes explosivos). Es incompatible con los accesorios detonadores (fulminantes, estopines, etc.) En condiciones adecuadas de almacenamiento, polvorines secos, frescos y bien ventilados, puede conservarse durante 1 año.

USO:

TOVEX* 700 es sensible al fulminante. Para iniciarse no necesita ser cebado. Es un extraordinario producto como carga de fondo, carga de columna, como cebo iniciador de otros explosivos o agentes explosivos y como explosivo para plasteos.

ventajas:

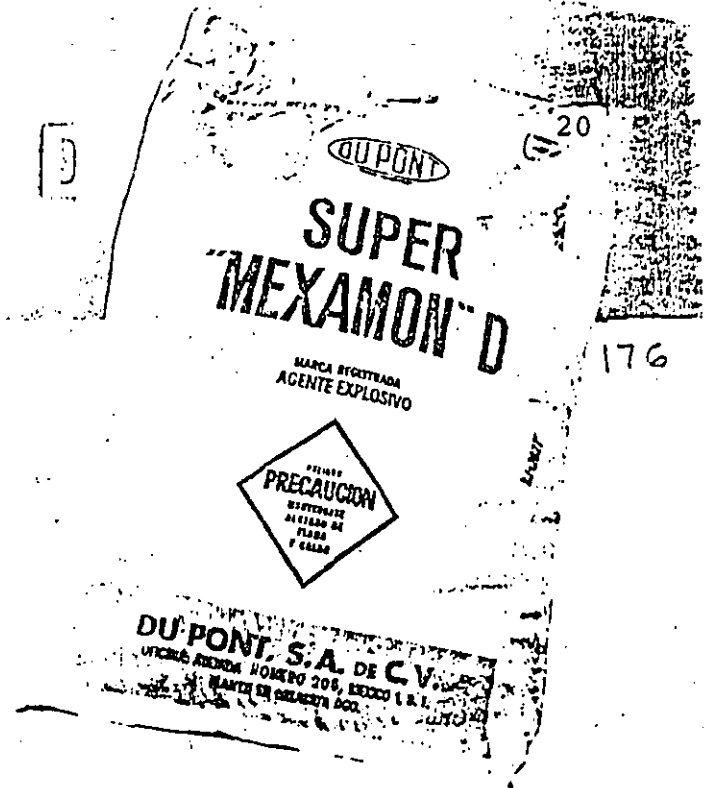
1. **Sensible al fulminante.** No requiere cebo suplementario.
2. **Versatilidad.** Adecuado para uso en barrenaciones de diámetro intermedio (desde 50 mm hasta 150 mm) en operaciones subterráneas y de superficie. Excelente para plasteo.
3. **Carga.** La variedad de diámetro en que es obtenible permite gran flexibilidad al diseño de voladuras y al cargado de barrenos.
4. **Gases tóxicos.** - Mínima producción de gases tóxicos y humo.
5. **Seguridad incrementada.** Menos sensibilidad al impacto, al golpe y al fuego.
6. **Resistencia al Agua.** Excelente. Superior a la de los explosivos tradicionales.
7. **Propagación entre Barrenos.** Está diseñado para minimizar la propagación entre barrenos en plantillas normales; por lo tanto, todo diseño de retardos con el fin de mejorar la fragmentación y de reducir la vibración, funcionará más apropiadamente.

Estas informaciones y sugerencias están basadas en la experiencia de Du Pont, S.A. de C.V. y se ofrecen como parte del servicio a sus consumidores. Se presupone que los productos explosivos serán usados por personas con el suficiente conocimiento técnico para poder apreciar el riesgo que acompaña su uso. La compañía Du Pont no garantiza resultados favorables ni asume responsabilidad alguna por cuanto a la interpretación de sus sugerencias. Esta información no se ofrece como autorización para usar o violar cualquier patente existente.

DU PONT, S.A. DE C.V. DEPARTAMENTO DE EXPLOSIVOS
HOMERO 206 MEXICO 5, D.F. TEL: 250-90-33



SUPER MEXAMON D



Super Mexamon* D reúne las características principales de los Agentes Explosivos: seguridad, economía y la eliminación de los malestares físicos producidos por las Dinamitas. Conjunta las propiedades principales de trabajo de los altos explosivos potencia y velocidad, pero con dos ventajas: baja densidad, que permite ahorros substanciales y resultados superiores, al hacer posible la mejor distribución de la carga explosiva en el barrenó. Además, un mínimo de gases tóxicos que lo hace indicado para uso subterráneo.

PROPIEDADES

Potencia: equivalente a Dinamita Extra 65%
 Densidad vaciado en el barrén: 0.65 gms./c.c.
 Densidad soplado-neumáticamente: 0.75 gms./c.c. (a 4.20 Kg./cm² ó 60 lbs./pulg.²)
 Velocidad: 3,800 mts./seg. (12,500 pies/seg.) aprox.

USOS

Super Mexamon* D proporciona buena fragmentación en roca de mediana dureza. Super Mexamon* D está diseñado para uso en minas bajo tierra. Fluye perfectamente con cargadores neumáticos y se compacta perfectamente aún en barrenaciones de contra-pozo. Super Mexamon* D es del todo recomendable para ser empleado a cielo abierto. Fluye con toda facilidad en barrenos inclinados.

VENTAJAS

1. Versatilidad: Super Mexamon* D puede usarse tanto en minas bajo tierra como en operaciones a cielo abierto.

2. Potencia: La velocidad de Super Mexamon* D y la energía que desarrolla por su gran volumen de gases de expansión lo equiparan en potencia a la Dinamita Extra 65%.
3. Distribución de la carga: Super Mexamon* D por su baja densidad permite la mejor distribución del explosivo en el barrén y en consecuencia, una mejor fragmentación.
4. No requiere mezclas adicionales: Super Mexamon* D es un Agente Explosivo cuidadosamente formulado e integralmente elaborado, listo para cargarse directamente de la bolsa, tal como se empaqueta. Resultado: economía, no hay desperdicio.
5. Sensibilidad: Super Mexamon* D ha demostrado ser más sensible a la onda de detonación que cualquier mezcla de Nitrato de Amonio y Aceite Diesel o combustible.
6. No es aceitoso: Super Mexamon* D por su elaboración integral, ofrece las máximas comodidades al usuario. Está libre de migraciones y evaporaciones.
7. Resultados reproducibles: Con Super Mexamon* D los resultados obtenibles, valadura tras valadura, son constantes y reproducibles siempre y cuando se cebe apropiadamente. Los resultados constantes no son posibles en las mezclas de Nitrato de Amonio o fertilizantes con combustibles, debido a las tantas variantes que intervienen en su preparación.
8. Seguridad: Super Mexamon* D no contiene nitroglicerina.
9. Economías: Super Mexamon* D puede en muchos casos sustituir ventajosamente a los otros explosivos, más altos en precio.

INICIACION

El iniciador o cebo recomendado para detonar el Super Mexamon* D debe ser un explosivo potente y violento, tal como: 1) Tovex 100 y 2) Tovex 700. El cebo de iniciación debe constituir un 15%.

aproximadamente, en peso, del total de la carga explosiva en el barreno. En barrenos largos es recomendable usar más de 1 cebo de iniciación y cordón detonante "Primacord" o "E-Cord" a lo largo del barreno, distribuyendo los cebos a intervalos máximos de 5 metros; es decir, debe distribuirse el cebo total a intervalos a lo largo del barreno dejando siempre en el fondo la mayor cantidad del cebo iniciador.

ALMACENAMIENTO

Super Mexamon* D debe almacenarse considerándolo para el caso, como cualquier otro explosivo. Es aconsejable dar rotación a las existencias almacenadas, usando siempre primero el material más antiguo.

CARGA

En operaciones a cielo abierto, Super Mexamon* D puede cargarse por gravedad, vaciado. La tabla o continuación muestra aproximadamente los kilos por metro lineal de barrenos de varios diámetros.

Diámetro Barreno cms. (pulg.)	Kg. por Metro Lineal de Barreno
2.54 (1)	0.329
5.08 (2)	1.318
7.62 (3)	2.964
10.16 (4)	5.270
12.70 (5)	8.234
15.24 (6)	11.857

EMPAQUE

Super Mexamon* D se envasa en bolsas de papel multicapas con forro interior de polietileno. Cada saco contiene 25 Kgs. netos.

Estas informaciones y sugerencias están basadas en la experiencia de Dupont, S.A. de C.V. y se ofrecen como parte del servicio a sus consumidores. Se presupone que los productos explosivos serán usados por personas con el suficiente conocimiento técnico para poder apreciar el riesgo que acompaña su uso. La compañía Du Pont no garantiza resultados favorables ni asume responsabilidad alguna por cuanto a la interpretación de sus sugerencias. Esta información no se ofrece como autorización para usar o violar cualquier patente existente.

DU PONT, S.A. DE C.V. DEPARTAMENTO DE EXPLOSIVOS
HOMERO 206 MEXICO 5, D.F. TEL: 250-90-33

... ..
... ..
... ..
... ..

... ..
... ..
... ..

... ..
... ..
... ..
... ..

... ..
... ..
... ..
... ..

... ..
... ..
... ..
... ..

... ..

... ..

Hay dos series básicas de retardos disponibles: de retardos cortos o milisegundos con incrementos de retardo de 25 m en el intervalo inferior y 50 m en el intervalo superior y, retardos largos a menudo llamados retardos lentos o simplemente retardos, con incrementos de retrdo de 0.5 seg y 1 seg.

Con los estopines de milisegundos se produce mejor fragmentación y se reduce la presión de aire y las vibraciones del terreno.

Los estopines de retardo se usan en lumbreras o túneles para dar tiempo suficiente al movimiento de la roca. Probablemente se produce fragmentación más gruesa que la obtenida con milisegundos.

Cordón detonante

El cordón detonante consiste de un tubo de plástico resistente al agua, que se protege con una cubierta o forro fabricado con una combinación de textiles, plástico y alambre a prueba de agua. Las cubiertas tienen diferentes grados de resistencia a la tensión, abrasión y flexibilidad.

Dentro del tubo de plástico está el núcleo o corazón constituido por un alto explosivo, usualmente PETN. La cantidad de PETN varía entre 1 gramo/pie a 400 gramos/pie, y se produce en diferentes potencias.

Todas las potencias de PETN pueden detonarse con una cápsula eléctrica y su velocidad de detonación es de 21 000 pies/seg.

Su notable insensibilidad contra impacto y fricción es ideal para su uso en la línea de encendido y líneas troncales.

Como los estopines eléctricos se sujetan al cordón detonante hasta el final justamente antes de la voladura, la mayor parte de una falla aleatoria por detonación se elimina.

Usualmente se usa el cordón de 25 gramos/pie y el de 50 gr/pie se usa en trabajos especiales.

El cordón detonante es un explosivo de alta potencia que explota con una gran producción de aire. Hay que tener cuidado con este efecto.

Un cordón detonante de 25 a 50 gramos/pie detona cualquier cápsula-sensitiva (primer o cebo y cápsulas de alta potencia, como son los boosters).

Cordón detonante Non-electric (NONEL)

Este es un cordón detonante muy útil para voladuras subterráneas, pues se eliminan las fallas por electricidad estática. También se usa en voladuras a cielo abierto para evitar vibraciones detonando barreno por barreno al igual que el cordón detonante y en zonas altas donde se generen tormentas eléctricas.

El NONEL detona en una sola dirección, por lo que hay que tener cuidado en su acoplamiento.

También existen conectores especiales de retardo constituidos por el mismo tubo de NONEL en longitudes de 2 pies con terminales de plástico.

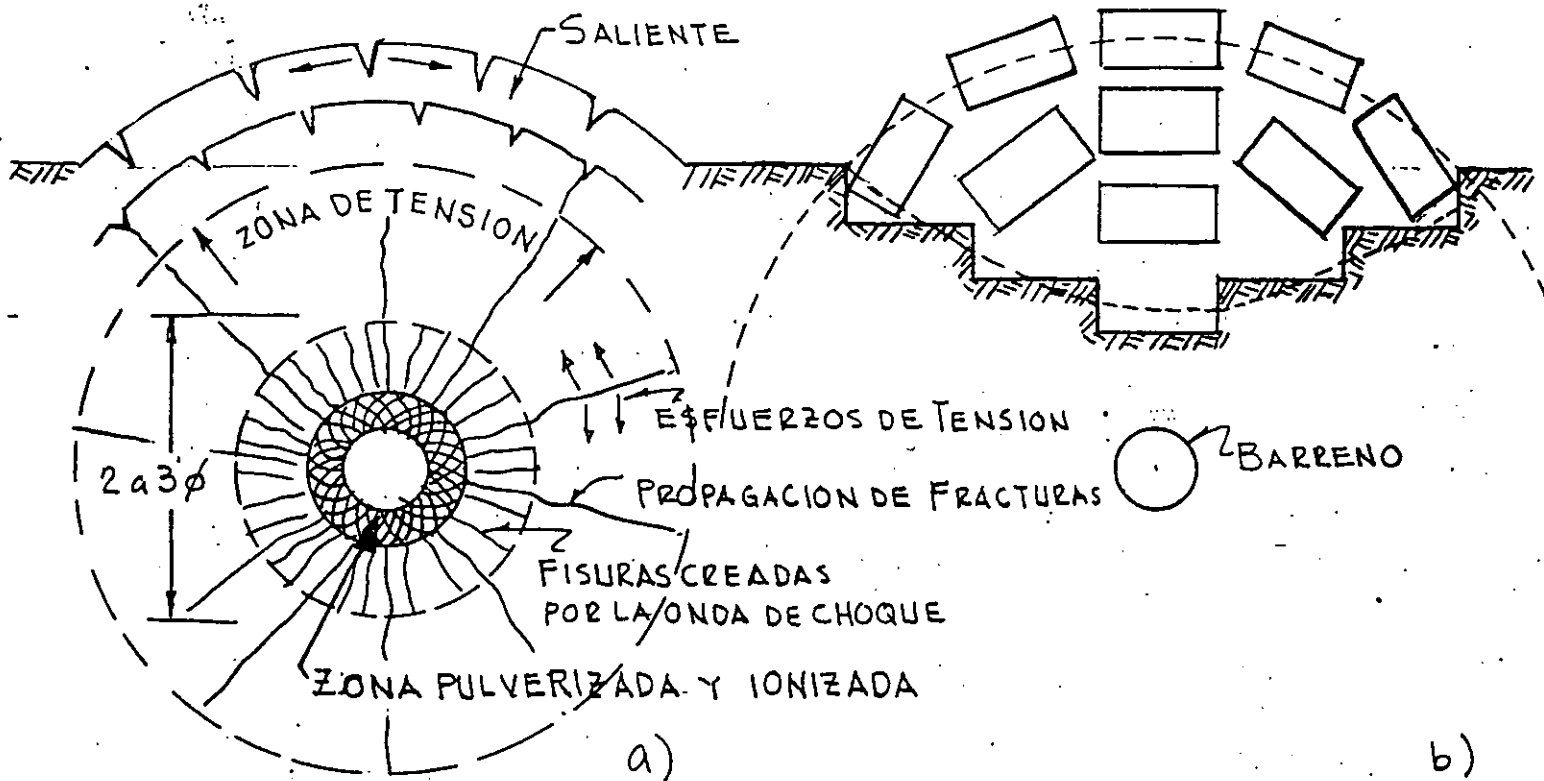
El NONEL tiene una gran resistencia al agua, ya que un extremo está sellado contra la cápsula de detonación y el otro está sellado contra una terminal de plástico.

El NONEL no explota, pudiendo sostenerse perfectamente con las manos.

El NONEL tiene una velocidad de 9000 pies/seg

Su composición química es:

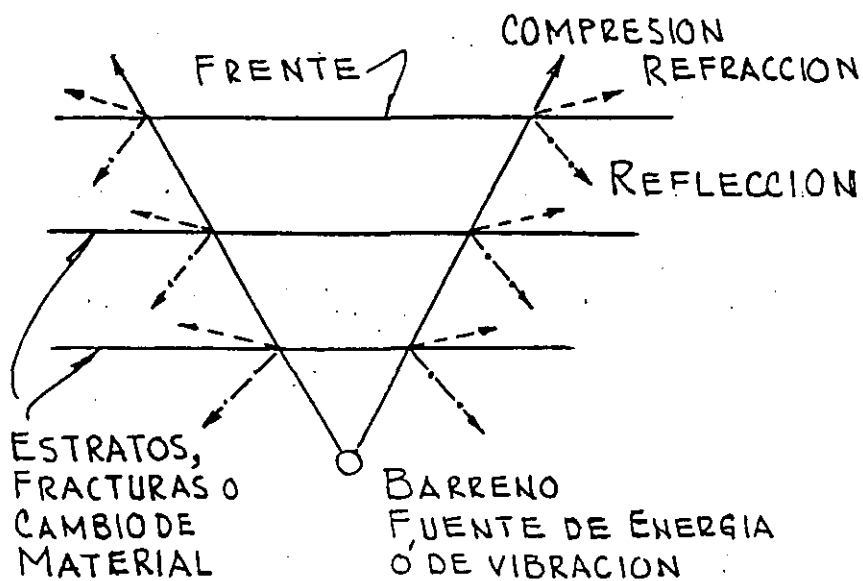
MECANISMO DE FRAGMENTACION



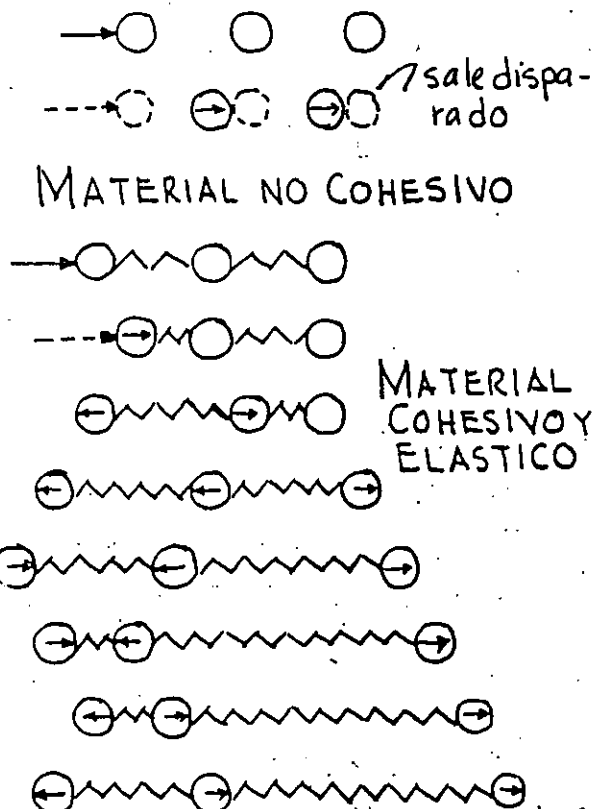
FRACTURAS RADIALES

SECUENCIA EN LA FORMACION DEL CRATER

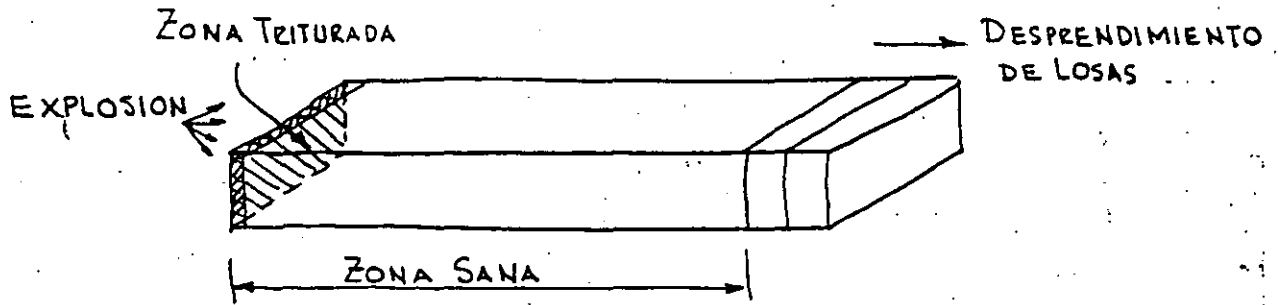
FRAGMENTACION Y DESPLAZAMIENTO =
FUERZA - DISTANCIA = TRABAJO



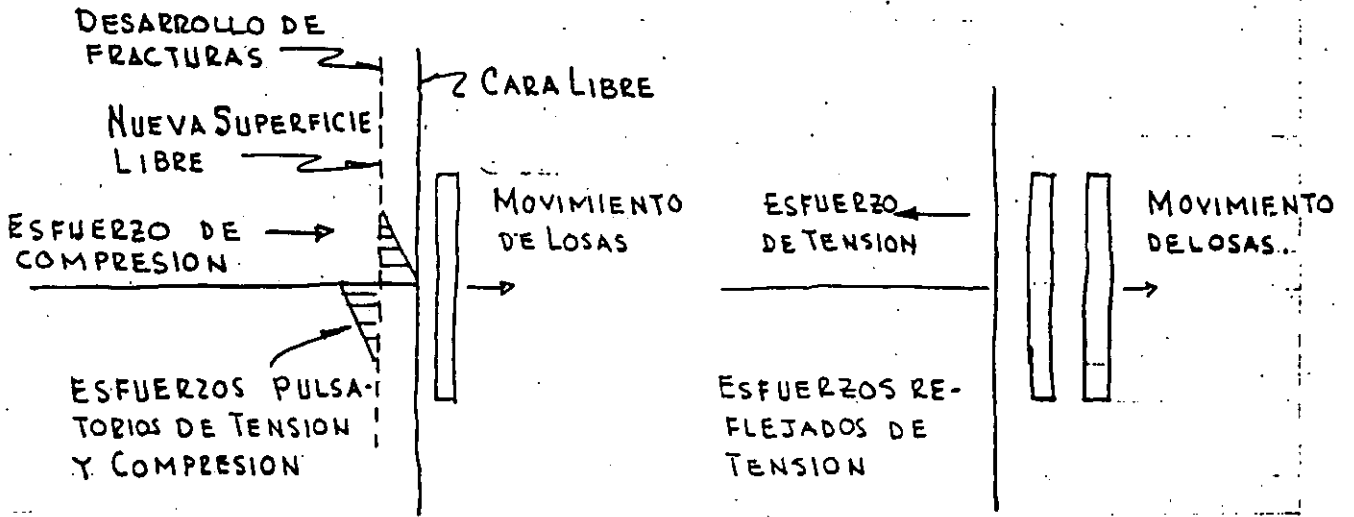
COMPONENTES DE LA ENERGIA
POR IMPACTO DEL EXPLOSIVO



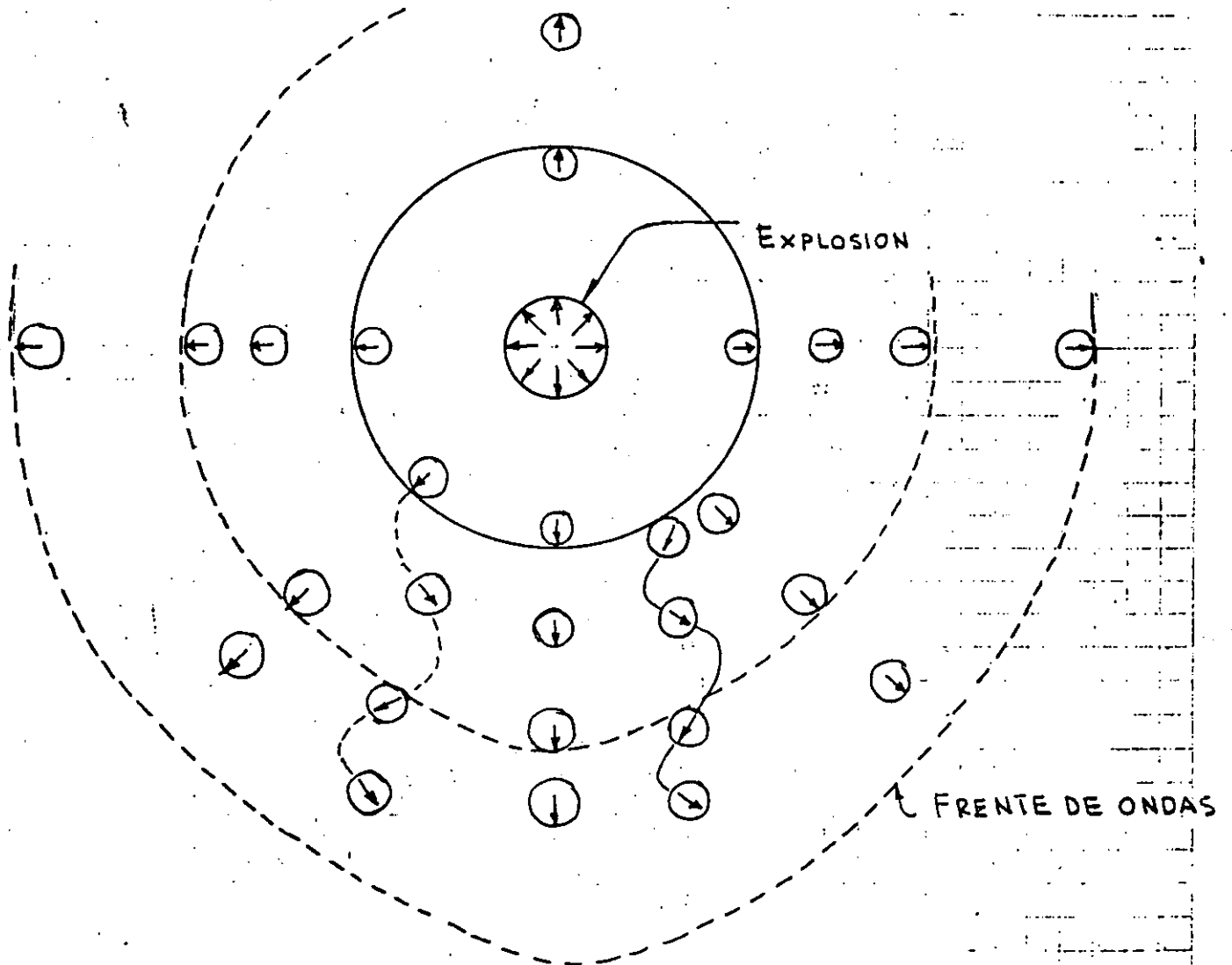
TRANSMISION DE ENERGIA EN MATERIALES
CON CARGAS DE BULSACION



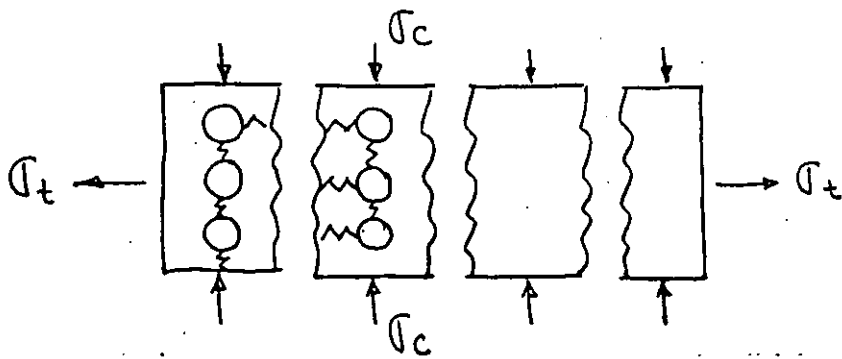
BARRA EXPERIMENTAL DE CONCRETO



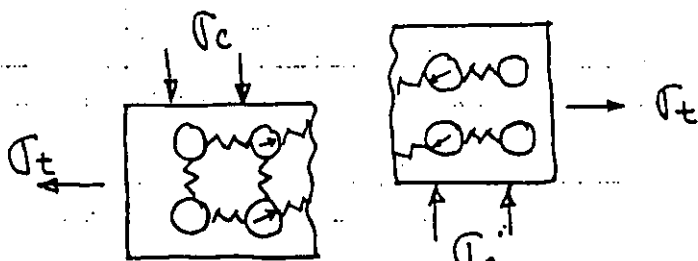
FRAGMENTAMIENTO DE TENSION POR REFLEXION DE IMPULSOS.



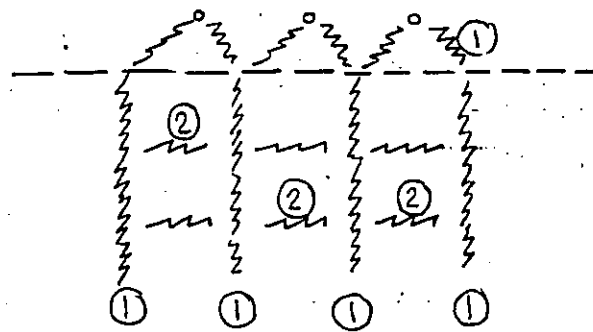
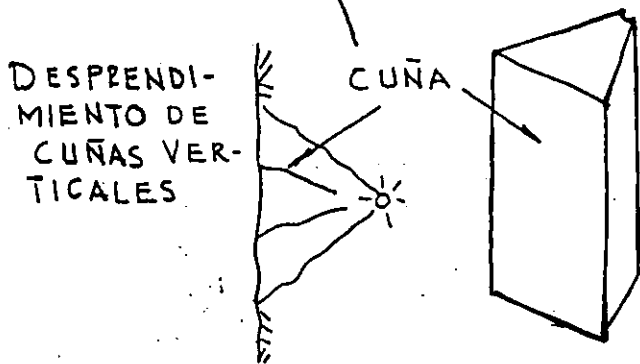
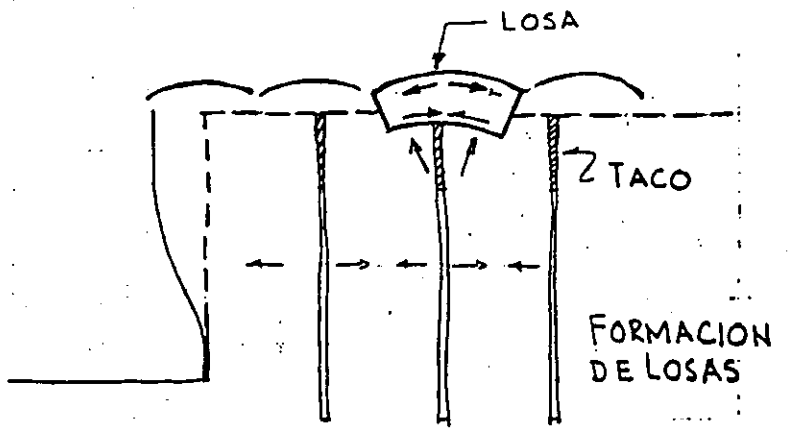
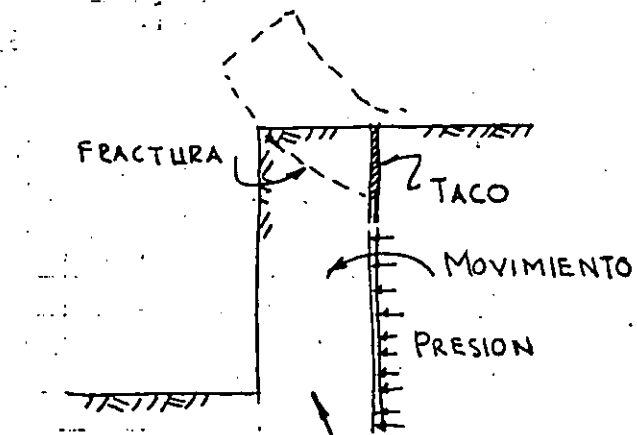
INFLUENCIA DEL PATRON ESTRUCTURAL DE LAS PARTICULAS



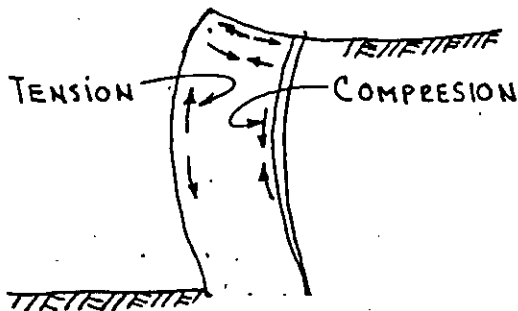
FRACTURAMIENTO POR COMPRESION O TENSION



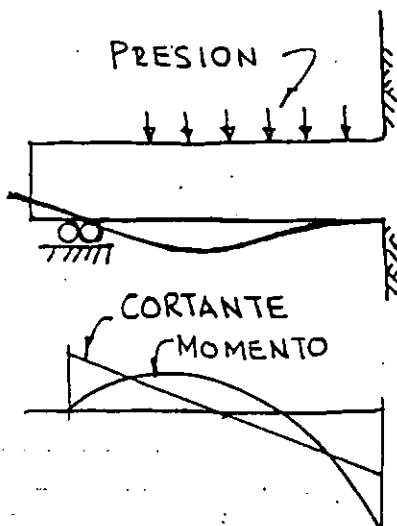
FRACTURAMIENTO POR CORTANTE



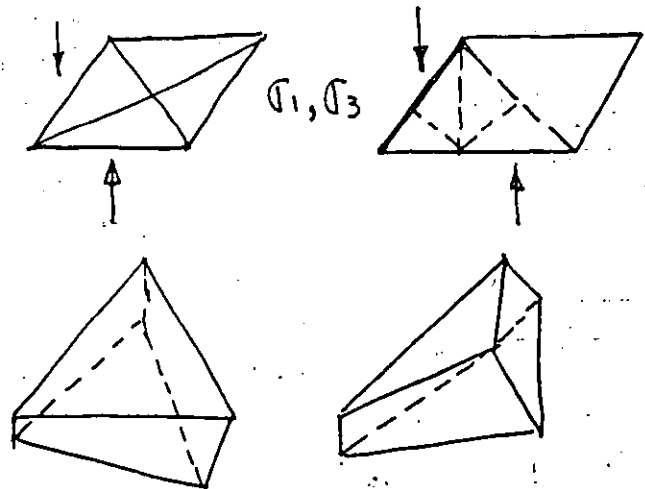
- ① FRACTURAS VERTICALES COMO CUÑAS
- ② FRACTURAS HORIZONTALES
- ③ SALIDA DE GASES



E FECTO DE VIGA



ANALOGIA DE LA VIGA



FRAGMENTOS EN FORMA DE TRIANGULOS

MECANISMO DE FRAGMENTACION

Las rocas normalmente son más resistentes en compresión y trituración que por tensión, por ejemplo: algunas calizas tienen resistencias a compresión entre 250 y 1500 kg/cm² y resistencias en tensión tan bajas como 35 a 150 kg/cm².

Por otro lado, los explosivos y agentes explosivos utilizados producen presiones muy altas que reaccionan con velocidades entre 2500 a 8000 m/seg (5300 a 17 000 mph).

La presión desarrollada súbitamente dentro del barreno alcanza valores desde 18 000 hasta 15 000 kg/cm² dependiendo del tipo de explosivo y de las condiciones de confinamiento.

El efecto del explosivo que reacciona contra la roca produce un impacto, o impulso, desde un golpe aplicado rápidamente, de extremadamente alta intensidad.

Cuando el explosivo está dentro de un barreno circular, se ejerce igual presión en todas direcciones a lo largo de todo el perímetro del agujero. La roca en toda esa región es comprimida y pulverizada hasta una distancia limitada del orden de $\phi/4$.

La aplicación súbita del impacto es seguida por la producción de alta presión que introduce ondas de esfuerzos compresionales que rápidamente penetran en forma de abanico a través del macizo rocoso como ondas elásticas. Esta acción se produce aún cuando las rocas son más bien frágiles, pero son algo elásticas. La velocidad con que viajan las ondas de choque a través de la roca, es función de la densidad del medio. Las rocas densas dan lugar a altas velocidades y las rocas blandas porosas o ligeras, a bajas velocidades.

Parte de la energía transmitida a través de las ondas compresionales es reflejada y refractada (flexionada) por cambios de densidad o discontinuidades de la estructura. Cualquier frente libre o cambio en el tipo de roca produce este efecto. El resto de la energía tiende a mantener su dirección original de viaje.

Los ángulos de reflexión son iguales a los que van hacia las fronteras. Los ángulos de refracción dependen de las características de los dos materiales. Esto es, que en cada cambio de densidad se produce reflexión y refracción de los impulsos de la energía, al equilibrarse la energía sigue viajando en su dirección original.

Si un golpe es ejercido a una partícula, la energía es transmitida en la dirección de aplicación del golpe hacia las partículas adyacentes, hasta que la energía es consumida como resultado del trabajo realizado y por efectos como fricción, amortiguamiento, fragmentación, etc.,

Los suelos granulares no tienen cohesión, de modo que tienen poca o ninguna atracción entre partículas, aún cuando cada partícula pueda tener un poco de elasticidad por sí misma.

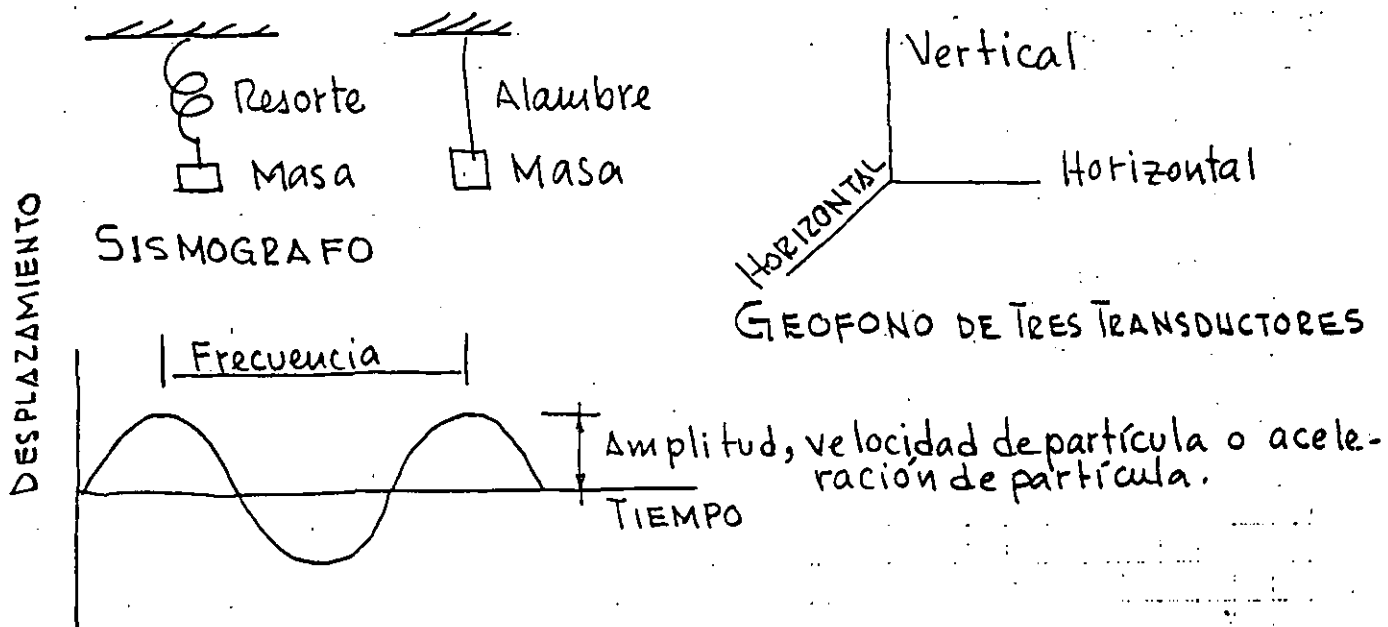
La mayor parte de las rocas es cohesiva y algo elástica, teniendo diferentes efectos que los producidos en fragmentos sueltos.

VIBRACIONES

Las vibraciones del terreno pueden medirse mediante los desplazamientos que se produzcan a una masa sujeta a un resorte o a un alambre. Los impulsos pueden ser proyectados en una pantalla de un osciloscopio, en el cual puede determinarse la velocidad de la partícula, su aceleración y la amplitud de su desplazamiento.

Generalmente la masa viene a ser el núcleo de un pequeño transformador lineal en el cual al desplazarse el núcleo, se producen cambios de voltaje y amperaje en el transformador pequeño que significan los desplazamientos de la masa.

Estos transformadores (LVDT) constituyen los geófonos y pueden instalarse en tres direcciones dentro de un geófono.



ONDAS SISMICAS

ONDAS DE CUERPO:

1. Compresional
Longitudinal
Primaria - P
De empuje
2. Corte
Onda transversal
Onda secundaria - S

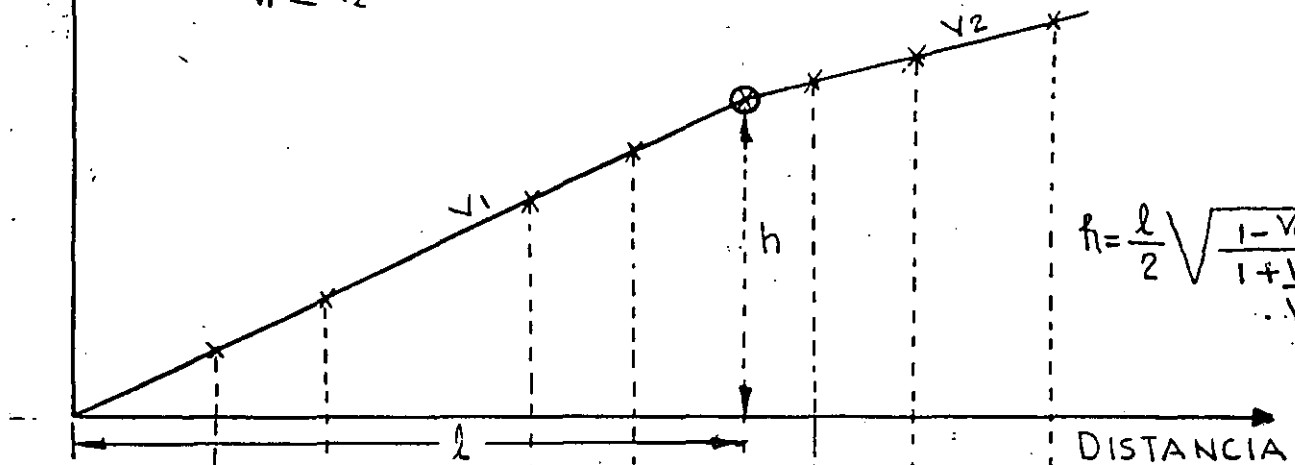
ONDAS DE SUPERFICIE:

3. Love
Rayleigh Igual de peligrosas que las P y S

En la figura 1 se presenta la transmisión de ondas de compresión por reflexión y refracción sísmica.

TIEMPO MS

$$V_1 < V_2$$



$$t = \frac{l}{2} \sqrt{\frac{1 - V_1/V_2}{1 + V_1/V_2}}$$

PUNTO DE VIBRACION

TRINCHERA

GEOFONOS

REFLEXION

ARRIBO FRENTE DE ONDAS

V_1

V_2

CAVERNA

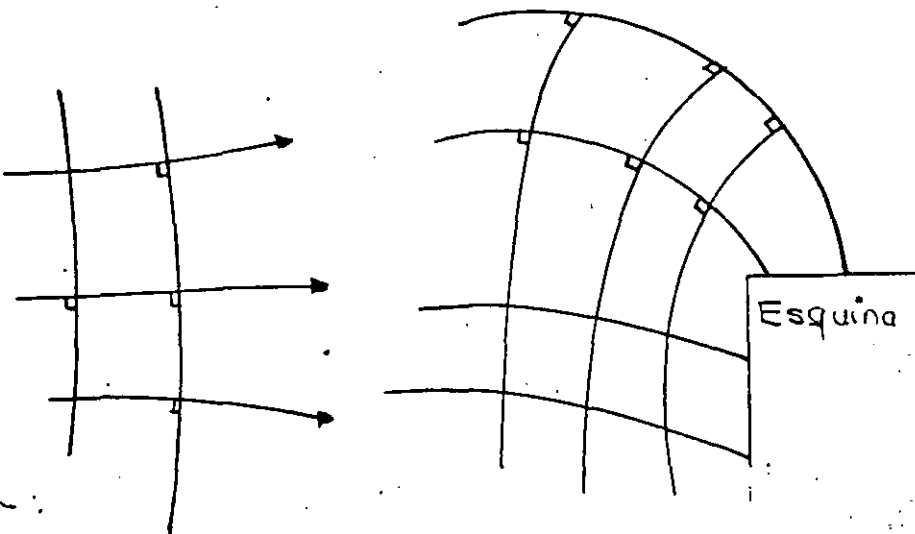
$V_1 = V_2$

$$V_L^2 = \frac{E(1-\nu)}{\rho(1+\nu)(1-2\nu)}$$

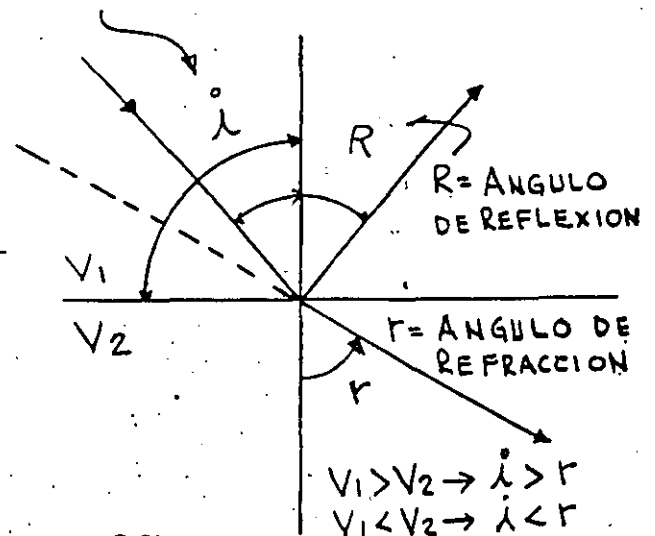
$$E = V_L^2 \rho \frac{(1+\nu)(1-2\nu)}{1-\nu}$$

REFLEXION Y REFRACCION DE ONDAS $V_T^2 = \frac{E}{\rho} \frac{1}{2(1+\nu)}$
 $E = V_T^2 \rho \cdot 2(1+\nu)$

$\dot{\lambda}$ = ANGULO DE INCIDENCIA



PRINCIPIOS DE REFLEXION



35

Apéndice 1

Distancia (m)	Carga, kg (detonación instantánea)						
	Grupo A	B	C	D	E	F	G
0.5				0.02	0.04	0.08	0.16
1	0.008	0.0015	0.03	0.06	0.12	0.25	0.50
2	0.025	0.05	0.09	0.2	0.4	0.7	1.4
3	0.040	0.08	0.16	0.33	0.65	1.3	2.6
4	0.06	0.12	0.25	0.5	1.0	2.0	4.0
5	0.09	0.18	0.36	0.73	1.4	2.8	5.6
6	0.12	0.23	0.47	0.95	1.9	3.8	7.2
7	0.14	0.27	0.57	1.15	2.3	4.6	9.2
8	0.18	0.36	0.72	1.45	2.9	5.8	11.6
9	0.2	0.42	0.85	1.70	3.4	6.8	13.6
10	0.25	0.5	1.0	2.0	4.0	8.0	16.0
12	0.3	0.6	1.3	2.5	5.2	10.5	21
14	0.4	0.8	1.6	3.2	6.4	13.0	26
16	0.5	1.0	2.0	3.9	7.8	15.5	31
18	0.6	1.2	2.4	4.7	9.4	19	38
20	0.7	1.4	2.8	5.6	11	22	44
	1.0	2.0	4.0	8.0	16	32	64
30	1.3	2.6	5.2	10.4	21	42	84
35	1.6	3.2	6.5	13	26	52	104
40	2.0	4.0	8.0	16	32	64	128
45	2.4	4.8	9.5	19	38	76	152
50	2.8	5.5	11	22	44	88	176
55	3.3	6.5	13	26	52	104	208
60	3.8	7.5	15	30	60	120	240
65	4.3	8.5	17	34	68	136	272
70	4.8	9.5	19	38	76	152	304
75	5.3	10.5	21	42	84	168	336
80	5.8	11.5	23	46	92	184	368
85	6.4	12.8	25.5	51	102	204	408
90	7.0	14.0	28	56	112	224	448
95	7.6	15.2	30	61	122	244	488
100	8.5	16.5	33	66	132	264	528
110	9.3	18.5	37	74	148	296	592
120	10.5	21.0	42	84	168	336	672
130	11.7	23.5	47	94	188	376	752
140	13.2	26.3	52.5	105	210	420	840
150	14.5	29.0	58	116	232	464	928
160	16.0	32.0	64	128	256	512	1024
170	17.5	35.0	70	140	280	560	1120
180	19.0	38.3	76.5	153	306	612	1224
190	20.7	41.5	83	166	332	664	1328
200	22.5	45.0	90	180	360	720	1440

Los grupos A-G dependen de la vibración de suelo permisible para construcción, instalación, etc.

El C es el grupo normal

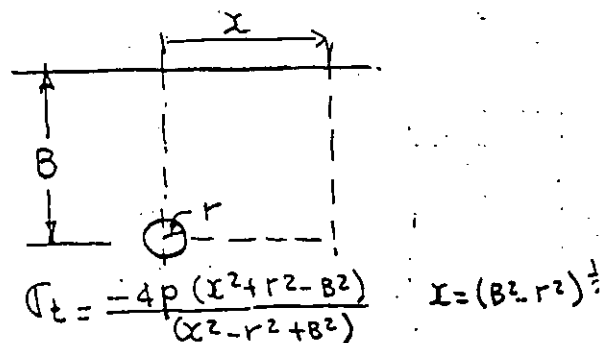
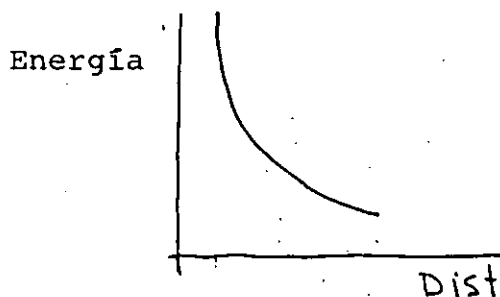
PROPAGACION DE ENERGIA

La energía se propaga disminuyendo con la distancia es directamente proporcional con la presión de detonación e inversamente proporcional al cuadrado de la distancia el Bordo:

$$B = K \left(\frac{Pe}{\sigma_t} \right)^{\frac{1}{2}}$$

en donde:

B bordo
K constante
P presión de detonación
 σ_t resistencia a tensión



El valor más significativo de la energía es la velocidad de la partícula. El Bureau of Mines usa la siguiente expresión:

$$v = H \left(\frac{D}{W^{\frac{1}{2}}} \right)^{-\beta}$$

Esta expresión puede graficarse en escala logarítmica como se presenta en la figura 2, en la cual la distancia escalada

$$SD = \frac{D}{W^{\frac{1}{2}}} \text{ o sea } W = \left(\frac{R}{SD} \right)^{\frac{1}{2}}$$

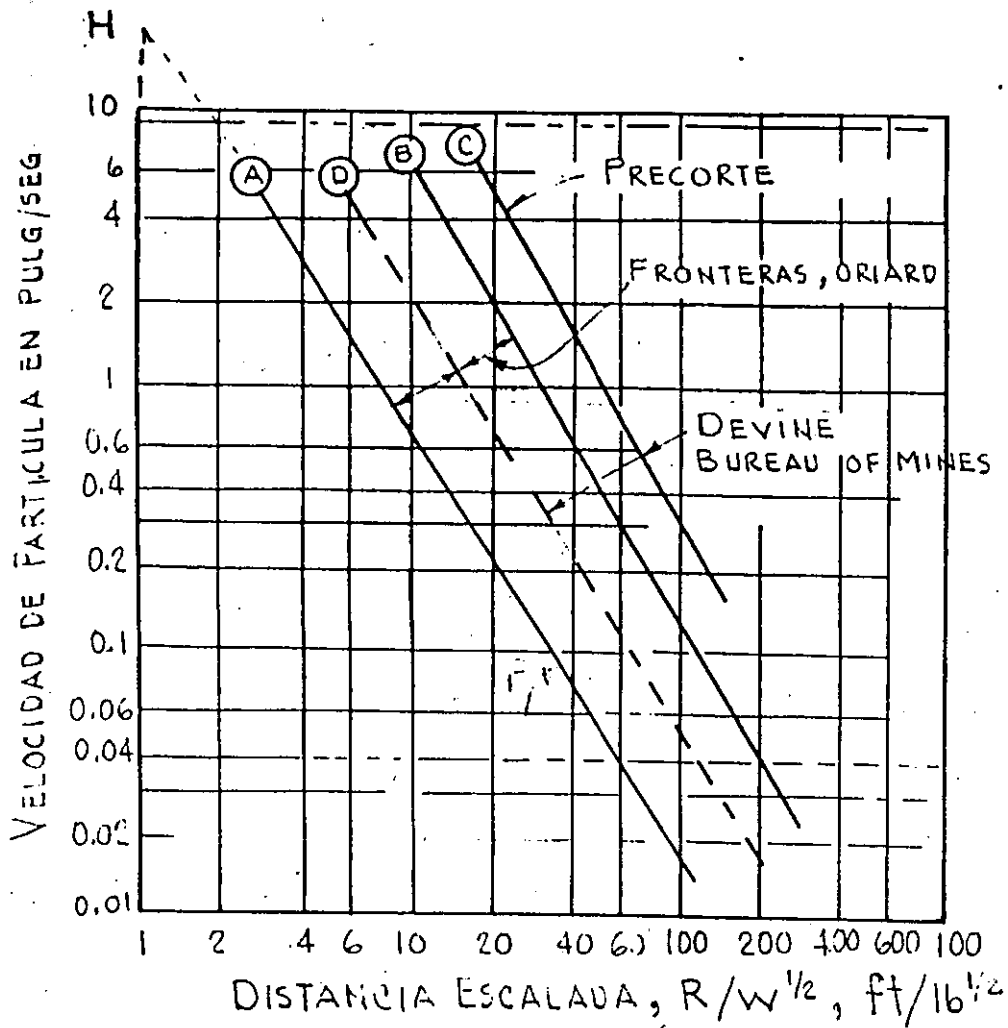
en donde

W máxima carga por retardo

La velocidad de partícula permisible es de 2"/seg.

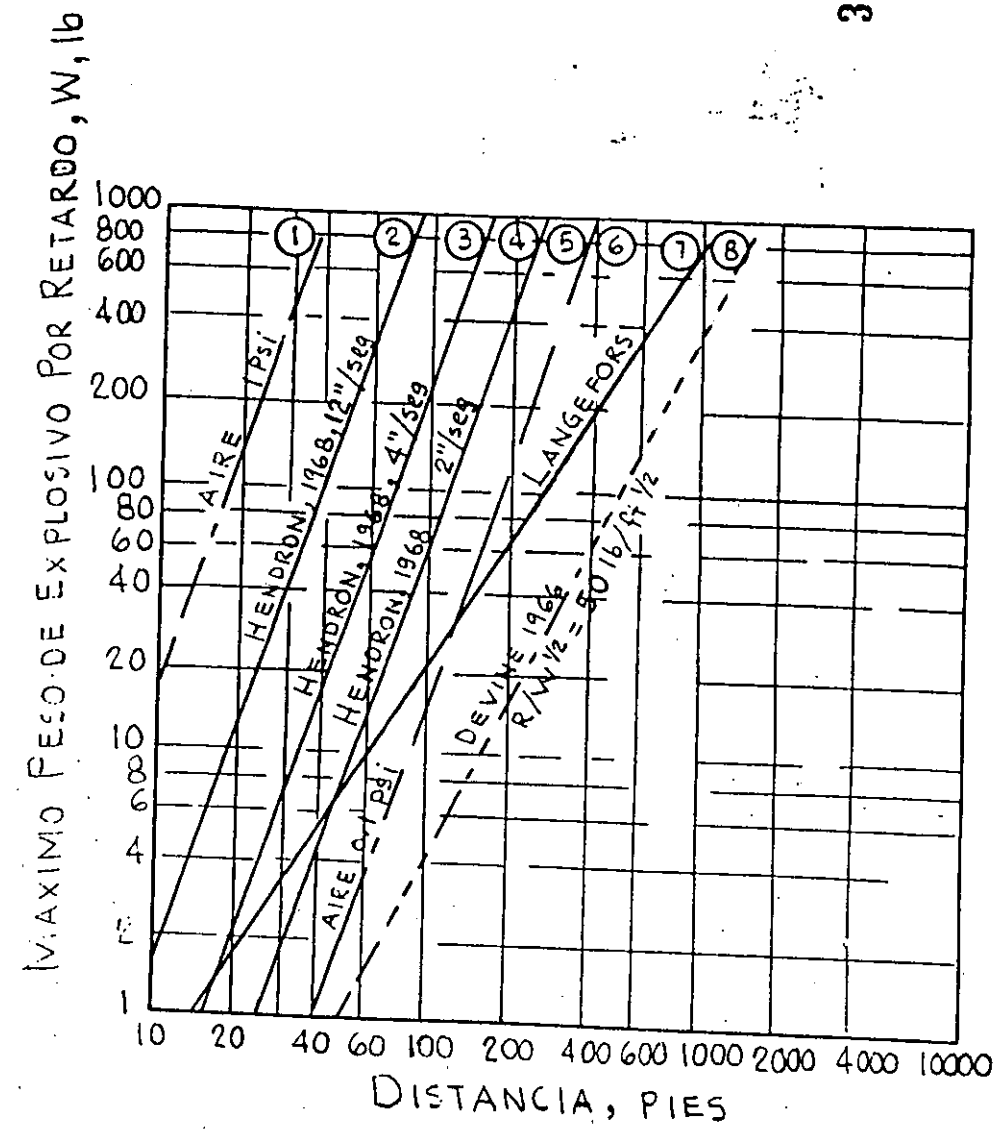
En la tabla I se presentan las cargas de explosivo máximas permisibles por retardo en Suecia.

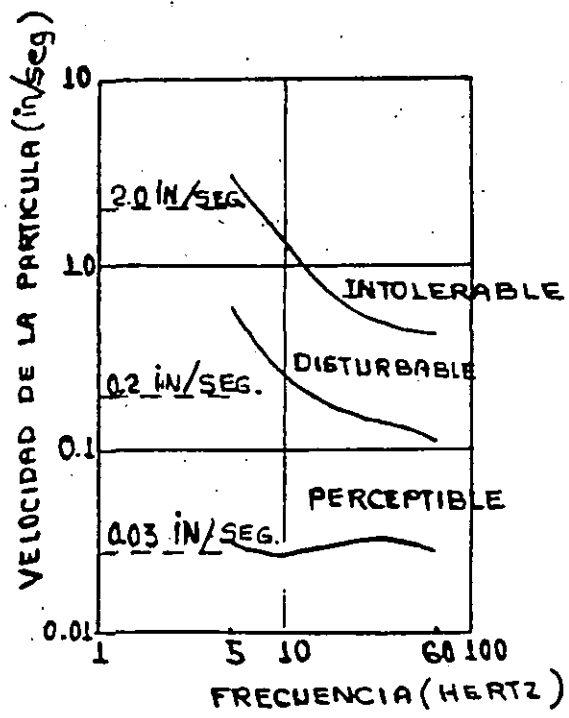
En la figura 3 se presentan los efectos de la velocidad de la partícula con la respuesta humana.



$$V = H \left(\frac{R}{W^{1/2}} \right)^{-\beta}$$

$$SD = \frac{R}{W^{1/2}} ; W = \left(\frac{R}{SD} \right)^2$$





RESPUESTA HUMANA A LA VIBRACION (SEGUN RATHBONE)

REDUCCION DE EFECTOS DE VIBRACIONES

Para reducir los efectos de las vibraciones deberán tomarse las siguientes acciones:

1. Seccionar la voladura (dividir el banco)
2. Reducir la carga por retardo
3. Cerrar el patrón de barrenación, y
4. Utilizar dos cargas por barreno.

ABBREVIATIONS AND SYMBOLS FOR EXPLOSIVE

ENGINEERING DESIGN

- a - Constant
- A - Blast area, sf
- Ap - Amplitude of incident compressive wave, ft.
- AS - Time used in adding steels for one drill cycle, min.
- b - Constant
- B - Optimum burden for charge, ft.
- B' - Minimum burden for charge, ft.
- B" - Maximum burden for charge, ft.
- c - Unit cohesion of material, psi
- C - Total weight of primary explosive charge, lb.
- C_d - Bucket capacity of power shovel, cy (broken material)
- d - Any distance, ft.
- d_e - Loading density of explosive, ppf
- d_p - Distance between primers, ft.
- d_p' - Minimum distance from collar to initial primer, ft.
- d_p" - Maximum distance between any two primers fired simultaneously, ft.
- d_r - Density of rock, pcf (solid)
- D - Time consumed in penetrating for one drill cycle, min.
- D_c - Critical diameter of an explosive, in.
- D_e - Diameter of explosive charge, in.
- D_h - Diameter of blasthole, in.
- D_p - Diameter of primer charge, in.
- DFR - Drill footage rate, fpm
- DPR - Drill penetration rate, fpm

- e - Voids ratio
- E - Total weight of blasthole explosive charge, lb.
- E_r - Modulus of elasticity for rock, psi
- f - Frequency, cps
- F - Total footage drilled for blast round, ft.
- g - Acceleration due to gravity, fps^2
- G_r - Modulus of rigidity, psi
- H - Length of blasthole, ft.
- H_w - Depth of water in blasthole, ft.
- H' - Minimum length of blasthole with single primer, ft.
- H'' - Maximum length of blasthole with single primer, ft.
- J - Depth of subdrilling, ft.
- KE - Kinetic energy, ft-lb
- K_B - Burden ratio or constant
- K_i - Refractive index of a material
- K_m - Bulk modulus of a material, psi
- K_r - Blastability coefficient for a rock
- K_S - Spacing ratio
- K_v - Velocity ratio
- L - Length of open face parallel with blasthole axis, ft.
- L_e - Length of explosive cartridge, ft.
- L_d - Maximum dumping height for power shovel, ft.
- L_m - Maximum cutting height for power shovel, ft.
- M - Time used for moving and setting-up for one drill cycle, min.
- n - Numer of blastholes per row

- N - Total number of blastholes
- p - Number of full passes (loading on both sides) for power shovel
- P - Weight of primer charge, lb.
- PC - Total length of explosive column in blasthole, ft.
- PF - Powder factor for single charge, tons/lb or lb/cy
- P_d - Detonation pressure, psi
- P_e - Explosion pressure, psi
- q - Number of explosive cartridges required to build out of water in blasthole.
- PR - Production rate, tph or cy/hr (Solid material)
- Q_e - Heat of explosion from an explosive reaction, Kcal/kg
- Q_p - Heat of formation for explosive products, Kcal/kg
- Q_r - Heat of formation for explosive reactants, Kcal/kg
- r - Number of blasthole rows
- R_c - Maximum radius of clean-up of floor level for power shovel, ft.
- R_d - Maximum dumping radius for power shovel, ft.
- R_m - Maximum cutting radius for power shovel, ft.
- R_r - Modulus of rupture of a material (tension or flexure), psi
- RE - Relative energy of explosive, ft-lb
- RS - Time for removing steels for one drill cycle, min.
- S - Spacing distance between blastholes within a row, ft.
- SC - Stick count of an explosive
- S_f - Swell factor of a material
- SG_e - Specific gravity of an explosive
- SG_r - Specific gravity of a rock

- t - Time, min.
 U - Total strain energy, ft-lb
 T - Length of stemming in a blasthole, ft.
 V - Volume, cf
 v - Linear velocity, fps
 v_b - Bar velocity of a material, fps
 v_e - Explosive's reaction velocity, fps
 v_i - Particle velocity, fps
 v_p - P-wave propagation velocity of a material, fps
 v_s - S-wave propagation velocity of a material, fps
 w - Width of cut of blast round, ft (measured horizontally and perpendicular to y)
 w' - Minimum cut width for loading by power shovel on one side only, ft.
 W - Total weight of rock, tons
 x - Constant factor
 y - Depth of cut or blast round, ft. (measured horizontally and perpendicular to w)
 z - Minimum horizontal spread of broken material from vertical bench, ft.
 Z - Acoustical impedance, lb-sec/cf
 Σ - Total or sum of
 α - Angle of incident and reflected P-wave, deg
 β - Angle of generated reflected S-wave, deg
 γ - Natural angle of repose, deg
 η - Porosity
 ϕ - Angle of internal friction, deg

- θ - Angle between normal stress and principal stress direction of no shear (x axis), deg
- ρ - Mass density, lb-sec²/ft⁴
- ϵ - Strain, in./in.
- σ_c - Compressive stress, or strength, psi
- σ_d - Stress at any distance, d, psi
- σ_e - Stress introduced into material from explosive, psi
- σ_n - Normal stress, psi
- σ_p - Compressive stress from P-wave, psi
- σ_t - Tensile stress, or strength, psi
- τ_s - Shear stress, or strength, psi
- μ - Poisson's ratio
- Ψ - Failure angle, deg
- v_f - Crack or fracture propagation velocity, fps
- v_m - Rock movement velocity, fps
- t_m - Time for rock to move out from solid, sec.
- t_f - Time for fracture to propagate, sec.

EXPLOSIVES ENGINEERING DESIGN RELATIONSHIPS

I. Explosives' Properties

1. $SG_e = 141/SC$
2. $d_e = 48D_e^2/SC, \text{ lb/ft}$
3. $d_e = 0.34D_e^2(SG_e), \text{ lb/ft}$
4. (a) $P_d = [(6.06 \times 10^{-3})v_e^2(SG_e)]/[1+0.80(SG_e)], \text{ psi}$
 (b) $P_e \cong P_d(\text{max.})/2, \text{ psi}$
5. $\rho_e = 62.4 (SG_e)/g, \text{ lb-sec}^2/\text{ft}^4$
6. $z_e = \rho_e v_e, \text{ lb-sec/cf}$

II. Material's Properties

7. $d_r = 62.4 (SG_r), \text{ pcf}$
8. (a) $\rho_r = d_r/g, \text{ lb-sec}^2/\text{ft}^4$
 (b) $\rho_r = 1.941 (SG_e), \text{ lb-sec}^2/\text{ft}^4$
9. $E_r = \sigma_c/\epsilon_c, \text{ psi}$
10. (a) $G_r = E_r/[2(1 + \mu)], \text{ psi}$
 (b) $G_r = \tau_s/\epsilon_s, \text{ psi}$
11. $K_m = E_r/[3(1 - 2\mu)], \text{ psi}$
12. $Z_r = \rho_r v_p, \text{ lb-sec/cf}$
13. $K_r = \sigma_c/\sigma_t$
14. (a) $v_p = [2G_r(1 - \mu)/\rho_r(1 - 2\mu)]^{1/2}, \text{ fps}$
 (b) $v_p = [E_r(1 - \mu)/\rho_r(1 + \mu)(1 - 2\mu)]^{1/2}, \text{ fps}$
15. (a) $v_s = (G_r/\rho_r)^{1/2}, \text{ fps}$
 (b) $v_s = [E_r/2\rho_r(1 + \mu)]^{1/2}, \text{ fps}$
16. (a) $v_b = (E_r/\rho_r)^{1/2}, \text{ fps}$
 (b) $v_b = [\sigma_c/(\epsilon_c \rho_r)]^{1/2}, \text{ fps}$

17. (a) $v_p = v_s [(2 - 2\mu)/(1 - 2\mu)]^{1/2}$, fps
 (b) $v_p = v_b [(1 - \mu)/(1 + \mu) (1 - 2\mu)]^{1/2}$, fps
18. (a) $K_i = v_p/v_s$
 (b) $K_i = [2(1 - \mu)/(1 - 2\mu)]^{1/2}$
19. $v_f = v_p/3$, fps
20. $\sigma_n = (\sigma_c/2) (1 - \sin \phi)$, psi
21. $\sigma_t = \sigma_c [(1 - \sin \phi)/(1 + \sin \phi)]$, psi
22. (a) $\tau_s = c + (\sigma_c/2) (1 - \sin \phi) \tan \phi$, psi
 (b) $\tau_s = (\sigma_c/2) \cos \phi$, psi
23. $c = (\sigma_c/2) [\cos \phi - (1 - \sin \phi) \tan \phi]$, psi
24. (a) $v_i = 2\pi f A_p$, fps
 (b) $v_i = v_p \epsilon_c$, fps (for plane wave)
25. (a) $\sigma_p = Z_r v_i$, psi
 (b) $\sigma_p = \rho_r v_p^2 \epsilon_c$, psi (for plane wave)
26. $Z = (1/2S_f^x) [L \cot \alpha + 2y (1 - S_f^x)]$, ft
27. $e = \eta/(1 - \eta)$
28. $\Psi = (\phi + 90^\circ)/2$, deg

III. Blasting Design

29. $E = d_e(PC)$, lb
30. $H = L + J$, ft
31. $PC = H - T$, ft
32. $J \cong B/3$, ft. (massive rock)
33. $T \cong 2B/3$, ft. (massive rock)
34. $B = K_B D_e^{1.2}$, ft
35. $K_B = 2.5(160/d_r)^{1/3} (SG_e/1.3)^{1/3} [v_e^2/(12,000)^2]^{1/3}$, ft
36. $K_v = v_e/v_p$

37. (a) $d_p' = 1.61B, \text{ ft}$
 (b) $d_p'' = 6K_v B, \text{ ft}$
38. (a) $B' = 3L/(6K_v + 1), \text{ ft. (single collar primer)}$
 (b) $B' = 3L/(18K_v + 1), \text{ ft. (single center-of-column primer)}$
 (c) $B' = 3L/(9K_v + 2), \text{ ft. (single floor-level primer)}$
39. $B'' = 0.62L, \text{ ft. (single floor-level primer)}$
40. $q = (H_w D_h^2)/(D_h^2 - D_e^2) L_e$
41. $A = wy, \text{ sf}$
42. $W = wyLd_r/2000, \text{ tons}$
43. (a) $PF = W/EN, \text{ tons/lb}$
 (b) $PF = 27EN/WyL, \text{ lb/cy}$
44. $DFR = H/(D + AS + RS + M), \text{ fpm}$
45. $DPR = H/D, \text{ fpm}$
46. $F = HN, \text{ ft.}$
47. (a) $S = (BH)^{1/2}, \text{ ft. (Simultaneous and short delay, } B < H < 4B)$
 (b) $S = 2B, \text{ ft. (Simultaneous and short delay, } H \geq 4B)$
 (c) $S = 1.41 B, \text{ ft. (Long delay, 90 deg crater)}$
 (d) $S = 1.15 B, \text{ ft. (Long delay, 60-120 deg, crater)}$

Loading Shovel Specifications

48. (a) $L_m = L/S_f^x, \text{ ft.}$
 (b) $L_m = 1.2C_d + 30, \text{ ft.}$
49. $L_d = 0.6C_d + 20 \text{ ft.}$
50. $R_c = 2C_d + 19, \text{ ft.}$
51. $R_m = 3C_d + 29, \text{ ft.}$
52. $R_d = R_m - 5, \text{ ft.}$
53. $w' = 2.5C_d + 24, \text{ ft.}$
54. (a) $w = R_c (2p - 1) + R_m, \text{ ft. (Rectangular box wt.)}$
 (b) $w = S_f^x \{R_c [1 + 2(p - 1)] + R_m - 0.5L_m\}, \text{ ft. (corner cut)}$

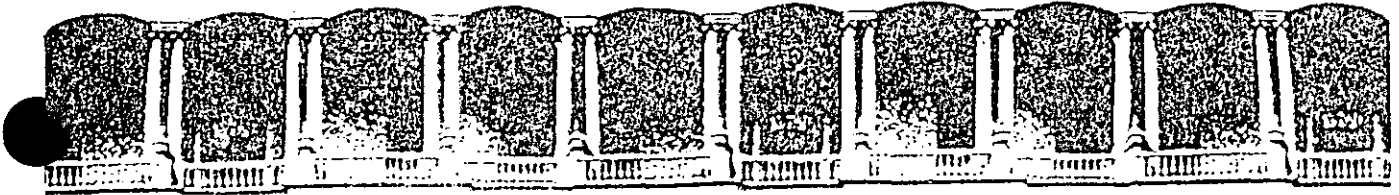
Note: Use w for frontal loading, y for parallel loading.

55. (a) $PR = 1.35 C_d S_f d_r$, tph (50-min. hour, 30-sec cycle)

(b) $PR = 100 C_d S_f$, cy/hr (50-min hour, 30-sec cycle)

Note: For $\gamma = 45$ deg and $S_f^x = 0.85$,

$$L = C_d + 26, \text{ ft, and } Z = 0.59(L + 0.3y), \text{ ft.}$$



**FACULTAD DE INGENIERIA U.N.A.M.
DIVISION DE EDUCACION CONTINUA**

CURSOS ABIERTOS

**IV. CURSO INTERNACIONAL DE INGENIERIA GEOLOGICA APLICADA A
OBRAS SUPERFICIALES Y SUBTERRANEAS**

CUARTO MODULO:

TECNOLOGIA SOBRE EL USO DE EXPLOSIVOS

Del 22 al 26 de junio de 1992

LAS TROJES COL.

PROCEDIMIENTO DE EXCAVACION DEL VERTEDOR

ING. RAUL CUELLAR BORJA

JUNIO - 1992

LAS TROJES, COL.

PROCEDIMIENTO DE EXCAVACION DEL VERTEDOR

860831

Raúl Cuellar Borja

1. TIPO DE ROCA

Origen: Ignea, piroclástica

Estructura: Pseudo estratificada, formada por estratos cuyo espesor varía entre 2 m y 10 m en actitud sensiblemente horizontal.

Clasificación: Brecha volcánica con fragmentos angulosos de andesitas de color gris y rosa cuyos tamaños varían desde 3 cm hasta 1 m, empacados en matriz vítrea andesítica de color gris, de bajo grado de cementación.

De esta manera se tiene una secuencia rítmica de estratos compuestos por brechas con matriz tobácea y tobas brechoides dependiendo del porcentaje relativo de matriz, apreciándose variaciones desde 50% matriz 50% fragmentos hasta 80 a 90% matriz y 10 a 20% fragmentos.

Resistencia: Los fragmentos o clastos andesíticos deben tener más o menos los siguientes valores:

Compresión simple: 300 a 700 kg/cm²

Dureza Mohs: 6.5

Índice de abrasión: 0.30

Índice de perforabilidad: 1.0

La matriz tobácea es blanda con grado de cementación variables desde deleznable a compacta.

Debe tener más o menos los siguientes valores de resistencia:

Compresión simple: 15 a 300 kg/cm²

Dureza Mohs: 6

Índice de abrasión: 0.6

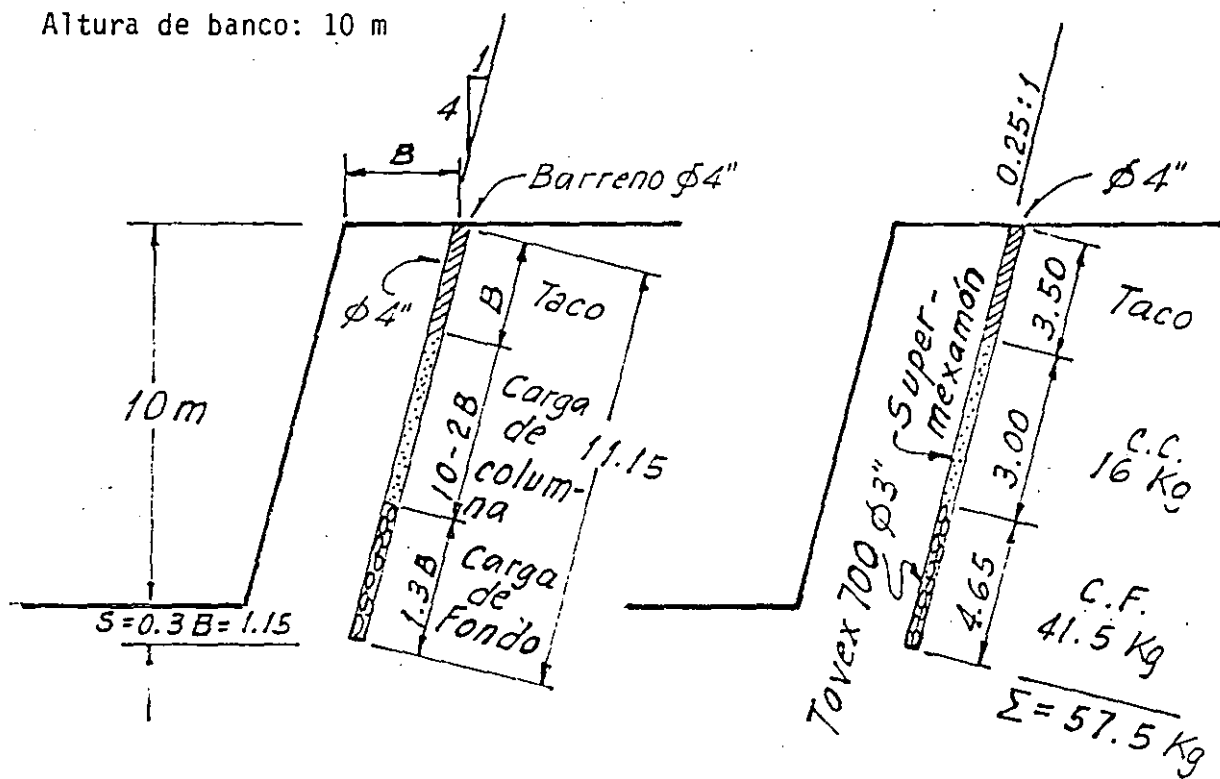
Índice de perforabilidad: 2.0

2. USO DE EXPLOSIVOS EN EL CANAL VERTEDOR

DATOS:

Constante de roca: 0.280 kg/m^3 Explosivo: Tovex 700; Densidad 1.2 g/cm^3 (teórica)Densidad 1.1 g/cm^3 (práctica)Anfomex: Densidad: 0.75 g/cm^3 , en saco; = 0.65 g/cm^3 , práct.

Altura de banco: 10 m

El bordo máximo en función de la potencia del Tovex 700 es 40ϕ Bordo_{máx} = 40ϕ ; Utilizando $\phi = 4''$ Bordo práctico = $B_1 = B_{máx} - \text{Falla de barrenación}$ Falla de barrenación = $F = (\text{error en emboquillado} + \% \text{ desviac.})$

$$\therefore B_{máx} = 40 \times 10.16 = \underline{406.4 \text{ cm}}$$

$$F = (0.10 + 0.05 \times 10) = 0.6 \text{ m}$$

$$\therefore B_1 = 406.4 - 60 = \underline{346.4 \text{ cm}}$$

Consideraciones sobre el bordo máximo

1) El bordo máximo teórico para el Tovex 700 es:

$$B = d \times 30 \sqrt{\frac{q \times S}{\bar{c} \times f \left(\frac{E}{F}\right)}} \quad \text{Fórmula actual}$$

en donde:

d = diámetro del barreno

q = densidad del explosivo, práctica

S = Potencia del explosivo en relación a la de un explosivo con NG = 40% y densidad $\rho = 1.4 \text{ g/cm}^3$: Para Tovex 700
S = 0.9

f = Factor de confinamiento = 1.02

E/B = 1.25

c = Constante de roca + 0.05 kg/m^3
(Factor de seguridad)

$$\therefore E_{\text{máx}} \text{ Tovex 700} = 10.16 \times 30 \sqrt{\frac{1.1 \times 0.9}{0.33 \times 1.02 \times 1.25}}$$

$$\therefore B_{\text{máx}} = 10.16 \times 30 \times 1.5339 = \underline{467.5 \text{ cm}}$$

e) Considerando el bordo máximo $B_{\text{máx}} = 45 \text{ c}$

$$E_{\text{máx}} \text{ Tovex 700} = B_{\text{máx}} \sqrt{\frac{\text{Pot. Tovex 700} \times \text{Densidad}}{\text{Pot. NG 40\%} \times \text{Densidad}}}$$

$$E_{\text{máx}} \text{ Tovex 700} = B'_{\text{máx}} \sqrt{\frac{\text{Factor de roca } 0.4}{\text{Factor de roca } 0.28}}$$

$$E_{\text{máx}} \text{ Tovex 700} = 45 \times 10.16 \sqrt{\frac{0.75 \times 1.1}{1.00 \times 1.4}} = 457.2 \times 0.77$$

$$= \underline{350.96}$$

$$\therefore E_{\text{máx}} = 350.96 \sqrt{\frac{0.4}{0.28}} = \underline{\underline{419.47 \text{ cm}}}$$

Utilizando el valor menor del bordo máximo se tiene:

$$B_{\text{máx}} = 406.4 \text{ cm}$$

Fallas en la barrenación $F = (0.10 + 0.05 \times 10) = 0.6 \text{ m}$

en donde 0.10 = falla de emboquillado y 0.05 es el % de desviación de la barrenación.

$$\therefore B_{\text{práctico}} = B_1 = B_{\text{máx}} - \text{Fallas}$$

$$B_1 = 406.4 - 60 = \underline{346.4 \text{ cm}}$$

Para un espaciamento $E_1 = 1.25 B_1$

resulta: $E_1 = 1.25 \times 346.4 = \underline{433 \text{ cm}}$

$$\therefore E_1 B_1 = 3.464 \times 4.33 = 15 \text{ m}^2$$

Utilizando $B_1 = 3.5 \text{ m}$

Resulta $E_1 = \underline{4.5 \text{ m}}$

Altura de carga de fondo = 1.3 B

Sub-barrenación = $\frac{1}{3} B = \frac{350}{3} \doteq 115 \text{ cm}$

Altura de carga de fondo = 1.3 B

$$\therefore \text{Altura de carga de fondo} = 1.3 \times 3.5 = 4.55 \text{ m}$$

$$\text{Carga de fondo} = 4.55 \times 8.107 \frac{\text{kg}}{\text{m}^3} \times 1.1 \frac{\text{kg}}{\text{kg}} = 40.58 \text{ kg}$$

Altura carga de columna = Altura banco - 2B

Altura carga columna = $10 - 2 \times 3.5 = 3 \text{ m}$

Carga de columna = $3 \text{ m} \times 8.107 \text{ kg/m} \times 0.65 \text{ kg/kg} = 16 \text{ kg}$

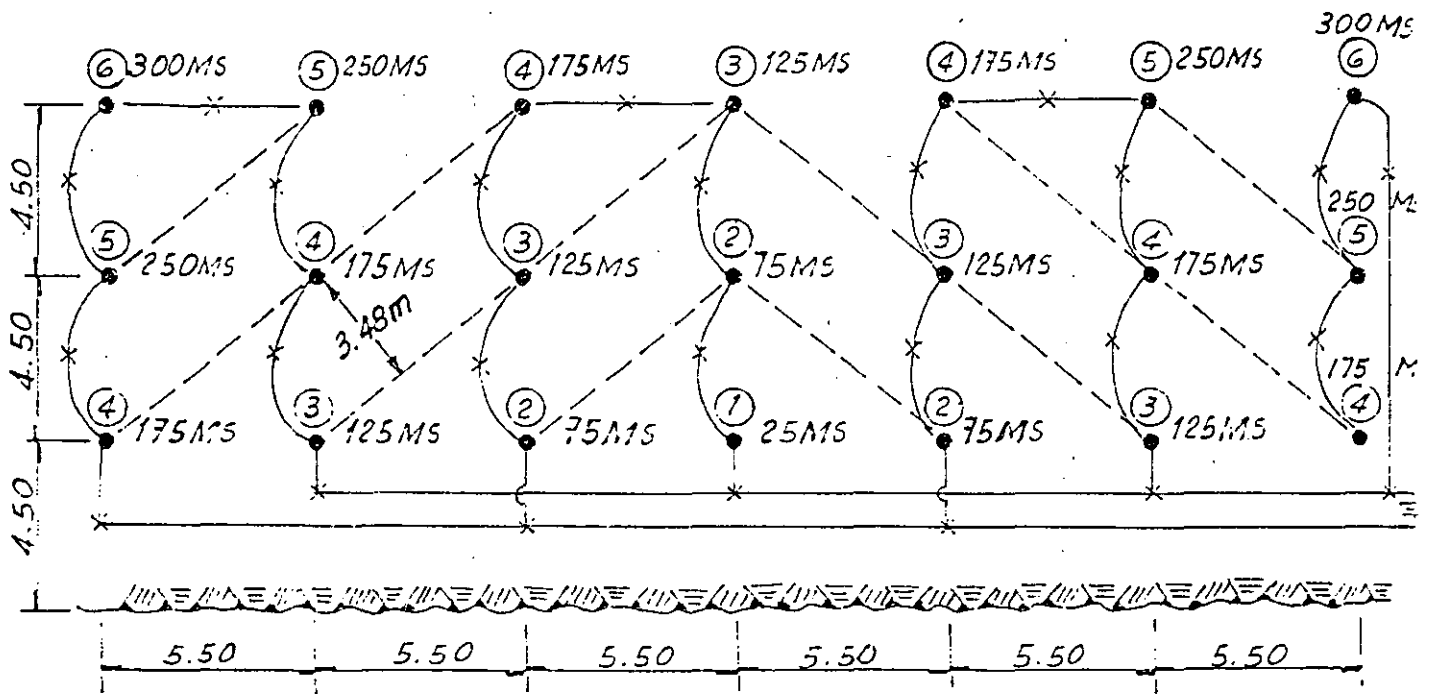
Carga total = $40.6 \text{ kg} + 16 \text{ kg} = 56.6 \text{ kg}$

$$\therefore \text{Factor de carga F.C.} = \frac{56.6}{10 \times 3 \times 3.5 \times 4.5} = 0.360 \text{ kg/m}^3$$

Realizando voladuras con sistema de ignición en V, se tiene:

$$B = 3.5 \times 1.414 = 4.95 \text{ m} \Rightarrow 4.5$$

$$\text{Factor de barrenación} = \frac{11.15}{10 \times 4.5 \times 5.5} = 0.0451 \text{ m/m}^3$$



PLANTA

$$\text{Factor de carga F.C.} = \frac{56.6}{10 \times 4.5 \times 5.5} = 0.229 \text{ kg/m}^3$$

Factor de perforabilidad:

Velocidad de perforación:

De los datos Ingersoll-Rand

Para una roca: Granito Barre

con Trackdrill CM 350 y perforadora VL-140

con Compresor DXL-750; $v = 44$ pies/hora

con Trackdrill ECM 350 y perforadora VL-140

con Compresor DXL-750; $v = 48$ pies/hora

Factor de perforabilidad de la brecha

Para matriz 50% y fragmentos 50% $(2 \times 0.5) = 1$

Para matriz 80% y fragmentos 20% $(2 \times 0.8) = 1.6$

Factor de perforabilidad promedio = 1.3

\therefore Velocidad de perforación = $44 \times 1.3 = 57.2$ pies/h

$$\therefore \underline{v = 17 \text{ m/h}}$$

Duración de brocas

Indice de abrasión = 0.6

Para el granito Barre la duración de brocas de 3" varía entre 400 a 900 ft;
promedio = 650

$$\therefore \frac{650}{0.6} = 1083 \text{ pies} = 330 \text{ m} \approx 350 \text{ m}$$

Duración de brocas = 350 m

3. PROPIEDADES DE LA ROCA

Resistencia en compresión simple; $R_C = 40$ a 80 kg/cm^2

Módulo elástico: $E = 20\,000 \text{ kg/cm}^2$; Toba

$E = 112,000 \text{ kg/cm}^2$; Andesita

Relación de Poisson: $\nu = 0.3$ supuesta; $\rho = 2.2 \text{ ton/m}^3$

Velocidad de transmisión de ondas de compresión V_L

$$V_L^2 = \frac{E(1-\nu)}{(1+\nu)(1-2\nu)} \times g$$

Para la Toba:

$$V_L^2 = \frac{200\,000 \frac{\text{ton}}{\text{m}^2} (1-0.3)}{2.2 \frac{\text{ton}}{\text{m}^3} (1+0.3)(1-0.6)} \times 9.81 \frac{\text{m}}{\text{seg}^2} = \frac{200\,000 \frac{\text{ton}}{\text{m}^2}}{2.2 \frac{\text{ton}}{\text{m}^3}} \times 1.3462 \times 9.81 \frac{\text{m}}{\text{seg}^2}$$

$$V_L^2 = 1\,200\,565 \frac{\text{m}}{\text{seg}^2} \quad \therefore \underline{V_L = 1100 \text{ m/seg} = 3600 \text{ pies/seg}}$$

Para $E = 112\,000 \text{ kg/cm}^2 = 1\,120\,000 \frac{\text{ton}}{\text{m}^2}$

$$\text{resulta: } V_L^2 = \frac{1\,120\,000}{2.2} \times 1.3642 \times 9.81 = 6\,723\,167 \text{ m}^2/\text{seg}^2$$

$$\therefore V_L = 2600 \text{ m/seg} = 8500 \text{ pies/seg}$$

DISENO DE UN SOLO BARRENO

DATOS:

Roca masiva

Altura de banco = 10 m = 32.8 pies

Densidad de roca $SGr = 2.2$ Velocidad ondas P: $V_p = 3600$ pies/seg; Rel. Poisson $\nu = 0.3$ Compresión simple = $80 \text{ kg/cm}^2 = 1140 \text{ lb/pulg}^2$ D_e = Diámetro del explosivo D_n = Diámetro del barrenoDensidad encartuchada del explosivo $SC = 117$ Diámetro crítico $D_c = 1"$

Velocidad confinada del explosivo:

$$V_e = 12\,500 \text{ pies/seg para } D_e = 3"$$

$$V_e = 15\,000 \text{ pies/seg para } D_e = 5"$$

SOLUCION

La relación entre V_e y D_e en el intervalo 1" a 5" puede determinarse por la expresión:

$$y = \frac{C_x}{a + bx} \quad \text{en donde } y = V_e; x = D_e - D_c$$

De donde:

$$V_e = \frac{C(D_e - D_c)}{a + b(D_e - D_c)}$$

Sabemos que $D_c = 1"$ y que: $V_e = 15000$ pies/seg para $D_e = 5"$

$$V_e = 12500 \text{ pies/seg para } D_e = 3"$$

$$\text{Para } D_e = 3''; \quad 12\,500 = \frac{C(3 - 1)}{a + b(3 - 1)} = \frac{2C}{a + 2b}$$

Suponiendo $C = 5000$ como valor de constante

$$\text{Se tiene: } a + 2b = \frac{2 \times 5000}{12\,500} = \frac{4}{5} = 0.8 \quad (1)$$

$$\text{y para } D_e = 5'' \quad 15\,000 = \frac{C(5 - 1)}{a + b(5 - 1)} = \frac{4C}{a + 4b}$$

$$a + 4b = \frac{4 \times 5000}{15\,000} = \frac{4}{3} = 1.33 \quad (2)$$

$$\text{Agrupando: } a + 2b = 0.8 \quad (1)$$

$$\underline{a + 4b = 1.33} \quad (2)$$

$$\text{Restando (1) de (2)} \quad 2b = 0.53 \quad \therefore b \cong 0.27$$

$$\text{Sustituyendo en I} \quad a + 2(0.27) = 0.8$$

$$\therefore a = 0.26$$

Por lo tanto: $a = 0.26$, $b = 0.27$ y $C = 5000$

$$\text{Empleando la expresión: } V_e = \frac{5000(D_c - 1)}{0.26 + 0.27(D_c - 1)}$$

con D_e variando desde 1" a 5"

Comprobación:

$$\text{Para } D_e = 3'': \quad V_e = \frac{5000(3 - 1)}{0.26 + 0.27(3 - 1)} = \frac{10\,000}{0.26 + 0.54}$$

$$\therefore V_e = \underline{12\,500 \text{ pies/seg}} - \text{O.K.}$$

$$\text{y para } D_e = 5'': \quad V_e = \frac{5000(5 - 1)}{0.26 + 0.27(5 - 1)} = \frac{20\,000}{0.26 + 1.08}$$

$$V_e = \underline{14\,900 \text{ pies/seg}} - \text{O.K.}$$

$$\text{Para } D_e = 2''; V_e = \frac{5000(2 - 1)}{0.26 + 0.27(2 - 1)} = \frac{5000}{0.26 + 0.27} = 9450 \text{ pies/seg}$$

$$\text{Para } D_e = 4''; V_e = \frac{5000(4 - 1)}{0.26 + 0.27(4 - 1)} = \frac{15\,000}{0.26 + 0.81} = 14\,000 \text{ pies/seg}$$

Presión de detonación:

$$P_d = \frac{6.06 \times 10^{-3} V_e^2 (SG_e)}{1 + 0.8(SG_e)}$$

$$\text{Densidad del explosivo: } SG_e = \frac{141}{SC} = \frac{141}{117} = \underline{1.2 \text{ g/cm}^3}$$

La densidad práctica del Tovex 700 es $SG_e = 1.1 \text{ g/cm}^3$

$$\text{De donde: } P_d = \frac{6.06 \times 10^{-3} \times 15\,000^2 \times 1.1}{1 + 0.8 \times 1.1} = \frac{6.06 \times 2.25 \times 10^5 \times 1.1}{1.88}$$

$$\therefore P_d \text{ máx} = 796\,790 \text{ lb/pulg}^2 = 56\,182 \text{ kg/cm}^2$$

$$\text{Para } D_e = 2''; P_d = P_d \text{ máx} \left(\frac{9450}{15000}\right)^2 = 796\,790 (0.397)$$

$$\therefore P_d = 316\,723 \text{ lb/pulg}^2 = 22\,304 \text{ kg/cm}^2$$

$$\text{Para } D_e = 4''; P_d = P_d \text{ máx} \left(\frac{14000}{15000}\right)^2 = 796\,790 (0.87)$$

$$\therefore P_d = 694\,077 \text{ lb/pulg}^2 = 48\,878 \text{ kg/cm}^2$$

$$\text{Para } D_e = 3''; P_d = P_d \text{ máx} \left(\frac{12500}{15000}\right)^2 = 796\,790 (0.69)$$

$$\therefore P_d = 554\,021 \text{ lb/pulg}^2 = 39\,016 \text{ kg/cm}^2$$

Determinación del bordo óptimo

Utilizando la expresión: $K_B = 30 \left(\frac{160}{d_r} \right)^{1/3} \left(\frac{SG_e}{1.3} \right)^{1/3} \left(\frac{V_e}{12000} \right)^{2/3}$

en donde:

$$d_r = 62.4 (SG_r) = 62.4 (2.2) = 137 \text{ lb/pie}^3$$

siendo:

d_r = peso volumétrico de la roca

SG_e = Densidad práctica del Tovex 700 = 1.1 g/cm³

V_e = Velocidad del explosivo Tovex 700 \approx 15 000 pies/seg

12 000 = Velocidad de un explosivo base

30 = Relación de bordo promedio = 30

1.3 = Densidad del explosivo base

$$\begin{aligned} \therefore K_B &= 30 \left(\frac{160}{137.3} \right)^{1/3} \left(\frac{1.1}{1.3} \right)^{1/3} \left(\frac{15000}{12000} \right)^{2/3} \\ &= 30(1.05)(0.95) \left(\frac{V_e}{12000} \right)^{2/3} = \underline{29.8} \left(\frac{V_e}{12000} \right)^{2/3} \end{aligned}$$

Para tener el bordo en pies:

$$B = \frac{K_B D_e}{12} = \frac{29.8}{12} \left(\frac{V_e}{12000} \right)^{2/3} D_e$$

$$\therefore B = \underline{2.48} D_e \left(\frac{V_e}{12000} \right)^{2/3}$$

Cálculo del bordo:

En forma general tenemos $B = 2.48 D_e \left(\frac{V_e}{12000} \right)^{2/3}$, pies

$$\text{Para } D_e = 2'' \quad B = 2.48 (2) \left(\frac{9450}{12000} \right)^{2/3} = 4.96 (0.85) = \underline{4.23 \text{ pies}}$$

$$\therefore B = \underline{25.4 \phi}$$

$$\text{Para } D_e = 4'' \quad B = 2.48 (4) \left(\frac{14000}{12000} \right)^{2/3} = 0.92 (1.11) = \underline{11 \text{ pies}}$$

$$\therefore B = \underline{33 \phi}$$

$$\text{Para } D_e = 5'' \quad B = 2.48 (5) \left(\frac{15000}{12000} \right)^{2/3} = 12.4 (1.16) = \underline{14.39 \text{ pies}}$$

$$\therefore B = \underline{34.5 \phi}$$

$$\text{Para } D_e = 6'' \quad B = 2.48 (6) \left(\frac{15000}{12000} \right)^{2/3} = 14.88 (1.16) = \underline{17.27 \text{ pies}}$$

$$\therefore B = \underline{34.5 \phi}$$

$$\text{Para } D_e = 3'' \quad B = 2.48 (3) \left(\frac{12500}{12000} \right)^{2/3} = 7.44 (1.03) = \underline{7.65 \text{ pies}}$$

$$\therefore B = \underline{30.6 \phi}$$

Velocidad de propagación de fracturas:

$$V_f = \frac{V_p}{3}; \quad V_f = \frac{3600}{3} = 1200 \text{ pies/seg}$$

Tiempo de arribo de fracturas al frente libre:

$$\text{Si } t = \frac{B}{V_f}; \quad \text{Para } D_e = 2''; \quad t_f = \frac{4.23}{1200} = 3.5 \text{ ms}$$

$$\text{Para } D_e = 4''; \quad t_f = \frac{11}{1200} = 9.2 \text{ ms}$$

$$\text{Para } D_e = 3''; \quad t_f = \frac{7.65}{1200} = 6.4 \text{ ms}$$

$$\text{Para } D_e = 5''; \quad t_f = \frac{14.39}{1200} = 12 \text{ ms}$$

Tiempo de arranque de la roca:

La velocidad de desprendimiento de la roca es $\approx \frac{1}{6}$ de la velocidad de propagación de las fracturas.

$$t = \frac{B}{V_d} \quad V_d = \frac{V_f}{6} = \frac{1200}{6} = \underline{200 \text{ pies/seg}}$$

Para: $D_e = 2''$; $t = \frac{4.23 \text{ pies}}{200 \frac{\text{pies}}{\text{seg}}} = 0.212 \text{ seg} \times 1000 = \underline{21.2 \text{ ms}}$

$D_e = 4''$; $t = \frac{11 \text{ pies}}{200} = 0.055 \text{ seg} \times 1000 = \underline{55 \text{ ms}}$

$D_e = 3''$; $t = \frac{7.65}{200} = 0.383 \text{ seg} \times 1000 = \underline{38.3 \text{ ms}}$

$D_e = 5''$; $t = \frac{14.39}{200} = 0.072 \text{ seg} \times 1000 = \underline{72 \text{ ms}}$

$D_e = 6''$; $t = \frac{17.27}{200} = 0.0864 \text{ seg} \times 1000 = \underline{86 \text{ ms}}$

Bordo Mnimo

Utilizando la relaci3n de bordo en funci3n de las velocidades de la roca y del explosivo se tiene:

$$K_v = \frac{V_e}{V_p}$$

donde: V_e = Velocidad explosivo

V_p = Velocidad roca

V_p = 3600 pies/seg

Tabulando valores:

D_e "	B, pies	V_e , pies/seg	K_v
1	0	0	0
2	4.23	9 450	2.63
3	7.65	12 500	3.47
4	11	14 000	3.89
5	14.39	14 900	4.14
6	17.27	15 000	4.17

Bordo mnimo para el primer o cebo a nivel del piso

$$B_1 = \frac{3L}{9K_v + 2} ; \quad L = 32.8 \text{ pies (altura banco)}$$

$$\text{Para } D_e = 5"; \quad B' = \frac{3 \times 32.8}{9 \times 4.14 + 2} = \frac{98.4}{39.26} = \underline{2.51 \text{ pies}}$$

De la tabla $B = 14.39 > 2.51$ Se puede reducir el dimetro

$$\text{Para } D_e = 6"; \quad B' = \frac{3 \times 32.8}{9 \times 4.17 + 2} = \frac{98.4}{39.53} = \underline{2.49 \text{ pies.}} \quad \text{Se puede reducir el dimetro}$$

Number of ...

...

...

...

...

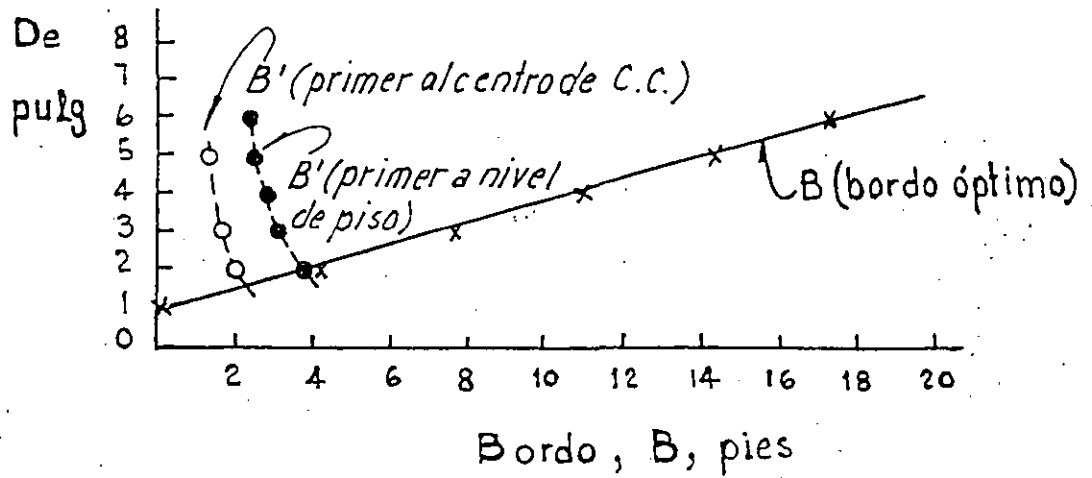
...

...

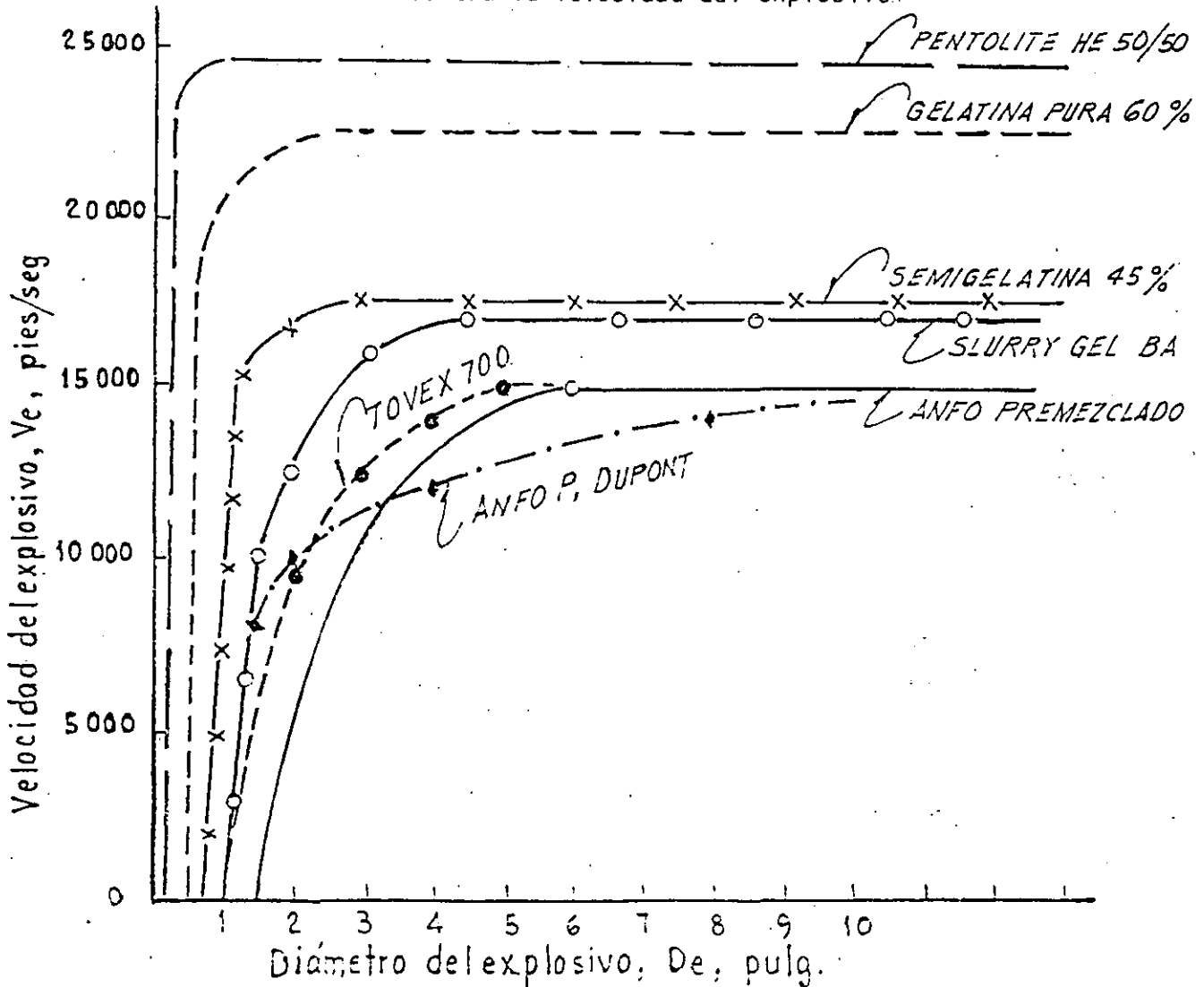
...

...

Graficando la relación entre los bordos y los diámetros se tiene:



Graficando el diámetro contra la velocidad del explosivo:



RESULTADOS:METODO SUECO

Diámetro de barreno $\phi = 4''$ (10.16 cm)

Bordo máximo = 346 cm = 34 ϕ

Bordo práctico = 350 cm

Espaciamiento = 350 x 1.25 = 437.5 \approx 450

Patrón de Barrenación

B = 3.5 m

E = 4.5 m

METODO AMERICANO

Diámetro barreno $\phi 4''$ (10.16 cm)

Bordo óptimo = 335 cm = 33 ϕ

Bordo práctico = 350

Espaciamiento = 335 x 1.25 = 418.75

Area = E x B = 3.35 x 4.1875 = 14.028 m²

Espaciamiento = 14.028/3.5 = 4.0 m

Patrón de Barrenación

B = 3.5 m

E = 4.0 m

RECOMENDACION

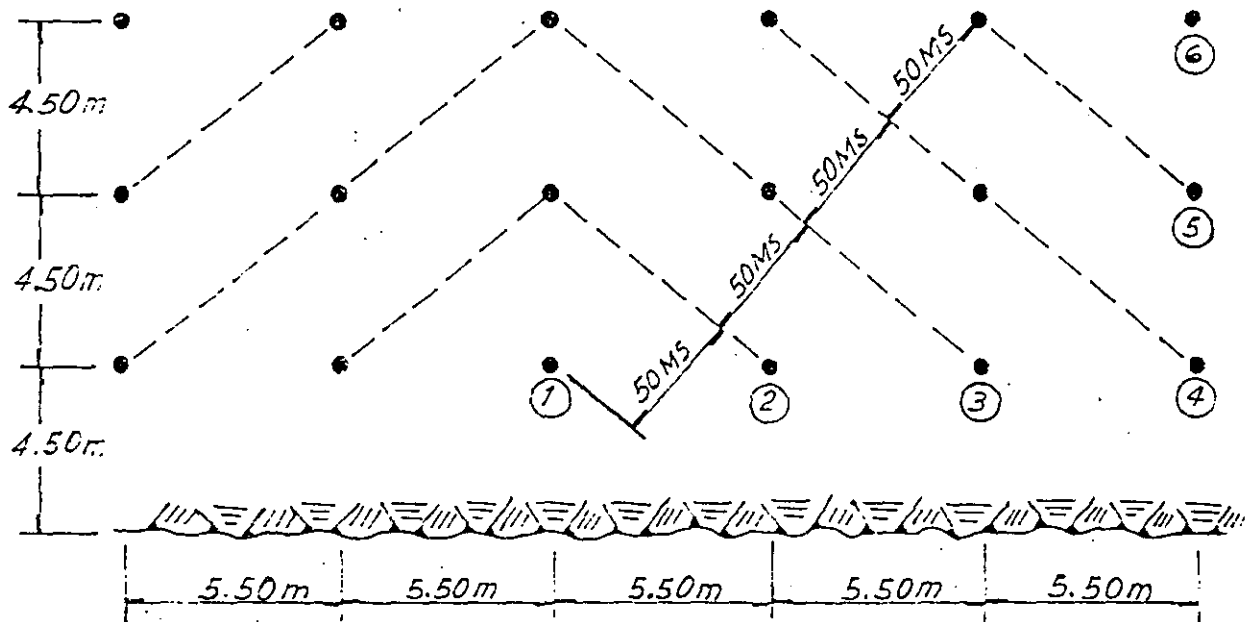
Utilizar el patrón resultante del Método Sueco realizando la voladura con secuencia de ignición en V, de manera que el bordo máximo se presente en forma diagonal resultando entonces un patrón rectangular de 4.5 x 5.5 que tiene un bordo diagonal de 3.48 m.

Resultando:

$$B = 4.5 \text{ m}$$

$$\text{Diámetro barreno } \phi = 4''$$

$$E = 5.5 \text{ m}$$

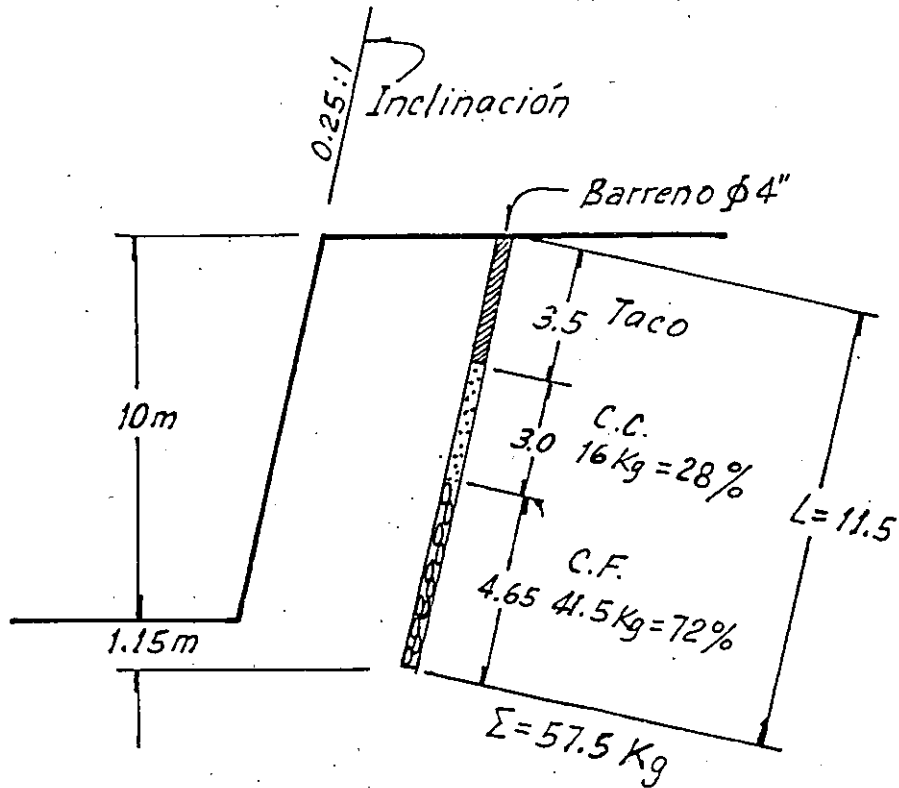


Explosivo: Tovex 700, 3" + Supermexamón

Carga de Fondo = 41.5 kg = 72%

Carga de columna = 16 kg = 28%

Total 57.5 kg



Factor de carga

$$F.C. = \frac{57.5 \text{ kg}}{10 \times 4.5 \times 5.5 \text{ m}^3} = 0.232 \text{ kg/m}^3$$

Factor de barrenación

$$F.B. = \frac{11.15}{10 \times 4.5 \times 5.5} = 0.045 \text{ m/m}^3 = 4.5 \text{ cm/m}^3$$

Velocidad de barrenación en $\phi 4'' \rightarrow 17 \text{ m/h}$

Duración de brocas: 350 m

NOTA: De la pág. 13 se observa que el tiempo de arranque de la roca para $\phi = 4''$ es de 55 ms por lo que se recomienda que la separación entre líneas sea de 50 ms.

COMENTARIOS

Las voladuras de Peñitas, Chis. tuvieron las siguientes características:

Diámetro de barreno: $\phi 2 \frac{1}{2}$ "

Patrón de barrenación:

2.5 x 3.0 m

2.75 x 2.75 m

3.0 x 3.0 m

Factor de carga: 0.180 a 0.36 kg/m³

Factor de barrenación: 0.12 a 0.14 m/m³

$$\text{Suponiendo un banco de } 10 \text{ m} = \frac{10.8}{10 \times 2.5 \times 3} = 0.14 \text{ m/m}^3$$

$$= \frac{10.8}{10 \times 3 \times 3} = 0.12 \text{ m/m}^3$$

Ejemplo: Patrón 3 x 3 m

F.C. = 0.256 Kg/m³

Barreno $\phi 2 \frac{1}{2}$ "

Relación de cargas:

C.F. = 29%

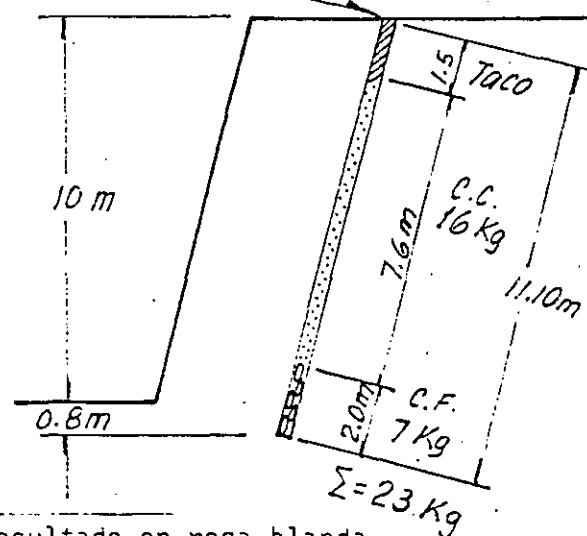
C.C. = 71%

Relación diámetro a bordo:

Para B = 2.5 m; $\phi 6.35$ cm; $K_v = 39$

B = 2.75 m; $\phi 6.35$ cm; $K_v = 43$

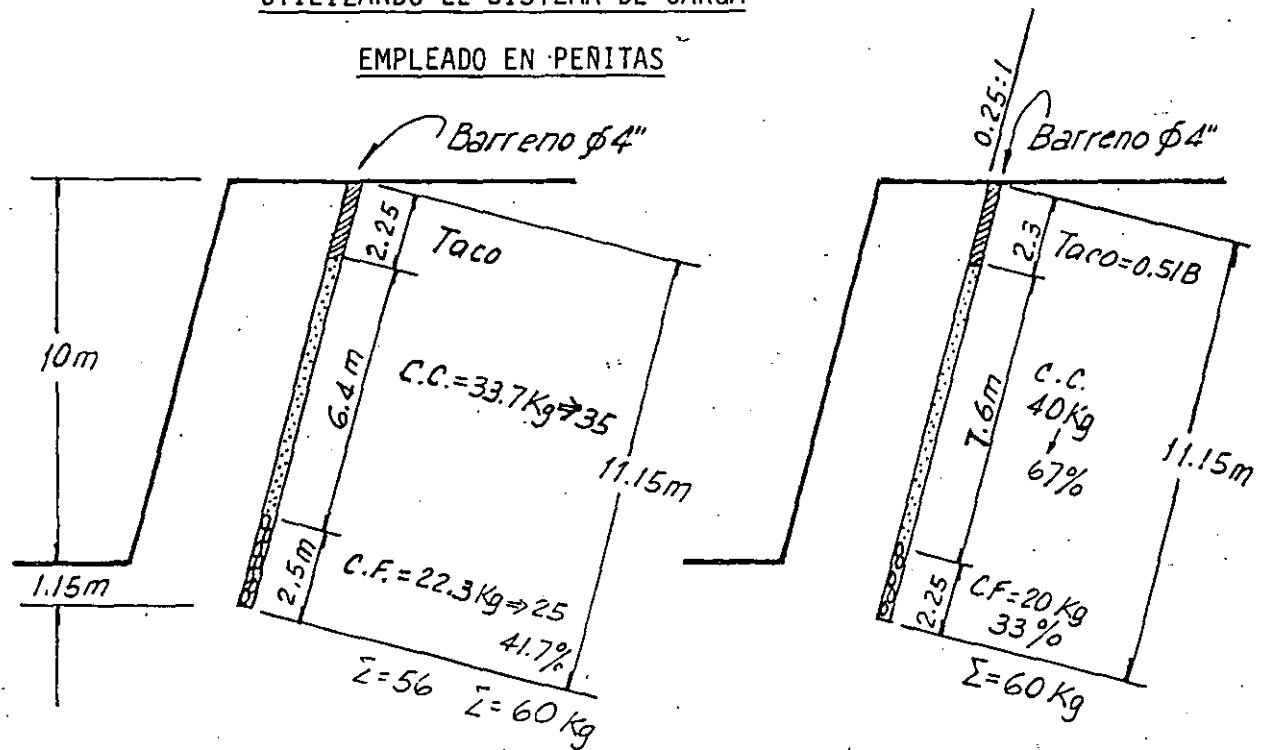
B = 3.00 m; $\phi 6.35$ cm; $K_v = 47$



NOTA: Se tiene la experiencia que dió buen resultado en roca blanda.

UTILIZANDO EL SISTEMA DE CARGA

EMPLEADO EN PENITAS



ALTERNATIVA 1

ALTERNATIVA 2

$$\text{Factor de carga} = \frac{60}{10 \times 4.5 \times 5.5} = 0.242 \text{ kg/m}^3$$

$$= \underline{242 \text{ g/m}^3}$$

$$\text{Factor de barrenación} = \frac{11.15}{10 \times 4.5 \times 5.5} = 0.045 \text{ m/m}^3$$

$$= \underline{4.5 \text{ cm/m}^3}$$

NOTA: Esta carga es más económica que la indicada en la pág. 20 y debe dar buen resultado ya que no se requiere explosivo muy potente, pues la roca es blanda y por tanto se debe usar la mayor cantidad posible de ANFO, recordando que conviene utilizar velocidad de explosivo igual a velocidad de roca. Es mejor la Alternativa 2.

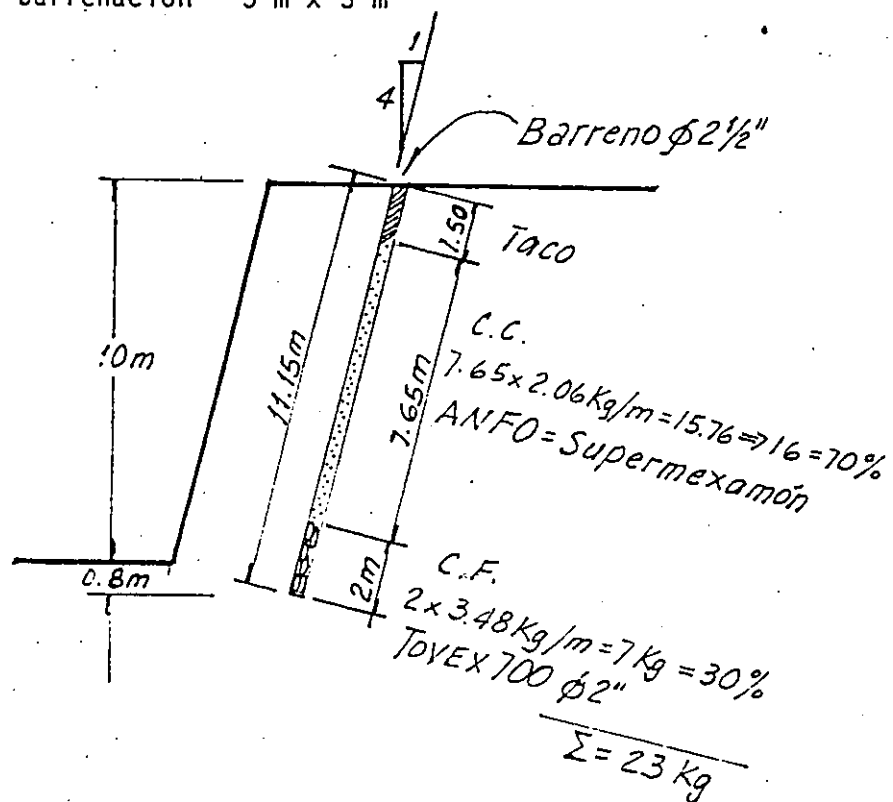
PROPUESTA:

VERTEDOR TROJES

Sept. 2, 1986

Diámetro de barreno ϕ 2 1/2" (6.35 cm)A = 31.67 cm²

Plantilla de barrenación 3 m x 3 m



$$\text{Factor de carga} = \frac{23 \text{ kg}}{10 \times 3 \times 3} = 0.256 \text{ kg/m}^3$$

$$\text{Coeficiente de barrenación} = \frac{11.15}{10 \times 3 \times 3} = 0.0124 \text{ m/m}^3 = 12.4 \text{ cm/m}^3$$

Rendimiento de barrenación = 17 m/h

Utilizar 5 tiempos: 25 ms, 50, 75, 100, 125 y 150 ms.

CANTERA TROJES

(CORTINA)

Sep. 2, 1986

Diámetro barreno = 3" (7.6 cm)

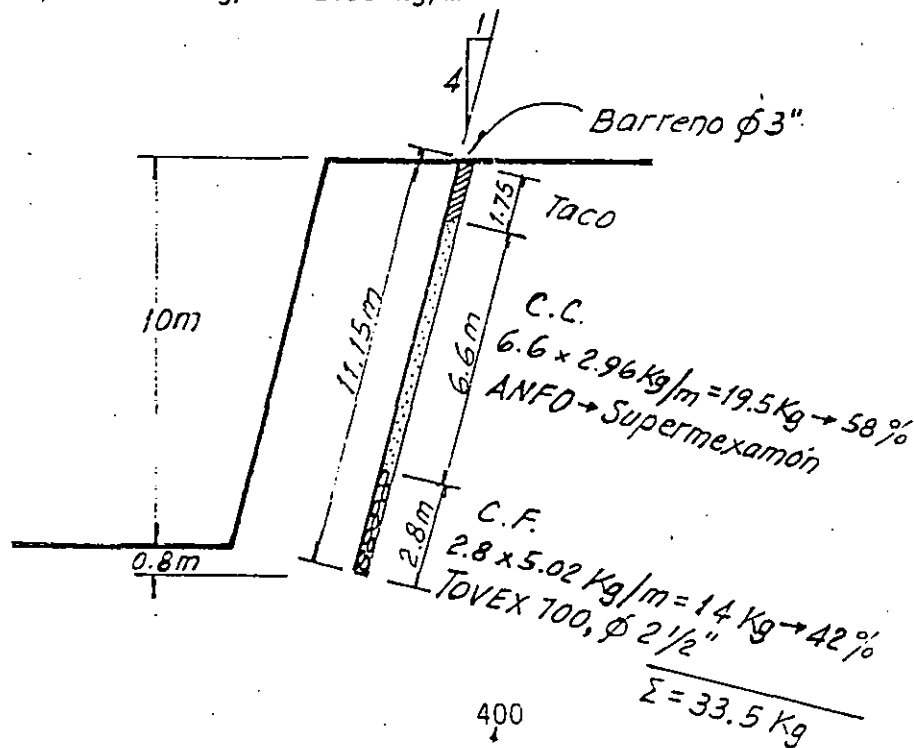
A = 45.6 cm²

Cambia a

Plantilla de barrenación 2.5 m x 2.5 m → 2.75 m x 3.0 m

Tovex 4.56 l/m x 1.1 kg/l = 5.02 kg/m

ANFO 4.56 l/m x 0.65 kg/l = 2.96 kg/m



$$\text{Factor de carga} = \frac{33.5}{10 \times \frac{2.75 \times 3}{2.5 \times 2.5}} = 0.536 \text{ kg/m}^3$$

$$\text{Factor de barrenación} = \frac{11.15}{10 \times \frac{2.75 \times 3}{2.5 \times 2.5}} = 0.18 \text{ m/m}^3$$

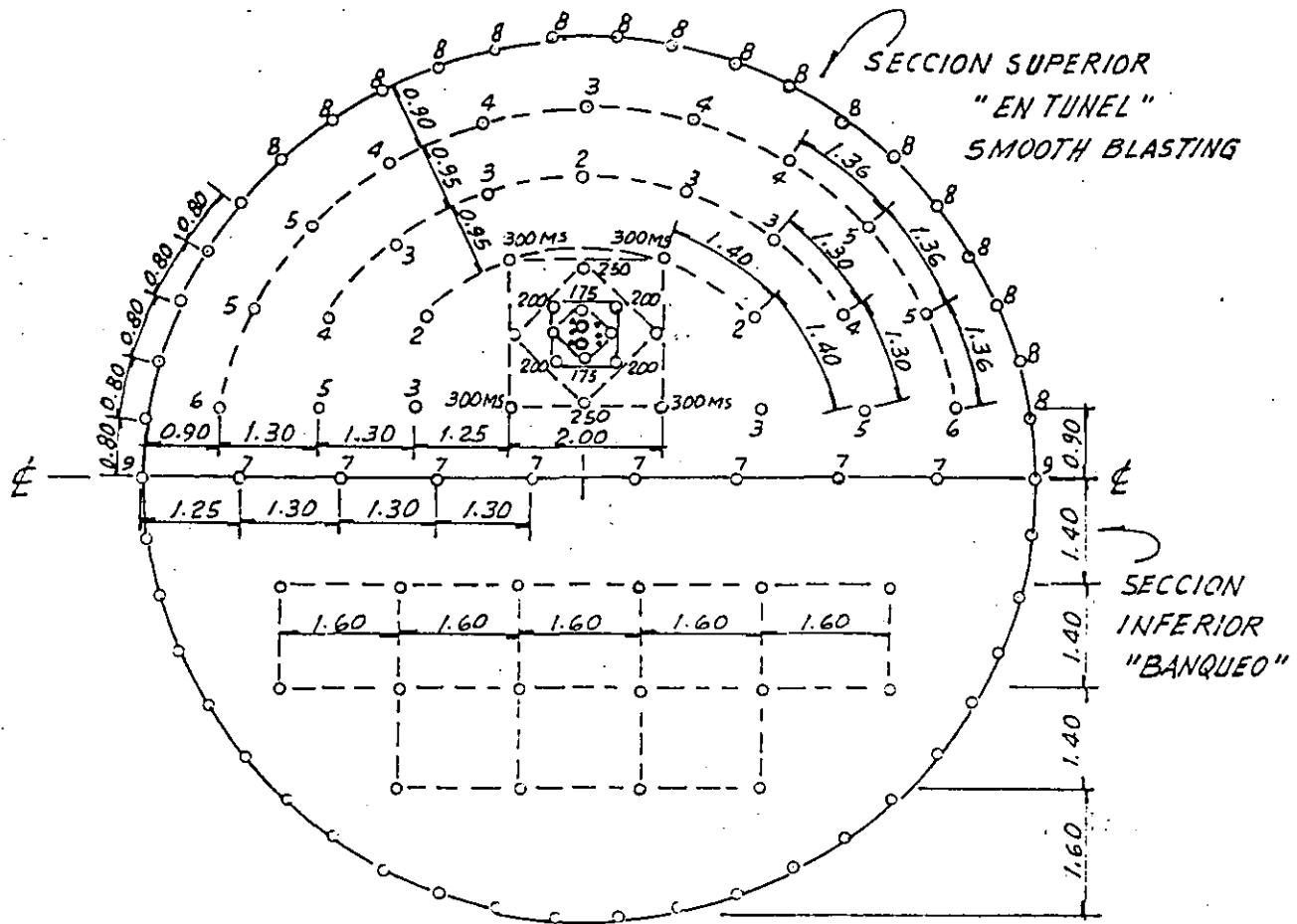
$$= 18 \text{ cm/m}^3$$

$$= 13.5 \text{ cm/m}^3$$

Rendimiento de barrenación: 12 m/h

Utilizar 6 tiempos: 25, 50, 75, 100, 125, 150 ms.

TUNEL DE DESVIO. P. TROJES, COLIMA

 ϕ 11.60 m

Longitud de Barrenación = 4 m

Avance real = 3.90 m

Sección Superior. Area = 52.84 m²

c Barreno 1 7/8"

Precorte: 24 x 1.2 kg = 28.80 kg

TOVEX 100 ϕ 1 7/8" x 8"

Piso: 8 x 7.35 kg = 58.80 kg

TOVEX 700 ϕ 1 3/4" x 16"

Abierta: 24 x 2.85 kg = 68.40 kg

24 x 2.4 kg = 58.5 kg

ANFO (SUPERMEXAMON)

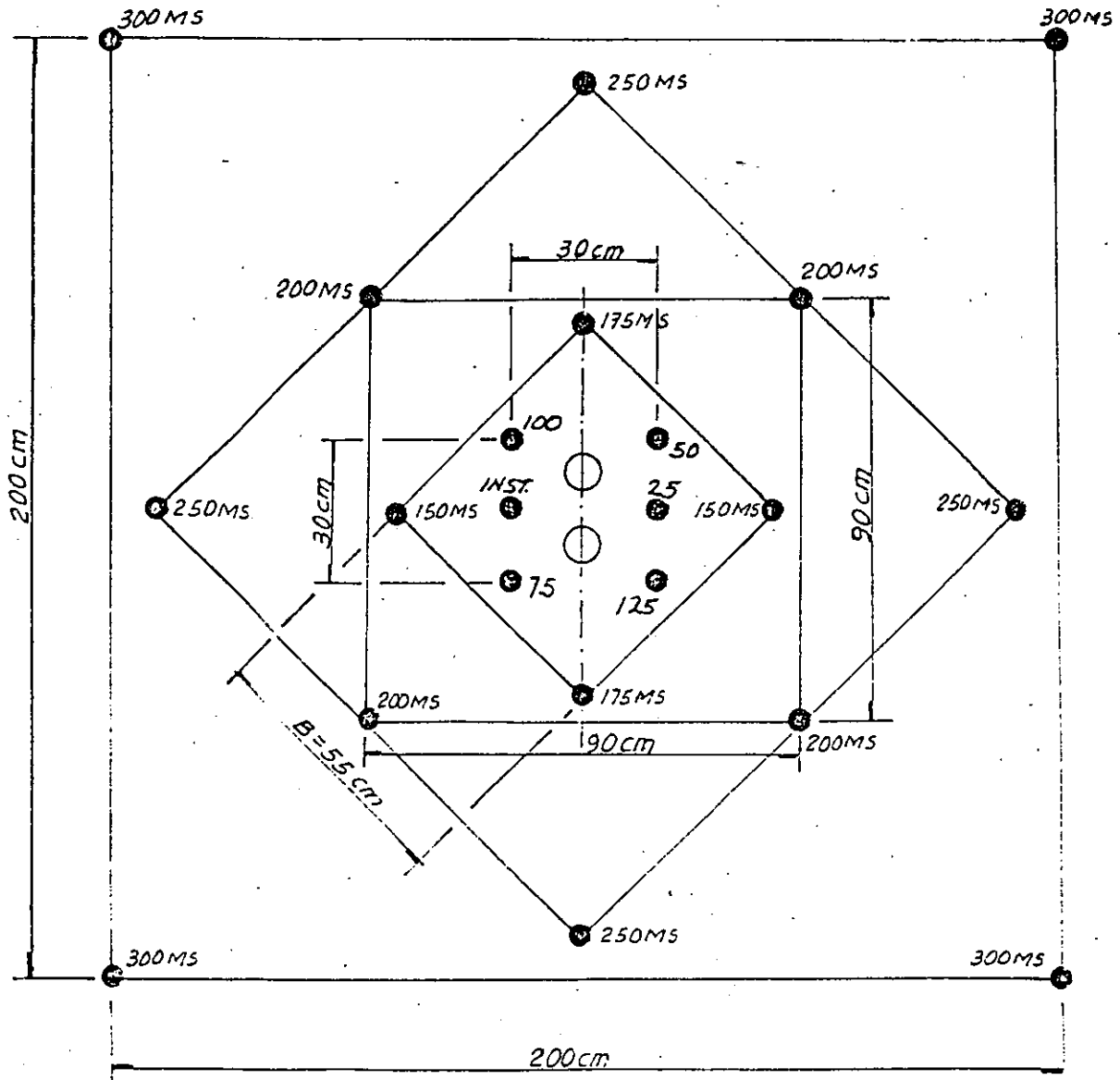
Contracuña: 12 x 3.40 kg = 40.70 kg

4 x 2.70 kg = 11.00 kg

TOVEX 700 ϕ 1 3/4" x 16"

Cuña: 6 x 2 kg = 12.00 kg

CUÑA DE EXPANSION DE BARRENOS PARALELOS
 CON 2 BARRENOS HUECOS DE $\phi 3''$



- ⊙ Barrano $\phi 1\frac{7}{8}''$ (22)
- Barrano $\phi 3''$ (2)

CANTIDAD DE EXPLOSIVO EN LA SECCION SUPERIOR

TOVEX 100	= 28.8 kg	→ 10.4%
TOVEX 700	= 190.9 kg	→ 68.6%
SUPERMEXAMON	= <u>58.5 kg</u>	→ 21.0%
Σ	= 278.2 kg	

No. DE BARRENOS

Barrenos con explosivo	= 78 ϕ 1 7/8"
Barrenos huecos	= 2 ϕ 3"
TOTAL	= 80 Barrenos

COEFICIENTE DE BARRENACION

$$C.B. = \frac{80 \times 4 \text{ m}}{\frac{\pi}{2} \times 5.8^2 \times 3.9} = \underline{\underline{1.55 \text{ m/m}^3}}$$

COEFICIENTE DE CARGA

$$C.C. = \frac{278.2}{\frac{\pi}{2} \times 5.8^2 \times 3.9} = \underline{\underline{1.35 \text{ kg/m}^3}}$$

CALCULO DE CARGAS DE EXPLOSIVO

ϕ barreno 1 7/8" = 4.8 cm Area = 18.1 cm²; Volumen = 1.81 ℓ/m

ϕ explosivo, TOVEX 700; Densidad = 1.18 g/cm³

ϕ 1 3/4"; Long. = 16" = 40.6 cm; Area = 15.5 cm²

Peso de 1 cartucho = 630.02 x 1.18 g/cm³ = 743.4 g

TOVEX 100 Densidad = 1.10 g/cm³

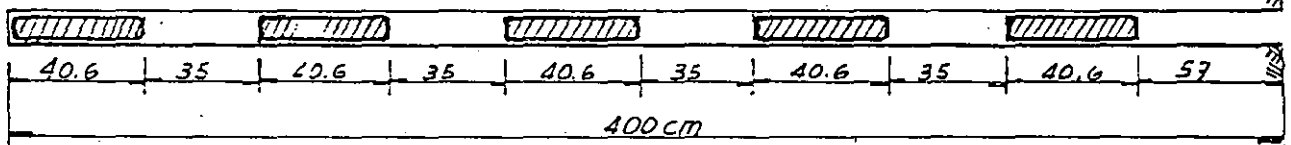
Peso de 1 cartucho = 120 g ϕ 1" x 8"

Peso de explosivo por metro de barreno

TOVEX 700 = 1.81 ℓ/m x 1.18 kg/ℓ = 2.14 kg/m

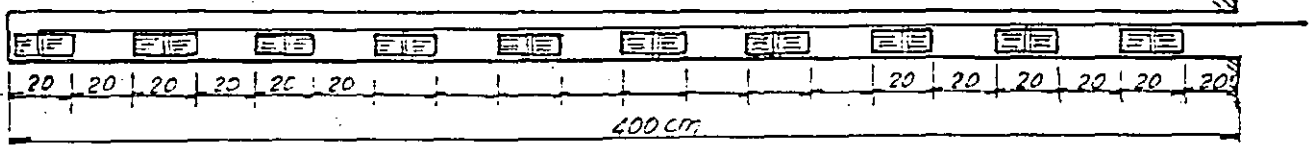
SUPERMEXAMON = 1.81 ℓ/m x 0.65 kg/ℓ = 1.18 kg/m

Peso de explosivo por metro de barreno en contra cuña (TOVEX 700)



Peso = 5 cartuchos x 0.743 kg = 3.72 kg; 3.72/4 = 0.93 kg/m

Peso de explosivo por metro de barreno en precorte (TOVEX 100)



Peso = 10 cartuchos x 120 = 1200 g → 1.2 kg/4 m = 0.30 kg/m

CARGA DE EXPLOSIVO A COLOCAR

- BARRENOS DE PISO Long. = 4 m

TACO DE 57 cm, BARRENOS LLENOS DE TOVEX 700

CARGA DE FONDO (TOVEX 700)

$$C.F. = 2.14 \frac{\text{kg}}{\text{m}} \times \frac{1}{3} \times 4 \text{ m} = 2.85 \text{ kg}$$

CARGA DE COLUMNA (TOVEX 700)

$$C.C. = 2.14 \text{ kg/m} (2/3 \times 4.00 - 0.57) = 4.5 \text{ kg}$$

$$\text{TOTAL} = 2.85 + 4.5 = 7.35 \text{ kg}$$

- BARRENACION ABIERTA Long. = 4 m

CARGA DE FONDO (TOVEX 700)

$$C.F. = 2.14 \text{ kg/m} \times 1/3 \times 4 = 2.85 \text{ kg}$$

CARGA DE COLUMNA (ANFO)

$$C.C. = 1.18 \text{ kg/m} \times (4 - 0.6 - 1/4 \times 4) = 2.44 \text{ kg}$$

- CONTRACUÑA

CONCENTRACION PARA B = 0.70, 1.15 kg/m

(TABLA I-22 CFE) B = 0.25, 0.75 kg/m

12 barrenos con 0.93 kg/m y 4 barrenos con 0.75 kg/m

$$12 \times 0.93 \times (4 - \frac{0.7}{2}) = 40.7 \text{ kg}$$

$$4 \times 0.75 \times (4 - 0.35) = 11.0 \text{ kg}$$

0) - CUÑA

CONCENTRACION = 0.65 kg/m (TABLA I-21 CFE)

NO. BARRENOS = 6 de ϕ 1 7/8"

6 x 0.55 kg/m (4 - 0.35) = 12 kg

- BARRENOS DE PRECORTE

TOVEX 100 ϕ 1" x 8" con 120 g c/u, de L = 20 cm

Densidad 1.10 g/cm³

10 cartuchos x 120 g = 1.2 kg

0) 12 kg/4 m = 0.30 kg/m (TABLA I-24 CFE)

No. de barrenos = 24

24 x 0.3 kg/m x 4 m = 28.8 kg

0)

MEMORANDUM

TO : SAC, NEW YORK

FROM : SAC, NEW YORK

SUBJECT: [Illegible]

[Illegible]

[Illegible]

[Illegible]

[Illegible]

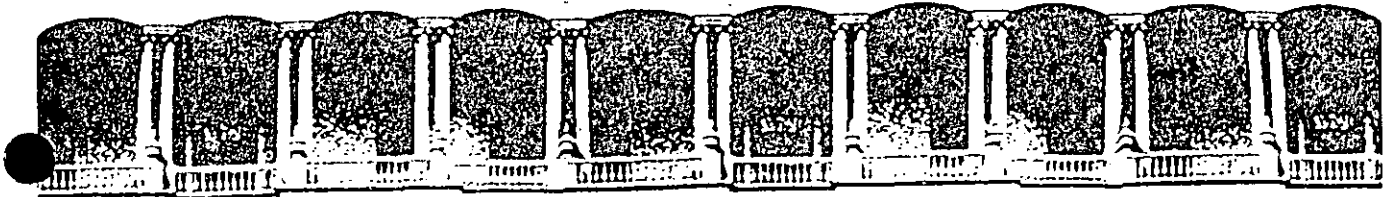
[Illegible]

[Illegible]

[Illegible]

[Illegible]

[Illegible]



**FACULTAD DE INGENIERIA U.N.A.M.
DIVISION DE EDUCACION CONTINUA**

CURSOS ABIERTOS

***IV. CURSO INTERNACIONAL DE INGENIERIA GEOLOGICA APLICADA A
OBRAS SUPERFICIALES Y SUBTERRANEAS***

CUARTO MODULO:

TECNOLOGIA SOBRE EL USO DE EXPLOSIVOS

Del 22 al 26 de junio de 1992

PROPIEDADES GEOMETRICAS Y MECANICAS DE LAS ROCAS

ING. RAUL CUELLAR BORJA

JUNIO - 1992

PROPIEDADES GEOMETRICAS Y MECANICAS DE LAS ROCAS

Raúl Cuéllar Borja

1.- PROPIEDADES GEOMETRICAS DE LOS MACIZOS ROCOSOS

1.1.- INTRODUCCION

En este capítulo se describen algunos de los sistemas usuales que se utilizan para describir ya sea en forma gráfica o escrita las características geométricas de la estructura de los macizos rocosos.

1.2.- Mapas geológicos

Estos mapas contienen la delimitación geográfica de las formaciones de roca existentes en el lugar y se aprovechan para señalar mediante una simbología las características de la estructura de los macizos rocosos como son: plegamientos, cabalgaduras, hundimientos, etc., así como los rasgos más significativos de las discontinuidades como son: fracturas o juntas, fallas, planos de estratificación, planos de foliación, oquedades, etc.

Es importante anotar la orientación (rumbo y echado) y espaciamiento de las discontinuidades, así como una descripción de las características de las caras o planos de discontinuidad. Por ejemplo: Los términos cerradas o abiertas se aplican para describir el grado

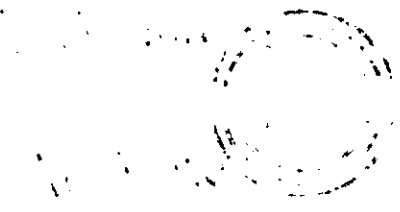
de estanqueidad de las discontinuidades, esta información debe acompañarse de una descripción del material de relleno. También deben anotarse las características de los plausos en los que están contenidas las caras de las juntas, por ejemplo: si el plauso es recto o alabeado y si las caras son lisas, rugosas o escalonadas. A estas características de los plausos de las juntas se les puede asignar un número en función de su resistencia al corte.

Existen dos formas básicas para representar las estructuras y los rasgos estructurales.

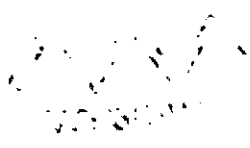
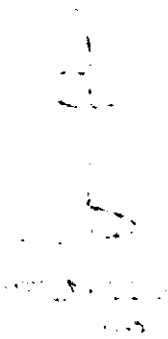
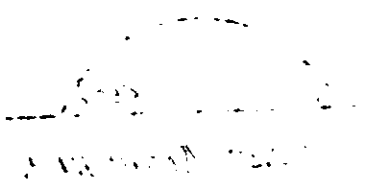
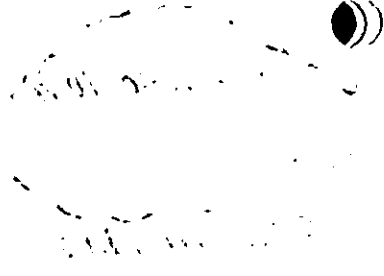
- 1) Mapas con la localización geográfica de estructuras y rasgos estructurales, anotando sus características físicas de orientación y posición y 2) Gráficas en las que se muestra la frecuencia relativa de las discontinuidades, mostrando el intervalo de variación de las orientaciones que ocurren en el sitio.

Ambos sistemas tienen sus ventajas y limitaciones.

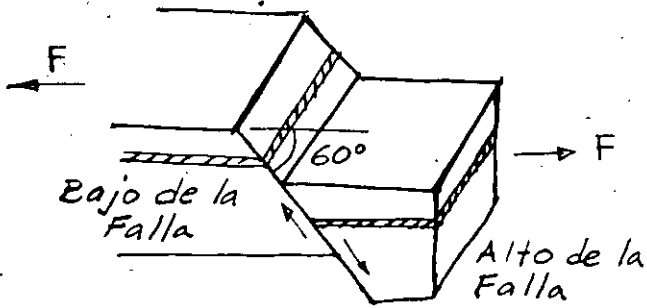
El primer sistema es preferido para usos generales. Permite la construcción de secciones transversales en cualquier área crítica particular del proyecto, ya sea una ladera o la pared de una excavación subterránea. De esta manera se puede identificar la presencia de alguna discontinuidad cuya orientación sea adversa a alguna excavación.



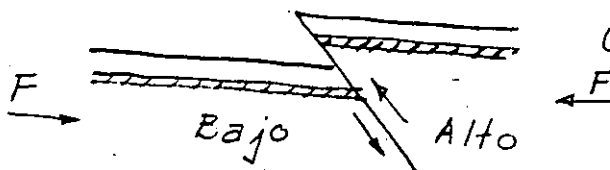
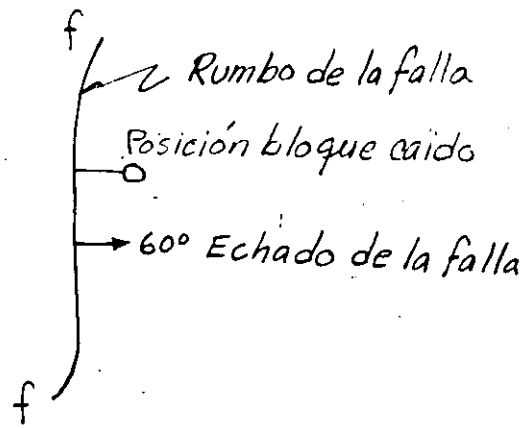
Handwritten text, possibly a label or note, located between the circular diagram and the diagram below it. The text is mostly illegible.



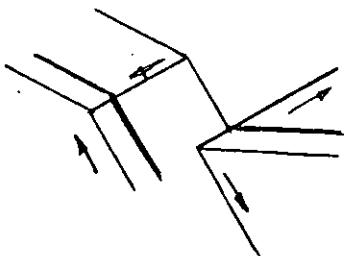
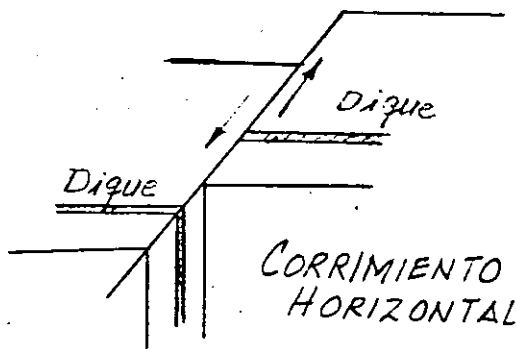
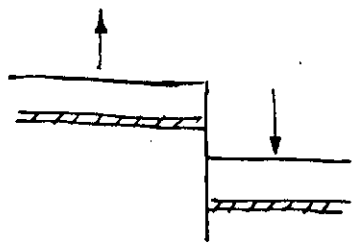
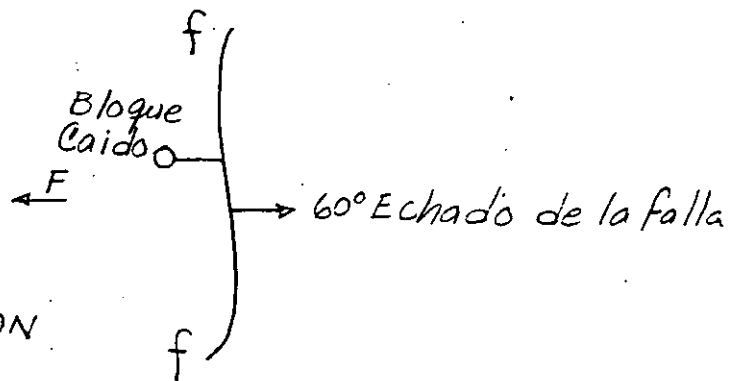
FALLAS



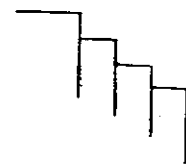
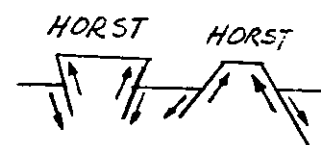
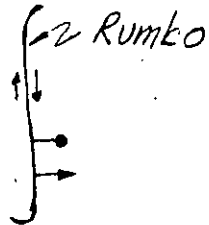
NORMAL O TENSION



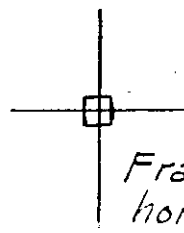
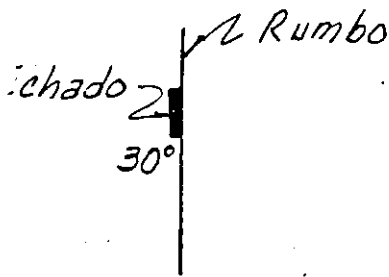
INVERSA O COMPRESION



OBLICUA



ESCALERA ECHELON



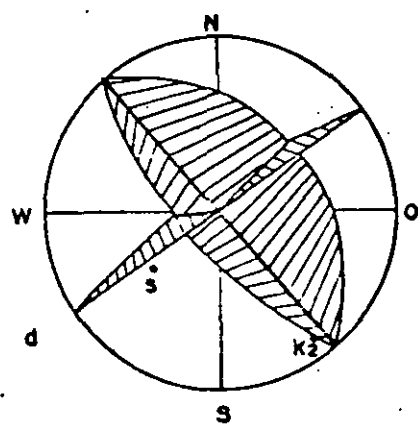
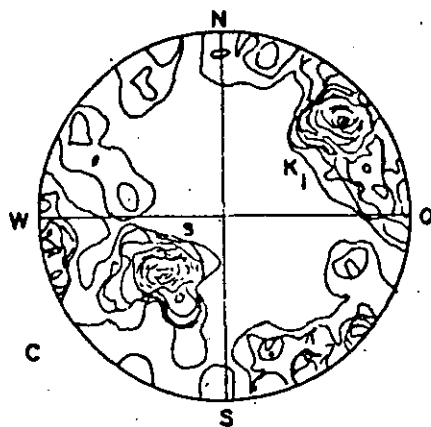
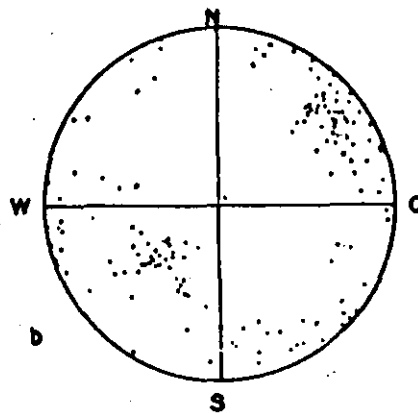
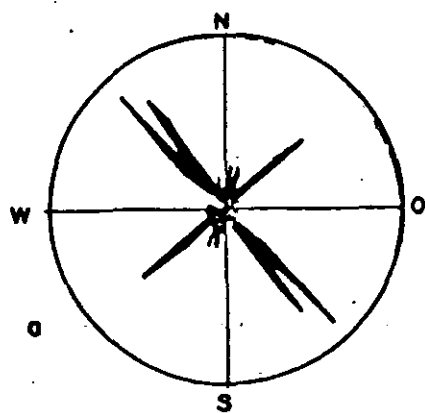
Fractura horizontal



Fractura vertical

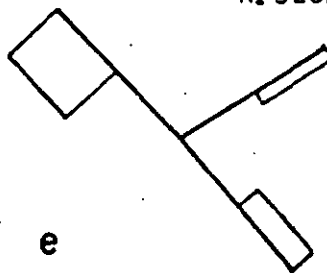
FIG. 2

Representación de planos estructurales —



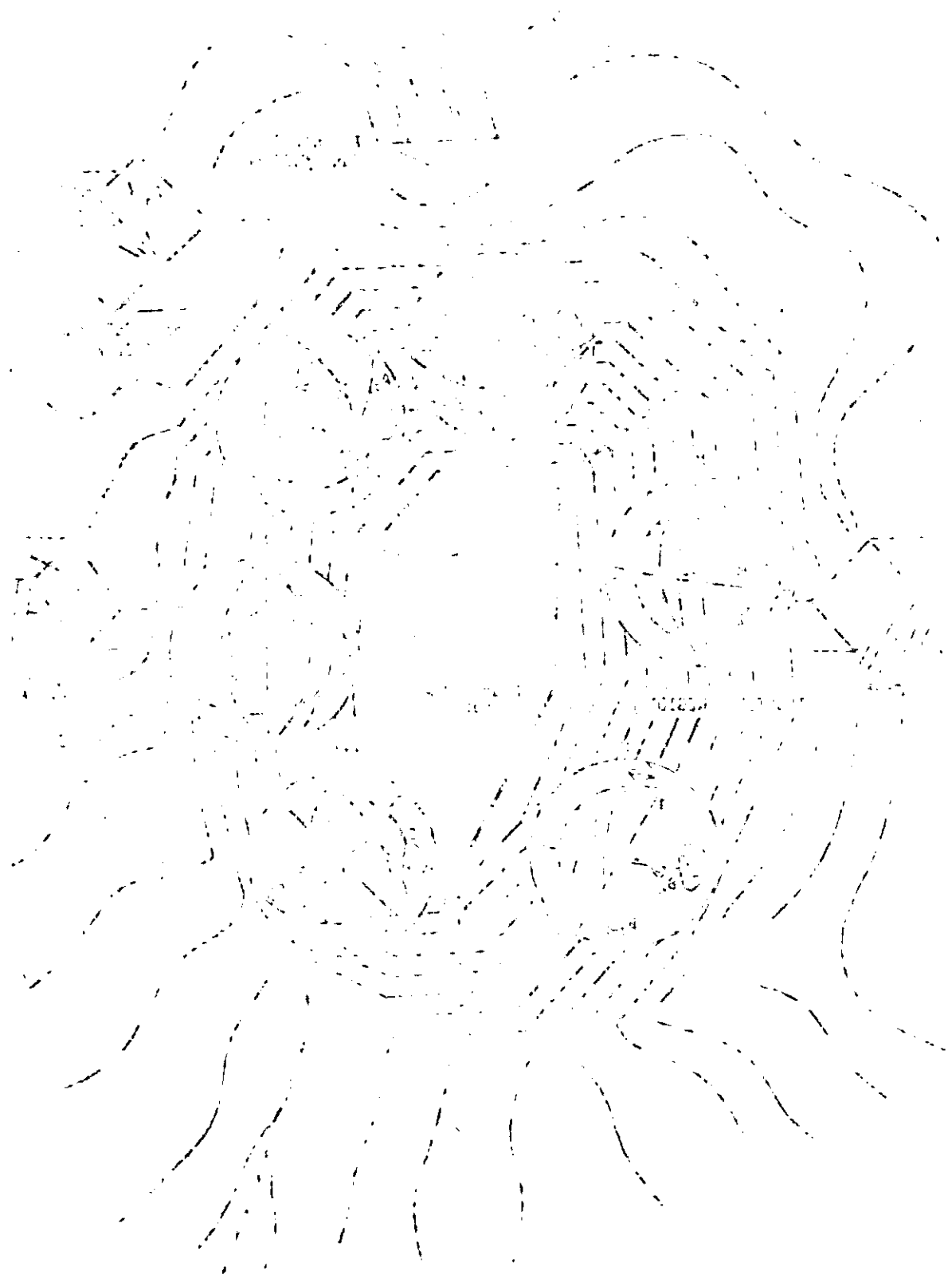
S 48/38

K₂ 325/80



K, 230/70

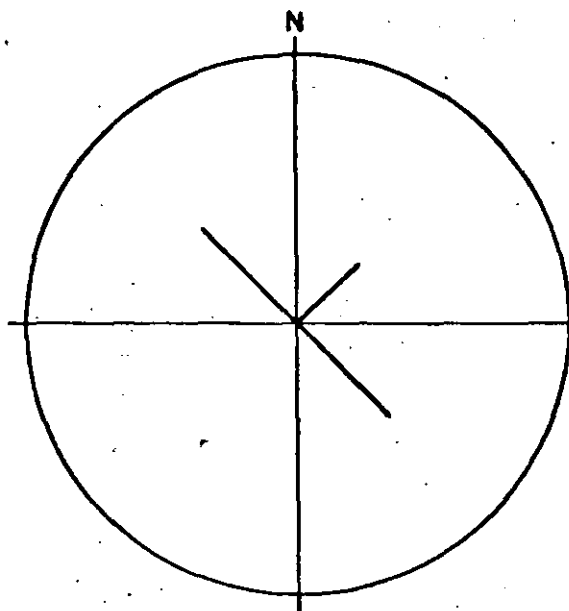
- a) Rosa de vientos b) Diagrama de puntos (polos)
 c) Diagrama de frecuencias d) Circulos grandes y polos
 e) Cuadrados unitarios segun MULLER



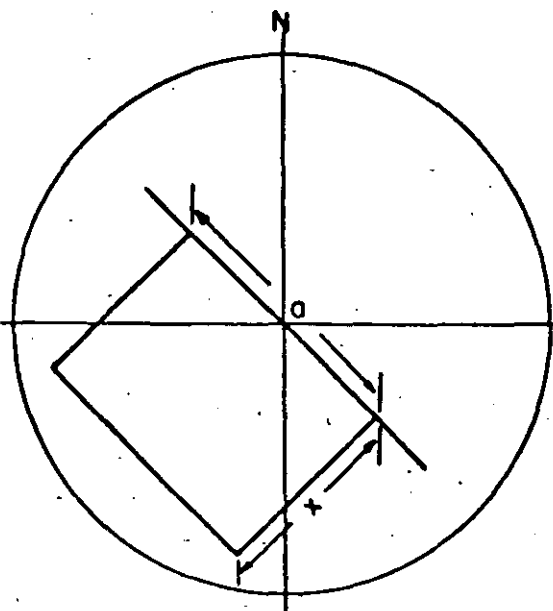
THE UNIVERSITY OF MICHIGAN LIBRARY

La banderola de MÖLLER

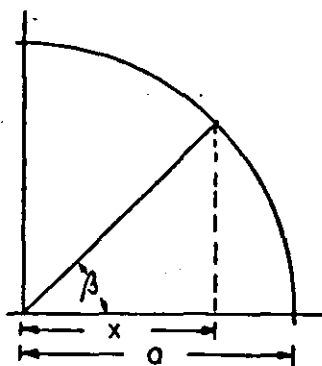
La representación de un plano geológico por medio del escorzo de un cuadrado unitario



Simbolo convencional

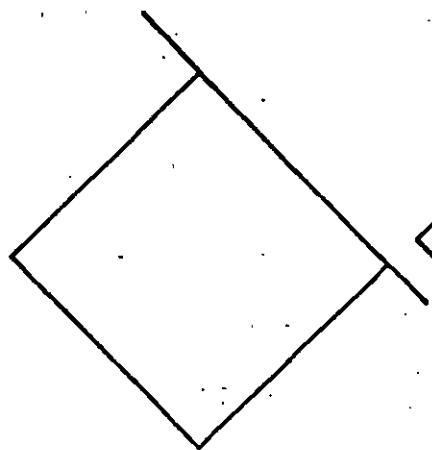


"Banderola de MÖLLER"

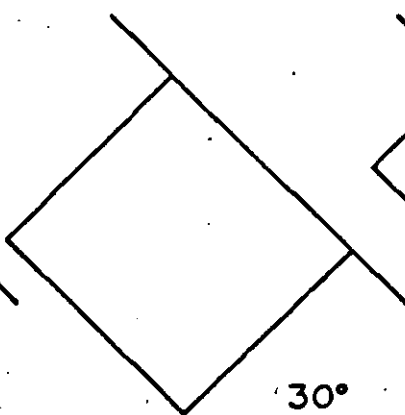


Determinación gráfica del escorzo x

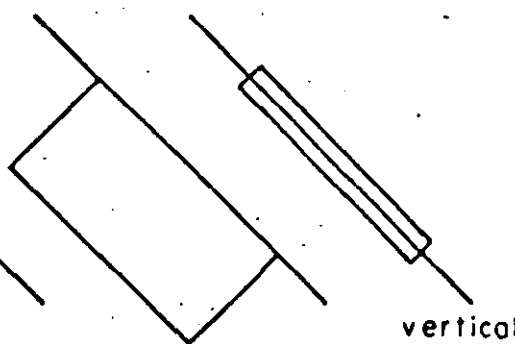
$$x = a \cdot \cos \beta$$



horizontal



30°



60°

vertical

... the ... of ...

... the ... of ...

... the ... of ...

... the ... of ...

... the ... of ...

... the ... of ...

1.3.1.- Índice de Calidad de la Roca, R.Q.D. (Rock quality designation)

El índice de calidad de la roca (RQD) está basado sobre un procedimiento de recuperación de núcleos modificado, el cual está apoyado indirectamente sobre el número de fracturas y la cantidad de alteración o suavidad de la roca como se observa en los núcleos recuperados en un barreno. En lugar de contar las fracturas, se obtiene una medida indirecta mediante la suma de todos los fragmentos duros y sanos con longitud ≥ 10 cm.

Ejemplo:

Recuperación
(pulg)

10

2

2

3

4

5

3

4

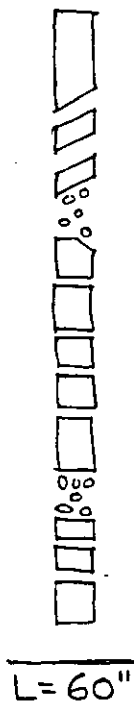
6

4

2

5

50"



Recuperación
modificada
(pulg)

10

4

5

4

6

5

34"

$$\% \text{ Recuperación} = \frac{50}{60} = 83\%$$

$$\text{RQD} = \frac{34}{60} = 57\%$$

En este caso la recuperación total es de 83% mientras que el índice de calidad de la roca es 57%.

Se ha visto que el RQD es un indicador más sensible de la calidad general de la roca que el porcentaje de recuperación total.

Si el núcleo se rompe por manejo o por efectos de la perforación p. ej. si la superficie de la fractura se observa fresca de berán unirse los dos fragmentos y considerarse como una sola pieza.

Este criterio puede cambiarse cuando se trate de rocas sedimentarias con estratificación delgada y rocas metamórficas foliadas. Sin embargo este sistema ha sido aplicado exitosamente aún para lutitas, siendo necesario realizar inmediatamente el registro después de sacar los núcleos del muestreador y antes del efecto de fracturamiento por secado al aire.

Este método penaliza la roca con pobre recuperación. Esto es apropiado porque una recuperación pobre generalmente coincide con una calidad pobre. Esto no siempre es cierto pues el equipo de perforación y la técnica empleada pueden ocasionar pobre recuperación. Por esta razón se recomienda el uso del doble barril giratorio con diámetro mínimo NX ($2\frac{1}{8}$ ")

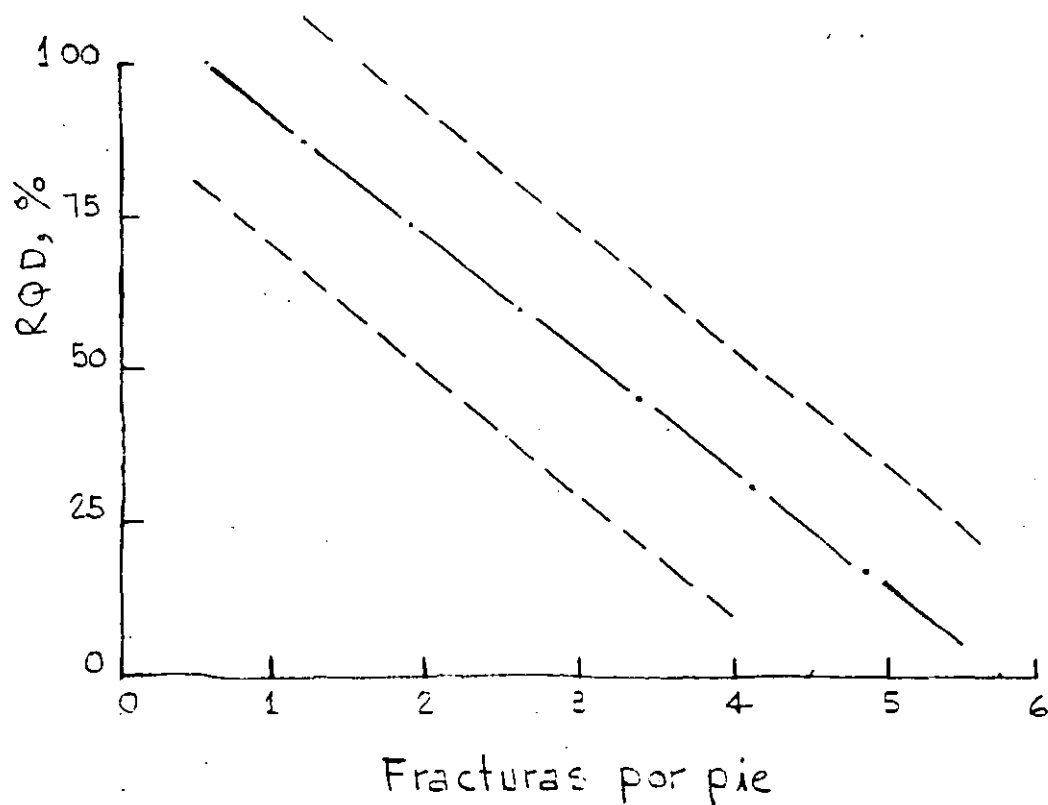
Tan simple como parece este método, se ha encontrado que existe una buena correlación entre los valores numéricos del RQD y la calidad ingenieril de las rocas.

El RQD usualmente ha sido utilizado por algunas Compañías Americanas, Consultores en Geotecnia y Contratistas para la evaluación de la calidad de la roca.

Indice de Calidad de roca RQD, %	Descripción de la Calidad
0 - 25	Muy pobre
25 - 50	Pobre
50 - 75	Regular
75 - 90	Buena
90 - 100	Excelente

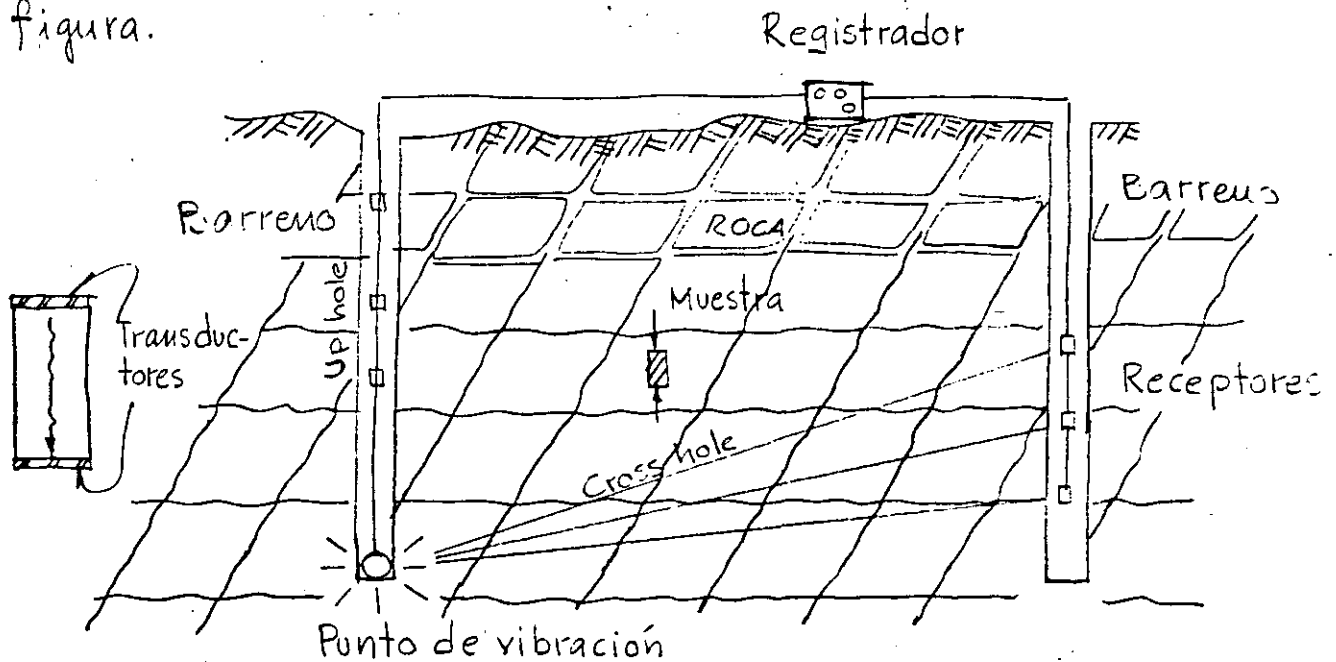
RELACION ENTRE EL RQD Y LA CALIDAD DE LA ROCA

A continuación se presenta la correlación entre la frecuencia de fracturas y la calidad RQD, observándose una correlación lineal con límites aceptables.



1.3.2. Relación de velocidades sísmicas

El efecto de las discontinuidades en la masa de roca puede ser estimado por comparación de la velocidad de la onda compresional "in situ" con la velocidad sónica de laboratorio obtenida en núcleos intactos de la misma roca como se observa en la siguiente figura.



RELACION DE VELOCIDADES COMO INDICE DE CALIDAD DE ROCA ;

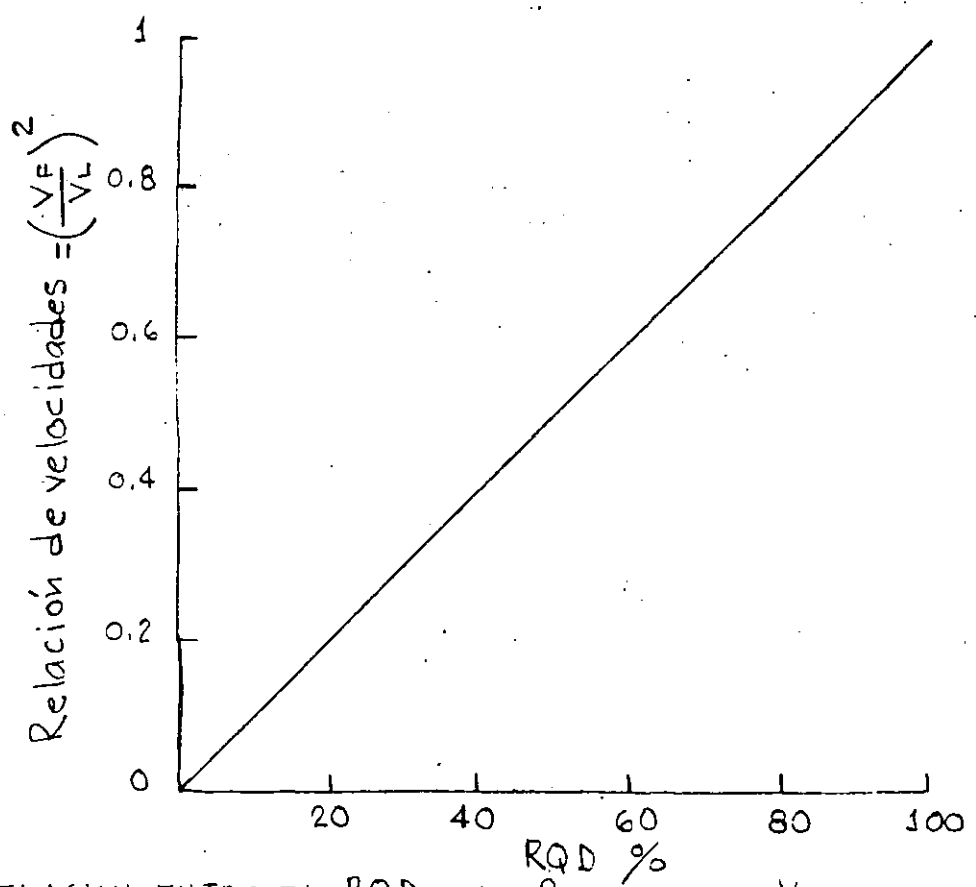
$$\text{Relación de velocidad} = \frac{V_F}{V_L} ; \begin{array}{l} \text{Velocidad de campo} \\ \text{Velocidad de lab.} \end{array}$$

La diferencia entre estas dos velocidades dilatantes es ocasionada por las discontinuidades estructurales existentes en el campo.

La relación entre estas ondas compresionales: V_F/V_L , donde V_F y V_L son las velocidades de ondas compresionales de la masa de roca "in situ" y de un espécimen intacto fue propuesto

por Onodera, 1963.

Para una roca masiva de alta calidad con pocas juntas, la relación de velocidades se aproxima a la unidad.



CORRELACION ENTRE EL RQD Y LA RELACION DE VELOCIDADES $(\frac{V_F}{V_L})^2$

La velocidad sísmica debe determinarse en núcleos sujetos a un esfuerzo axial igual al que produce la cobertura de roca a la misma profundidad a la que fue tomada la muestra y con un contenido de agua equivalente al de la roca "in situ". La velocidad sísmica es mejor obtenida entre barrenos con el sistema "Up-hole" o "Cross-hole" que mediante refracción superficial.

Parece que el cuadrado de la relación de velocidades es intercambiable con el RQD, pero todavía hay poca información.

2.- PROPIEDADES MECANICAS DE LA ROCA

2.1.- Introducción

En muchos problemas de la mecánica de rocas las propiedades ingenieriles de la roca intacta son de importancia primordial. En otros casos resulta más importante el comportamiento de la roca "in situ" con sus inherentes discontinuidades geológicas.

2.2.- Propiedades ingenieriles de la roca intacta.

2.2.1.- Resistencia en tensión

La determinación de la resistencia a la tensión por extensión directa de un espécimen cilíndrico ha sido difícil de realizar, pues los dispositivos de sujeción introducen flexiones.

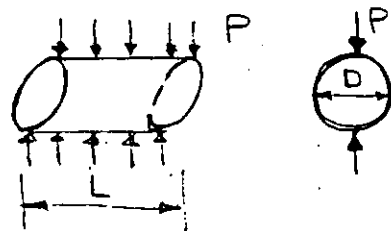
A causa de la dificultad arriba mencionada es más rápido obtener la resistencia en tensión en forma indirecta mediante la prueba "Brasileña". En esta prueba la probeta cilíndrica se ensaya acostada aplicando una carga lineal diametralmente opuesta.

La resistencia a la tensión σ_t se calcula mediante la expresión:

$$\sigma_t = \frac{2P}{\pi DL}$$

en donde:

P = carga a la falla ; D = diámetro
 L = longitud del espécimen



Otra prueba indirecta para determinar la resistencia en tensión de la roca es la "Carga puntual" que se realiza aplicando una carga puntual de compresión sobre la superficie curva de un espécimen cilíndrico con eje horizontal. Esta carga produce esfuerzos de tensión perpendiculares al eje de carga. La resistencia a la tensión σ_t está dada por una expresión empírica:

$$\sigma_t = \frac{0.96 P}{D^2}$$

en donde:

P = carga de falla en lb. y D = diámetro en pulg.

Miller relacionó esta resistencia en tensión de punta con la resistencia uniaxial de compresión mediante la siguiente expresión:

$$\sigma_c(\text{ult}) = 21 \sigma_t + 4000 \text{ lb/pulg}^2$$

en donde $\sigma_c(\text{ult})$ = resistencia en compresión y

σ_t = resistencia en tensión bajo carga puntual.

Para propósitos ingenieriles se tiene suficiente aproximación suponer una resistencia a la tensión comprendida entre 5 y 10% de la resistencia en compresión.

No se requiere mayor aproximación en la determinación en vista del amplio intervalo de variación en la resistencia, sobre todo en rocas metamórficas y sedimentarias con estratificación delgada.

2.2.2.- Resistencia en compresión simple

El comportamiento de la roca intacta bajo compresión uniaxial esta influenciada por las características intrínsecas de la prueba como son la relación de esbeltez, la velocidad de carga y las condiciones de fricción de los apoyos.

En especímenes con relación de esbeltez pequeña no pueden desarrollarse los planos de cizalla por el efecto de fricción de los apoyos, resultando un valor mayor de la resistencia en compresión. Obert y Duvall han encontrado una relación empírica entre la resistencia a la compresión y la relación de esbeltez como sigue:

$$\sigma_{a(L/D)} = \sigma_{aL} \left(0.778 + \frac{0.222}{L/D} \right)$$

en donde: $\sigma_{a(L/D)}$ = resistencia en compresión para $L/D \neq 1$
y σ_{aL} es la resistencia en compresión para $L/D = 1$

Se recomienda una relación de esbeltez entre 2 y 2.5 para asegurar una distribución de esfuerzos más o menos uniforme en la muestra alejándose también del efecto de fricción de los cabezales. En la Fig se presenta en forma gráfica la relación entre la resistencia en compresión simple y la esbeltez del espécimen.

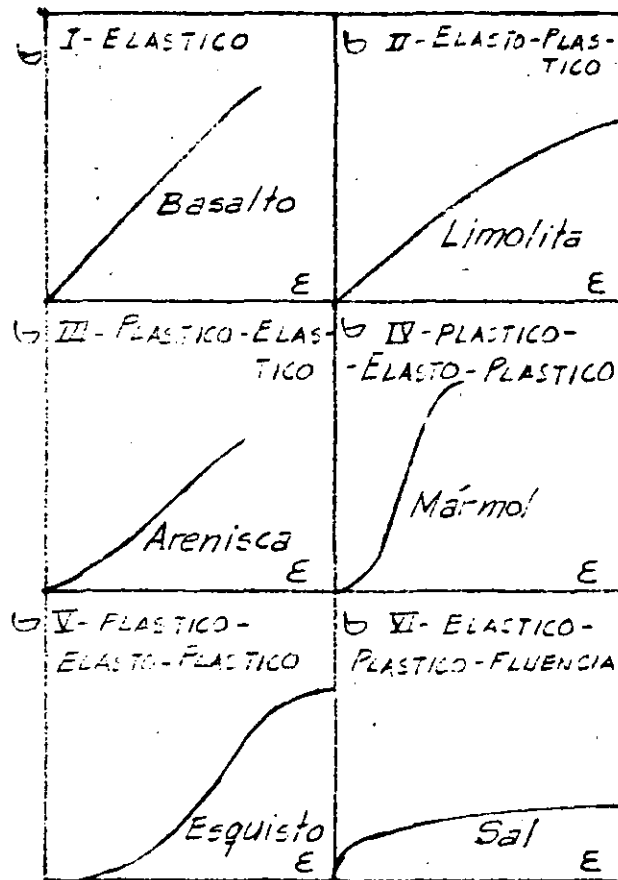
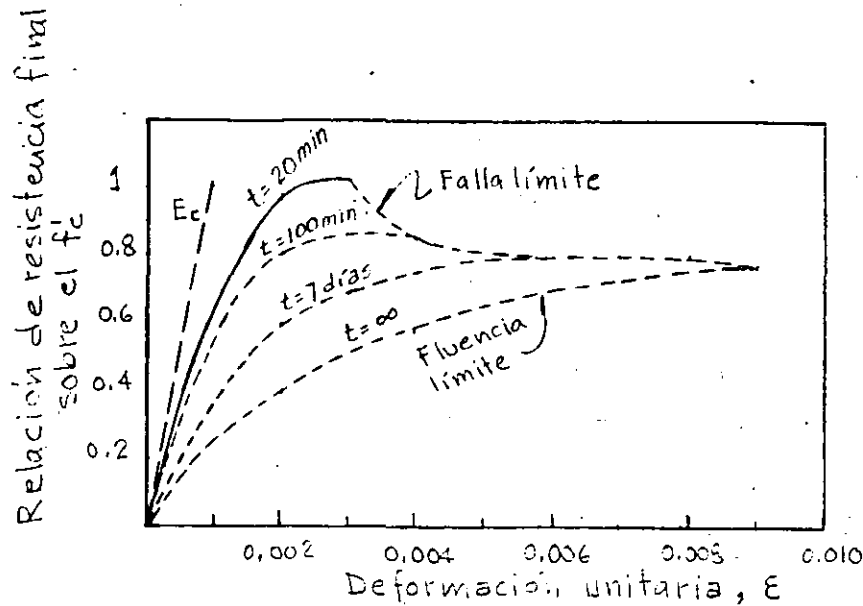


Fig. CURVAS ESFUERZO-DEFORMACION TÍPICAS PARA ROCAS A LA FALLA EN COMPRESIÓN SIMPLE



INFLUENCIA DE LA VELOCIDAD DE CARGA EN LA RESISTENCIA Y MÓDULO EN ESPECIMENES DE CONCRETO

En la Fig. ... se presenta varios gráficos esfuerzo-deformación en ensayos de compresión simple para varios tipos de roca.

A continuación se presentan algunos valores de resistencia obtenidos en varios tipos de roca

TIPO DE ROCA	$\sigma_{c(ult)}$ (lb/pulg ² × 10 ³)	c, Cohesión (lb/pulg ² × 10 ³)	ϕ (grados)	$N_s = K$	
Granito	Intervalo	10-40	1.4-5.8	51-58	8-17
	Promedio	25	3.6	55	11
Calizas	Intervalo	3-20	0.5-5	27-53	4-13
	Promedio	15-20	2.5-3.3	50	8
Areniscas	Intervalo	3-30	0.6-6	48-50	6-7
	Promedio	8-20	1.6-4.1	48	6

$$N_s = \frac{1 + \sin \phi}{2}$$

○

The first part of the document discusses the importance of maintaining accurate records of all transactions. It emphasizes that every entry should be supported by a valid receipt or invoice. The text also mentions the need for regular audits to ensure the integrity of the financial data.

In the second section, the author details the various methods used for data collection and analysis. This includes the use of statistical software and manual calculations. The document highlights the challenges of handling large volumes of data and the importance of using appropriate sampling techniques.

The third part of the document focuses on the results of the study. It presents a series of tables and graphs that illustrate the trends and patterns in the data. The author concludes that the findings are significant and provide valuable insights into the subject matter.

○

The following table shows the distribution of data points across different categories. The data is presented in a clear and concise manner, allowing for easy comparison and analysis.

Category	Frequency	Percentage
A	15	15%
B	25	25%
C	30	30%
D	10	10%
E	20	20%

The results indicate that category C is the most frequent, followed by category B. This suggests a higher prevalence of this category in the overall dataset.

The document also includes a discussion on the limitations of the study. It acknowledges that the sample size may not be representative of the entire population, and that there may be other factors influencing the results.

○

In conclusion, the study has provided a comprehensive overview of the data and its implications. The findings are consistent with previous research and offer new perspectives on the topic.

Further research is needed to explore the underlying causes of the observed trends and to develop more effective strategies for data management and analysis.

2.3 Propiedades ingenieriles de la roca "in situ"

En la Fig se presenta la variación del factor de reducción contra calidad de la roca (RQD) a partir de pruebas de placa flexible de 34" de diámetro en granitos de la Presa Dworshak, considerando al factor de reducción como la relación entre módulos elásticos de campo y laboratorio.

Se observa que los módulos de deformación son consistentemente más altos con la profundidad que los módulos superficiales, y que a mayor calidad de roca el factor de reducción va aproximándose a la unidad.

En la Fig se presenta la variación entre la calidad de roca, RQD, o, $(V_F/V_L)^2$ contra el factor de reducción observándose que para valores de RQD menores de 65% el factor de reducción varía más o menos entre 0.1 y 0.2 y que para valores de RQD mayores de 65% se tiene una relación lineal con el factor de reducción. Para valores de RQD entre 90 y 100% el factor de reducción varía entre 0.8 y 1.



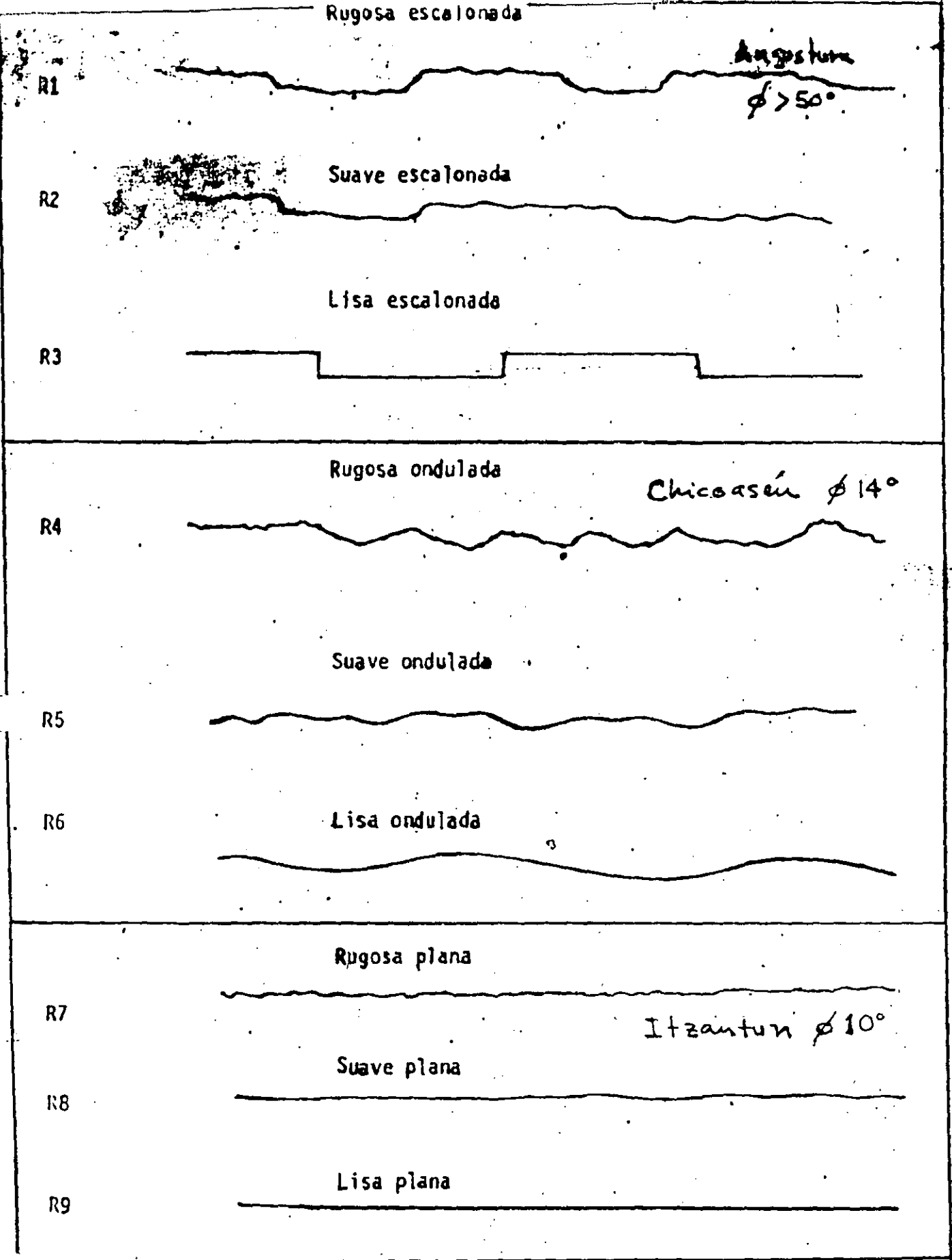


FIGURA N° .- JUNTAS RUGOSAS CERRADAS.

1. The first part of the document discusses the importance of maintaining accurate records of all transactions. It emphasizes that proper record-keeping is essential for the integrity of the financial system and for the ability to detect and prevent fraud. The text notes that without reliable records, it would be difficult to track the flow of funds and identify any irregularities.

2. The second part of the document focuses on the role of internal controls. It explains that internal controls are designed to ensure that transactions are recorded accurately and in a timely manner. These controls include procedures for authorizing transactions, verifying the accuracy of data, and reconciling accounts. The document stresses that strong internal controls are a key component of an effective risk management strategy.

3. The third part of the document addresses the issue of transparency. It argues that transparency is crucial for building trust and confidence in the financial system. By providing clear and accessible information about transactions and financial performance, organizations can demonstrate their commitment to ethical practices and accountability. The text suggests that transparency can also help to identify areas for improvement and reduce the risk of mismanagement.

2. Internal Controls

4. The fourth part of the document discusses the importance of regular audits. It explains that audits provide an independent and objective assessment of the organization's financial records and internal controls. Regular audits can help to identify weaknesses in the system and provide recommendations for improvement. The text notes that audits are also a key tool for detecting and preventing fraud.

5. The fifth part of the document focuses on the role of technology in financial reporting. It explains that technology can greatly enhance the accuracy and efficiency of financial reporting. By using automated systems, organizations can reduce the risk of human error and ensure that data is recorded consistently and in a timely manner. The document suggests that investing in technology is a key strategy for improving financial reporting and risk management.

6. The sixth part of the document addresses the issue of data security. It explains that data security is a critical concern for organizations that rely on financial data. Strong data security measures are essential to protect sensitive information from unauthorized access and theft. The text notes that data security is also a key component of an organization's overall risk management strategy.

7. The seventh part of the document discusses the importance of employee training. It explains that employees play a key role in maintaining accurate records and implementing internal controls. Regular training and education are essential to ensure that employees understand their responsibilities and are equipped with the skills and knowledge needed to perform their duties effectively. The document suggests that investing in employee training is a key strategy for improving financial reporting and risk management.

8. The eighth part of the document focuses on the role of external audits. It explains that external audits provide an independent and objective assessment of the organization's financial statements. External audits can help to identify weaknesses in the system and provide recommendations for improvement. The text notes that external audits are also a key tool for detecting and preventing fraud.

9. The ninth part of the document discusses the importance of communication. It explains that clear and effective communication is essential for ensuring that all stakeholders are aware of the organization's financial reporting and risk management practices. Regular communication can help to build trust and confidence and ensure that everyone is working towards the same goals. The document suggests that investing in communication is a key strategy for improving financial reporting and risk management.

10. The tenth part of the document concludes by emphasizing the importance of a strong financial reporting and risk management framework. It notes that a strong framework is essential for ensuring the integrity of the financial system and for the ability to detect and prevent fraud. The document suggests that organizations should focus on improving their internal controls, transparency, and data security to build a strong and resilient financial reporting and risk management framework.

conditions, it is possible to make reasonable approximations of the energy capabilities of various kinds of explosives and the estimated level of the transmitted stresses at any distance d from the explosion center. With respect to the relative energies of explosives with different densities but having a constant charge diameter and velocity of reaction, the following expression can be used:

$$RE_2 = RE_1 (SG_{e2}/SG_{e1})$$

In the case where explosives' densities, charge diameters, and reaction velocities all differ, the general relationship for making the comparison would be

$$RE_2 = RE_1 (d_{e2}^2 v_{e2}^2 / d_{e1}^2 v_{e1}^2)$$

For all practical considerations, the comparisons would be reasonably valid for all center-initiated 1-ft long charges with diameters that would vary from 2 to 72 inches. This is because the range of values for L_c/D_e and its reciprocal, or D_e/L_c , would not exceed 6, which was defined earlier as the limitation for a point charge.

The significance of the foregoing relationships becomes apparent when one considers their application for cratering in materials. The problem, in gist, is one involving the accomplishment of mechanical work, whereby the energy supplied by the explosive (Q_e) is used for fracturing the materials by overcoming their strength properties and then displacing the broken particles. In general, the required diverged value of dQ_e , or dQ_e at distance d from the explosion's center, will be unique for any given type of material.

The specific depth of charge burial, which would correspond with the maximum limit for distance d , at which optimum crater results will be achieved is called the burden, B . The volume of the developed crater (V_c), in turn, will always be a function of B , as well as the explosive's Q_e . For example, V_c for a simple cone-type crater with one free surface is $\pi r^2 B/3$, but the value for the crater radius r is dependent on the material's properties and is related to B . Thus, as a general rule one can assume that $V_c = B^3 = Q_e$ for approximation purposes. From the previous discussions it was shown that $Q_e = RE_e = SG_e = D_e^3$. Therefore, for any confined explosive charge it can be concluded that

$$B = V_c^{1/3} = RE_e^{1/3} = SG_e^{1/3} = D_e$$

$$\text{and } B_2 = B_1 (RE_2/RE_1)^{1/3} \text{ or } B_2 = B_1 (D_{e2}/D_{e1})$$

In summation, the cube-root law describes the effect of three-dimensional divergence in reducing the stress energy produced by a confined explosive charge as the energy propagates in all directions.

through a material. As a result, the ideal optimum depths of burial (or burden) and the resultant crater volumes produced by confined explosive charges in a given blasting environment will be proportional to the charge diameters and the cube root of their respective relative energies.

The Square-Root Law

Because the energy of an explosive is released as a pressure or stress, i.e., P_e or σ_e , it will exert itself over the entire surface of the charge. For the concentric or point charge the total outer surface at which the pressure acts is equal to $4\pi r_e^2 = \pi D_e^2$. Therefore, the total energy from the explosion (Q_e) will be equal to $\sigma_e(\pi D_e^2)$. By similar analysis, from the explosion center the stress transmitted through a material a distance d will be distributed over a surface area equaling $4\pi d^2$, in which the total energy at that location Q_d times the area would be related in the form of $Q_d = \sigma_d(4\pi d^2)$. Assuming there are no losses because of absorption, etc., or $Q_e = Q_d$, it follows then that

$$\sigma_e(\pi D_e^2) = \sigma_d(4\pi d^2),$$

$$\text{or} \quad \sigma_d = \sigma_e (D_e/2d)^2.$$

If $d = B$ for the optimum crater produced, then

$$B = (D_e/2) (\sigma_e/\sigma_B)^{1/2}$$

Because the stresses transmitted into a material are proportional to the pressure released by the explosion, or $\sigma_e = P_e$, the transmitted stresses for the production of a crater must equal or exceed the material's strength properties, or σ_t or τ_s depending on which would be the most critical. Thus, one can conclude that

$$B = P_e^{1/2} = \sigma_t^{-1/2} \text{ or } \tau_s^{-1/2}.$$

In brief, then, the square-root law of energy divergence, when used to predict requirements for the production of craters, states that the optimum depths of burial (or burden) and the resultant crater volumes for confined explosive charges in any given blasting environment will vary directly with the square root of their respective explosion pressures and inversely with the square root of the pertinent materials' strengths.

TABLE I. Strength Data For Some Competent Rocks (13).

Rock Type	Compressive Strength psi x 10 ³	Elasticity Modulus (Compression) psi x 10 ⁶	Tensile Strength psi $\frac{Tens.}{Comp.}$	C psi	ϕ deg.	Equation of Mohr's Envelope (ref. Fig. 3)	% Compressive Strength
Chert	29.3	8.15	8200.002550	2550	71.5	$Y = 2550 + 3.0 x$	0.0870
Coal	6.2	-	-	1600	38.5	$Y = 1600 + 0.8 x$	0.258
Granite	28.0	3.17	4100.0176	1720	76.5	$Y = 1720 + 4.2 x$	0.0614
Green Stone	29.1	8.82	3800.0130	1700	77.5	$Y = 1700 + 4.5 x$	0.0584
Greywacke	7.9	1.80	7000.0666	1200	59.5	$Y = 1200 + 1.7 x$	0.1519
Limestone	21.3	9.50	3500.0164	1320	75.5	$Y = 1320 + 3.9 x$	0.0620
Marble	30.8	7.15	8630.0279	2650	71.0	$Y = 2650 + 2.9 x$	0.0860
Salt Rock	2.2	1.35	850.0386	210	72.5	$Y = 210 + 3.2 x$	0.0954
Sand Stone	14.8	2.00	2300.0155	900	76.0	$Y = 900 + 4.0 x$	0.0606
Shale	5.2	1.09	1538.0.2957	1420	31.0	$Y = 1420 + 0.6 x$	0.2731
Silt Stone	5.0	12.60	440.0.0880	750	59.5	$Y = 750 + 1.7 x$	0.1500

C - Cohesion
 ϕ - Angle of Internal Friction
 Y - Shear Stress, τ_s
 x - Normal Stress, σ_n

1. The first part of the document discusses the importance of maintaining accurate records of all transactions. It emphasizes that this is crucial for ensuring the integrity of the financial statements and for providing a clear audit trail. The text notes that any discrepancies or errors in the records can lead to significant complications during an audit and may result in legal consequences for the company.

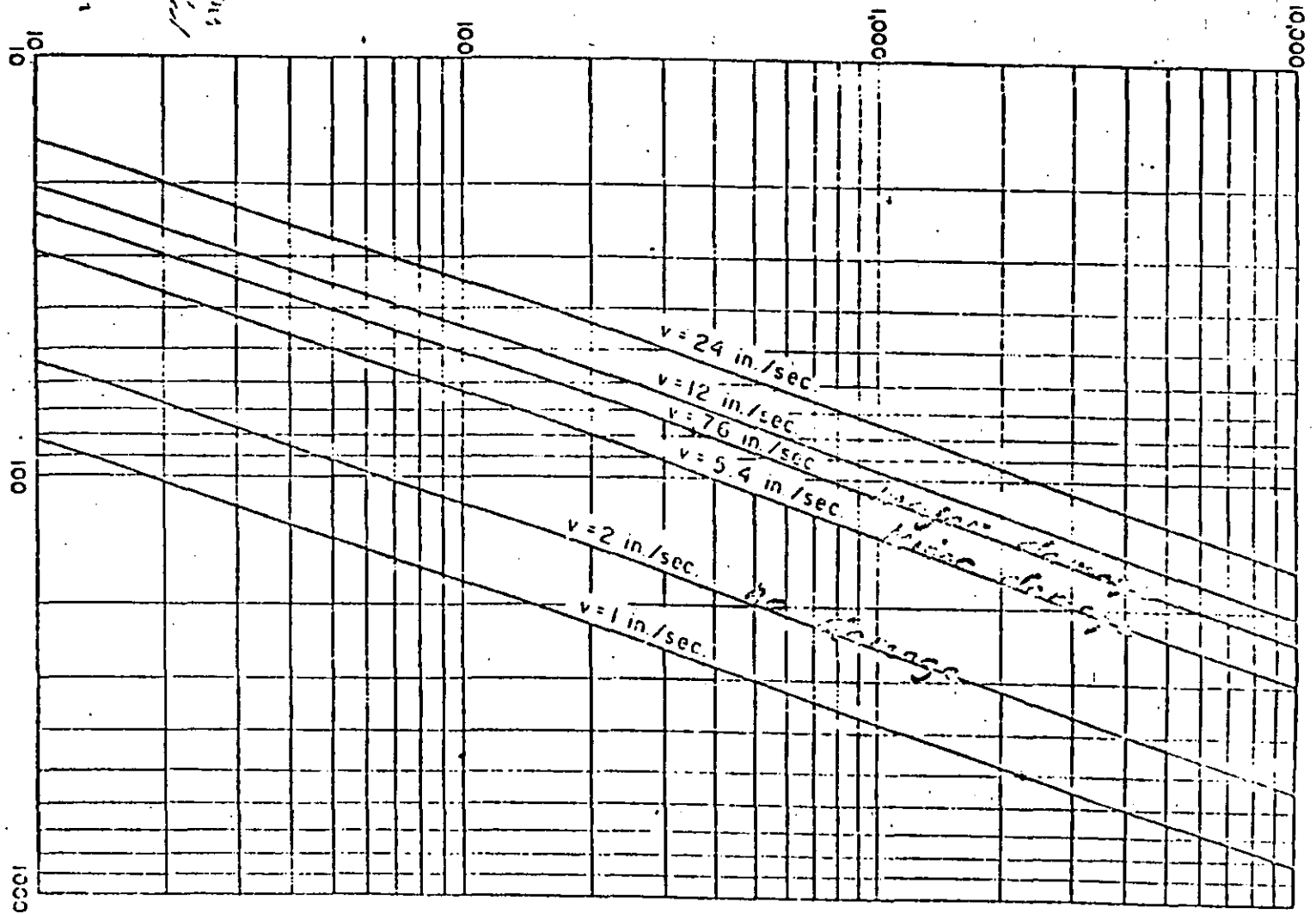
2. The second part of the document outlines the specific procedures that should be followed when recording transactions. It details the steps from identifying the transaction to the final entry in the accounting system. Key points include the need for proper documentation, such as invoices and receipts, and the importance of timely recording to avoid errors and omissions. The text also mentions the role of the accounting department in ensuring that all transactions are properly classified and recorded.

3. The third part of the document addresses the issue of internal controls. It explains how a strong system of internal controls can help prevent fraud and reduce the risk of errors. The text describes various control measures, such as segregation of duties, authorization requirements, and regular reconciliations. It stresses that these controls are essential for maintaining the reliability of the financial information and for protecting the company's assets.

4. The fourth part of the document discusses the importance of transparency and communication in the financial reporting process. It highlights the need for clear and concise reporting to all stakeholders, including management, investors, and regulatory bodies. The text notes that transparency is not only a legal requirement but also a key factor in building trust and confidence in the company's financial performance. It encourages the company to provide detailed explanations for any significant changes or fluctuations in the financial data.

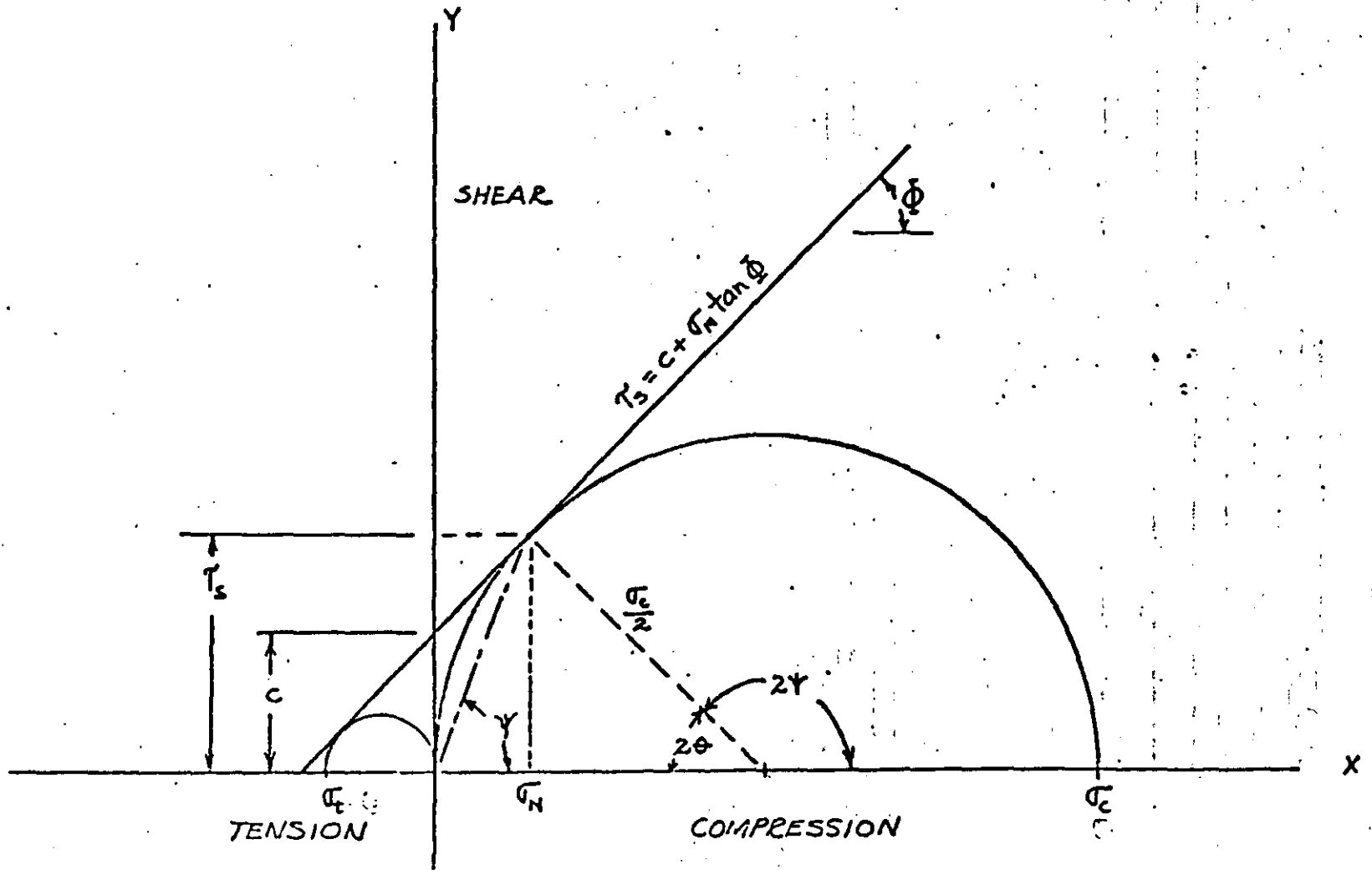
5. The fifth and final part of the document provides a summary of the key points discussed and offers some concluding thoughts. It reiterates the importance of accuracy, proper procedures, strong internal controls, and transparency in the financial reporting process. The text concludes by stating that these principles are fundamental to the success of any business and are essential for ensuring long-term growth and stability.

Maximum Weight of Charge Per Delay W, lbs.



Distance from Blast, D, ft.

is a nomograph
Major damage: serious wall cracking, plastic pellets
Minor damage: fine plastic cones, opening of air cracks
is a nomograph
Major damage: serious wall cracking, plastic pellets
Minor damage: fine plastic cones, opening of air cracks



MOHR'S FAILURE ENVELOPE

NOTE: @ $\phi = 36.8^\circ$, $\tau_s = \sigma_c = \sigma_c / A$; AND $\psi = (90^\circ + \phi) / 2$

SOLUTION (CONT.)

C.(1) From Eq. 36, $K_v = \frac{V_c}{V_p}$. Thus, from part B and determining K_v fr. the respective V_c values fr each D_c from 1 to 6 inches, inclusive, the following summary table can be prepared:

D_c , in.	B , ft.	V_c , fps	K_v
1	0	0	0
2	4	9450	0.56
3	7	12,500	0.74
4	10.3	14,000	0.82
5	13.5	14,900	0.85
6	16.2	15,000	0.85

(a) Floor Priming

$$\text{From Eq. 38(a), } B' = \frac{3L}{9K_v + 2}$$

1. At $D_c = 5$ in.,

$$B' = 3(30) / (9 \times 0.85 + 2) = 90 / 9.9 = 9.1 \text{ ft.}$$

From above Table, $B = 13.5$ ft.

Thus, $B > B'$ or $13.5 > 9.1$. Diameter can be reduced.

2. At $D_c = 4$ in.,

$$B' = 3(30) / (9 \times 0.82 + 2) = 90 / 9.4 = 9.6 \text{ ft.}$$

From Table, $B = 10.3$ ft.

Thus, $B > B'$ or $10.3 > 9.6$. Diameter can be reduced.

3. At $D_c = 3$ in.,

$$B' = 3(30) / (9 \times 0.74 + 2) = 90 / 8.66 = 10.4 \text{ ft.}$$

From Table, $B = 7$ ft.

Thus, $B < B'$ or $7 < 10.4$. Diameter too small.

Note that at $D_c = 4$ in., optimum burden B and the minimum burden B' at which misfire might occur are approximately equal. Therefore, use $D_c = 4$ in. \leftarrow

1900

1901

1902

1903

1904

1905

1906

1907

1908

1909

1910

1911

1912

1913

1914

1915

1916

1917

1918

1919

1920

SOLUTION (CONT.)

B(2) (CONT.)

(a) $D_c = 2 \text{ in.}$

$$P_d = P_{d_{\max}} \left(\frac{9450}{15,000} \right)^2 = 835,000 (0.397)$$

or $P_d = 331,000 \text{ psi}$ ←

(b) $D_c = 4 \text{ in.}$

$$P_d = P_{d_{\max}} \left(\frac{19,000}{15,000} \right)^2 = 835,000 (0.57)$$

or $P_d = 730,000 \text{ psi}$ ←

B(3) From Eq. 4(b),

$$P_c = P_{d_{\max}} / 2$$

This, (a) $D_c = 2 \text{ in.}$, and (b) $D_c = 4 \text{ in.}$,

$$P_c = 835,000 / 2 = 417,500 \text{ psi} \quad \leftarrow$$

B(1) From Eq. 35,

$$K_B = 30 \left(\frac{160}{d_r} \right)^{\frac{1}{3}} \left(\frac{S_{h_c}}{1.3} \right)^{\frac{1}{3}} \left(\frac{V_c}{12,000} \right)^{\frac{2}{3}}$$

From Eq. 7,

$$d_r = 62.4 (S_{h_r}) = 62.4 (2.9) = 181 \text{ pc}$$

Substituting for values of d_r and S_{h_c} , then

$$\begin{aligned} K_B &= 30 \left(\frac{160}{181} \right)^{\frac{1}{3}} \left(\frac{1.2}{1.3} \right)^{\frac{1}{3}} \left(\frac{V_c}{12,000} \right)^{\frac{2}{3}} \\ &= 30 (0.96) (0.97) \left(\frac{V_c}{12,000} \right)^{\frac{2}{3}} \end{aligned}$$

or $K_B = 28 \left(\frac{V_c}{12,000} \right)^{\frac{2}{3}}$

But from Eq. 34,

$$B = \frac{K_B D_c}{12} = \frac{28}{12} \left(\frac{V_c}{12,000} \right)^{\frac{2}{3}} D_c$$

SOLUTION (CONT.)

3 (1) (cont.)

Therefore, basic velocity equation for the explosive is

$$V_e = \frac{5000 (D_c - 1)}{0.26 + 0.27 (D_c - 1)}$$

with the D_c range of values from 1 to 5 inches.

Check: @ $D_c = 3$ in.

$$V_e = \frac{5000 (3-1)}{0.26 + 0.27 (3-1)} = \frac{10,000}{0.26 + 0.54} = 12,500 \text{ fps} \quad \underline{OK}$$

@ $D_c = 5$ in.

$$V_e = \frac{5000 (5-1)}{0.26 + 0.27 (5-1)} = \frac{20,000}{0.26 + 1.08} = 14,900 \text{ fps} \quad \underline{OK}$$

(a) $D_c = 2$ in.

$$V_e = \frac{5000 (2-1)}{0.26 + 0.27 (2-1)} = \frac{5000}{0.26 + 0.27} = 9450 \text{ fps} \quad \leftarrow$$

(b) $D_c = 4$ in.

$$V_e = \frac{5000 (4-1)}{0.26 + 0.27 (4-1)} = \frac{15,000}{0.26 + 0.81} = 14,000 \text{ fps} \quad \leftarrow$$

B (2) From Eq. 4 (a)

$$P_d = \frac{6.06 \times 10^{-3} V_e^2 (S_{hc})}{1 + 0.80 (S_{hc})}$$

From Eq. 1

$$S_{hc} = \frac{141}{30} = \frac{141}{117} = 1.2$$

Then

$$P_{d_{max}} = \frac{6.06 \times 10^{-3} + 1.5^2 \times 10^8 \times 1.2}{1 + 0.80 (1.2)} = \frac{6.06 + 2.25 \times 10^5 \times 1.2}{1.96}$$

or $P_{d_{max}} = 835,000 \text{ psi}$

SOLUTION (cont.)

B(1) First determine relationship of V_c with D_c
from $y = \frac{cx}{a+bx}$ where $y = V_c$ and $x = D_c - D_c$

$$\text{Then } V_c = \frac{c(D_c - D_c)}{a + b(D_c - D_c)}$$

It is given that $D_c = 1$ in., $V_c = 12,500$ fps @ $D_c = 3$ in.,
and $V_c = 15,000$ fps @ $D_c = 5$ in.

$$\text{Then @ } D_c = 3 \text{ in.}, \quad 12,500 = \frac{c(3-1)}{a + b(3-1)} = \frac{2c}{a + 2b}$$

Assume $c = 5000$,

$$\text{Then } a + 2b = \frac{2(5000)}{12,500} = \frac{4}{3} = 0.80 \quad (\text{I})$$

$$\text{For } D_c = 5 \text{ in.}, \quad 15,000 = \frac{c(5-1)}{a + b(5-1)} = \frac{4c}{a + 4b}$$

$$\text{or } a + 4b = \frac{4(5000)}{15,000} = \frac{4}{3} = 1.33 \quad (\text{II})$$

$$\begin{aligned} \text{Regrouping } a + 2b &= 0.80 \quad (\text{I}) \\ a + 4b &= 1.33 \quad (\text{II}) \end{aligned}$$

Subtracting I from II,

$$2b = 0.53$$

$$\text{or } b = 0.27$$

Substituting value of b in I and II,

$$a + 2(0.27) = 0.80 \quad (\text{I})$$

$$\text{or } a = 0.26$$

$$\text{and } a + 4(0.27) = 1.33 \quad (\text{II})$$

$$\text{or } a = 0.25$$

For all practical purposes, then, $a = 0.26$ and $b = 0.27$
when $c = 5000$.

SOLUTION TO SINGLE BLASTHOLE DESIGN PROBLEM

A (1) From Eq. 21,

$$\sigma_y = \sigma_c \left(\frac{1 - \sin \phi}{1 + \sin \phi} \right)$$

Then

$$\frac{1750}{25,000} = \frac{1 - \sin \phi}{1 + \sin \phi}$$

or

$$0.07(1 + \sin \phi) = 1 - \sin \phi$$

$$0.07 + 0.07 \sin \phi = 1 - \sin \phi$$

$$1.07 \sin \phi = 0.93$$

or

$$\sin \phi = 0.87$$

Thus,

$$\phi = 60 \text{ deg}$$

From Eq. 22(b),

$$\sigma_s = \frac{\sigma_c}{2} (\cos \phi)$$

$$= \frac{25,000}{2} (0.5)$$

or

$$\sigma_s = 6250 \text{ psi}$$



A (2) From Eq. 14(b)

$$V_p = \left[\frac{E_r (1 - \mu)}{\rho_r (1 + \mu)(1 - 2\mu)} \right]^{1/2}$$

From Eq. 8(b)

$$\rho_r = 1.941 SGr$$

Thus, substituting given values of V_p , μ , and SGr and squaring both sides of Eq. 14(b),

$$(17,000)^2 = \frac{E_r (1 - 0.25)}{1.941 (2.9) (1 + 0.25) (1 - 2 \cdot 0.25)}$$

Rearranging

$$E_r = \frac{1.7^2 \times 10^8 (1.941)(2.9)(1.25)(0.5)}{0.75}$$

or

$$E_r = 13.5 \times 10^8 \text{ psf} = 9.4 \times 10^6 \text{ psi}$$



SINGLE BLASTHOLE DESIGN PROBLEM

A deposit is quarried in 30-ft high benches for crushed stone. The rock is quite massive and has the following properties:

$$SG_r = 2.9, \quad v_p = 17,000 \text{ fps}, \quad \mu = 0.25, \quad S_f = 0.7,$$

$$\gamma = 45 \text{ deg.}, \quad \sigma_c = 25,000 \text{ psi}, \text{ and } \sigma_t = 1750 \text{ psi}.$$

Blasted rock is loaded by a 5 cy front-end loader. The blastholes are drilled vertically and bulk loaded ($D_g = D_a$) with an explosive having an $SO = 117$, $D_c = 1$ in., and confined velocities of 12,500 fps at 3 in. and 15,000 fps at 5 in. and larger charge diameters. The relationship between v_a and D_a in the 1 to 5 in. range can be assumed to be in the form of

$$y = \frac{cx}{a + bx}$$

Drainage at the operation is such that blastholes generally are always dry, and there is no free parting in the rock available that can serve as a floor. For estimating purposes the average blast area A of material cratered by a single blasthole would be equal to $1.4B^2$.

A. Considering the foregoing information, find the following properties for the intact rock:

(1) σ_3 , and (2) E_r .

B. For charge diameters D_c of (a) 2 in., and (b) 4 in., determine each of the following estimates:

(1) v_a , (2) P_d , (3) P_g , (4) B , (5) T , (6) J ,
 (7) E , (8) W , (9) t_f , and (10) t_1 .

C. At the given bench height L determine the respective D_c values that define each of the following conditions:

(1) The B' that insures all of the explosive column will react before any cracks will have propagated to any open face when using a single primer located at (a) Floor level, and at (b) The Center of the charge column.

(2) The B'' at which overbreak quite likely may begin to occur when the primer is placed at floor level.

Faint, illegible text in the top left column.

Faint, illegible text in the middle left column.

Faint, illegible text in the bottom left column.

Faint, illegible text in the top middle column.

Faint, illegible text in the middle middle column.

Faint, illegible text in the bottom middle column.

Faint, illegible text in the top right column.

Faint, illegible text in the middle right column.

Faint, illegible text in the bottom right column.



The Mechanics of ROCK BREAKAGE

STANDARDS FOR BLASTING DESIGN

Part II of a Series

It is not enough just to understand what happens during blasting. Probably the most important thing to the average person is to know how blast effects can be controlled to suit the requirements of his operation. In this respect there are available five basic standards upon which to evaluate blasts, all of which are unitless (dimensionless) ratios. They can be applied to both underground and surface blasting with equal success. For simplicity, however, their use will be discussed as applied to surface (open-pit) blasting conditions. The standards are defined as follows:

1. **Burden Ratio (K_B)**—the ratio of the burden distance in feet to the diameter of the explosive in inches, equal to $12 B/D_e$.

2. **Hole-Depth Ratio (K_H)**—the ratio of the hole depth to the burden, both measured in feet, or H/B .

3. **Subdrilling Ratio (K_J)**—the ratio of the subdrilling used to that of the burden, both expressed in feet, or J/B .

4. **Stemming Ratio (K_T)**—the ratio of the stemming, or collar distance to that of the burden, both measured in feet, or T/B .

5. **Spacing Ratio (K_S)**—the ratio of the spacing dimension to that of the burden, both measured in feet, or S/B .

Burden Ratio The most critical and important dimension in blasting is that of the burden. There are two requirements necessary to define it properly. To cover all conditions, the burden should be considered as the distance from a charge measured perpendicular to the nearest free face and in the direction in which displacement will most likely occur. Its actual value will depend on a combination of variables, including the rock characteristics, the explosive used, etc. But when rock is completely fragmented but displaced little or not at all, one can assume the critical value has been approached. Usually, an amount slightly less than the critical value is preferred by most blasters.

There are many formulas that

provide approximate burden values, but most require calculations that are bothersome or complex to the average man in the field. Many also require knowledge of various qualities of the rock and explosives, such as tensile strengths and detonation pressures, etc. As a rule, the necessary information is not readily available, nor is it understood.

A convenient guide that can be used for estimating the burden, however, is the K_B ratio. Experience shows that when $K_B=30$, the blaster can usually expect satisfactory results for average field conditions (Table 1). Thus, for a 3-in. diameter explosive, a 7½-ft. burden ($30 \times 3/12$) would be a reasonable approximation. To provide greater throw, the K_B value could be reduced below 30, and subsequent finer sizing is also expected to result.

Light density explosives, such as field-mixed AN/FO mixtures, necessarily require the use of lower K_B ratios (20 to 25), while dense explosives, such as the slurries and gelatins, permit the use of a K_B near 40. The final value selected should be the result of adjustments made to suit not only the rock and explosive types and densities but also the degree of fragmentation and displacement desired.

To estimate the desired K_B value, one should know that densities for explosives are rarely greater than 1.6 or less than 0.8 gm./cc. Also, for most rocks requiring blasting, the density in gm./cc rarely exceeds 3.2, nor is it less than 2.2, with 2.7 (165 lb. per cu. ft. in the solid) by far the most common value. Thus, by first approximating the burden, make simple estimations toward 20 at a K_B of 30, the blaster can then

Table 1—Standard Blasting Ratios for Vertical Blastholes
(All Types of Surface Blasting, 20 Different Rock Types, Hole Depths From 5 to 260 ft., and Hole Diameters From 1½ to 10½ in. for All Grades of Explosives)

All Operations				All Operations but Coal Strippings			
K_B Group	Frequency	K_B Group	Frequency	K_B Group	Frequency	K_B Group	Frequency
		0.0-0.9	0			0.10-0.19	0
10-13	0	1.0-1.9	43			0.20-0.29	6
14-17	5	2.0-2.9	70	0.00-0.09	15	0.30-0.39	12
18-21	13	3.0-3.9	56	0.10-0.19	18	0.40-0.49	18
22-25	51	4.0-4.9	45	0.20-0.29	27	0.50-0.59	18
26-29	74	5.0-5.9	22	0.30-0.39	25	0.60-0.69	25
30-33	66	6.0-6.9	22	0.40-0.49	25	0.70-0.79	19
34-37	44	7.0-7.9	11	0.50-0.59	2	0.80-0.89	13
38-41	20	8.0-8.9	4	0.60-0.69	6	0.90-0.99	6
42-45	7	9.0-9.9	2	0.70-0.79	2	1.00-1.09	14
46-49	4	10.0-10.9	8	0.80-0.89	0	1.10-1.19	7
50-53	0	11.0-11.9	0			1.20-1.29	7
		12.0-12.9	1			1.30-1.39	3
						1.40-1.49	2
						1.50-1.59	2
Total	284	Total	284	Total	125	Total	152
Mean	30	Mean	4.0	Mean	0.23	Mean	0.74
Mode	38	Mode	2.6	Mode	0.24	Mode	0.65
Median	29	Median	3.4	Median	0.27	Median	0.67

*Note—Rf: Ash, R. L., and Pearse, T. E.—"Velocity, Hole Depth Related to Blasting Results." *Mining Engineering*—September, 1952, p. 75.

Faint, illegible text on the left side of the page, possibly bleed-through from the reverse side.

Faint, illegible text in the middle section of the page, appearing as a vertical column.

Faint, illegible text on the right side of the page, including several circular marks that resemble hole punches or stamps.

ROCK BREAKAGE

By **RICHARD L. ASH, P.E.**
School of Mines and Metallurgy
University of Missouri

ual characteristics of each ingredient determine whether it may be desirable for use in a mixture. Table 3 gives a partial listing of the many ingredients that might be included in an explosive. It can be recognized that certain compounds may be highly explosive by themselves or may be normally inert; but when combined, the entire mix may form an explosive. For this reason the compounding of explosives should not be attempted by the average person.

Explosive Reactions

To be an explosive, the reactions change in form from liquid or solid, or a combination of both, to that of a gas, or gas and solid, must be an exothermic reaction, or one from which heat is released. For most explosives, the quantity of heat released is quite large (Table 4). The gases formed, in turn, quickly produce very high pressures, with the reaction being called either deflagration or detonation.

The distinction between the two

types of reaction is that deflagration consists of a burning action at a high rate of speed, the chemical reaction of which causes gaseous formation and pressure expansion along with the burning. Thus, a heaving action from the pressures produced is experienced at nearly the same rate as that of the burning. This type of reaction is characteristic of low explosives, of which black powder is one particular type.

Detonation, on the other hand, consists of the propagation of a shock wave through the explosive, accompanied by a chemical reaction that furnishes energy to sustain the shock-wave propagation in a stable manner, with gaseous formation following shortly thereafter. The shock wave is characterized by a very sharp rise in pressure (Figure 11), in front of which there is a zone in which all immediate matter is ionized. The pressures developed by detonation (shock) are nearly double those produced by the gaseous expansion that follows. All high explosives are designed to detonate.

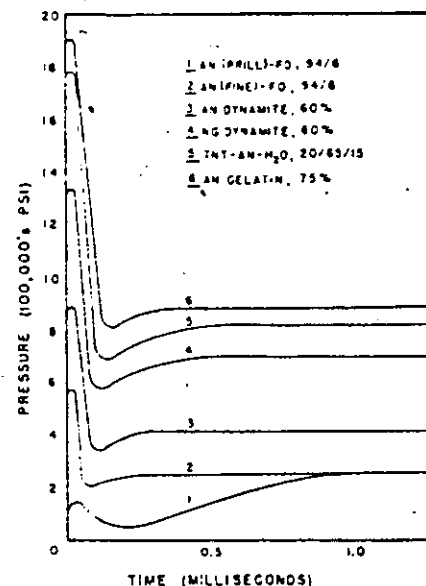


Figure 11—Curves of calculated pressure developed by some selected explosives under perfect confinement.

all low explosives will deflagrate; and blasting agents may exhibit one or the other type of reaction, according to their specifications and conditions of use. The important thing to remember about the reactions is that the effects of one type are very much different from those of the other, detonation producing higher energy and much higher velocities.

To accomplish a desired reaction, certain temperature and pressure conditions must be met, most explosives being designed for use under confinement, e.g., in blastholes. If the temperature required for a proper reaction is not present, no detonation may occur, with only burning or possible deflagration resulting. In practical terms, this means that even though the designed chemical composition calls for detonation, inadequate initial heat from an initiator or primer or a loss in confinement conditions can result in lower blast energy being developed from the explosive charge, or even in complete failure, causing a misfire.

For this reason, control over the confinement and the selection of primers with adequate heat energy and initiating power are particularly important. One should recognize then, which of the explosives need strong priming and which need very little heat for initiating their reactions, not only for reasons of blasting efficiency but for safety considerations as well. (Turn page)

Table 4—Available Heat Energies (Q) for Certain Selected Explosives

Explosive	SG	SC	Q (Cal gm)
Nitroglycerin (NG)	1.6	88	1420
PETN	1.6	88	1400
RDX	1.6	88	1320
Composition B	1.6	88	1140
Tetryl	1.6	88	1010
NG gelatin 40%	1.5	94	820
Slurry (TNT-AN-H ₂ O, 20/65/15)	1.5	94	770
NG gelatin 100%	1.4	101	1400
NG gelatin 75%	1.4	101	1150
AN gelatin 75%	1.4	101	990
NG dynamite 40%	1.4	101	930
AN gelatin 40%	1.4	101	800
NG dynamite 60%	1.3	109	990
PETN	1.2	118	1200
Semigelatin	1.2	118	940
Extra dynamite 60%	1.2	118	880
Amatol, 50/50	1.1	128	890
DX	1.0	141	1280
ST	1.0	141	960
TNT-AN, 50/50	1.0	141	900
TNT	1.0	141	870
AN-FO, 94/6	0.9	157	890
AN low-density dynamite	0.8	176	880
AN	0.8	176	350

To better understand the requirements just described, Table 5 illustrates the approximate temperature characteristics of two basic ingredients used in many commercial explosives. It should be noted that a very low temperature NG begins to decompose, boiling occurring shortly thereafter. Flame from a fuse, heat released by blasting caps, a relatively warm blasthole (such as one just recently drilled), friction from metal objects, and similar effects, can all provide quite easily the relatively low temperature needed to provide dangerous conditions. If the NG is confined, e.g., in a blasthole, the initial decomposition will be accelerated to result in detonation.

On the other hand, AN requires a fairly high temperature before it will begin to decompose and fume, necessitating a large amount of initial heat. However, once decomposition begins, detonation or deflagration will follow with a very small temperature rise. By combining the two ingredients, as is done in the ammonia dynamites, a compromise effect is achieved, the grades having the most NG being the easier to fuse.

Important Properties Of Explosives Most manufacturers supply catalogs and other information concerning the specifications of their products. However, certain properties are particularly important to quarry blasting. A review and explanation of their practical aspects should therefore be of special interest to the operator.

Water Resistance For all explosives, the presence of water in blastholes tends to promote chemical unbalance, as well as retard the heating reaction. Water supplies additional hydrogen and oxygen and requires additional heat to be vaporized into steam. If water is flowing through the ground, a leaching action can occur, whereby certain salts that may be easily dissolved could be removed from the explosive mixture. Explosives may be protected internally from water action by gelatinizing the mix or externally by cartridgeing. The ingredients added for gelatinizing are usually included in the chemical bal-

Table 5—Comparison of Approximate Reaction Temperatures (°F) of NG and AN

	NG	AN
Detonate	420	460
Boil	290	—
Decompose	140	410
Freeze	50	340

ance, as with the use of nitrocellulose in the gelatin grades.

Similarly, the paper, wood fiber, paraffin, or polyethylene used for external cartridgeing are generally included in the chemical balance. For this reason explosives that are made for use in cartridges should not be removed if preservation of the oxygen balance is to be maintained.

If an explosive is properly compounded initially, but detrimental effects occur from water, the action will be noticeable by the formation of brown nitrous-oxide fumes and a low blasting action. If these effects are observed, the explosive grade should be changed or other appropriate action taken. Primers must of necessity possess unlimited water resistance.

Fumes Most explosives are given a fume rating, the classification of which is based on the amounts of poisonous gases produced by the explosive reaction. Limits are set by many of the states, the U. S. Bureau of Mines, and certain other agencies. Where inadequate ventilation and exposure of personnel to toxic gases may exist, care must be taken to ensure that the explosives used give amounts below the established limits.

This property is particularly important for underground blasting; but for open-cut operations the problem could also be quite serious. Fumes may lie inside piles of broken rock. Such material, when stirred up by loading equipment, will release the fumes, to contaminate the air in which men are working. The problem may be aggravated by atmospheric conditions, deep cuts, and similar factors that hinder air circulation. Men will become ill and nauseated if this situation is present.

A person should understand the distinction between fumes and smoke, the latter of which is composed of liquid or solid particles

suspended in the air. Usually when white smoke is observed from blasts, it is quite likely composed primarily of the steam from the reaction.

Sensitivity This property actually refers to two related characteristics. It defines the relative ease with which an explosive reaction can be initiated and the relative ease with which the reaction is propagated through an entire charge. Several tests are used to rate sensitivity, the most common of which is the minimum booster required for initiation. Usually the total number of No. 6 strength blasting caps required for initiation is used to classify sensitivity.

However, an explosive may initiate easily but in small diameters the reaction may not propagate and dies out. For this reason explosives may not be manufactured below specific diameters. A critical diameter, or that below which propagation of a reaction will not continue, exists for practically all commercial products. Some blasting agents have a large critical diameter; most high explosives have a small one. By definition, blasting agents cannot be sensitive to initiation by a single No. 6 blasting cap, while high explosives all are one-cap sensitive.

On the other hand, an explosive may be quite insensitive to initiation but propagate easily when above the critical diameter. For safety reasons this situation is the more desirable; it is a definite advantage offered by many of the blasting agents. However, adequate priming is mandatory for their use. If propagation is difficult or impossible through a column of explosives, boosters may be used to sustain the reaction. But it should be recognized that both boosters and primers must be sensitive to initiation.

The sensitivity of an explosive is a function of the ingredients, their particle sizing, the charge diameter, the degree of confinement, and certain other factors. For example, ammonium-nitrate explosives may become quite sensitive in time by particle degradation due to the process of cycling. AN has the characteristic whereby it will change its crystalline form with changes in temperature; two of the changes often encountered in normal field blasting are at 0 and 90 deg. F. Constant

changes through those temperatures causes the particles to break into smaller sizes. The smaller particles offer more contact surfaces between ingredients, making it easier for particles to be consumed by the explosive reaction. The result is to permit easier initiation and subsequent more rapid propagation through a charge. Blasting agents that would normally be insensitive become quite sensitive to initiation by a single No. 6 blasting cap, similar to that expected of high explosives.

Larger charge diameters also propagate reactions more easily because of the greater surface area available. Confinement tends to concentrate the reaction's force along the charge length rather than permit the action to spread.

Certain hydrocarbons have an adverse effect on some types of explosives, principally those with free NG, as do the straight and extra grades of dynamites (Table 6). Since some of the blasting agents have liquid hydrocarbons as one of their ingredients, e.g., FO, one should be particularly cautious in his choice of primer explosive. Under certain conditions there could be an accumulation of the hydrocarbon in the blastholes, particularly at the bottoms, which in turn may lead to misfires when charges are bottom-primed. This situation can be avoided by using gelatins or simigelatins or high explosives containing no NG for priming. Furthermore, it is simply good practice to avoid the use of excessive FO in any blasting agent, to avoid upsetting the oxygen balance.

Density Explosives are manufactured and sold on a weight basis, the densest explosives usually being the strongest. The density, or weight per unit volume, of an explosive is therefore one of its most important properties. In industry this property may be specified in three ways: (a) by specific gravity (SG) expressed as a unitless number or in gm/cc; (b) by stick count (SC) or the number of 1¼ x 8-in. cartridges per 50-lb. box; and (c) by loading density (d_s) or the pounds of explosive per foot of charge length. The value for the loading density, however, is a function of the explosive's charge diameter

Table 6—Percent by Weight of Diesel FO Additive Where Detonation Fails

Explosive	Pct. Add.	Qt. FO/lb. of Expl.
Extra dynamite 40%	1.5	0.008
Extra dynamite 60%	2.5	0.014
Low-density dynamite (SC 120)	4.0	0.022
AN gelatin 60%	8.0*	0.05*
NG gelatin 60%	39.0*	0.21*

*Amounts applied, but detonation successful; no failures.

(D_s), which should then also be specified easily for clarity.

The various measures for density can be calculated easily for rapid use in the field, provided that the charge diameter (D_s), expressed in inches, and one of the density values are known. The relationships are as follows:

$$d_s = 48D_s^2/SC \quad (1)$$

$$d_s = 0.34D_s^2(SG) \quad (2)$$

$$SG = 141/SC \quad (3)$$

These formulas provide a very convenient means for estimating explosive quantities, in that most explosive manufacturers supply the SC or SG for their products. For example, if a free-flow AN-FO mixture with an SC of 176 were to be used in a 10-in. diameter blasthole, one would expect slightly in excess of 27 lb. per foot of hole (or $d_s = 48 \times 10^2$ divided by 176 = 27 lb./ft.). (The relationships are illustrated graphically by Figure 12.)

It will be noted that an SC of 176 corresponds to an SG of 0.8, which could also be determined from

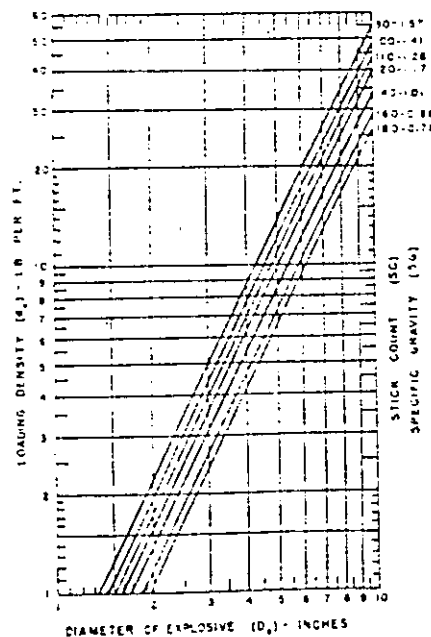


Figure 12—Relationships between densities of explosives.

Expression (3), above. Since the SG of water is 1 and its equivalent SC value is 141, any explosive with an SG greater than 1 or an SC less than 141 could be expected to sink in wet blastholes. It should be pointed out, however, that D_s is the diameter of the explosive, not that of the blasthole. These diameters are equal only in the case of free-flowing explosives or charges composed of cartridges that are thoroughly tamped.

Because certain ingredients may be included in explosives that do not contribute to the energy produced, there is no distinct relationship between density and pressures developed. In fact, some manufacturers make a 40 percent Extra type dynamite, for example, that is denser than the 60 percent of the same type of explosive. Similarly, a 90 percent gelatin is lighter than a 30 percent gelatin. But as a general rule it is reasonably approximate to relate the energy developed by explosives to their relative densities. This is because explosives are characterized by general density groups that correspond to their various types, e.g., gelatins, dynamites, etc. The denser types as a group produce more energy than the lighter ones, even though there may be exceptions to the rule between grades within the same type.

Velocity The rate, usually expressed in feet per second (fps), at which a reaction propagates through an explosive is considered by many as the most important quality of an explosive. It is often called the detonation velocity, but this is not always technically correct. Its importance can be better appreciated when it is understood that the energy produced by any explosive is a function of the product of its density and velocity characteristics. Since the initial reaction for most explosives used in commercial blasting is detonation with subsequent gaseous expansion, the action would be considered dynamic.

Thus, impulsive and momentive forces are produced as a result of the kinetic energy of the reaction, which can be expressed by the relationship $KE = \frac{1}{2}Mv^2$, where M is the mass and v, is the velocity of the explosive's reaction. The rela-

relationship is given to illustrate that the value of the velocity is squared. Thus, energy releases are affected much more by changes in velocity than by changes in density. For example, if one of two different explosives has *double the density* of the other but both have the *same velocity*, the denser one could be expected normally to produce twice the work. However, if both explosives have the *same density*, but one has *double the velocity* of the other, the faster explosive would produce *four times* the work possible from the other.

Contrary to common belief, all high explosives do *not* react with high velocities, which may vary from about 20,000 fps to as low as 5,000 fps. The velocity of an explosive is related to the sensitivity in some respects, being dependent on the particular ingredients used, their particle sizing, the density, the charge diameter, and the degree of confinement under which it is used. As explained earlier, the smaller the particles the greater the density, which in turn usually increases the amount of energy-producing material per unit of volume and the number of contact surfaces between particles, thereby increasing the over-all rate of reaction. The combined effect is to increase the energy potential of the explosive.

Explosives are given two velocity ratings, one for use in the open or unconfined, the other if it is confined. For many grades and types, the unconfined velocities are 20 to 30

percent lower than those achieved under confinement. In a practical sense one could then assume that an explosive would produce only 60 to 70 percent of the total work possible if used unconfined. It is, therefore, particularly important to know which velocity value is specified for a product.

The technique known as cushion blasting utilizes the principle of reduced velocities resulting from less confinement. It can be used to prevent shattering. In this method an annular air space is left around the explosive, if used in cartridges, or air pockets are left at prescribed intervals between deck charges placed along the length of a blasthole.

Strength The least understood and often the most improperly specified property for describing an explosive is its strength. It is usually expressed as a percentage, and it was originated when all commercial high explosives contained NG as the primary energy-producing ingredient. In the beginning, the percentage meant the actual amount of NG in the total weight of explosive, which would be applicable for most of the straight dynamites. However, for all other types of explosives other ingredients may be used to supply a part or all of the energy. In addition, there are two strength ratings given to explosives; and unless this is clearly understood by users, it can lead to very serious difficulties.

The first method for rating—*weight strength*—means that a pound of a particular explosive can do the same work as a pound of straight NG dynamite of equivalent strength when used under certain specified conditions. Since densities of explosives vary considerably although the explosive or blasthole diameter may not be changed, a method for rating strength on an equal volume basis would be necessary.

The bulk, cartridge, or *volume strength* rating provides the necessary comparison, but its value is determined by calculation. The two strength ratings, by weight and by volume, are considered equal when the stick count (SC) is near 100, as it would be for most straight dynamites. To assist in the correla-

tion between the two ratings, the nomograph in Figure 13 can be used.

If the weight strength of an explosive having an SC of 150 is 60 percent, a pound of it will provide energy equivalent to that of a pound of 60 percent straight dynamite. However, from Figure 13, the cartridge strength is indicated as only 30 percent, which means that if the explosive was used on an equal volume basis, it would have the energy of only a 30 percent straight dynamite. Unfortunately, some explosives are sold and designated by weight strength, and others by bulk or volume strength; and still others are specified by letter or number, with a weight strength given for the general class or type of explosive in which it is but one of the grades.

The operator can understand that he could be badly mistaken if he were not careful to distinguish between the two strengths in using this property as a primary basis for selecting an explosive. To avoid confusion and possible serious difficulties, it is generally much simpler to judge an explosive's relative strength according to its density and velocity characteristics. The quantities of both are usually available from the manufacturer's information.

Correlating Explosive's Properties to Blasting Standards Since the burden is the most important single di-

mension for successful blasting, and that upon which the design standards are based, its determination must take into account the individual characteristics of the particular explosive selected for use on a job. A convenient method for estimating its value is to employ the relative-energy comparison technique. Because all properties may be considered relative for comparison purposes, an explosive with an SG of 1.3 and a v_d of 12,000 fps could be considered the standard, or one with characteristics near that, for 40 percent to 60 percent Extra dynamites, which long have been considered appropriate explosives for quarry blasting. However, it should be understood that any standard might be used for making a comparison.

To estimate the relative energy potential of an explosive, the diameter (D_s), density (SG), and velocity

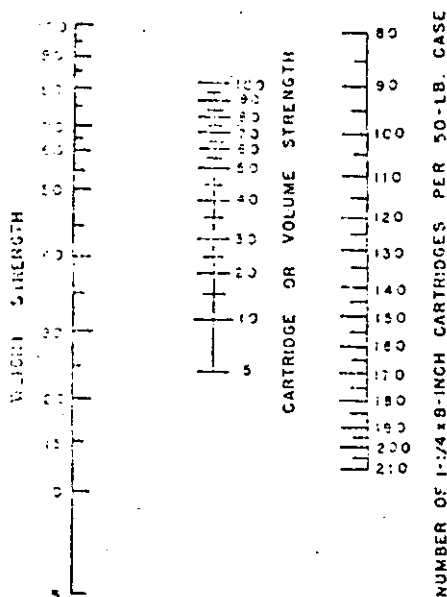


Figure 13—Chart for correlating explosive strengths.

(v_1) must be known, or approximated. Furthermore, to simplify calculations, one can assume blast-holes would be filled across their entire diameter, or $D_2 = D_1$. This condition ensures little or no energy losses, or dampening, for a complete energy transfer from the explosive's reaction into the surrounding rock to be blasted.

The relative energy (RE) and that exerted to the rock could then be expressed by a simplified kinetic-energy relationship, or $RE = a(SG)v_1^2$. The "a" is a conversion factor to permit the use of specific gravity instead of mass, and it assumes that the explosives will be used in the same diameter. For any set of similar field conditions the "a" will be a particular constant number, making it then possible to omit it from the relationship when explosives are compared under identical field conditions. Thus, the following expression can be used for comparing two or more explosives, based on their energies:

$$RE_2/RE_1 = (SG_2)(v_{2,2})^2 / (SG_1)(v_{1,1})^2 \quad (4)$$

If Explosive No. 1 represented the average explosive ($SG_1 = 1.23$ and $v_{1,1} = 12,000$ fps) and Explosive No. 2 had $SG_2 = 1.5$ and $v_{2,2} = 18,000$ fps, the relative energy of the second compared to the first according to Expression (4) would be as follows: $RE_2/RE_1 = (1.5)(18,000)^2 / (1.23)(12,000)^2 = 2.8$

The RE value shows then that the second explosive has 2.8 times the energy potential of the standard explosive. Since the comparison is made between explosives used for blasting the same material, the comparative blast results in the rock would vary as the cube root of their relative energy value. The cube root is used rather than the direct ratio because of the spherical fan effect for energy propagation through homogenous materials. This relationship then tells us that the K_B ratios and therefore the burdens will vary in proportion to the cube root of the explosives' relative energies. To provide a simple formula for illustrating the relationship, the following may be used:

$$K_{B2} = K_{B1}(RE_2/RE_1)^{1/3} \quad (5)$$

If one assumes that average rock will be blasted, a K_B value of 30 would represent the average explosive (Figure 7). The burden used

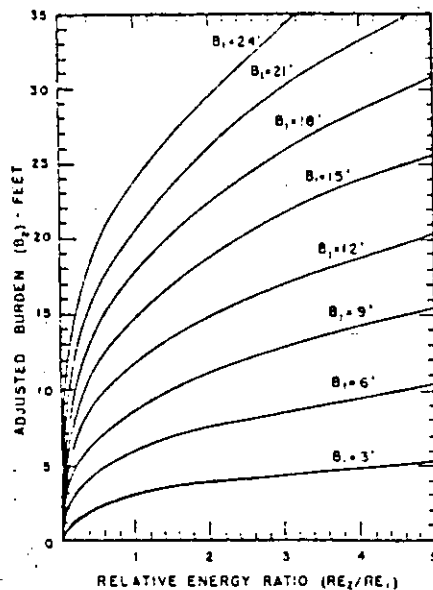


Figure 14—Relationships between burden dimensions for explosives according to their relative energy and when used under field conditions.

would be $7\frac{1}{2}$ ft. for a 3-in. diameter explosive, since $K_{B1} = 30 = 12B_1/D_1$, which gives $B_1 = 30D_1/12 = 30 \times \frac{3}{4} = 7\frac{1}{2}$ ft.

For Explosive No. 2, then, using Expression (5), one can approximate that $K_{B2} = 42.1$ or $K_{B2} = 30(2.8)^{1/3}$. The burden for the second explosive would then be $10\frac{1}{2}$ ft., since $B_2 = 42D_2/12 = 3\frac{1}{2} \times 3$. For direct calculation of the burdens for explosives used in the same diameters and under identical field conditions the following may be used:

$$B_2 = B_1(RE_2/RE_1)^{1/3} \quad (6)$$

The relationships given by Expressions (5) and (6) are shown on Figure 14, which permits one to determine the approximate new burden for any explosive as compared to the average explosive when used under identical field conditions.

Although the example given illustrates ideal conditions and one should recognize that many variables enter into making the final selection of a K_B ratio and its related subsequent burden dimension, the relative-energy comparison technique gives a realistic approximation. As a matter of interest, for most explosives used in blasting the maximum density variation is from 0.7 to 1.6, with a velocity variation from 8,000 to 20,000 fps, the heavier densities having the higher reaction rates. Therefore, the weakest explosives possess only 26 percent of the energy available, while the strongest have 370 percent of the energy available,

as compared to that available from the average explosive. Converted to K_B values and using a $K_B = 30$ for the average explosive in average rock, the lower and upper limits for K_B values would be 19 and 46, respectively. From Table 1 it can be seen that these values satisfy results from actual field experiences.

The Mechanics of

ROCK BREAKAGE

MATERIAL PROPERTIES, POWDER FACTOR, BLASTING COST

Part IV of a Series

THEIR PROPERTIES AND INFLUENCE

Materials requiring blasting are not homogeneous nor are their properties the same throughout. Of all the physical properties, there are essentially five that predominantly influence blasting results. These include in order of their importance the following characteristics: (1) structure, (2) resilience, (3) strength, (4) density, and (5) velocity of energy propagation. Blastability, elasticity, hardness, toughness, and other terms may also be used to describe a material, but often such expressions are too indefinite and difficult for the ordinary quarry man to understand. Drillability, or ease of drilling, should in no way be confused with the manner in which a material can be blasted.

Structure The structural features of a material usually have the greatest influence on blast effects. To better understand their importance one should recognize that rock, as we think of it, is essentially an accumulation of small particles bonded together. The constituents are oriented in definite structural patterns, established during the formation and alteration processes. Of primary importance to blasting is compression jointing, existing within all rocks (igneous, sedimentary, and metamorphic) and composed of planes along which there is no resistance to separation. Igneous rock may also have tension jointing, formed during the cooling process.

Sedimentary rocks are unique in that they have stratification planes (in addition to joints), which were originally horizontal and formed by

interruptions in the initial deposition of sediments. Stratification and jointing are not the same thing. For metamorphic rocks, the relationship of their jointing to schistosity is similar to that between jointing in sedimentary rocks and their stratification, both in angular position and mechanical development.

Jointing is usually easily detected, the planes being generally smooth and often short distances apart. One set of planes is parallel with the dip and strike of the rock formation, with two or more sets being nearly perpendicular to the first set. Rocks when broken will separate into blocks of a shape characteristic of their particular jointing pattern, and the new faces produced from blasting tend to follow the jointing directions. (See Figures 3, 4, 8, 10, and 15.)

For the sedimentary rocks there is one particular direction along which jointing is the most pronounced, the other planes being less dominant. The horizontal angles between the vertical jointing planes are usually near 75 and 105 degrees, which form rhombohedrons when the rock is broken. Igneous rocks, however, have jointing planes of uniform strength, the angles between planes being most often near 60 degrees. The fragments produced from blasting are generally hexagons or pyramids in shape.

Jointing directions can be found quite easily if it is recognized that most faults, cliffs, mud seams, caves, etc., produced by weathering and the other geologic actions tend to

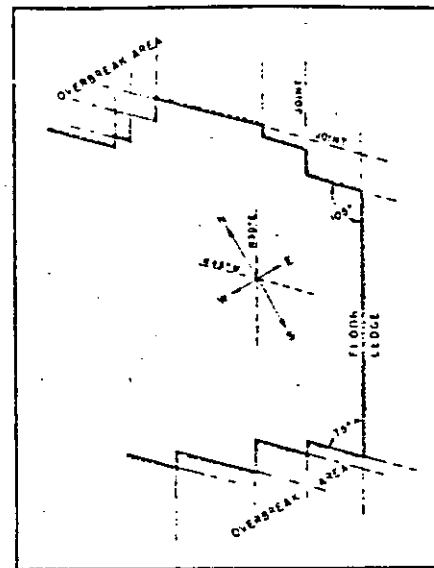


Figure 15—A representative plan sketch of a quarry in a sedimentary rock formation, showing tight (75-degree) and open (105-degree) corners.

follow the jointing planes. It is particularly important that the blaster endeavor to locate the planes before laying out a drill pattern. Blast-holes located in tight corners will generally overbreak, opening large cracks in the ledge. Subsequent blasts will usually do no more in those areas than give large boulders, and possibly be quite violent. It can be seen from Figure 15, which illustrates a representative quarry in a sedimentary rock formation, that there are tight (75-degree) and open (105-degree) corners. This means that normal blasts under those conditions should be directed out of the open angles in so far as possible, or toward the east or west. If blasting is done in the other directions, or to the north or south, cracking of the solid ledge will occur along the planes forming the tight angles.

Another structural feature that is

By RICHARD L. ASH, P.E.
School of Mines and Metallurgy
University of Missouri

very important, particularly to rock fracturing, is the type and strength of the bonding between individual grains. For example, rock may have pronounced jointing at widely separated distances, but the material between joint planes may be strongly bonded, or massive in character. Large boulders invariably result when blasting is carelessly done under this condition. On the other hand, rocks may be highly laminated or stratified, or the bond between grains may be very weak, so that fragmentation is always easily accomplished by merely moving the material from its original place.

Resilience This property, sometimes called sponginess or toughness, refers to the elasticity of a material. It is used to express the capability of a rock to resist shock and recover its original position and shape without being ruptured. If a rock on being dropped, for example, makes a dull thud and does not rebound, it would be very difficult to break by impact. Brittle rocks, however, shatter easily, particularly those types having a high silica (quartz) content. A blaster can generally determine quite easily whether or not a material will break into small sizes or large coarse fragments by conducting a simple drop test. Furthermore, the test provides a clue as to the energy absorption power of the material, which is important for estimating the amount of additional charge, or energy, that would be necessary to overcome expected energy losses.

Strength Of the characteristic strengths of materials, blasting is normally concerned only with that of tension. Most rocks are very weak in tension, more resistant to shear, and strongest in compression, having approximately only one-tenth the resistance to tensile rupture that they have to failure by compression (Table 7). However, shear is not actually a force by itself but rather the result of two forces, either two tensile or two compressive forces, or a combination of one of each, which act along different lines and directions.

To know the actual strengths of a material, samples must be tested in a laboratory. (Regular tensile-

Table 7—Properties of Various Selected Materials

Name and Location	Compressive Strength (psi)	Modulus of Rupture (psi)	Specific Gravity (SG)	Density (d.) (ton/cu. ft.)	Longitudinal Velocity (v.) (fps) \sqrt{p}
Amphibolite (fine grain, India)	61,400	7,400	3.12	0.097	19,000
Basalt (New York)	46,600	8,000	2.94	0.092	18,700
Basalt (Michigan)	33,400	3,800	2.85	0.089	15,200
Basalt glass	—	—	2.81	0.088	21,000
Diabase (fine grain, Michigan)	44,200	5,300	2.94	0.092	16,700
Dolomite (Missouri)	8,800	1,000	2.80	0.087	—
Dolomite (Tennessee)	46,700	3,800	2.84	0.089	17,900
Gabbro (altered, New York)	40,200	5,400	2.93	0.091	17,600
Granite (Georgia)	28,000	2,000	2.64	0.082	8,900
Granite (Vermont)	33,200	2,900	2.66	0.083	11,100
Granite (Nevada)	39,500	3,900	2.63	0.082	14,500
Granite (North Carolina)	30,400	1,600	2.60	0.081	8,600
Greenstone (Michigan)	45,500	3,300	3.30	0.103	16,600
Gypsum (Indiana)	3,200	1,200	2.52	0.072	—
Limestone (Ohio)	28,500	2,900	2.69	0.084	15,400
Limestone (Utah)	28,000	2,200	2.78	0.087	15,900
Limestone (fossiliferous, Indiana)	10,900	1,600	2.31	0.072	12,400
Limestone (West Virginia)	23,000	1,900	2.68	0.084	16,400
Marble (Maryland)	30,800	2,800	2.37	0.074	13,700
Marble (New York)	18,400	1,700	2.72	0.085	14,500
Obsidian	—	—	2.35	0.073	16,100
Quartzite (taconite, Minnesota)	91,200	3,400	2.75	0.086	18,200
Rock salt (Louisiana)	5,000	Negligible	2.50	0.078	—
Sandstone (Ohio)	10,400	500	2.06	0.064	5,600
Sandstone (West Virginia)	19,400	3,400	2.50	0.078	12,900
Sandstone (Utah)	11,500	620	2.17	0.068	8,400
Sandstone (Alabama)	26,800	2,200	2.76	0.086	12,500
Shale (Utah)	31,300	2,500	2.81	0.083	14,900
Shale (West Virginia)	11,600	4,200	2.40	0.075	13,600
Syenite (New York)	34,300	2,800	2.72	0.085	14,500
Alluvium, broken rock, loess	—	—	1.3-1.5	0.044	2,300
Clay	—	—	2.53	0.081	5,900
Air	—	—	0.0012	—	1,080
Water	—	—	1.00	0.031	4,750

strength tests are usually difficult to conduct.) However, tests for what is known as the modulus of rupture are much easier to perform; yet they provide information that is just as useful in providing tensile-strength data of equal practical value. In fact, the laboratory test for the modulus breaks samples in tension by bending test slabs until they fracture, much in the same manner that rock is stretched and broken at an open face during blasting (Figure 3).

Quite often it is impossible or quite impracticable for quarry operators to have tests conducted. Also, test results on samples may not necessarily provide information on the over-all strength of a rock deposit, except when the material is homogeneous and very massive. Nevertheless, if tests could be made, the data would aid greatly in determining the stress levels (psi) required for fracture. It is the resistance to tensile rupture that must be exceeded by the energy pulses at

the free faces, and thus, if known, could also give an approximation of the required burden dimension and the explosive pressures needed for proper breakage. In the event specific test data cannot be obtained, the operator may find the information in Table 7 quite useful. From the various moduli listed for many of the representative rock-types, a practical estimate can be made that will approximate the characteristics of his particular deposit.

Density Denser materials require greater amounts of work energy to be satisfactorily broken and displaced, and heavier explosives or large charges will therefore be needed. However, from Table 7 it can be concluded that for most rocks there is a very narrow range of density differences, with SG values varying from 2.3 to 3.3 in most instances. The materials generally requiring blasting have densities confined to the 2.5-2.9 SG range. This can be interpreted to mean that the

influence of rock density alone has a limited effect on blasting, the extreme conditions being within 15 percent of the average 2.7 SG. One may then reasonably assume that rock density by itself is of little importance to blasting and would not appreciably affect a K_B value or burden dimension.

Its importance, however, lies in the fact that it does influence costs and the other physical properties. Although densities are most often given by specific gravity, for calculations in costing and powder factor determinations it is more convenient to use the density ratio, d_r , expressed in units of tons/cu. ft. of solid material. If the d_r value is not known, one can utilize the following expression for converting any SG that may be given:

$$d_r = SG(62.4/2000) = 0.0312(SG), \text{ tons/cu. ft. (7)}$$

Velocity The velocity of energy transmission in rock, v_p , is like the reaction velocity for explosives, v_r , in that it increases as rock density becomes greater. The denser rocks are often the least porous and are generally composed of small grains, which permit easier propagation of energy through the material. For this reason most dense rocks have smaller energy losses due to dampening, and they often have a tendency to shatter rather than break into slabs. Most brittle rocks also transmit energy at very high rates, except in the unique case of certain sandstones. The characteristic low velocities of many of the sandstones are due to a peculiarity in their composition: the matrix bonding the sand grains may be clay, lime, or other energy-absorbing substances. However, if the matrix is silica, the velocity is quite high.

Velocities for materials are usually specified as longitudinal velocities, v_l , as are also those given in Table 7. But these values are normally slightly lower than the velocity of energy propagation, v_r . The two velocities are related by the following expression:

$$v_l = v_r \left[\frac{(1-\mu)}{(1+\mu)(1-2\mu)} \right]^{1/2} \quad (8)$$

Because μ , or Poisson's Ratio, is usually considered as 0.25 for estimations, it is more convenient to

convert velocities by using $v_r = 1.095v_l$ for approximations. However, it is more practical and will not introduce any great error if the two velocities are considered equal.

The importance of velocity in rocks on blasting is that it has a strong influence on the amount and manner in which a material will be stressed. In order that the momentive forces be conserved, there should be nearly perfect coupling of the energy from an explosive's reaction with the surrounding material. The matching of the momentive energies is considered necessary theoretically for the most efficient blasting results. This condition is known as acoustical coupling. Since the energy required for stressing strong and dense rocks would be relatively large compared to that needed for lighter materials, the use of denser, fast-reacting explosives is generally advisable.

The velocity of a rock will determine the time it takes the stress energy to reach free faces and return. The velocity of an explosive, on the other hand, will determine the total time it takes for an entire charge to complete its reaction. The relationship of the two velocities, called the velocity ratio or $K_r = v_r/v_p$, has a very important influence on the manner in which an entire blast will function. This is because the K_r ratio defines the shape of the composite wave produced by all the individual stresses introduced into the rock from each point along a charge column (see Figure 6, PIT AND QUARRY, September, 1963, page 119) the primer positions thus controlling which faces are fractured first and the direction in which the composite wave will travel in the rock.

The K_r ratio, primer location, and general design features of a blast must follow certain definite relationships, if results are to be satisfactory. In particular, the influence of rock velocity is such that there will be a certain optimum of critical hole depth for each blasting situation. For example, when a charge is bottom-primed, there will be a specific *minimum* hole depth. If the depth is less than the minimum value, blast effects will begin near the collar region, which quite likely may promote violence and air blast. In some instances, toe will be left

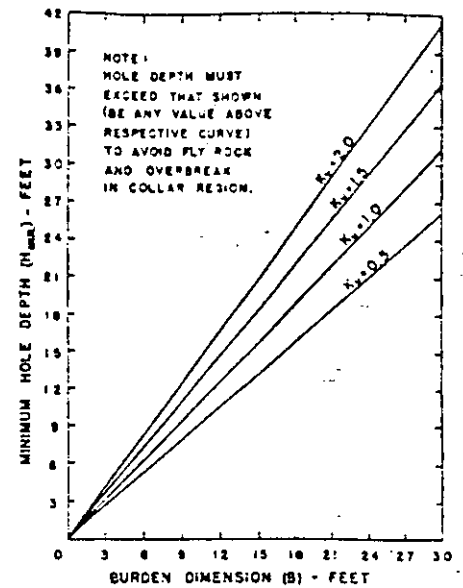


Figure 16—A graphic presentation of the relationship between minimum hole depth and burden dimension.

at the floor. However, when holes are deeper than the minimum value, stressing and rock movement will always begin at the ledge bottom before action occurs in the collar region. The particular minimum required depth of hole can be determined from the following expressions: Collar-Primed, $H^* = T + J$ (9a); Bottom-Primed, $H^*_{min} = K_r [(B^2 + J^2)^{1/2} - T] + T$ (9b). The relationship is illustrated graphically in Figure 16, in which $K_r = 0.7$ and $K_r = 0.5$ are considered average conditions. The values for the H^*_{min} represent balanced stressing at both the toe and collar regions.

If charges are collar-primed, stressing will always begin in the collar region, unless the amount of stemming used exceeds the burden dimension. Even under that condition, collar overbreak and air blast may occur, with possible toes resulting, if a particular *maximum* hole depth is exceeded. This limiting condition can be determined from the following relationships:

$$H^*_{max} = K_r(T - B) + T \quad (10)$$

From a practical viewpoint, the expression shows that under no circumstances should the stemming dimension be less than that for the burden in blasting massive rock. Otherwise, collar cratering and air blast can be expected. The condition becomes particularly critical when detonating fuse is used and initiation is done on the surface, since the fuse on detonating has the

$$\text{Collar-Primed } H^* = T(2K_r + 1) \quad (9c)$$

$$\text{Bottom-Primed } H^* = 2K_r(B^2 + J^2)^{1/2} + T \quad (9d)$$

tendency to loosen the stemming. For deep holes, collar priming would definitely be undesirable under conditions where massive cap rock occurs in the collar region and where column loading is practiced; i.e., the charges are continuous from just below the stemming to the hole bottoms.

An unusual situation exists when the K_v is less than 1, or when the rate of travel of the compressive stress-wave in the rock exceeds the speed of the detonation wave in the charge column (Figure 6). Stress waves will reach free faces before the explosive has completed its reaction, with rock at the faces being repeatedly stressed by the pressures produced by the still reacting explosive column. The action reinforces the stresses and reduces the resistance of the rock to fracture, giving the impression that the explosive is stronger than it actually is. Under certain conditions, blasts are extremely efficient, but they are usually difficult to control, producing greater heave or throwing action.

Since there are critical hole depths for each blasting condition, the best results can often be insured by first estimating the particular K_v value for the conditions present, and then placing primers accordingly. Control for very deep holes, for example, is achieved by using primers both near the collars and in the hole bottoms; or primers may be placed at strategic intervals throughout the columns, with or without the use of deck charges. Either detonating fuse or close-interval delay blasting caps can be

used for initiating the primers, those near the collar being preferably of a longer delay. The composite effect of using primers at both the collar and hole bottom is that it extends the optimum hole depth and better distributes the stresses in the ledge, notably in the toe and collar regions.

POWDER FACTOR AND ITS SIGNIFICANCE

A guideline used by many for estimating and evaluating blasting is the Powder Factor, Pf, an expression which relates the yield of material blasted to the quantity of explosives used. For quarry work and mining, the Pf is most often stated in tons/lb., or vice versa, while for most construction excavation it is customarily expressed in lb./cu. yd., or cu. yd./lb. The latter ratio is also commonly used for much of the work in overburden removal for coal and metal-ore operations. Of all the different ratios in common use, only those utilizing weights, e.g., tons/lb., take into account any of the properties of the materials being blasted.

Because of its extremely variable character Pf is not normally a sound index upon which to judge blasting efficiency or design blasts, as many believe. Different values will be obtained by merely changing the blast-hole pattern or configuration, and values will also change for other reasons, such as variable hole depths

and deck loading. Also, the many different standards employed tend to confuse rather than assist persons in evaluating results. The most practical value of Pf is in cost analysis, because explosives are sold by weight, and payment for materials mined or removed is generally made on a weight or volume basis.

One of the ways in which the powder factor can vary is shown by the examples given in Figure 17. These sketches illustrate four possible ways of blasting with a single charge and six different patterns utilizing a V-cut arrangement for multiple charges. All the blasts are conducted under identical conditions except for the relative positions of open faces. Pertinent data for Figure 17 are given in Table 8. The information there given is merely representative and used for comparative purposes. It may or may not fit actual blasting situations.

In determining the possible yields given in Table 8 for the various blasts shown in Figure 17, the surface blast areas, A, were approximated based on the locations of open faces, assumed rock structural features, and the particular mechanics of how each specific blast would be expected to function. The excavation volume would then be the product of the blast area and the ledge height, L, not the hole depth, H, as some might assume. Simple conversion to tonnage yield, W, was accomplished by multiplying the volume by the material density, d_r , using the following relationship:

$$W = AL(d_r), \text{ tons} \quad (11)$$

The quantity of explosives used, E,

Figure 17—These sketches show four possible ways of blasting with a single charge and six patterns utilizing a V-cut arrangement for multiple charges.

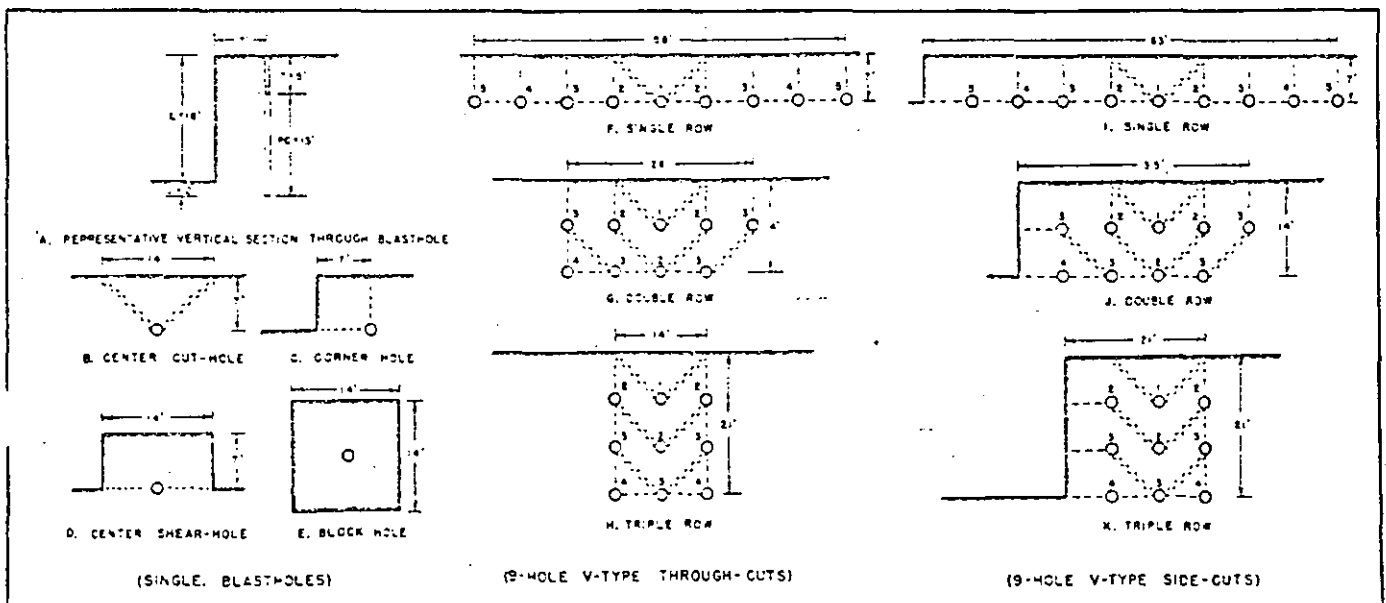


Table 8—Change in Powder Factor (Pf) With Variation In Drill-Pattern Configuration (a)

(For blasting limestone with $d. = 0.084$ ton/cu. ft. (b) by Extra 60% dynamite, $D. = 2$ inches (c), and blastholes located according to average K_b ratio of 30 (d).)

	Total No. Blastholes	Total Yield (tons)	Total Expl. Used (lb.)	Powder Factor (tons/lb.)
Single charges:				
(B) Center cut-hole (2 free faces)...	1	66	22.7	2.91
(C) Corner hole (3 free faces)	1	66	22.7	2.91
(D) Center shear-hole (4 free faces) ..	1	132	22.7	5.82
(E) Block hole (5 free faces)	1	264	22.7	11.64
Multiple charges: V-type through-cut:				
(F) Single row	9	528	205	2.58
(G) Double row	9	462	205	2.25
(H) Triple row	9	396	205	1.93
Multiple charges: V-type side-cut:				
(I) Single row	9	594	205	2.90
(J) Double row	9	627	205	3.06
(K) Triple row	9	594	205	2.90

Notes: (a)—See Figure 17 for design specifications.
 (b)—Rf. Table 7.
 (c)—Rf. Figure 12.
 (d)—Rf. Table 2.

would be the product of the explosive's loading density, $d.$, the total average length of one charge, PC , and the total number of blastholes, N , calculated as follows:

$$E = (d.) (PC) N, \text{ lb.} \quad (12)$$

The powder factor, Pf , would then be the ratio of the above two expressions, or

$$Pf = W/E, \text{ tons/lb.} \quad (13)$$

In studying Figure 17 and Table 8, it will be noticed that the number of free faces has a very pronounced influence on the value of the Pf . For multiple-hole blasts, when there is a free face added on one side, the over-all Pf 's for all blasts will usually be the same as that for a single corner or cut hole. However, the Pf may be affected by the initiation-timing pattern employed, which may change the blast area outline, as shown in Figure 17J and line J of Table 8. For the particular blast in point, the additional tonnage results from overbreak in the tight corner of the second row of holes. If a later-interval initiation delay were used in the corner hole, the blast would then be expected to cut squarely without any overbreak, to give the same yield as for the other two examples (Figures 17I and 17K).

Estimating or evaluating an entire blast on a single-hole Pf basis can be very misleading, but unfortunately it is a practice often followed. For the design and evaluation of underground face-blasting,

the errors produced would be even more serious and costly when based on a single-hole Pf . This is because there is an automatic elimination of potential tonnage for one complete row of holes. The row may be considered as serving merely to shear the cut out of the solid without achieving any effective production. It is also very important to recognize that in all blasting, when rows are added into the solid, with a subsequent reduction in the number of open faces, the Pf value will continue to change toward lower yields even though all other fundamental blasting relationships and the resulting rock fragmentation may remain substantially the same.

In surface or open-pit blasting the hole depths may vary within a particular cut or excavation, with no other changes being made in any

of the other design dimensions. If column loading is practiced, the Pf will change with the hole-depth variations. The trend is illustrated by data given in Table 9, in which the values represent conditions for the 9-hole blast shown in Figure 17F. The cause for the Pf variations is the result of changes in the ratio of the amount of hole used for stemming relative to the total hole depth. To counteract the lowering of yields, deck loading could be used, a practice commonly followed for deep holes particularly. This practice produces no detrimental effects on fragmentation when the decking is done properly.

Blasters should be cautioned regarding difficulties that may result from reducing the explosive loading density as a means for improving their Pf , or use of lighter grades or smaller diameter explosives. Attempts to extend drill-pattern dimensions by increasing burdens, etc., will produce similar difficulties for the same reason. Rather than sacrifice good fragmentation and displacement effects by decreasing the explosive energy, adjusting the blasthole arrangement is generally preferred. This can be done by redesign, so that more free faces are made available and charges are located more advantageously.

COST OF BLASTING

The primary concern of the quarry operator is to make a profit. To do this, costs must be kept to the minimum. Some costs, however, are interdependent, so that no single cost reduction may necessarily guarantee an over-all decrease in production expenses. It is the composite effect with which one must be

Table 9—Change in Powder Factor (Pf) With Variation of Hole Depth (H)

(9-hole single-row V-type through-cut, using Extra 60% dynamite with 2-in. $D.$ column loaded and drill pattern dimensions* constant for blasting limestone with SG of 2.69)

Avg. H (ft.)	Avg. PC (ft.)	Avg. L (ft.)	Total Expl. Used (lb.)	Yield (tons) Total	Pf (tons/lb.)
10	5	8	79	264	3.34
12	7	10	110	330	3.00
14	9	12	142	396	2.79
16	11	14	173	462	2.67
18	13	16	205	528	2.58
20	15	18	235	594	2.52
22	17	20	268	660	2.47
24	19	22	300	726	2.42

Note: *See Figure 17 for drill pattern specifications.

concerned. In this respect many different costs and their effects on one another must be considered, some of which include the following: drilling, primary blasting, secondary breakage, loading, haulage, crushing, screening, stockpiling and reclaiming, loading and weighing for delivery to customers, supervision and engineering, maintenance, equipment and materials purchases and replacements, insurance, depletion and depreciation allowances, sales and other administrative services, royalties, stripping expenses (including ground breaking and removal), and taxes. Of all costs or expenses, the first seven (and in some instances those for stripping) generally constitute the major portion of costs for quarry production.

The percentage of total production costs attributed to drilling and blasting may be as low as 10 percent or as high as 40 percent. The relative importance of primary and secondary breakage costs to loading, haulage, crushing, etc., will depend largely on the properties of the deposit, equipment and plant operating characteristics, and results achieved from the primary blasting.

Studies on quarry efficiency show that in most cases hourly production rates for well-blasted material are nearly double that achieved for poorly blasted rock. Similar results are obtained in the other types of mining and in heavy construction work. Crushing and screening costs are likewise appreciably reduced if the material is well blasted at the very beginning. Because of these effects the trend today is to spend more for primary blasting, because the savings realized from all the other production phases more than compensate for the initial added cost for blasting. This fact is evidenced by the lower powder factor yields obtained in a great many operations.

Primary blasting expense is normally considered to be composed of costs for both drilling and explosives, including all charges for labor and material used. Before the advent of the new high-speed highly mobile drills, the respective costs for drilling and blasting were about equal. But with the new types of drilling equipment, drilling costs of many operations are only half as much as the explosive with conventional high explosives.

Table 10—Blasting Cost Analysis, Showing Effects from Changing the Type of Explosive (V-type side-cut^(a) for vertical holes in a limestone ledge with constant P_f)

A Assumed Conditions:		B Unit Costs (a):		
(1) Kept constant are $K_r = 0.7$, $K_j = 0.3$, $K_s = 1.0$, $D_r =$ $D_H = 3$ in., $L = 20$ ft., and $d_r = 0.084$ ton/cu. ft. ^(b)		(1) Drilling at \$0.363/ft. ^(c)		
(2) $E_1 =$ Extra 60% dynamite with $SG = 1.28$ and $v_r = 12,200$ fps ^(c)		(2) Extra 60% at \$0.22/lb.		
(3) $E_2 =$ field-mixed AN-FO, 94/6, with $SG = 0.85$ and $v_r = 11,100$ fps ^(d)		(3) AN-FO, 94/6 at \$0.05/lb.		
(4) All holes drilled with 4½-in. hammer track-mounted air-drill with 500 cfm compressor at av- erage drilling rate of 400 ft. per 8-hour shift ^(e)		(4) 30-ft. MS delay EBC at \$0.62		
		(5) 6-ft. instant EBC at \$0.17		
		(6) Regular Primacord at \$0.32/ft.		
		(7) MS delay Primacord connector at \$0.50		
		(8) Cast booster (¼-lb. primer) at \$0.50		
C Blasting Data Calculations:				
<u>E_1 (Extra 60% dynamite)</u>		<u>E_2 (Field-mixed AN-FO, 94/6)</u>		
$RE_1 = (1.28)(12,200)^2 = 191 \times 10^6$		$RE_2 = (0.85)(11,100)^2 = 105 \times 10^6$		
If $K_{a1} = 30$, then $B_1 = 7½$ ft. for equivalent drill pattern of 10 x 10 ft. ^(f)		$RE_2/RE_1 = 105/191 = 0.55$, ^(g) or $K_{a2} = 24½$, ^(h)		
$T_1 = K_r B_1 = (0.7)(7.5) = 5$ ft.		Thus, $B_2 = 6$ ft. ⁽ⁱ⁾ for equivalent square drill pattern of 8 x 8½- ft. ^(j)		
$J_1 = K_j B_1 = (0.3)(7.5) = 2½$ ft.		$T_2 = K_r B_2 = (0.7)(6) = 4$ ft.		
$H_1 = L + J_1 = 20 + 2½ = 22½$ ft.		$J_2 = K_j B_2 = (0.3)(6) = 2$ ft.		
$PC_1 = H_1 - T_1 = 22½ - 5 = 17½$ ft.		$H_2 = L + J_2 = 20 + 2 = 22$ ft.		
Since the blast consists of 3 rows of 3 holes each, or $N_1 = 9$ holes, then		$PC_2 = H_2 - T_2 = 22 - 4 = 18$ ft.		
$W_1 = A \cdot L(d_r) = 10(10)(9)(20)$ (0.084) ^(k)		To drill a complete pattern there should be 4 rows of 4 holes each, or $N_2 = 16$ holes.		
or $W_1 = 1510$ tons		Thus, $W_2 = A \cdot L(d_r) = 8(8½)(16)$ (20)(0.084) ^(k)		
If $d_{r1} = 3.9$ lb./ft. ^(k) and		or $W_2 = 1830$ tons		
$E_1 = d_r(PC_1)N_1$, ^(l) then		If $d_{r2} = 2.6$ lb./ft. ^(k) and		
$E_1 = (3.9)(17½)(9) = 615$ lb.		$E_2 = d_r(PC_2)N_2$, ^(l) then		
Thus, if $P_f = W_1/E_1$, ^(m) then		$E_2 = (2.6)(18)(16) = 750$ lb.		
$P_f = 1510/615 = 2.46$ tons/lb.		Thus, if $P_f = W_2/E_2$, ^(m) then		
The total required drill footage, or		$P_f = 1830/750 = 2.44$ tons/lb.		
$H \cdot N_1 = (22½)(9) = 203$ ft.		The total required drill footage, or		
		$H \cdot N_2 = (22)(16) = 352$ ft.		
D Blasting Cost Comparison: (Calculated from B and C. above):				
Method of Initiation:	<u>E_1 (Extra 60% dynamite)</u>		<u>E_2 (Field-mixed AN-FO, 94/6)</u>	
	<u>Electric</u>	<u>Nonelectric</u>	<u>Electric</u>	<u>Nonelectric</u>
Drilling:	(203) \$ 73.69	(203) \$ 73.69	(352) \$127.78	(352) \$127.78
Explosives:				
Dynamite	(615#) 135.30	(615#) 135.30	—	—
AN-FO	—	—	(750#) 37.50	(750#) 37.50
Primers	—	—	(16) 8.00	(16) 8.00
Initiators:				
30' MS EBC.	(9) 5.58	—	(16) 8.12	—
6' Inst. EBC.	—	(2) 0.34	—	(2) 0.34
Primacord	—	(300') 9.60	—	(505') 16.16
Primacord MS connectors.	—	(9) 4.50	—	(16) 8.00
Misc.:				
Connecting wire	1.25	—	1.25	—
Labor for loading and firing blast	2.00	1.80	3.50	3.00
Total blasting cost:	\$217.82	\$225.23	\$186.15	\$200.78
Cost per ton:	0.144	0.149	0.102	0.109
E Percentage Distribution of Blasting Costs:				
Drilling	33.8	32.8	68.6	63.7
Explosives (Excl. primers)	62.2	60.1	20.1	18.7
Primers	—	—	4.3	4.0
Initiators	2.6	6.3	4.4	12.1
Misc.	1.4	0.8	2.6	1.5
Total	100.0	100.0	100.0	100.0

Special Notes—Table 10

- (a)—See Figure 17K for general drill pattern and initiation-timing system.
- (b)—Rf. Table 7.
- (c)—Rf. Table 1, p. 63, *Blasters' Handbook*, 14th edition. E. I. duPont de Nemours & Co.
- (d)—Rf. Figure 6, p. 8, Technical Bulletin AG-2, Nov., 1960, Monsanto Chemical Co.
- (e)—Rf. *A Field Man's Guide to Drilling Costs*, A. W. Foster, Atlas Chemical Industries, Inc.
- (f)—Rf. Table 2
- (g)—Rf. Formula (4)
- (h)—Rf. Formula (5)
- (i)—Rf. Formula (6) and Figure 14
- (j)—Rf. Formula (11)
- (k)—Rf. Formula (2) and Figure 12
- (l)—Rf. Formula (12)
- (m)—Rf. Formula (13)
- (n)—Explosive unit costs based on schedule 1960 prices

With the introduction of inexpensive AN blasting agents, however, the drilling-explosive cost ratio has been reversed. Even though the less dense blasting agents appreciably increase the cost of drilling because of the increased number of blast-holes required, the over-all drilling and blasting cost in most instances has been materially reduced. This is because of the tremendous savings in costs of explosives. Such blasting agents often cost only 20 to 30 percent as much as the conventional high explosives.

To illustrate the effect of the various components that determine primary drilling and blasting cost, Table 10 presents representative data for a typical quarry blast. Only the type of explosive has been changed, with the powder factor, drill-pattern general arrangement, and initiation-timing system kept the same. It should be noted from the data, however, that for conventional dynamite, i.e., Extra 60 percent, a typical 10- by 10-ft. pattern is used.

In order to use a regular AN-FO 94/6 blasting agent (field-mixed), the pattern dimensions are changed to an 8- by 8½-ft. arrangement. This is done according to the principles outlined earlier in the discussion on correlating the properties of explosives to the blasting standards. In this instance, the net result is that 16 blastholes are required for the AN-FO blast, compared to only nine holes for when Extra 60 percent is used. Because of the difference in the required true-burden dimension, other design dimensions necessarily must be adjusted to give a properly balanced blast. However, the basic K_T , K_B , K_S , and K_H ratios are kept closely to the same values for both blasts, only the K_a

ratios being adjusted to suit the various characteristics of the explosives.

From the costs indicated in Table 10, one would logically conclude that everyone should change to AN-FO blasting agents. However, it must be kept in mind that individual circumstances may greatly change the over-all cost relationships. The factors that have the greatest influence on the final values would be the unit costs for drilling and explosives materials used and the par-

ticular properties of the explosives themselves, since the latter decide the final required drill pattern dimensions, i.e., the K_B . Furthermore, some explosives simply would not be suitable for use under certain quarry operating conditions. One should, therefore, recognize that for making a cost analysis, the actual values for expenses and properties of materials peculiar to the local circumstances should be used, not general estimates, as was done for Table 10 data.

The influence of the properties of explosives on final costs cannot be overemphasized; this is true particularly of the velocity of the explosive, since it has a very prominent effect on the most desirable drill pattern. As described earlier, the manufacturer's specifications may not clearly define whether the velocity is for unconfined or confined blasting, nor which charge diameter applies. As one can see from Table 11, specifications vary considerably, a fact which in turn greatly affects estimates for designing blasts based on energy potential (RE) of the prod-

Table 11—A Comparison of Published Explosives Specifications
(For competitive grades equivalent to 60% ammonia dynamite when used with D=3 in. and based on published data)

	American(a) Ammonia Dyna- mite	Apache(b) Stand- ard Dyna- mite	Atlas(c) Extra Dyna- mite	Du Pont(d) Red Cross Extra	Hercu- les(e) Extra Dyna- mite	Olin(f) Spe- cial Dyna- mite	Trojan(g) Stand- ard Explo- sive
Velocity (fps)	10,800	12,800	10,600	12,200	12,450	13,600	12,600
Open (O) or confined (C):	Not given	(O)	(O)	Not given	(O)	Not given	(O)
Charge diameter (inches):	Not given	1¼	1¼	1¼	1¼	Not given	1¼
Stick count:	110	110	110	110	110	108	116
Specific gravity	1.28	1.28	1.28	1.28	1.28	1.30	1.22
RE factor (X10 ⁶)	149	210	128	191	198	241	193
Relative energy Ratio (RE _a /RE _b):(h) ..	0.78	1.10	0.67	1.00	1.04	1.26	1.01
Adjusted burden (B ₂ in feet):(i)	6.5	8.0	6.2	7.5	7.7	8.2	7.5
Equivalent drill Pattern (square):	8x9	10x11	8x8	10x10	10x11	11x11	10x10

References:

- (a)—p. 2, Ammonia Dynamites specification sheet, A-2141-300-4/61, American Cyanamid Co.
- (b)—p. 16, Apache Explosives catalog, third revision, Apache Powder Co.
- (c)—p. 21, Atlas Explosives Products, Catalog No. 13, 1957, Atlas Chemical Industries, Inc.
- (d)—p. 63, Table 1, *Blasters' Handbook*, 14th edition, 1958, E. I. du Pont de Nemours & Co.
- (e)—p. 4, Hercules Explosives, Blasting Agents and Blasting Supplies, catalog, 1959, Hercules Powder Co.
- (f)—p. 9, Olin Explosives Products catalog, fourth edition, 1955, Olin Mathieson Chemical Co.
- (g)—p. 4, Trojan Explosives and Blasting Supplies, Catalog No. 101, Trojan Powder Co.
- (h)—Relative energy ratios calculated on basis of Du Pont Red Cross Extra 60% as unity.
- (i)—Figures 7 and 14, with $K_B=30$ for Du Pont Red Cross Extra 60%.

uct. The suggested drill-pattern arrangements will not give the same powder factor yields but should produce comparable blast results, if the published specifications are not in error.

The expenses for primers and initiators may have a greater influence on final costs than one might expect, from the data indicated in Table 10. For blastholes with deck charges and those having extremely short depths, the costs for primers and initiators may constitute a considerable share of the over-all cost. Nevertheless, under such conditions the inherent savings resulting from higher powder factor yields usually compensate for the added costs. As experience has clearly shown, it is simply good practice always to use the best primers available. As a rule, the total required quantity of powerful high-energy primers is much smaller than that needed when cheaper low-energy explosives are used for priming. Initiator costs are also normally relatively low; so if improved blasting results can be insured by using additional initiators,

the added expense could be considered insignificant, as compared to the benefits received.

As powder factor yields are reduced, costs will be increased proportionately. But irrespective of the actual powder factor value, blasts should always be designed to give the yield most suitable for maximum production at the least expense. In this respect, the percentage of usable material from a blast must also be given consideration. Well-blasted rock does not mean it must necessarily be pulverized. On the contrary, the required particle sizing and its uniformity must be such that maximum recovery is achieved. If, for example, 10 percent of the production is lost due to spoiling or waste, which in quarrying is quite common, the loss must be included in the final cost analysis. If recovery is reduced in order to increase rates of production, the value of the wasted material should logically be less than the savings accomplished from the lower operating costs for the material salvaged.

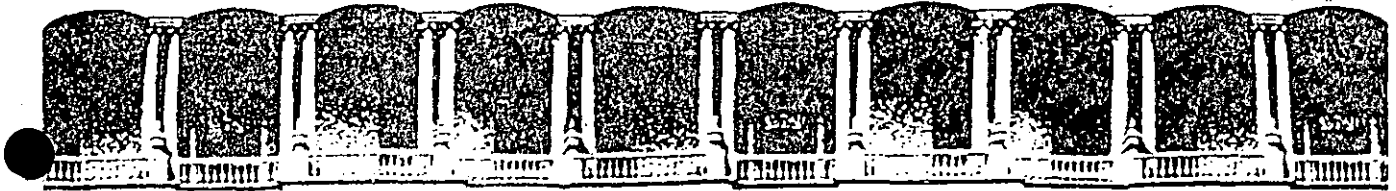
CONCLUSIONS

Effective blasting depends largely on a knowledge of how materials fracture, the particular characteristics of those materials, qualities of the various explosives that may be used, and recognition that the secret of efficient, economical, and safe results lies essentially in the suitable placement of charges where they will do the most good. Since explosives are merely very powerful tools for performing work, they should always be used accordingly.

As has been shown by these discussions, there are no easy, simple methods for solving blasting problems. The mechanisms and factors involved are too complex and numerous to permit clear-cut solutions. Each situation must be handled according to its own requirements, with the prudent use of one's best judgment. However, with a reasonable amount of study and understanding of operating conditions, blasters can evaluate results and make adjustments toward improvements by using certain basic standards. It has been the purpose of this article, therefore, to outline those standards and explain how they can be adjusted to apply to on-the-job conditions. But it must be realized that there can be no substitute for initial tests to ascertain what may be expected.

The burden dimension is the most critical of the important factors in blasting. Its value must suit the characteristics of the material being blasted and the properties of the explosives, and it must produce the desired degree of fragmentation and displacement. All other blasting standards are controlled by the burden value, and they should be designed on that basis. It should be, therefore, of primary concern to all blasters first to establish the best burden for their particular needs.

It has been shown that the powder factor as such has little meaning except as a relative basis for cost comparisons. For many years it has been used all too frequently, and unfortunately, as a means of judging blast efficiency. But under no circumstances can it be used as a reliable index for judging what one can expect in rock breakage or control of throw. Its value in costing is even questionable under many conditions.



**FACULTAD DE INGENIERIA U.N.A.M.
DIVISION DE EDUCACION CONTINUA**

CURSOS ABIERTOS

**IV. CURSO INTERNACIONAL DE INGENIERIA GEOLOGICA APLICADA A
OBRAS SUPERFICIALES Y SUBTERRANEAS**

CUARTO MODULO:

TECNOLOGIA SOBRE EL USO DE EXPLOSIVOS

Del 22 al 26 de junio de 1992

NOTES ON DETONATION PHYSICS

AUTOR: P.D. KATSABANIS

EXPOSITOR: ING. RAUL CUELLAR BORJA

JUNIO - 1992

NOTES ON DETONATION PHYSICS

by

P.D. Katsabanis

Department of Mining Engineering

Queen's University

Kingston, Ontario

Canada

K7L 3N6

Tel. # (613) 545 2197

© 1989

CHAPTER 1

THE DETONATION PROCESS

1.1 Introduction

According to Persson⁽¹⁾ steady state detonation along a cylindrical charge can be regarded as a self propagating process in which the axial compressive effect of the shock front discontinuity changes the state of the explosive so that exothermic reaction sets in with the requisite velocity.

This reaction in homogeneous liquid explosives such as nitroglycerin is completed in a time interval of the order of 10^{-12} seconds⁽¹⁾. In high explosives, such as RDX and PETN it is completed in about $1\mu\text{sec}$. In composite explosives containing AN the reaction times are considerably longer. The significance of this will be demonstrated later.

1.2 Shock waves

Compressional waves of small intensity are propagated in gases at the velocity of the sound. Let us suppose that a column of gas is set in motion by a piston which is accelerated into it. Let us also consider that the velocity of the piston is a staircase function of time. Each step transmits a small compressional wave which advances through the gas already set in forward motion and heated by the previous waves. Since the velocity of the wave is larger at elevated temperatures, the new wave overtakes the previous⁽²⁾. Therefore the velocity, pressure and temperature gradients in the front of the wave grow steeper

with time. If there is no dissipative mechanism (e.g. heat diffusion) the gradients become infinite⁽²⁾.

This type of wave, in which a discontinuity has developed is known as a shock wave. The area of pressure rise is called the shock front. The front advances with a speed higher than the sound speed. The shock velocity depends on the conditions behind. If the piston continues accelerating so does the front. If the piston maintains a constant velocity, the front maintains a constant velocity as well. If the piston decelerates a wave of rarefaction is formed ahead of it. Finally this wave overtakes and weakens the shock front.

It follows that the velocity of the front is determined by the conditions behind the front. The wave does not maintain itself. Rather it depends on the support provided by the piston.

1.3 Detonation waves

However from our experience we know that steady detonation waves exist. In this case the role of the piston is played by the reaction taking place in the detonation wave.

Let us consider a plane detonation wave which has been established in an explosive (Figure 1). The wave front advances into the unconsumed explosive with a constant velocity D and it is followed by the reaction zone. If an observer is moving with the velocity D of such a front, the wave will appear to him/her as in Figure 1. Undetonated explosive flows into the shock front AA' with constant velocity $U_0 = -D$. Its pressure, temperature and density and internal energy per unit mass are P_1, T_1, ρ_1, E_1 at all points to the right of AA' . The wave front is considered to

be a discontinuity in comparison to the changes occurring behind it. Therefore at AA' these values change to values P_2 , T_2 , ρ_2 , E_2 . These values change at some later stage.

The apparent velocity of the mass leaving the front is $(D-U_p)$ where U_p is the particle velocity (mass velocity) in the zone between AA', BB', relative to the fixed coordinates.

If we consider a region of flow surrounded by a tube of unit sectional area and two planes, one just before the detonation front and one right after it, the mass flowing in must equal the mass flowing out (conservation of mass). The mass flowing in per unit time is $\rho_1 D dt$. The mass flowing out is $\rho_2 (D-U_p) dt$. Therefore :

$$\rho_1 D = \rho_2 (D-U_p) \quad (1)$$

Furthermore the difference in momentum should be equal to the impulse of the net force. Thus:

$$\rho_1 D dt D - \rho_2 D dt (D-U_p) = (P_2 - P_1) dt$$

$$\text{or } P_2 - P_1 = \rho_1 D U_p \quad (2)$$

P_1 is very small compared to the detonation pressure.

Therefore it can be ignored and equation (2) can be written as :

$$P_2 = \rho_1 D U_p \quad (3)$$

From equation (1), one can obtain:

$$U_p = (1 - \rho_1/\rho_2) D \quad (4)$$

According to Cook⁽³⁾ U_p/D and ρ_1/ρ_2 are slowly variable functions of the original density. Thus:

$$U_p = f(\rho_1) D \quad (5)$$

where $f(\rho_1) = 1 - \frac{\rho_1}{\rho_2}$

Therefore equation (3) can be written as:

$$P_2 = \rho_1 f(\rho_1) D^2 \quad (6)$$

For most cases (explosives having a density between 0.9 -

1.4g/cc) it is sufficiently accurate to assume $f(\rho_1) = 4.0$. Under this approximation, the detonation pressure in atmospheres when the velocity of detonation is given in meters per second, is given by the following equation⁽⁸⁾:

$$P_2 = 0.00987 \rho D^2/4 \quad (7)$$

This is a relationship of great practical value. It allows the estimation of the detonation pressure when only the detonation velocity and the initial density are known. It is worth mentioning that the detonation velocity can be measured accurately in the laboratory.

Apart from equations (1) and (2) other equations are used in the theory of detonation. Many of these fall outside the area of interest of these notes. They are mentioned in the following to assist the reader in further studies.

The conservation of energy is expressed by the following equation:

$$E_2 - E_1 = \frac{1}{2} (P_2 + P_1)(V_2 - V_1) \quad (8)$$

This is known as the Rankine-Hugoniot equation.

A fourth equation is the equation of state of the reaction products of the explosive.

The above four basic equations are not enough to calculate the five unknown quantities behind the detonation front (energy, density, detonation velocity, pressure and particle velocity). A fifth condition is necessary. This is the Chapman-Jouguet hypothesis stating that the detonation velocity equals the local sound speed plus the particle velocity at the detonation state. Therefore:

$$D = C + U_p \quad (9)$$

Equations (1), (2), (8), (9) and the equation of state of the

detonation products are essential for the calculation of the detonation parameters in the thermohydrodynamic codes.

1.4 The Detonation Head Model (3,4)

Practical explosives are used normally in the form of cylindrical charges. Cook's detonation head model illustrates the sequence of events taking place. Figure 2 shows the detonation head formation in a cylindrical unconfined charge. With strong priming a detonation wave travels out from the primer and along the charge. This is responsible for the promotion of the necessary exothermic detonation reactions within the explosive charge. At the back of the primer the high pressure gases expand into the surrounding air. As this expansion takes place it permits a release wave or a rarefaction wave to travel down the charge behind the detonation front. This always lags the detonation front for reasons which were explained earlier. In a similar manner at the sides of the charge immediately after the detonation wave the gases expand into the atmosphere. Again two release waves are travelling into the charge. The detonation front, rear release wave and side release waves define a region called the detonation head. The detonation head is a region associated with high pressure and high density. The shape of the detonation head depends on the geometry of the charge and changes as it travels out from the initiation source. This is due to the approximately constant relationship between the release wave velocity and the detonation velocity. Initially the shape is that of a section of a truncated cone with curved front and rear surfaces. Further away from the initiation the length of the

detonation head grows so that it is controlled from the side release waves which meet on the axis of the charge forming a cone. It has been found (X ray radiography) that the length of the cone when the detonation is fully developed is approximately equal to the diameter of the charge. The density inside the detonation head is constant and approximately equal to $4/3 \rho_1$ where ρ_1 is the initial density of the explosive. The distance from the initiator to the point where the full head is formed is approximately equal to $3 \frac{1}{2}$ charge diameters for unconfined charges. As the explosive enters the detonation head it reacts. If it is in a granular form (e.g ANFO prills) the reaction starts at the surface and proceeds radially towards the centre of the prill. As it was mentioned in the previous the energy liberated supports the detonation. If the reaction is not completed inside the head the energy liberated is less than the maximum available and the detonation velocity is less than the maximum. This is what is normally known as non-ideal detonation. It is worth mentioning that non ideal detonations can be stable; indeed a great number of commercial explosives used by the mining industry today detonate at non ideal velocities at the diameters at which they are used.

The detonation velocity is the most important parameter of the detonating explosive. It is well known that the velocity of detonation is a constant characteristic of a particular explosive when the other parameters are kept constant. It was explained that the knowledge of the detonation velocity can lead to fairly accurate estimates of the detonation pressure which is of particular importance and cannot be measured directly. In the next chapter the parameters influencing the detonation velocity will be discussed.

1.5 References

1. Johansson, C.H. and Persson, P.A.: "Detonics of High Explosives", Academic Press, London, New York, 1970.
2. Taylor, J.: "Detonation in Condensed Explosives", Oxford at the Clarendon Press, 1952.
3. Cook, M.A.: "The Science of High Explosives", Reinhold Book Corporation, New York, 1958.
4. Bauer, A.: "Explosives Technology Notes", Queen's University, Kingston, 1981.
5. Zerilli, F.: "Notes from Lectures on Detonation Physics", Naval Surface Weapons Center, Silver Spring, Maryland, 1981.

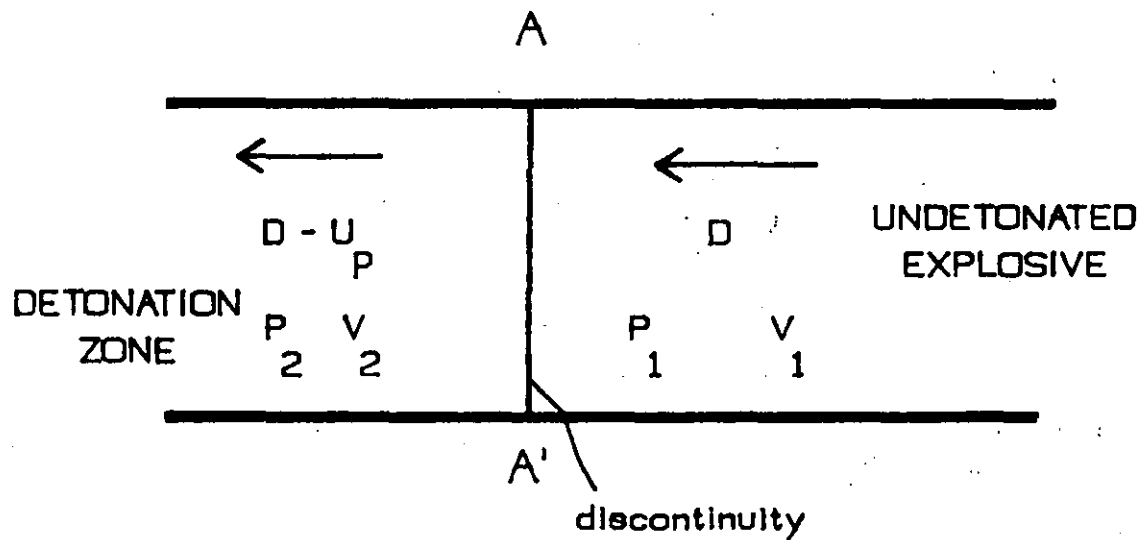


FIGURE 1: SECTIONAL DIAGRAM OF A DETONATION WAVE

Observer moves to right at wave velocity D .

The discontinuity is at rest

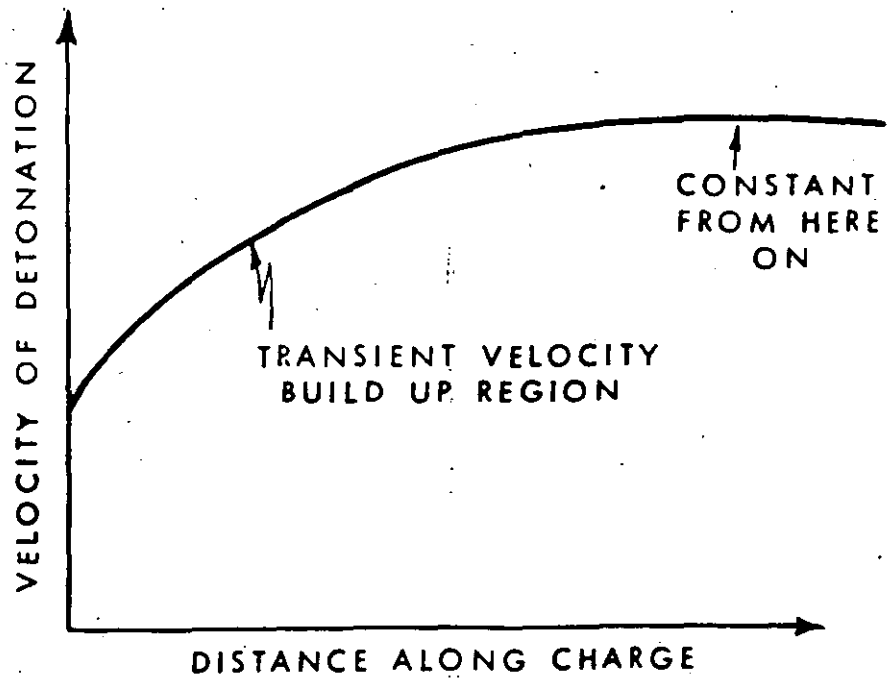
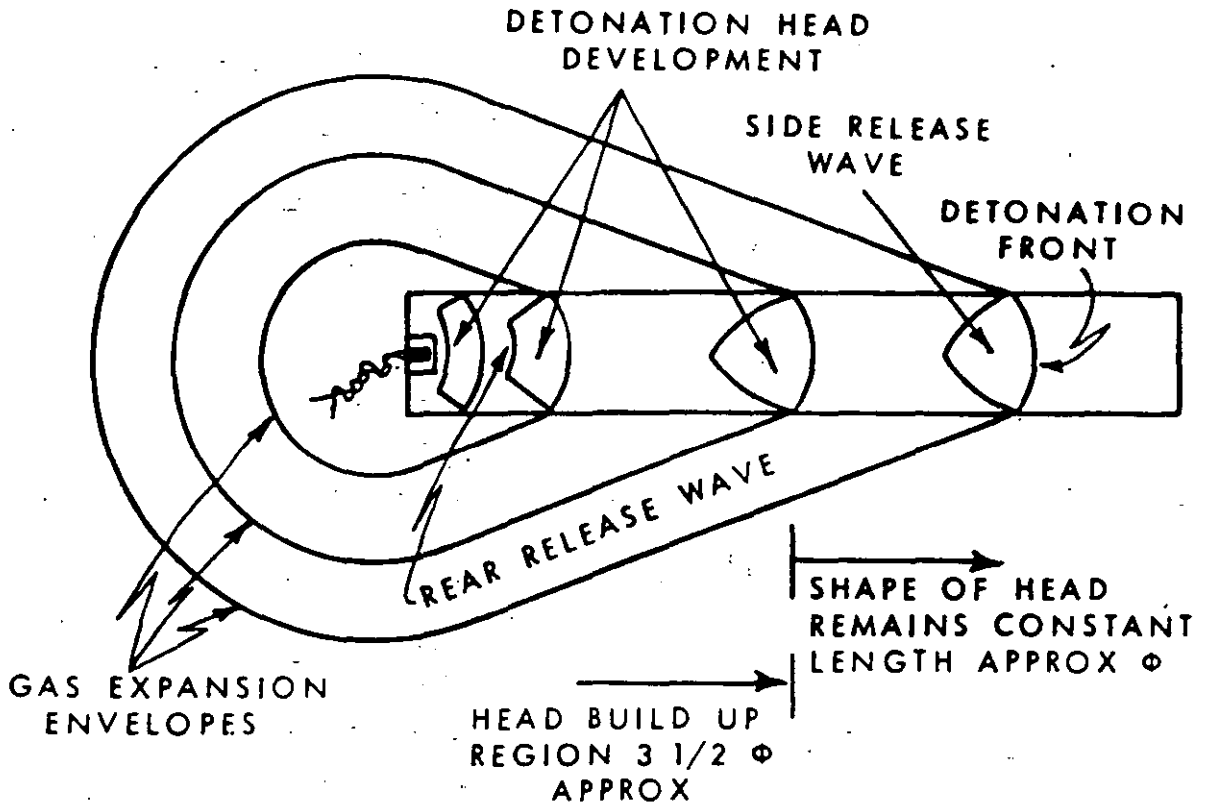


FIGURE 2: DETONATION HEAD FORMATION
(AFTER COOK AND BAUER)

EQUATIONS OF STATE

An equation of state is normally a pressure - volume - temperature relationship. Ideal gases have an equation of state expressed as:

$$PV = nRT$$

where P is the pressure
 T is the temperature
 n is the number of moles of gas
 R is the universal gas constant and
 V is the volume.

However real gases do not always behave according to the previous equation. It is obvious that a real gas cannot be cooled to zero volume. Under certain conditions gases turn into liquids or solids.

The origin of the deviations from ideality is the interaction between particles. Molecules exercise attractive forces when they are separated by some distance and repulsive forces when they are very close together.

Repulsive forces are short term interactions while attractive forces have a relatively long range. Figure 1 provides a plot of the compression factor $Z = PV/RT$ against pressure applied on the gas. One can obtain an indication of the imperfection at different pressures. For a perfect gas $Z = 1$ under all conditions. For a real gas the case is somewhat different. At very low pressures all gases behave almost ideally ($Z = 1$). At high pressures the repulsive forces dominate and $Z > 1$, while at moderate pressures $Z < 1$ due to the attractive forces. Obviously an equation of state for the detonation products has to reproduce this behaviour of real gases.

EQUATIONS OF STATE FOR DETONATION PRODUCTS.

The equations of state used for detonation calculations are of two types: those which do not treat chemistry explicitly and those which do. The latter contain individual equations of state for the component molecules and a mixture rule for combining them to give an equation of state for any composition. The composition of the detonation products is calculated by assuming chemical equilibrium.

At this point it is worth mentioning that much of the work involving the development of an equation of state has been employed in an inverted form. Experimental values are used to calibrate an assumed form of an equation of state. Attempts to develop a general, completely theoretical equation of state have failed to produce a good result.

The most common equations of state for detonation products are:

1. The Abel Equation of State.

The Abel equation of state is a form of the Van der Waal's equation of state. It can be expressed as:

$$P(V-\alpha) = nRT$$

where α is a constant.

It was found that this form did not produce acceptable results for many cases of condensed explosives. Cook⁽¹⁾ provided a modification expressing α as a function of the volume of the

detonation products without considering their chemical composition. He showed that the empirical values of the covolume fall in a common $\omega(V)$ curve.

2. The Becker - Kistiakowsky - Wilson Equation of State.

The most popular equation of state is the BKW equation. The equation has the following form:

$$\frac{PV}{RT} = 1 + xe^{E-x}$$

where $x = \frac{K}{V(T+\theta)^\alpha}$

and $K = \sum k_i x_i$

with α, E, K, θ and k_i empirical constants. The constants k_i of each molecular species are the covolumes. For the mixture each k_i is multiplied by x_i , the mole fraction of species 1, and summed to find the effective covolume.

According to a parameter study performed by the Los Alamos Laboratory, one may adjust the BKW parameters α, E, K and θ and the covolumes of the detonation products. Cowan and Fickett² have shown that for a given α and E one may adjust K to obtain the experimental velocity of detonation. The slope of the curve relating detonation velocity and density can be changed by changing E .

By using one explosive as a standard it was possible to obtain a set of parameters which can be used for a variety of explosives. BKW has been calibrated for RDX and TNT. The most common parameters used today are shown in Table 1^(3,4). It has been found that the RDX parameters result in realistic values of the detonation parameters (pressure and velocity of detonation). The parameters which have been developed based on TNT as the standard produce reliable results for very oxygen deficient systems which produce large amounts of carbon in the detonation products.

The best fit for RDX parameters should not be used in predictions of the detonation state parameters. This set was developed in order to have $(dP/dT)_V > 0$ at pressures of the order of 0.5 Mbar. It has been found that this set of parameters results in poorer predictions than the RDX set.

3. Other Equations of State

Other equations of state have been developed by Fickett and by Jacobs, Cowperthwaite and Zwisler⁽⁴⁾.

These equations are similar and they are based on statistical mechanics. They use the Lennard-Jones potentials to describe the interactions between the molecules. The general form of the intermolecular potential energy is shown in Figure 2. When the molecules are squeezed together, the nuclear and electronic repulsions dominate the attractive forces. The repulsions increase steeply with decreasing separations. One approximation is the hard sphere potential where it is assumed that the potential energy rises abruptly to infinity as soon as the

particles come within some separation distance σ (collision diameter).

Normally the intermolecular potential is written as:

$$V = C_n/R^n - C_6/R^6$$

This is the Lennard-Jones (n,6) potential. Often the (12,6) potential is written in the form:

$$V = 4\varepsilon[(\sigma/R)^{12} - (\sigma/R)^6]$$

where ε is the depth of the potential well and

σ is the separation distance at which $V=0$.

REFERENCES

1. Cook, M.A.: "The Science of High Explosives", Reinhold Book Corporation, New York, 1958.
2. Mader, C.: "Detonation Properties of Condensed Explosives Computed Using the Becker-Kistiakowsky-Wilson Equation of State", Los Alamos Scientific Laboratory, LA-2900, 1963.
3. Mader, C.: "Numerical Modelling of Detonation", University of California Press, 1981.
4. Cowperthwaite M. and Zwisler, W.H.: "Tiger Program Documentation", Stanford Research Institute, 1974.
5. Atkins, P.W.: "Physical Chemistry", W.H. Freeman and Company, 1986.

FIGURE 1: COMPRESSION FACTOR VS PRESSURE

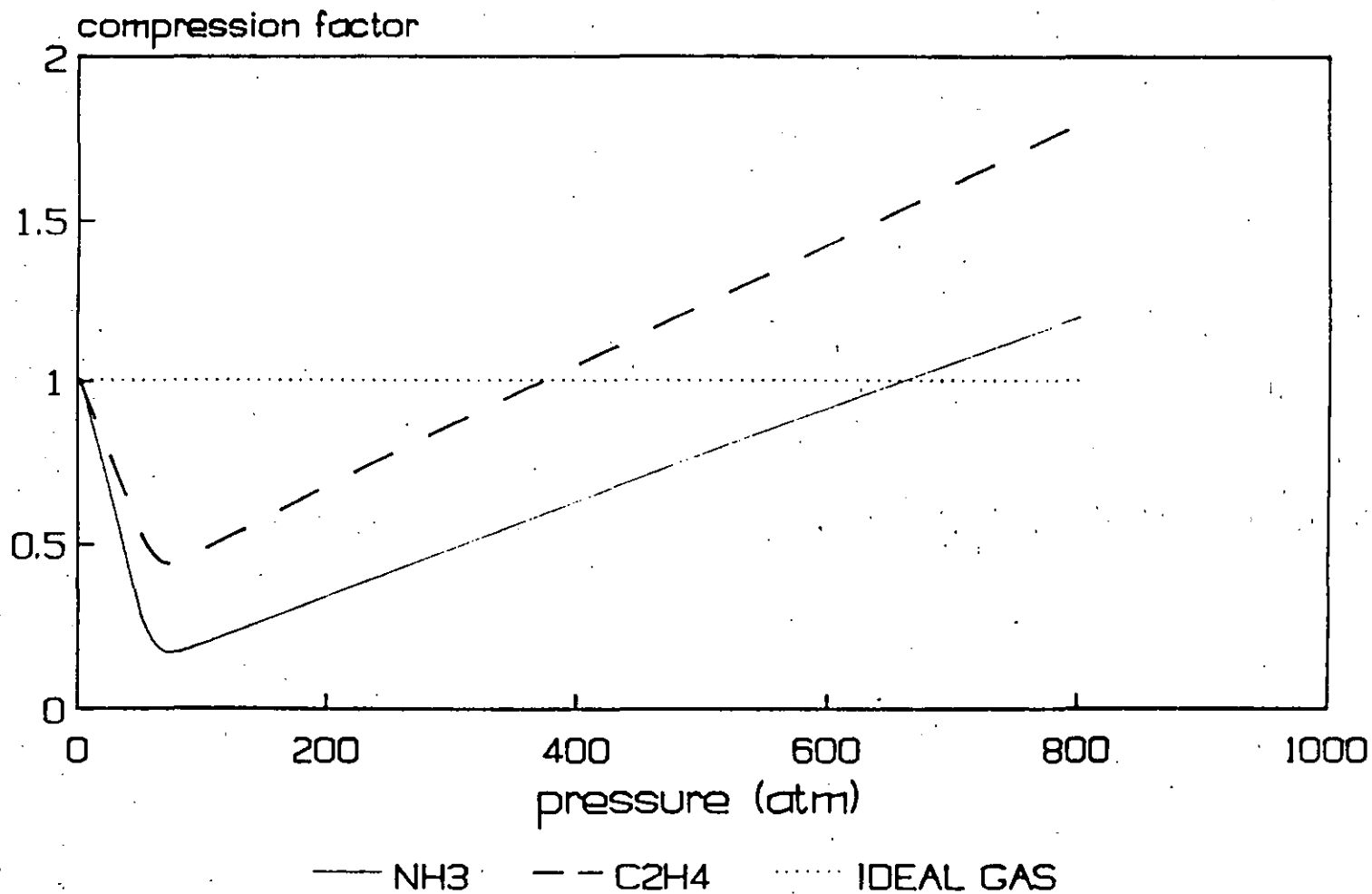


FIGURE 2: POTENTIAL ENERGY BETWEEN MOLECULES

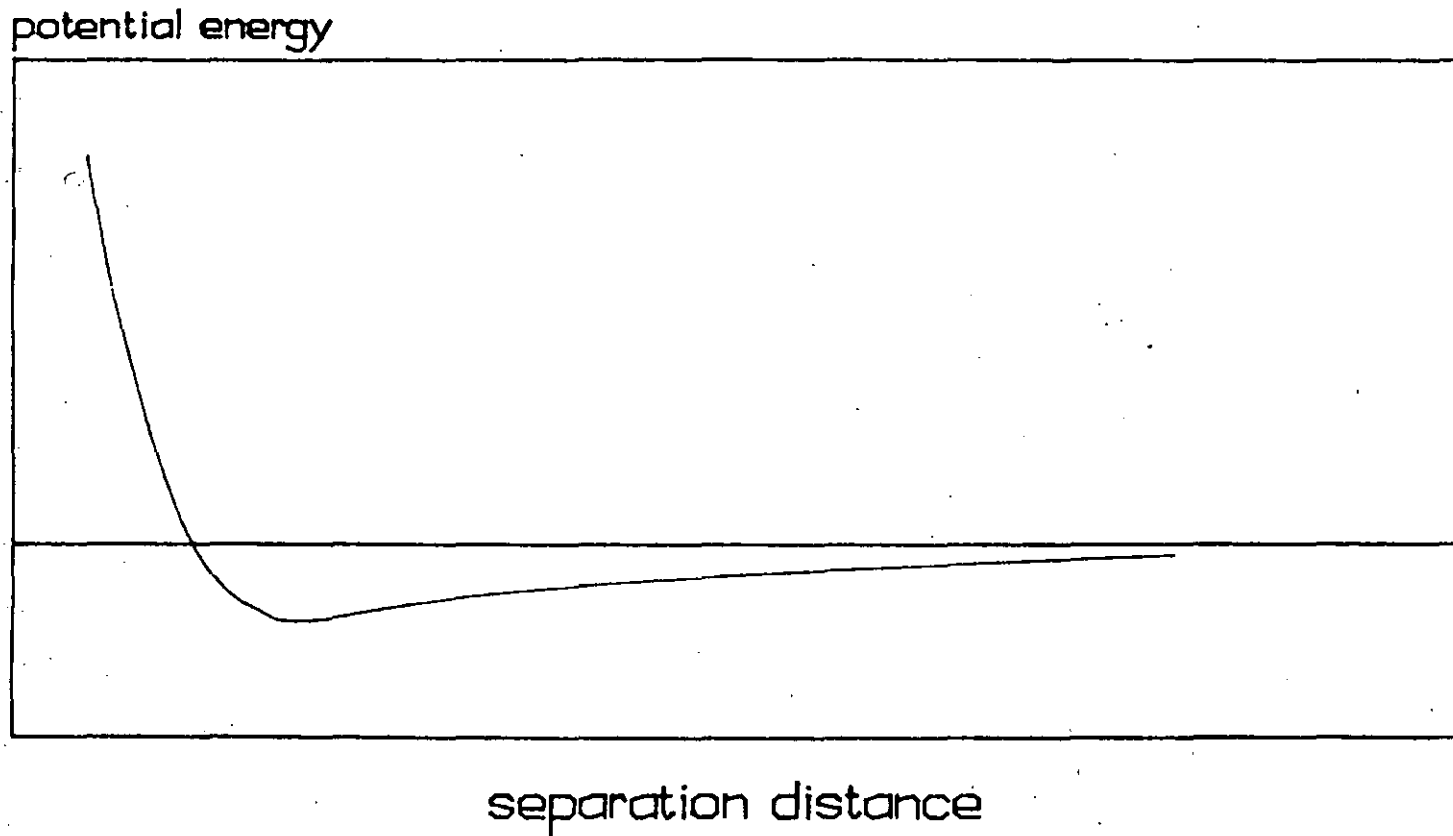


TABLE 1

COMMONLY USED BKW PARAMETERS FOR HIGH DENSITY
EXPLOSIVES

NO.	PARAMETER SET	β	κ	α	θ
1	Fitting RDX	0.181	14.15	0.54	400
2	Fitting TNT	0.09585	12.685	0.50	400
3	Best fit for RDX with $(\partial P / \partial T)_v > 0$	0.16	10.91	0.50	400
4	Default parameters	0.10	11.85	0.50	400

CHAPTER 3

EXPLOSIVE PROPERTIES

3.1 Introduction

A variety of factors influence the explosives selection process. This chapter discusses the most important of them and the parameters which influence them.

3.2 Velocity of Detonation

The velocity of detonation is the velocity at which the detonation wave travels through an explosive charge. The detonation wave travels at speeds above the normal sound speed of the unreacted material. Typical detonation velocities for commercial explosives range from 2500 to 7000 m/sec. The detonation velocity is the most important property of the explosive. It can be measured easily and accurately and it can be used for the calculation of the detonation and borehole pressures which are of importance in explosive applications. The velocity of detonation of a particular explosive depends on factors such as charge diameter, confinement, density and particle size.

3.1.1 The effect of charge Diameter

Let us consider a typical velocity of detonation - diameter curve as shown in Figure 1⁽²⁾. If the diameter is too small the explosive fails to detonate. At some minimum diameter stable detonation occurs. This minimum diameter is called the critical diameter of the explosive.

As the charge diameter is increased the detonation velocity

is increased as well. However when a certain diameter is reached, further increase in diameter does not result in an increase of the detonation velocity. At this point a maximum detonation velocity of the explosive is reached. This velocity is called the ideal detonation velocity of the explosive and is the value predicted by thermohydrodynamic codes.

The detonation head model as developed by Cook⁽¹⁾ can be useful in explaining the shape of the observed detonation velocity - diameter curves. Figure 1 illustrates the length of the established detonation heads in charges of various diameters and indicates what happens when a solid particle of explosive enters the detonation head. For the small diameters, the degree of reaction is small and the energy liberated is not enough to support a detonation. As the diameter is increased the detonation head length is increased and for the same size of particle the degree of reaction increases. At the critical diameter the degree of reaction is sufficient to support stable detonation. If the diameter is increased further a larger amount of explosive reacts in the detonation head. When the ideal detonation occurs, the full amount of explosive reacts in the detonation head.

3.2.2 Effect of Confinement

The effect of confinement is to lower the rate of expansion of the gases off the side of the charge⁽²⁾. This in turn slows down the rate at which the lateral rarefaction travels into the reaction region. As a result it takes longer for the side release waves to meet on the charge axis. The length of the detonation head is thus increased. This is shown in Figure 2⁽¹⁾, where the development of the detonation head is outlined for both the

confined and the unconfined cases. Therefore, if the explosive was not reacting fully at a particular charge diameter, the effect of confinement would be to increase the degree of reaction and consequently the detonation velocity at this diameter. Similarly, confinement will reduce the critical charge diameter (Figure 3)⁽²⁾.

However confinement cannot be quantified. Steel, glass, various kinds of rock and soil will produce a different effect. For this reason most of the tests are done with the explosive charge unconfined.

3.2.3 Effect of Particle Size

If the size of the explosive particles is reduced at a given charge diameter in the non ideal velocity region, the degree of reaction is enhanced because of the increase of the surface area. Furthermore since the grains are smaller, they are consumed faster in the detonation head. As a result the critical diameter is decreased and the explosive reaches ideal detonation at a smaller diameter (Figure 4)⁽²⁾.

3.2.4 Effect of Density

If the density is increased, the specific energy is increased; as a result the ideal detonation velocity is increased. It has been found that the detonation velocity and the density are related linearly. Figure 5⁽³⁾ shows the detonation velocity density relationship for various explosives.

However if the density is increased beyond a critical point, steady state detonation is not possible. The phenomenon is called dead packing and a qualitative explanation can be given by the

fact that the volume of the entrapped air is insufficient to provide enough hot spots for the reaction to proceed⁽²⁾.

The relationship between critical diameter and density is shown in Figure 6⁽⁵⁾. It is obvious that apart from the density in which the material is dead packed there is a critical density below which the explosive will not shoot.

3.2.5 Effect of Temperature

The initial temperature of the explosive has a small influence on the velocity of detonation at diameters well above the critical. However the critical diameter is dependant on the initial temperature. Figure 7 shows the effect of the temperature on the critical diameter powdered TNT⁽⁴⁾.

In the case of commercial liquid explosives the effect is more pronounced. Figure 8 shows the effect of low temperatures on the critical diameter of typical slurry explosives⁽⁵⁾. The effect on solid explosives is almost negligible.

3.2.6 Effect of Water

Generally dynamites are not affected by the presence of water inside boreholes. Ammonium nitrate mixed with fuel oil has no water resistance. The product absorbs water and soon becomes desensitized. Generally performance drops drastically as the weight of water in the composition is increased.

3.3 Detonation Pressure

The detonation pressure is a very important parameter. It is an indicator of the ability of the explosive to produce the

A. Permitted explosives (USBM)

Fume class	Toxic Gas ft ³ /lb	Toxic Gas l/kg
A	< 1.25	< 78
B	1.25 - 2.50	78 - 156
C	2.50 - 3.75	156 - 234

B. Rock blasting explosives

Fume class	Toxic Gas ft ³ /lb	Toxic Gas l/kg
1	< 0.16	10
2	0.16 - 0.33	10 - 21
3	0.33 - 0.67	21 - 42

Canada uses the same standards. However explosives of class 2 or 3 cannot be used in underground mines unless special application has been made to and permission is received from the authorities (EMR).

It is worth mentioning here that the relative toxicity of the fumes is important and this is not shown in the above tables. NO₂ is much more toxic than CO (about 6 times as much)⁽⁸⁾.

It has been found that the fumes depend on⁽²⁾:

1. The oxygen balance
2. Marginal priming
3. Water attack
4. Critical diameter
5. Gaps in loading
6. Deflagrations.

3.6 Energy of Explosives

Explosives are substances that rapidly liberate their chemical energy as heat to form gaseous and solid decomposition products at high temperature and pressure. The hot and dense detonation products produce shock waves in the surrounding medium and upon expansion impart kinetic energy to the surrounding medium. The energy released in the detonation process is given by the following formula:

$$Q = \Delta H_f(\text{products}) - \Delta H_f(\text{reactants})$$

where ΔH_f is the heat of formation.

The energy per unit weight is called the weight strength of the explosive.

The energy per unit volume is called the bulk strength of the explosive.

Sometimes it is useful to express the weight and the bulk strengths as relative values obtained by dividing the strength (weight or bulk) to the corresponding strength of a standard explosive. The commercial industry normally uses AN/FO as the standard explosive.

3.7 Shelf Life

The shelf life of an explosive determines the maximum time period the explosive can be in storage. Various explosives age and their use is unsafe or they cannot be detonated reliably.

3.8 Pressure Desensitization

Commercial explosives can be susceptible to hydrostatic

heads. Hydrostatic heads can compress the explosive to high densities and "dead packing" can result.

3.9 Measurement of the Detonation Properties

3.9.1 Detonation Velocity

There are various methods of measuring detonation velocities. These are outlined in the following:

i. The continuous probe method.

The system consists of the explosive charge, along the central axis of which a uniform resistance probe is inserted, a constant current source, a triggering source and an oscilloscope.

The resistance probe consists of a resistance wire inserted into a small diameter brass tube. The resistance wire is a nichrome wire having an accurately known linear resistance.

The oscilloscope is connected in parallel to both the current source and the probe (Figure 9)⁽⁵⁾. At detonation the wire resistance probe is consumed. However the circuit remains closed due to the fact that the detonation wave is sufficiently ionized. The circuit follows Ohm's law. Therefore, since current is constant, the voltage change with time shown on the oscilloscope, is proportional to the resistance. Knowing the full voltage drop across the probe and the length of the probe, the voltage drop can be converted to distance along the charge. Therefore the velocity of detonation can be calculated by interpreting the voltage drop - time record provided by the oscilloscope.

ii. Start-stop method

Two probes are placed at a known distance apart in the explosive. Each probe consists of two wires placed in close proximity. When the detonation wave contacts each probe it shortens the circuit by bringing the two wires in contact. By measuring the signals obtained by either a counter or an oscilloscope one can measure the detonation velocity.

iii. Streak camera method

The method is shown in Figure 10⁽⁹⁾. The streak camera uses a mirror which rotates at the centre of the drum. The film is placed on the drum. The field of view of the camera lens is masked except for a narrow slit. The charge is aligned so that its axis is parallel to the slit of the camera. The light generated by the detonation front enters through the slit and after being reflected on the rotating mirror, leaves a mark on the film. Thus the streak camera trace is essentially a time distance record. The slope of the trace made by the luminous wave provides the velocity of detonation. A typical streak camera record is shown in Figure 11⁽¹⁰⁾.

iv. D'Autriche Method

This is the least sophisticated method. It is outlined in Figure 12⁽⁹⁾. The method uses a detonating cord both ends of which are inserted in the explosive at a known distance apart. A metal witness plate is placed close to the middle of the detonating cord. The detonation wave in the charge initiates the detonating cord at both ends. When the detonation waves travelling in opposite directions in the detonating cord collide,

they leave a dent in the witness plate. This helps to find the position in the detonating cord at which the collision took place. Thus, the distance, and therefore the time, each wave travelled in the detonating cord can be found. The difference in the times the two waves travelled in the cord provides the time it took the detonation wave in the test charge to travel the distance l .

3.9.2 Detonation Pressure

The measurement of the detonation pressure is normally based on photographic techniques. These techniques require a streak camera and accurate experiments (aquarium technique). In the aquarium technique, a transparent liquid serves as a pressure gauge for measuring transient pressures. The transparent liquid has to be selected in such a way that the reflected wave at the gauge-liquid interface is either a weak shock or a very weak rarefaction. The technique, as described by Cook⁽⁸⁾ consists of the following two stages:

- i. Initially the Hugoniot of the liquid which serves as a gauge is determined. The experimental set up is shown in Figure 13. The method consists of the simultaneous measurement of the shock velocity at the free surface and the free surface velocity as the shock emerges from the transparent medium. Observations of the shock velocity and the free surface velocity are made by using a streak camera. By changing the height (h) of the liquid inside the container, one changes the shock velocity and the free surface velocity. By assuming that the particle velocity of the liquid at the interface is half of the free surface velocity the relationship between shock velocity and the particle velocity in the liquid (Hugoniot) is obtained.

ii. The experimental set up for the second part of the technique is shown in Figure 14. In this experiment, the velocity of detonation in the explosive charge and the initial transmitted shock velocity in the liquid are measured. From the transmitted shock velocity in the liquid and the known Hugoniot of the liquid, the initial pressure in the liquid can be calculated. The corresponding pressure in the detonation head is calculated by using the following relationship:

$$P_d = P_{il} [(\rho U_s)_{il} + \rho_{ie} U_{se}] / (2(\rho U_s)_{il})$$

where

P_d is the detonation velocity

ρ_{ie} is the initial density of the explosive

U_{se} is the detonation velocity

$(\rho U_s)_{il}$ is the initial impedance of the liquid and

P_{il} is the initial pressure in the liquid.

The initial pressure in the liquid is calculated by the well known relationship

$$P_{il} = \rho_1 U_{sl} U_{pl}$$

where P_{il} is the pressure in the liquid

U_{sl} is the shock velocity

U_{pl} is the particle velocity and

ρ_1 is the initial density of the liquid.

Because of the difficulty in measuring detonation pressures it is often necessary to calculate the detonation pressure from the detonation velocity by using the approximate formula:

$$P = \frac{\rho D^2}{4}$$

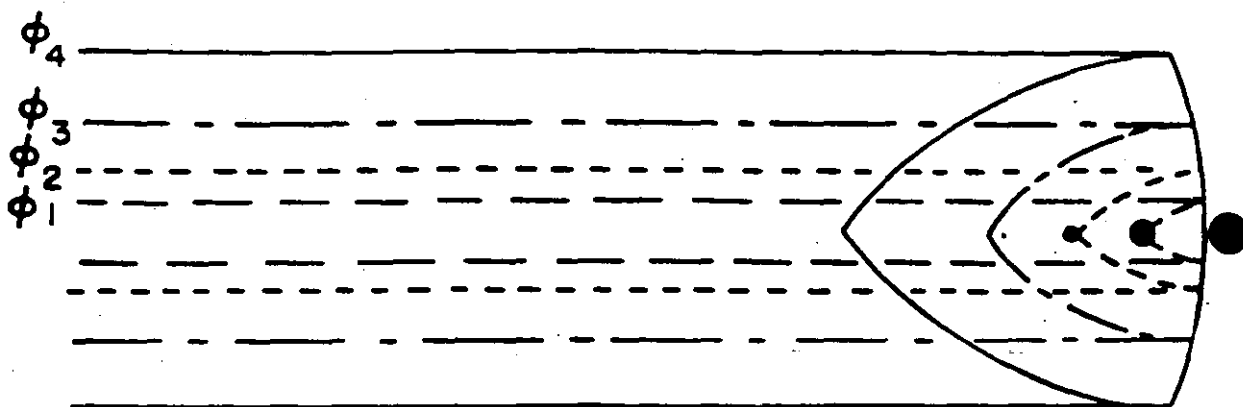
where P is the detonation pressure

ρ is the initial density of the explosive and

D is the measured detonation velocity.

3.10 References

1. Cook, M.A.: "The Science of High Explosives", Reinhold Book Corporation, New York, 1958.
2. Bauer, A.: "Explosives Technology Notes", Queen's University, Kingston, 1981.
3. Mader, C.: "LASL Explosives Property Data", Los Alamos Scientific Laboratory, University of California Press, 1981.
4. Johansson, C.H. and Persson, P.A.: "Detonics of High Explosives", Academic Press, London, New York, 1970.
5. Katsabanis, P.D.: "A Comparative Study of Emulsion and Slurry Explosives", M.Sc. Thesis, Queen's University, 1983.
6. Mader, C.: "Numerical Modelling on Detonation", University of California Press, 1981.
7. Meyer, R.: "Explosives", Verlag Chemie, Weinheim, New York, 1977.
8. Cook, M.A.: "The Science of Industrial Explosives", IRECO Chemicals, Salt Lake City, Utah, 1974.
9. Engineering Design Handbook, Principles of Explosives Behaviour, Headquarters, US Army Materiel Command, AMCP 706-180, 1972
10. Katsabanis, P.D.: "Studies on the Numerical Modelling of Explosives Performance and Sensitivity", Ph.D. Thesis, Dept. of Mining Engineering, Queen's University, 1987.
11. Atlas Powder Company : "Explosives and Rock Blasting", 1987.



DETONATION HEAD IN UNCONFINED CHARGES OF INCREASING DIAMETER AND THE REACTION OF A SOLID PARTICLE OF EXPLOSIVE

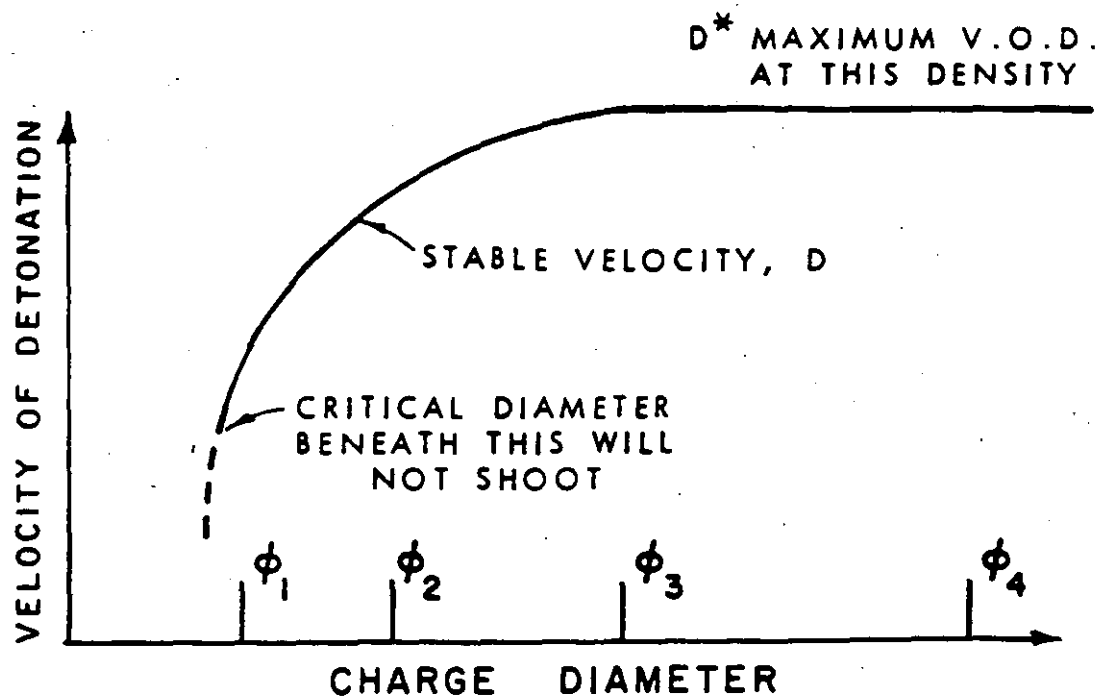


FIGURE 1: TYPICAL VELOCITY OF DETONATION CHARGE DIAMETER CURVE FOR A GRANULAR EXPLOSIVE (AFTER BAUER)

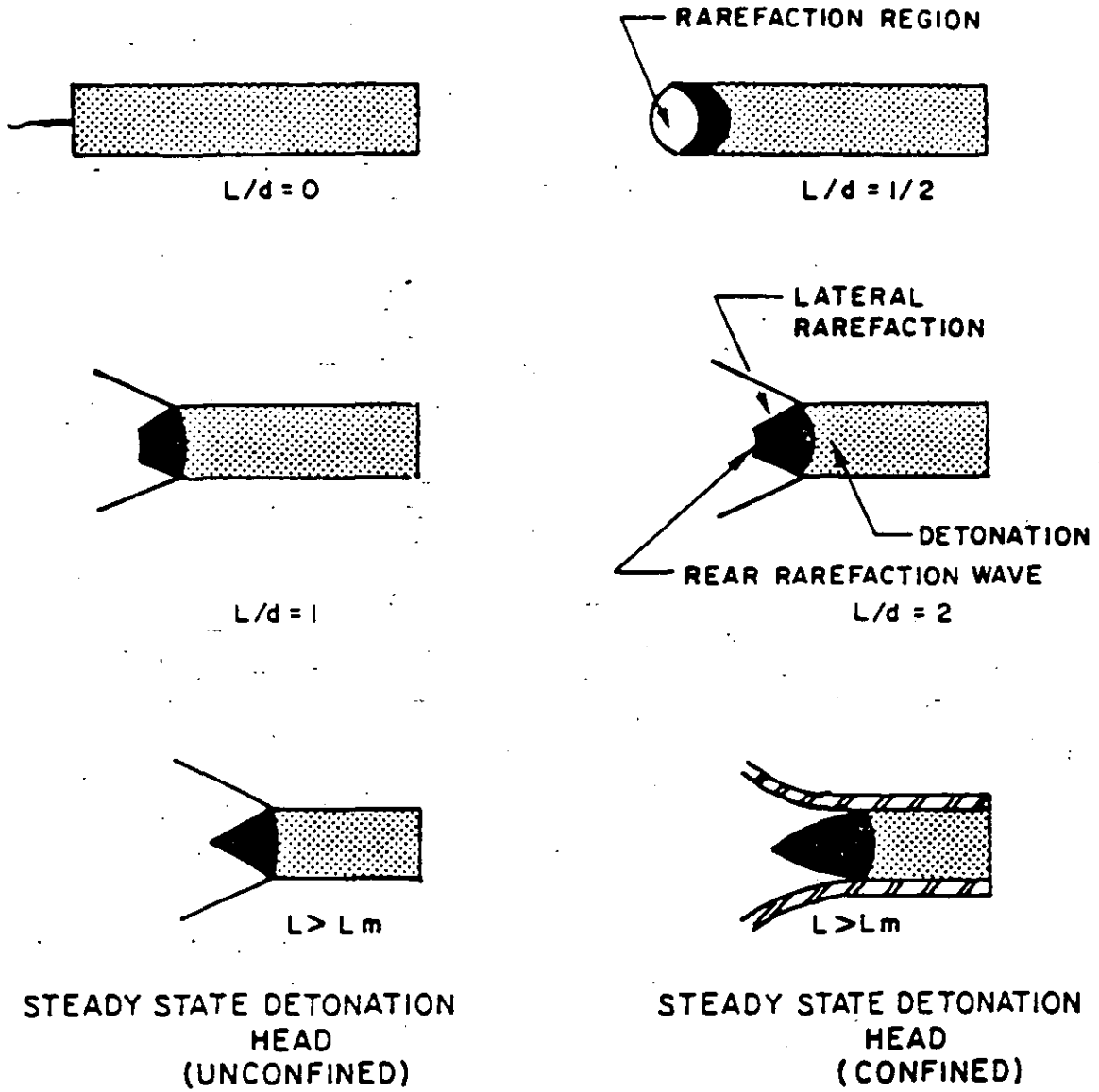
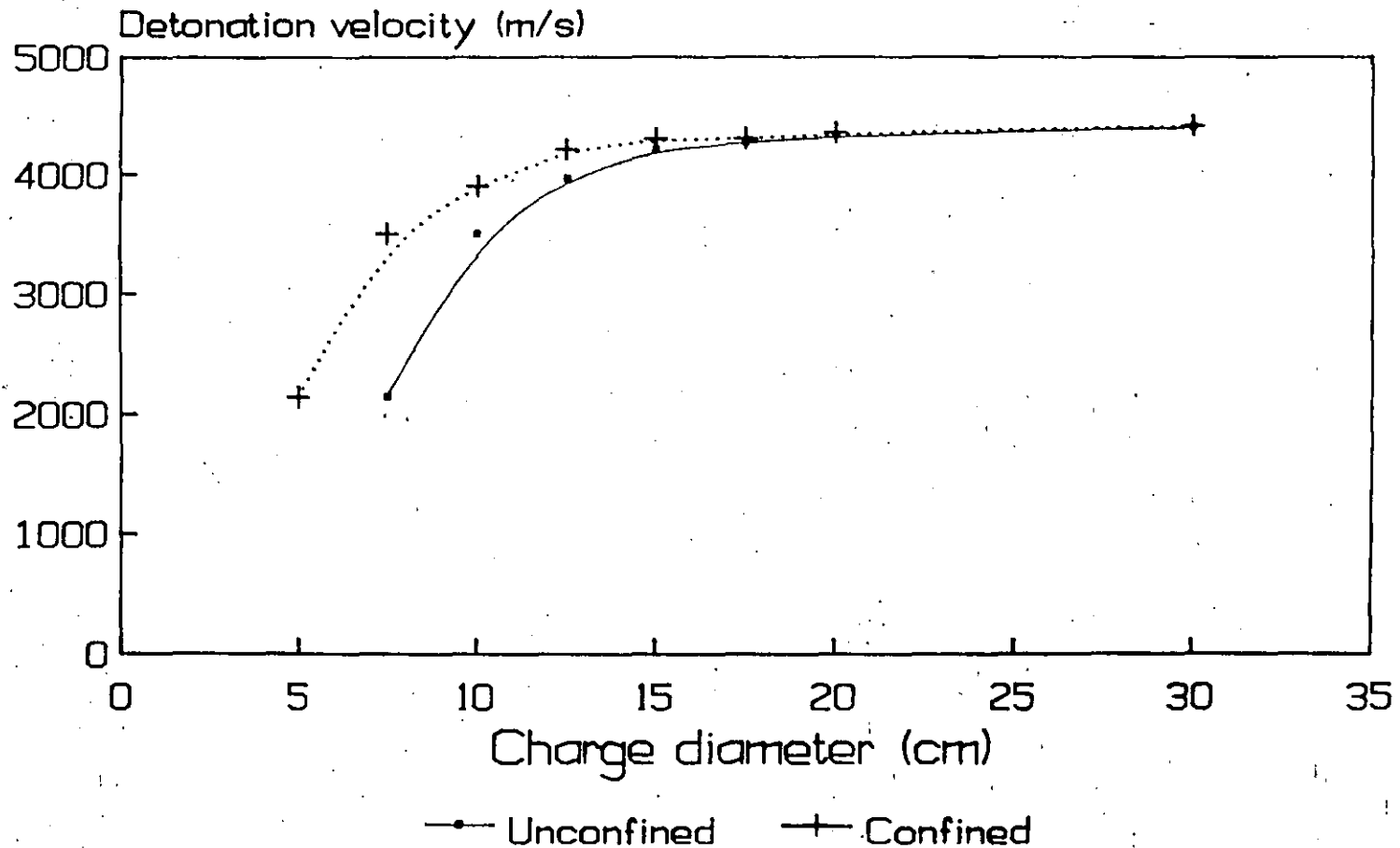


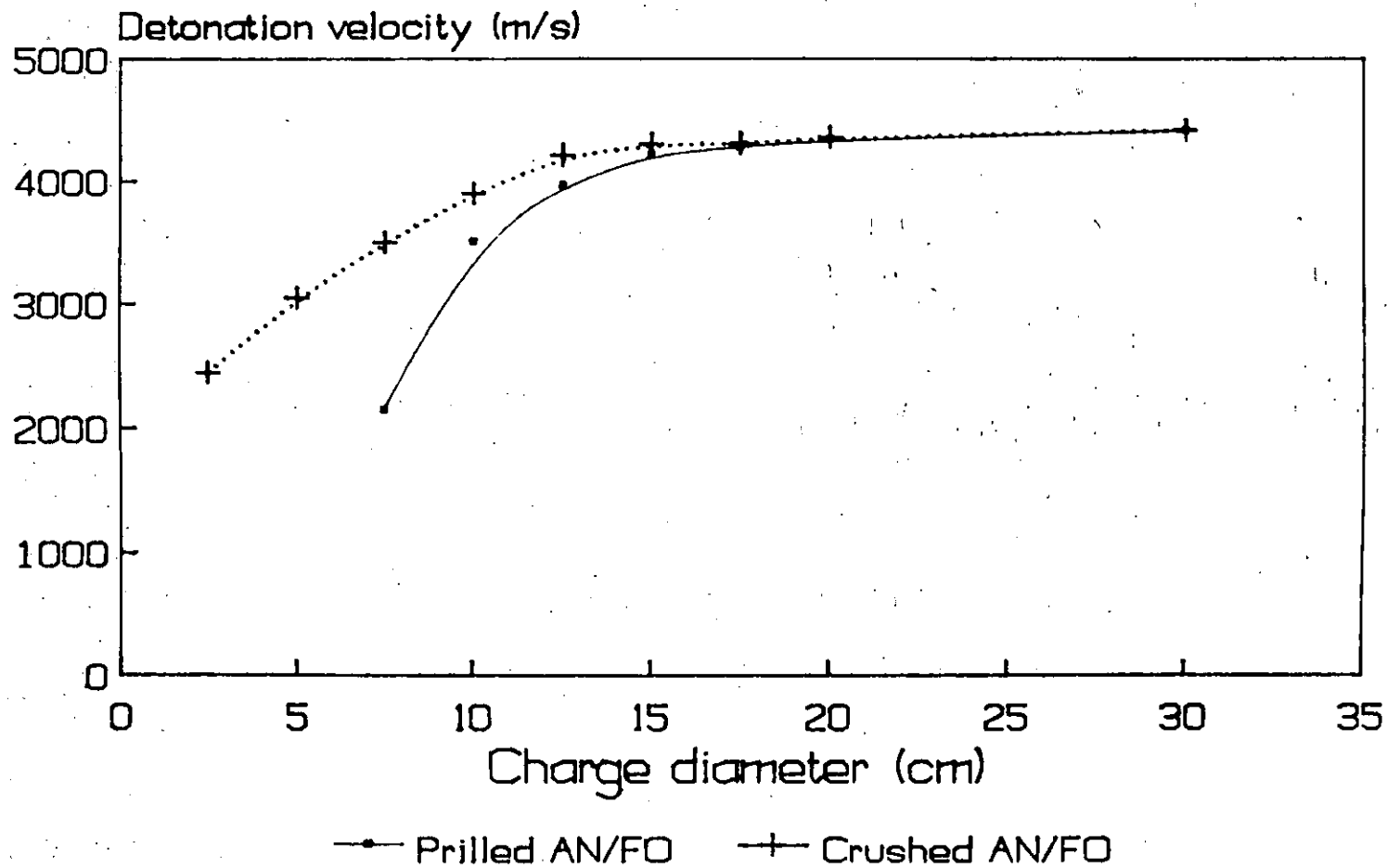
FIGURE 2: DEVELOPMENT OF THE DETONATION HEAD (AFTER COOK, 1958)

FIGURE 3: VOD - CHARGE DIAMETER CURVES FOR CONFINED AND UNCONFINED ANFO



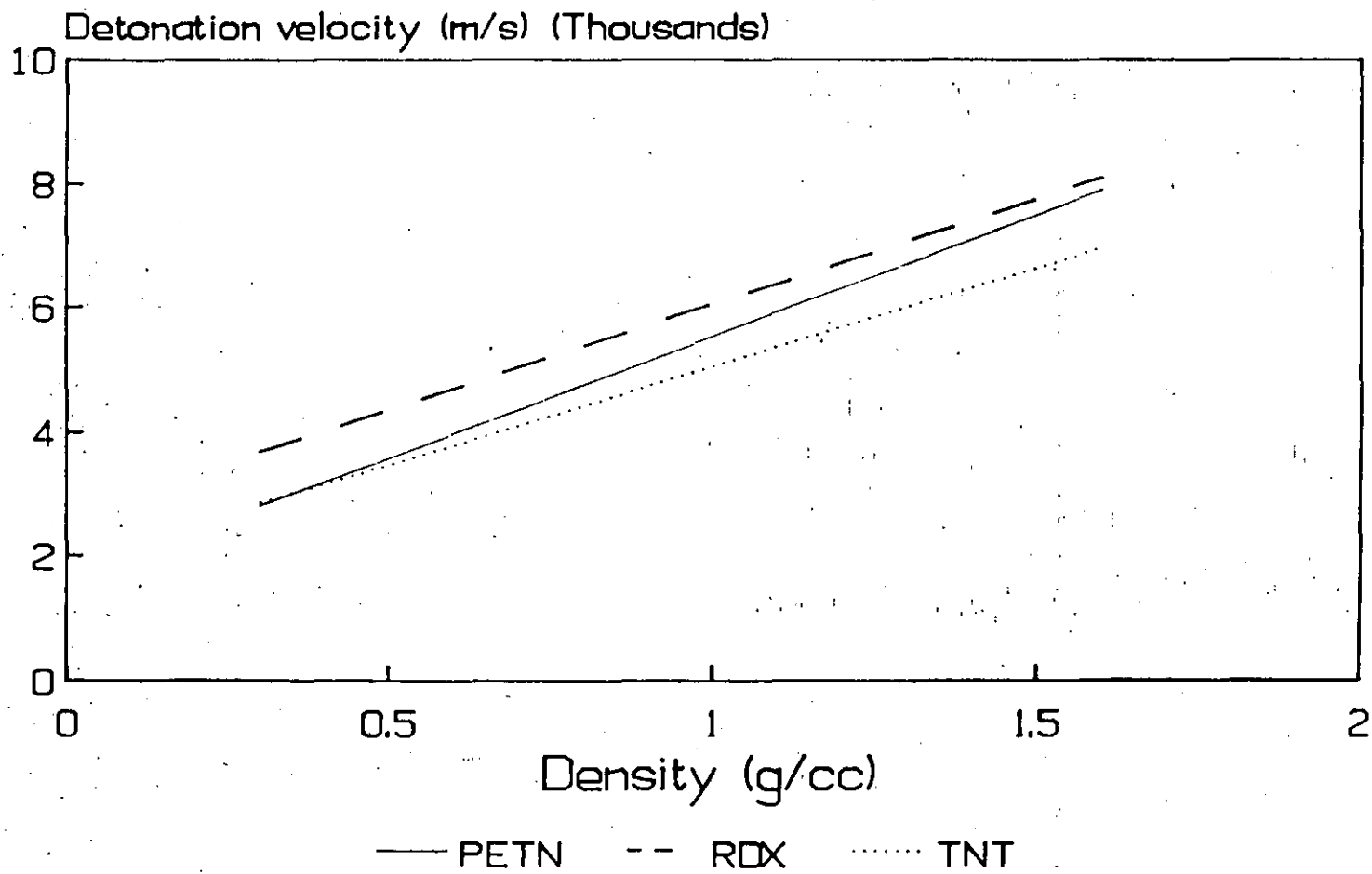
density = 0.85g/cc

FIGURE 4: EFFECT OF THE PARTICLE SIZE ON THE VELOCITY - DIAMETER CURVE OF AN/FO



density = 0.85g/cc

FIGURE 5: DETONATION VELOCITY - DENSITY
RELATIONSHIPS



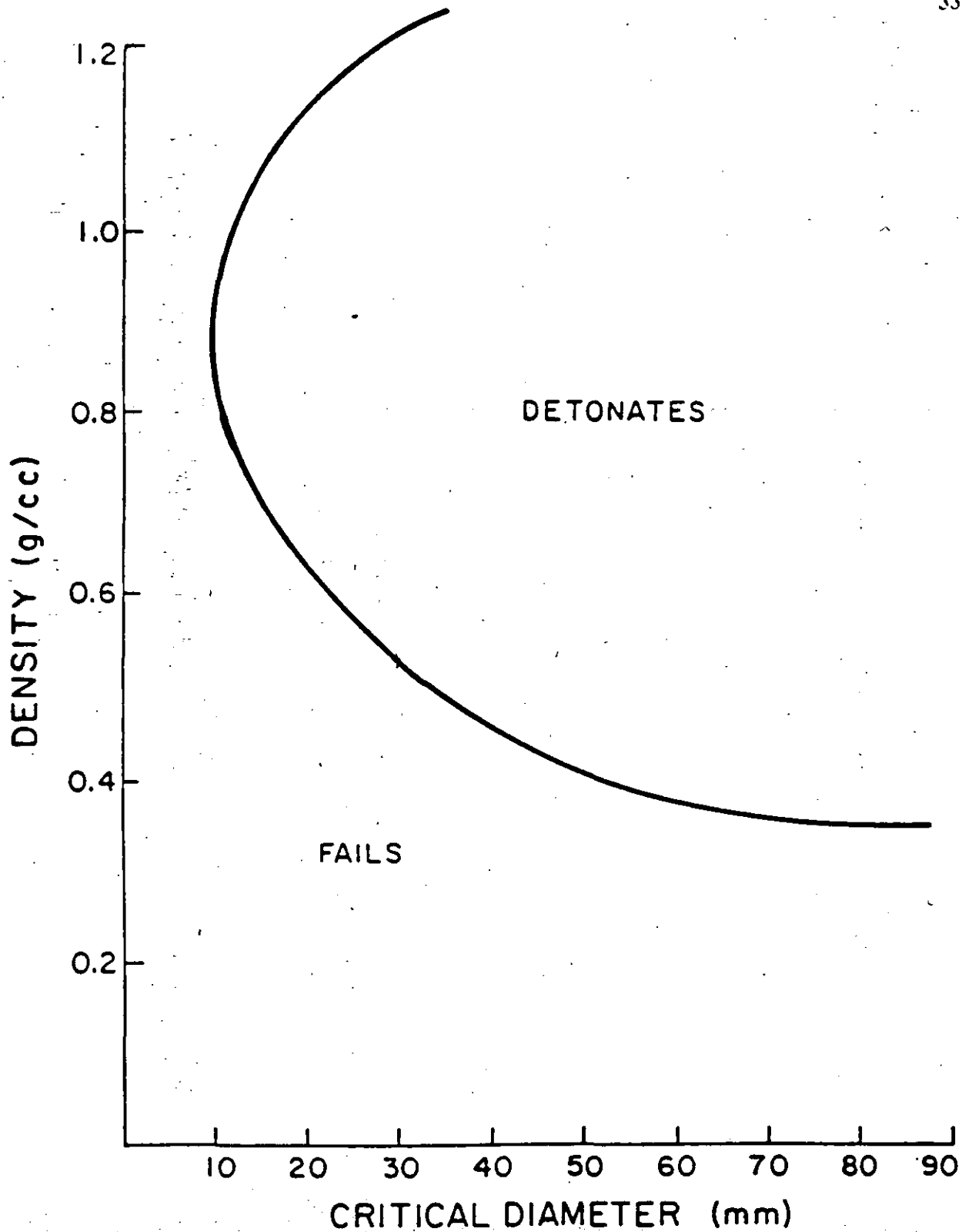


FIGURE 6: EFFECT OF THE DENSITY OF A TYPICAL EMULSION ON THE UNCONFINED CRITICAL DIAMETER

FIGURE 7: EFFECT OF TEMPERATURE ON THE CRITICAL DIAMETER OF TNT

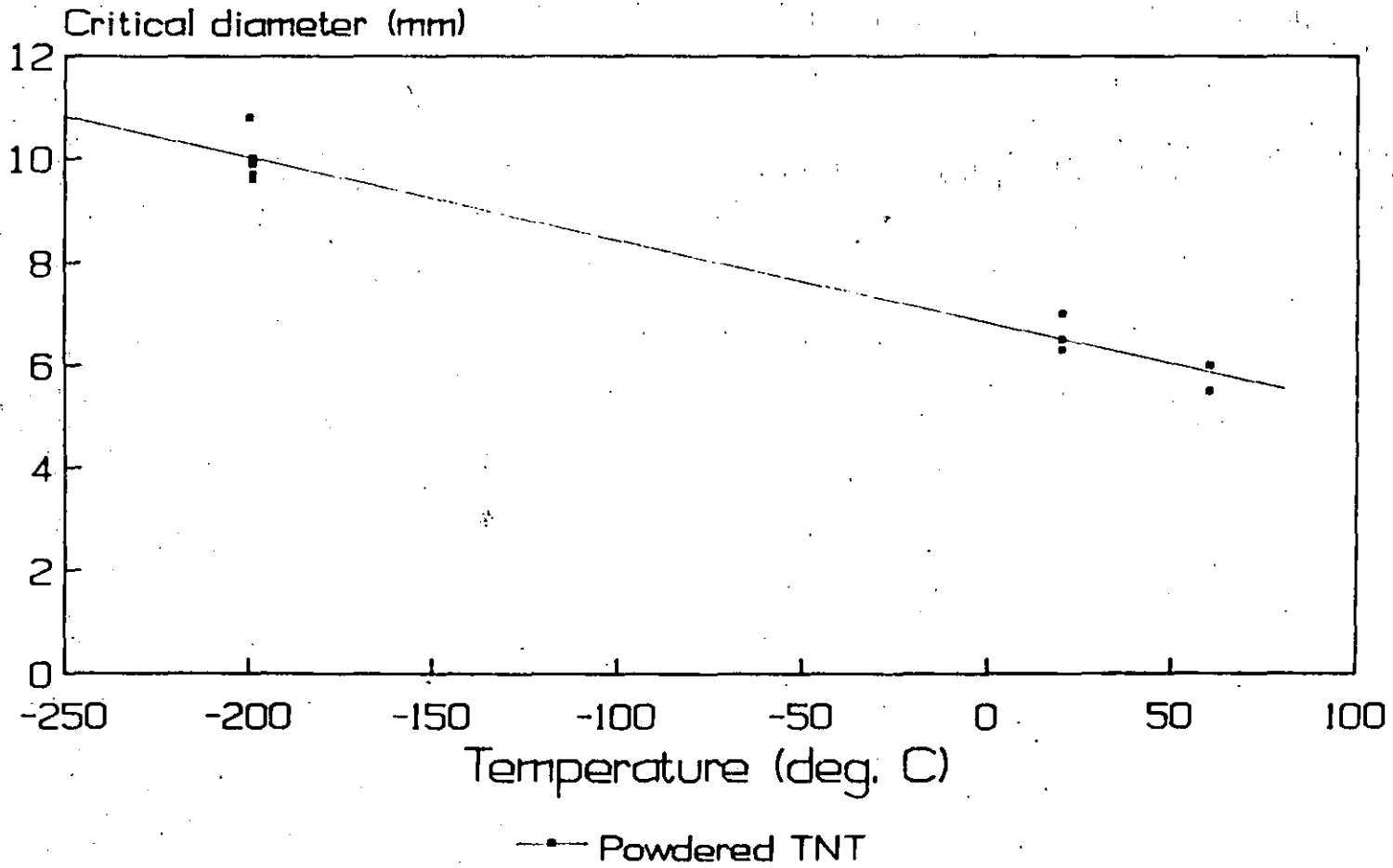
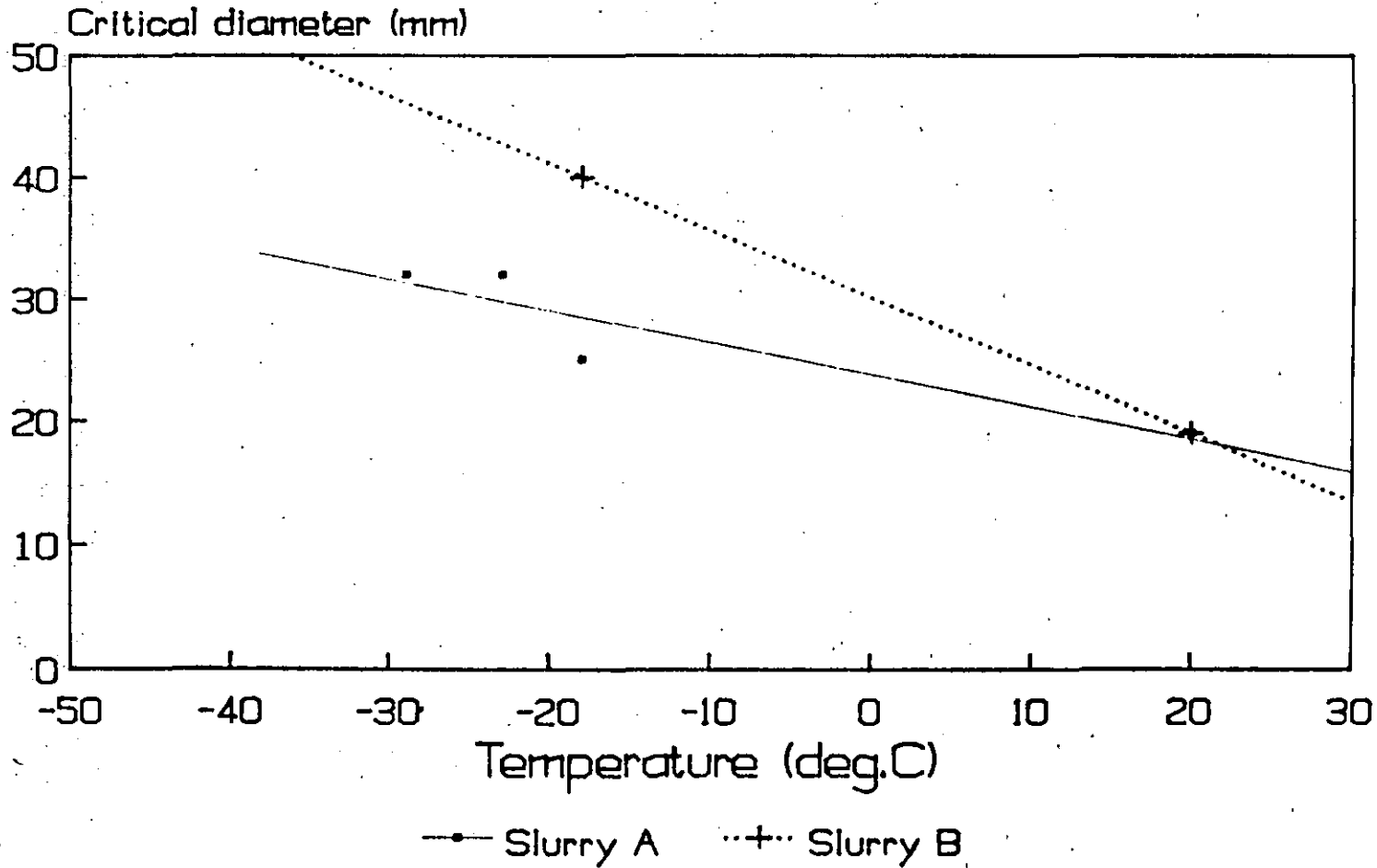


FIGURE 8: EFFECT OF TEMPERATURE ON THE CRITICAL DIAMETER OF SLURRIES



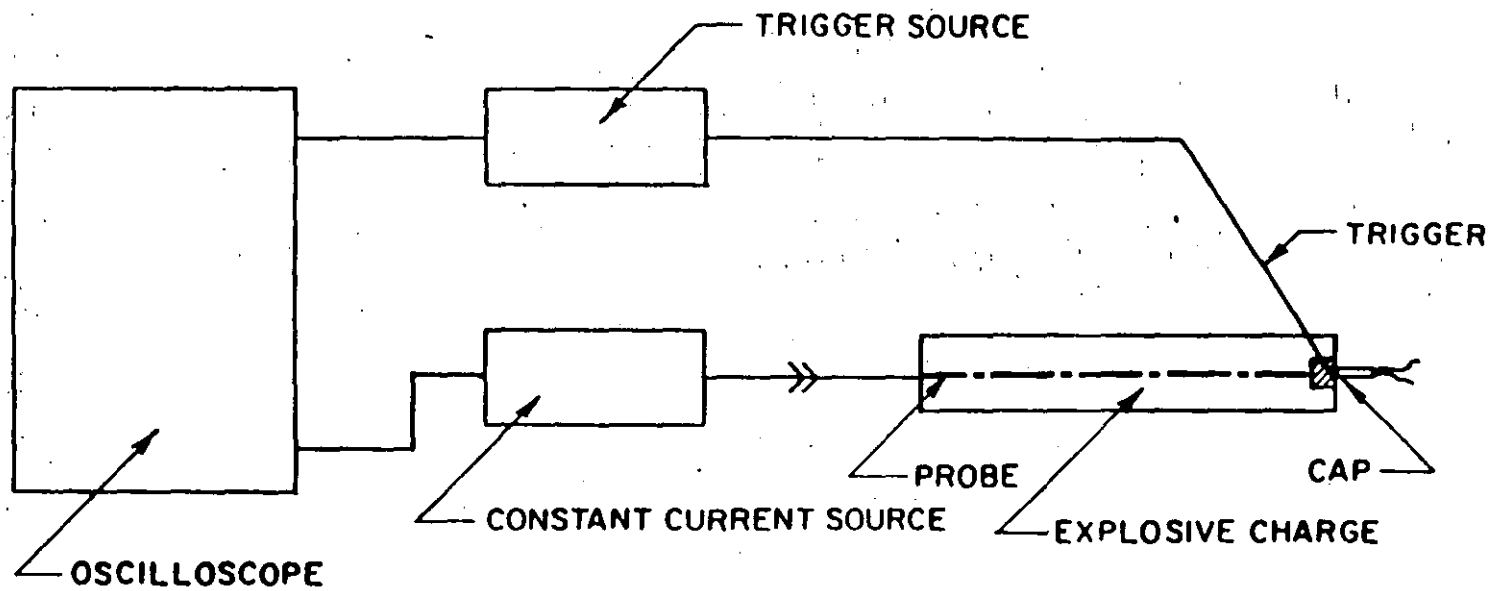


FIGURE 9. SCHEMATIC REPRESENTATION OF THE CONTINUOUS VELOCITY SYSTEM FOR THE MEASUREMENT OF THE VELOCITY OF DETONATION

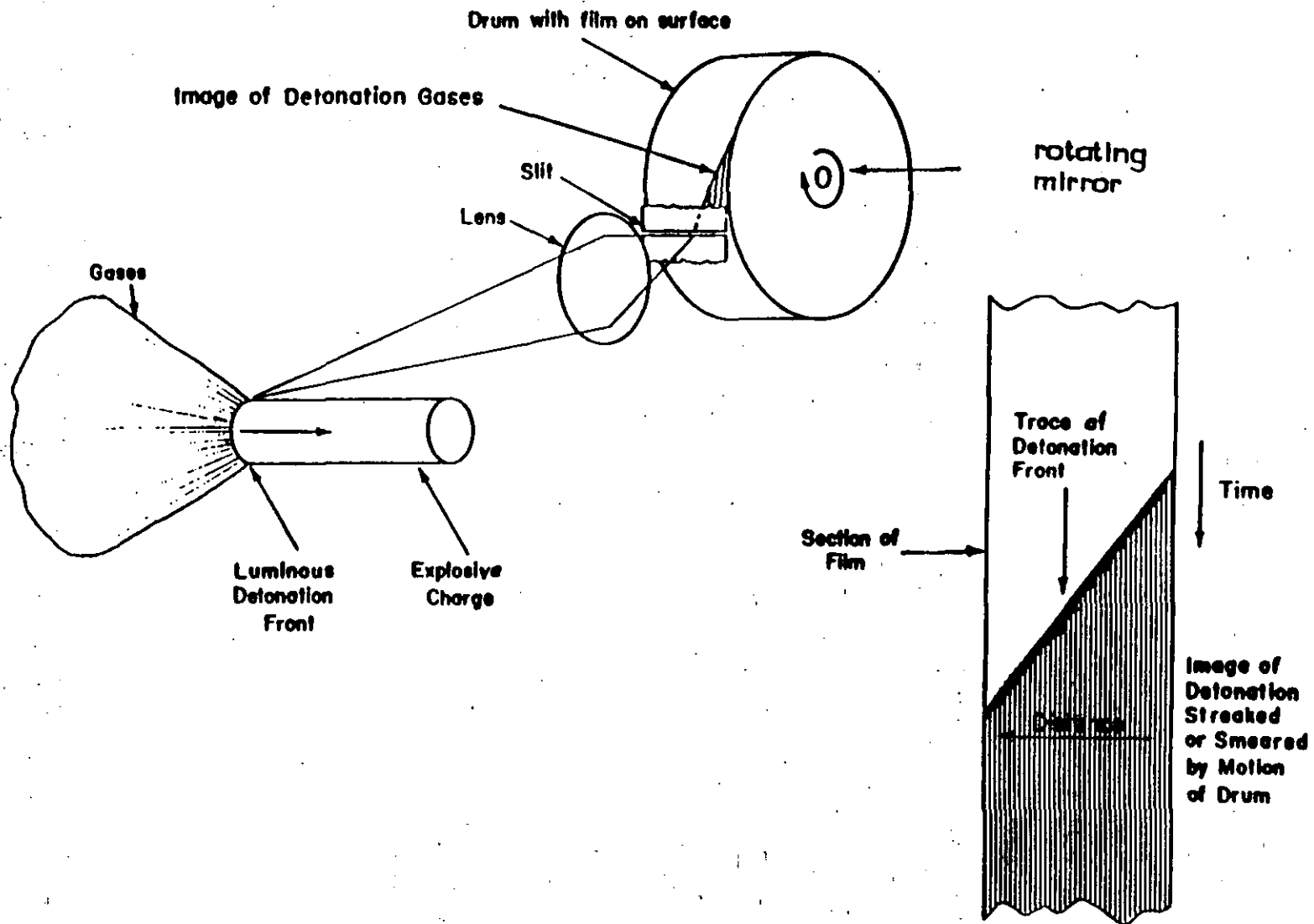


FIGURE 10: MEASUREMENT OF THE VELOCITY OF DETONATION BY USING A STREAK CAMERA (ref. 9)

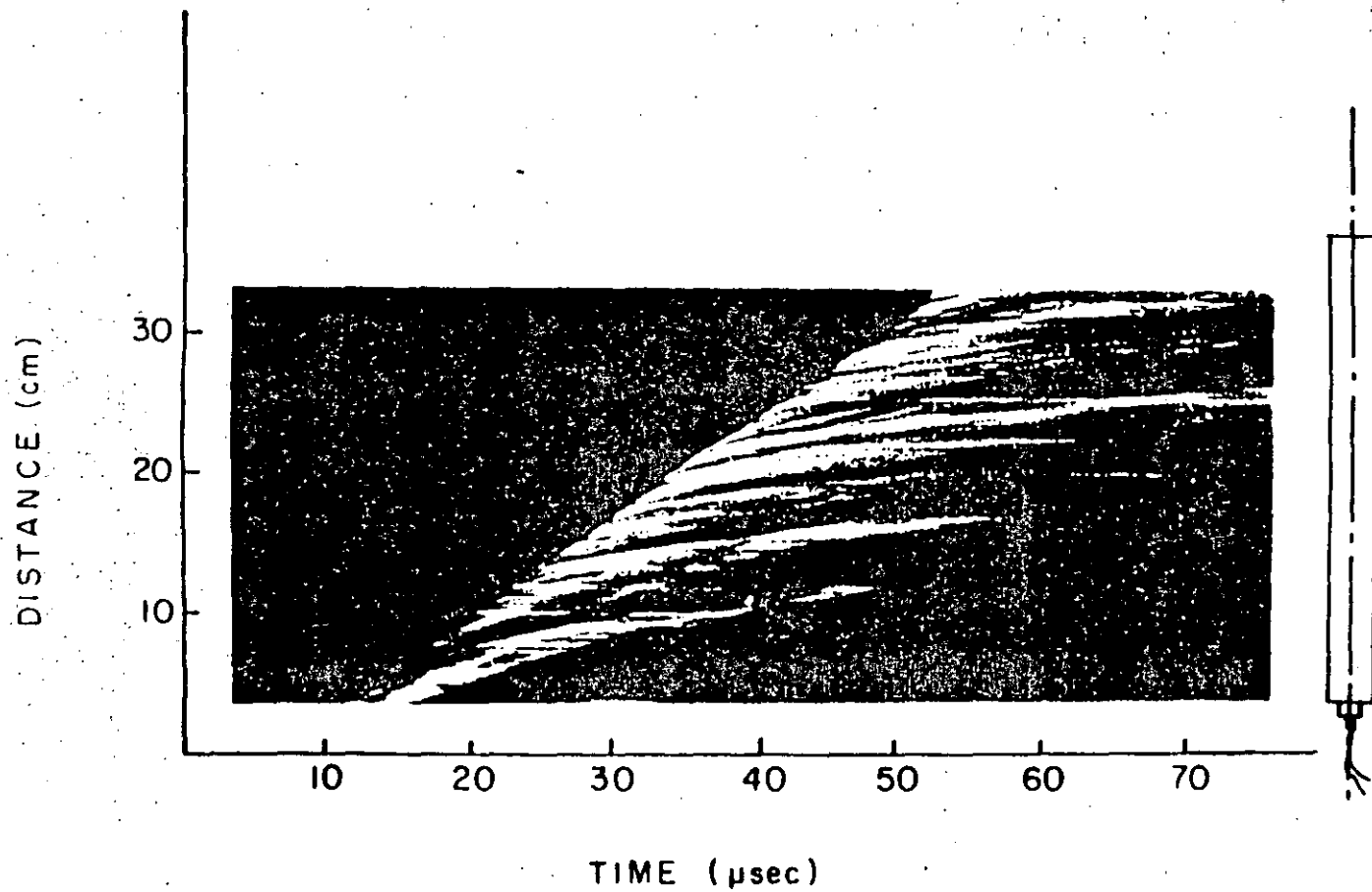


FIGURE 11: TYPICAL STREAK CAMERA RECORD FOR THE MEASUREMENT OF THE VELOCITY OF DETONATION OF PENTOLITE

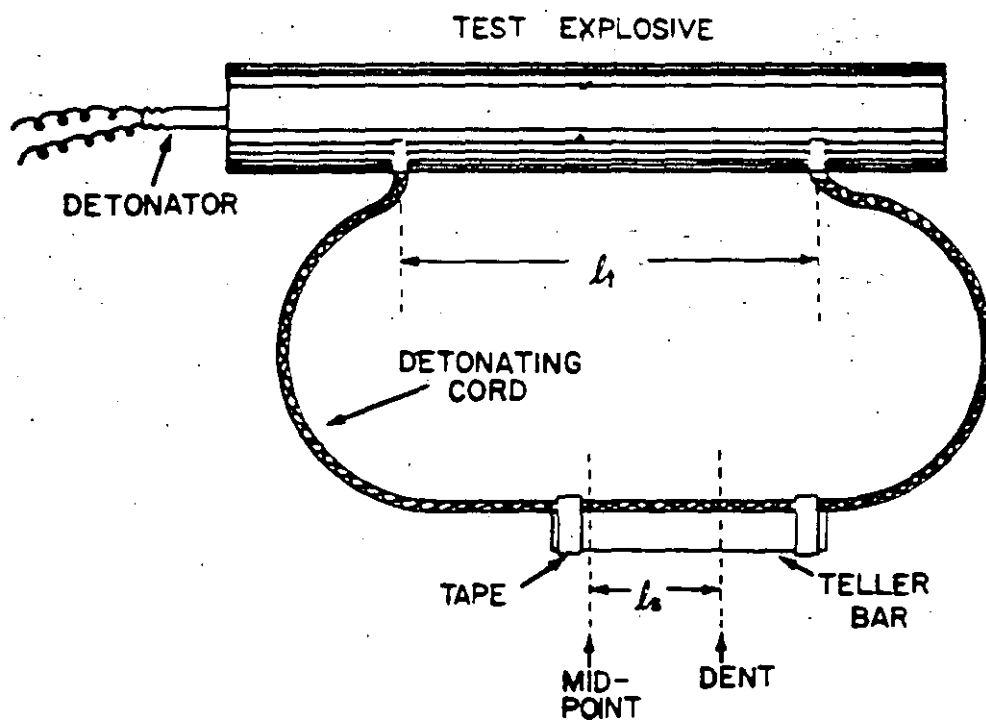


FIGURE 12. D'AUTRICHE METHOD FOR THE MEASUREMENT OF THE VELOCITY OF DETONATION

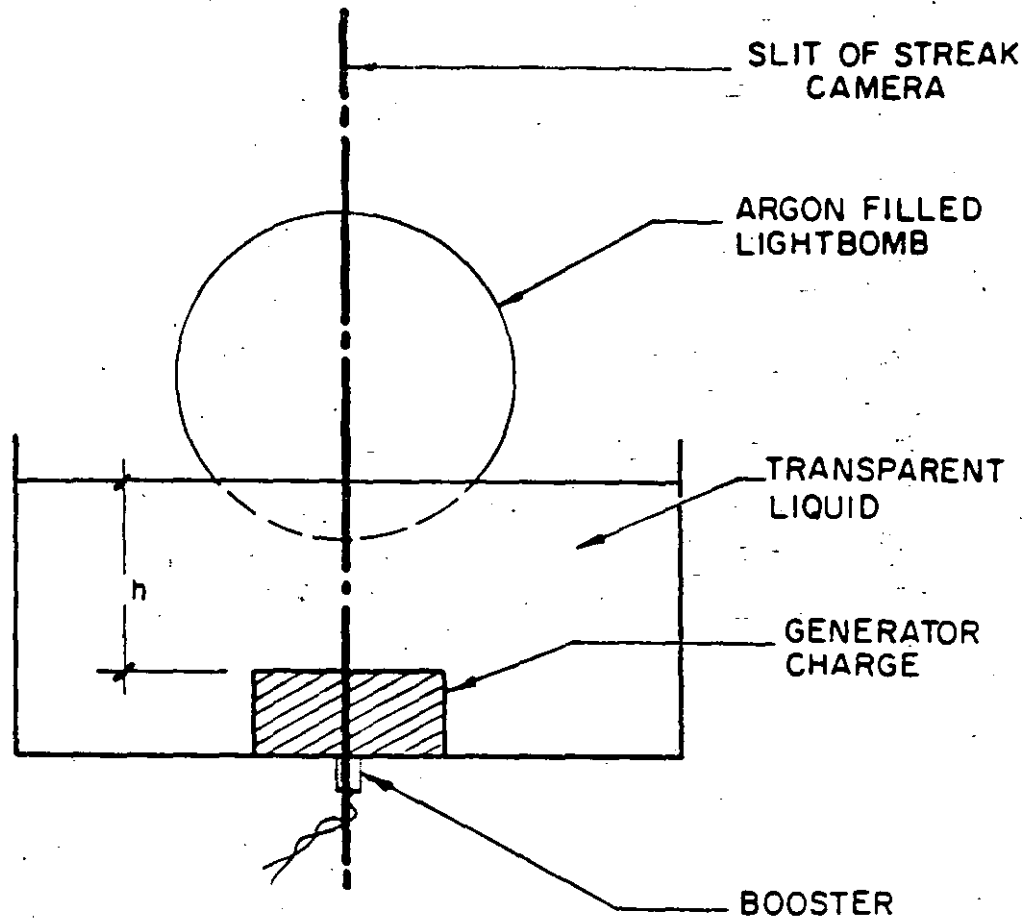


FIGURE 13: EXPERIMENTAL SET UP FOR DETERMINING THE HUGONIOT OF THE TRANSPARENT LIQUID

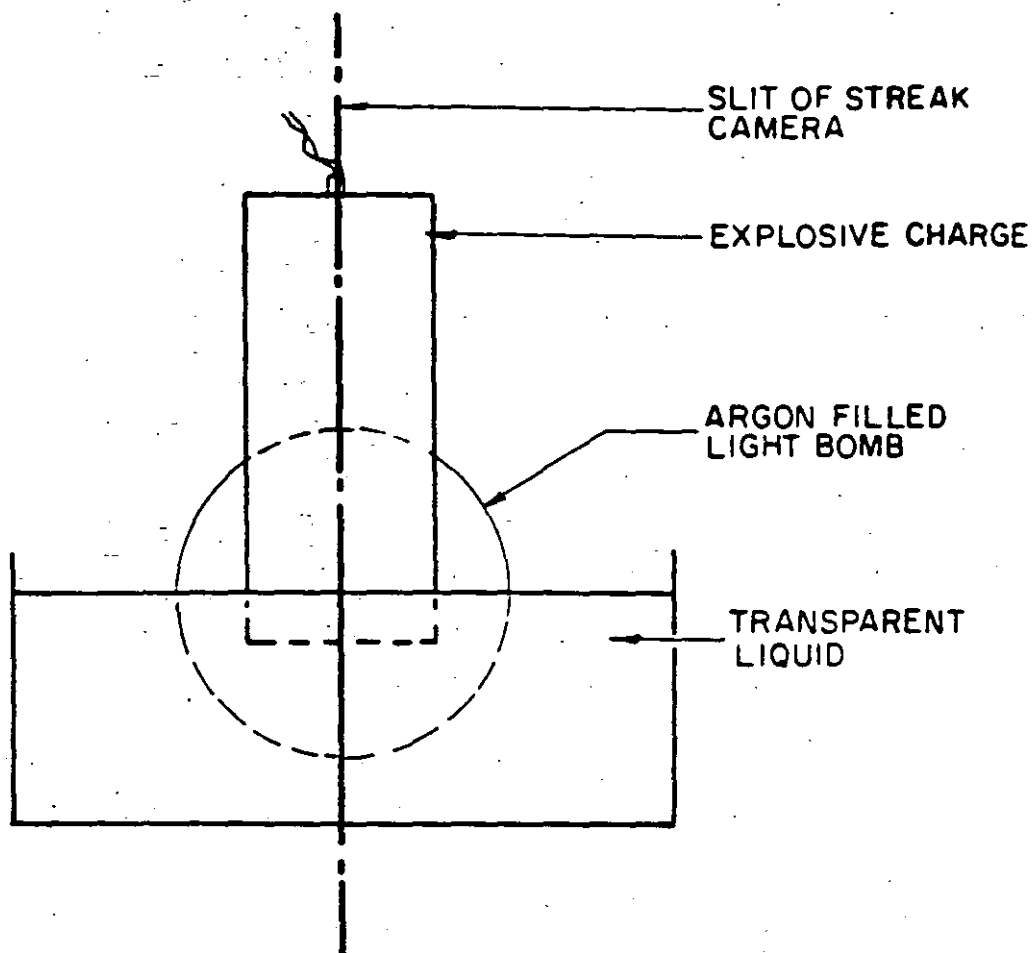


FIGURE 14: EXPERIMENTAL SET UP FOR THE MEASUREMENT OF THE DETONATION VELOCITY AND THE INITIAL SHOCK VELOCITY IN THE TRANSPARENT LIQUID

CHAPTER 4

GAP AND FRICTION SENSITIVITY OF EXPLOSIVES

4.1 Introduction

The gap sensitivity of explosive represents its ability to propagate through barriers. The gap sensitivity of an explosive is an important property to be considered in blasting operations. If the sensitivity is low, the detonation in the borehole can be interrupted because of obstacles (rocks) or air gaps. On the contrary, an explosive which is very sensitive can be dangerous to handle and can detonate sympathetically in the boreholes. Cross propagation of adjacent holes is very undesirable since this eliminates the effects of delays and results in excessive vibrations and poor fragmentation.

However one has to differentiate between solid gap and air gap sensitivity because the phenomena involved in each case are considerably different.

The friction sensitivity determines the safe handling of explosive charges. Charges can be subjected to friction forces when loaded in blastholes. These can be of a significant magnitude especially where pneumatic loaders are used.

4.2 Underdriven and Overdriven Detonations

The detonation state (C-J state) represents a dynamic stable condition. If the detonation wave encounters a small gap in the explosive charge, it will weaken temporarily and will come back to the original stable condition once the perturbation is passed.

The same will happen if the detonation wave encounters a part of the explosive which has greater energy. Temporarily it will strengthen but later it will reach the stable condition.

Consider the situation shown in Figure 1 a. A detonation is transmitted from a donor explosive to an acceptor explosive. In this case there are three possibilities; the shock wave transmitted in the acceptor can be stronger than the detonation wave in the acceptor, the shock wave can be of equal magnitude to the detonation wave in the acceptor or the shock wave can be of a smaller magnitude than the detonation wave in the acceptor. The first case is called overdriven and the last case underdriven detonation. It has been found that in the case of an overdriven wave the strength always decays until the C-J condition is reached. In the case of the underdriven wave the detonation builds up to the C-J value. However, there is a limiting strength below which the wave decays and detonation does not propagate. This limiting strength is of importance since it determines the conditions required for safe handling and reliable initiation of explosive materials.

4.3 The Gap Test

Experimentally a simple way to determine the sensitivity of an explosive to initiation is represented in the gap test. The gap test is shown in Figure 1 b. The experiment consists of a donor charge, an attenuator and an acceptor charge. By varying the attenuator thickness, different underdriven waves are transmitted to the acceptor. The thickness of the attenuator at which 50% of the times the acceptor detonates is called critical

gap thickness. At that thickness the shock wave in the acceptor has a limiting value above which the acceptor has a high probability of detonation. The gap material is normally a standard solid material. Air gaps are not desirable because hot decomposition products of the donor explosive will impinge directly on the acceptor.

The result of the gap test depends on the geometry of the donor and acceptor charges as well as the attenuator material and the donor explosive. For this purpose various laboratories standardize gap tests by using the same donor and the same attenuator material. Thus the results of the tests are indicative of the explosives shock sensitivity.

Typical gap tests are shown in Figures 2 and 3.

The following factors affect the result of a standard gap test:

1. Density. The effect of density is shown in Figure 4⁽²⁾ where the critical gap pressure is plotted against the percent of the theoretical maximum density. It is obvious that the explosive becomes less sensitive as the theoretical maximum density is approached. This is a general trend obtained in a variety of explosive compositions⁽²⁾.

2. Temperature. The effect of temperature is shown in Figure 5. This is a general trend for any material in which the reaction rate increases with temperature⁽²⁾.

3. Composition. It is obvious that the result of the gap test is composition dependant. It has been found that if wax is added to RDX or TNT, the shock sensitivity is decreased. However if wax is added to ammonium nitrate, the sensitivity is drastically increased. This happens because of the combination of an oxidizer

with a fuel and the dominant factor is the oxidation-reduction reaction. Figure 6 is typical of this phenomenon⁽²⁾.

4. Acceptor diameter. Initiation is controlled not only from the magnitude of the impacting shock wave but from its duration as well. The reduction of the diameter of the acceptor has changed the duration of the shock wave. It is recommended that the charges are tested at a diameter above the minimum diameter for ideal detonation, where this is possible. According to Price the critical initiating pressure - diameter relationship should follow a curve as in Figure 7⁽⁵⁾. Experimental results by Moulard indicate the same trend for Composition B⁽⁶⁾.

5. Confinement. Price has found that confinement of the acceptor in the test prevents the lateral rarefaction from producing a large disturbance. The confinement gives a result which is comparable to that which would be obtained for a very much larger diameter unconfined charge. The result may approach that which would be obtained in the one dimensional flow⁽²⁾. In Figure 8 the critical gap pressures for confined charges are compared to the critical cap pressures of unconfined charges. It is obvious that confinement increases the sensitivity of explosives.

4.4 Air Gap Sensitivity

This term denotes the initiation of an explosive charge without a priming device by the detonation of another charge in the neighbourhood. The transmission mechanism is complex. The important parameters are the shock wave, the hot reaction products of the donor and the flying parts from the casing of the donor charge. Various tests are conducted to determine the air gap

sensitivity of explosives. In Europe the smallest diameter of manufacture is used in the test charges which are tested unconfined⁽³⁾. This will provide the largest gap below which detonation will always be observed. Confinement however affects the result. For this purpose coal mining explosives are tested in pipes which simulate boreholes. It is recommended that gap tests simulating the conditions of application are performed to determine the gap sensitivity of a particular product.

4.5 Initiation by Friction

The mechanism of heating by friction has been investigated by Bowden and co-workers. When solid bodies are pressed against each other contact will occur only at the summits of the surface irregularities. The total area of contact is a small fraction of the total surface area⁽⁴⁾. When the bodies are sliding against each other heat is developed at the regions of contact. Hot spots are created at the points of contact and their temperature depends on the pressure, sliding velocity and heat conductivity of the sliding material. The contact material with the lowest melting point determines the hot spot temperature. When melting occurs its supporting capacity is taken over by other points⁽⁴⁾. According to Bowden if the melting point of the slider is below the critical hot spot temperature for the explosive, detonation does not occur.

Several friction tests have been developed. The Swedish⁽⁴⁾ developed a friction test in which the explosive is subjected to stresses similar to those when the explosive is charged in boreholes. The test consists of a block of granite which has a semi-cylindrical groove. A thin layer of explosive is placed in

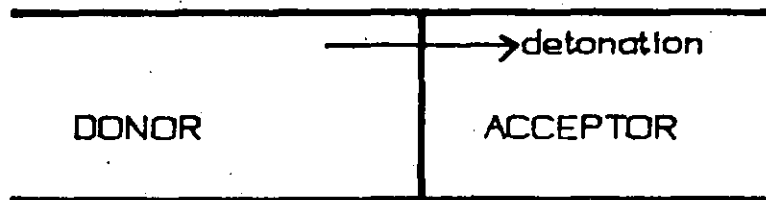
the groove and a slider moves on top. Various loads are put on the slider. The slider moves at a constant speed and the result is recorded as a function of the load.

In Germany a sample is placed on a roughened porcelain plate⁽³⁾. The sample is put on top of it and a porcelain cylinder is placed on top with various loads. The plate moves at a certain speed and the result is recorded as a function of the load.

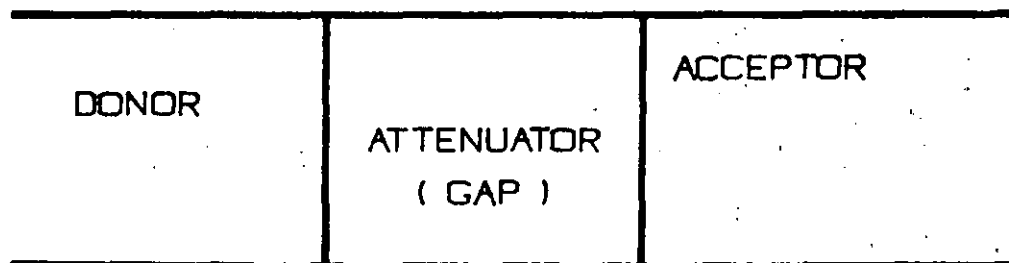
Similar tests have been developed in other countries.

4.6 References

1. U.S. Army: "Engineering Design Handbook. Principles of Explosives Behaviour", AMXP 706-180, 1972.
2. Zerilli, F.: "Notes from Lectures on Detonation Physics", Naval Surface Weapons Laboratory, 1981.
3. Meyer, R.: "Explosives", Verlag Chemie, Weinheim, New York, 1977.
4. Johansson, C.H. and Persson, P.A.: "Detonics of High Explosives", Academic Press, London, New York, 1970.
5. Price, D.: "Critical Parameters for Detonation Propagation and Initiation of Solid Explosives", Naval Surface Weapons Center, 1981.
6. Moulard, H.: "Critical Conditions for Shock Initiation of Detonation by Small Projectile Impact", Seventh International Symposium on Detonation, Maryland, 1981.



(a)



(b)

FIGURE 1: TYPICAL GAP TEST CONFIGURATION

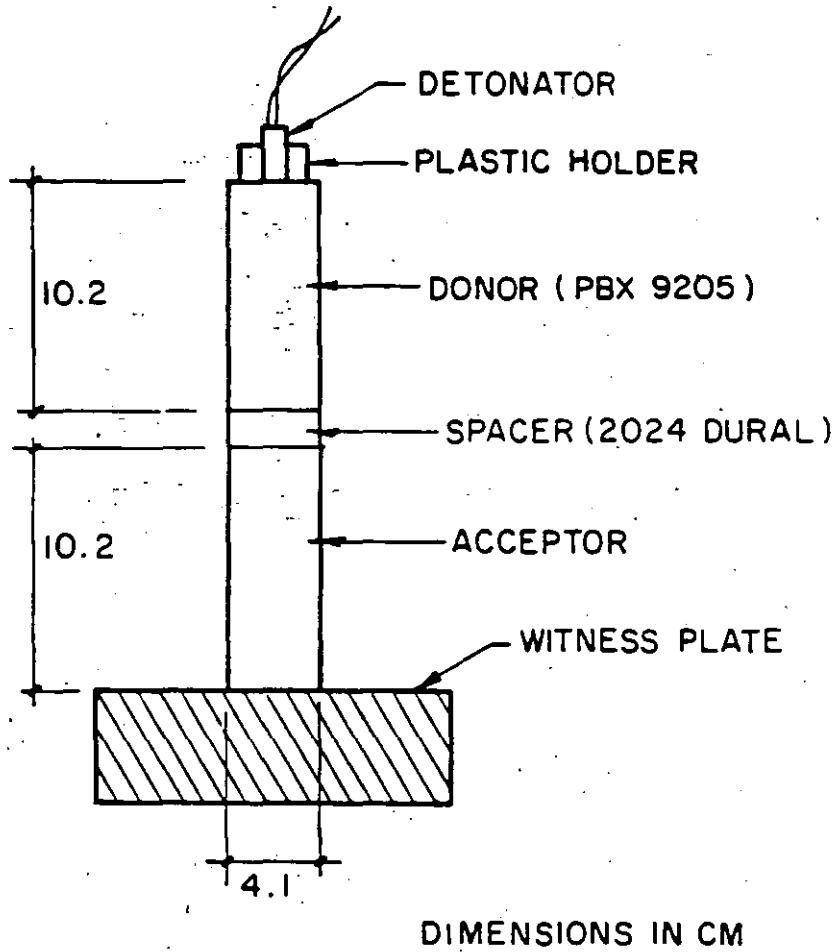


FIGURE 2: THE LOS ALAMOS LARGE GAP TEST

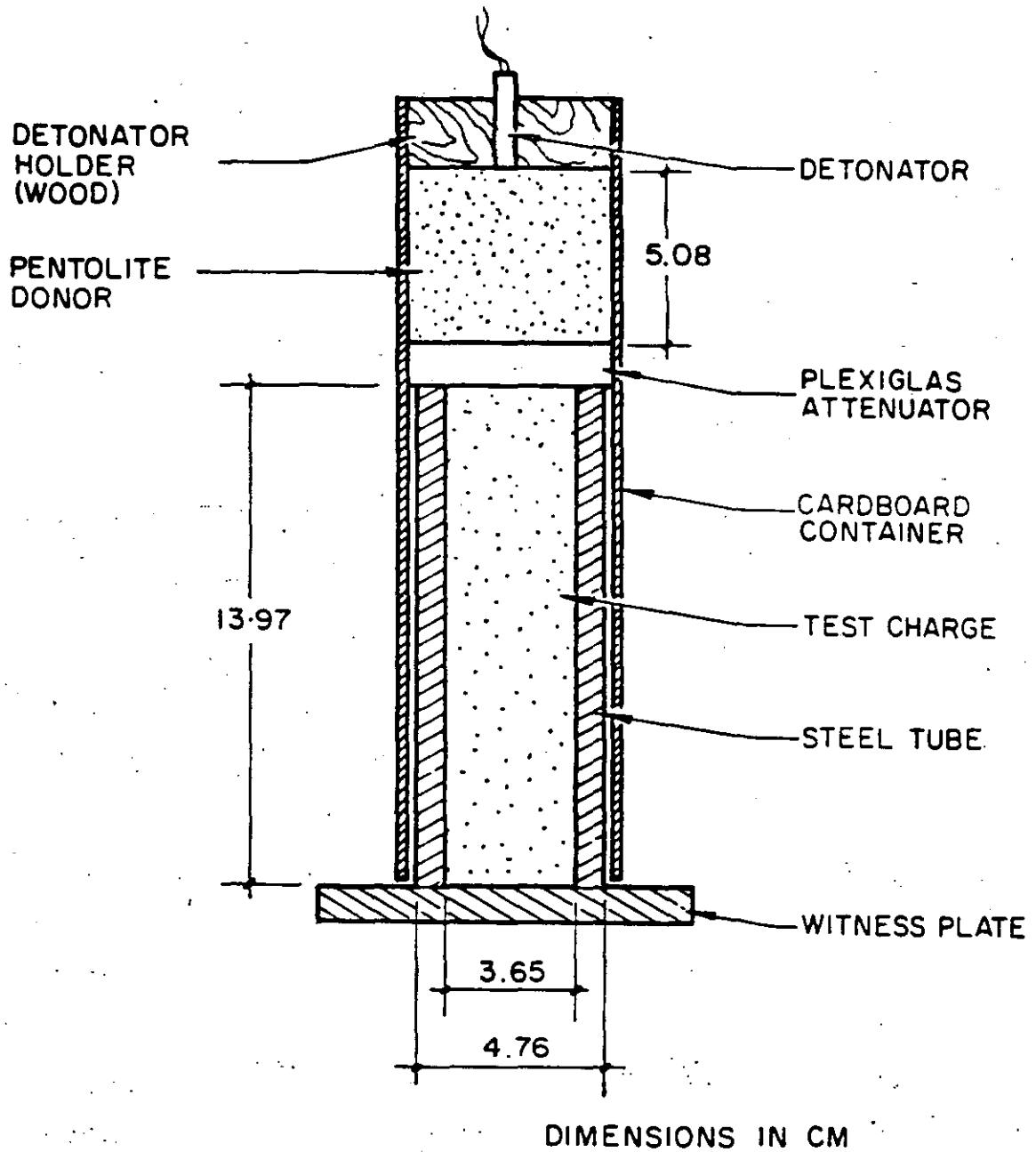


FIGURE 3: THE NOL GAP TEST

FIGURE 4: EFFECT OF DENSITY ON
CRITICAL GAP PRESSURE

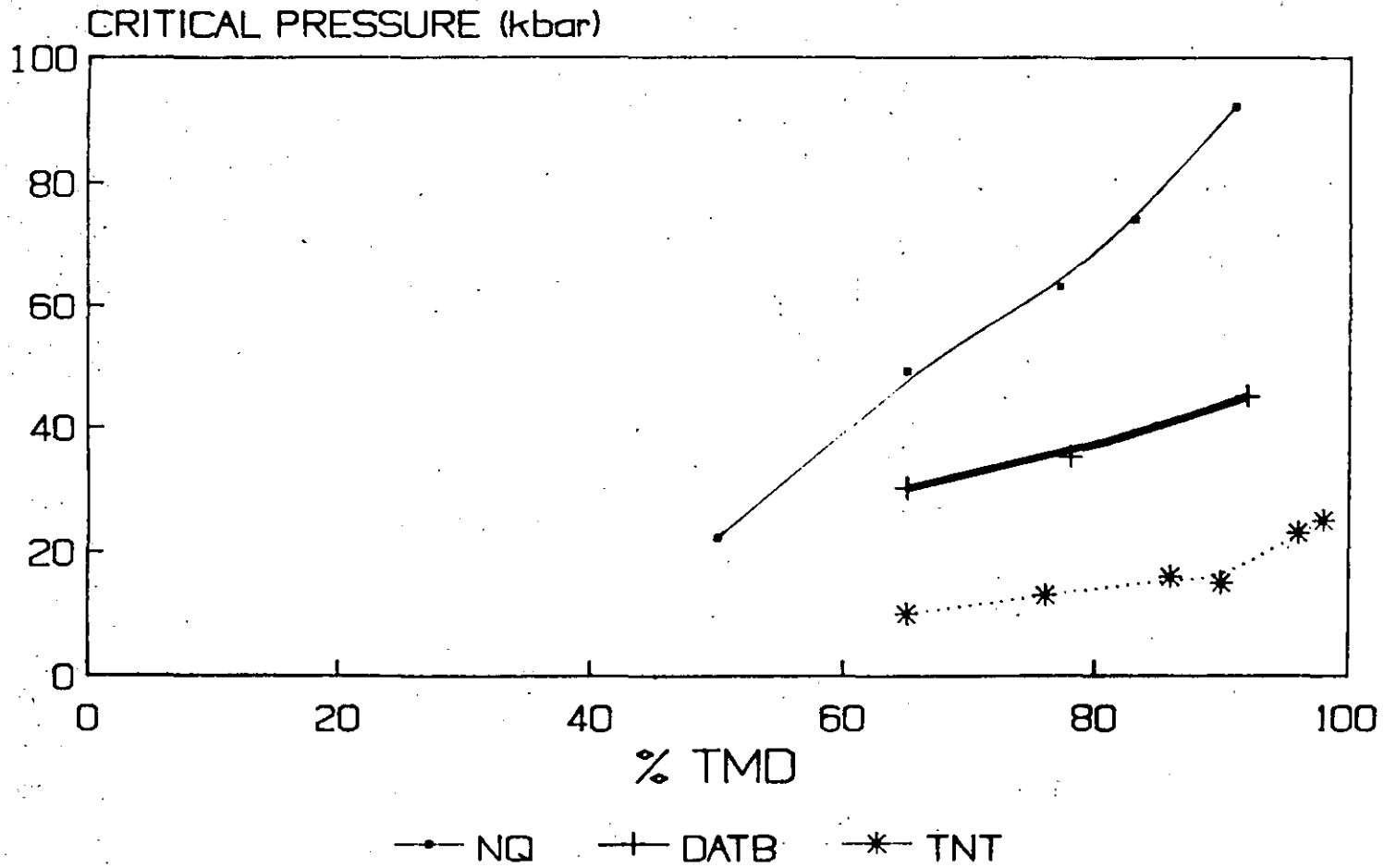


FIGURE 5: EFFECT OF THE COMPOSITION ON CRITICAL GAP PRESSURE

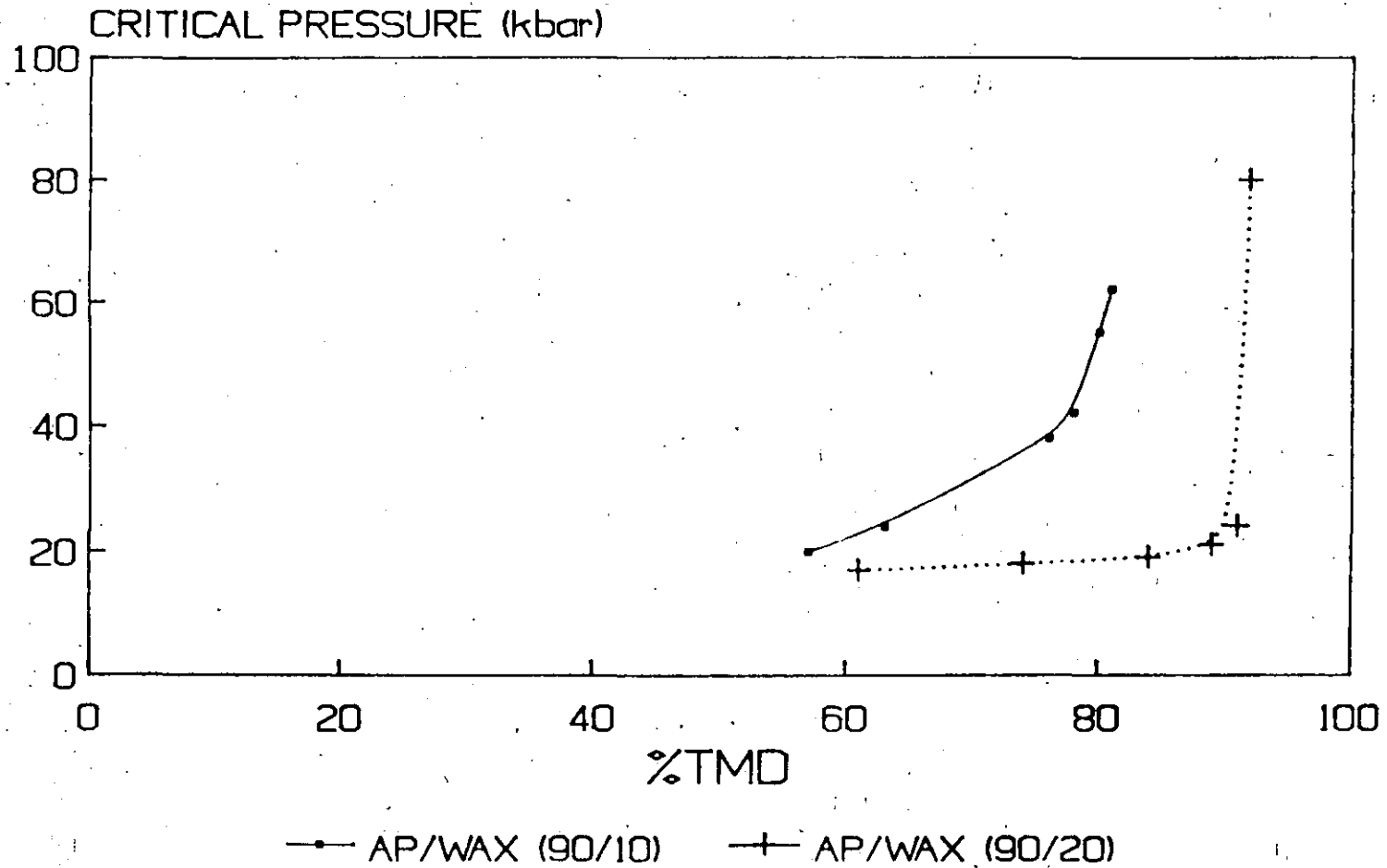
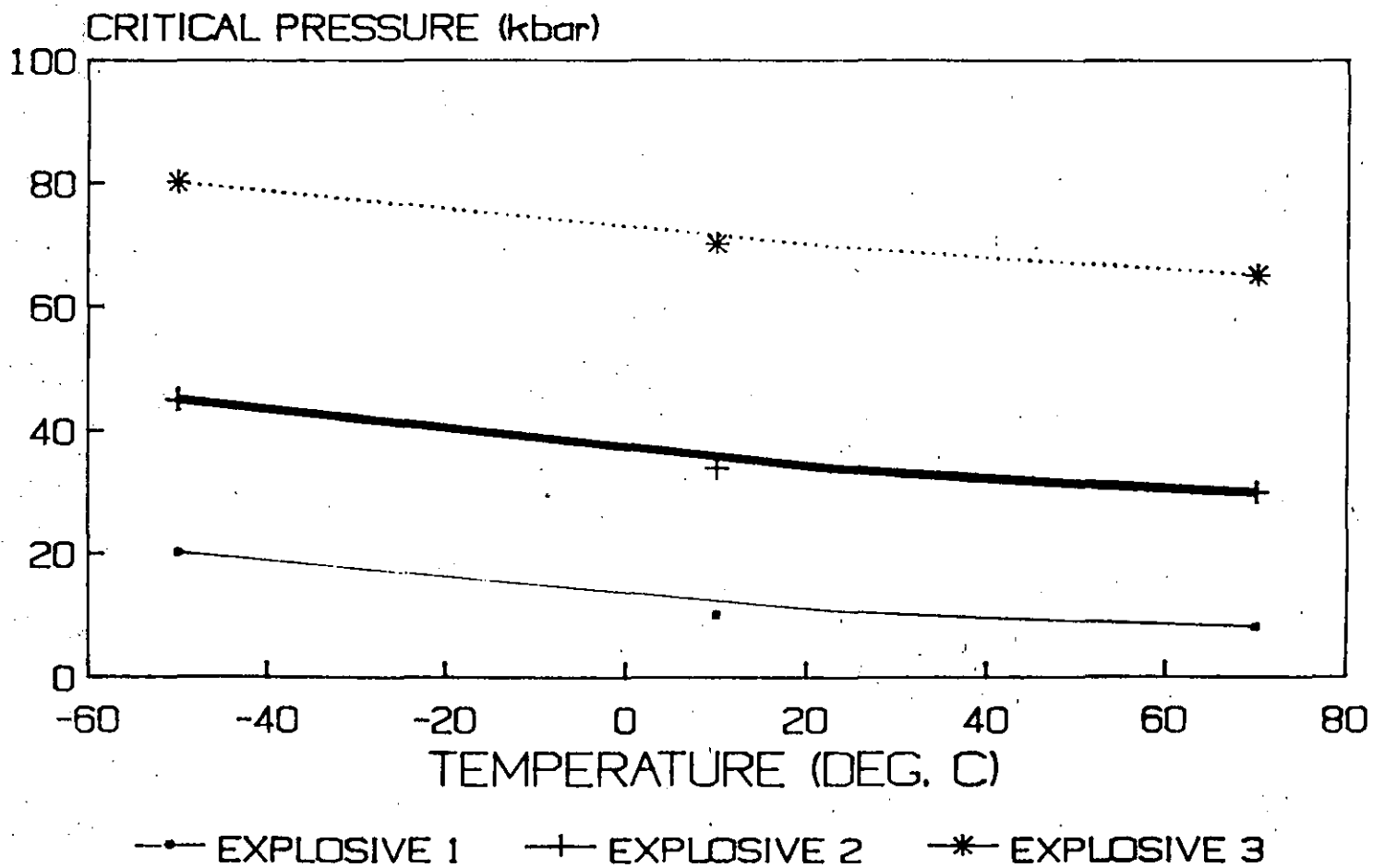


FIGURE 6: EFFECT OF TEMPERATURE ON THE CRITICAL GAP PRESSURE



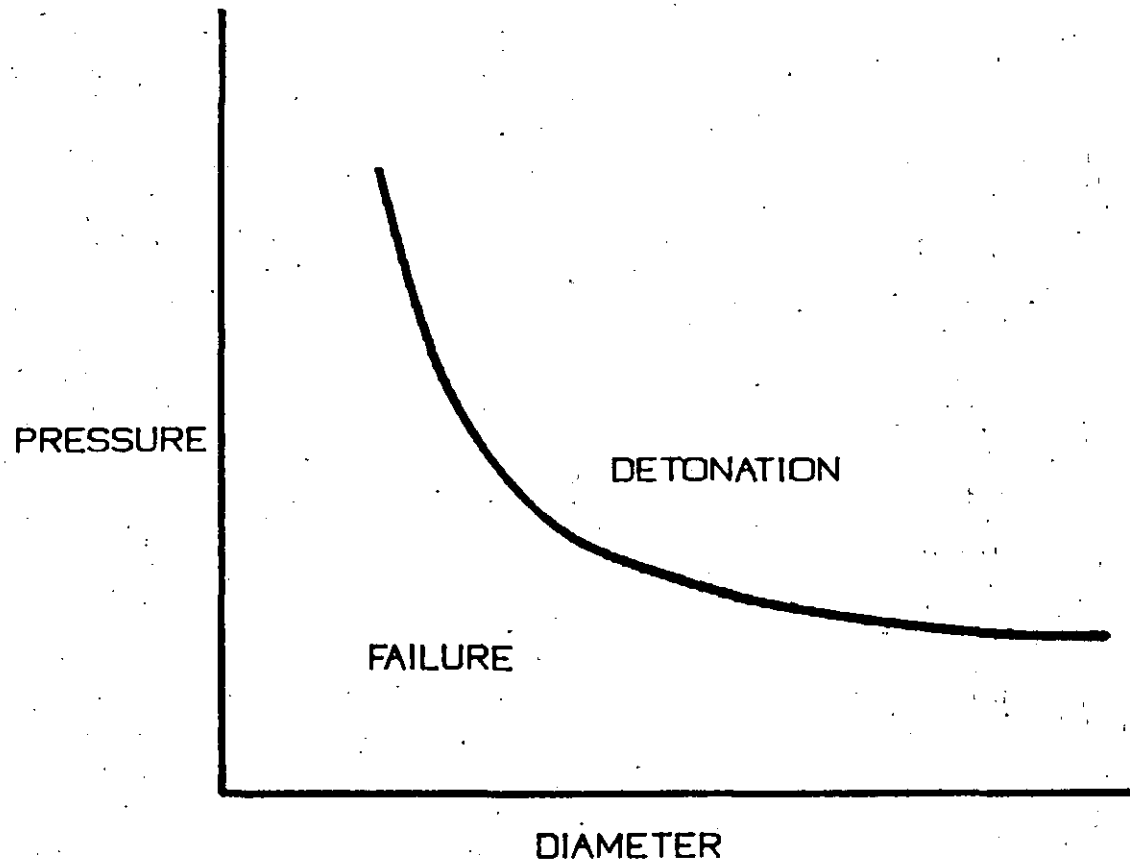
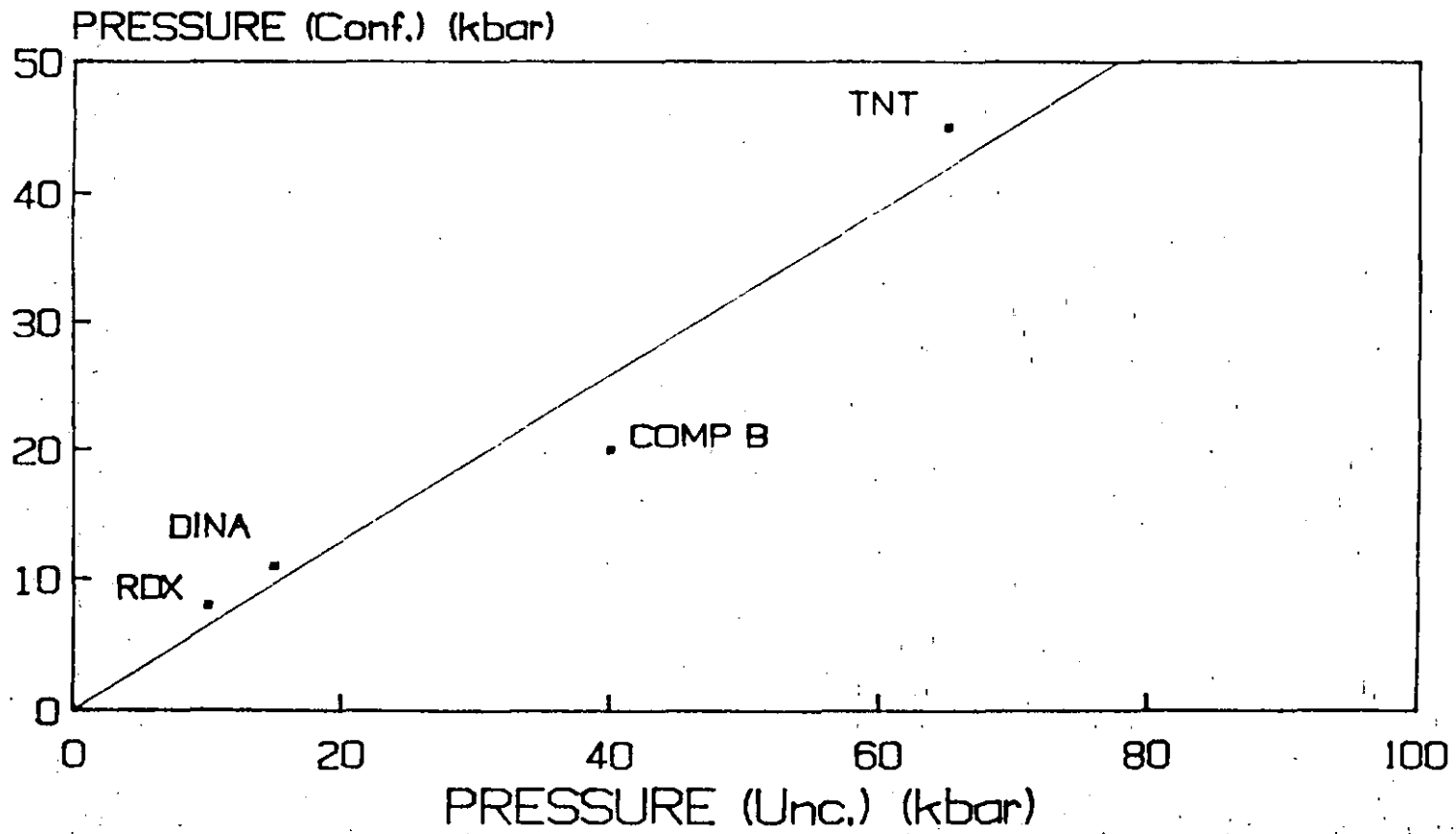
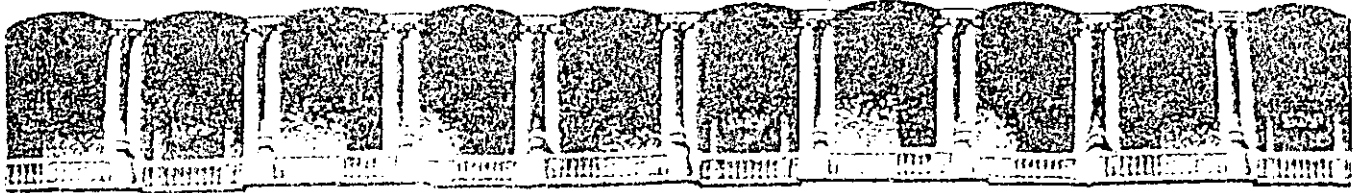


FIGURE 7: VARIATION OF CRITICAL PRESSURE WITH DIAMETER

FIGURE 8: EFFECT OF CONFINEMENT ON CRITICAL GAP PRESSURE





FACULTAD DE INGENIERIA U.N.A.M.
DIVISION DE EDUCACION CONTINUA

CURSOS ABIERTOS

**IV. CURSO INTERNACIONAL DE INGENIERIA GEOLOGICA APLICADA A
OBRAS SUPERFICIALES Y SUBTERRANEAS**

CUARTO MODULO:

TECNOLOGIA SOBRE EL USO DE EXPLOSIVOS

Del 22 al 26 de junio de 1992

*THE VELOCITY OF DETONATION RECORDER A NEW BLAST AND SHOCK
WAVE DIAGNOSTIC TOOL FOR COMMERCIAL USE*

AUTOR: GARY KAHN

EXPOSITOR: ING. RAUL CUELLAR B.

JUNIO - 1992

**THE VELOCITY OF DETONATION RECORDER
A NEW BLAST AND SHOCK WAVE DIAGNOSTIC TOOL FOR COMMERCIAL USE**

By

Gary Kahn

EG&G Special Projects
2450 Alamo Ave. SE
Albuquerque, NM 87106
(505) 243-2233

The knowledge of how and when your explosives go off can help you make intelligent decisions regarding future application of explosives thus removing some of the black magic associated with blasting. The net result will be intelligently set-up shots with timing, explosive charges, and placement more accurately done. Lower operational costs can be achieved when the correct combinations are applied.

This article describes a technique for accurately measuring explosive detonation time, burn rates, and shock wave propagation in a straightforward and simply implemented fashion. Further, application of this technique can be used to collect information from large scale blasting operations where there are multiple holes and sequenced firings of explosive.

The technique has been used for many years in underground nuclear tests. The technology (Time Domain Reflectometry, TDR) is well understood and is a standard diagnostic technique in many fields. In the nuclear field the technology fielded is called CORRTEX for Continuous Reflectometry for Radius versus Time Experiments. Developed at and fielded from Los Alamos National Laboratory, New Mexico, its major use has been to estimate the yield from underground nuclear explosive detonations both in the U.S. and in the Soviet Union. This technology also has a useful and important role in the explosive industry, however, and will be particularly useful when high timing accuracy detonators are readily available.

The concepts involved are similar to that of RADAR where a pulse of radio waves are sent out and a echo or reflected pulse is returned to give ranging information. The technique uses a coaxial cable to carry a fast rise-time electrical pulse back and forth. The time between the sending of the

pulse and its return is accurately measured. Knowing how the time changes from pulse to pulse gives an accurate picture of the length of the cable in time. This is the underlying concept for the CORRTEX and of the Velocity of Detonation Recorder (VODR), the commercial version of the CORRTEX.

In the measurement of explosive performance the coaxial cable is laid out along the length of the explosive with the far end of the cable near the detonator (see Figure 1).

As the explosive is detonated (and burns), the cable becomes progressively shorter. The VODR accurately measures the time interval and therefore the length of the cable from moment to moment.

The collected information can then be processed into a useful form which may be tabular or graphical in nature (see Figure 2). From the displayed data both burn rates and timing information can be obtained and compared to expected information.

To further understand the technology involved you need to know something about pulses traveling along electrical cables. First they travel a little bit slower than the speed of light which travels at 299 million meters per second. This is many times faster than the fastest explosive burn rate. Secondly, the electrical pulses are reflected back by discontinuities in the transmission line. Thus, a pulse is reflected at the point where the cable is crushed or severed by the explosive shock wave. The return pulse then contains useful information about exactly where the shock wave is passing.

To measure distances very accurately using time you must have a high resolution timer. For the unit designed, the resolution is down to 125 picoseconds for a two-way transit distance on an electrical cable of about 0.6 inches. The fine resolution is useful for examining events occurring close to the detonator.

The unit sends pulses down the electrical cable up to 100,000 times a second at its maximum pulse rate. Consider an explosive with a burn rate of 6000 meters a second. In the 10 microseconds between pulses the explosive can burn about 2.4 inches. Thus, the time resolution of 125 picoseconds is about the correct resolution considering that most explosives have a significantly slower burn rate.

COMMERCIAL CORRTEX

The Commercial version of CORRTEX, the VODR is smaller and more highly integrated than some of the earlier units built for underground nuclear yield monitoring. The commercial unit is a self contained unit about the size of a large suitcase. An external 24 volt, 15 amp-hour battery is used for power allowing it to operate for about 5 hours. The external battery charger will allow the battery to be completely charged in about three hours from a 120 volt 60 Hz source.

An operator communicates with the VODR with a standard IBM personal computer keyboard. A graphics liquid crystal display permits both the display of alphanumeric characters as well as graphics. The combination of the IBM style keyboard and the display makes for an easy operator interface. A 5-inch wide thermal graphics printer allow easy hard copies of the data.

APPLICATION OF THE REPETITIVE TIME DOMAIN REFLECTOMETER

For explosions involving multiple detonations, the cabling is laid out so the end of the cable is located where the first detonation begins and is then laid out so the next detonation and shock wave sequences make the cable progressively shorter to where the VODR instrumentation is located (see Figure 3).

Often several different channels of data may be required to fully instrument a shot. Repetitive Time Domain Recorder has the capability to collect data from two different coaxial cables. The frequency at which each cable is sampled is reduced, however.

In addition to the time domain reflectometer capabilities the VODR has remote analog recording capabilities that may be used for various environmental measurements having an influence on shot performance parameters. Examples of such data are temperatures and pressures. It is not intended at this time that analog recordings be made at the same time as the operation of the time domain unit reflectometry unit.

FIBER OPTIC TIME DOMAIN REFLECTOMETRY

Fiber optic cables use light waves for the transmission of data down a thin thread of glass. As with electrical cables, part of the light is reflected off the end of a broken fiber. The time between the transmission of the light and the return of the reflected pulse is a strong indication of how long the fiber is.

Except for the fiber optic cables and the special interface board the fiber optic system operates in the same fashion as the coaxial cable unit.

At the present time the fiber optic version of the CORRTX unit is under development.

In the system EG&G has developed, we have considered the needs of the blasting engineer. Data is available in the raw form, and in a graphical mode both processed and unprocessed. Hard copies of the data are available from a 5-inch wide thermal printer. Additionally, the data can easily be loaded into a lap top personal computer for permanent storage.

For more exacting technical information, see the technical description note.

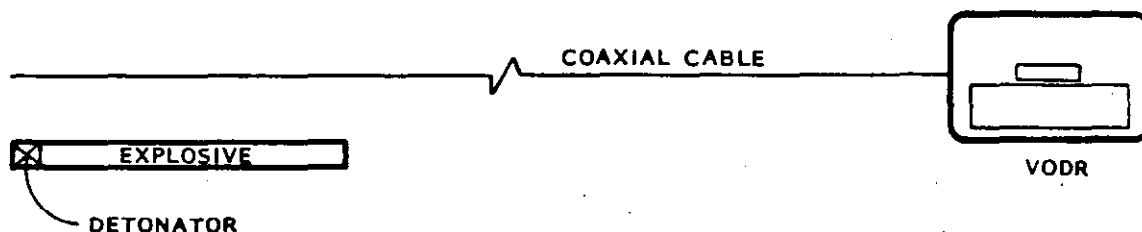
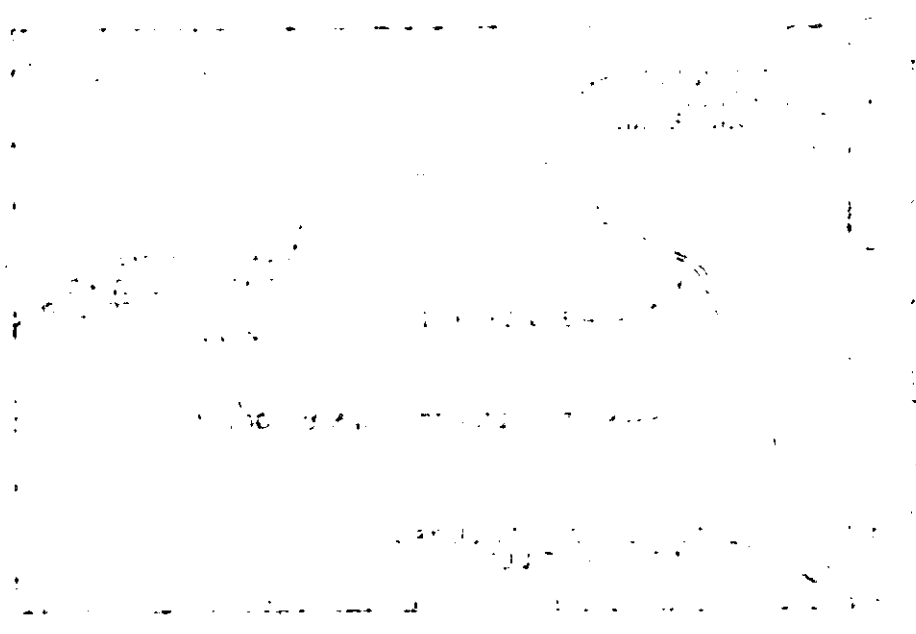
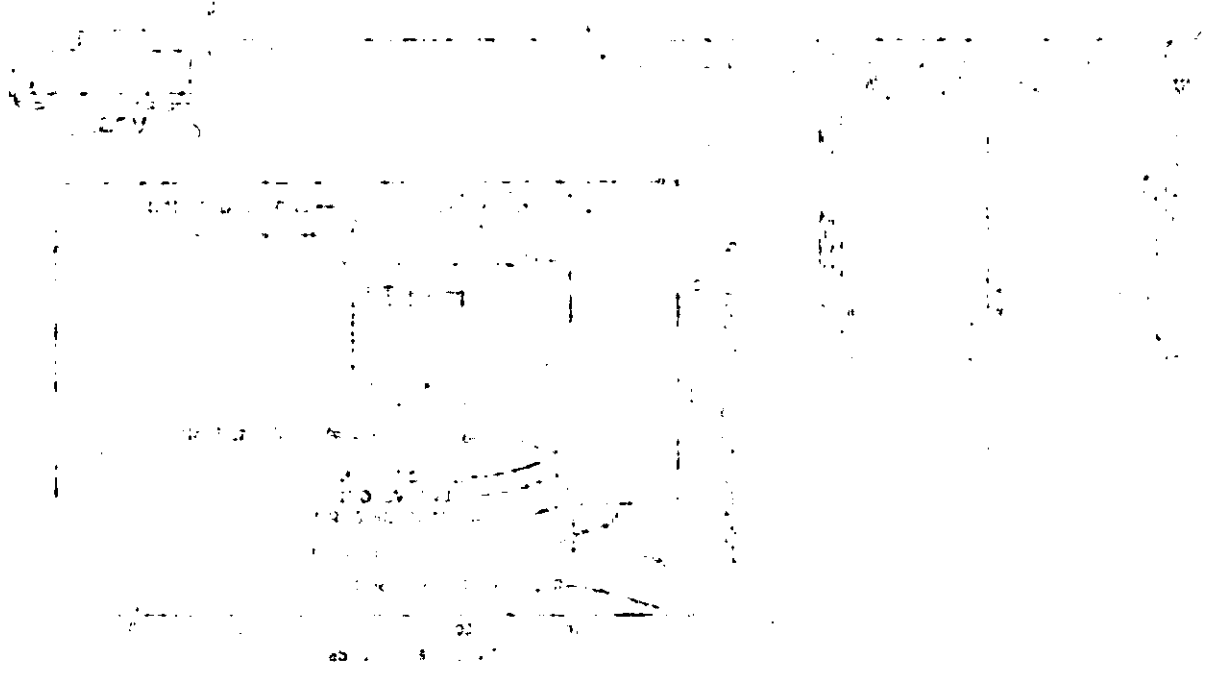


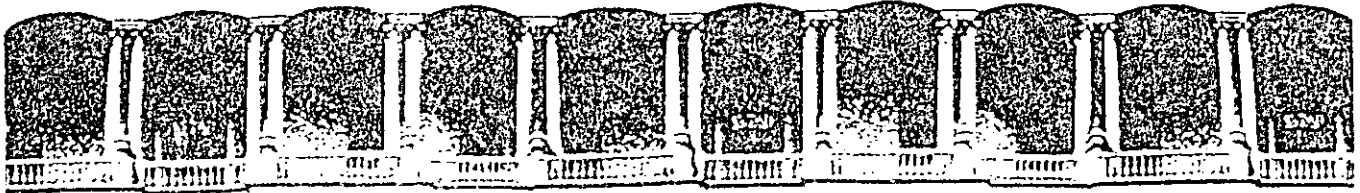
Figure 1. Principle of Operation



Technical drawing or diagram showing a cross-section of a mechanical part, possibly a shaft or a component of a machine. The drawing is very faint and difficult to discern.



Technical drawing or diagram showing a cross-section of a mechanical part, possibly a shaft or a component of a machine. The drawing is very faint and difficult to discern.



**FACULTAD DE INGENIERIA U.N.A.M.
DIVISION DE EDUCACION CONTINUA**

CURSOS ABIERTOS

**IV. CURSO INTERNACIONAL DE INGENIERIA GEOLOGICA APLICADA A
OBRAS SUPERFICIALES Y SUBTERRANEAS**

CUARTO MODULO:

TECNOLOGIA SOBRE EL USO DE EXPLOSIVOS

Del 22 al 26 de junio de 1992

*BLAST DESIGN CONSIDERATIONS FOR UNDERGROUN MINING AND
CONSTRUCTION OPERATIONS*

ING. RAUL CUELLAR BORJA

JUNIO - 1992

Blast design considerations for underground mining and construction operations

31

Étude d'abatage—considérations pour les opérations souterraines d'exploitations minières ou de construction

Sprengarbeitsentwürfe—Erwägungen für den Untertagebau und für Bauarbeiten

T. N. HAGAN, Principal, Blasting Engineer, Golder Associates Pty. Ltd, Melbourne, Australia

Because the great majority of completely new fractures are created by tension, the dynamic tensile breaking strain (ϵ_c) is an important property of massive rocks. As the degree of natural fissuring increases, the influence of ϵ_c decreases whilst that of the pre-existing cracks becomes greater. Important and highly controllable blast parameters include the diameter and length of blastholes; the type and configuration of charges; the shape, condition and development of effective faces; the available expansion volume for broken rock; the type and dimensions of the blasthole pattern; and initiation sequence and delay timing. The effects of these several parameters on blast design, the results of blasting (and especially fragmentation and overbreak) and excavation costs are presented. Greatest consideration is given to tunnelling, sub-level open stoping and the excavation of caverns.

Jusqu'en grande majorité les fractures entièrement nouvelles sont créées en tension, la déformation dynamique de rupture en tension (ϵ_c) est une propriété importante des roches massives. Quand le degré de fissuration naturelle croît, l'influence de ϵ_c diminue alors que celle des fissures pré-existantes grandit. Parmi les paramètres de sautage à la fois importants et faciles à contrôler on trouve le diamètre et la longueur des trous de tir; la configuration des charges et leur espèce; la forme, la condition et le développement des fronts de taille effectifs; le volume d'expansion disponible pour la roche brisée; les dimensions et le genre du plan de tir; et la séquence d'initiation et la durée des retards. Les effets de ces paramètres sur l'étude, les résultats de l'abatage (et surtout sur la fragmentation et le surabatage) et les coûts d'excavation sont présentés. Les considérations les plus grandes ont été données à l'excavation de tunnels, de cavernes et à l'abatage souterrain.

Da völlig neue Rupturen meistens durch Spannkraften hervorgerufen werden, ist die Bruchgrenze der dynamischen Zugspannung (ϵ_c) eine wichtige Eigenschaft massiver Felsen. Mit der Vergrößerung der natürlichen Spaltungstendenz verringert sich der Einfluss von ϵ_c , während sich der Einfluss vorherbestehender Risse vergrößert. Unter den wichtigen und höchstregulierbaren Spannungsparametern befinden sich der Durchmesser und die Länge der Sprenglöcher, die Art und Anordnung der Sprengladungen, die Form und die Beschaffenheit, sowie die Entwicklung zweckmässiger Stöße, das zur Verfügung stehende Ausdehnungsvolumen für Bruchgestein, die Art und Mäße der Sprenglochanordnung, die Zündfolge und Zündverzögerung. Die Auswirkungen dieser verschiedenen Parameter auf den Sprengarbeitsentwurf, die Folgen der Sprengung (insbesondere die Zerkleinerung und der Mehrausbruch) und die Ausschachtungskosten werden hier vorgelegt. Die Hauptbetrachtungen beziehen sich auf die Tunnelarbeiten, den offenen Teilsohlenbau und die Ausschachtung von unterirdischen Hohlräumen.

NOTATION

B, B ₀	- actual and optimum burden distance
d, d _c	- blasthole diameter and charge diameter
ϵ_c	- explosion-generated strain
ϵ_c^*	- rock's dynamic tensile breaking strain
E _f	- explosion energy per m ³ of rock
m	- face height
l _c	- charge length
l _{sc}	- length of stemming or collar
S, S ₀	- actual and optimum blasthole spacing
CR ₀	- vertical crater retreat

INTRODUCTION

In underground construction and metal mining, blasting is the dominant method of excavating rock and ore (hereinafter referred to collectively as rock). Therefore, in order to maximise the cost-effectiveness of most of these operations, it is first necessary to optimise blasting. Any blast optimisation programme can show appreciable progress only after a clear understanding of the effects of the principal blast parameters has been developed and carefully applied.

- overbreak control,
- (b) the blasthole length and/or face height (H) and, very importantly,
 - (c) the general reduction in drilling costs associated with increases in d.

Where d is small, the costs of drilling, charging, priming and stemming operations are high. If d is too small, these disadvantages outweigh the benefit of the slightly lower energy factor which results from the superior energy distribution within the rock to be broken. Where d is too large, the correspondingly larger blasthole pattern may well lead to inadequate fragmentation, especially in rocks which are strong and massive or contain widely spaced open discontinuities.

If the degree of fragmentation is to remain unchanged, an increase in d must be accompanied by an increase in EF. The required increase in EF is greatest for blocky rocks and least for highly fissured rocks. In entirely massive rocks, an intermediate increment in EF is needed.

In rocks which exhibit widely-spaced open discontinuities, fewer larger-diameter blastholes intersect a smaller percentage of effective blocks. Where such discontinuities are parallel to blastholes, they partially reflect explosion-generated strain waves. This provides better fragmentation between a charge and its adjacent discontinuity, but tends to produce oversize material beyond these discontinuities. Blocks which do not contain a charge experience strain waves which have been dissipated appreciably by the discontinuities through which the waves have been transmitted. Therefore, isolated blocks tend to be poorly fragmented. Such oversize material retards mucking rates and increases the wear, downtime and maintenance costs for materials handling equipment. Where the blocks between consecutive discontinuities are larger than those that can be handled by the available equipment, S should be restricted to a small multiple of the mean discontinuity spacing. If this is not done, any cost saving in drilling (achieved by increasing d) is usually outweighed by the higher combined cost of secondary blasting, digging, hauling and crushing.

In metal mines, it is unlikely that d will increase beyond the currently common range of 150-200mm. As d increases

- (a) there tends to be more wastage of drilling capacity (in already planned stopes at least) as a result of the stope width not being an exact multiple of the desired blasthole spacing;
- (b) it is more difficult to control damage to (adjacent) pillars, fill, draw points and haulage drives; and
- (c) it becomes necessary to increase the number of charge decks per blasthole which, in turn, complicates and increases the costs of charging, priming and stemming operations.

Although it is an important factor in the study of overbreak control, blasthole diameter, per

se, does not have an influence of the magnitude generally ascribed to it. For strong massive rocks, at least, overbreak can be well controlled even with blastholes having the following diameters, provided that other influential parameters (e.g., initiation sequence; delay timing, charge concentration in perimeter blastholes, etc.) are given sufficient attention:

- (a) 55-65mm blastholes in large-diameter tunneling, and
- (b) 60-90mm blastholes in benching (in cavern excavation).

If, in somewhat weaker rock benches, the use of larger-diameter blastholes is found to give considerable cost savings in excavation but also significant increases in overbreak, a highly compatible system may well be developed

- (a) by presplitting the walls of the bench, and/or
- (b) by using two individually delayed deck charges in blastholes within a certain distance of the walls.

Effects of Blasthole Alignment

Where deep 150-200mm downholes are drilled, the accuracy of blasthole alignment is most important in slot development, and especially for those earliest firing blastholes which are required to shoot to a raise (and particularly when the raise is bored rather than blasted).

When excavating caverns with downhole benches, the optimum blasthole inclination can vary between 0° (i.e., vertical) and about 25°. For benches with heights of about 4m and less and blasts which are always fired to a free face (i.e., a clean rock-air interface), satisfactory muckpiles can often be obtained by drilling vertical blastholes. As H increases, vertical front-row blastholes become progressively overburdened at bench floor level. Therefore, the replacement of vertical by inclined blastholes maintains toe burdens at their design values. In benches higher than about 4m, blastholes are usually angled at 10-25°.

In the common situation in which downhole bench blasts are fired into a buffer of broken rock, and especially in 4-10m high benches in strong massive rock, angled blastholes are much more effective. Because the buffer virtually prevents lateral movement of the blasted rock, blastholes must be aligned so that their charges provide sufficient upward displacement to leave well fragmented and loose muck. The upward heaving action with angled blastholes is appreciably greater than that with vertical blastholes. The optimum blasthole inclination increases with both bench height and rock strength.

Effects of Blasthole Length

The face height or desired depth of pull should be such that the driller has a high degree of control over blasthole deviation and, hence, over both B and S for the toes of charges. If blastholes are too long, both B and S will exhibit considerable variability. Where B and/or S is too small, fragmentation of an inadequate

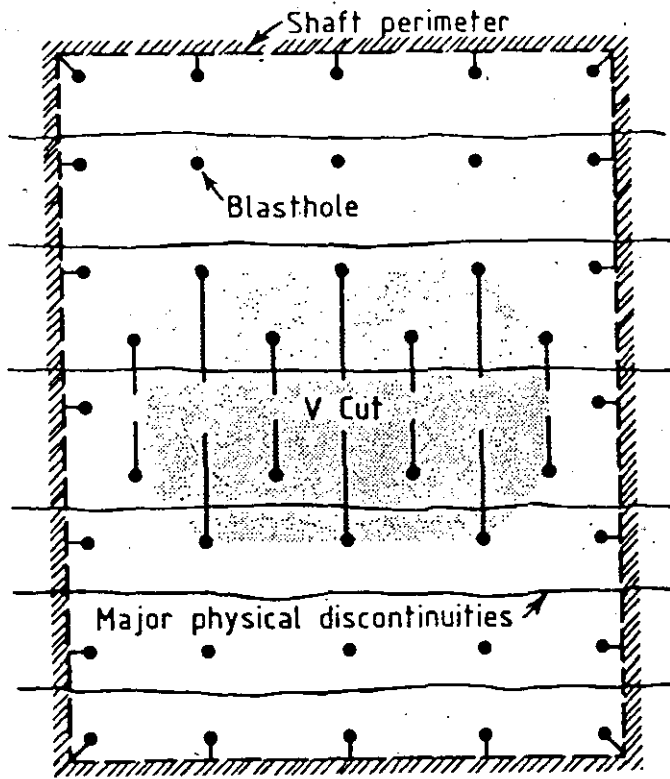


Fig. 1. Shaft round with V cut suitably aligned with dominant physical discontinuities.

EFFECTS OF ROCK PROPERTIES

The design and results of blasts are affected by numerous factors, most of which are controllable. Unfortunately, the most influential single blast parameter, rock properties, can be effectively controlled only to the limited extent that the direction of firing relative to that of the dominant physical discontinuities within the rock mass can be varied somewhat by changing the initiation sequence.

Effect of Dynamic Tensile Breaking Strain (ϵ_c)

If the fragmentation of blasted rock is to remain unchanged, any increase in ϵ_c (this being the effective resistance to breakage of a truly massive rock) necessitates

- (a) increases in energy factor (EF=explosion energy yield per m³ of rock), and
- (b) decreases in burden distance (B), blasthole spacing (S), stemming length (L) and, in some tunnelling and shaft sinking operations, depth of pull.

Increases in ϵ_c also have the important effect of reducing overbreak.

Where the strength of rock varies along the length of an excavation, efforts should be made to progressively modify the blast design, so that any particular design is highly compatible with the rock strength at that location.

Effects of Structural Properties

Any increase in the mean spacing between physical discontinuities demands that a greater degree of (new) breakage is created in the

blast. In massive rocks, therefore, EF values should be higher and B, S and L values lower than those in highly fissured rocks. When tunnelling in the latter rocks, it is usually easier and less costly to achieve the desired depth of pull. Where a tunnel is driven through rock that is very highly fissured, however, the depth of pull may need to be reduced so as to limit the area of unsupported back (i.e., roof).

In tunnelling, longer rounds can generally be pulled where the dominant discontinuities are normal to (cf. parallel to) the tunnel's axis. Where V cuts are used in sinking rectangular shafts, best results are usually obtained where the dominant discontinuities are parallel to the line joining the bottoms of the Vs (see Fig. 1).

Effects of structural properties on overbreak control

Highly-fissured rocks often cause problems associated with overbreak and the stabilities of the back and/or walls of the excavation. The associated costs of support and/or linings tend to increase with the number of discontinuities unless this potential problem is given extra consideration during both the design and execution phases of blasting.

Perimeter blasting techniques are most successful in massive rocks and in formations in which tight discontinuities are normal to the axes of blastholes. In rocks which exhibit closely spaced discontinuities, some overbreak will occur (principally along the discontinuities), irrespective of the steps taken to prevent it. The very blasting technique that produces the desired effect in a massive rock may be quite unsuitable in a highly fissured rock. Because they need to change with rock properties, the spacings and charge concentrations for perimeter blastholes are site specific.

The need for overbreak control increases with a decrease in the effective strength of the rock. The absence or a small percentage of half blastholes on the back of a tunnel in weak rock does not necessarily indicate that the performance of smoothwall blasts is poor; if smoothwall blasting were to be discontinued, overbreak would probably be much greater.

Smoothwall blasting is almost invariably better than presplitting in tunnelling and shaft sinking. Provided that the rock is either strong and massive or has tight/well cemented discontinuities normal to the blastholes, presplitting can be used to advantage to create sound smooth surfaces

- (a) in tunnel portals and, more importantly,
- (b) alongside benches in the excavation of caverns, crusher chambers, etc.

EFFECTS OF DRILLING

Effects of Blasthole Diameter

The blasthole diameter (d) is governed by (a) the required degrees of fragmentation and

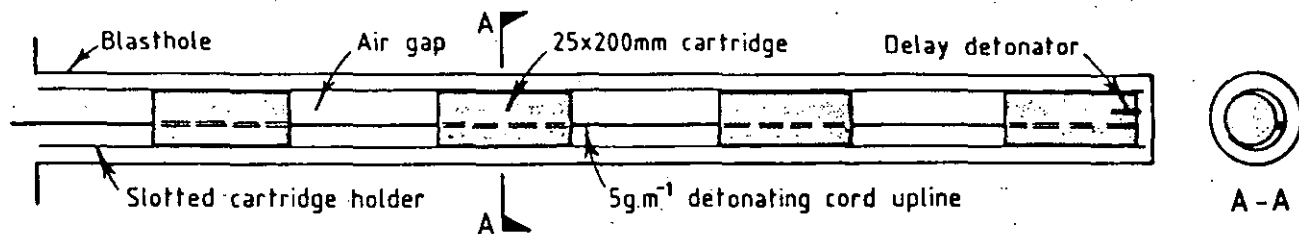


Fig. 2. An assembled slotted cartridge holder in a perimeter blasthole.

volume of rock will be excessive, and an appreciable proportion of the explosion energy will be manifested as air vibrations and flyrock. Where B and/or S is excessive, fragmentation will be sub-optimum. In those situations in which blastholes are tight and, therefore, drilled on close centres (e.g., in burn cuts in tunnelling), blasthole deviation is a strong restricting influence upon blasthole length.

Where fans of downholes are drilled in an orebody bounded by a weak footwall and/or hangingwall, the base of any charge should not be within the weak wall. If blastholes are knowingly drilled too long, they should be backfilled with drill cuttings so as to provide a stand-off distance of about $4d$ between the charge and the ore/waste contact. Should the base of the charge detonate within the waste or with an inadequate stand-off distance, some of the waste will be broken and intermixed with the

causing appreciable dilution. If the waste contains persistent physical discontinuities which run parallel to the contact, explosion gases could well stream into, wedge open and extend these causing

- (a) very considerable dilution by slabbing and, quite possibly,
- (b) a major stability problem.

EFFECTS OF CHARGE PROPERTIES

Effects of Explosive Type

Explosives are and should be selected on the basis of cost-effectiveness rather than technical efficiency. Currently, the energy yield per unit cost is usually greater for ANFO than for any other explosive. Largely for this reason, ANFO is used in nearly all operations with dry blastholes, even though the technical efficiency of ANFO may be somewhat lower than that of a more costly explosive.

In mines that drill deep 100-200mm blastholes, there is an incentive to maximise the percentage of blastholes that break through (at their bottoms). These self drain, thereby increasing the use of ANFO, with the option of using unmineralised ANFO (for increased energy yield) and ANFO/polystyrene (ANFOPS) mixtures (for reduced energy yields in perimeter blastholes).

Because they can be bulk loaded and their density varied between about 0.12 and 0.90g.cm^{-3} ANFOPS mixtures represent a useful tool for controlling overbreak and, thus, for reducing support requirements and increasing the load-

bearing capacity of pillars. In large ($>150\text{mm}$) diameter blastholes, polystyrene contents as high as 85% (volume basis) can be used without endangering the propagation stability of the detonation wave. In 45mm blastholes, 75% polystyrene would appear to be the upper practicable limit.

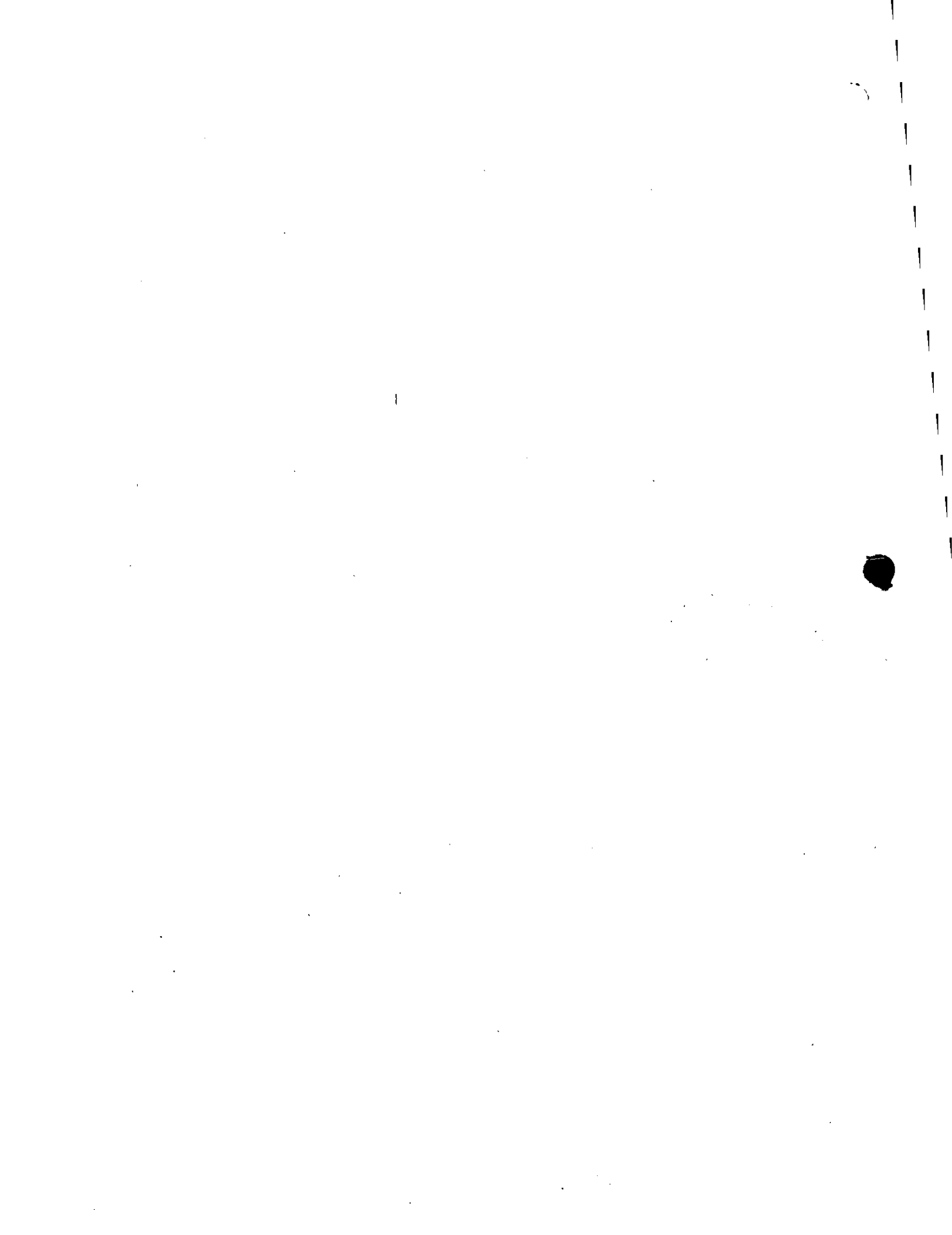
In vertical crater retreat (VCR) mining, there is a need, for all but the weakest rocks, to maximise the effective explosion energy yield per unit length of charge. This requirement is best met by using an explosive which exhibits high bulk strength and the ability to fill the entire cross-sectional area of the blasthole. Because stemming columns in VCR blasts are short, a high percentage of the resultant breakage is brought about by the explosive's strain wave energy. For this reason, the explosive should also exhibit a high velocity and acceleration to its steady-state velocity within a short distance from the primer. Currently, these several requirements are best met by TNT-sensitised watergel blasting agents. As the effective strength of the rock decreases, however, the performance of watergels with lower bulk strengths and velocities becomes more acceptable. Except in the weakest rocks, ANFO is unsuited to VCR blasting.

In order to achieve the required smoothwall effect in tunnels, it is usually necessary to charge those perimeter blastholes along the back and walls with an explosive which exhibits a relatively low energy yield per metre of charge length. Where blastholes are dry and the rock's effective strength is sufficiently high, ANFOPS mixtures can be used. In damp or wet conditions, special small-diameter smoothwall cartridges (which provide a low but, unfortunately, constant energy concentration) can be employed.

Where smoothwall blasting is necessary in tunnels which pass through rocks having highly variable strength and wetness, it is preferable to use perimeter charges which exhibit

- (a) an energy yield per unit length which can be varied between wide limits, and
- (b) a high degree of water resistance (so as to cope with the wettest possible conditions).

These two requirements are best met by using 25x200mm cartridges of a watergel (or gelatine dynamite) explosive which are spaced out within a slotted cartridge holder (see Fig. 2). The energy yield per unit length is reduced simply by increasing the length of the air gap between cartridges. Because one cannot rely upon the detonation wave to consistently propagate from one cartridge to the next across wide gaps, it is necessary to trace each charge with a strand



of detonating cord. The operator's degree of control over energy concentration is better with the slotted cartridge holder than with either ANFOPS or special smoothwall cartridges.

Effects of Charge Configuration

Where blastholes are short, continuous charges should be used, as these are more practicable and cost-effective than deck charges. In long blastholes, highest cost-effectiveness is usually achieved with deck charges. The lengths of stemming decks should increase with decreases in the effective strength of the rock.

The explosion-generated strain (ϵ) in the rock alongside a charge increases as the length:diameter (l/d) ratio of the charge increases in the approximate range 0-20; ϵ remains constant for $l/d \geq 20$. As l/d decreases below about 20, therefore, the optimum burden distance (B) for the charge decreases. When a charge becomes very short, B needs to be reduced appreciably. A centre-initiated charge with $l/d = 20$ also causes considerable breakage within an almost hemispherical zone off each of its ends. The extent of end breakage is such that overall fragmentation by a continuous charge with $l/d = 52$ is little if any better than that for two deck charges with $l/d = 20$ separated by a stemming deck with a length:diameter ratio of 12.

In operations in which H/d is less than about 60, blastholes are not long enough to hold two such deck charges. Because any move to smaller-diameter blastholes is to be avoided (on account of the associated higher drilling costs), such operations would need to increase H in order to employ deck charges. Where $H/d > 60$, the use of individually delayed deck charges reduces both overbreak and ground vibrations.

EFFECTS OF INITIATION AND PRIMING

Where detonation of a downline does not desensitise the explosive, toe-initiated charges have the following advantages over collar-initiated charges.

- (a) The detonation wave and conical strain wave front propagate towards the uncharged collar section of the blasthole, where two or more planar faces promote fragmentation. If this wave front were to propagate towards the toe of the blasthole, its energy would be gradually dissipated in the rock mass beyond the base of the blasthole, where the absence of faces would suppress the translation of strain energy into fragmentation.
- (b) Where a charge is collar primed, the pressure in that part of the blasthole near the primer has started to fall by the time the base of the charge detonates. When the gases are created in the base of the blasthole, they tend to stream along the blasthole towards the zone of low pressure. With toe priming, therefore, gases in the base of the blasthole fall from their initial pressure at a rate which is less than that for collar priming.

This assists in achieving the fragmentation and displacement required along a plane normal (or nearly so) to the base of the charge (the plane along which a strong blast effect is most needed).

The difference between collar and toe priming is greatest for long charges which are poorly stemmed or unstemmed. However, the advantage of toe priming is finite even for short unstemmed charges.

Where deck charges are used in deep large-diameter blastholes, the primer should be positioned at the mid-point of the charge. This priming geometry ensures

- (a) that the superposition of strain waves from simultaneously detonating charge elements is maximised, and
- (b) that the entire charge has been transformed into gases before the stemming at each end of the charge realises that a detonation has taken place.

EFFECTS OF BLAST GEOMETRY

Effects of Shape and Condition of Face(s)

Good fragmentation and displacement are more difficult to achieve where the face

- (a) is at an unfavourably large angle to the blasthole's axis,
- (b) subtends a small angle at the blasthole,
- (c) has not been cracked by one or more previous blasts, and/or
- (d) is choked with previously broken rock.

A decrease in the angle between a blasthole and its face causes increases in fragmentation and muckpile looseness, best results being obtained where blastholes are parallel to the face. Therefore, although the VCR system may have cost-effective application at some mines, the blasting component of this system tends to exhibit a poor technical efficiency.

The angle subtended at a blasthole by that part of the face which is reasonably near should be as large as possible. Where maximum fragmentation for a given energy factor is sought, the best practicable configuration is that provided by the blasthole/initiation pattern shown in Fig. 3. The biplanar effective faces created during such blasts explain why the fragmentation produced is significantly better than that achieved by say square V firings (in which effective faces are planar - Hagan, 1983).

In benching-type operations, blasting is facilitated by both irregularities in the face and cracks in the burden rock created by the previous blast. Where smooth unfractured faces exist, fragmentation is achieved with greater difficulty, especially where the face curves away from the blasthole. When blasting to a relief hole commences in a burn cut, good initial fragmentation is discouraged for reasons which include the following.

- (a) Even where the relief hole has a diameter as large as 200mm, it provides a face which has a very restricted area and an unfavourable shape.

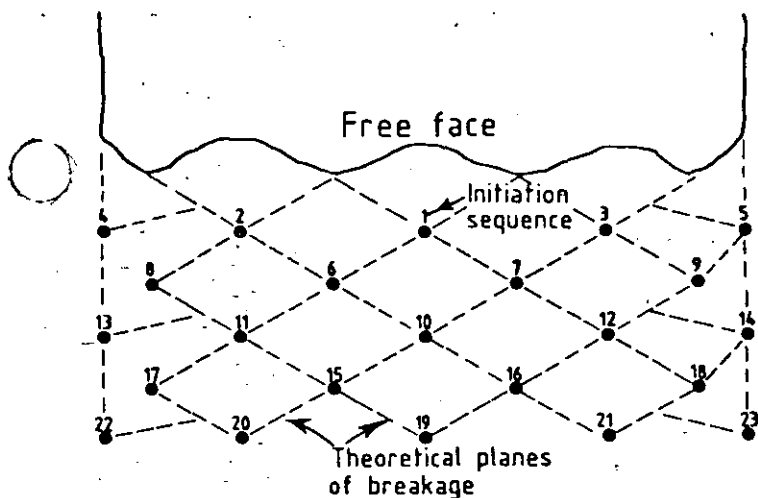


Fig. 3. Recommended blasthole/initiation pattern for downhole benching

(b) The rock immediately around the relief hole contains few if any cracks created by previous blasts, especially near the base of each blasthole.

This explains why the earliest firing charge has to be located very close to the relief hole(s). Excessive burden distances tend to cause rifling and/or dislocation of (and possible ejection of charges from) adjacent later-firing blastholes. For the above reasons, the burden distances in burn cuts (and for the earliest-firing charges around bored raises) must be appreciably less than those which are employed when identical charges shoot to an extensive parallel planar (or biplanar) face. Because a relief hole represents a relatively poor face, burn cuts should be designed so that each of the early firing blastholes can shoot to at least two equidistant relief holes. The combined cross-sectional area of relief holes should be increased when attempting to pull longer rounds.

Where good fragmentation and muckpile looseness are to be achieved at the lowest possible cost of drilling and blasting, blasts should be fired to a free face rather than to a buffer of rock broken by a previous blast. Buffer blasting

- (a) requires slightly smaller blasthole patterns and higher energy factors for the same degree of fragmentation and muckpile looseness, and
- (b) produces more overbreak, higher ground vibrations and, hence, an increased probability of instability.

Effects of Available Expansion Volume

When broken, all rocks expand. If the available expansion volume is less than about 15% of the volume of the solid rock in a blast, all fragmentation mechanisms will proceed to completion, but the particles of broken rock will still be highly interlocked and, therefore, will not flow/rill readily to the drawpoints. If the expansion volume is $\ll 15\%$, one or more of the later-acting breakage mechanisms may not even proceed to completion. Where mass pillar blasts are fired into slots, a minimum expansion volume

of 25% is usually required if consistently rapid mucking without hang-ups is to be achieved.

If the void volume provided by the relief hole(s) in a burn cut is too small, recementation of the finely fragmented rock tends to take place. Wherever possible, the void volume should be $\leq 15\%$ of the volume of the cut. In rocks which have a tendency to freeze, the void volume should be as great as is practicable if the probability of leaving long butts is to be minimized. Burn cuts with very small void volumes can still be pulled to full depth provided that the energy factor (in the cut) is increased sufficiently; but rounds are pulled more consistently and to greater depths through the application of finesse rather than brute force.

Effects of Type of Blasthole Pattern

Ideally, blastholes should be drilled on equilateral triangular grids, since these provide the optimum distribution of energy within the rock mass to be broken and, hence, the best fragmentation. Where blastholes are vertical, $S = (1.15)B$, but when they are angled at θ° to the vertical, $S = (1.15)B \cos \theta$.

Effects of Burden Distance (B) and Blasthole Spacing (S)

For a given set of blast conditions, there is an optimum burden (B_0) for which the volume of suitably fragmented and loosened rock is maximum and toe conditions are acceptable. Normally, B_0 lies in the 20d-35d range; the coefficient of d tends to increase with a decrease in d and depends upon the properties of the explosive and, more particularly, the rock.

When B falls below B_0 , strain-wave fracturing increases and breakage by heave energy decreases. For a very small burden, strain-wave fracturing occurs so rapidly directly in front of the charge that much of the heave energy is lost as airblast and excessive kinetic energy of rock displacement before it is able to contribute fully to fragmentation.

When B increases beyond B_0 , the crack pattern around each charge fails to be extended to the face; beyond the limit of radial cracking, a bridge of unbroken rock extends across the face. Equally important is the fact that heave energy is unable to provide adequate displacement and its associated breakage. Gases are bottled up within blastholes for periods of time that are longer than optimum. In effect, the energy saved through the reduction in displacement is manifested as an increase in ground vibrations. In their struggle to escape to the atmosphere, these gases are obliged to stream into, wedge open and extend both natural discontinuities and strain wave-induced cracks all the way around the blasthole; forward-facing fissures and cracks are not preferentially extended. (Forward-looking cracks are extended preferentially when $B = B_0$).

In benching and sub-level open stoping with parallel blastholes, S is necessarily a function of the width of the blast block. As this width decreases and/or d increases, the number of blastholes in each row decreases. In narrow blasts with large-diameter blastholes, therefore, S may need to be considerably less than the (desired) optimum spacing (S_0) for those particular conditions. If $S < S_0$, then B should also be $< B_0$. The prevention of such inefficiencies should be a significant consideration when selecting d for a given situation. It should also be recognised that less overbreak can be achieved by selecting a spacing for perimeter blastholes which is 15-25% less than that for other blastholes in the row or ring (see Fig. 3).

Should the walls of bench blasts be presplit, it is important to ensure

- (a) that the distance between the end production blastholes and the presplit plane lies in the $(0.35)S - (0.5)S$ range (the optimum value being determined by closely supervised trials on site), and
- (b) that the presplit plane extends at least two burden distances beyond the longitudinal extremity of the blast.

Effects of Size and Shape of Blast

In sub-level open stoping and downhole benching, blasts should be as large as is practicable. Where small numbers of large blasts are fired, there are fewer boundaries between blasts. Fragmentation at such boundaries tends to be poorer than that within the heart of a blast block; this is largely due to

- (a) large rock fragments (their size being controlled largely by pre-existing discontinuities) falling off the newly created backs, walls and faces after the blast, and
- (b) gases liberated in front-row blastholes escaping rapidly through cracks (resulting from overbreak caused by the previous blast) and thus contributing less to fragmentation and muckpile looseness.

In the interests of productivity, there is usually an incentive to fire as many rows of blastholes as possible in a single shot. Fragmentation generally improves with an increase in the number of rows. In massive or blocky rocks, single-row blasts often give inadequate fragmentation. Unfortunately, however, overbreak and ground vibrations increase with the number of rows. This is because progressive relief of burden is achieved with greater difficulty towards the back of a deep blast. Where there are too many rows, back-row charges will not see an effective free face. The overbreak and ground vibrations created by such (overconfined) back-row charges are considerably greater than those for charges which can displace their burden rock forwards with reasonable ease.

Ideally, blast blocks should have a length: width ratio > 3 . With such elongated blasts, lateral movement of the burden rock is not

suppressed appreciably by the drag forces imposed by the (stationary) rock alongside the blast block. Where the number of rows of blastholes exceeds the number of blastholes within a given row, the blast becomes a trench-type shot in which forward movement is restricted, particularly towards the back of the blast. Wherever forward movement is less than a certain critical value, fragmentation and especially muckpile looseness are reduced. In extensive trench-type shots, therefore, EF should be increased so as to counteract the adverse effect of the low length: width ratio of the blast block, thereby encouraging forward displacement which, in turn, promotes looseness and low-cost mucking.

EFFECTS OF INITIATION SEQUENCE AND DELAY TIMING

In any multi-row blast (including tunnelling rounds), it is most important that charges detonate with the sequence and timing which maximise the successive development of free faces which are as extensive as possible (and preferably concave) and reasonably near. When allocating delay numbers in initial designs, operators should construct theoretical lines of breakage for each charge. By doing this, any instances of poor sequencing are exposed, and alternative superior delay allocations can then be made.

The rock fragmented by the first one or few charges in a burn cut is ejected laterally into the void provided by the relief hole(s) before being swept outwards along the tunnel's axis. The time taken for these rock fragments to be completely swept from the cut is considerable (typically ≥ 100 ms). It follows, then, that the delay between consecutive detonations should exceed 100ms if the probability of choking is to be minimised. Where charges are fired on consecutive numbers of a millisecond series of delay detonators, good progressive relief of burden is not achieved and, as a consequence, there is a higher risk of choking and a frozen cut.

Events in the cut are often so remote from the perimeter of a tunnel blast that there is a tendency to believe that their effects on overbreak are insignificant. But such is not the case. If progressive relief is not achieved in the cut, all later-firing charges will be effectively overconfined as a result of the choked conditions in front of them. Each charge will then create more overbreak. Minimal blast damage requires that every charge fragments and displaces its burden rock forwards with reasonable ease.

In benching, initiation should commence at or close to the centre of the first row. Delays should be allocated so as to maximise progressive relief and to minimise overbreak and ground vibrations. If possible, the delay allocation should ensure the successive development of biplanar free faces for the highest possible percentage of charges in the blast (see Fig. 3). Charges should not be fired in a square

V or rectangular V formation, especially when downhole bench blasts with a length:width ratio < 1 shoot into a buffer of broken rock. Muckpile characteristics will be promoted by selecting a blasthole/initiation pattern like that shown in Fig. 3.

CONCLUSIONS

Man's control over the results of blasts (and especially fragmentation, muckpile looseness and overbreak-induced instability) and, hence, over the costs of underground mining and construction operations is strongly geared to

- (a) his understanding of the effects of rock properties and each of the more controllable blast parameters, and
- (b) his ability to synthesize the elements of this knowledge into a totally compatible blast design for the particular operating conditions/restraints.

Such expertise is not gained lightly. If its momentum is to be maintained or, preferably, increased, progress in blasting will continue to require the unified application of relevant engineering principles and experience to both

the design and execution phases of blasting. There is a need for blasting engineers to work in closer technical cooperation with engineering geologists and stability specialists. If blast designs are based upon a paucity of obtainable data and/or are applied without sufficient care and precision, the potential value of accumulated knowledge will not be realised and the costs of underground excavations will be unnecessarily and irresponsibly high.

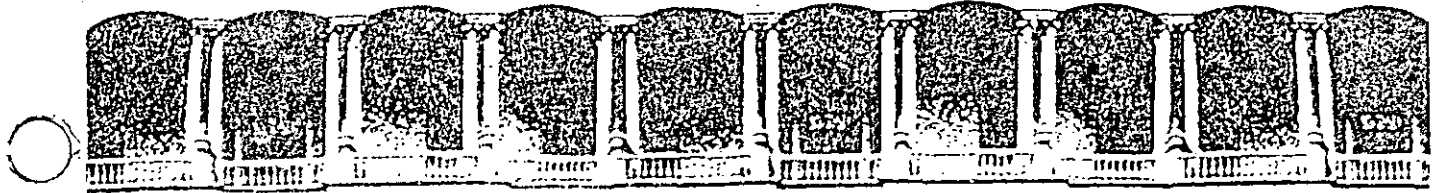
ACKNOWLEDGEMENT

The author gratefully acknowledges the contributions made by his colleagues and clients to many of the blast design principles and concepts presented in this paper.

REFERENCE

- Hagan T.N. The influence of controllable blast parameters on fragmentation and mining costs. Proc. First Int. Symp. on Rock Fragmentation by Blasting, Lulea, Sweden, Vol.1, p.31-51 (1983).





**FACULTAD DE INGENIERIA U.N.A.M.
DIVISION DE EDUCACION CONTINUA**

CURSOS ABIERTOS

**IV. CURSO INTERNACIONAL DE INGENIERIA GEOLOGICA APLICADA A
OBRAS SUPERFICIALES Y SUBTERRANEAS**

CUARTO MODULO:

TECNOLOGIA SOBRE EL USO DE EXPLOSIVOS

Del 22 al 26 de junio de 1992.

SURFACE BLAST DESIGN

ING. RAUL CUELLAR BORJA

JUNIO _ 1992

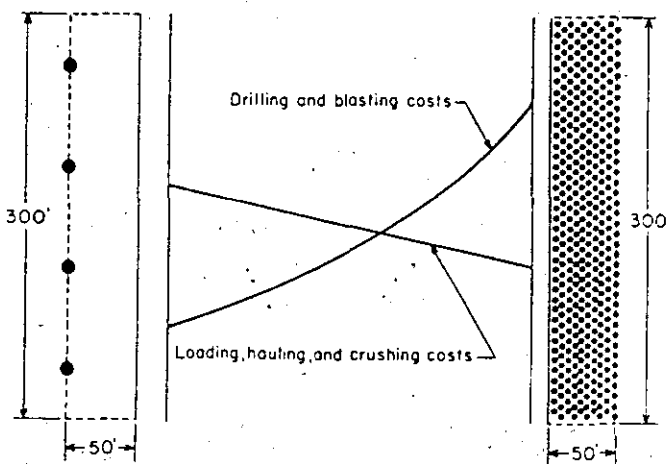
SURFACE BLAST DESIGN

This article is an excerpt from Bureau of Mines circular IC 8925,
"Surface Blast Design."

BLASTHOLE DIAMETER

The size of blasthole is the first consideration of any blast design. The blasthole diameter, along with the type of explosive being used and the type of rock being blasted, will determine the burden. All other blast dimensions are a function of the burden. This discussion assumes that the blaster has the freedom to select the borehole size. In many operations one is limited to a specific size borehole based on available drilling equipment.

Practical blasthole diameters for surface mining range from



Blast area = 15,000 sq ft
Borehole diameter = 20 in
Number of holes = 4
Total borehole area = 1,256 sq in
Burden = 50 ft
Spacing = 75 ft

Blast area = 15,000 sq ft
Borehole diameter = 2 in
Number of holes = 400
Total borehole area = 1,256 sq in
Burden = 5 ft
Spacing = 7.5 ft

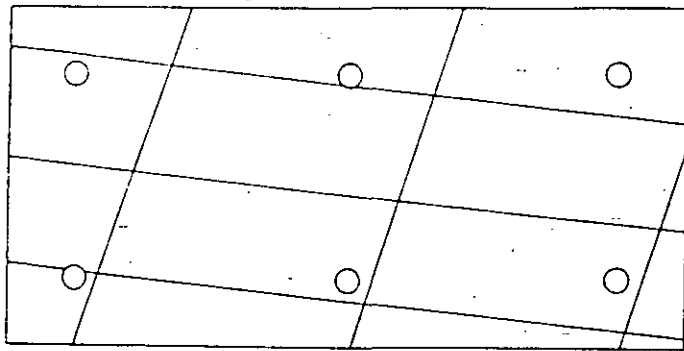
Figure 65.—Effect of large and small blastholes on unit costs.

2 to 17 in. As a general rule, large blasthole diameters yield low drilling and blasting costs because large holes are cheaper to drill per unit volume and less sensitive, cheaper blasting agents can be used in larger diameters. However, larger diameter blastholes also result in large burdens and spacings and collar distances and hence, they tend to give coarser fragmentation. Figure 65 illustrates this comparison using 2- and 20-in-diameter blastholes as an example. Pattern A contains four 20-in blastholes and pattern B contains 400 2-in blastholes. In all bench blasting operations some compromise between these two extremes is chosen. Each pattern represents the same area of excavation, 15,000 sq ft, each involves approximately the same volume of blastholes, and each can be loaded with about the same weight of explosive.

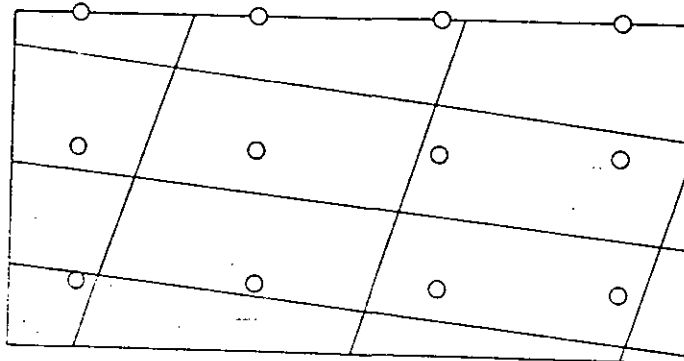
In a given rock formation, the four-hole pattern will give relatively low drilling and blasting costs. Drilling costs for the large blastholes will be low, a low-cost blasting agent will be used, and the cost of detonators will be minimal. However, in a difficult blasting situation, the broken material will be blocky and nonuniform in size, resulting in higher loading, hauling, and crushing costs as well as requiring more secondary breakage. Insufficient breakage at the toe may also result.

On the other hand, the 400-hole pattern will yield high drilling and blasting costs. Small holes cost more to drill per unit volume, powder for small-diameter blastholes is usually more expensive, and the cost of detonators will be higher. However, the fragmentation will be finer and more uniform, resulting in lower loading, hauling, and crushing costs. Secondary blasting and toe problems will be minimized. Size of equipment, subsequent processing required for the blasted material, and economics will dictate the type of fragmentation needed, and hence the size of blasthole to be used.

Geologic structure is a major factor in determining blasthole diameter. Planes of weakness such as joints and beds, or zones of soft, incompetent rock tend to isolate large blocks of rock in the burden. The larger the blast pattern, the more likely these blocks are to be thrown unbroken into the muckpile.



Larger holes



Smaller holes

Figure 66.—Effect of jointing on selection of blasthole

Note that in the top pattern in figure 66 some of the blocks are not penetrated by a blasthole, whereas in the smaller bottom pattern all of the blocks contain at least one blasthole. Owing to the better explosives distribution, the bottom pattern will give better fragmentation.

As more blasting operations are carried out near populated areas, environmental problems such as airblast and flyrock often occur because of an insufficient collar distance above the explosive charge. As the blasthole diameter increases, the collar distance required to prevent violence increases. The ratio of collar distance to blasthole diameter required to prevent violence varies from 14:1 to 28:1, depending on the relative densities and velocities of the explosive and rock, the physical condition of the rock, the type of stemming used, and the point of initiation. A larger collar distance is required where the sonic velocity of the rock exceeds the detonation velocity of the explosive or where the rock is heavily fractured or low in density. A top-initiated charge requires a larger collar distance than a bottom-initiated charge. As the collar distance increases, the powder distribution becomes poorer resulting in poorer fragmentation of the rock in the upper part of the bench.

Ground vibrations are controlled by reducing the weight of explosive fired per delay interval. This is more easily done with small blastholes than with large blastholes. In many situations where an operator uses large-diameter blastholes near populated areas, several delayed decks must be used within each hole to control vibrations.

Large holes with large blast patterns are ideally suited to an operation with the following characteristics: A large volume of material to be moved; large loading, hauling, and crushing equipment; no requirement for fine, uniform fragmentation; an

easily broken toe; few ground vibration or airblast problems (few nearby neighbors); and a relatively homogeneous, easily fragmented rock without excessive, widely spaced planes of weakness or voids. Many blasting jobs, however, present constraints that require smaller blastholes.

In the final analysis, the selection of blasthole size is based on economics. It is important to consider the economics of the overall excavation or mining system. Savings realized through indiscriminate cost cutting in the drilling and blasting program may well be lost through increased loading, hauling, and crushing costs and increased litigation costs owing to disgruntled neighbors.

TYPES OF BLAST PATTERNS

There are three commonly used drill patterns; square, rectangular, and staggered. The square drill pattern (fig. 67) has equal burdens and spacings, while the rectangular pattern has a larger spacing than burden. In both the square and rectangular patterns, the holes of each row are lined up directly behind the holes in the preceding row. In the staggered pattern (fig. 67), the holes in each row are positioned in the middle of the spacings of the holes in the preceding row. In the staggered pattern, the spacing should be larger than the burden.

The staggered drilling pattern is used for row-on-row firing; that is, where the holes of one row are fired before the holes in the row immediately behind them as shown in figure 68. The square or rectangular drilling patterns are used for firing V-cut (fig. 69) or echelon rounds. Either side of the blast round in figure 69 by itself would be called an echelon blast round. In V-cut or echelon blast rounds the burdens and subsequent rock displacement are at an angle to the original free face. Looking at figure 69, with the burdens developed at a 45° angle with the original free face, you can see that the originally square drilling pattern has been transformed to a staggered blasting pattern with a spacing twice the burden. The simple patterns discussed here account for the vast majority of the surface blasts fired.

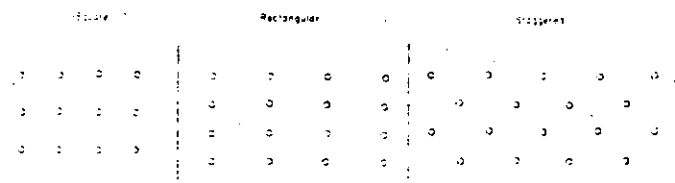


Figure 67.—Three basic types of drill pattern.

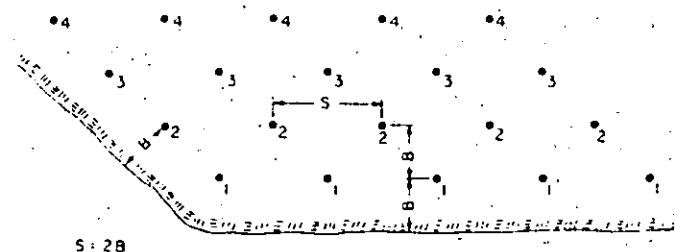


Figure 68.—Corner cut staggered blast pattern—Simultaneous initiation within rows (blasthole spacing, S, is twice the burden, B).

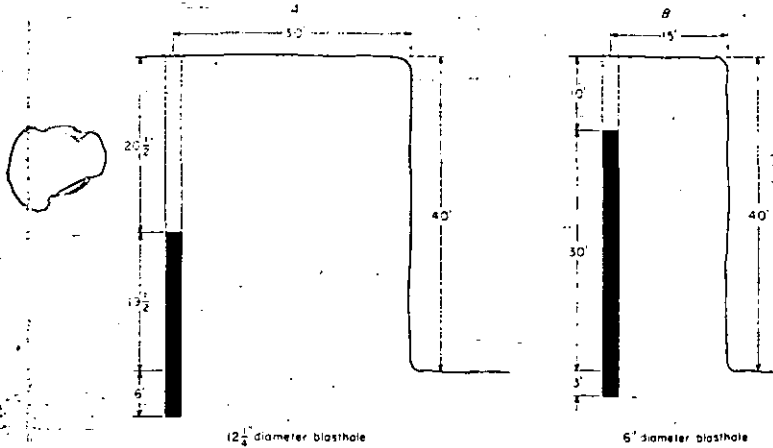


Figure 71.—Comparison of a 12¼-in-diameter (A) blasthole (stiff burden) with a 6-in-diameter (B) blasthole (flexible burden) in a 40-ft bench.

Priming the explosive column at the toe level gives maximum confinement and normally gives the best breakage. Other factors being equal, toe priming usually requires less subdrilling than collar priming.

Too much subdrilling is a waste of drilling and blasting expense and may also cause excessive ground vibrations owing to the high degree of confinement of the explosive in the bottom of blasthole, particularly when the primer is placed in the bottom of the hole. In multiple-bench operations, excessive subdrilling may cause undue fracturing in the upper portion of the bench below, creating difficulties in collaring holes in the lower bench. Insufficient subdrilling will cause high bottom, resulting in increased wear and tear on equipment and expensive secondary blasting. Table 5 summarizes the recommended subdrilling approximations.

Table 5.-Approximate J/B ratios for bench blasting

	Ratio
Open bedding plane at toe	0
Easy toe	0.1-0.2
Normal toe3
Difficult toe4- .5

B Burden J Subdrilling

**COLLAR DISTANCE
(STEMMING)**

Collar distance is the distance from the top of the explosive charge to the collar of the blasthole. This zone is usually filled with an inert material called stemming to give some confinement to the explosive gases and to reduce airblast. Research has shown that crushed, sized rock works best as stemming but it is common practice to use drill cuttings because of economics. Too small a collar distance results in excessive violence in the form of airblast and flyrock and may cause back-break. Too large a collar distance creates boulders in the upper part of the bench. The selection of a collar distance is often a tradeoff between fragmentation and the amount of airblast and flyrock that can be tolerated. This is especially true where the upper part of the bench contains rock that is difficult to break. In this situation the difference between a violent shot and one that fails to fragment the upper zone properly may be a matter of only a few feet of stemming. Collar priming of blastholes normally causes more violence than center or toe priming, and requires the use of a longer collar distance.

Field experience has shown that a collar distance equal to 70 pct of the burden is a good first approximation except where collar priming is used. Careful observation of airblast, flyrock, and



**Brings You . . .
State of The Art
Packaged Blasting Agents . . .**



Featuring . . .

- Controlled Density
- Accurate Oil Content
- Multiple Energy Levels
- Optional Packaging
- Wide Selection of Sizes
- Consistent Performance

NORTHERN DIVISION
Saginaw, MI
517/790-7477

WESTERN DIVISION
Pittsfield, IL
217/285-5531

EASTERN DIVISION
Upper Sandusky, OH
419/294-1946

SOUTHERN DIVISION
Evansville, IN
271/285-5531

fragmentation will enable the blaster to further refine this dimension. Where adequate fragmentation in the collar zone cannot be attained while still controlling airblast and flyrock, deck charges or satellite holes may be required.

A deck charge is an explosive charge near the top of the blasthole, separated from the main charge by inert stemming. If boulders are being created in the collar zone but the operator fears that less stemming would cause violence, the main charge should be reduced slightly and a deck charge added. The deck charge is usually shot on the same delay as the main charge or one delay later. Care must be exercised not to place the deck charge too near the top of the blasthole, or excessive flyrock may result. As an alternative, short satellite holes between the main blastholes can be used. These satellite holes are usually smaller in diameter than the main blastholes and are loaded with a light charge of explosives.

From the standpoint of public relations, collar distance is a very important blast design variable. One violent blast can permanently alienate neighbors. In a delicate situation, it may be best to start with a collar distance equal to the burden and gradually reduce this if conditions permit. Collar distances greater than the burden are seldom necessary.

SPACING

Spacing is defined as the distance between adjacent blastholes, measured perpendicular to the burden. Where the rows are blasted one after the other as in figure 68, the spacing is measured between holes in a row. However, in figure 69, where the blast progresses on an angle to the original free face, the spacing is measured at an angle from the original free face.

Spacing is calculated as a function of the burden and also depends on the timing between holes. Too close a spacing causes crushing and cratering between holes, boulders in the burden, and toe problems. Too wide a spacing causes inadequate fracturing between holes, accompanied by humps on the face and toe problems between holes (fig. 72).

When the holes in a row are initiated on the same delay period, a spacing equal to twice the burden will usually pull the round satisfactorily. Actually, the V-cut round in figure 69 also illustrates simultaneous initiation within a row, with the rows being the angled lines of holes fired on the same delay. The true spacing is twice the true burden even though the holes were originally drilled on a square pattern.

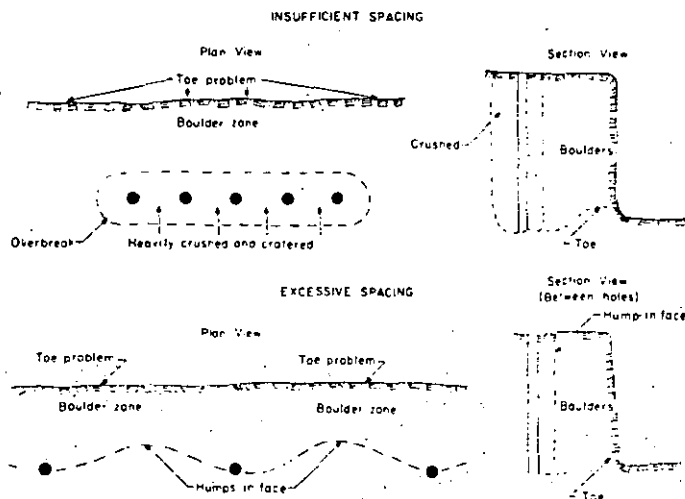


Figure 72.—Effects of insufficient and excessive spacing.

Field experience has shown that the use of millisecond delays between holes in a row results in better fragmentation and also reduces the ground vibrations produced by the blast. When

millisecond delays are used between holes in a row, the spacing-to-burden ratio must be reduced to somewhere between 1.2 and 1.8, with 1.5 being a good first approximation. Various delay patterns may be used within the rows, including alternate delays (fig. 73) and progressive delays (fig. 74). Generally, large-diameter blastholes require lower spacing-to-burden ratios (usually 1.2 to 1.5 with millisecond delays) than small-diameter blastholes (usually 1.5 to 1.8). Because of the complexities of geology, the interaction of delays, differences in explosive and rock strengths, and other variables, the proper

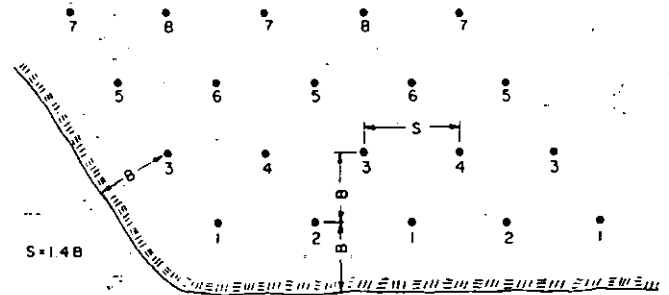


Figure 73.—Staggered blast pattern with alternate delays (spacing, S, is 1.4 times the burden, B).

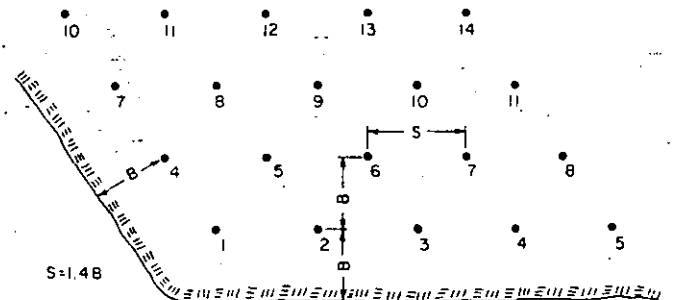


Figure 74.—Staggered blast pattern with progressive delays (spacing, S, is 1.4 times the burden, B).

spacing-to-burden ratio must be determined through onsite experimentation, using the preceding values as first approximations.

Except when using controlled blasting techniques such as smooth blasting and cushion blasting, the spacing should never be less than the burden.

HOLE DEPTH

In any blast design it is important that the burden and the blasthole depth (or bench height) be reasonably compatible. As a rule of thumb for bench blasting, the hole depth-to-burden ratio should be between 1.5 and 4.0. Hole depths less than 1.5 times the burden cause excessive airblast and flyrock and, because of the short, thick shape of the burden, give coarse, uneven fragmentation. Where operational conditions require a ratio of less than 1.5, the primer should be placed at the toe of the bench to assure maximum confinement. Keep in mind that placing the primer in the subdrill can cause increased ground vibrations. If an operator continually finds use of a hole depth-to-burden ratio of less than 1.5 necessary, consideration should be given to increasing the bench height or using a smaller drill.

Hole depths greater than four times the burden are also undesirable. The longer a hole is in respect to its diameter the more error there will be in its location at toe level, which is the most critical portion of the blast. A poorly controlled blast will result. Extremely long, slender holes have even been known to intersect.

High benches with short burdens also create hazards, such as a small drill having to put in the front row of holes near the edge of a high ledge or a small shovel having to dig at the toe of a precariously high face. The obvious solution to this problem is to use a lower bench height. There is no real advantage to a high bench height. Lower benches give more efficient blasting results, lower drilling cost and chances for cutoffs, and are safer from an equipment operation standpoint. If it is impractical to reduce the bench height, larger drilling and rock handling equipment should be used, which will effectively reduce the blasthole depth-to-burden ratio.

A major problem with long slender charges is the greater potential for cutoffs in the explosive column. Where it is necessary to use blast designs with large hole depth-to-burden ratios, multiple priming should be used as insurance against cutoffs.

DELAYS

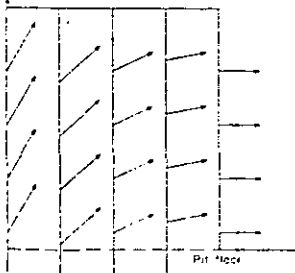
Millisecond delays are used between charges in a blast round for three reasons:

1. To assure that a proper free face is developed to enable the explosive charge to efficiently fragment and displace its burden.
2. To enhance fragmentation between adjacent holes.
3. To reduce the ground vibrations created by the blast.

There are numerous possible delay patterns, several of which were covered in figures 68, 69, 73, and 74.

Andrews, of du Pont, conducted numerous field investigations to determine optimum delay intervals for bench blasting and reached the following conclusions.

INADEQUATE DELAYS



ADEQUATE DELAYS

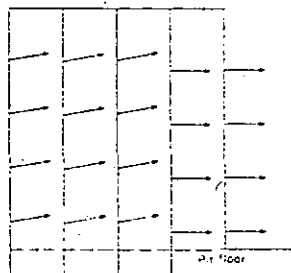


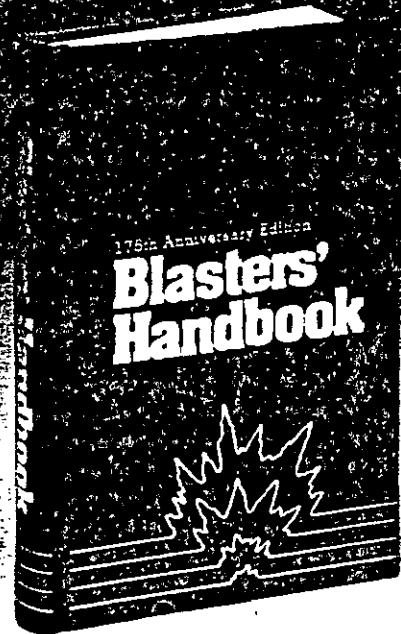
Figure 75.—The effect of inadequate delays between rows.

1. The delay time between holes in a row should be between 1 and 5 ms per foot of burden. Delay times less than 1 ms per foot of burden cause premature shearing between holes, resulting in coarse fragmentation. If an excessive delay time is used between holes, rock movement from the first hole prevents the adjacent hole from creating additional fractures between the two holes. A delay of 3 ms per foot of burden gives good results in many kinds of rock.

2. The delay time between rows should be two to three times the delay time between holes in a row. This is longer than most previous recommendations. However, in order to obtain good fragmentation and control flyrock, a sufficient delay is needed so that the burden from previously fired holes has enough time to move forward to accommodate broken rock from subsequent rows. If the delay between rows is too short, movement in the back rows will be upward rather than outward (fig. 75).

3. Where airblast is a problem, the delay between holes in a row should be at least 2 ms per foot of spacing. This will prevent airblast from one charge from adding to that of subsequent charges as the blast proceeds down the row.

**500 pages
of explosives
know-how...
only \$24.**



Latest edition. A practical guide on the latest and safest techniques for using modern explosives, including: initiating systems and firing techniques, water gels,* ANFO and dynamite.

Special sections on applications, equipment, accessories and practices.

Conveniently organized in textbook style; handy thumb index.

Sums up 175 years of Du Pont explosives experience: the how-to guide for explosives users.

Available by mail only. Send your check for \$24 to:

BLASTERS' HANDBOOK

Du Pont Company
Room G40052
Wilmington, DE 19898

*Only Du Pont and its licensees manufacture and sell TOVEX, the original water gel explosive.

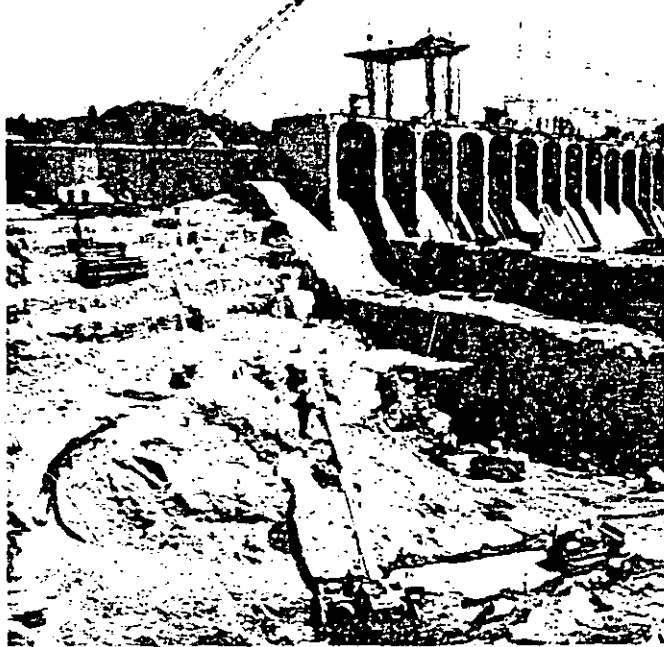
Order your copy now!





Here's Hercudet™

nonelectric delay blasting system

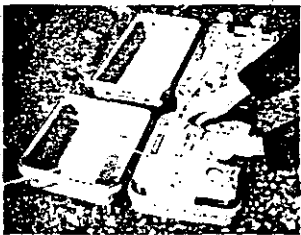


Mitchell Dam Redevelopment Project, Coosa River, Alabama, where Hercudet provided safe, cost-effective blasting.

For construction blasting, you can't beat Hercudet.

Plastic tubing replaces wires. There's no worry about stray currents, static electricity or radio frequency energy. And Hercudet is the only nonelectric system with circuit test capability.

A combustible gas enters the tubing only *after* shot preparations are complete. Hookup is *inert* until then. At firing time, the gas is ignited and the ignition travels noiselessly at 8,000 ft./sec. to initiate the high-strength Hercudet® caps. There's no airblast from the tubing.



Hercudet™ Blasting Machine

The use of Hercudet permits once-a-day firing. Hercudet eliminates the shot-size restrictions many users encounter with sequential timers. More holes can be fired in a single shot while vibrations are still held down.

Hercudet provides vibration control with tubing and fuse element delays and is totally sequential. It is more economical than detonating cord and other nonelectric systems.

For details contact your Hercules representative or Hercules Incorporated, Hercules Plaza, Wilmington, DE 19899, Attn: H. Citino, (302) 575-6500 and ask for Extension 3941.



XC B2-4

4. For the purpose of controlling ground vibrations, most regulatory authorities consider two charges to be separate events if they are separated by a delay of 9 ms or more.

Following these recommendations should yield good blasting results. However, when using surface delay systems such as detonating cord connectors and sequential timing blasting machines, the chances for cutoffs will be increased. To solve this problem, in-hole delays should be used in addition to the surface delays. For instance, when using surface detonating cord connectors, one might use a 100-ms delay in each hole. This causes ignition of the in-hole delays well in advance of rock movement, thus minimizing cutoffs. With a sequential timer, the same effect can be accomplished by avoiding the use of electric caps with delays shorter than 75 to 100 ms.

From the standpoint of simplicity in blast design it is best if all the explosive in a blasthole is fired as a single column charge. However, it is sometimes necessary, where firing large blastholes in populated areas, to use two or more delayed decks within a blasthole to reduce ground vibrations. Blast rounds of this type can become quite complex, and should be designed under the guidance of a competent person.

All currently used delay detonators employ pyrotechnic delay elements. That is, they depend on a burning powder train for their delay. Although these delays are reasonably accurate, overlaps have been known to occur. Therefore, when it is essential that one charge fires before an adjacent charge, such as in a tight corner of a blast, it is a good idea to skip a delay period. Development of blasting caps with electronic delays is a good future possibility.

POWDER FACTOR

Powder factor, in the opinion of the authors, is not the best tool for designing blasts.

Blast designs should be based on the dimensions discussed earlier in this chapter. However, powder factor is a necessary calculation for cost accounting purposes. In blasting operations such as coal stripping or construction work where the excavated material has little or no inherent value, powder factor is usually expressed in terms of pounds of explosive per cubic yard of material broken. Powder factors for surface blasting can vary from 0.25 to 2.5 lb/cu yd, with 0.5 to 1.0 lb/cu yd being most typical.

Powder factor for a single blasthole is calculated by the following formula:

$$P.F. = \frac{L(0.3405d)(D^2)}{(B)(S)(H)(27)}$$

where P.F. = powder factor, pounds of explosive per cubic yard of rock,

L = length of the explosive charge, feet,

d = density of the explosive, grams per cubic centimeter,

D = charge diameter, inches,

B = burden dimension, feet,

S = spacing dimension, feet,

and H = bench height, feet.

Many explosives companies publish tables that give loading densities in pounds per foot of blasthole for different combinations of d and D. Powder factor is a function of type of explosive, rock density, and geology. Table 6 gives typical powder factors for surface blasting.

Higher energy explosives, such as those containing large amounts of aluminum, can break more rock per pound than lower energy explosives. However, most of the commonly used explosive products have fairly similar energy values and thus have similar rock breaking capabilities. Soft, light rock requires less explosive per yard than hard, dense rock. Large-hole

patterns require less explosive per yard of rock blasted because a larger proportion of stemming is used. Of course, larger blastholes frequently result in coarser fragmentation because of poorer powder distribution. Massive rock with few existing cracks or planes of weakness requires a higher powder factor than a formation that has numerous, closely spaced geologic flaws. Finally, the more free faces a blast has to break to, the lower will be the powder factor. For instance a corner cut, with two vertical free faces, will require less powder than a box cut with only one vertical free face; and a box cut will require less powder than a sinking cut, which has only the ground surface as a free face. In a sinking cut it is desirable, where possible, to open a second free face by using a V-cut somewhere near the center of the round.

Table 6.-Typical powder factors for surface blasting

Degree of difficulty in rock breakage	Powder factor, lb/cu yd
Low	0.25-0.40
Medium40- .75
High75-1.25
Very high	1.25-2.50

When blasting materials that have an inherent value per ton, such as limestone or metallic ores, powder factors are sometimes expressed as pounds of explosive per ton of rock or tons of rock per pound of explosive.

**SECONDARY
BLASTING**

Some primary blasts, no matter how well designed, will leave boulders that are too large to be handled efficiently by the loading equipment or large enough to cause plugups in crushers or preparation plants. Secondary fragmentation techniques must be used to break these boulders.

In the case of boulders too large to be handled, the loader operator will set the boulders aside for treatment. Identifying material large enough to cause plugups is not always quite so apparent. The operator must be instructed to watch for material that is small enough for convenient loading but which is large enough to cause a bottleneck later in the processing cycle.

Secondary fragmentation can be accomplished in four ways:

1. A heavy ball suspended from a crane may be dropped repeatedly on the boulder until the boulder breaks. This is a relatively inefficient method, and breaking a large or tough (nonbrittle) rock may take a considerable period of time. This method is adequate where the number of boulders produced is not excessive.

2. A hole may be drilled into the boulder and a wedging device inserted to split the boulder. This is also a slow method but may be satisfactory where only a limited amount of secondary fragmentation is necessary. An advantage of this method is that it does not create the flyrock associated with explosive techniques or, to some degree with drop balls.

3. Loose explosive may be packed into a crack or depression in the boulder, covered with damp earthen material, and fired. This type of charge is called a mudcap, plaster, or adobe charge. This method is inefficient because of a lack of explosive confinement, and relatively large amounts of explosives are required. The result is considerable noise and flyrock, and often, an inadequately broken boulder. The system is hazardous because the primed charge, lying on the surface, is prone to accidental initiation by external impacts from falling rocks or equipment. External charges should be used to break boulders only where drilling a hole is impractical, and when used, extreme

caution concerning noise, flyrock, and accidental initiation through impact must be exercised. If it is found necessary to shoot a multiple mudcap blast, long delays or cap and fuse are not recommended.

4. The most efficient method of secondary fragmentation is through the use of small (1- to 3-in) boreholes loaded with explosives. The borehole is normally collared at the most convenient location such as a crack or a depression in the rock, and is directed toward the center of mass of the rock. The hole is drilled two-thirds to three-fourths of the way through the rock. Because the powder charge is surrounded by free faces, less explosive is required to break a given amount of rock than in primary blasting. One-quarter pound per cubic yard will usually do the job. Careful location of the charge is more important than its precise size. When in doubt it is best to estimate on the low side and underload the boulder. With larger boulders it is best to drill several holes to distribute the explosive charge, rather than placing the entire charge in a single hole. All secondary blastholes should be stemmed. As a cautionary note, secondary blasts are usually more violent than primary blasts.

Any type of initiation system may be used to initiate a secondary blast. For connecting large numbers of boulders, where noise is not a problem, detonating cord is often used. Electric blasting is also frequently used.

Although secondary blasting employs relatively small charges, its potential hazards must not be underestimated. Flyrock is often more severe and more difficult to predict than with primary blasting. Secondary blasts require at least as much care in guarding as do primary blasts. Secondary blasting can truly be called an art, with experience being an important key to success.

SEC

**NEW COST SAVING
BLASTING
TECHNIQUES**

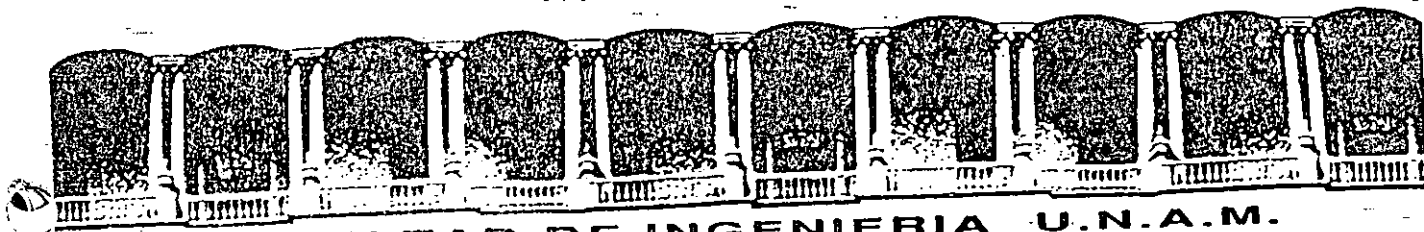
**LEARN TO SELECT EXPLOSIVES
AND PATTERNS AND TO BLAST
THE SIZE ROCK YOU WANT.**

**INVESTIGATE OUR
SEMINARS
TRAINING PROGRAMS &
CONSULTING SERVICES**

CONTACT: CALVIN KONYA

PRECISION BLASTING SERVICES
P.O. BOX 189 - MONTVILLE, OHIO 44064
PHONE (216) 474-6700





**FACULTAD DE INGENIERIA U.N.A.M.
DIVISION DE EDUCACION CONTINUA**

CURSOS ABIERTOS

**IV. CURSO INTERNACIONAL DE INGENIERIA GEOLOGICA APLICADA A
OBRAS SUPERFICIALES Y SUBTERRANEAS**

CUARTO MODULO:

TECNOLOGIA SOBRE EL USO DE EXPLOSIVOS

Del 22 al 26 de junio de 1992

**CHARGE CALCULATION METHODS FOR
TUNNEL BLASTING**

ING. RAUL CUELLAR BORJA

JUNIO - 1992

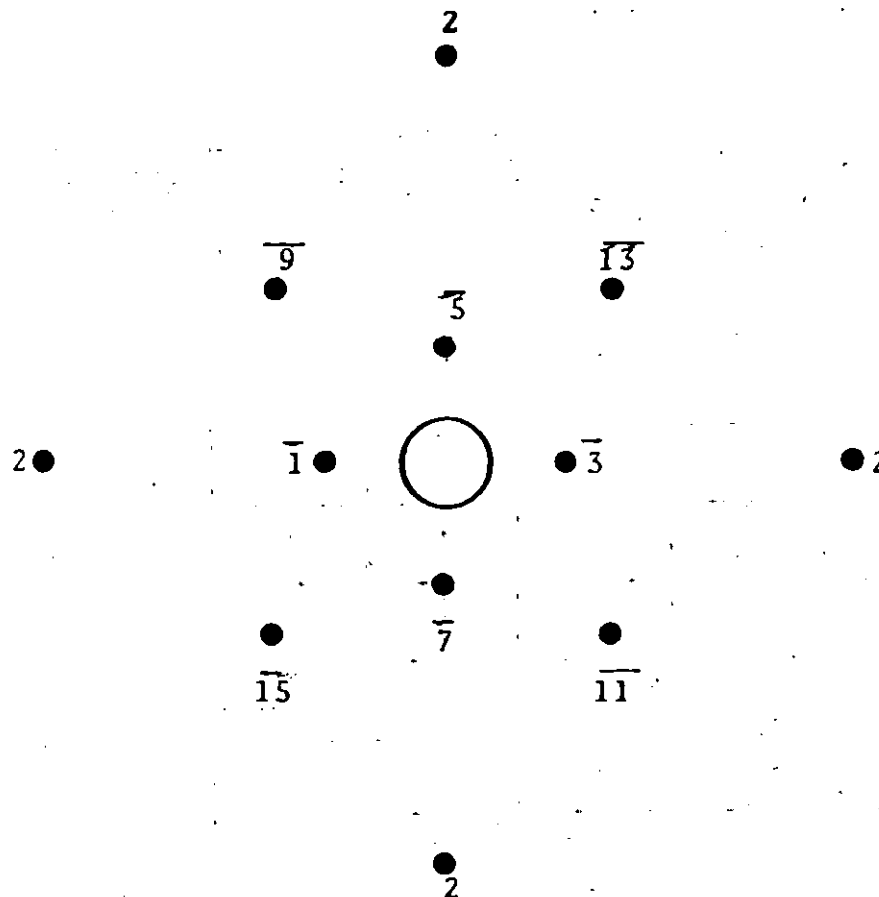
Knowing V' , hole depth H and the concentration of the bottom charge l_b , the table below provides burden V , spacing E , height of bottom charge h_b , concentration of column charge l_p and uncharged part h_o .

HOLE TYPE	V (m) $\times V'$	E (m) $\times V$	h_b (m) $\times H$	l_p (kg/m) $\times l_b$	h_o (m) $\times V$
Floor	1	1.1	1/3	1.0	0.2
Wall	0.9	1.2	1/6	0.4	0.5
Roof	0.9	1.2	1/6	0.3	0.5
Stopping $\uparrow \rightarrow$	1	1.1	1/3	0.5	0.5
Stopping \downarrow	1	1.2	1/3	0.5	0.5

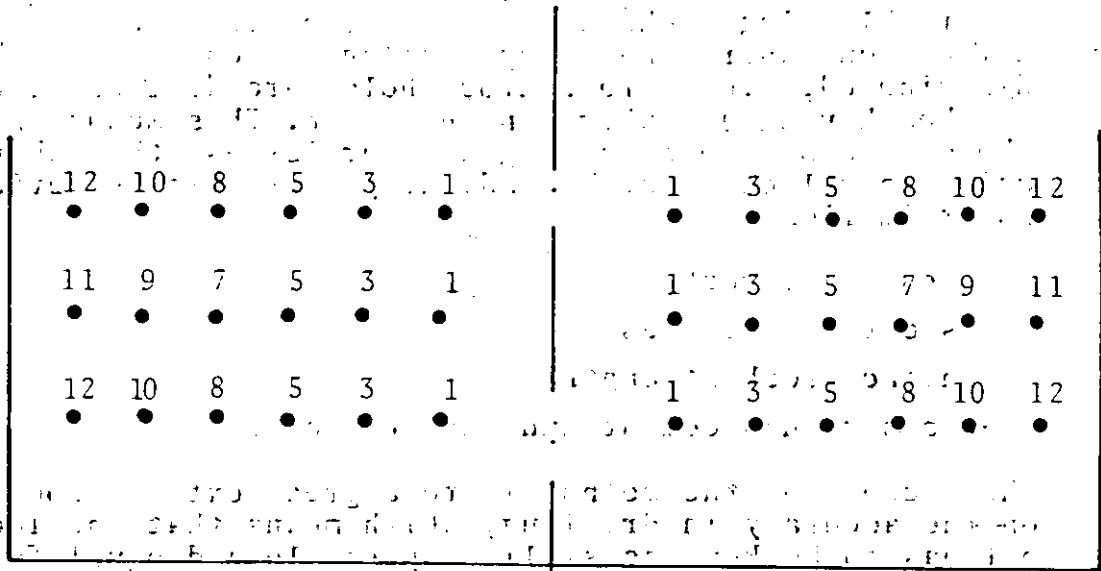
The design of the drilling pattern can now be carried out and the cut is fitted into the cross section in the most suitable way.

5. EXAMPLES OF IGNITION PATTERNS

Parallel hole cut

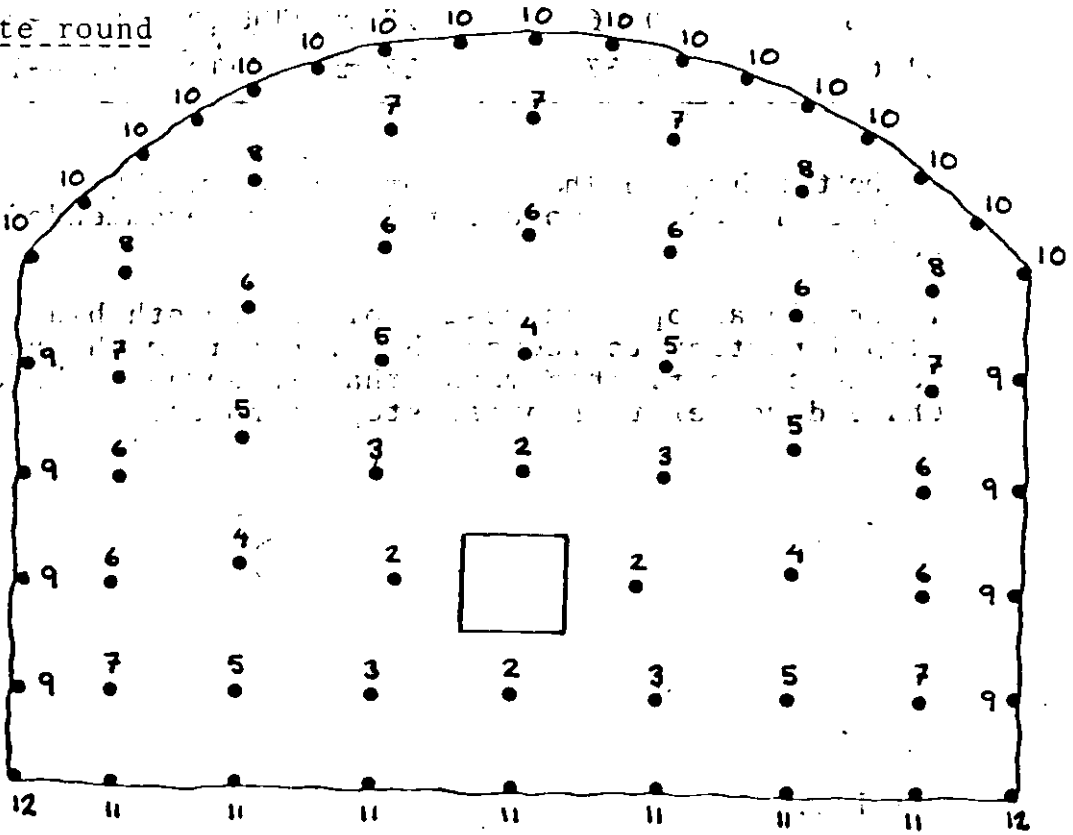


V-cut



MS-detonators

Complete round



MS-detonators

circumstances it was proved that the delay time must be at least 50 ms. As for the other holes this time could be reduced to 25 ms according to fig. 9. It must be pointed out that these delay times is an absolute minimum and ought to be somewhat higher to be sure on a good result.

RECOMMENDATION

At drifting and tunnelling one try to obtain the best total economical result. This is achieved as a rule at an advance per round of 95% or more of drilled depth.

Drilling and charging calculations shall be made so, that the conditions for a big advance per round increase, fig. 10. This is achieved by the following steps.

- Choose a large hole diameter in relation to the hole depth, which gives at least 95% advance per round and gladly more. If the drilling equipment is not suitable for drilling large holes, make more holes with less diameter according to the formula

$$D = d \cdot \sqrt{n}$$

D = fictitious large hole diameter

d = used large hole diameter

n = number of large holes

- Calculation of the conditions in relation to large hole diameter, alternatively opening width, according to the following

First quadrant $V = 1,5 \emptyset$

V is the largest burden = c/c-distance large hole/
small hole (m)

\emptyset is the diameter (m) of the large hole

Other quadrants $V = B$

V is the largest burden (m)

B is opening width (m)

- Always calculate with faulty drilling. A useful formula is

$$F_c = V (0,1 + 0,03 H) = 10,237 \cdot 0,03 \cdot 70 = 0,06 \text{ m}$$

F = faulty drilling

V = the largest burden

H = hole depth (m)

- Always drill the hole to a contemplated plan. A too deep hole damages the rock and if the hole is too shallow rock parties remain undestroyed. The result is poorer conditions for next round and a reduced advance per round.

- Always calculate the charges after the largest burden and always calculate with a certain safety margin.
- Choose interval number in a way that enough time is obtained for the rock to move. The two first holes are the most important.

Difference
in costs
per cu.m of rock

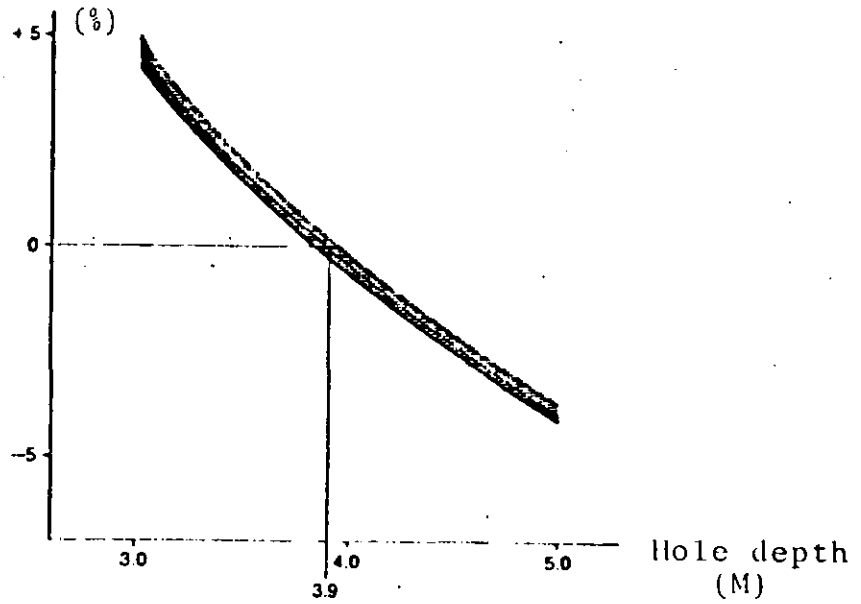


Fig 1. Change in costs per cu.m of rock at different hole depths and at the same percentage of advance per round.

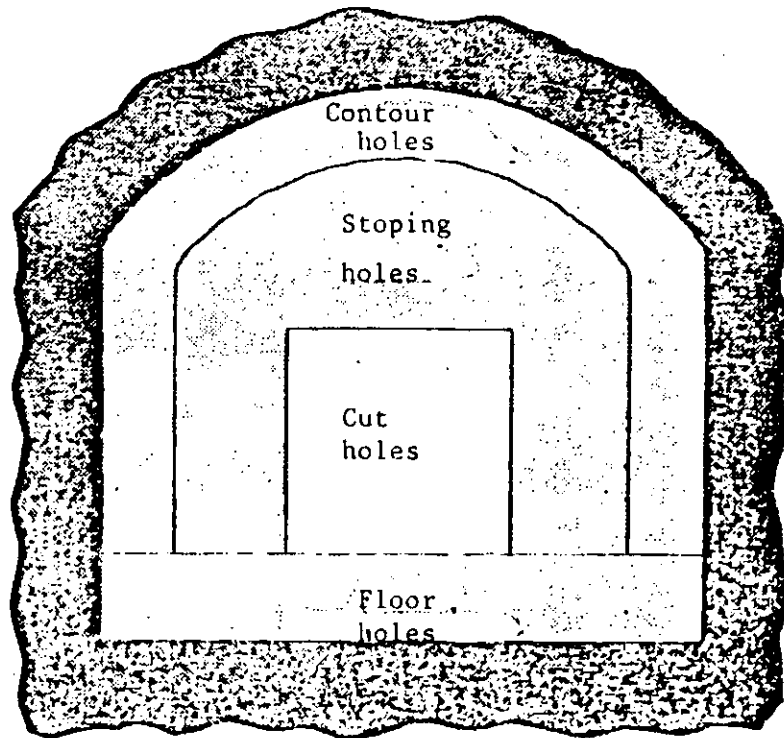


Fig 2. When blasting a tunnel round the result is very much depending on how you manage with the cut.

Advance
per round

(%)

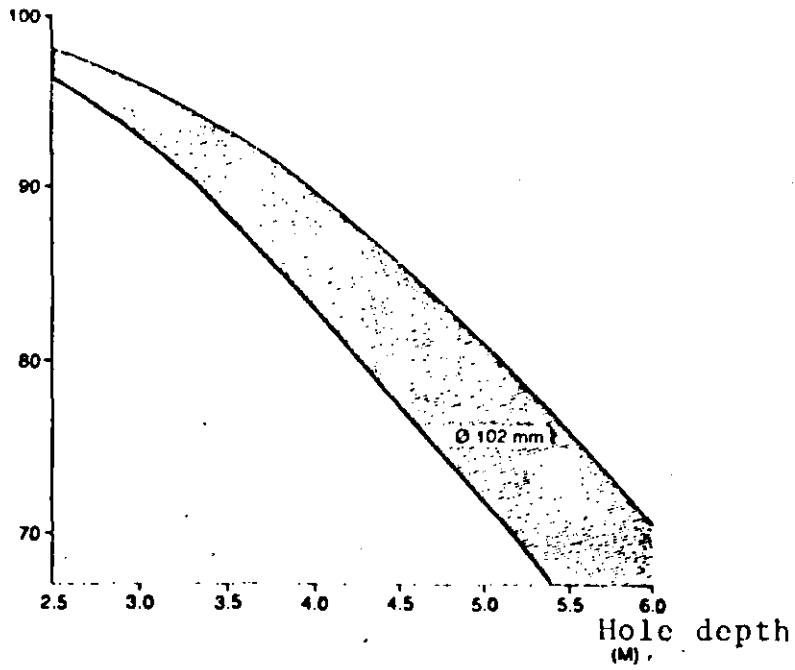


Fig 3. The relation between percentage of advance per round and hole depth at 102 mm large hole diameter.

Difference
in costs
per cu.m of rock
(%)

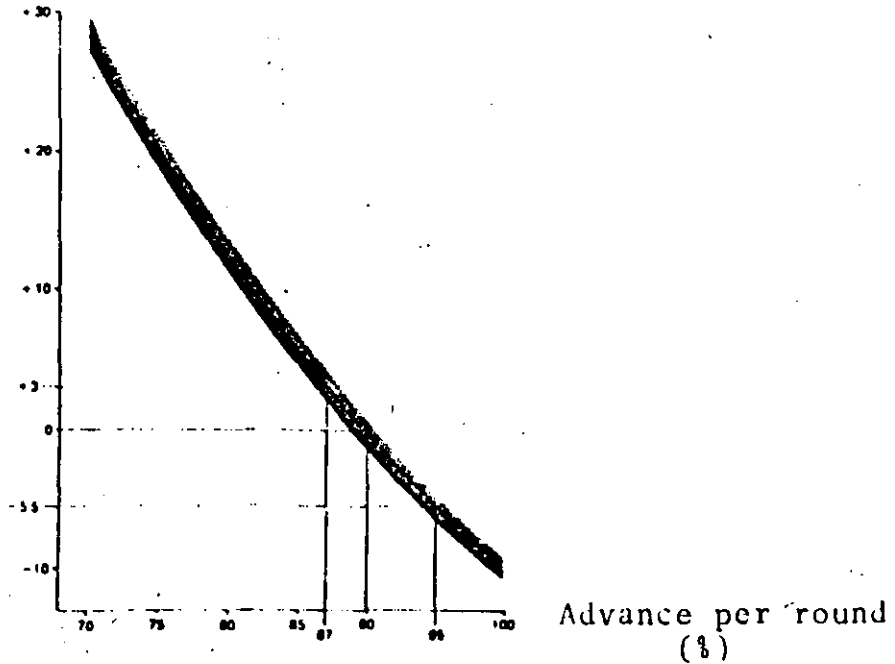


Fig 4. The change in costs for drilling/blasting per cu.m of rock at a changed percentage of advance per round but with the same hole depth.

Four section cut

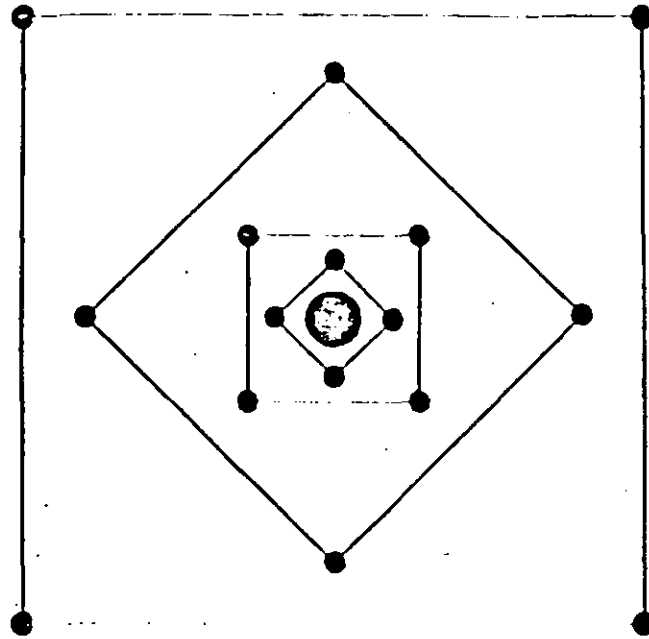


Fig 5. Parallel hole cut with a large hole surrounded by small hole with small burdens placed in a number of squares.

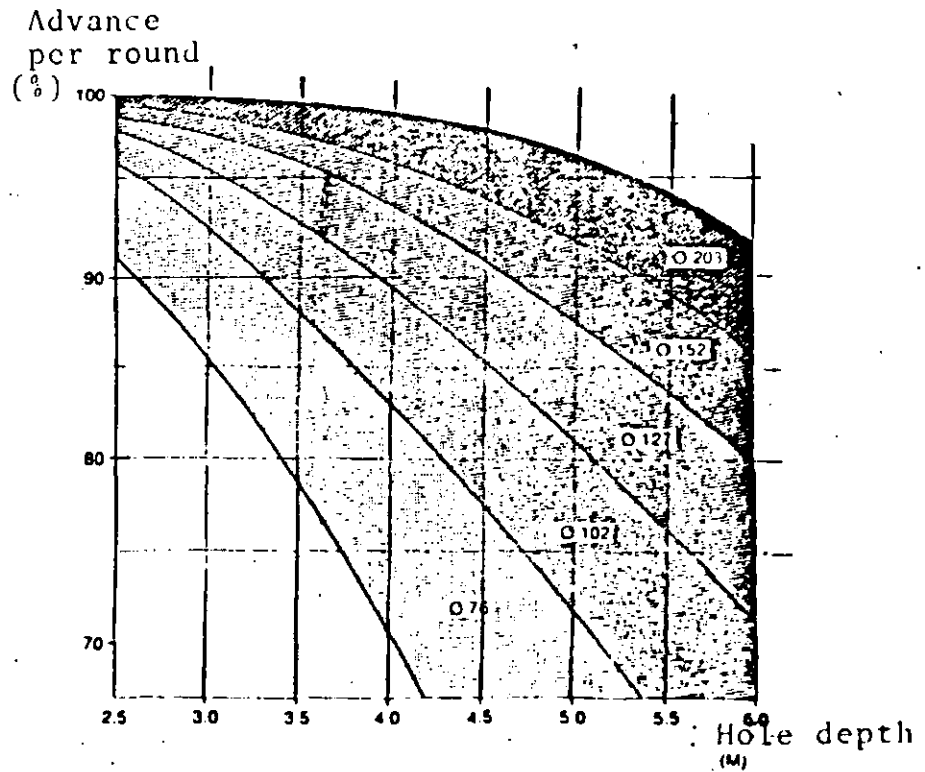


Fig 6. The relation between percentage of advance per round and the hole depth at different large hole diameters.

Charge concentration l_b

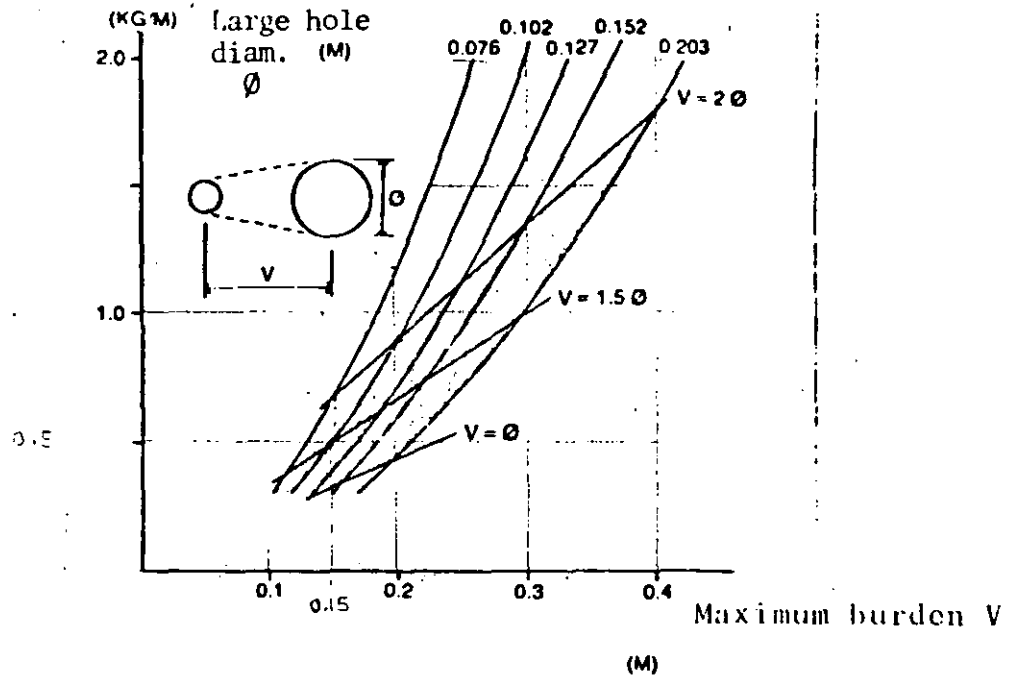


Fig 7. The relation between charge concentration (l_b) and largest burden (V) at different hole diameters (ϕ). As basic value is normally $V=1.5$ used.

Charge concentration l_b (KG/M)

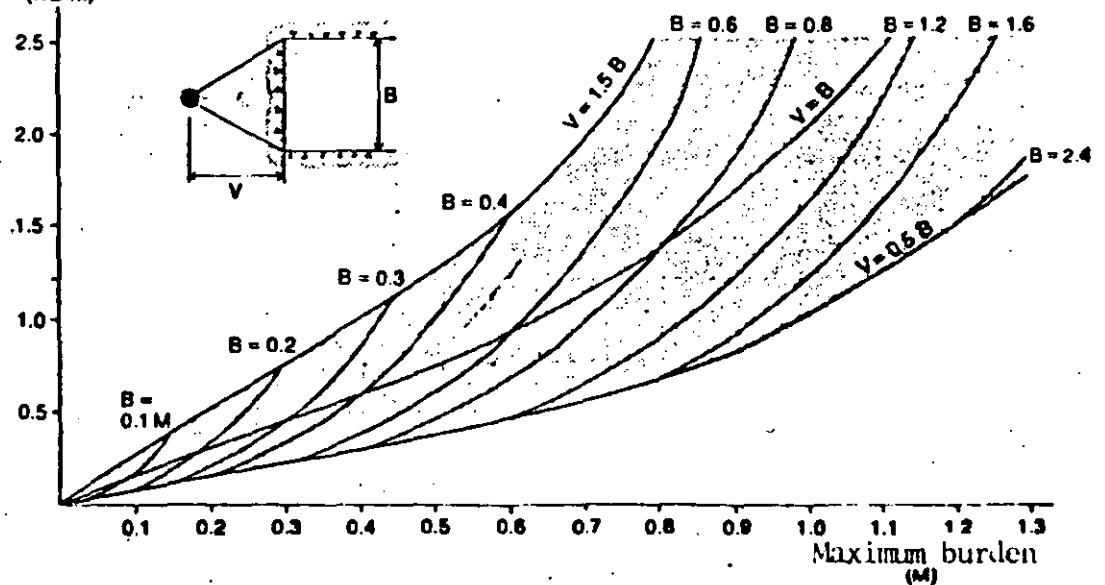
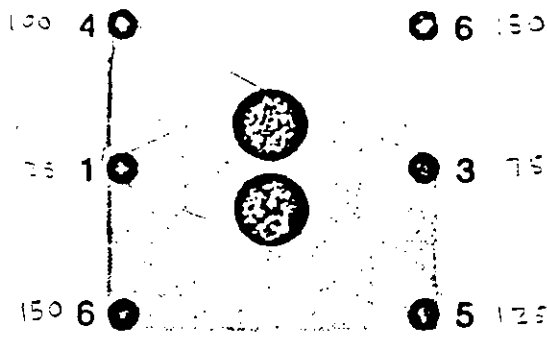


Fig 8. The relation between charge concentration (l_b) and largest burden (V) at different width of opening. As basic value is normally $V = B$ used.



MILLISECOND DETONATORS

<u>DELAY NUMBERS</u>	<u>DELAY TIMES</u>
1	25 MS
3	75 MS
4	100 MS
5	125 MS
6	150 MS

Fig 9. Shortest delay time for a large hole cut with 2 large holes of 76 mm.

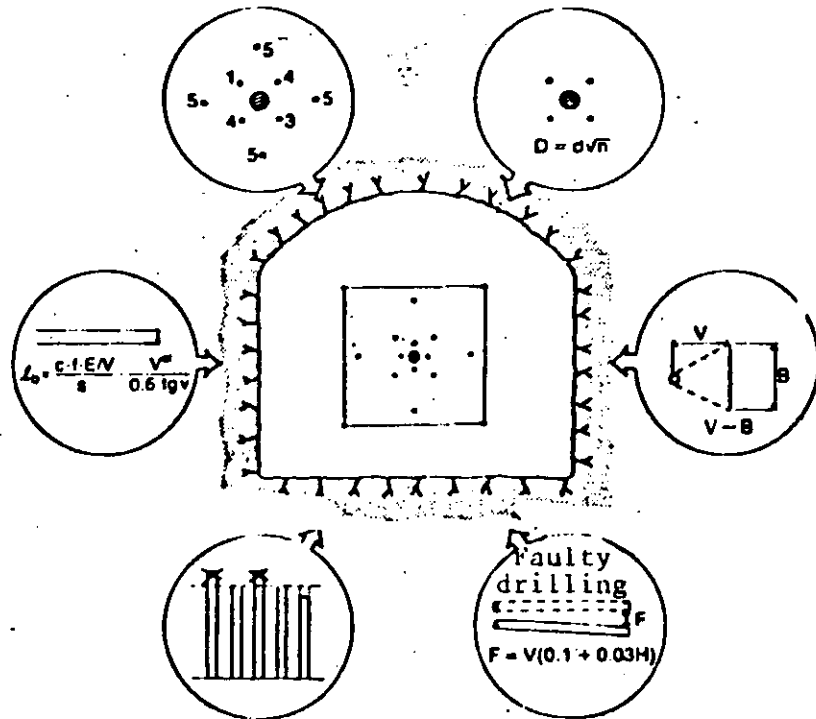


Fig 10. Recommendations to achieve a maximum advance per round.

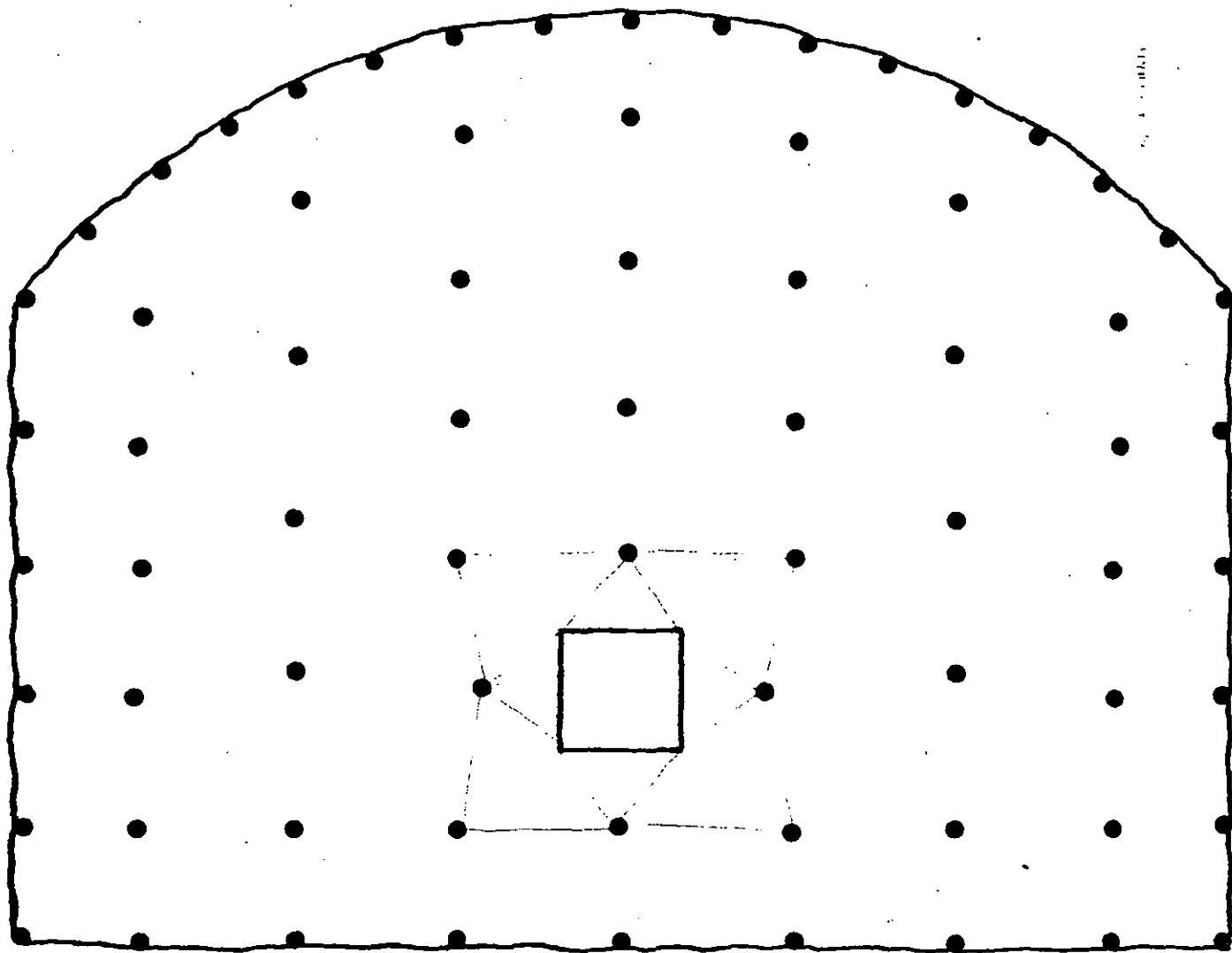
TUNNEL BLASTING

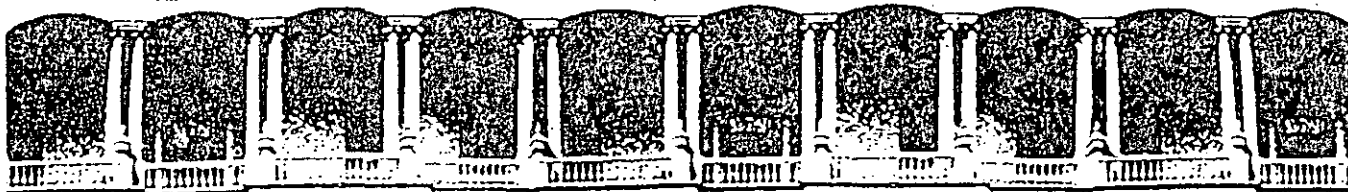
Calculation example

Conditions:

Cross section	53 m ²
Width	8.55 m
Abutment height	4.65 m
Height of arch	2.00 m
Hole diameter	45/102 mm
Hole depth	3.9 m

Smooth blasting to be carried out of the roof, using 17 mm GURIT.





**FACULTAD DE INGENIERIA U.N.A.M.
DIVISION DE EDUCACION CONTINUA**

CURSOS ABIERTOS

***IV. CURSO INTERNACIONAL DE INGENIERIA GEOLOGICA APLICADA A
OBRAS SUPERFICIALES Y SUBTERRANEAS***

CUARTO MODULO:

TECNOLOGIA SOBRE EL USO DE EXPLOSIVOS

Del 22 al 26 de junio de 1992

A N E X O I

JUNIO - 1992

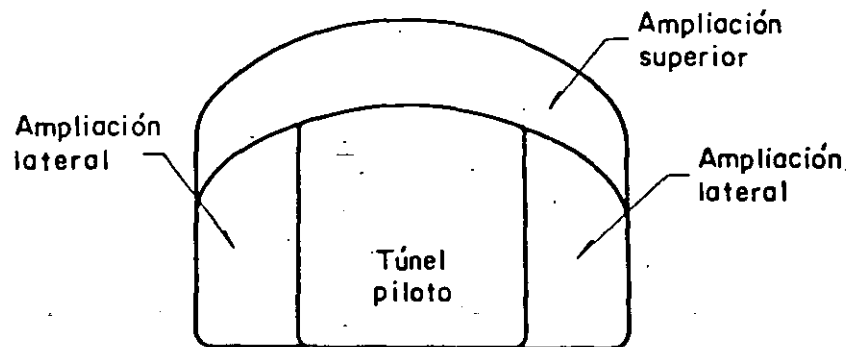


FIG I.27 Túnel piloto y ampliaciones laterales y superior

7.2.1.3 Cuñas iniciales

En los socavones y túneles el frente de avance es la única cara de liberación de la voladura. Es por este confinamiento de los barrenos cargados, que la carga específica es mayor en los túneles de pequeña sección y túneles pilotos que en los banqueos o en las excavaciones a cielo abierto. A fin de dar mayor eficiencia a la voladura se produce una abertura a todo lo largo del avance previsto, creando así un espacio vacío que permite la expansión y fragmentación de la roca removida por las sucesivas etapas de la voladura. Es obvio que este espacio inicial no es suficiente para acomodar la expansión y movimiento de toda la roca de la voladura completa. Por tanto, la mayor parte de la roca se proyecta hacia la zona previamente excavada. El espacio producido inicialmente se ha denominado "cuña".

Los principales tipos de cuña son dos: la cuña de barrenos paralelos y la cuña en "V". Cada tipo de cuña tiene una variedad de diseños para ajustarse a cada formación particular.

La cuña inicial es la parte más crítica en el diseño de voladuras en túneles.

Es muy difícil determinar un tipo de cuña inicial que resulte el adecuado

para el terreno por excavar sin haber efectuado algunas voladuras previas.

a) Cuña de barrenos paralelos o cuña quemada

La cuña de barrenos paralelos consiste de uno o más barrenos vacíos y uno o más barrenos cargados, paralelos unos a otros, que son perforados en el centro del frente, y con la profundidad del tramo de avance fijado. Las perforaciones que rodean la cuña están dispuestas en tal forma que se disparan después de abierta la cuña. Es muy importante para lograr una fragmentación eficiente, que se mantenga el paralelismo de los barrenos de la cuña. Una barrenación inapropiada puede dar lugar a la propagación entre los barrenos cercanos, destruyendo así la secuencia de detonación prevista y provocando zonas de fragmentación deficiente por exceso de confinamiento.

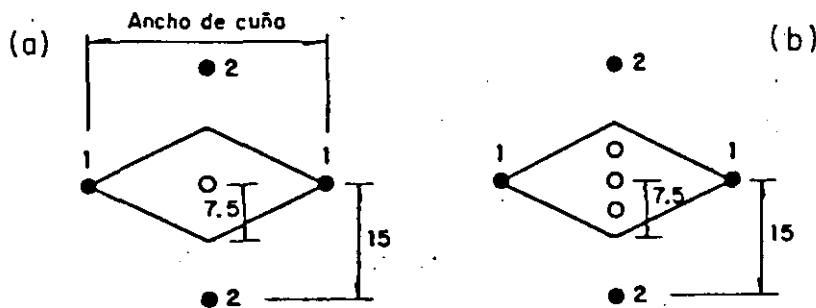
La cuña quemada es empleada casi exclusivamente en túneles de sección transversal menor de 10 m^2 y permite voladuras más profundas. En túneles reducidos el espacio resulta pequeño para acomodar las máquinas para perforar con cualquier ángulo, lo cual limita la longitud del tramo excavado empleando cuñas en "V".

La cuña quemada queda emplazada en la zona central del frente, pero no exactamente al centro sino que se va cambiando su posición en voladuras sucesivas para evitar que la perforación de la cuña se ejecute en la parte más fracturada del frente. Además, la rotación del sitio de la cuña resulta una medida de seguridad, ya que, la zona de la cuña es el sitio donde con más alta probabilidad pueden quedar explosivos sin disparar. El diseño de la cuña quemada depende de las características de la roca, del tipo de los explosivos empleados y del diámetro de los barrenos. Toda roca tiene un determinado porcentaje de expansión que varía con el tamaño de los fragmentos producidos por la voladura. Por tanto, el diseño de la cuña quemada debe tomar en cuenta un espacio vacío para permitir esta expansión. Un 15 por ciento del área de influencia de los barrenos que disparan en primer término es el espacio mínimo que ha resultado adecuado para una fragmentación y desalojo apropiados. Este porcentaje varía de acuerdo con la

formación rocosa. Sin embargo, a medida que el espacio vacío proporcionado es mayor, mayor es también la probabilidad de que la voladura actúe eficientemente en la longitud total de las perforaciones.

En una cuña con barrenos de 41.3 mm ($1\frac{5}{8}$ pulg) de diámetro con un área de influencia de 225 cm² (fig I.28) si el espacio vacío está constituido por un barrenó central (fig I.28a) proporcionará únicamente el 5.9 por ciento para la expansión. Si con la misma área de influencia se dejan vacíos tres barrenos (fig I.28b) el porcentaje para expansión será, entonces, de 17.8 por ciento. La mayor longitud de los tramos de avance que se logran cuando se deja un espacio de expansión suficiente compensa con amplitud el tiempo invertido en la perforación de los barrenos adicionales.

Para lograr la remoción de la cuña en toda la longitud de la perforación se recomienda cargar el tercio interior del barreno con la mitad de la carga total del barreno. Además para una adecuada expulsión del material fragmentado, la columna de explosivos debe alcanzar casi hasta la boca del barreno con menor densidad en la carga.



Acotaciones, en cm
1,2 Secuencia de disparo

FIG I.28 Cuña quemada cuadrada: a) con un barreno vacío central; b) con tres barrenos vacíos

Si no se reduce la densidad de la carga en la mitad exterior del barreno se corre el riesgo de impedir la acción eficiente de la carga del interior para expulsar el material fragmentado. Cuando este error se comete el avance só lo se logra hasta donde la cuña es fragmentada y desalojada.

El tipo de cuña quemada se determina a partir de la experiencia y de acuerdo al tipo de terreno. Las cuñas quemadas de 15 a 25 cm de ancho son, por lo general, las usadas en rocas sanas y rígidas y las de 25 a 35 cm en rocas blandas y laminadas.

A fin de reducir la densidad de explosivos en la zona de la cuña es frecuente emplear espaciadores de madera de 20 cm de longitud. Es también conveniente utilizar un explosivo de densidad baja y un sistema de retardos.

Para establecer cuál es el mejor tipo de cuña quemada para las condiciones de un sitio particular deben probarse varias de las distribuciones usuales.

→ En la fig I.29 se muestran algunos de los tipos de cuñas usadas actualmente en minas subterráneas. Cuando estos tipos de cuñas quemadas se acompañan con barrenos de alivio (que son los que disparan inmediatamente después de la cuña) emplazados en sitios apropiados, actúan eficientemente en cualquier tipo de roca. Si alguno de estos arreglos no expulsara convenientemente la cuña son recomendables los barrenos de alivio inclinados o barrenos diagonales (fig I.30). Los barrenos diagonales se perforan con un cierto ángulo y con una ubicación tal que el extremo interior quede de 20 a 30 cm de distancia de los barrenos de la cuña.

La perforación de uno o más barrenos vacíos de mayor diámetro (fig I.31) es cada vez más frecuente. Este procedimiento permite tramos de avance más largos y menor riesgo de expulsión deficiente de la cuña.

En el método de la cuña quemada se incluye la iniciación con periodos de retardo. Los primeros periodos corresponden a los barrenos de la cuña. Es importante dejar el tiempo suficiente entre el disparo de los barrenos de la cuña y los barrenos de alivio. En la fig I.32 se muestra un arreglo típico para un túnel de 3 por 3 m, utilizando la serie de retardos denominada "Acudet". Cada distribución de barrenos para una voladura debe diseñarse de manera que cada secuencia de barrenos dispare hacia el espacio previamente vaciado en las secuencias anteriores.

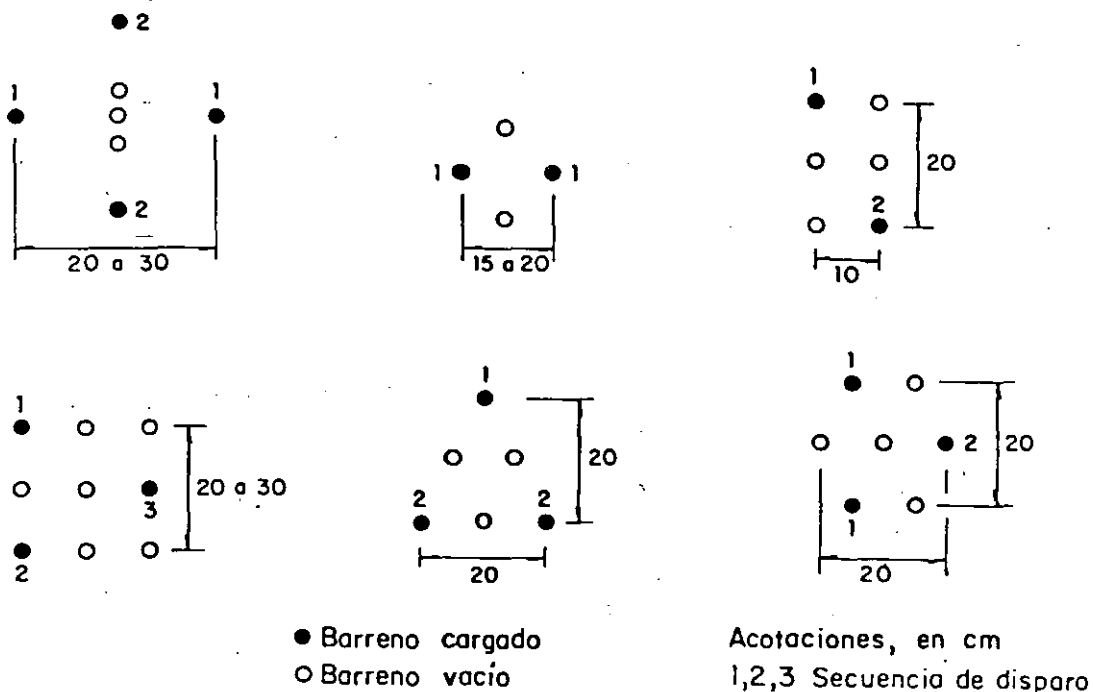


FIG I.29 Algunos diagramas típicos de cuñas quemadas

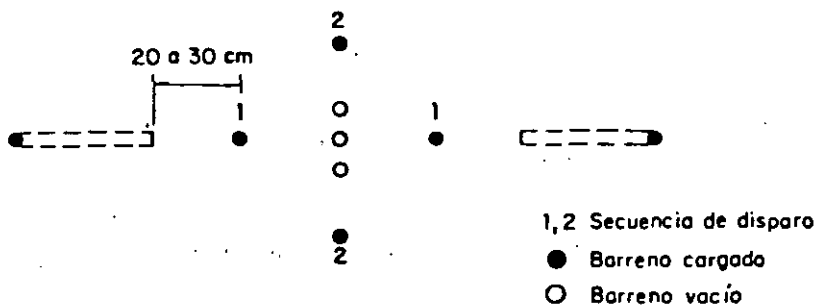


FIG I.30 Barrenos de alivio inclinados o diagonales

Los barrenos de la cuña y los de alivio se cargan dejando, en general, 30 cm para el retacado. Los barrenos restantes se retacan en un tramo de longitud igual al espaciamiento entre los mismos.

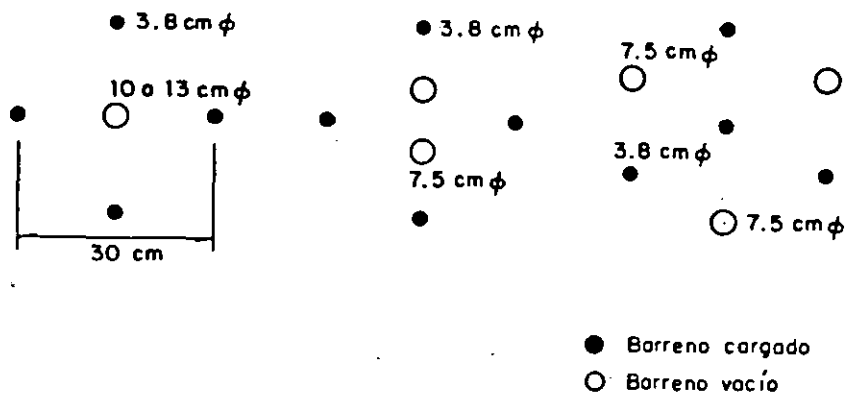


FIG I.31 Cuñas quemadas con barrenos vacíos de mayor diámetro

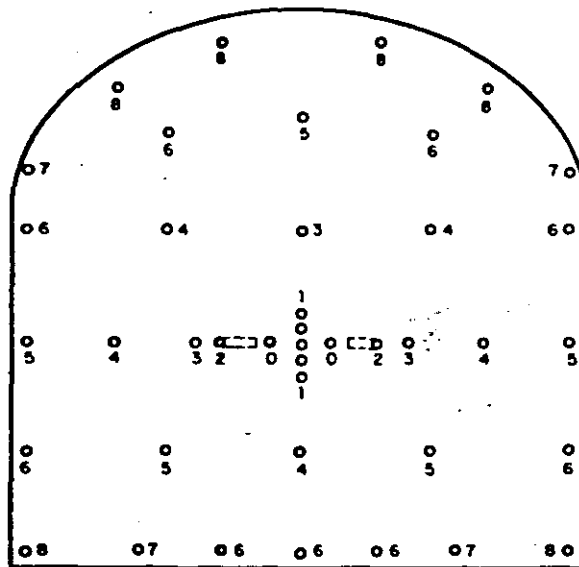


FIG I 32 Distribución típica de retardos en un frente de 3 por 3 m

b) Cuña en V

Este tipo de cuña es el más utilizado en túneles mayores de 20 m², aunque recientemente ha podido notarse una tendencia hacia la cuña paralela.

La cuña en V es simétrica. Esto permite una mejor organización del trabajo en el frente respecto a los tipos de cuñas no simétricas. La cuña en V,

por otra parte, no exige una barrenación tan perfecta como la cuña paralela para lograr un avance razonable. El ángulo mínimo recomendable para la cuña es de 60° . Este requisito limita el avance por tronada a la mitad del ancho del túnel (fig I.33).

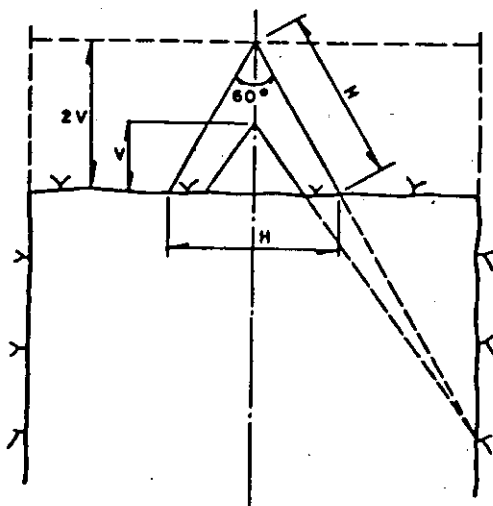


FIG I.33 Barrenos inclinados de la cuña en V

La cuña puede estar formada por uno o más pares de barrenos en V perforados en planos paralelos. El número de estos pares de barrenos depende de la estructura o estratificación de la roca. Cuando el avance por tronada es muy grande o en roca muy resistente cada V de barrenos se integra con uno o dos pares de barrenos de menor longitud.

Todos los barrenos de la cuña en V deben dispararse simultáneamente para obtener mejores resultados, particularmente en roca muy resistente.

En frentes muy grandes deben emplearse retardos mayores para lograr el desplazamiento y la fragmentación adecuados.

7.2.1.4 Cálculo de la carga

El cálculo de cargas en túneles es menos sistemático que el de las voladuras de bancos a cielo abierto. Se emplea la información teórica y experimental

de las voladuras de banco a cielo abierto, aplicando factores de aumento de carga para ajustarla a la voladura en túneles. Este aumento se debe al mayor confinamiento de las voladuras en túneles, de tal manera que, a medida que el frente de ataque es menor, mayor es el confinamiento. Por tanto, a menores dimensiones del túnel corresponde una mayor carga específica.

A continuación se darán reglas para la estimación de los espaciamientos y de las cargas en las cuñas de barrenos paralelos, en las cuñas en V y en los barrenos que no pertenecen a la cuña.

a) Barrenos que no pertenecen a la cuña

En esta sección se supone que ya está abierta y expulsada la zona de la cuña y se tiene una cavidad de 1.40 por 1.40 m. Este es el espacio generalmente requerido en barrenos para el fracturamiento y expulsión de la roca hacia esa abertura. Si los barrenos son de diámetro mayor de 3 cm puede ser necesario aumentar las dimensiones de la cavidad a 2 por 2 m.

En la fig I.34 se presentan gráficas que permiten calcular la distancia máxima que debe fijarse entre la cavidad y los barrenos según su diámetro.

Todos los barrenos de la periferia, ya sean del piso, del techo y de los hastiales, deben orientarse de manera que lleguen más allá del contorno (fig I.35) y proporcionen espacio para la perforación de la voladura siguiente.

Los principios de cálculo descritos en esta sección están basados en experiencia obtenida de casos particulares.

La fig I.36 muestra el valor de las cargas específicas que se utilizan normalmente en túneles en función del área de la sección transversal de los mismos. Los valores indicados en las figs I.36 y I.37 son valores promedio; existen ejemplos de valores que se desvían debido a la forma del túnel, condiciones de la roca, etc.

A continuación se dan recomendaciones para el diseño de las cargas y espa-

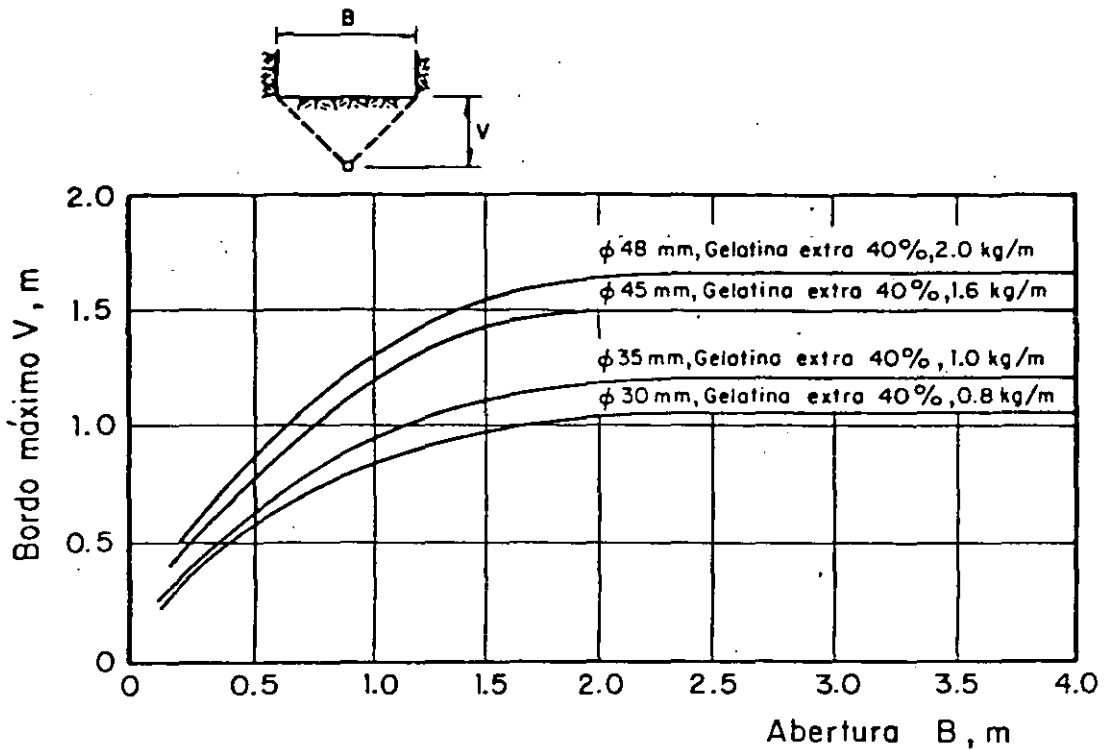


FIG I.34 Relación entre abertura, B, concentración de carga y bordo máximo, V

ciamientos de los barrenos de cada una de las zonas del túnel que se señalan en la fig I.38.

-Barrenos ayudantes con proyección horizontal o hacia arriba

El bordo o distancia entre los barrenos y la cavidad central no debe ser mayor que la mitad de la profundidad del barreno menos veinte centímetros. No deberá tomarse esta condición como base para el cálculo.

El espaciamiento de los barrenos debe ser igual a 1.1 veces el bordo.

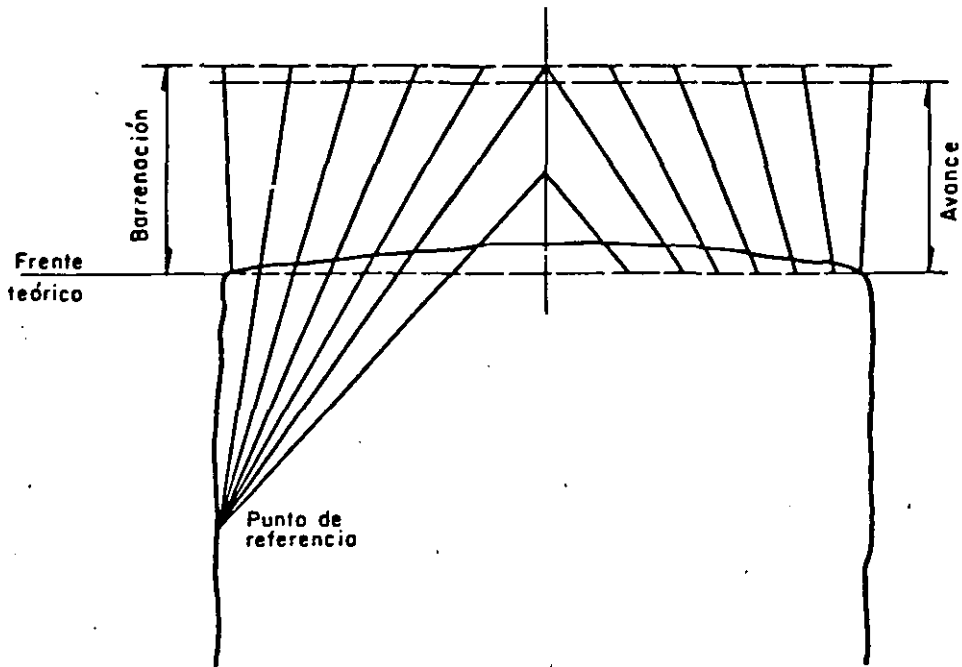


FIG I.35 Distribución en planta de los barrenos de la cuña y los de fuera de la cuña

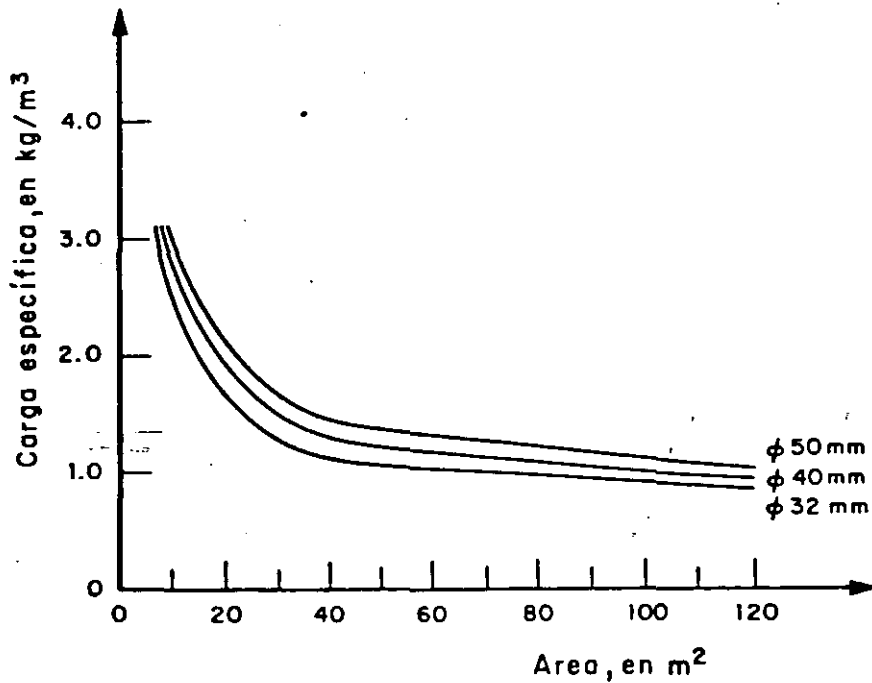


FIG I.36 Cargas específicas utilizadas normalmente en túneles

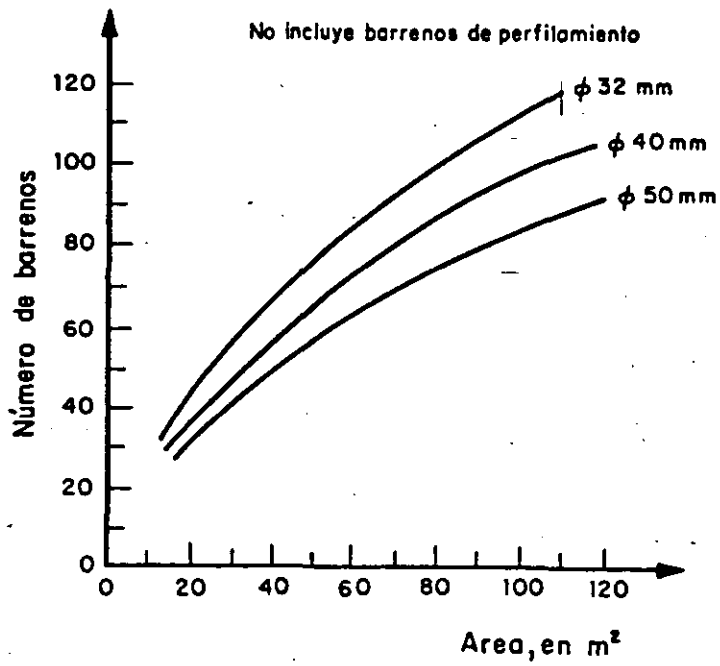


FIG I.37 Número de barrenos en función del área del frente

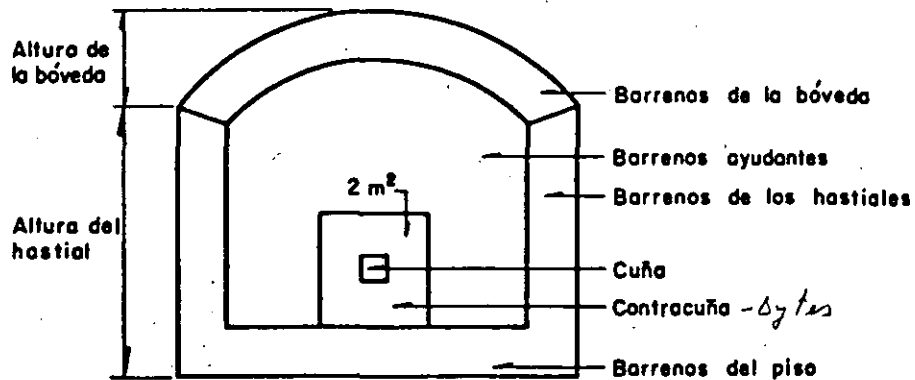


FIG I.38 Zonas de distribución de los barrenos

La carga de fondo ocupa el tercio inferior del barreno con la carga específica de la tabla I.12.

La concentración de la carga de columna en kg/m puede tomarse igual a la mi

tad de la concentración de la carga de fondo. La zona de retaque debe ser igual a la mitad del bordo.

TABLA I.12 Carga específica de fondo

Diámetro de los barrenos, en mm	Carga específica, en kg/m ³
30	1.1
40	1.3
50	1.5

En la tabla I.13 se muestran los espaciamentos calculados de acuerdo con las cargas específicas de fondo necesarias, considerando explosivos de peso volumétrico de 1.3 g/cm³ y el diámetro de barrenos de la tabla I.12.

TABLA I.13 Espaciamentos y bordos en función de los diámetros de los barrenos

Diámetro de barreno, en mm	Area por barreno, en m ²	Bordo, en m	Espaciamento, en m
32	0.91	0.90	1.00
35	1.00	0.95	1.05
38	1.15	1.00	1.15
45	1.44	1.15	1.25
48	1.57	1.20	1.30*
51	1.71	1.25	1.35*

* Estos espaciamentos son sólo para túneles de gran diámetro; en el caso de áreas menores su magnitud es menor como se muestra en las gráficas de la fig I.34.

Las concentraciones y cargas de fondo y de columna de la tabla I.14 han sido calculadas a partir de las recomendaciones anteriores, en función del diámetro de los barrenos. Estos datos han sido obtenidos de la práctica e incluyen los errores normales de perforación.

TABLA I.14 Cargas, espaciamientos y bordos en barrenos ayudantes con proyección horizontal o hacia arriba

Taco

Diámetro barreno, mm	Profundidad barreno, m	Bordo m	Espaciamiento m	Carga de fondo		Carga de columna		Zona de retaque m
				kg	kg/m	kg	kg/m	
33	1.6	0.60	0.70	0.60	1.10	0.30	0.40	0.30
32	2.4	0.90	1.00	0.80	1.00	0.55	0.50	0.45
31	3.2	0.90	0.95	1.00	0.95	0.85	0.50	0.45
38	2.4	1.00	1.10	1.15	1.44	0.80	0.70	0.50
37	3.2	1.00	1.10	1.50	1.36	1.15	0.70	0.50
45	3.2	1.15	1.25	2.25	2.03	1.50	1.00	0.55
48	3.2	1.20	1.30	2.50	2.30	1.70	1.15	0.60
48	4.0	1.20	1.30	3.00	2.30	2.45	1.15	0.60
51	3.2	1.25	1.35	2.50	2.60	1.95	1.30	0.60
51	4.0	1.25	1.35	3.40	2.60	2.70	1.30	0.60

-Barrenos de piso

El bordo y el espaciamiento de estos barrenos debe calcularse del mismo modo que los barrenos ayudantes. Sin embargo, debe considerarse en el bordo una corrección debido al emboquille de preparación para la voladura siguiente. Por ejemplo, con un bordo de 1.00 m y un margen para emboquille de 0.20 m, la segunda fila de barrenos del piso debe estar 0.80 m arriba de la entrada de los barrenos de la primera fila. La zona de retaque debe ser de 0.20 veces el bordo, es decir, mucho menor que en los barrenos ayudantes y la concentración de la carga de columna se fija hasta de un 70 por ciento de la concentración de la carga de fondo.

En la tabla I.15 se presentan las concentraciones de carga de fondo y de columna, el espaciamiento, el bordo y la zona de retaque para distintos diámetros de barrenos.

-Barrenos ayudantes con proyección hacia abajo

Debido a la ayuda de la gravedad, estos barrenos requieren una menor carga específica que los anteriores. La carga específica de fondo puede ser la de la tabla I.16.

TABLA I.15 Cargas, espaciamentos y bordos en barrenos de piso.

Diámetro barreno mm	Profundi- dad barre- no, m	Bordo m	Espacia- miento m	Carga de fondo		Carga de columna		Zona de retaque m
				kg	kg/m	kg	kg/m	
33	1.6	0.60	0.70	0.60	1.10	0.70	0.75	0.10
32	2.4	0.90	1.00	0.80	1.00	1.00	0.70	0.20
31	3.2	0.90	0.95	1.00	0.95	1.30	0.65	0.20
38	2.4	1.00	1.10	1.15	1.44	1.40	1.00	0.20
37	3.2	1.00	1.10	1.50	1.36	1.80	0.95	0.20
45	3.2	1.15	1.25	2.25	2.03	2.60	1.40	0.25
48	3.2	1.20	1.30	2.50	2.30	3.00	1.60	0.25
48	4.0	1.20	1.30	3.00	2.30	4.25	1.60	0.25
51	3.2	1.25	1.35	2.70	2.60	3.20	1.80	0.25
51	4.0	1.25	1.35	3.40	2.60	4.75	1.80	0.25

TABLA I.16 Carga específica de fondo

Diámetro de los barrenos, en mm	Carga específica, en kg/m ³
30	1.0
40	1.2
50	1.4

El espaciamento de estos barrenos puede ser de 1.2 veces el bordo. Las de más características son las señaladas para los otros barrenos ayudantes.

En túneles de sección transversal pequeña las cargas deberán aumentarse y el bordo y el espaciamento disminuirse de acuerdo con las funciones de las gráficas que se presentan en las figs I.34, I.36 y I.37.

En la tabla I.17 se presentan las cargas, bordos y espaciamentos de estos barrenos. Los espaciamentos indicados son aplicables siempre que la con-

B.I

centración de carga en el fondo alcance, asimismo, el valor señalado. Si la concentración de carga resulta menor, el espaciamiento deberá reducirse para obtener la carga específica requerida.

Los valores de espaciamientos y bordos indicados en la tabla I.17 pueden aumentarse, particularmente cuando la roca es fácil de excavar y cuando los túneles tienen un área de más de 70 m². También es frecuente en estos casos utilizar los espaciamientos señalados pero con menores concentraciones de carga.

TABLA I.17 Cargas, espaciamientos y bordos en barrenos ayudantes con proyección hacia abajo.

Diámetro barreno, mm	Profundidad barreno, m	Bordo, m	Espaciamiento, m	Carga de fondo		Carga de columna		Zona de retaque, m
				kg	kg/m	kg	kg/m	
33	1.6	0.60	0.70	0.60	1.10	0.30	0.40	0.30
32	2.4	0.90	1.10	0.80	1.00	0.55	0.50	0.45
31	3.2	0.85	1.10	1.00	0.95	0.85	0.50	0.45
38	2.4	1.00	1.20	1.15	1.44	0.80	0.70	0.50
37	3.2	1.00	1.20	1.50	1.36	1.15	0.70	0.50
45	3.2	1.15	1.40	2.25	2.03	1.50	1.25	0.55
48	3.2	1.20	1.45	2.50	2.30	1.70	1.15	0.60
48	4.0	1.20	1.45	3.00	2.30	2.45	1.15	0.60
51	3.2	1.25	1.50	2.70	2.60	1.95	1.30	0.60
51	4.0	1.25	1.50	3.40	2.60	2.70	1.30	0.60

-Barrenos de los hastiales

Las voladuras de los hastiales y de la bóveda corresponden por lo común al tipo de voladuras denominado recorte o poscorte perimetral (inciso 7.2.1.5). En esta sección se tratan los casos que no son voladuras de recorte.

El bordo, considerando el emboquille de preparación para la voladura siguiente, se toma igual a 0.90 veces el bordo de los barrenos ayudantes.

El espaciamento que mejores resultados ha aportado en la práctica es 1.2 veces el bordo; la longitud de la carga de fondo un sexto de la profundidad del barreno; la zona de retaque la mitad del bordo; y la concentración de la carga de columna de 0.40 veces la carga de fondo. La tabla I.18 está elaborada con las especificaciones anteriores.

TABLA I.18 Cargas, espaciamentos y bordos en barrenos de los hastiales

Diámetro barreno mm	Profundidad barreno, m	Bordo m	Espaciamento m	Carga de fondo		Carga de columna		Zona de retaque m
				kg	kg/m	kg	kg/m	
33	1.6	0.55	0.65	0.30	1.10	0.45	0.45	0.30
32	2.4	0.80	0.95	0.40	1.00	0.65	0.40	0.40
31	3.2	0.80	0.95	0.50	0.95	0.90	0.40	0.40
38	2.4	0.90	1.10	0.60	1.44	0.85	0.60	0.45
37	3.2	0.90	1.10	0.75	1.36	1.20	0.55	0.45
45	3.2	1.00	1.20	1.10	2.03	1.80	0.80	0.50
48	3.2	1.10	1.30	1.20	2.30	2.00	0.90	0.55
48	4.0	<u>1.10</u>	1.30	1.50	2.30	2.50	0.90	0.55
51	3.2	1.15	1.40	1.40	2.60	2.10	1.00	0.60
51	4.0	1.15	1.40	1.70	2.60	2.70	1.00	0.60

-Barrenos de la bóveda (tabla I.19)

En estos barrenos la carga de columna se reduce a 0.30 veces la concentración de la carga de fondo. Las demás características son iguales a las de los barrenos de los hastiales.

b) Resumen de las características de los barrenos que no pertenecen a la cuña

Nomenclatura:

V bordo o separación de la cavidad previamente abierta, en m

V₁ bordo práctico, en m

B.I

- H profundidad del barrenado, en m
- q carga específica, en kg/m³
- d diámetro del barrenado, en mm
- Q_{bk} concentración de la carga de fondo, en kg/m
- Q_{pk} concentración de la carga de columna, en kg/m
- h_b altura de la carga de fondo, en m
- h_o longitud del retaque, en m
- E Distancia entre barrenos, en m

TABLA I.19 Cargas, espaciamentos y bordos en barrenos de la bóveda

Diámetro barrenado mm	Profundidad barrenado, m	Bordo m	Espaciamento m	Carga de fondo		Carga de columna		Zona de retaque m
				kg	kg/m	kg	kg/m	
33	1.6	0.55	0.65	0.30	1.10	0.35	0.35	0.30
32	2.4	0.80	0.95	0.40	1.00	0.50	0.30	0.40
31	3.2	0.80	0.95	0.50	0.95	0.70	0.30	0.40
38	2.4	0.90	1.10	0.60	1.44	0.70	0.45	0.45
37	3.2	0.90	1.10	0.75	1.36	0.90	0.40	0.45
45	3.2	1.00	1.20	1.10	2.03	1.30	0.60	0.50
48	3.2	1.10	1.30	1.20	2.30	1.45	0.80	0.55
48	4.0	1.10	1.30	1.50	2.30	1.95	0.90	0.55
51	3.2	1.15	1.40	1.40	2.60	1.70	0.80	0.60
51	4.0	1.15	1.40	1.70	2.60	2.25	0.80	0.60

-Barrenos ayudantes con proyección horizontal o hacia arriba

d(mm)	q(kg/m ³)
30	1.1
40	1.3
50	1.5
h _b	H/3

$$v_1 < \frac{H - 0.40m}{2} \quad (\text{ésta es una condición y no es una base de cálculo}) \quad (I.4)$$

B.I

$$E = 1.1 \text{ V} \quad (\text{I.5})$$

$$Q_{pk} = 0.50 Q_{bk} \quad (\text{I.6})$$

$$h_o = 0.5 \text{ V} \quad (\text{I.7})$$

-Barrenos de piso

Las mismas características de los anteriores, excepto

$$h_o = 0.2 \text{ V} \quad (\text{I.8})$$

$$Q_{pk} = 0.70 Q_{bk} \quad (\text{I.9})$$

-Barrenos ayudantes con proyección hacia abajo

Las mismas características de los ayudantes con proyección horizontal o hacia arriba, excepto

$$E = 1.2 \text{ V} \quad (\text{I.10})$$

-Barrenos de los hastiales

Las mismas características de los anteriores, excepto

$$V = 0.90 \times (\text{bordo de los barrenos anteriores}) \quad (\text{I.11})$$

$$Q_{pk} = 0.40 Q_{bk} \quad (\text{I.12})$$

$$h_b = H/6 \quad (\text{I.13})$$

-Barrenos de la bóveda

Las mismas características de los anteriores, excepto

$$Q_{pk} = 0.30 Q_{bk} \quad (\text{I.14})$$

c) Cuñas de barrenos paralelos

Debe calcularse la separación entre el barreno vacío central y los barrenos cargados de la cuña de manera que el área del barreno vacío sea de cuando menos un 15 por ciento del área de influencia de los barrenos de la cuña, que disparan en primer término (inciso 7.2.1.3a, fig I.31). La separación así calculada no debe rebasar la que se muestra en la tabla I.20.

TABLA I.20 Separación entre los barrenos vacíos y cargados de la cuña de barrenos paralelos

Diámetro del barreno central, mm	Diámetro de los barrenos cargados, mm	Bordo o separación entre barrenos, mm	Distancia entre centros, mm
57	32	40	85
76	32	53	107
76	45	53	113
2 x 57*	32	80	125
2 x 57*	45	80	131
2 x 76*	32	106	160
2 x 76*	45	106	167
100	45	70	143
100	51	70	146
125	51	88	176

* Dos barrenos centrales.

Las cargas que se presentan en la tabla I.21 son, en general, adecuadas para los barrenos más próximos al barreno central.

- Los barrenos denominados de contracuña, situados fuera de ésta, son adaptados al área de la sección transversal del túnel.

La carga de los barrenos de la contracuña es muy elevada debido a su gran confinamiento. La fig I.39 muestra la disposición de la contracuña para una cuña de dos barrenos centrales.

TABLA I.21 Cargas asignadas a los barrenos más próximos al central

Diámetro de los barrenos cargados, mm	Carga asignada (kg/m)	Diámetro del barreno central, mm
32	0.25	de 57 a 2 x 76
35	0.30	de 76 a 2 x 76
38	0.36	de 76 a 2 x 76
45	0.45	de 2 x 76 a 125
48	0.55	de 2 x 76 a 125
51	0.55	de 2 x 76 a 125

En la tabla I.22 se presentan valores de cargas que han dado buenos resultados en barrenos de contracuña.

TABLA I.22 Valores empíricos de carga en barrenos de contracuña (Ayuda s)

Bordo o separación entre barrenos m	Carga de fondo kg	Carga de columna en kg/m para diámetros de los barrenos cargados de:			
		32 mm	38 mm	45 mm	48 mm
0.20	0.25	0.30	0.45	0.60	0.75
0.30	0.40	0.30	0.45	0.60	0.75
0.40	0.50	0.35	0.50	0.70	0.80
0.50	0.65	0.50	0.70	1.00	1.15
0.60	0.80	0.50	0.70	1.00	1.15
0.70	0.90	0.50	0.70	1.00	1.15

* Longitud sin carga (taco) = 0.5 V.

d) Cuña en V

En esta sección se proporcionan reglas generales para el cálculo de cargas considerando una cuña de vértice interior de 60°. Si este ángulo es menor la carga debe incrementarse.

La dimensión V de la cuña (fig I.40) es función de la cantidad de explosivos que pueden cargarse en los barrenos con arreglo a su diámetro. En la

B.I

- Acotaciones, en mm
- Barreno vacío
- Barreno cargado

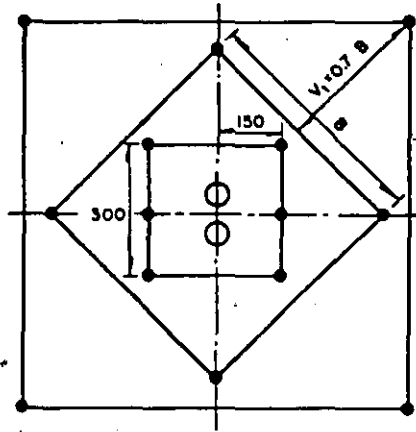


FIG I.39 Cuña de dos barrenos centrales y contracuña

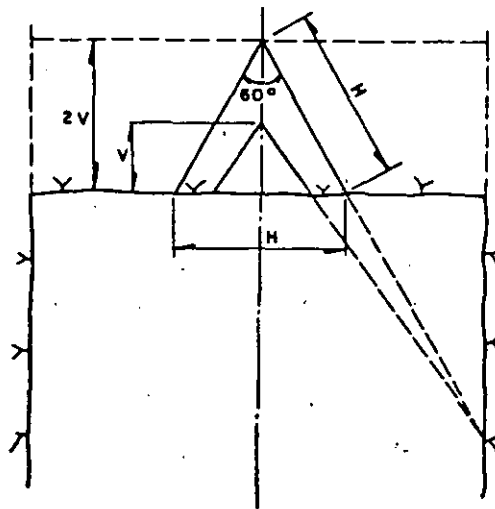


FIG I.40 Cuña en V

tabla I.23 se proporcionan valores que pueden servir de orientación en la determinación de la dimensión y carga de la cuña en V.

En cuñas en V la longitud de la carga de fondo debe ser de cuando menos un tercio de la profundidad del barreno. La carga de columna debe ser igual a la mitad de la carga de fondo. La zona de retaque debe ser un tercio de la dimensión V de la cuña, pero debe ser adaptada al espaciamiento de los barrenos de manera que no haya exceso de carga en la parte de la columna.

TABLA I.23 Dimensiones y cargas de la cuña en V

Diámetro de los barrenos mm	Altura de la cuña m	Bordo V (fig I.34) m	Concentración de la carga de fondo kg/m	Número de filas horizontales
30	1.5	1.0	0.9	3
38	1.6	1.2	1.4	3
45	1.8	1.5	2.0	3
51	2.8	2.0	2.6	3

La concentración de la carga de columna es igual al 40% de la concentración de la carga de fondo.

El bordo o separación de barrenos no debe ser superior a $(Prof. \text{barreno} - 0.40 \text{ m}) / 2$, lo que implica que en voladuras de poca profundidad la separación de barrenos es menor.

Los barrenos de la contracuña se perforan inclinados (fig I.35) para facilitar la remoción total hasta la profundidad de barrenación.

Los barrenos de la cuña y de la contracuña deben iniciarse con estopines de milisegundos a fin de mejorar la interacción entre los barrenos.

7.2.1.5 Poscorte perimetral

El poscorte perimetral también llamado recorte convencional tiene por objeto proteger la superficie de roca alrededor de la voladura.

Este método consiste en la aplicación de concentraciones de carga reducidas y una mayor densidad de perforación para producir un agrietamiento menor en la superficie perimetral del túnel. Al disparar instantáneamente o con un retardo mínimo entre barrenos se obtiene una acción cortante perimetral que desprende el bordo final con un daño reducido de las paredes (fig I.41).

Estos barrenos se disparan después de los barrenos de piso para asegurar

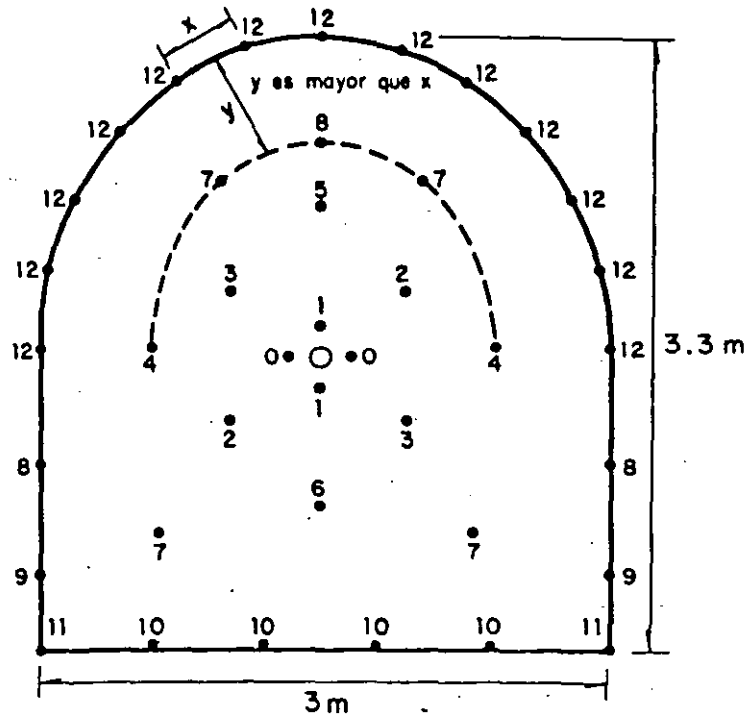


FIG I.41 Distribución típica de retardos en un túnel

que la roca fragmentada ya ha sido desplazada, ofreciéndoles un espacio de alivio suficiente. Este alivio permite una voladura del bordo final con un sacudimiento mínimo.

En la tabla I.24 se proporcionan valores prácticos recomendados de espaciamientos, bordos y concentraciones de carga promedio para dos diámetros de barreno, utilizando explosivos de 1.2 a 1.3 g/cm³ de peso volumétrico.

TABLA I.24 Poscorte perimetral

Diámetro barreno mm	Espaciamiento m	Bordo m	Concentración total de carga en el barreno kg/m
38 - 45	0.60	0.90	0.18 - 0.38
51	0.75	1.05	0.18 - 0.38

Los cartuchos largos de diámetro pequeño de explosivos de baja densidad, permiten una distribución adecuada de la carga a lo largo del barrenos. Los cartuchos de 20 cm de longitud se han empleado con éxito en voladuras de poscorte perimetral utilizando espaciadores entre cartuchos para reducir la carga total en kg/m; sin embargo, este procedimiento da como resultado concentraciones de carga relativamente altas en distintos puntos.

7.2.1.6 Precorte

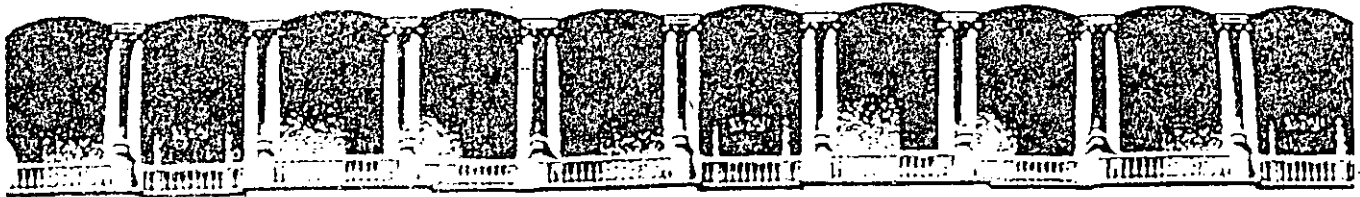
En el precorte los barrenos de contorno se disparan antes de efectuar la voladura propiamente dicha. El precorte produce una grieta entre los barrenos de contorno. Esta grieta evita que las ondas de choque de la voladura principal se transmitan en toda su intensidad hacia la pared terminada y minimiza la profundidad de la fragmentación en la roca. Como los barrenos están muy próximos entre sí, las grietas se forman siguiendo las líneas de barrenos, y los mismos barrenos constituyen el inicio del agrietamiento. Esto significa que la inclusión de barrenos vacíos entre los cargados, puede mejorar los resultados.

En la tabla I.25 se indican algunas cargas y espaciamientos en función del diámetro de los barrenos.

Si no existen limitaciones en las vibraciones del terreno se utiliza el encendido instantáneo; por lo contrario, si es necesario limitar la magnitud de las vibraciones del terreno se utilizan microretardos. La formación de grietas resulta menos eficiente que con la iniciación instantánea, a menos que se reduzca el espacio entre barrenos. Si el tiempo de retardo es muy grande no se logra el precorte.

TABLA I.25 Precorte

Diámetro del barreno mm	Espaciamiento m	Concentración de carga kg/m
25 - 32	0.20 - 0.30	0.08
25 - 32	0.35 - 0.60	0.18
40	0.35 - 0.50	0.18
51	0.40 - 0.50	0.36
64	0.60 - 0.80	0.38



**FACULTAD DE INGENIERIA U.N.A.M.
DIVISION DE EDUCACION CONTINUA**

CURSOS ABIERTOS

**IV. CURSO INTERNACIONAL DE INGENIERIA GEOLOGICA APLICADA A
OBRAS SUPERFICIALES Y SUBTERRANEAS**

CUARTO MODULO:

TECNOLOGIA SOBRE EL USO DE EXPLOSIVOS

Del 22 al 26 de junio de 1992

A N E X O 2

JUNIO - 1992

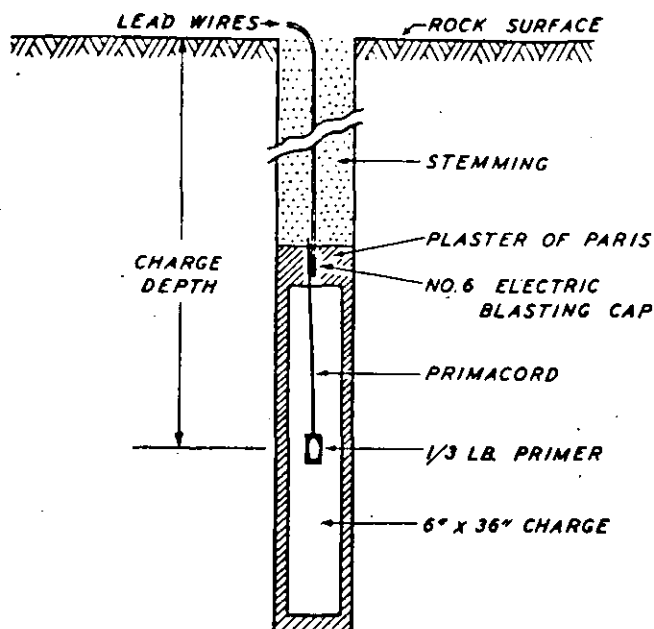


FIG. 1. Typical Dow volume crater charge showing position of explosives charge, detonators and stemming.

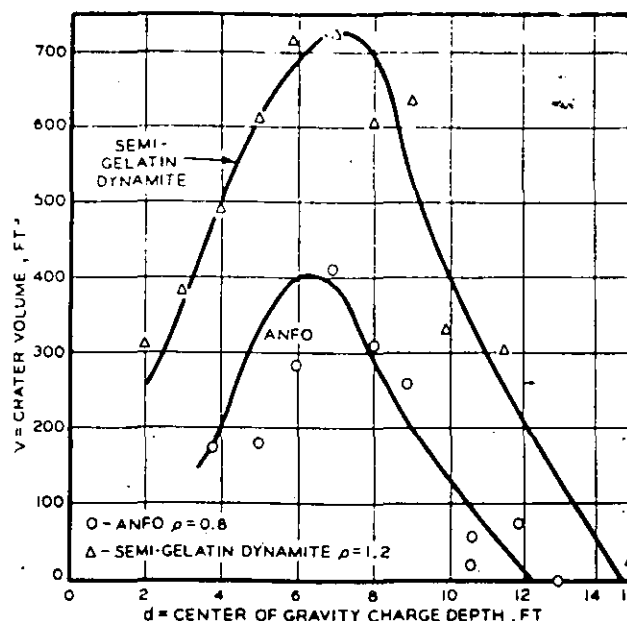


FIG. 2. Crater depth relationships for semi-gelatin dynamite are compared with those for ANFO charges.

Simplified Explanation of Crater Method

CHARLES H. GRANT

Editor's Note: Widespread interest in the "explosives algebra" article published in E&MJ, August 1964, prompted us to ask Mr. Grant for a more complete explanation of the cratering methods employed in introducing Dow's new metallized blasting agents. Mr. Grant prepared this article to assist readers in understanding the crater method.

AT THE RISK OF RIDICULE from some of my fellow engineers, I am going to try to reduce the principles and practices of rock cratering with explosives to the simplest possible terms for two reasons:

1) Because, too often, crater methods are ignored or misunderstood at field level which is where they should be best known; and, as a result, new explosives are usually tested in full-scale production blasting where poor performance can result in heavy losses.

2) Because only if those at field level have an understanding of cratering, can we at Dow (or anyone else) bring out the true characteristics of any new blasting agent or explosive as proved in the only proper laboratory for a rock-breaking material—that of rock itself.

Let's start out by giving full credit to the untiring enthusiasm of consultant C. W. Livingston, whose efforts to put his original theories into practical applications were so significant in gaining recognition for all crater methods. Credit must also be given to Messrs. Duvall, Rinehart, Nichols and Atchison of the U.S. Bureau of Mines, M. A. Cook of the University of Utah, Allen Bauer of C.I.L., K. Hino of Japan, and many others who have helped to increase this knowledge.

All of us who have gotten involved in cratering, however, have often forgotten that the work which seems so close and clear to us is almost a foreign language to those whose daily job is planning and executing the primary blasting which our investigations have endeavored to improve.

So this is an effort at communication, in the hope that

Mr. Grant is Manager of Marketing & Development, Industrial Explosives Section, The Dow Chemical Co.

proper testing methods will replace production blasting as a proving ground for new explosives and blasting agents.

For many years "Curly" Livingston's methods for determining explosives performance in rock were simply branded as "theories" and not given the practical application they deserved. It took much patient work before he established their validity and gained justly deserved recognition. Before stating the Livingston formula let's simply say that it measures how far down in a blast hole you can detonate a given weight of explosive and still pull rock at the top of the hole. The depth at which the explosive no longer breaks rock is called the critical depth. Its algebraic symbol is N.

The trick is to take this critical depth, N, and find some reproducible relationship between it and the explosive being used, and the size of the crater formed. Livingston determined theoretically and experimentally that there was a constant factor between critical depth and the cube root of the weight of the explosive. He expressed it this way:

$$N = EW^{1/3}$$

That E is called the strain energy factor. You could also call it a weight crater constant. It is simply there. You have the critical depth and the cube root of the weight of your explosive, and between them there is this factor. You can transpose the equation and solve for this factor as follows:

$$E = \frac{N}{W^{1/3}}$$

A practical application of this might work out this way. Say you have an 8-lb charge of explosive and in a series of crater tests you establish that the critical depth for this explosive in this rock is 6 ft. You solve for the strain energy factor (or weight crater constant) as follows:

$$E = \frac{N}{W^{1/3}} = \frac{6}{8^{1/3}} = \frac{6}{2} = 3$$

Now what do you have? Nothing yet, but since you have measured volumes of various craters you have blasted in searching for the critical depth of the explosive, you have found a certain depth at which the explosive produced the greatest volume of crater, and this gives you

another relationship. The depth at which the explosive produced the largest crater you can call the optimum depth, and there is a ratio you can form between this depth and the critical depth. This can be stated as follows:

$$\text{Optimum Depth Ratio} = \frac{\text{Optimum Depth}}{\text{Critical Depth}}$$

Say you found that a given explosive in a certain rock had a critical depth of 10 ft and an optimum depth of 5 ft. Then you have this equation:

$$\text{Optimum Depth Ratio} = \frac{5 \text{ ft}}{10 \text{ ft}} = .5$$

With this ratio, you can go to the practical application of the weight crater method which is expressed in this formula:

$$W = \left(\frac{\text{Distance}}{\text{Optimum Depth Ratio} \times E} \right)^3$$

Here Distance equals the number of feet to the center of gravity of the explosive charge. Now you have something you can take right into the pit to determine the charge you want to put into a specific blast hole or series of blast holes.

According to H. E. Farnam, manager of operations of the Iron Ore Co. of Canada, "From this point on, bench geometry becomes a problem of mathematically turning the crank, substituting numbers for burdens, spacing, and depth." In calculating bench geometry, a number of burden distances are arbitrarily chosen and substituted for Distance in the above equation. Then Iron Ore Co. engineers solve for the number of pounds of explosive required for each chosen burden. With the burden and the explosive weight known, the depth of hole and the spacing are calculated, and thus they solve a number of bench configurations for a specific rock and a specific explosive.

Using a typical example, the above equation can be easily applied. In an iron formation with a C.I.L. slurry, the strain energy factor has been determined as being 4.26 and the optimum depth ratio as being .52. Substituting an 18-ft burden for distance, we have:

$$W = \left(\frac{18}{.53 \times 4.26} \right)^3$$

$$\left(\frac{18}{2.25} \right)^3 \text{ or } (8)^3$$

W = 512 lb of slurry per hole (when burden equals depth of center of gravity of the charge)

In practice, Iron Ore Co. furnishes pit foremen with pre-calculated cards designating the type of material and explosive and listing information on bench height, burden, hole spacing, depth of hole, weight of explosive per hole, height of explosive column in the borehole, and the height from the top of the explosive column to the collar. With the cards (Table I) the foremen are able to lay out blast patterns for any bench in any of Iron Ore Co.'s rock types for any of their available explosives. The cards allow a margin of safety in the burden calculations to guard against underloading.

According to Farnam, this system of calculating bench and blast configurations is the first systematic method Iron Ore Co. has tried that has produced satisfactory results, increasing broken rock yield 30% per foot of drilled borehole and reducing blasting cost 40% with numerous other benefits.

"The system is not perfect, however, and considerable work must be done to perfect the theoretical aspects of the procedure," Farnam has reported.

This was the situation we at Dow faced when we first tried to gain accurate measurements of the effectiveness of our line of metallized blasting agents. We found that the existing crater methods which compared explosive using charges of constant weight made it necessary to vary the

charge size in accordance with the density of each explosive being tested. If we kept the boreholes at a uniform diameter, this uniform weight changed the shape of each explosive charge, and we found that this shape affected our results. This got us into an intensive investigation of charge geometry. Results from underwater testing showed that with some explosive compositions there was a significant variation in performance with changes in the length-to-diameter (L/D) ratio of the charge, up to an L/D ratio of 4.

A series of cratering experiments comparing performance of charges at L/D ratios of 2 and 6 with both ANFO and semi-gelatin dynamite, showed that a difference in performance also manifested itself in rock. At an L/D ratio of 2, more rock was broken per unit of explosive. At an L/D ratio of 6, the depth at which any explosive would affect the surface of the rock (critical depth) was greater. But of most significance for the purposes of the study, data obtained at an L/D of 6 was more reproducible and acted more like the typical column charge used in actual production blasting. Therefore, we determined that this charge geometry was essential for valid testing, and an L/D ratio of 6 was selected for all comparative work.

But this was not the only reason we began comparing explosives and blasting agents on the basis of a constant explosive volume and shape rather than a constant weight basis. Many other factors indicated that a volume method would give us more meaningful comparative data on explosive performance.

Using a constant volume, we avoid the problem of having to scale charges by weight and we can correlate the data with a single function. More important, the use of a constant volume of explosive means that each sample faces an identical rock resistance, and this also helps reproducibility.

To ensure that all experiments would be conducted with a charge diameter greater than critical diameter for the least sensitive composition expected to be evaluated, a constant diameter of 6 in. was selected.

These considerations committed us to a charge geometry for all experiments of 6x36 in.—a massive charge for cratering but possessing many advantages. The charge is of sufficient size so that the effect of the priming system does not distort our results. The effect of minor variations in rock structure is overcome. And, from the point of view of cost, having all holes of the same diameter simplifies our drilling problem. Fig. 1 shows a typical Dow volume crater charge as loaded.

In making a crater test with the volume method, the weight of the explosive varies with its density, and this is recorded. The charge is primed with a 1/2-lb high density pentolite primer placed at the center of the 6x36 in. cartridge. The primer is initiated with 100-grain detonating fuse. The fuse extends only to the top of the charge where the electric blasting cap is attached. The charge is cemented into the borehole with plaster of paris to ensure good con-

TABLE FOR PIT FOREMEN

MATERIAL—IRON FORMATION				EXPLOSIVE—HYDROMEX		
E = 4.26 Δ = 0.53						
BH	BURDEN	SPACING	DEPTH	WEIGHT	COLUMN	COLLAR
21	17	24	25	506	10	15
24	18	25	28	603	12	16
26	19	26	30	710	14	16
28	20	28	32	825	17	16
31	21	29	35	958	19	16
33	22	31	37	1102	22	16
36	23	32	40	1258	25	15
39	24	34	43	1476	29	14

TABLE I. This is the card which the Iron Ore Co. of Canada gives to pit foremen to solve blasting problems.

tact between the explosive and the rock. The hole is stemmed with finely crushed rock or tailings. After the charge has been shot, the crater, if one is obtained, is carefully excavated and cleaned, and its volume is calculated from measurements taken in a meticulous sectioning procedure.

As in the weight crater method, the critical depth is determined as the charge depth where the rock just starts to fail at the surface by cracking or spalling. At all depths less than critical, of course, craters will result.

With the volume crater method we use a somewhat different set of symbols than those in the weight crater method. The symbol N for critical depth stays the same, but instead of E (the strain energy factor or *weight* crater constant) we use the symbol Σ or sigma; to stand for the *volume* crater constant. And instead of taking the cube root of the *weight* of the explosive, we work in terms of the cube root of the volume, for which we use the symbol v —the explosives volume in cubic inches. Thus the Dow crater formula appears as follows:

$$N = \Sigma v^{1/3}$$

or in solving for Σ it can be written

$$\Sigma = \frac{N^3}{v^{1/3}}$$

Since the volume of the explosive in cubic inches is expressed as v , the volume of the crater in cubic feet is expressed as V . This can be plotted against the center of gravity depth of the explosive charge, d , which is expressed in feet. This is shown in Fig. 2, which compares a semigelatin dynamite with ANFO.

Three features of the curves may be noted:

1) Crater values at relatively shallow depths are not meaningful, because of the lack of confinement in this region, which is referred to as the airblast range.

2) The peaks of the curves represent the optimum depth, as described under the weight crater method but here determined volumetrically.

3) The point at which no crater is produced and the confinement of explosives energy is complete in the critical depth and will ordinarily be different for different explosives.

All this, as you can see, is relatively close to the weight crater method, but at this point the symbols and reasoning of the volume method begin to differ somewhat from conventional methods.

One difference is in the use of the symbol Δ (delta) to express the ratio of the center of gravity of the charge depth to the critical depth, or

$$\Delta = \frac{d}{N}$$

Table II Symbols

d	= Center of gravity charge depth, ft
v	= Explosive volume, cu in.
W	= Explosive weight, lb
ρ	= Explosive density, lb per cu in.
V	= Crater volume, cu ft
N	= Critical depth, ft (to center of gravity of charge)
E	= Weight crater constant
Σ	= Volume crater constant
Σ	= $E\rho^{1/3}$ when $W = \rho v$
Δ	= Reduced charge depth = d/N
$K(\Delta)$	= Reduced crater volume = V/N^3
$K(\Delta)'$	= A variation of $K(\Delta) = \frac{V}{d^3} = \frac{K(\Delta)}{\Delta^3}$

In conventional weight crater calculations, the delta sign represents optimum depth only. We at Dow, and a growing number of other crater testers, find there is a greater flexibility in our calculations when we use delta to express the ratio of d/N wherever the charge may be placed in the hole—at depths either more or less than critical. If the center of gravity of the charge depth is halfway to the collar from critical depth, we have a delta of .5. If it is below critical depth we have a delta of over 1.

Thus, it is convenient to call delta the reduced crater depth and think of it simply as the ratio of center of gravity charge depth, d , to the critical depth, N . It represents points of constant interrelationship of rock and explosive, or points of equal relative confinement.

Another ratio which comes in handy in finer crater calculations is the relationship of the actual crater volume, V , to the cube of the critical depth. We call this the $K(\Delta)$, and the formula for finding it is expressed as follows:

$$K(\Delta) = \frac{V}{N^3}$$

Being nothing but ratios, both Δ and $K(\Delta)$ are dimensionless. $K(\Delta)$ has the same value for any explosive at points of equal relative confinement and so may be considered a function of the reduced charge depth, Δ .

Our object in working out these ratios was to reduce the large number of experiments required to define a complete cratering curve.

In Fig. 2, you can see that the general shape of the two cratering curves is the same. You might say that only the dimensions are different. Therefore, it is mathematically possible to drop the dimensions and keep only the relationships. Since these relationships are constants, the curves can become the same. Fig. 3 shows what happens when we plot the Δ and $K(\Delta)$ ratios of the tests in Fig. 2.

In Fig. 3, within experimental error, a common curve is obtained over the major portion of the range. Values for ANFO drop off in the range of poor confinement, apparently because ANFO does not detonate well in this range. Normally crater experiments are performed in the range between optimum and critical depth to avoid the uncertainties of the airblast region.

The objective of all this is to compare explosive performance by comparing the crater volumes produced at points of equal relative confinement. In Fig. 3, this condition is satisfied for craters obtained at equal values of Δ or, because of the dependency of $K(\Delta)$ on Δ , at equal values of $K(\Delta)$. To compare two craters formed by equal volumes of explosive 1 and explosive 2,

$$K(\Delta)_1 \text{ must equal } K(\Delta)_2 \text{ or } \frac{V_1}{N_1^3} = \frac{V_2}{N_2^3} \text{ or } \frac{V_1}{V_2} = \frac{N_1^3}{N_2^3}$$

The ratio of the cubes of the critical depths has the same value as the ratio of crater volumes and is an equivalent measure of relative explosive performance.

Although in practice it is usually more convenient to determine the critical depth and make the comparison on this basis, it is now theoretically possible to shoot one crater with a new explosive and from the values of crater volume, V , and depth of charge, d , to determine the critical depth, N , for the explosive. The data point must be moved by trial and error on Fig. 3 until its location on the reduced crater curve gives a value of N that satisfies the values of both Δ and $K(\Delta)$ at that point.

For instance, if you had an explosive (say ANFO) which gave you a crater volume (V) of 200 cu ft at a depth (d) of 9 ft, you could assume various critical depths to find the one which would satisfy the values in Fig. 3. The only critical depth which would do this would be 12 ft:

$$\Delta = \frac{d}{N} = \frac{9}{12} = .75$$

and

$$K(\Delta) = \frac{V}{N^3} = \frac{200}{1728} = .108$$

— or with a semi-gelatin you would find that only an assumed critical depth of 15 ft, based on a charge depth of 10 ft and a crater volume of 400 cu ft would give you a correlation of Δ and $K(\Delta)$ as follows:

$$\Delta = \frac{10}{15} = .67$$

$$K(\Delta) = \frac{400}{3475} = .108$$

To avoid trial and error solutions, another parameter or ratio, $K(\Delta)'$, can be defined in terms of the experimentally determined crater volumes and charge depth

$$K(\Delta)' = \frac{V}{d^3} = \frac{K(\Delta)}{\Delta^3}$$

$K(\Delta)'$ is a mathematical variation of $K(\Delta)$; it has the advantage that it can be determined directly from field data.

Fig. 4 is a plot of $K(\Delta)'$ against $K(\Delta)$ using data for the calibrating explosives ANFO and semi-gelatin dynamite. Having calculated $K(\Delta)'$ from the experimental data for a single shot, a value of $K(\Delta)$ can be found that will enable us to determine Δ from the reduced crater curve (Fig. 3) hence the critical depth.

As an example, if a given explosive produces 1000 cu ft of crater at a depth of 10 ft,

$$K(\Delta)' = \frac{V}{d^3} = \frac{1000}{10^3} = \frac{1000}{1000} = 1$$

But $K(\Delta)'$ also equals $\frac{K(\Delta)}{\Delta^3}$, so we can determine that

$$1 = \frac{K(\Delta)}{\Delta^3}$$

and by employing the rock function curve to determine that $K(\Delta)$ is .185 [dropping down from $K(\Delta)' = 1$ on a finer calibration than shown here] we find

$$\begin{aligned} \Delta^3 &= .185 \\ \text{or } \Delta &= .57 \\ \text{hence } N &= 17.5 \end{aligned}$$

This can be checked against the reduced crater curve, Fig. 3, if you don't trust your algebra.

Those unfamiliar with "explosives algebra" may find the latter part of this analysis somewhat confusing. Actually $K(\Delta)'$ can be plotted against Δ to obtain the critical depth from a single curve, but this presentation attempted to trace the manner in which the method developed.

In practice, because of the experimental error inherent in crater work, data from more than one shot with a test explosive are used in comparing explosive performance.

To make comparison more meaningful, results of experiments comparing various explosives are reported in terms of the volumes of standard explosive equivalent in crater performance to one volume of the test explosive. This is equal to the inverse ratio of the cubed critical depths.

$$\frac{V_1}{V_2} = \frac{N_2^3}{N_1^3}$$

Examples of such comparisons are given in Table III.

That about wraps up the basic algebra involved in volume crater testing. Now all you have to do is translate all

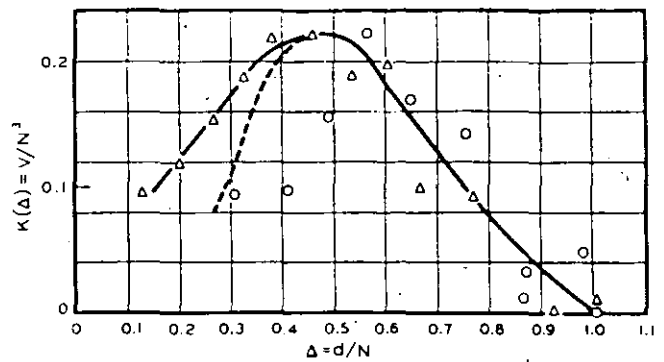


FIG. 3. Reduced crater curve. Data are plotted for both ANFO and semi-gelatin dynamite.

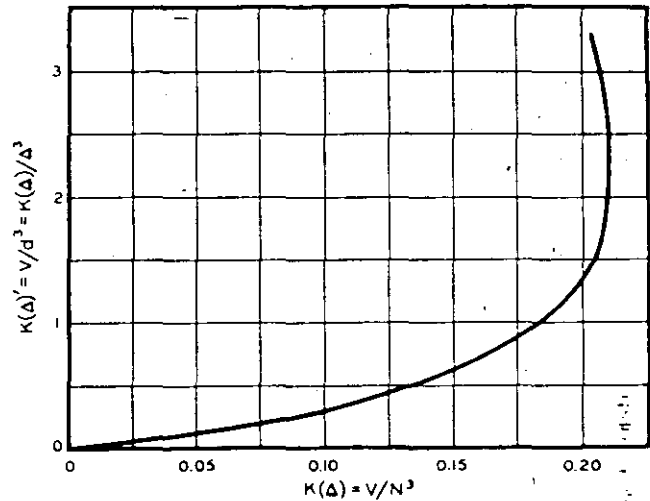


FIG. 4. Rock function curve derived from ANFO and semi-gelatin dynamite data.

this into action in your rock with the explosives or blasting agents available at your operation. With these techniques, you should be able to determine the best explosive for your job without gambling a single production blast.

Along with certain other companies, Dow offers the services of experienced crater technicians on a per diem—excess cost basis to conduct crater tests in the user's rock formation or to assist in the loading and firing of trial production blasts.

Bibliography

1. A. Bauer, "Application of the Livingston Theory," QUARTERLY OF THE COLORADO SCHOOL OF MINES, Vol. 36, No. 1, January 1961.
2. R. H. Cole, UNDERWATER EXPLOSIVES, Princeton University Press, 1948.
3. W. I. Duval, and T. C. Atchison, "Rock Breakage by Explosives," USBM Report of Investigation 5356, September 1957.
4. Kumao Hino, "Fragmentation of Rock Through Blasting," JOUR. IND. EXPLOSIVES SOC., Japan, Vol. 17, No. 1, 1956.
5. C. W. Livingston, "Fundamental Concepts of Rock Failure," QUARTERLY OF THE COLORADO SCHOOL OF MINES, Vol. 51, No. 3, July 1956.
6. D. J. Selleck, BASIC RESEARCH APPLIED TO THE BLASTING OF CHERTY METALLIC IRON FORMATION, 1961 International Symposium on Mining Research, Vol. 1, Pergamon Press, 1962.

Results of Minnesota and Georgia Crater Shooting in Granite

Explosive Type	Density, g per cc	V AN-FO per V Explosive	Wt AN-FO per Wt Explosive
Ammonium nitrate and fuel oil	.80	1.00	1.00
Hi-Explosive slurries nonmetallized	1.5	1.0 - 1.65	.53 - .88
Hi-Explosive slurries iron-metallized	1.7	1.1 - 2.2	.52 - 1.04
Hi-Explosive slurries metallized with aluminum	1.5	2.6	1.48
Slurried explosive metallized with aluminum (containing no Hi-Explosives)	1.20	5.0 ± .2	3.33

TABLE III. Comparison of various blasting agents on the basis of weight and volume, using the inverse ratio of their

cubed critical depths as derived by the Dow volume-crater method described in this article.



**FACULTAD DE INGENIERIA U.N.A.M.
DIVISION DE EDUCACION CONTINUA**

CURSOS ABIERTOS

**IV. CURSO INTERNACIONAL DE INGENIERIA GEOLOGICA APLICADA A
OBRAS SUPERFICIALES Y SUBTERRANEAS**

CUARTO MODULO:

TECNOLOGIA SOBRE EL USO DE EXPLOSIVOS

Del 22 al 26 de junio de 1992

A N E X O 3

JUNIO - 1992

NITRO

**EXPLOSIVOS
S.A. DE C.V.**

MORELOS 1854
SECTOR HIDALGO
GUADALAJARA, JALISCO
MEXICO
TELS. (9136) 30-11-18
26-77-16
16-48-98



Bill Cravitt
BILL CRAVITT
887 1900

POWDERMAN

Características de la emulsión sensitiva

CONCEPTO

Densidad (g/cc)	1.15-1.20
Velocidad de detonación km/seg. al aire libre (*)	4.5-4.7
Presión de detonación kbars (confinado)	115
RWS (Potencia relativa al peso)	81
RBS (Potencia relativa al volumen)	120
ASV kj/100 gr.	305
Eficiencia % (**)	90
Energía útil kj/100 grs.	274.5
Sensitividad a la cápsula No. 6	sí
Sensibilidad	-10°C
Resistencia al agua	Buena
Vida	6 meses en condiciones normales de almacenamiento

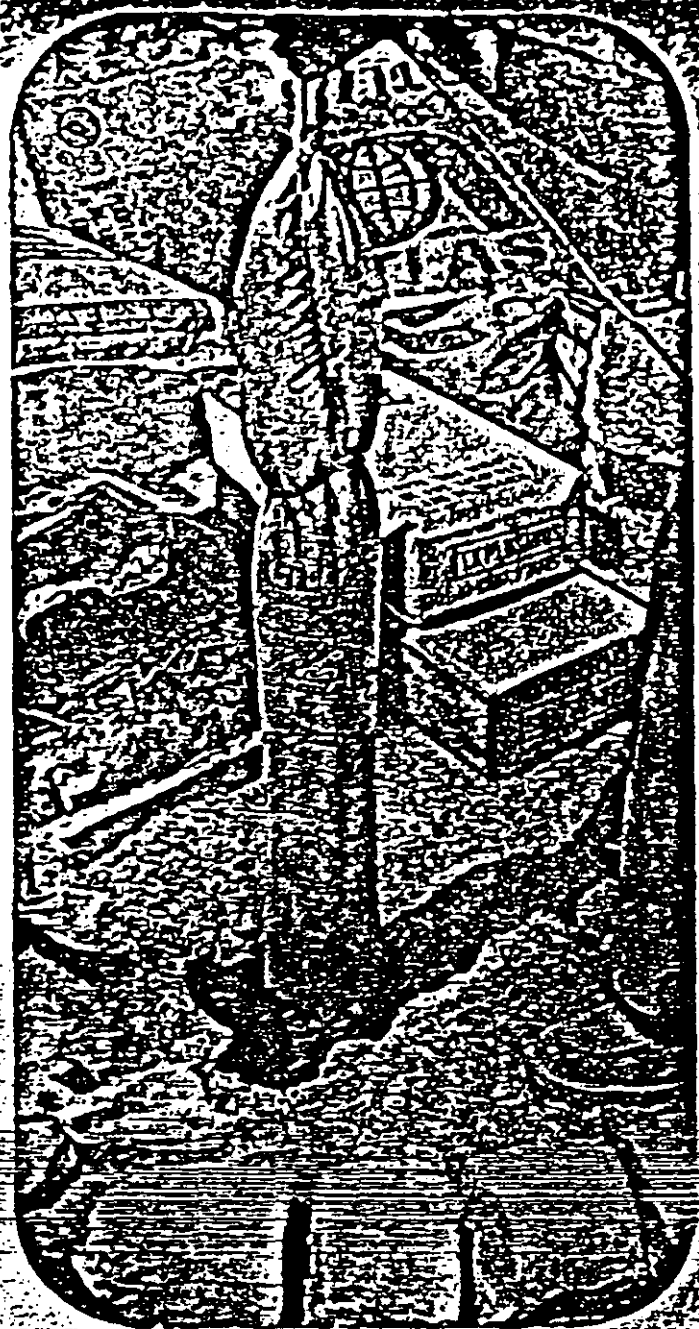
* La velocidad de los explosivos se incrementa en un 40% cuando esta confinado en el barreno.

** El concepto de eficiencia se refiere a la efectividad de la reacción de detonación de los explosivos.



BOLETIN TECNICO

DIVISION
EXPLOSIVOS



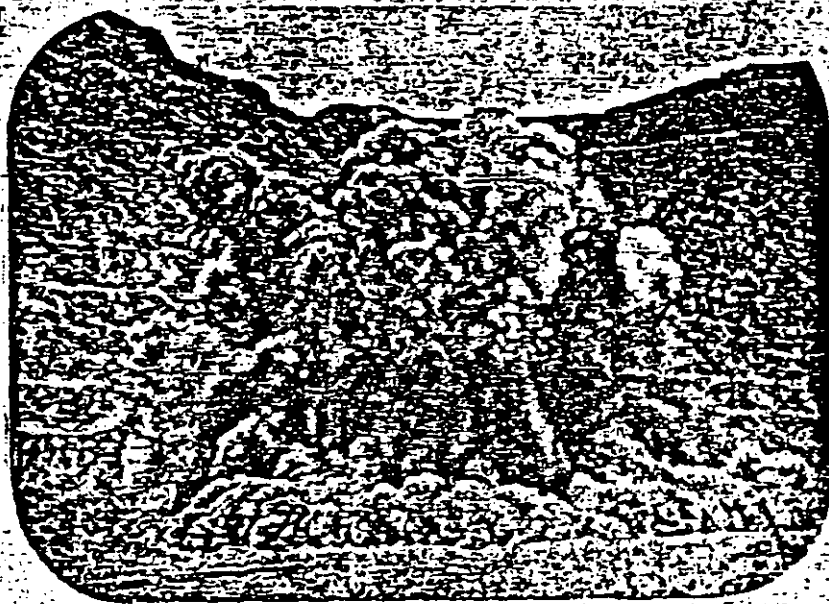
GODYNE

EXPLOSIVO
ALUMINIZADO

PRODUCTOS

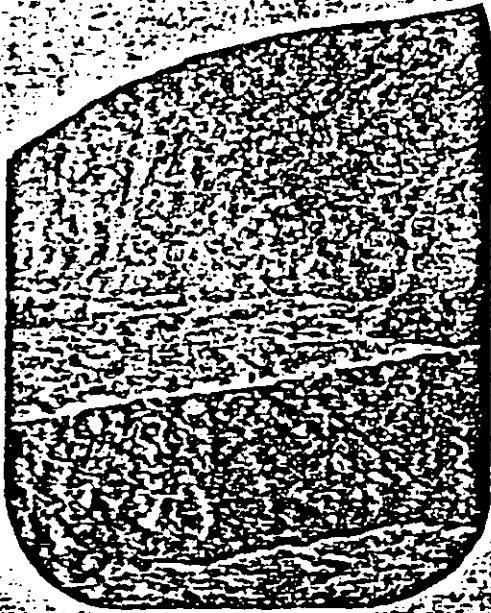
 **ATLAS
DE MEXICO, S.A.**

SAN LORENZO 1009 3er. PISO
COL. DEL VALLE • MEXICO 12, D.F.
TEL. 575-70-11



**CORTE
SIN PATA**

**BUENA
FRAGMENTACION**



PRODUCTO

CARACTERISTICAS

PRODUCTO	Diametros Equivalentes		Densidad	Potencia	Car- tuchos en Caja	Velocidad de iniciación		Unidades Energía	Resistencia al Agua
	cm	pulgadas				ft	mts		
GODYNE DIAMETRO PEQUEÑO	2.22	7/8"	1.18	60%	290	12.500	3.787	111	Envoltura de papel explosivo de excelente resistencia al agua
	2.54	1"	1.15	60%	260	13.500	4.090	111	
	2.857	1 1/8"	1.15	60%	190	13.500	4.090	111	
	3.175	1 1/4"	1.15	60%		14.500	4.393	111	
GODYNE DIAMETRO INTERMEDIO	4.44	1 3/4"	1.15	60%	33	14.500	4.393	104	Envoltura de plástico, excelente resistencia al agua
	5.08	2"	1.15	60%	26	15.500	4.696	104	
	6.35	2 1/2"	1.15	60%	16	15.500	4.696	104	
GODYNE EXTRA GRANDES DIAMETROS	7.63	3"	1.15	60%	13	15.500	4.696	104	
	12.70	5"	1.13	50%	2	14.300	4.333	94	
	15.24	6"	1.13	50%	2	14.300	4.333	94	

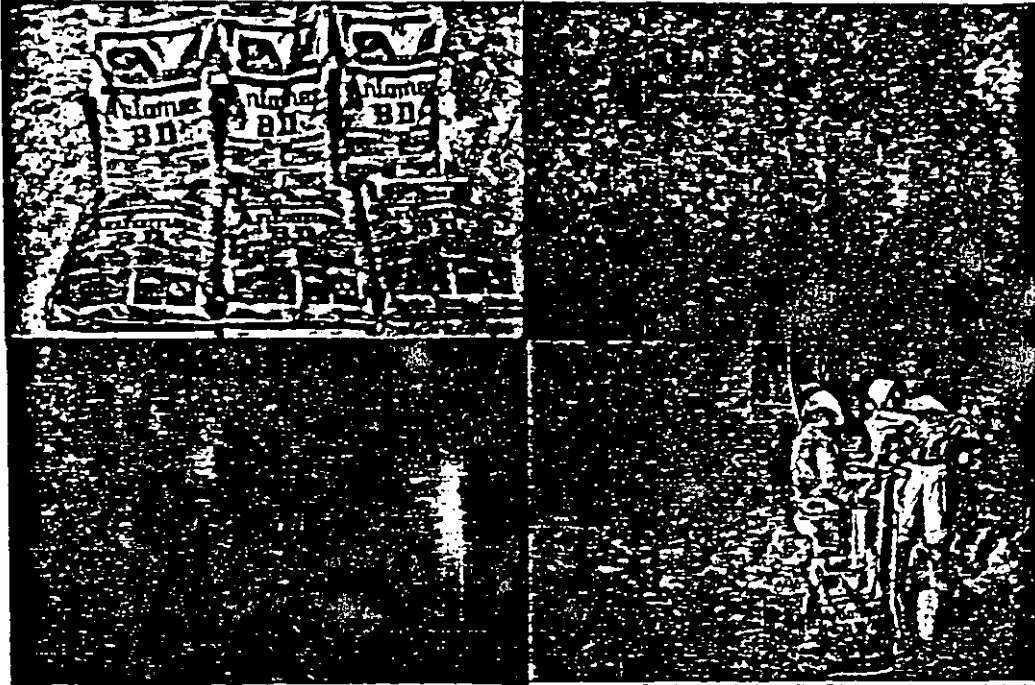
LINEA COMPLETA DE EXPLOSIVOS Y ACCESORIOS



SAN LORENZO 1009 3er. PISO • COL. DEL VALLE • MEXICO 12, D.F. • TEL. 575-70-11



ANFOMEX B.D. Agente Explosivo



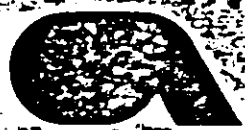
Ventajas para el cliente

- Más energía por su dinero
- Mejor fragmentación
- Menos kgs/m³ lineal cargado, con resultados óptimos
- Menor cantidad de gases nocivos
- Mayor fluidez a la hora de cargar
- Menor costo total operativo

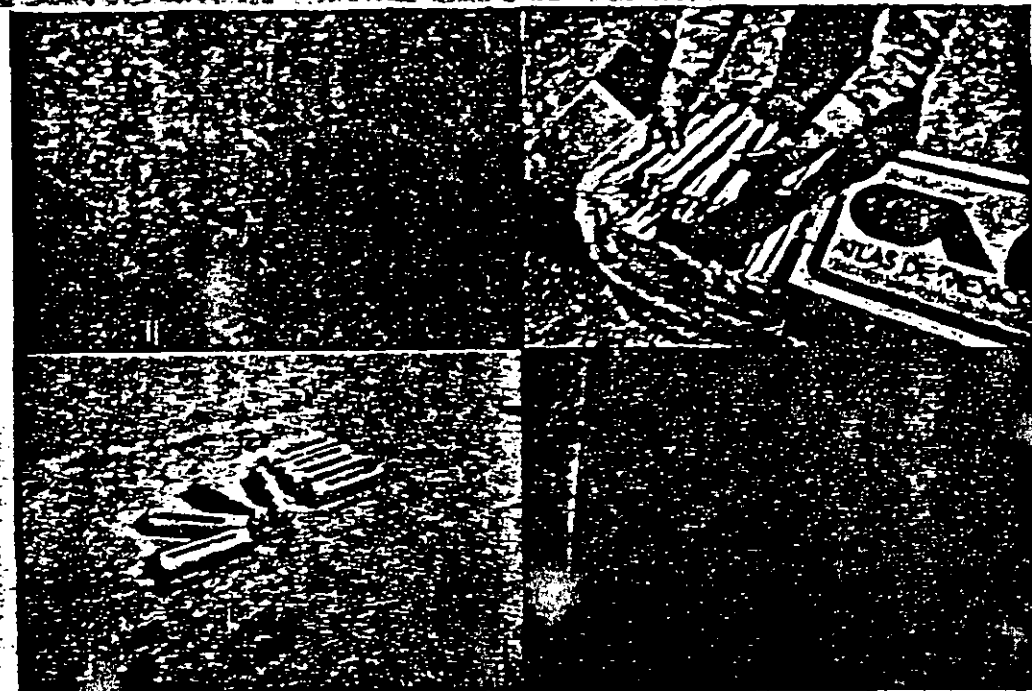
Características

- a) ASV = 361
- b) RWS = 96
- c) RBS = 14
- d) V.O.D. 2.7-2.8 km/seg
- e) Densidades reales de carga neumática de 83-87 g/cc
- e) Densidad 0.65-0.85 g/cc
- g) Clasificación de gases #1 (contiene materiales aligerantes que producen menos gases nocivos)
- h) Balance de oxígeno - 2.76
- i) Prueba al impacto de bala 30'06
- j) Prueba de fuego
- k) Mejor fluidez del producto: no se aglomera ni se apelmaza al cargar neumáticamente

- a) — ASV: Energía en KJ/100 grs.
- b) — RWS: Potencia relativa al peso.
- c) — RBS: Potencia relativa al volumen.
- d) — VOD: Velocidad de detonación al aire libre (ésta se incrementa hasta en un 40% cuando está confinado en el barreno).



GODYNE Diámetro pequeño Alto explosivo



Ventajas para el cliente

- Más energía por su dinero
- Mejor fragmentación
- Mejor sensibilidad
- Mayor seguridad
- Resistencia al agua
- Mejor propagación
- Menor cantidad de gases en combinación con el uso del AN/FO B.D.

Características

- a) ASV = 433 KJ/100 g
- b) RWS = 115
- c) RBS = 157
- d) Densidad = 1.2 g/cc
- e) Temperatura crítica $-8 \pm 2^\circ\text{C}$
- f) V.O.D. 32 a 33 km/seg
- g) ϕ crítico $-5/16"$
- h) Prueba de sensibilidad al cordón
- i) Prueba al impacto de bala 30'06
- j) Clasificación de gases # 1
- k) Prueba de fuego
- l) No contiene químicos orgánicos
- m) Prueba de gap. 1" a 2 1/2" a 25°C

- a) — ASV: Energía en kJ/100 grs.
- b) — RWS: Potencia relativa al peso.
- c) — RBS: Potencia relativa al volumen.
- f) — VOD: Velocidad de detonación al aire libre (ésta se incrementa hasta en un 40% cuando está confinado en el barreno).

SUPER "MEXAMON" D

edades

POTENCIA: equivalente a dinamita extra 65%

DENSIDAD VACIADO EN EL BARRENO: 0.65 g/cc.

DENSIDAD SOPLADO NEUMATICAMENTE: 0.75 g/cc.
(a 4.20 kg/cm² o 60 lb/plg²)

VELOCIDAD: 3 800 m/seg (12 500 pies/seg) aprox.

Super "Mexamon" D proporciona buena fragmentación en roca mediana dureza; está diseñado para uso en minas bajo tierra. Se emplea perfectamente con cargadores neumáticos y se compacta fácilmente aun en barrenaciones de contra-pozo. Super "Mexamon" D es del todo recomendable para ser empleado a cielo abierto. Fluye con toda facilidad en barrenos inclinados.

ventajas

VERSATILIDAD. Super "Mexamon" D puede usarse tanto en minas bajo tierra como en operaciones a cielo abierto. El mínimo de gases tóxicos que produce le conceden tal virtud.

POTENCIA. La velocidad de Super "Mexamon" D y la energía que desarrolla por su gran volumen de gases de expansión lo equiparan en potencia a la de la Dinamita Extra 65%.

DISTRIBUCION DE LA CARGA. Super "Mexamon" D, por su baja densidad, permite la mejor distribución del explosivo en el terreno y en consecuencia produce mejor fragmentación.

NO REQUIERE MEZCLAS ADICIONALES. Super "Mexamon" es un agente explosivo cuidadosamente formulado e integralmente elaborado, listo para cargarse directamente de la bolsa, tal como se recibe. Resultado: economía, no hay desperdicio.

INSIBILIDAD. Super "Mexamon" D ha demostrado ser más insensible a la onda de propagación que cualquier mezcla de nitrato de amonio o fertilizante y aceite diesel o combustible.

NO ES POLVOSO NI ACEITOSO. Super "Mexamon" D por su elaboración integral, ofrece las máximas comodidades al usuario. Está libre de migraciones y evaporaciones.

RESULTADOS REPRODUCIBLES. Con Super "Mexamon" D los resultados obtenibles, voladura tras voladura, son constantes y re-

nto o fertilizantes con combustibles debido a las tantas variantes que intervienen.

- 8. **SEGURIDAD.** Super "Mexamon" D es un agente explosivo y como tal, su empleo implica una mayor seguridad que con cualquier Dinamita.
- 9. **ECONOMIA.** Super "Mexamon" D puede en muchos casos, sustituir ventajosamente a las dinamitas, más altas en precio.

Iniciación

El iniciador o cebo recomendado para detonar el Super "Mexamon" D debe ser un explosivo potente y violento; tal como: 1. Gelatina extra 60%; 2. Gelamex No. 1; 3. Dinamita extra 60%. El cebo de iniciación debe constituir un 15% aproximadamente, en peso, del total de la carga explosiva en el barreno. En barrenos largos es recomendable usar más de un cebo de iniciación y cordón detonante "Primacord" o "E-Cord" a lo largo del barreno, distribuyendo los cebos a intervalos máximos de 5 metros; es decir, debe distribuirse el cebo total a intervalos a lo largo del barreno, dejando siempre en el fondo la mayor cantidad del cebo iniciador.

Carga

En operaciones a cielo abierto, Super "Mexamon" D puede cargarse por gravedad, vaciado. La tabla a continuación muestra aproximadamente los kilos por metro lineal de barrenos de varios diámetros:

Diámetro barreno cm (plg)	kg por metro lineal de barreno
2.54 (1)	0.329
5.08 (2)	1.318
7.62 (3)	2.964
10.16 (4)	5.270
12.70 (5)	8.234
15.24 (6)	11.857

Empaque

Super "Mexamon" D se envasa en bolsas resistentes de papel con cubierta interior de polietileno. Cada saco contiene 25 kg netos.

Almacenamiento

Super "Mexamon" D debe almacenarse considerándolo para el caso, como una Dinamita. Es aconsejable dar rotación a las existencias almacenadas, usando siempre primero el material más antiguo.

idades

- POTENCIA: equivalente a dinamita extra 65%
- DENSIDAD VACIADO EN EL BARRENO: 0.65 g/cc
- DENSIDAD SOPLADO NEUMATICAMENTE: 0.75 g/cc (a 4.20 kg/cm² o 60 lb/plg²)
- VELOCIDAD: 3 800 m/seg (12 500 pies/seg) aprox.

Super "Mexamon" D proporciona buena fragmentación en roca mediana dureza; está diseñado para uso en minas bajo tierra. Se compacta perfectamente con cargadores neumáticos y se compacta aún en barrenaciones de contra-pozo. Super "Mexamon" D es del todo recomendable para ser empleado a cielo abierto. Fluye con toda facilidad en barrenos inclinados.

VERSATILIDAD. Super "Mexamon" D puede usarse tanto en minas bajo tierra como en operaciones a cielo abierto. El mínimo de gases tóxicos que produce le conceden tal virtud.

POTENCIA. La velocidad de Super "Mexamon" D y la energía que desarrolla por su gran volumen de gases de expansión lo equiparan en potencia a la de la Dinamita Extra 65%.

DISTRIBUCION DE LA CARGA. Super "Mexamon" D, por su baja densidad, permite la mejor distribución del explosivo en el barreno y en consecuencia produce mejor fragmentación.

NO REQUIERE MEZCLAS ADICIONALES. Super "Mexamon" D es un agente explosivo cuidadosamente formulado e integralmente elaborado, listo para cargarse directamente de la bolsa, tal como se recibe. Resultado: economía, no hay desperdicio.

INSIBILIDAD. Super "Mexamon" D ha demostrado ser más insensible a la onda de propagación que cualquier mezcla de nitrato de amonio o fertilizante y aceite diesel o combustible.

NO ES POLVOSO NI ACEITOSO. Super "Mexamon" D por su elaboración integral, ofrece las máximas comodidades al usuario. Está libre de migraciones y evaporaciones.

RESULTADOS REPRODUCIBLES. Con Super "Mexamon" D los resultados obtenibles, voladura tras voladura, son constantes y re-

nio o fertilizantes con combustibles debido a las altas variaciones que intervienen.

- 8. **SEGURIDAD.** Super "Mexamon" D es un agente explosivo y como tal, su empleo implica una mayor seguridad que cualquier Dinamita.
- 9. **ECONOMIA.** Super "Mexamon" D puede en muchos casos, sustituir ventajosamente a las dinamitas, más altas en precio.

Iniciación

El iniciador o cebo recomendado para detonar el Super "Mexamon" D debe ser un explosivo potente y violento, tal como: 1. Gelatina extra 60%; 2. Gelamex No. 1; 3. Dinamita extra 60%. El cebo de iniciación debe constituir un 15% aproximadamente, en peso, del total de la carga explosiva en el barreno. En barrenos largos es recomendable usar más de un cebo de iniciación y cordón detonante "Primacord" o "E-Cord" a lo largo del barreno, distribuyendo los cebos a intervalos máximos de 5 metros; es decir, debe distribuirse el cebo total a intervalos a lo largo del barreno, dejando siempre en el fondo la mayor cantidad del cebo iniciador.

Carga

En operaciones a cielo abierto, Super "Mexamon" D puede cargarse por gravedad, vaciado. La tabla a continuación muestra aproximadamente los kilos por metro lineal de barrenos de varios diámetros:

Diámetro barreno cm (plg)	kg por metro lineal de barreno
2.54 (1)	0.329
5.08 (2)	1.318
7.62 (3)	2.964
10.16 (4)	5.270
12.70 (5)	8.234
15.24 (6)	11.857

Empaque

Super "Mexamon" D se envasa en bolsas resistentes de papel con cubierta interior de polietileno. Cada saco contiene 25 kg netos.

Almacenamiento

Super "Mexamon" D debe almacenarse considerándolo para el caso, como una Dinamita. Es aconsejable dar rotación a las existencias almacenadas, usando siempre primero el material más antiguo.



**FACULTAD DE INGENIERIA U.N.A.M.
DIVISION DE EDUCACION CONTINUA**

CURSOS ABIERTOS

**IV. CURSO INTERNACIONAL DE INGENIERIA GEOLOGICA APLICADA A
OBRAS SUPERFICIALES Y SUBTERRANEAS**

CUARTO MODULO:

TECNOLOGIA SOBRE EL USO DE EXPLOSIVOS

Del 22 al 26 de junio de 1992

CHAPTER 11

BLASTING THEORY

AUTOR: R. FRANK CHIAPPETTA

EXPOSITOR: ING. RAUL CUELLAR BORJA

JUNIO - 1992

CHAPTER 11

BLASTING THEORY

by R. Frank Chiappetta

1. INTRODUCTION

Blasting theory is perhaps one of the most interesting, thought provoking, challenging and controversial areas of our industry. It encompasses many areas in the science of chemistry, physics, thermodynamics, shock wave interactions, and rock mechanics. In broad terms, rock breakage by explosives involves the action of an explosive and the response of the surrounding rock mass within the realms of energy, time and mass. Past, current and new blasting theories are presented along with the factors affecting fragmentation and general blast design criteria. The chapter content has been carefully selected to emphasize the concepts associated with each blasting theory rather than a rigorous mathematical, physical, or chemical treatment through formulae. Where formulae are introduced, they are merely to enhance the concepts presented.

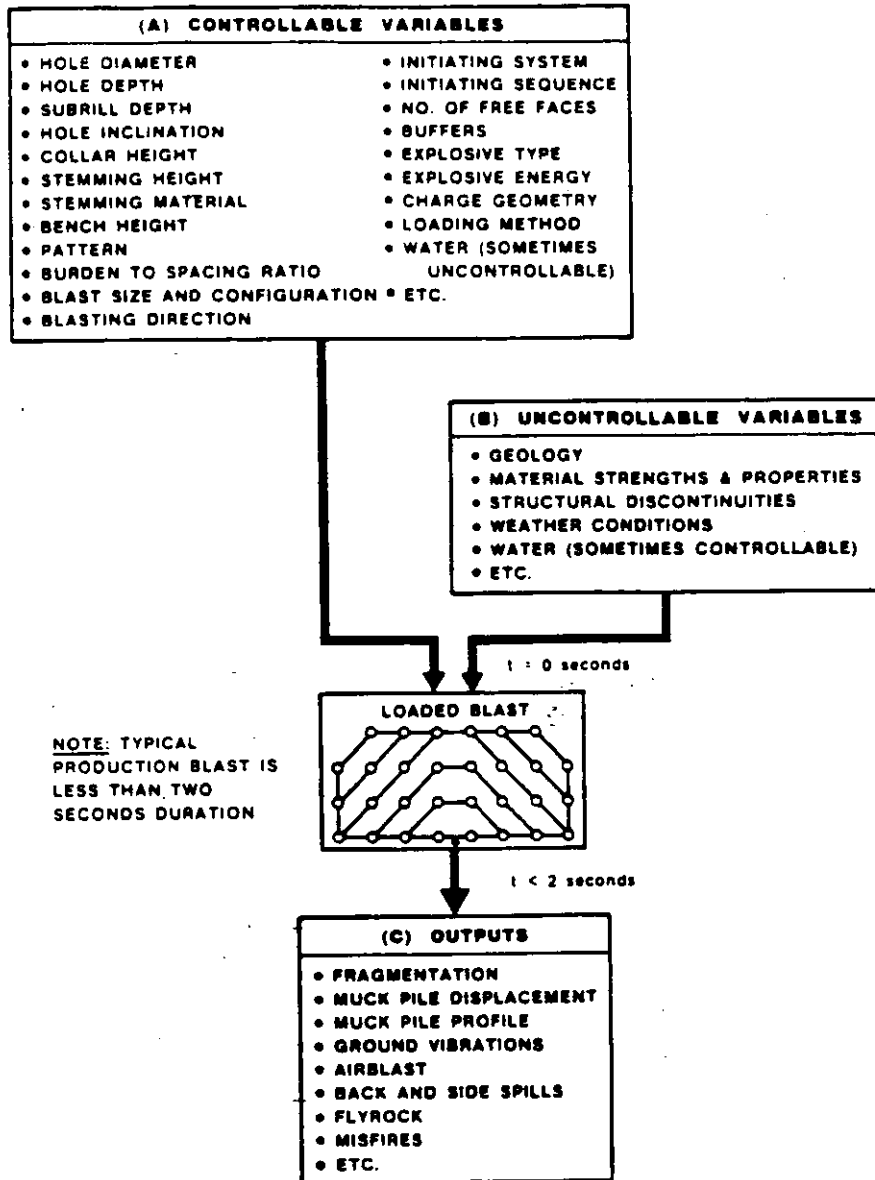
In spite of the tremendous amount of research conducted in the last few decades, no single blasting theory has been developed and accepted that adequately explains the mechanisms of rock breakage in all blasting conditions and material types. Given specific test environments, conditions and assumptions, individual researchers have contributed valuable information and insight as inputs into blasting theories, although a simple "plug-in" type formula for predicting "optimum fragmentation" is still largely unresolved. There is as yet no consistent and widely applicable theory of blasting, but only a number of limited and disconnected theories, many of which are empirical in nature and based on ideal blasting conditions. Blasting theories have been formulated and based on pure speculation, years of blasting experience on a trial and error approach, laboratory testing, field investigations, and mathematical and physical models adapted from other disciplines of science.

Primary breakage mechanisms have been based upon:

- Compressional and tensile strain wave energy
- Shock wave reflections at a free face
- Gas pressurization on the surrounding rock mass
- Flexural rupture
- Shear waves
- Release-of-load
- Nucleation of cracks at flaws and discontinuities
- In-flight collisions

Since so many schools of thought surround blasting theory, one must be prepared to investigate not only the theories, but the overall field input

variables that are inherent in any blast design to have any practical meaning. Given the diverse nature of field conditions encountered and the overwhelming number of blast design variables to select from, blast results may not always be easily predicted as is outlined in Figure 11-1. Where one theory is successful in one specific environment or application, it may not be as predictive in another.



FIELD MODEL ILLUSTRATING BLAST DESIGN INPUTS AND OUTPUTS

FIGURE 11.1

Often more than one theory is needed to clarify or explain certain results. Parallel this approach to the physicist trying to explain light with only one theory, that is, the wave theory. With the passage of time it became apparent that everything associated with light could not always be adequately explained with this theory alone and hence, another theory, the particle or "packets of energy" theory was developed to explain the phenomena of light in which the first theory failed. With both theories, the physicist could now explain many of the mysteries surrounding light which eventually led to new developments such as the laser. Similarly, in trying to define the mechanisms of rock breakage by explosives, more than one theory or explanation is often needed. In any case, a blasting theory should not only attempt to explain and predict the breaking process, but more importantly, it should suggest and allow new methods and techniques to improve on current blasting practices.

2. TIME EVENTS FOR THE BREAKING PROCESS

There are basically four time frames designated as T1 to T4 in which breakage and displacement of material occur during and after complete detonation of a confined charge.

The time frames are defined as follows:

- T1 — Detonation
- T2 — Shock or Stress Wave Propagation
- T3 — Gas Pressure Expansion
- T4 — Mass Movement

Each time frame is first discussed separately, and then discussed in conjunction with blasting theories for an overall, more detailed explanation and meshing of events. Although these are treated as discrete events, it should be emphasized that in a typical shot hole or production blast, one event phase can occur simultaneously with another at specific time intervals.

a. T1 — DETONATION

Detonation is the beginning phase of the fragmentation process. The ingredients of an explosive consisting of a fuel and oxidizer combination; upon detonation, are immediately converted to high pressure, high temperature gases. Pressures just behind the detonation front are in the order of 9 Kbars to 275 Kbars, while temperatures range from approximately 3000° to 7000°F.⁽²⁾

Detonation pressure is generally expressed as a function of the velocity of detonation and density of the explosives as,

$$P_D = (2.325 \times 10^{-7}) \times \rho \times VOD^2$$

Where P_D = detonation pressure in Kbars
 ρ = density in g/cc
 VOD = velocity of detonation in ft/sec.

To change detonation pressure from Kbars to lb/in², multiply Kbars by 14,700. Generally, explosives yielding higher detonation pressures are required to fracture materials which are massive, fine grained, hard, tightly bonded and strongly consolidated with heavy burdens. Typical values of detonation pressure for selected explosives are presented in Table 11-1.

TABLE 11.1
 DETONATION PRESSURES FOR SELECTED EXPLOSIVES

Explosive	Density (g/cc)	VOD (ft/sec)	Detonation Pressure (Kbars*)	Pressure (psi)
ANFO	0.81	12,000	27.00	396,900
POWERMAX 420	1.19	19,000	100.00	1,470,000
HI-PRIME	1.40	20,000	130.00	1,911,000
"G" BOOSTER	1.60	26,000	251.00	3,689,700

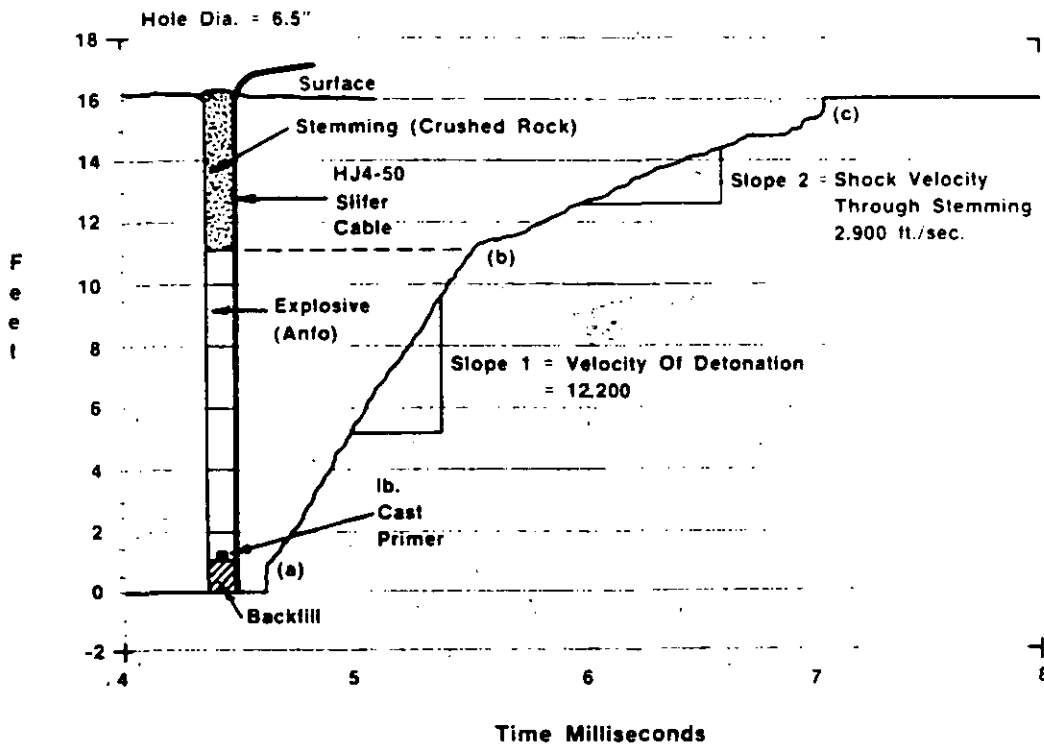
*1 Kbar = 14,700 PSI

The detonation wave starts at the point of primer initiation in the explosive column and travels at supersonic speeds. Supersonic refers to velocities which are faster than the speed of sound in the explosive. Typical velocities of detonation for commercial explosives range from 8,000 to 26,000 ft/sec. This velocity, sometimes referred to as the steady-state velocity, remains fairly constant for a given explosive, but varies from one explosive to another, depending primarily on the composition, particle size and density of the explosive. To a lesser extent, the steady state velocity is also affected by the degree of confinement and explosive diameter.

Since the velocity of detonation is greater than the velocity of sound in the explosive, the explosive material directly in front of the

detonation head is totally unaffected until the detonation head passes through it. In a typical 30 foot explosive column loaded with an explosive having a characteristic velocity of detonation of 10,000 ft/sec, complete detonation and energy release within the entire column would occur in about 3 milliseconds. For an explosive with a velocity of detonation of 20,000 ft/sec, detonation and energy release would be complete in 1.5 milliseconds. Detonations of this kind are self-sustaining due to the inertia of the explosive itself that provides confinement necessary to maintain conditions for fast chemical reaction rates.

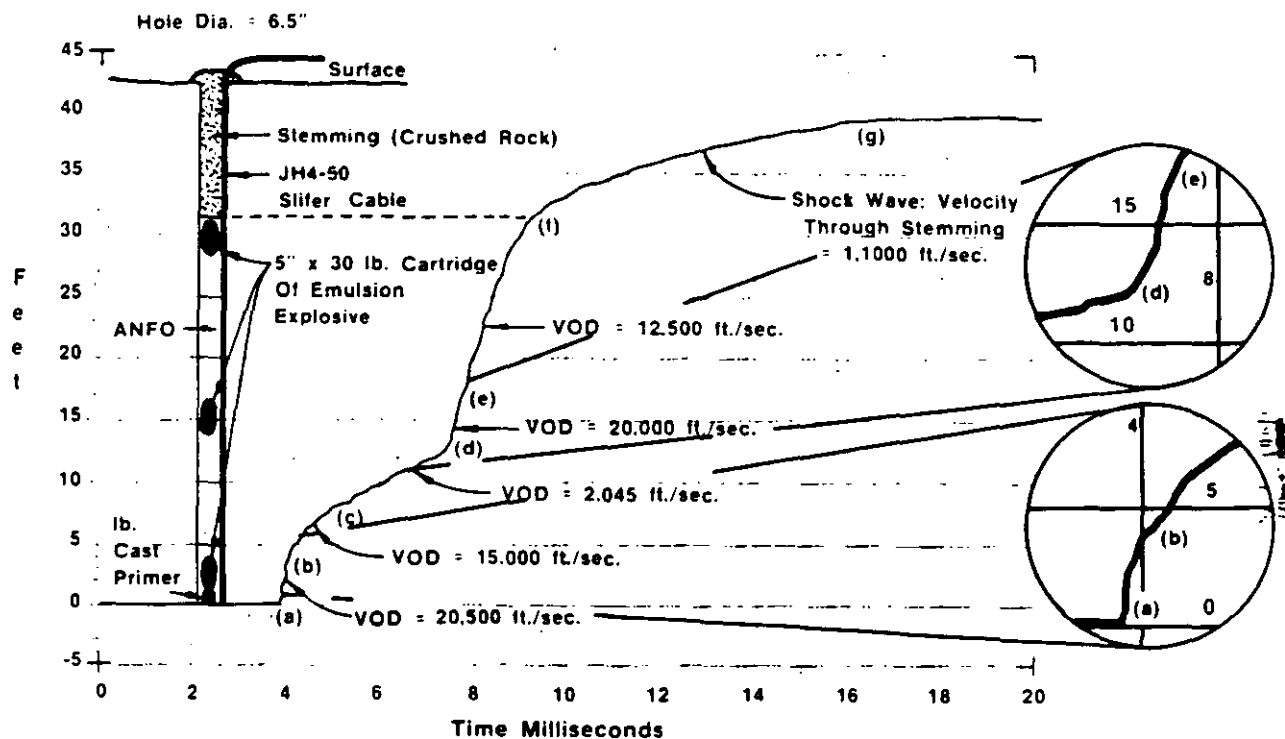
Figure 11-2 and 11-3 illustrate two typical hole load configurations. Velocity of detonation within the explosive column was measured with the SLIFER System developed at SANDIA NATIONAL LABORATORIES. For a continuous 11 foot column of cartridge ANFO, the velocity of detonation was measured to be 12,200 ft/sec as indicated by the slope of the straight line segment between point (a) and (b) in Figure 11-2. The straight line is indicative of a consistent explosive composition, constant density and a stable velocity of detonation. As detonation progresses along the column, not only is a



VELOCITY OF DETONATION MEASUREMENT USING THE SLIFER SYSTEM DEVELOPED AT SANDIA NATIONAL LABORATORIES
FIGURE 11.2



shock wave imparted into the surrounding medium adjacent to the borehole wall, but is also imparted into the stemming as indicated by the slope of the straight line segment between points (b) and (c). In this case, the shock wave velocity through the stemming was measured to be 2,900 ft/sec. or approximately $\frac{1}{4}$ that of the velocity of detonation.



**VELOCITY OF DETONATION MEASUREMENT
USING THE SLIFER SYSTEM DEVELOPED
AT SANDIA NATIONAL
LABORATORIES.**

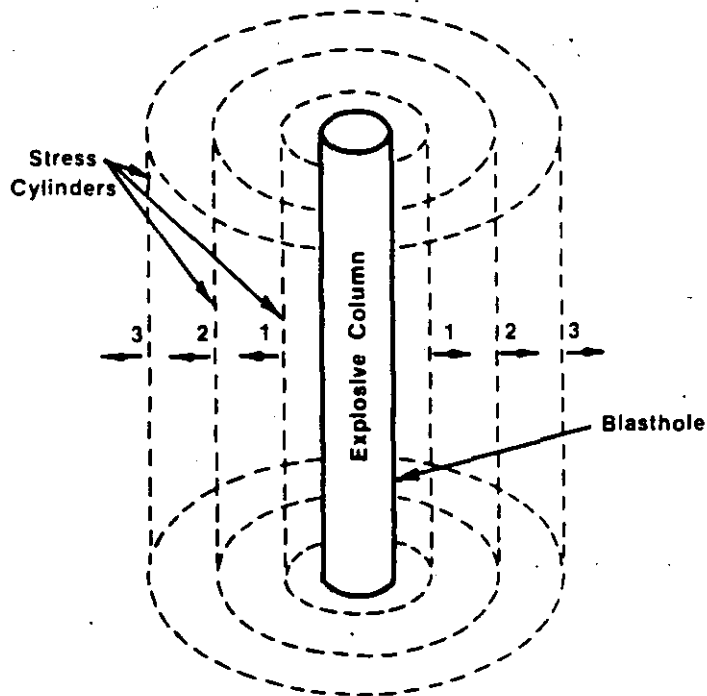
FIGURE 11.3

In Figure 11-3, results are shown using ALTERNATE VELOCITY techniques with a hole loaded with ANFO as the main charge, with cartridges of APEX 260 emulsion spaced 11-12 feet along the column. Without direct measurements of the continuous velocity of detonation, much of the information would not have been discernable in the field by direct observation. Many important points are noteworthy in the results. Between points (a) and (b), the velocity of detonation for the 3 foot length of emulsion cartridge is 20,500 ft/sec. Between (b) and (c) the velocity of detonation is reduced from 20,500 ft/sec to 2,045 ft/sec within the ANFO and the detonation is sustained at the lower velocity until point (d) is reached. At point (d) the detonation head encounters another emulsion cartridge, which when detonated, at 20,000 ft/sec between points (d) and (e), brings ANFO back up to its normal velocity of detonation of 12,500 ft/sec. Thus, even a

low order ANFO detonation can act as a very effective primer for the emulsion cartridge. The decrease in velocity between points (b) and (c) is attributed to water trickling into the bottom part of the hole from the surrounding rock mass. Although ANFO can tolerate up to a 10% water saturation level, it does so at the cost of blasting efficiency. If the center emulsion cartridge was not present, one of two things would have occurred. It may have sustained a low order ANFO detonation with a velocity of 2,045 ft/sec throughout the remaining explosive column, or it would have soon failed. It has been demonstrated in field trials that where an explosive of higher velocity of detonation is embedded sparingly within the column of a main explosive with a lower velocity of detonation, that better results are generally achieved. The greater the difference in detonation velocities and the harder the material to be blasted, the more pronounced are the results.

b. T2 – SHOCK AND STRAIN WAVE PROPAGATION

The second phase, immediately following detonation or in conjunction with the detonation phase of T1, is the shock and strain wave propagations throughout the rock mass. This disturbance or emitted



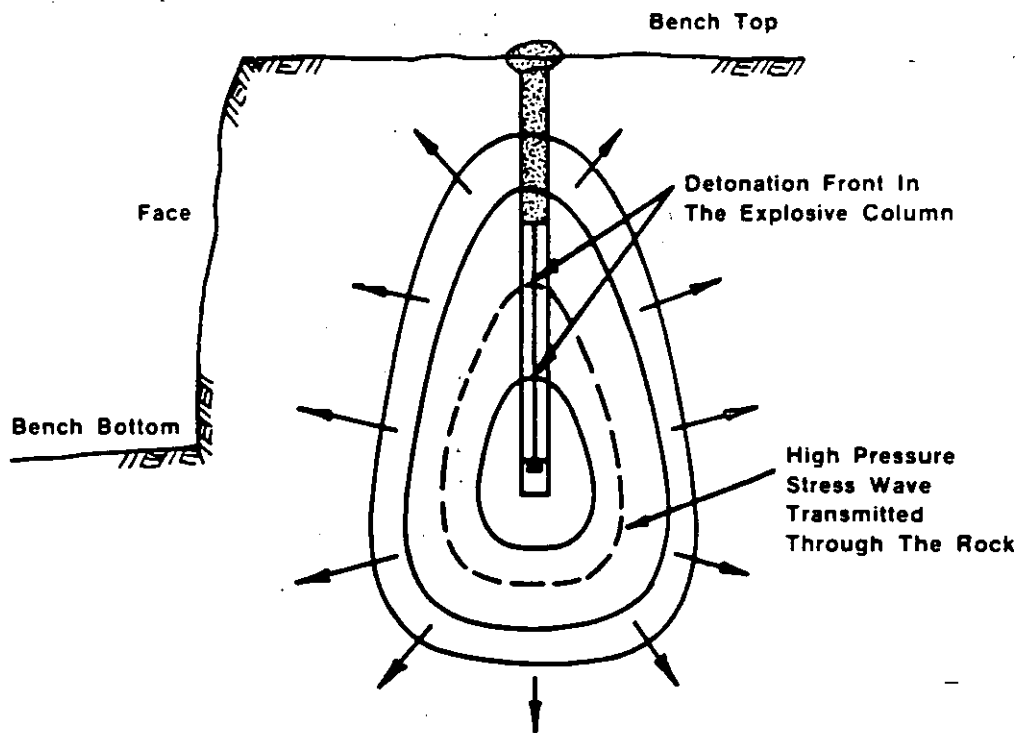
1,2,3 Successive Positions Of Stress Wave

THEORETICAL POSITIONS OF THE OUTBOUND DISTURBANCE FROM A COLUMN CHARGE

FIGURE 11.4



pressure wave(s) emitted into the rock mass results, in part, from the rapidly expanding high-pressure gas impacting the borehole wall. The geometry of dispersion depends primarily on the shape of the charge. If the charge is shot, with a length to diameter ratio of less than or equal to 6:1, then the disturbance is propagated in the form of an expanding sphere. If the charge is long, with a length to diameter ratio of greater than 6:1, then the disturbance is propagated in the form of an expanding cylinder. (Figure 11-4). However, in a typical, bottom primed, cylindrical shot hole normally encountered in bench blasting, the strain waves originally formed near the point of initiation are already in progress and propagating into the surrounding medium, while the detonation is still progressing within the explosive column. Thus, close to the shot hole, strain wave propagation is neither perfectly spherical nor cylindrical but more like that shown in Figure 11-5.



**SECTION THROUGH THE FACE DURING
 DETONATION SHOWING EXPANDING
 STRESS WAVE FRONT**

FIGURE 11.5

The pressure next to the borehole wall will rise instantaneously to its peak and then rapidly decay exponentially. The quick decay is due to cavity expansion of the borehole and increased gas cooling. Cavity expansion around the borehole can occur through crushing, pulverization, and/or displacement of material and can range anywhere from about one to three hole diameters depending on the medium and explosive used. Generally, extensive compressive, shear and tensile failure occur as a region of pulverized material since the wave energy is at its maximum near the borehole wall.

As the strain wave front proceeds outward, it has a tendency to compress the material at the wave front through a volume change. At right angles to this compressive front, there exists another component referred to as the tangential or "hoop" stress. The tangential stress, if large enough, can cause tensile failures at right angles to the direction of propagation. The largest tensile failures are expected to occur close to the borehole where the tangential stress is high enough for failure to occur. Both the compressive and tensile components of the wave front decay with distance from the borehole.

When the compressive wave front encounters a discontinuity or interface, some of the energy is transferred across the discontinuity and some reflected back to its point of origin.⁽⁴⁾ For the most part, the partitioning of energy depends on the ratio of the acoustic impedance of the materials on either side of the interface, as illustrated in Figure 11.6. Acoustic impedance, Z , for any material is defined as:

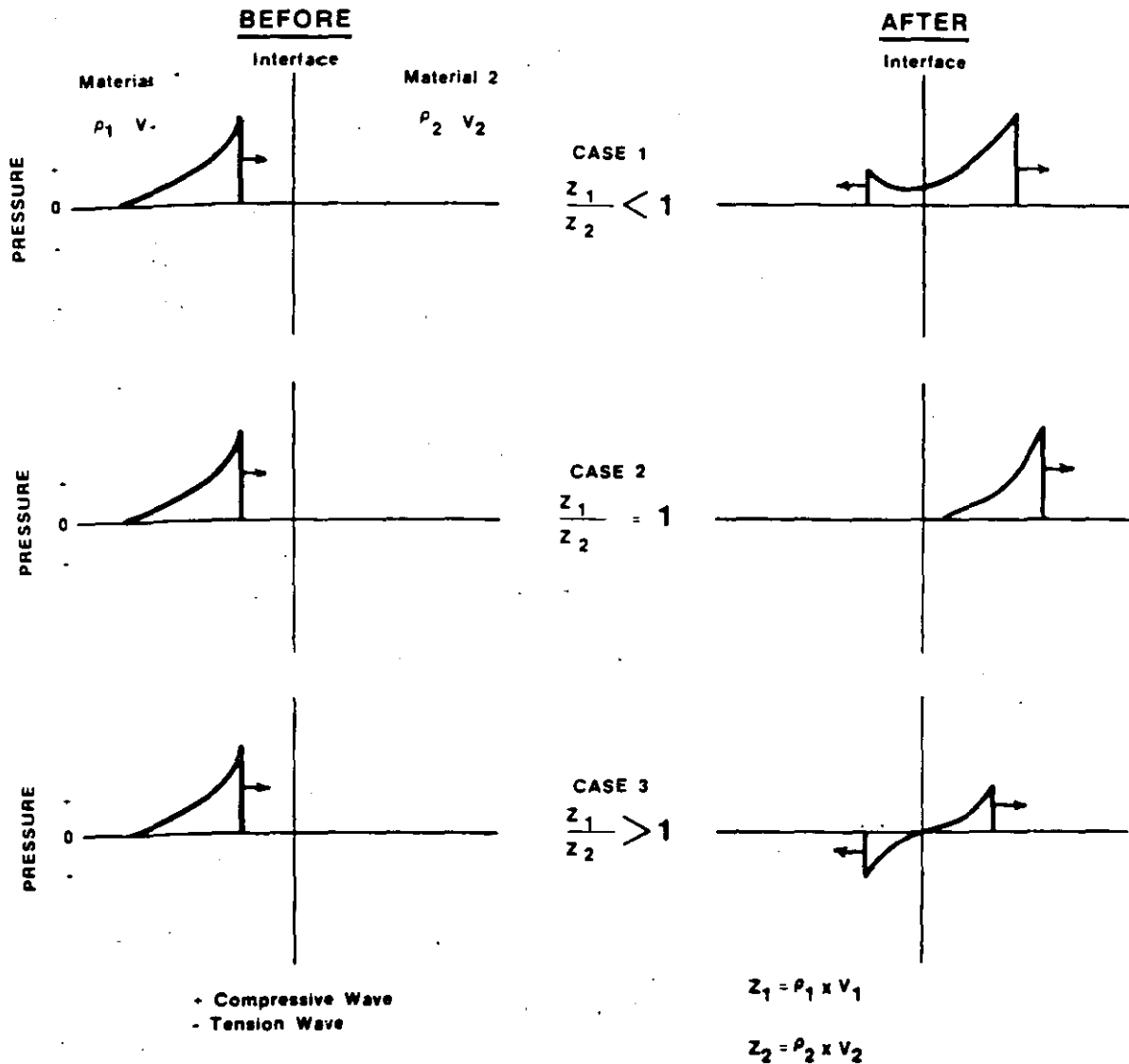
$$Z = \rho \times V_p$$

where: Z = acoustic impedance
 ρ = density of material
 V_p = sonic velocity of material

In reference to Figure 11-6, where the ratio of the acoustic impedance of material 1 to material 2 is less than one, some of the wave energy is transferred into material 2 and some reflected back, but both waves remain compressional. When the acoustic impedance ratio is 1, all of the energy is transferred into material 2 and no reflected wave occurs. When the impedance ratio is greater than 1, then some of the energy gets transferred into material 2 as a compressive wave and the remaining energy gets reflected at the interface as a tensile wave. When a compressive wave travelling through rock encounters an interface such as a free face, nearly all of the energy will be reflected back as a tensile wave. If the burden distance between the free face and explosive column is relatively small in

contrast to normal burdens for a chosen explosive, then most of the energy is consumed in spalling at the free face.

The interaction of stress waves in the outgoing compressive and reflected tensile modes around discontinuities and flaws within the rock mass is an area of intense research and is considered to be quite important in some of the newer blasting theories.



**INTERACTION OF STRESS WAVES
 AT AN INTERFACE
 FIGURE 11.6**

0

c. **T3 – GAS PRESSURE**

During and/or after strain wave propagation, the high pressure, high temperature gases impart a stress field around the blasthole that can expand the original borehole, extend radial cracks and jet into any discontinuity. It is during this phase where some controversy exists as to the main mechanism of fragmentation. Some believe that the fracture network throughout the rock mass is completed while others believe that the major fracturing process is just beginning. In any case, it is the gases that have jetted into discontinuities and the fracture network that is either fully developed or being developed, which are responsible for the displacement of broken material.

It is not clear as to the exact travel paths that gases take within the rock mass, although it is agreed that they will always take the path of least resistance. This means that gases will first migrate into existing cracks, joints, faults, and discontinuities, in addition to seams of material which exhibit low cohesion or bonding at interfaces. If a discontinuity or seam between the borehole and free face is sufficiently large, the high pressure gases will immediately vent to the atmosphere, rapidly reducing the total confinement pressures, and results in reduced displacement of broken and fragmented material.

The confinement time of gas pressures within a rock mass vary significantly depending on the amount and type of explosive, material type and structure, fracture network, amount and type of stemming, and burden. ATLAS studies, with the use of high-speed photography in full scale bench blasts, have shown that gas confinement times before the onset of movement can vary from a few milliseconds to tens of milliseconds.⁽³⁾ To date, confinement times have been measured to range from 5 to 110 milliseconds for a variety of materials, explosives and burdens. Generally, but not always, confinement times can be decreased by employing higher energy explosives, decreasing the burden, or a combination of both. This applies equally to material at the bench face or at the bench top, as in the case of stemming blowouts or cratering. Refer to Figures 12.35 and 12.36 Vibration/Airblast for specific examples of gas confinement times for stemming blowouts. It is evident that only suitably burdened and well stemmed charges can deliver their full potential of additional gas extension fracturing and mass movement.

d. **T4 – MASS MOVEMENT**

Mass movement of material is the last stage in the breaking process. The majority of fragmentation has already been completed

through compressional and tensile stress waves, gas pressurization or a combination of both. However, some degree of fragmentation, although slight, occurs through in-flight collisions and also when the material impacts the ground. Generally, the higher the bench height, the greater is this type of breakage owing to increased impact velocities of individual fragments when falling onto the bench floor. Similarly, material ejected from opposite rows of a "V-shot" design upon head-on collisions can result in increased fragmentation. This phenomenon was evidenced and documented with the use of high-speed photography of bench blasts.

Mass burden movement of fragmented material is shown in Figure 11-7 for a number of typical face conditions encountered in bench blasting operations. Face profiles and velocities are based on the results of high-speed photographic analysis performed at the ATLAS POWDER COMPANY. Where no subdrilling is utilized, (a and b), two types of face movement may be encountered. In 11-7a the entire length of face burden, directly in front of the explosive column, moves out similar to a plane wave and the face velocity at any point is constant. This behavior is usually encountered where material is very competent, quite brittle, and structured with well defined, largely spaced joints, much greater than the spacings or burdens employed in blast designs. When the material is soft, highly fissured, and/or closely jointed as might be found in coal and some sedimentary deposits, face profiles resembling that of flexural rupture is more likely. In this case, the greatest displacement and velocity occur adjacent to the center of the explosive column with the least amount of movement occurring at the toe and crest. When identical conditions in 11-7b are assumed and when subdrilling is employed, face movement results in much the same way except that the toe burden is displaced upwards faster and at a greater angle to the horizontal.

The first three cases assumed a relatively straight face between the crest and toe, however, in many bench blasting operations, the condition is more like that illustrated in Figure 11-7d, where toe burden is considerably greater than the crest burden. The toe burden is too great for the explosive selected, hence, very little movement occurs at the toe while the greatest displacement results in the upper half of the bench.

Three options are available to increase toe movement:

- Employ angle drilling in an attempt to maintain constant burdens from the crest to the toe
- Use a higher energy bottom charge in the current vertical drill holes
- Decrease the burden with the current vertical drill holes

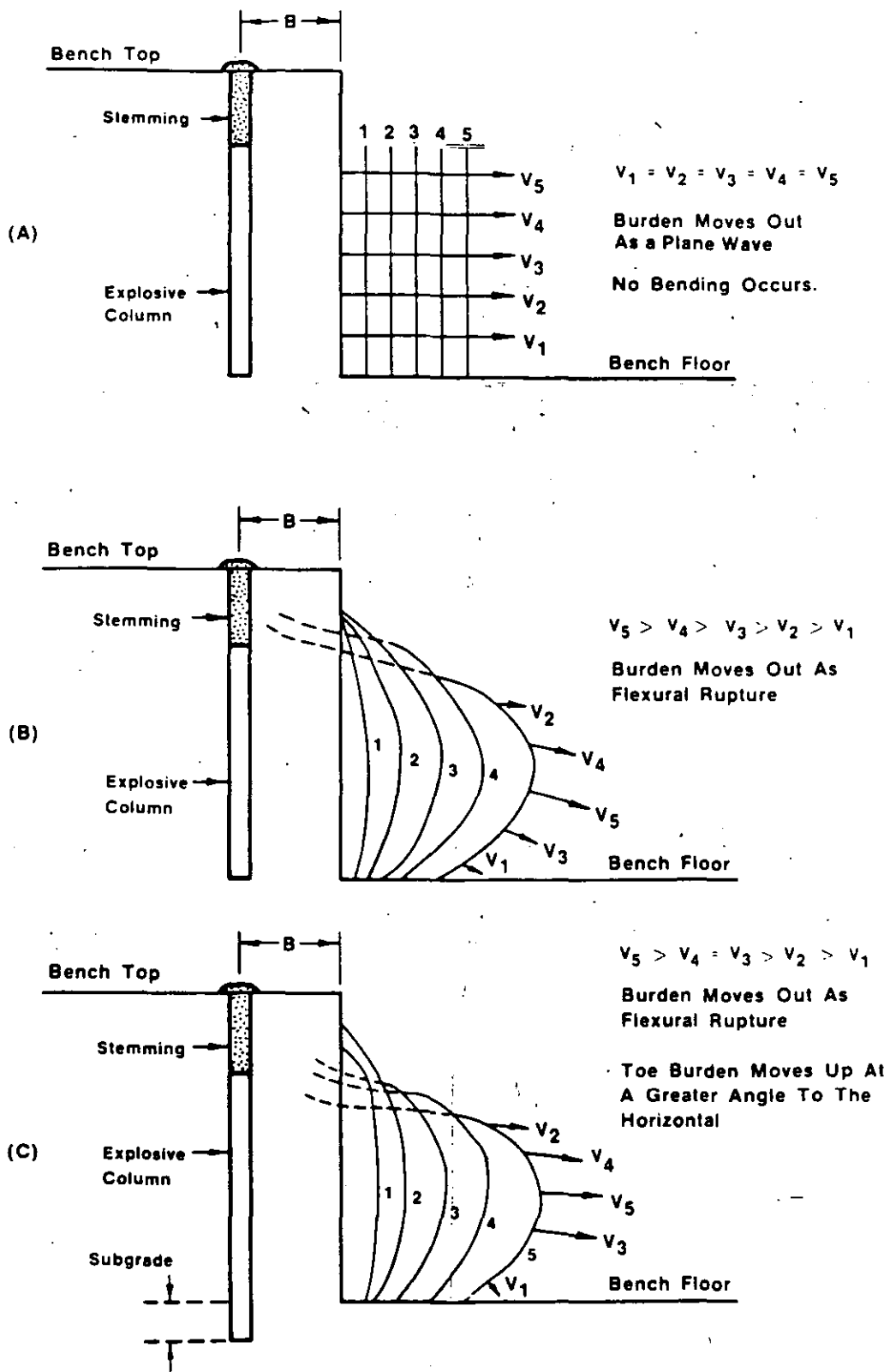


FIGURE 11.7

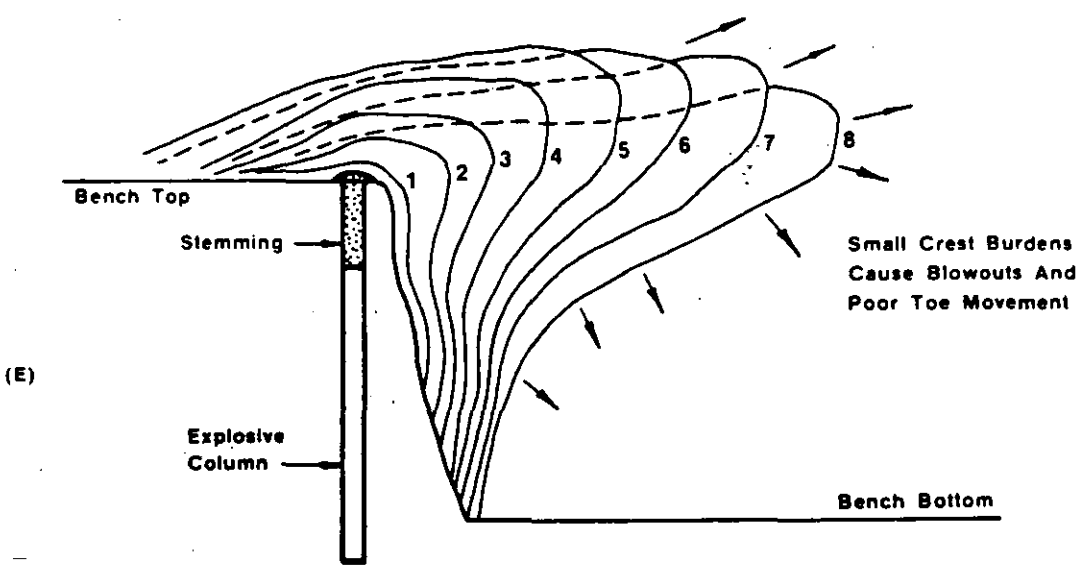
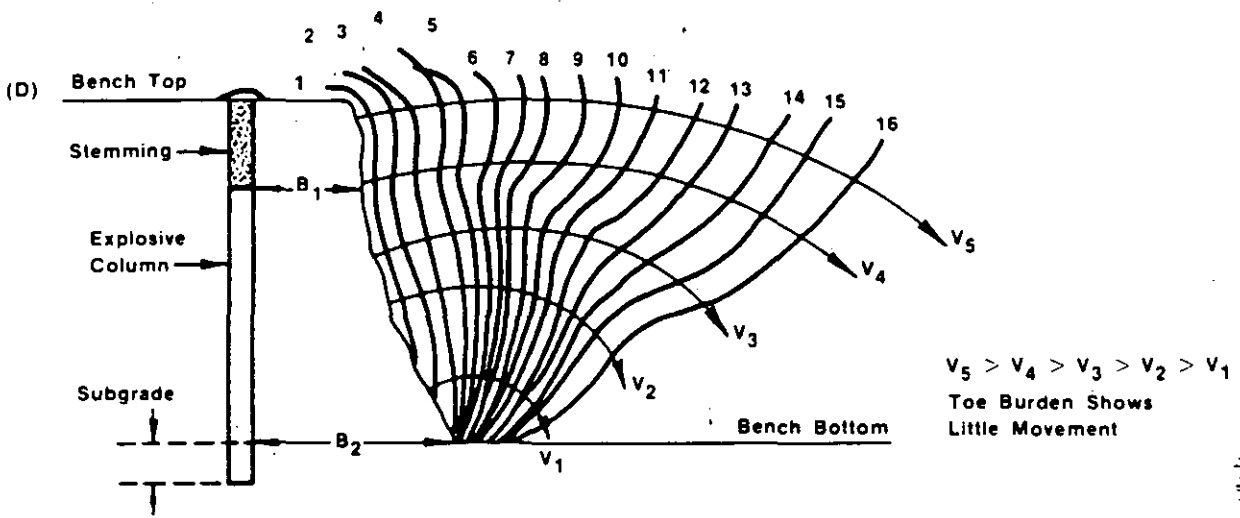


FIGURE 11.7 (Cont'd)

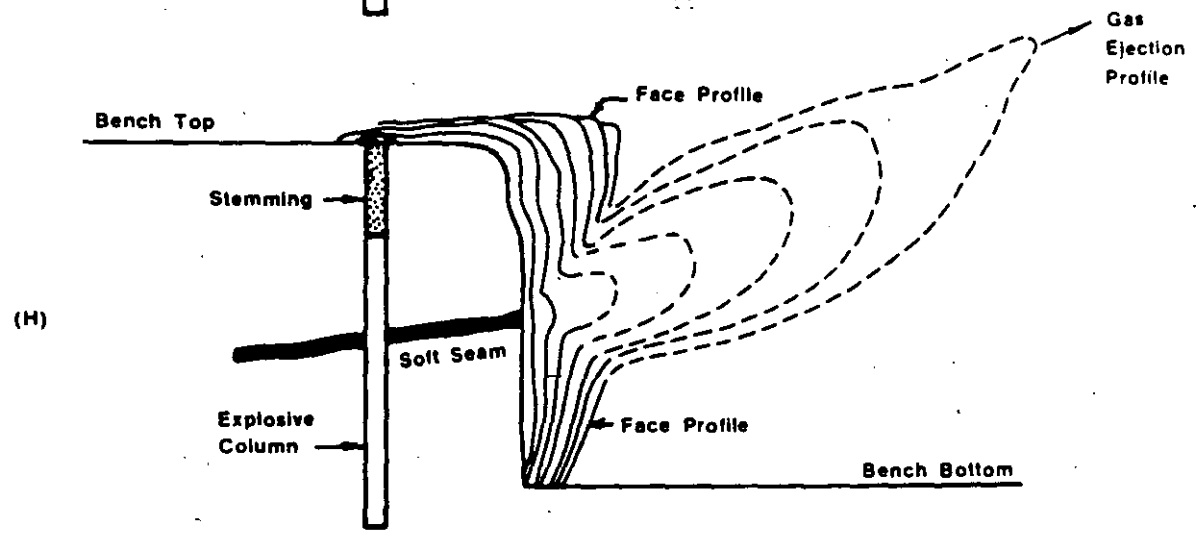
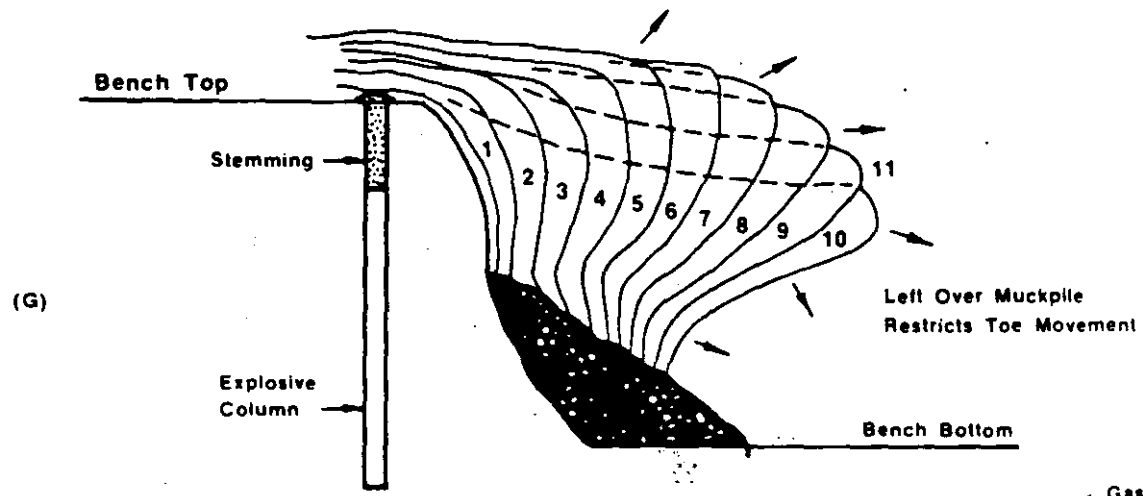
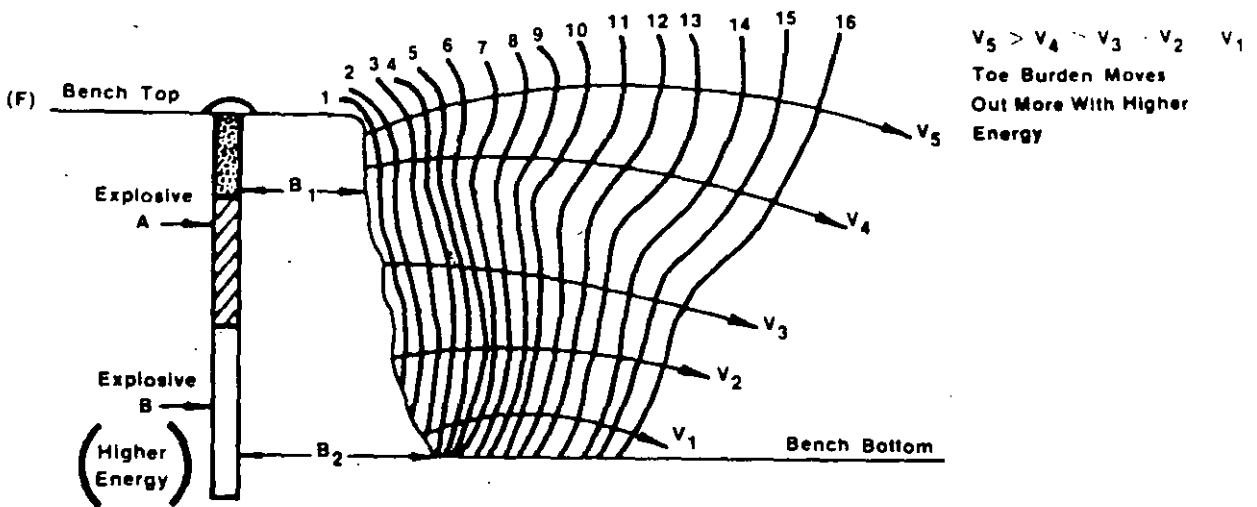


FIGURE 11.7 (Cont'd)

In selecting the latter, care should be exercised so as not to decrease the burden to the point of obtaining the condition shown in Figure 11-7e. The toe burden is now correct for the explosive selected, but the crest burden is substantially reduced. This may bring about many adverse conditions near the crest burden such as flyrock, blowouts, and increased airblast complaints. Because confinement pressures are released near the crest (in this case, a path of least resistance relative to the toe burden), restricted toe movement will result. It is better to use the same burden, but with a higher energy bottom charge near the toe. This load configuration as shown in Figure 11-7f tends to pressurize more of the burden mass for longer periods without adverse effects, and adequate toe movement generally results.

Where large leftover muckpiles are left against the face, Figure 11-7g, toe movement will be restricted and increased ground vibration levels are likely. Unless the situation requires a buffer, such as when blasting in the vicinity of mining equipment or to avoid dilution of an ore blast adjacent to a waste muckpile, it should be avoided.

Where seams are encountered in a blast, Figure 11-7h, tremendous gas ejections with velocities up to 600 ft/sec can occur. When such gas venting occurs, it will adversely affect other parts of the burden to displace adequately and inevitably leads to poor overall blasting results. A stemming deck immediately adjacent to the seam will give better results.

e. **TIME EVENTS T1-T4 COMBINED**

Up to this point, time events T1 to T4 have been discussed more or less as separate isolated events. However, in a real blasting environment, more than one event can occur at the same time.

Consider a single vertical hole in a quarry face with the primer located near the bottom of the hole as is illustrated in Figure 11-8. Assume the explosive used is 40 feet of ANFO with a velocity of detonation equal to 13,000 ft/sec, the material blasted is limestone with a sonic wave velocity of 15,000 ft/sec and a density of 2.3 g/cc. Upon initiation of the primer, it takes only a few microseconds and a distance of 2 to 6 hole diameters up the column to form a full detonation head. When a full detonation head is formed, it travels up the explosive column with a velocity characteristic of the steady-state velocity, (in this case 13,000 ft/sec). It takes approximately 3.0 ms for the 40 foot column of ANFO to be completely detonated.

Within this 3.0 ms, many other things have occurred. Starting at the bottom of the hole and progressing up the column, borehole

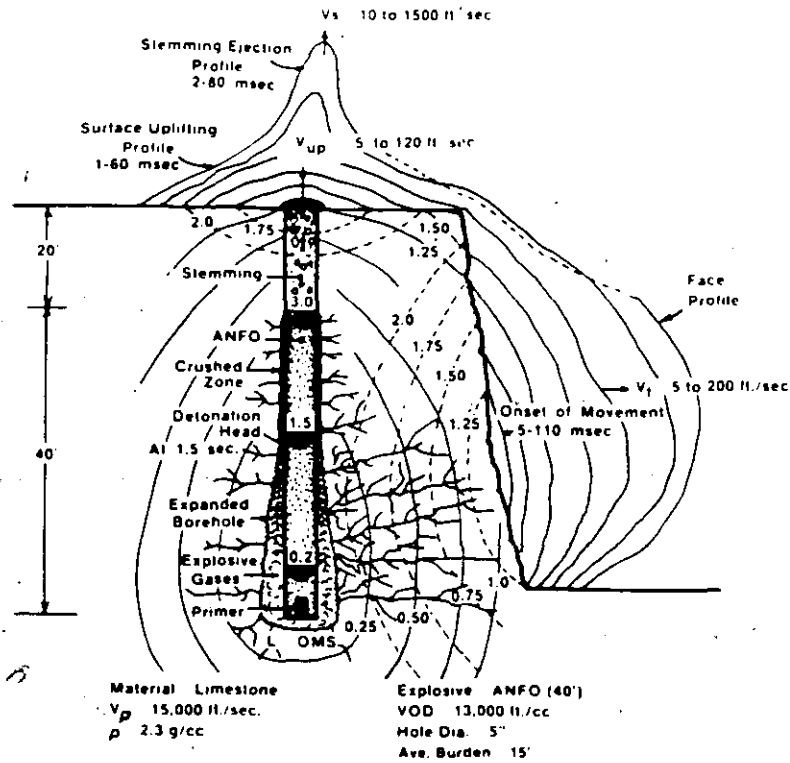


**ILLUSTRATION SHOWING THE INTERACTION OF
TIME EVENTS T1 TO T4 IN A
TYPICAL QUARRY BENCH
FIGURE 11.8**

expansion through crushing of the borehole walls has taken place. This produces compressive stress waves with tangential components emanating from the borehole walls and progressing outward in every direction with a velocity characteristic of the sonic wave velocity of limestone. It takes approximately 1.0 msec for the compressive strain wave to transverse 15 feet of burden to the free face. Behind the strain wave propagation some radial cracks start to develop in the crushed zone region of the borehole with a velocity ranging from 25 to 50% of the P-wave velocity for limestone. If the intensity of the compressive strain pulse is high enough, new cracks and/or extensions of pre-existing cracks and flaws can be initiated anywhere between the crushed zone next to the borehole and the free face. The greatest number of cracks are generally found closest to the borehole

When the compressive wave strikes a free face, it is immediately converted to a tensile strain wave which starts at the free face and travels back through the rock mass towards the borehole. Owing to

the new fractures created from the outgoing compressive strain wave, the tensile strain wave will take somewhat longer to travel the same burden distance of 15 feet. If the burden is small enough and the intensity of the reflected strain wave is large enough, then some spalling at the free face or bench top is expected, although no significant mass movement will occur.

At 3 ms after detonation and complete reaction of ANFO, the original high temperature, high pressure gases have reached a new equilibrium due to borehole expansion. Both temperature and pressure have dropped significantly resulting in an energy reduction ranging from 25 to 60% of the theoretical energy originally available. This remaining energy acts on the surrounding "preconditioned" rock mass to displace it in the direction of least resistance. Further fragmentation can occur at this stage from gases entering and extending preexisting cracks or discontinuities. It is at this stage where some blasting theories are contradictory. Some believe that the major fracture network is completed within about 3 ms due to the interaction of stress waves on the surrounding material, while others believe that the major fracture network is just beginning.

Regardless of which time frame is responsible for the development of a fracture network, mass movement and displacement of material at the bench top or face occurs much later in time due to the confinement of gas pressure within the rock mass. The onset of mass movement depends on the material response in conjunction with the strain and gas pressure stimulus generated from the explosive. For typical stemming and burdens encountered in the field, bench top swelling occurs between 1 to 60 ms, stemming ejections between 2 to 80 ms and bench burdens between 5 to 110 ms. Surface-uplifting velocities around the collar region of a hole occur between 5 and 120 ft/sec, stemming ejections between 10 to 1500 ft/sec and burden velocities between 5 to 200 ft/sec. Gas ejection velocities at discontinuities have been recorded as high as 700 ft/sec and often occur in less than 5 ms.

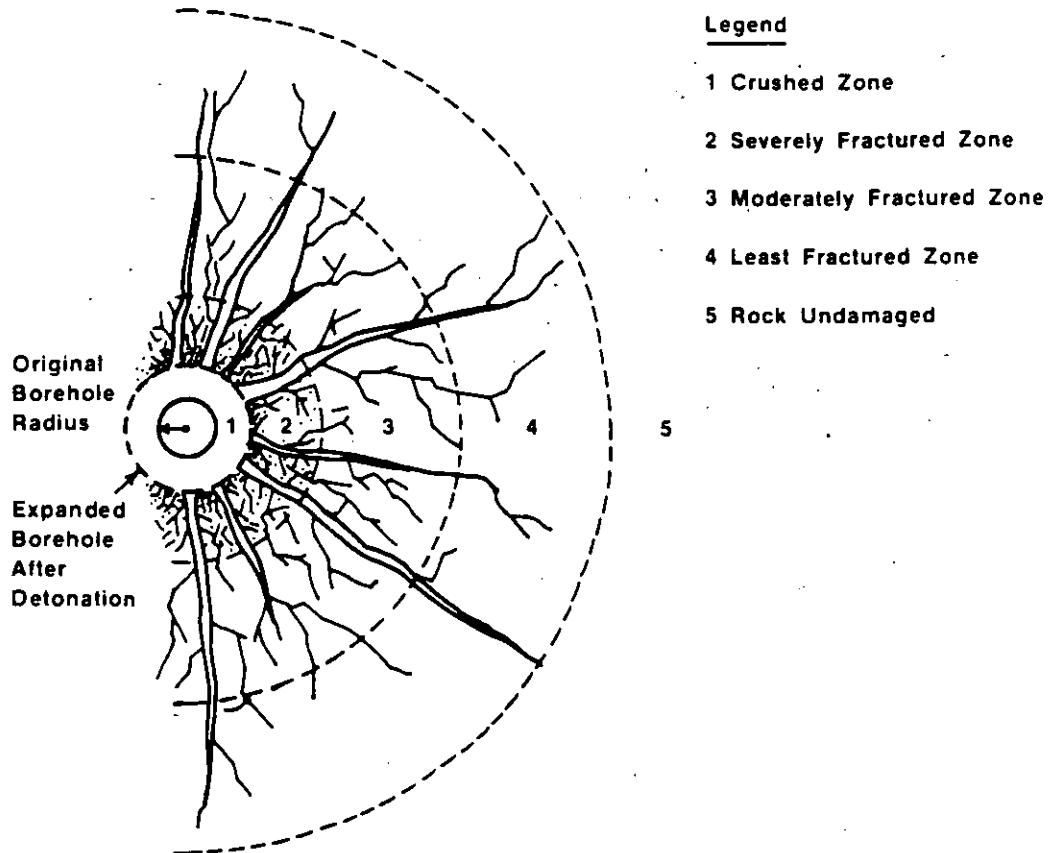
3. RUPTURE RADIUS

The degree of damage and fracturing around a borehole can be characterized by four zones as illustrated in Figure 11-9. In the crushed zone immediately around the borehole, the explosive induced pressures and stresses exceed the dynamic compressive strength of the rock by factors ranging from 40 to 400. These high pressures acting against the borehole wall will crush, pulverize and shatter the surrounding rock mass, causing



intense damage. This zone is also referred to as the hydrodynamic zone in which the elastic rigidity of the rock becomes insignificant. (6)

Next to the crushed zone is a region defined by a severely fractured zone referred to as the non-linear zone. Here fracturing can range from severe crushing through partial fracturing, to plastic deformation. Extension



ZONES OF RUPTURE RADIUS
FIGURE 11.9

of cracks can occur from previously formed cracks by the tangential component (hoop stress) of the shock wave, infiltration of gas pressure and at flaw sites.

In zones 3 and 4 (elastic zones) tensile failures and crack extensions occur in a less intense mode because the stress wave amplitude has attenuated significantly. Much of the original energy from the detonation has been consumed in the form of heat, friction, and fracturing in zones 1 and 2. The peak amplitude of the compressive stress is now much smaller than the compressive strength of the rock so no new fractures are likely in this wave type. However, the tangential stress component of the wave is still substan-



tially larger than the tensile strength of the rock. Since the tensile strength of rock is about 1/15 to 1/10 of the compressive strength, the tangential stress of the wave is large enough to cause radial fractures. These new fractures are formed from the extension of cracks in the non-linear zone (zone 2) or from cracks initiated from microfractures and flaws inherent in a typical rock mass.

Once the tangential stress has attenuated below the critical tensile strength of the rock, no further breakage occurs beyond this point as illustrated in zone 5 (Figure 11-9). Once the wave or disturbance passes into and through this zone, the individual particles of the medium will oscillate and vibrate about their rest positions within the elastic limits of the rock and so no permanent damage results. It is this region where seismic waves are carried considerable distances and are responsible for ground vibrations.

Table 11-2 gives an idea of the degree of maximum damage found around the crushed and fractured zones in terms of charge radii for a number of conditions. Results are based on the works of many researchers, conducted in a number of different materials with varying explosives. For a given explosive, the rupture radius is greater in soft rock than hard rock. Given the same rock, the rupture radius is greater for higher strength explosives than lower strength ones. Thus, the degree of radial rupture is influenced by the explosive, material properties and structure.

TABLE 2
DEGREE OF DAMAGE AROUND A
BOREHOLE IN TERMS OF CHARGE RADII

SOURCE	EXPLOSIVE	EXPLOSIVE AMOUNT	CHARGE SHAPE	MATERIAL OR ROCK TYPE	CRUSHED ZONE IN CHARGE RADII (MAX)	RADIUS OF DAMAGE IN CHARGE RADII (MAX)	COMMENTS
Olsen (7)	C4	0.25 kg 2.00 kg	S	Granite	—	18	
Siskind (8)	60% Dynamite	—	C	Granite	—	20	
	ANFO	—	C	Shale	—	45-55	
Cattermole (9)	60% Dynamite	—	C	Shale	—	15-22	
	—	—	C	Tuffaceous Pyroclastic	3.0	20-30	
Colorado (10) School of Mines	—	—	—	Soft Rock	—	26-29	
	—	—	—	Hard Rock	—	20-23	
Dertlich (11)	Nuclear (TNT)	—	—	Granite	1.9	4.9	
Atchison (12)	—	3.6 kg (max)	C	Granite	3-4.5	—	
D'Andrea (13)	C4	0.00 216 kg to 0.467 kg	S	Granite	2.3	—	
Siskind (14)	ANFO	—	C	Granite	—	14	
Kutter et al (8)	Underwater	—	S	Plexiglass & Rock	—	6	Theoretically Calculated
	Sparks Discharge	—	C	Plexiglass & Rock	—	9	
Yosh et al (15)	—	—	—	Granite, Limestone & Concrete	8-12	30-50	Theoretically Calculated
Borg (16)	Nuclear	—	—	Competent	2.7-3.5	—	Horizontal Fracturing Below Shot Point
					2.0	—	

4. BLASTING THEORIES (Past & Present)

In this section, blasting theories of the past and present are discussed in concept form. Table 11-3 is a list of some of the more common thoughts regarding breakage mechanisms and the researchers responsible for their introduction. This list is by no means complete, but it does illustrate how certain thoughts on blasting theory started with the simple reflection theory after World War II and progressed to the more complex nuclei or stress-wave flaw theory of the present.

Since each theory has inherent strengths and weaknesses, the main concepts of each theory are best explained with a brief description. Blasting theories discussed are:

- a) Reflection Theory (Reflected Stress Waves)
- b) Gas Expansion Theory
- c) Flexural Rupture
- d) Stress Waves & Gas Expansion Theory
- e) Stress Waves, Gas Expansion & Stress-Wave/Flaw Theory
- f) Nuclei or Stress-Wave/Flaw Theory
- g) Torque Theory
- h) Cratering Theory
- i) Cratering Mechanisms

a. REFLECTION THEORY (Reflected Stress Waves) (17, 18, 19, 20)

One of the first attempts to explain, analytically, how rock breaks when a concentrated explosive charge is detonated in a borehole near a free surface was with the reflection theory. The concept was simple, straight forward, and based strictly on the well known fact that rock is always less resistant in tension than in compression. A compressive strain pulse is generated by the detonation of an explosive charge, moves through the rock in all directions with a decaying amplitude, and is reflected only at a free surface. At the free surface, the compressive strain pulse is converted into a tensile strain pulse that progresses back to its point of origin. (See Figure 11-10). Since rock is weakest in tension, it is easily pulled apart by the reflected tensile strain pulse and damage at the face appears in the form of spalling. The high pressure, expanding gases, are not deemed directly responsible for the major degree of fracturing that occurs.

A more detailed explanation follows: Detonation of an explosive charge in rock generates a large quantity of high temperature, high pressure gas in a very short time. Typically, this occurs in a few microseconds for small cylindrical charges and in a few milliseconds

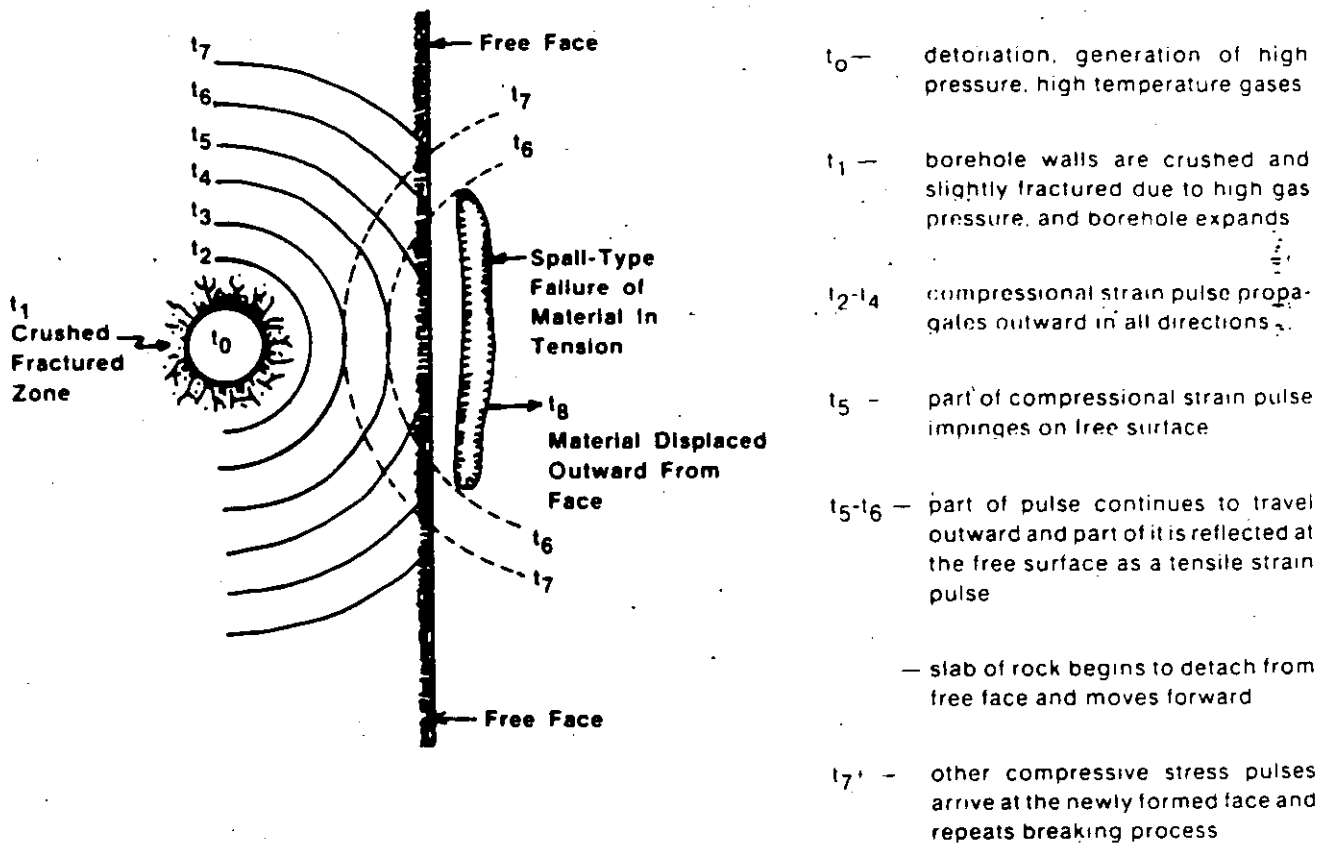
**TABLE 11.3
BLASTING THEORIES AND
THEIR BREAKAGE MECHANISM**

DATE	RESEARCHER(S)	BREAKAGE MECHANISMS				
		TENSILE REFLECTED WAVES	COMPRESSSIONAL STRAIN WAVES	GAS PRESSURE	FLEXURAL RUPTURE	NUCLEI STRESS-FLAW
1949	Obert, Duvall (17) (18)	1				
1956	Hind (19)	1				
1957	Duvall, Atchison (20)	1				
1958	Rinehart (21)	1				
1963	Langfors, Kihlstrom (22)		2	1		
1966	Starfield (23)	1				
1970	Porter, Fairhurst (24)		2	1		
1970	Persson, Lunborg, Johansson (25)		1			
1971	Kutter, Fairhurst (6)		1	1		
1971	Field, Ladegarrd - Pederson (26)		1	1		
1972	Johansson, Persson (27)	2		1		
1972	Lang, Faureau (28)	4	2	1		3
1973	Ash (29)			1	1	
1974	Hagan (30) (31)		1			
1978	Barker, Fourney, Dally (32) (33) (34)					1
1983	Winzer, Anderson, Ritter (35)					1
1983	Adams, Margolin (36) (37)					1
1983	McHugh (38)					1

for long cylindrical charges found in normal bench blasting. This gas pressure acting against the borehole wall generates a compressive strain or stress pulse of high amplitude which will crush and/or fracture rock next to the borehole. This stress pulse travels radially outward in all directions from the shot point at speeds equal to or greater than the velocity of sound in the medium. Due to wave divergence and energy absorption by the rock, the pulse amplitude decreases very rapidly. Thus, the extent of the crushed zone immediately next to the borehole is relatively small.

When a longitudinal compressive stress strikes a free surface, two reflected pulses are generated, a tensile and shear pulse. The amount of energy imparted to each depends on the angle of incidence of the compressional stress pulse. Of the two reflected pulses, the tensile one predominates in breaking rock as it moves back into the rock.

The effective transfer of detonation pressure to stress in the rock depends on the impedance match of the explosive to rock. A smaller explosive to rock impedance ratio was shown to provide a more effective transfer of this pressure to stress. The concept of reflection breakage is illustrated in Figure 11-10. The time order of key events are:



**REFLECTION THEORY
TENSILE FRACTURE BY REFLECTION
OF A COMPRESSIVE STRAIN
PULSE AT A FREE SURFACE**

FIGURE 11.10

Slabs broken off closer to the hole are displaced with lower velocities.

b. GAS EXPANSION THEORY (25) (39)

The pressure acting on the walls of an explosive filled hole, upon detonation, will be approximately one-half of the detonation pressure due to expansion of the borehole. This pressure will propagate out from the borehole into the rock as a shock wave. The material between the borehole and the shock front is compressed and flows elastically or plastically, depending on the pressure and strength of the rock. Some radial cracks form next to the borehole wall starting at about two hole radii out and then propagate radially inwards as well as outward. The greatest frequency of radial cracks are next to the borehole, but a few extend farther out. When no free face exists, a small number of these radial cracks become very much larger than the others.

By the time the shock wave reaches the free surface, radial crack lengths formed are less than one quarter of this distance. At this stage the longest of cracks have extended inwards and reached the borehole wall. Gas pressure is now capable of entering these cracks and if the pressure is high enough can reach out towards the crack tips, thus further elongating the cracks. This has the effect of aiding cracks that interact with the returning tensile wave and cause them to reach the free surface. Up to this point, acceleration of the rock mass between the hole and free face has been negligible. Only after the cracks have reached the free surface is the rock accelerated by the remaining gas pressure.

The key point of the gas expansion theory are:

- Radial cracks are initiated not immediately next to the borehole but about two hole radii out and extend inwards toward the hole as well as outwards towards a free face.
- Rock displacement does not occur until pressurized radial cracks extend to the free surface.

c. FLEXURAL RUPTURE (A Gas Expansion Theory) (29)

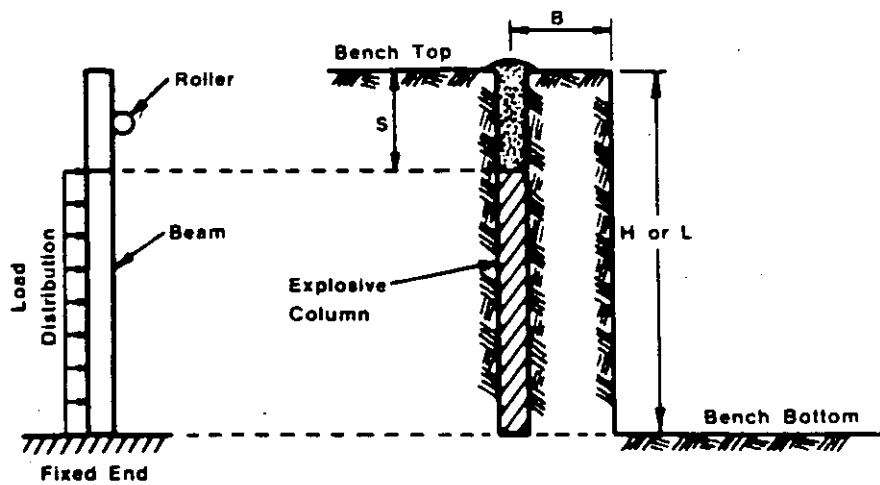
During detonation of an explosive confined in a borehole, two distinct pressures are formed; one from the detonation itself and the other from the highly heated gases acting on the borehole walls. In

this theory, ninety percent of the total energy to break rock is in the latter. Detonation pressure acts only momentarily against any one part of the borehole's internal surface area, while gas pressure is sustained considerably longer until some form of cavity volume change occurs. Gas pressure, then, is the major component responsible for fragmentation and flexural rupture.

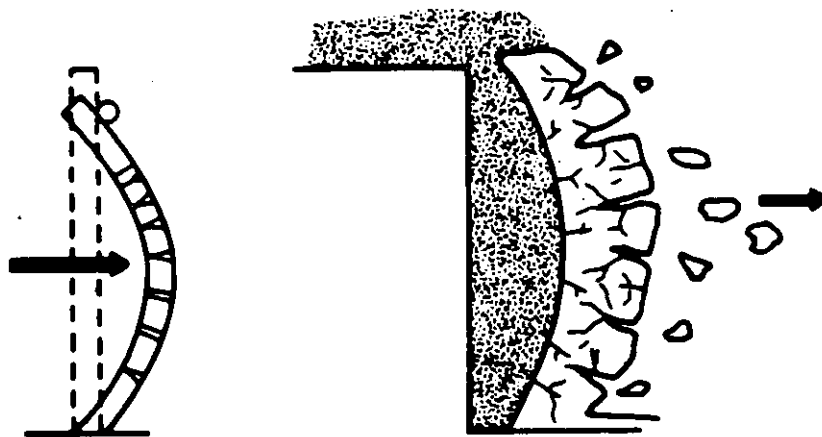
Radial cracks form only in planes parallel with the borehole axis. No cracks develop where the explosive is not in immediate contact, thus most cracks form adjacent to the borehole wall where tangential stresses are produced within the borehole's wall as the cavity is pressurized. Providing strain energies at crack tips are adequate, extension of fractures continue. Breakage by reflection of strain energy at a free face is considered negligible. Gas pressure drives the radially produced cracks through the burden to the free face and displaces rock through bending and in the direction of least resistance generally following naturally occurring planes of weakness. It is during this final stage where the major breakup of intact material takes place.

Breaking of rock by flexural rupture is analogous to bending and breaking a beam as illustrated in Figures 11-11 and 11-12. A rectangular beam is used to represent the field configuration of bench height, H, and burden, B, in the form of a modified cantilever beam model. The fixed end of the beam represents toe conditions while a roller, placed directly opposite the center of the stemming column, represents the stemming function. The roller allows the collar region to rotate and move longitudinally but does not allow deflection normal to the borehole axis. Although not shown for clarity of concept, the beam thickness in Figures 11-11 and 11-12 is actually equal to the burden. Borehole pressure is represented as a load distributed along the length of blasthole containing the explosive. Rock weight of the bench segment is considered negligible relative to the load resulting from the borehole gas pressure. Maximum contribution of total rock load acting at floor level is only at a ratio of about 1:100,000 or more compared to gas pressure.

The degree of fragmentation is controlled by the stiffness property of the burden-rock mass. This stiffness depends on existing restraints to movement, rock (Young's modulus), radially-cracked block's geometric shape as defined by its average thickness, width, and length. In terms of blast configuration, burden, spacing, and bench height are the controlling factors for any given rock.



BEAM BENDING MODEL BEFORE DETONATION
FIGURE 11.11



BEAM BENDING MODEL AFTER DETONATION
FIGURE 11.12

To achieve adequate flexural rupture, the burden to length (B/L) ratio becomes critical because stiffness varies with the third power of this ratio. For a given explosive diameter and reflective B value, decreasing the bench height L has the effect of,

- i) stiffening the burden rock
- ii) reduces fragmentation
- iii) inhibits the necessary lateral and upward displacements needed to break collar material and remove toes

Reducing burden for a given bench height has the opposite effect. Doubling the bench height for a given burden, or reducing the burden by one-half for a constant bench height has the effect of reducing the stiffness theoretically some eight times, although in practice a B/L ratio of 1/3 is often adequate.

d. STRESS WAVE AND GAS EXPANSION THEORY (6)

In 1971, Kutter and Fairhurst combined the concepts of strain wave induced fracturing and gas pressure as the main mechanisms to fragment rock. Their experiments were performed with homogeneous plexiglass and rock models.

After detonation, an intense pressure wave is emitted into the rock from the impact of the rapidly expanding high pressure gas. This pressure rises immediately to its peak and can be assumed to be one-half to one-quarter of the detonation pressure. Due to cavity expansion around the borehole and the cooling of the gases, the pressure decays exponentially. In spite of the decay, the pressure is sufficient to exert a quasi-static pressure on the rock boundary for a relatively long time.

The amount of energy in the shock wave is calculated to be only a fraction of the total energy released by the explosive. In granite this was measured to range between 10 to 18 percent while in salt it was only 2 to 4% of the total energy released. The remaining energy is contained in the gas pressure. However, the compressional wave energy is sufficiently high next to the borehole to cause extensive breakage.

A radially fractured zone is the first fracture pattern to develop around the new expanded cavity. Next to develop is a ring of wider spaced radial cracks.

This width of radially fractured zone depends on:

- the tensile strength of the rock
- wave velocity of the rock
- input pressure of the explosive
- detonation velocity of explosive
- extent of energy absorption in the rock mass

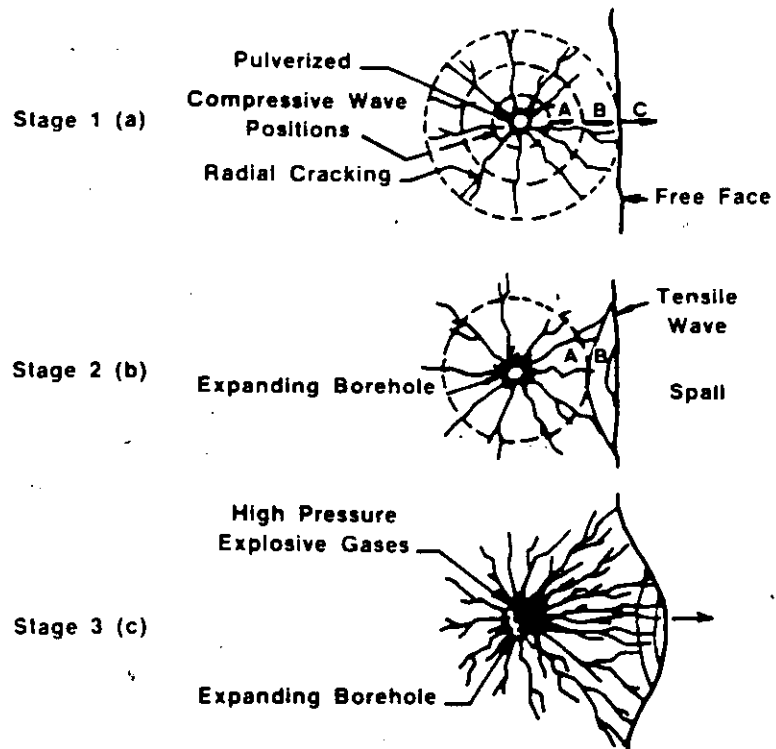
The diameter of the fractured zone was theoretically calculated to be around six hole diameters for a spherical charge and nine hole diameters for a cylindrical charge. It is in this expanded or equivalent cavity that the gas pressure becomes active and not in the original borehole. Thus cracks are pressurized and free to extend toward a free face. The original stress wave functions only to precondition the rock by initiating (in tension) radial cracks at the borehole wall.

The main points of interest of the stress wave and gas expansion theory are:

- Both stress waves and high pressure gases play an important role in fragmenting material. Neither the strain wave or gas pressure alone is responsible for rock fragmentation in blasting.
- Radial cracks originate at the borehole wall.
- Pre-existing cracks would reinitiate under stress, but no new cracks would form in the area occupied by an old crack.
- Presence of a free surface favors extension of gas pressurized radial cracks in that direction.
- In-situ stresses affect the direction in which radial cracks travel.
- For a given borehole size, an increase of explosive charge beyond an optimum amount does not increase the fractured zone, but results only in additional crushing around the cavity.

e. **GASEXPANSION, STRESS WAVES, STRESS-WAVE FLAW, AND REFLECTION — (Combined Theory) (28)**

Stage 1—On detonation of the explosive the high pressure shatters the rock in an area adjacent to the drill hole. The outgoing shock wave traveling at 9,000 to 17,000 feet per second sets up tangential stresses that create radial cracks which move out from the region of the hole. The first radial cracks develop in one to two milliseconds. (Figure 11-13a)



**FRACTURES OPENED UP AND PROPAGATED BY GAS EXPANSION
PRODUCING AN ISOLATED FRAGMENTED ROCK MASS OR CRATER
FIGURE 11.13**

Stage 2—The pressure associated with the outgoing shock wave of the first stage is positive. If the shock wave reaches a free face it will reflect, but in so doing the pressure falls rapidly to negative values and a tension wave is created. This tension wave travels back into the rock and since this material is less resistant to tension than to compression, primary failure cracks will develop due to the tensile strength of this reflected wave. If these tensile stresses are sufficiently intense they may cause scabbing or spalling at the free face. (Figure 11-13b)

In rock breaking this spalling effect appears to be of secondary importance. It has been calculated that the explosive load must be in the order of 8 times the normal load to cause failure of the rock by reflected shock wave alone.

In the first and second stages, the function of the shock wave energy is to condition the rock by inducing numerous small fractures. In most explosives the shock wave energy theoretically amounts to only 5 to 15% of the total energy of the explosive. This strongly suggests that the shock wave is not directly responsible for any signifi-

cant amount of rock breakage, but it does provide the basic conditioning for the last stage of the breakage process.

Stage 3—In this last stage the actual breakage of rock is a slower action. Under the influence of the exceedingly high pressure of the explosion gases, the primary radial cracks are enlarged rapidly by the combined effect of tensile stress induced by radial compression and by pneumatic wedging. When the mass in front of the borehole yields and moves forward, the high compressive stresses within the rock unload in much the same way as a compressed coil spring being suddenly released. The effect of unloading is to induce high tension stresses within the mass which complete the breakage process started in the second stage. The small fractures and threshold fracture conditions created in the second stage serve as zones of weakness to initiate the major fragmentation reactions. (Figure 11-13c)

f. NUCLEI OR STRESS WAVE—FLAW THEORY (32, 33, 34, 35, 37, 38)

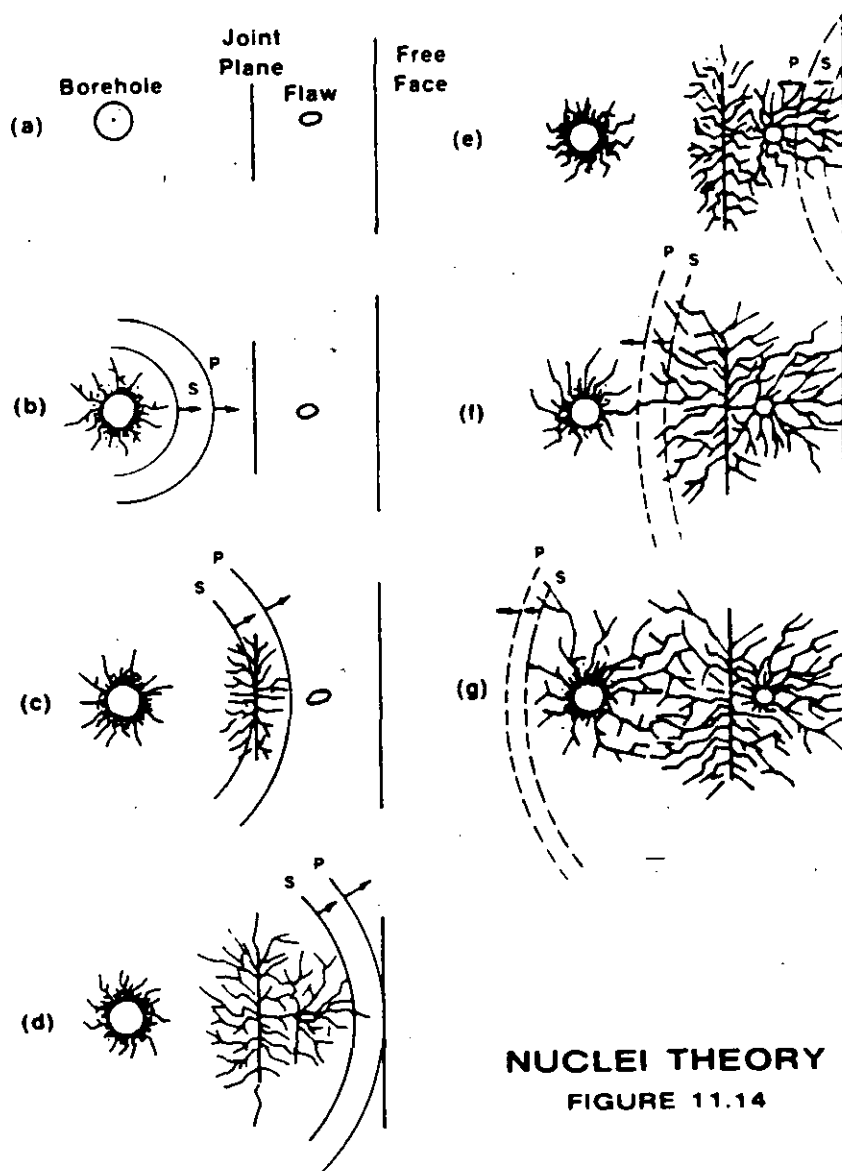
This relatively new theory was formulated at the University of Maryland in the fracture mechanics laboratory. Laboratory tests were conducted in homolite-100 models, both unflawed and flawed, by simulating many of the geologic structures and discontinuities (joints, fractures, bedding planes) typically found in large scale bench blasting. Results showed that stress waves were quite important in the fragmentation process and caused a substantial amount of crack initiation at regions rather remote from the borehole. These regions consisted of small or large flaws, joints, bedding planes, and other discontinuities that acted as a nuclei for crack formation, development or extension. This new stress wave dominated mechanism of fragmentation is referred here as the nuclei theory.

The theory and actual mechanisms of stress wave propagation and interaction in a flawed medium are quite complex. They involve many phases such as: (40)

- detonation and crack nucleation around borehole
- crushed zone extension
- dynamic crack stability
- activation of flaws
- coalescence of wave velocities and strains
- branching of cracks
- interaction of cracks and reflected wave systems
- instability of crack direction
- random progressive failure

In more simple terms, the important points of the theory are explained with the illustration in Figure 11-14. A borehole is located behind a free face with two discontinuities, a joint plane and a small flaw, located between the borehole and free face. Assume all other areas in the medium to be homogeneous and flaw free.

In unflawed material, only 8 to 12 dominant cracks emerge from a dense radial network around the borehole. These dominant cracks can travel significant distances and consequently form large pie shaped segments, that alone are not conducive for good fragmentation. Stress waves continuing away from the fractured zone around the borehole result in no further damage.



In flawed material or sections of the material which contain flaws, fragmentation is quite different. Consider the P and S waves propagating away from the fracture network around the borehole in Figure 11-14b and 11-14c. Refer to Chapter 12—Vibration/AirBlast section for a discussion on Seismic Waves. No fracturing takes place until the flaw (joint plane) is initiated by the P wave tail and the leading front of the S wave, (Figure 11-14c). The remainder of the S wave has sufficient energy to keep the crack from arresting. A similar effect occurs as the P and S waves move past the small flaw between the joint plane and the free face, (Figure 11-14d). It is important to note that cracks are initiated at flaw sites remote from the borehole region by the combined action of the P wave tail and the S wave front. Flaws initiated in the immediate borehole vicinity of these waves have only a small effect. Note also, that the outward directed P and S waves can initiate flaws anywhere independent of the presence of a free surface.

When a P wave encounters a free face (Figure 11-14d and 11-14e), it is reflected and travels back into the medium as a tensile wave to meet the outcoming S wave. At this stage, constructive interference can occur which allows for further crack initiation or extension of cracks previously formed. New wave systems (PP, PS, SP, SS, PP, and S, PS, and S) will also form from the original outgoing wave system upon reflection at a free surface or discontinuity. These new wave systems can also contribute to crack extensions. Figure 11-14f and 11-14g illustrate further crack extensions when all wave systems have been reflected back towards the hole.

The important points of the nuclei or stress-wave flaw theory are:

- the fracture network spreads with the speed of the P and S waves, which initiate fracture around flaws remote from the borehole
- in highly flawed material, fragmentation results from the nucleation of new cracks at flaws and reinitiation of old cracks from the reflected stress wave systems
- gas pressurization does not contribute significantly to the fragmentation process

Computational models incorporating stress wave/flaw interaction as a mechanism of nucleating and extending cracks is growing in popularity. (32-38, 40) Although the models differ in approach and/or details, the main idea is that shock and/or stress waves fragment

material and gas pressure acts to displace the broken material. Stress wave functions not only to initiate fractures at or near the borehole wall, but also initiate fractures throughout the rock mass being blasted.

Recent work in full scale production shots and in large blocks added further insight into this phenomena. (35) Stress wave induced fracturing at flaws and discontinuities removed from the borehole was found to be considerably greater than either spalling or borehole radial tensile failure documented by earlier works. Gas pressurized radial fracturing, in typical bench blasting operation, was found to be only a minor contributor to the overall fragmentation of the rock mass.

Some key points of Winzer's theory and observations are:

- i) new fractures are seen to form at the face at about twice the time it takes for the P wave to traverse the burden distance
- ii) old fractures are the loci of new fractures or are re-initiated themselves early in the event; they continue to be active for several tens of milliseconds after detonation of the explosive
- iii) fragmentation continues in blocks of rock, following detachment from the main rock mass, by trapped stress waves
- iv) the fracture pattern on the free face is well developed prior to the expected time of arrival of radial cracks from the borehole
- v) in blasted faces from production-scale shots, fractures are observed to have initiated at, and propagated from, joint and bedding planes, suggesting the same operating mechanism(s) as those observed in homolite models at the University of Maryland
- vi) gas venting occurs through already open cracks relatively late in the event, indicating that the majority of fractures observed on the free face are not gas pressurized
- vii) in more massive rock stress waves are transmitted with higher velocity and less attenuation, but fewer fractures will form because there are few fracture sites. However, more radial fractures will form in massive rock, while fewer fractures form at a distance from the borehole



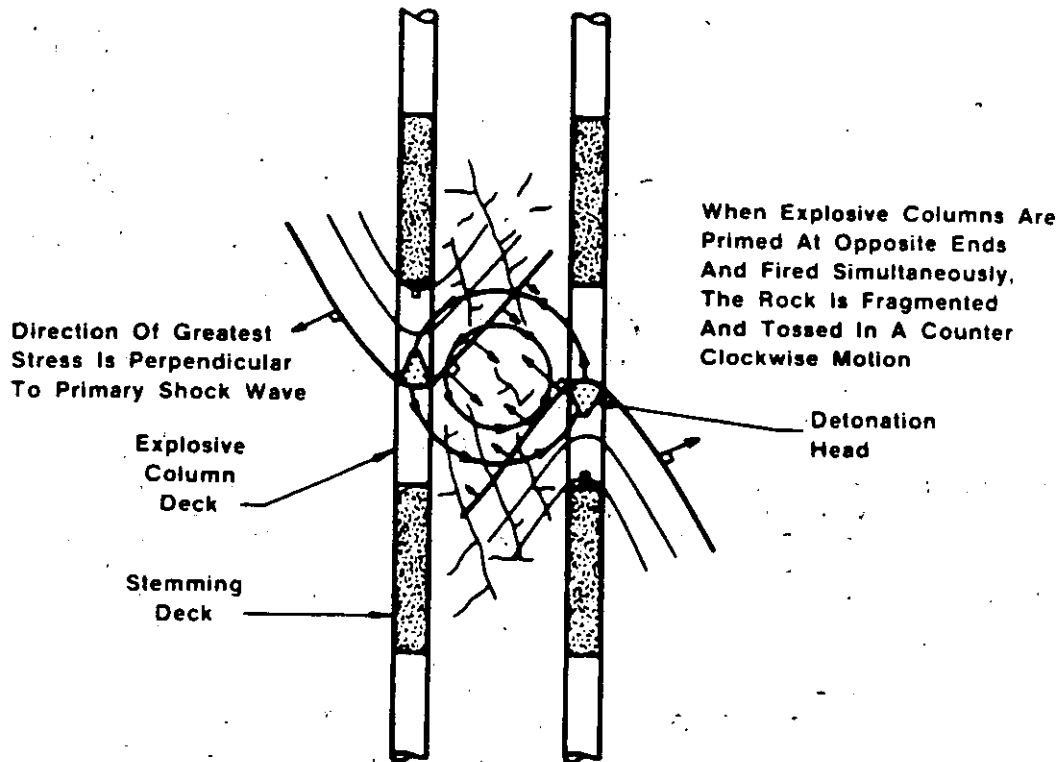
- viii) large fragments will form early in the event, and as they move and fractures open, large segments of the rock mass will be effectively isolated from further stress energy
- ix) in more heavily fractured rock, the stress wave velocity will be lower and attenuation higher, but there are more fractures to serve as initiation sites
- x) the stress wave takes longer to penetrate the mass, and movement of the rock can be expected to be slower as more energy is absorbed by the rock mass
- xi) cracks open more slowly, and smaller masses of rock are isolated early in the event, so that later arriving stress waves can continue to increase crack initiation and propagation

g. TORQUE THEORY

The success of this theory is totally dependent on the absolute, accurate timing of initiators. When two adjacent explosive columns are initiated simultaneously from opposite ends, a compressional shock wave from each column traveling parallel but in opposite directions is formed. (Figure 11-15) The greatest stress is always directed perpendicular to the primary shock front. This stress is also assumed to be greatest near the detonation head in the explosive and diminishes with distance away from the detonation head. An uneven stress distribution is formed between explosive columns when the columns are fired simultaneously and from opposite directions. This action tends to toss the fragmented rock between explosive columns in a counterclockwise motion. Reversing the primers of each explosive column will toss the material in a clockwise motion. This action is precisely what is needed to obtain uniform fragmentation and avoid tight muck piles such as in the case of in-situ retorting. For this theory to work, exact initiators are crucial; nothing less will do, especially when using explosives with very high velocity of detonation.

h. CRATERING THEORY (41-45)

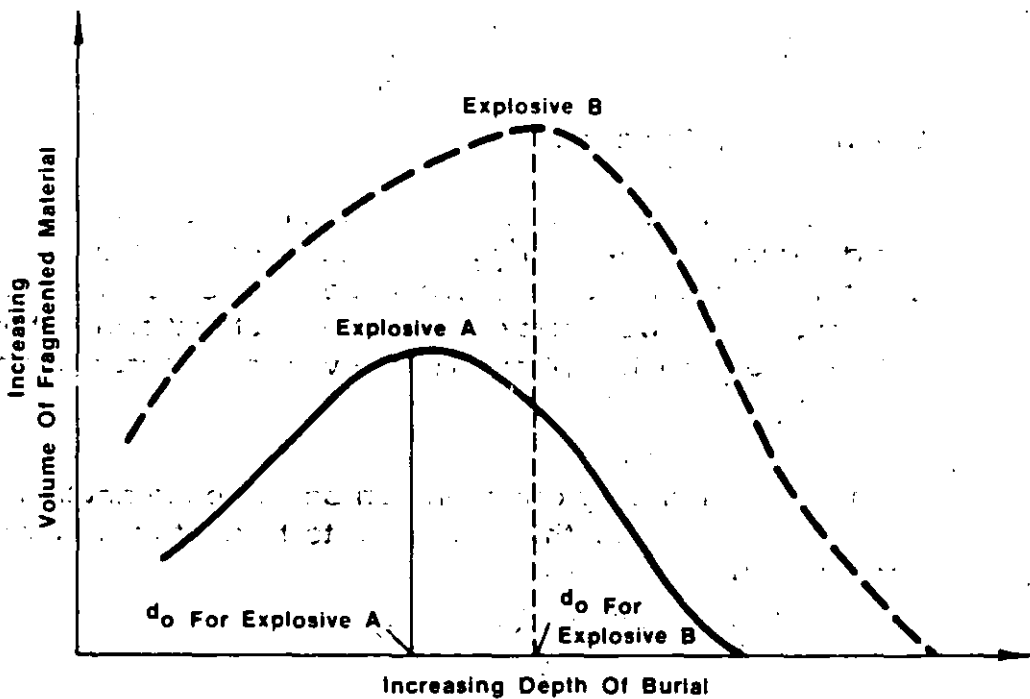
The concept of cratering, its development, and resulting applications were originally proposed by C.W. Livingston and later modified by others such as Lang and Bauer. (41) (43) (44) It involves a spherical charge of length to diameter ratio of less than or equal to 6 to 1, detonated at an empirically determined distance beneath the sur-



**APPLICATION OF NEW BLASTING
THEORY TO IN-SITU RETORTS
BLASTING
FIGURE 11.15**

face to optimize the greatest volume of permanently fragmented material between the charge and free surface. This implies that given a specific explosive and material, there exists a burden distance between the charge and free surface which yields the largest crater (Figure 11-16d). This burden is referred to as the optimum burden or depth. Similarly, there exists another burden distance referred to as the critical distance, which is too far below the surface to result in any crater or expulsion of material at the surface, other than minor radial cracks. This is the point where material at the surface just begins to show evidence of failure, (Figure 11-16b).

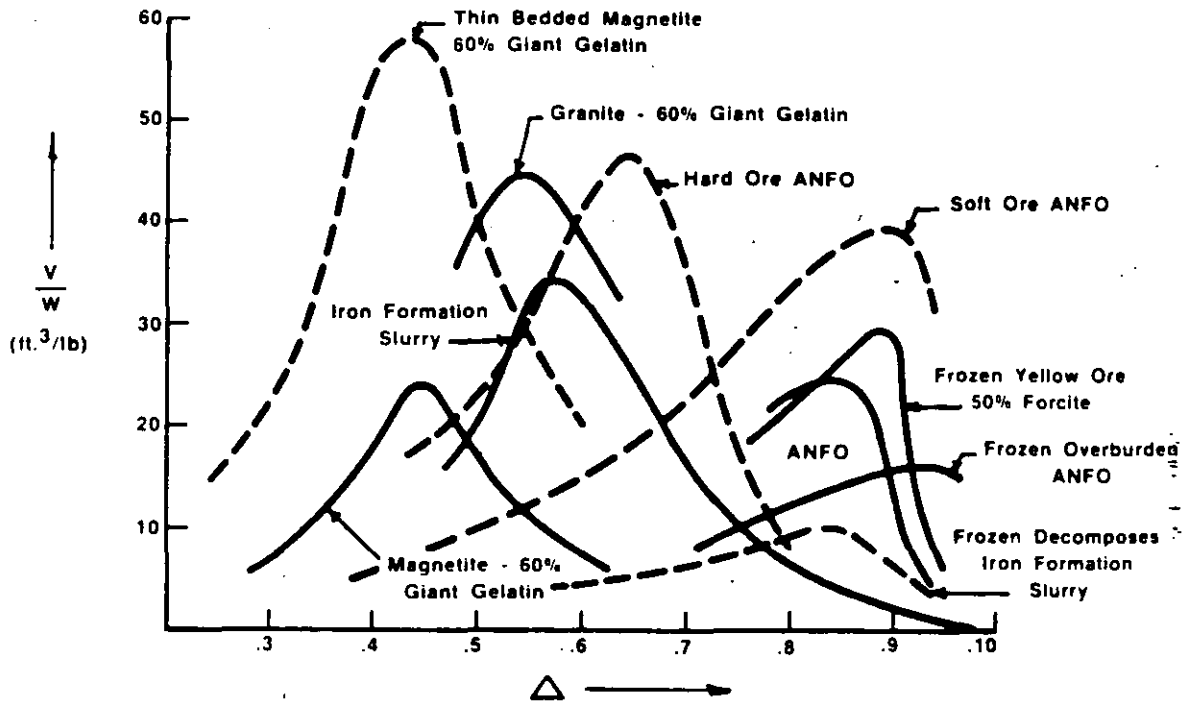
Crater data can be plotted in a number of different ways. Figure 11-17 illustrates the effect of two explosives, A and B on the amount of fragmented material that each is capable of achieving at different depths of burials. Note that the higher energy explosive always fragments a greater volume of material at the same depth of burial as explosive A, but that the optimum depth of burial differs for each explosive.



**VOLUME OF FRAGMENTED MATERIAL VERSUS
DEPTH OF BURIED FOR TWO EXPLOSIVES IN
THE SAME MATERIAL
FIGURE 11.17**

Another method of representing crater data on a common base is by plotting V/W on the y-axis and the depth ratio on the x-axis as shown in Figure 11-18. (44) V is the volume of broken material in cubic feet, W is the weight of explosive in pounds, and the depth ratio has been defined as the depth of burial divided by the critical depth. The important thing to note is that the optimum depth ratio, (Δ_0), varies with each explosive-rock combination. The advantage of performing such field experiments is that one would obtain crater data specifically suited to the user environment for a number of different explo-

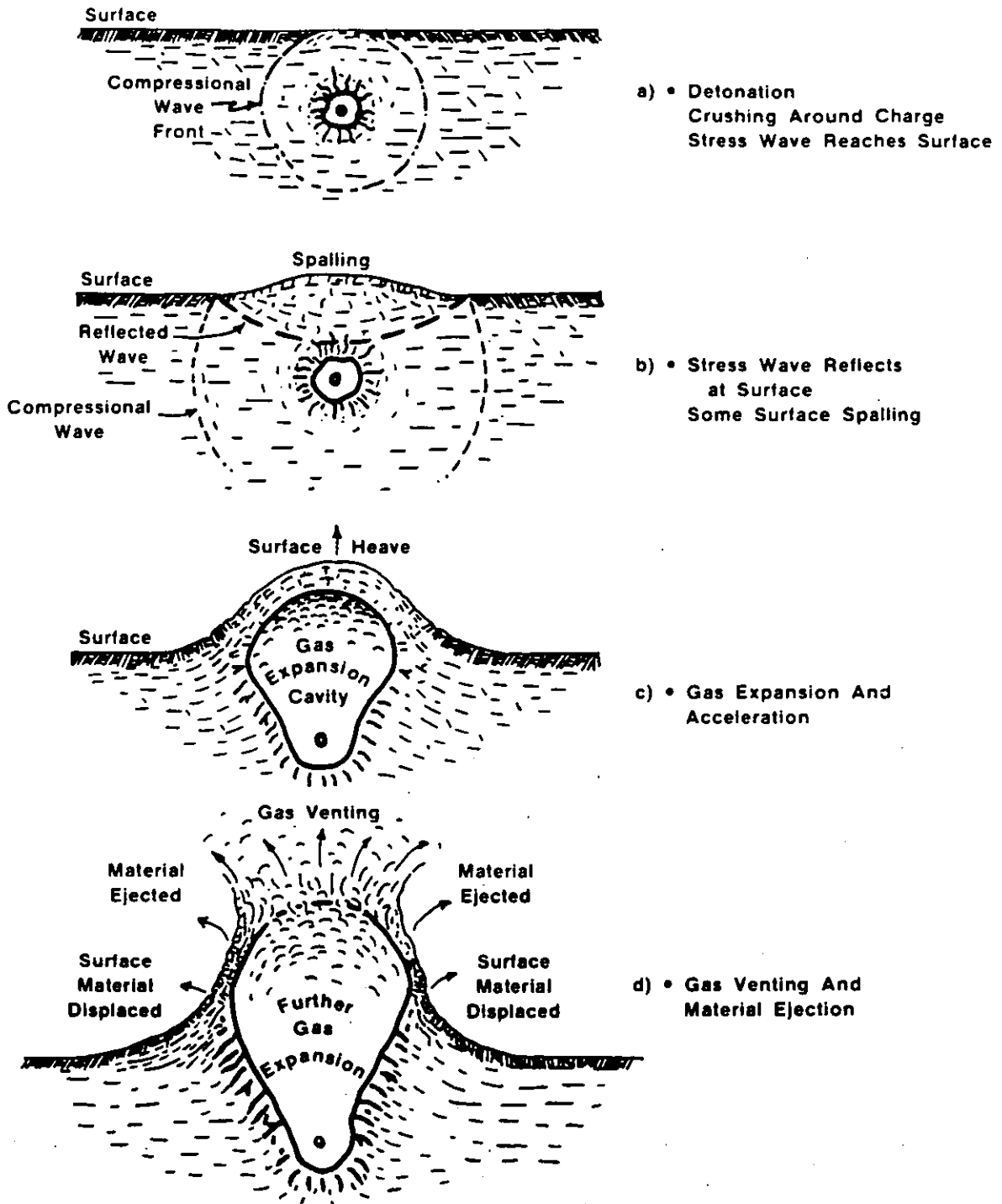
sives. Although the curves in Figure 11-18 are fitted as smooth curves, one should remember that some scatter of data is always present and it is important to take this into account for crucial applications of cratering.



ROCK REMOVED IN CU. FT. PER LB. OF EXPLOSIVE VS DEPTH RATIO
 FIGURE 11.18 (44)

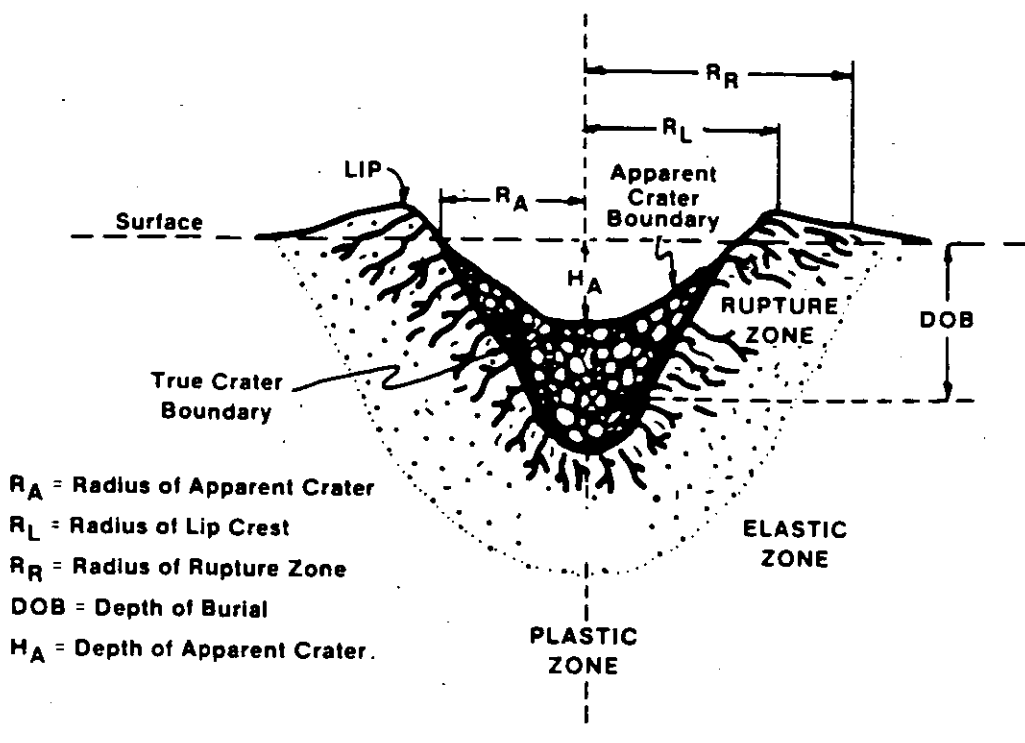
i. CRATERING MECHANISMS (4) (45)

As the high pressure explosive gases expand against the medium immediately surrounding the explosion, a spherical shock wave is generated causing crushing, compaction and plastic deformation. (Figure 11-19a) For commercial explosives the initial shock pressures are on the order of 100 to 200 thousand atmospheres (one atmosphere = 14.7 pounds per square inch). As the shock front moves outward in a spherically diverging shell, the medium behind the shock front is put into radial compression and tangential tension. This results in the formation of radial cracks directed outward from the cavity. The peak pressure in the shock front becomes reduced due to spherical divergence and the expenditure of energy in the medium. For shock pressures above the dynamic crushing strength



CRATERING EVENTS AND MECHANISMS
FIGURE 11.19

of the medium, the material is crushed, heated and physically displaced, forming a cavity. In regions outside this limit the shock wave will produce permanent deformation by plastic flow, until the peak pressure in the shock front has decreased to a value equal to the plastic limit of the medium. This is the boundary between the plastic and elastic zones shown in Figure 11-20.



EMPLOYMENT OF ATOMIC DEMOLITION MUNITIONS
 DEPARTMENT OF THE ARMY, WASHINGTON, D.C. AUG. 1971
 FIGURE 11.20

When the compressive shock front encounters a free face, it must match the boundary condition that the normal stress or pressure be zero at all times. This results in the generation of negative stress, or rarefaction wave which propagates back into the medium (Figure 11-19b). Thus the medium which was originally under high compression is put into tension by the rarefaction wave. This phenomenon causes the medium to break up and fly upward with a velocity characteristic of the total momentum imparted to it. In a loose soil material, this spalling makes almost every particle fly into the air individually, while in a rock

medium the thickness of the spalled material is generally determined by the presence of pre-existing fracture patterns and zones of weakness. As the distance from surface increases, the peak negative pressure decreases until it no longer exceeds the tensile strength of the medium. The velocity of spalled material also decreases in proportion to the peak pressure. This breakage mechanism is predominant only for charges placed at very shallow depths of burial.

The two mechanisms described so far are short term, lasting only a few milliseconds. The gas acceleration mechanism, however, is a much longer lasting process which imparts motion to the medium around the detonation by the expansion of gases trapped in the explosion-formed cavity. (Figure 11-19c and 11-19d) These gases are produced in the surrounding material by vaporization and chemical changes induced by the heat and pressure of the explosion. Venting occurs because the material is no longer cohesive enough to contain the explosion gases. As the gases are released, fragments assume free ballistic trajectories. At depths of burial at which crater dimensions are maximum, the gases produced will give appreciable acceleration to overlying material during its escape or venting through cracks extending from the cavity to the surface. At shallow depth of burials the spall velocities are so high that the gases are unable to exert any pressure before venting occurs. For very deep explosions the weight of the overburden precludes any significant gas acceleration of the overlying material. Gas acceleration is the dominant mechanism at optimum depth of burial. With a constant weight of explosive, the optimum depth of burial varies with the surrounding material.

At deep depths of burial, the mechanism of overburden collapse (subsidence) becomes dominant. This effect is closely linked to the crushing, compaction and plastic deformation mechanism which produces an underground cavity. At these depths of burial, spall and gas acceleration will not impart sufficient velocity to the overlying material to physically eject it from the crater. Most throwout returns to the crater as fallback material. In a rock medium the bulking action of the rock, when it is disoriented from its original fracture pattern, could produce a volume greater than the underground cavity. This could result in no crater or a mound above the ground rather than a crater.

At even deeper depths of burial, about twice or deeper of that of optimum, another type of subsidence occurs. In this case the spall and gas acceleration has no significant effect on the overlying material. Only an underground cavity is formed. When the pressure in the cavity decreases below overburden pressure, the roof of the cavity begins to collapse. In most media this collapse will continue upward

forming a chimney of collapsed material. In soil, where the density of the material will not significantly change after it has fallen, the volume of the underground cavity will be transmitted to the surface.

Figure 11-21 illustrates surface time profiles after detonation of a 40 pound equivalent charge of ANFO, buried 8.0 feet in an unconsolidated, sedimentary type material. (46) High-speed photography was

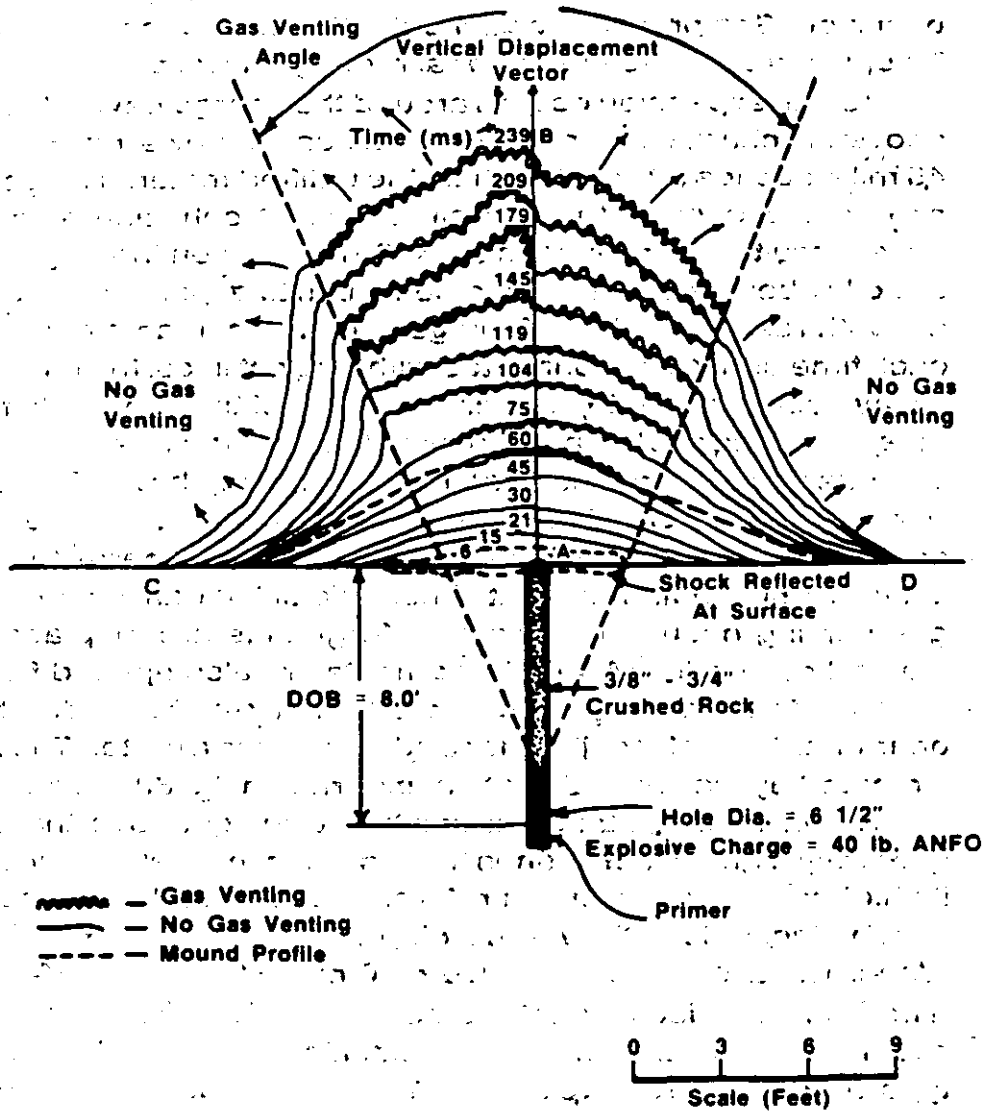
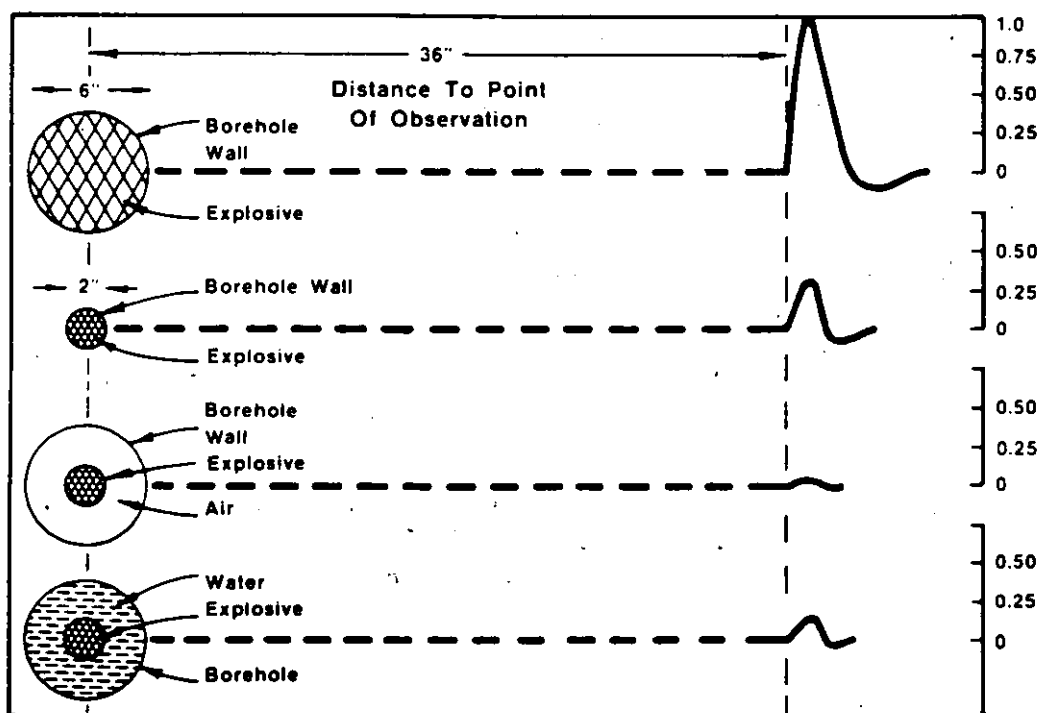


FIGURE 11.21

or tensile strengths. Ideally, the borehole pressure should be somewhere between the compressive and tensile strength of the rock, so as to avoid extensive crushing at the borehole wall, yet provide enough pressure to extend a single predominant crack between any two perimeter holes in the control line of holes.

A good example of decoupling in air and water in relation to fully coupled holes is illustrated in Figure 11-23. (47) The pressure imparted in the rock mass at 36" away for the same explosive is shown for four conditions:

- i) a 6" diameter explosive in a 6" hole
- ii) a 2" diameter explosive in a 2" hole
- iii) a 2" diameter explosive in a 6" hole (air decoupled)
- iv) a 2" diameter explosive in a 6" hole (water decoupled)



**EFFECT OF AIR AND WATER DECOUPLING
VS FULLY COUPLED HOLES
FIGURE 11.23 (47)**

All measured stress levels are compared relative to the 6" diameter explosive in a 6" diameter hole. A number of important points are immediately evident. The greatest stress level was achieved with a fully coupled

explosive in a 6" diameter hole. The next highest stress level was achieved, again, with a fully coupled explosive, even though the hole diameter was reduced three-fold to a 2" diameter. Water decoupling followed next and air decoupling produced the smallest stress level. Thus, an air decoupled charge is the most effective means of reducing borehole pressure and consequently the peak stress level within the rock mass.

A reasonably reliable method of calculating the borehole pressure is with the following formula which takes into account two decoupling ratios. (48) (49) (50)

$$P_b = 1.69 \times 10^{-3} \times \rho \times VOD^2 \times \left[\frac{c \times d_e}{d_h} \right]^{2.6}$$

where:

P_b = Borehole pressure in PSI.

ρ = Density of explosive in g/cc

VOD = Velocity of detonation in ft/sec

c = Percentage of explosive column loaded expressed as a decimal

d_e = Explosive diameter (in.)

d_h = Hole diameter (in.)

This formula is best suited for explosives which contain no metallic elements or relatively small amounts, since the addition of energizing metals lowers the detonation velocity of the explosive and hence, the borehole pressure as calculated by this equation. Computer codes such as TIGER and EXPLODE are used to calculate borehole pressures from explosives containing metallic elements.

6. REFERENCES

- 1) CHIAPPETTA, R.F., BORG, D.G., **Increasing Productivity Through Field Control and High-Speed Photography**, First International Symposium on Rock Fragmentation by Blasting, Lulea, Sweden, Aug., 1983, pp. 301-331
- 2) DAVIS, W.C., **High Explosives**, Los Alamos Science, 1983, pp. 48-52

- 3) CHIAPPETTA, R.F., BAUER, A., BURCHELL, S.L., **The Use of High-Speed Motion Picture Photography in Blast Evaluation and Design**, Proceedings 9th Annual Conference on Explosives and Blasting Techniques, Society of Explosives Engineers, 1983
- 4) MAJOR JOHNSON, M.S., **Explosive Excavation Technology**, U.S. Army Engineer Nuclear Cratering Group, Livermore, California, June, 1971, NCG Technical Report No. 21, TID-4500
- 5) ATLAS POWDER COMPANY, Field Technical Operations, Tamaqua, PA, USA, Internal unpublished data, 1981-1985
- 6) KUTTER, H.K., FAIRHURST, C., **On the Fracture Process in Blasting**, Int. J. Rock Mech. Min. Sci., Vol. B, pp. 181-202, Pergamon Press, 1971, Great Britain
- 7) OLSON, J.J., WILLARD, R.J., FOGELSON, D.E., HJELMSTAD, K.E., **Rock Damage from Small Charge Blasting in Granite**, USBM, RI 7754, 1973, 44pp.
- 8) SISKIND, D.E., STECKLEY, R.C., OLSEN, J.J., **Fracturing in the Zone Around a Blasthole**, White Pine, Michigan, USBM, RI 7753, 1973, 20pp.
- 9) CATTERMOLE, J.M., HANSON, W.R., **Geologic Effects of the High Explosives Test in U.S.G.S.**, Tunnel Area, Nevada Test Site, U.S. Geol. Survey, Prof. Paper 382-B, 1962, 29pp.
- 10) Colorado School of Mines, **Underground Explosion Test Program**, Ser. I and Ser. II experiments, December 1948
- 11) DERLICH, S., **Underground Nuclear Explosion Effects in Granite Rock Fracturing**, Proc. Symposium of Engineering with Nuclear Explosives, Las Vegas, Nevada, January, 1970, pp. 508 and 518
- 12) ATCHISON, T.C., TOURNAY, W.E., **Comparative Studies of Explosives in Granite**, USBM RI 5509, 1959, 28pp.
- 13) D'ANDREA, D.V., FISCHER, R.L., HENDRICKSON, A.D., **Crater Scaling in Granite for Small Charges**, USBM RI 7409, 1970, 28pp.
- 14) SISKIND, D.E., FUMANTI, R.R., **Blast Produced Fractures in Lithonia Granite**, USBM RI 7901, 1974, 38pp.

- 15) VOVK, A.A., MIKHALYUK, A.V., BELINSKI, I.V., **Development of Fracture Zones in Rocks during Camouflet Blasting**, translated from FIZLKO-TEKLINICHESKIE PROBLEMY ROZRABOTKI POLEZRYKH ISKI-PAEMYKH, No. 4, pp. 39-45, July-Aug., 1973
- 16) BORG, I.Y., **Extent of Pervasive Fracturing Around Underground Nuclear Explosions**, Int. J. Rock Mech. Mining Science, 10, 11-18, 1973
- 17) OBERT, L., DUVALL, W.I., **A Gauge and Recording Equipment for Measuring Dynamic Strain in Rock**, U.S. Dept. Int., Bureau of Mines, RI 4581, 1949
- 18) OBERT, L., DUVALL, W.I., **Generation and Propagation of Strain Waves in Rock**, USBM RI 4663, 1950
- 19) HINO, U., **Frangmentation of Rock through Blasting**, Q. Colorado School of Mines, 51, 189, 1956
- 20) DUVALL, W.I., ATCHISON, T.C., **Rock Breakage by Explosives**, USBM RI 5356, 1957
- 21) RINEHART, J.S., **Fracturing Under Impulse Loading**, University of MO-Rolla, School of Mines and Met, Bulletin, Tech Ser., 95, 46, 1958
- 22) LANGFORS, U., KIHLMSTROM, B., **The Modern Technique of Rock Blasting**, John Wiley and Sons, NY, 405pp., 1963
- 23) STARFIELD, A.M., **Strain Wave Energy in Rock Blasting**, Proc. 8th Symposium on Rock Mech., Univ. of Minnesota, 1966
- 24) PORTER, D.D., FAIRHURST, C., **A Study of Crack Propagations Produced by the Sustained Borehole Pressure in Blasting**, Proc. 12th Symposium Rock Mech., Univ. of Missouri, Rolla, 467, 1970
- 25) PERSSON, P.A., LUNDBORG, N., JOHANSSON, C.H., **The Basic Mechanism in Rock Blasting**, Proc. 2nd Congress Int. Society for Rock Mech., Belgrade, 1970
- 26) FIELD, J.E., LADEGAARD-PEDERSON, A., **The Importance of the Reflected Stress Wave in Rock Blasting**, Int. J. Rock. Mech. Min. Sci., 1971

- 27) JOHANSSON, C.H., PERSSON, P.A., **Frangmentation Systems**, Proc. and Papers of Int. Society of Rock Mech., 3rd Congress, Denver, CO, Sept. 1-4, 1974
- 28) LANG, L.C., FAVREAU, R.F., **A Modern Approach to Open Pit Blast Design and Analysis**, CIM Bulletin, pp. 37-44, June, 1974
- 29) ASH, R.L., **The Influence of Geological Discontinuities on Rock Blasting**, PhD. Thesis, Univ. of Minnesota, June, 1973
- 30) HAGEN, T.N., **Rock Breakage by Explosives**, Australian Geomechanics National Symposium on Fragmentation, Adelaide, 1974
- 31) HAGEN, T.N., JUST, G.D., **Rock Breakage by Explosives—Theory, Practice, Optimization**, Proc. 3rd Congress Int. Society for Rock Mechanics, Denver, CO, Sept. 1-4, 1974
- 32) BARKER, D.B., FOURNEY, W.L., DALLY, J.W., **Photoelastic Investigation of Fragmentation Mechanisms, Part I — Borehole Crack Network**, Univ. of Maryland, MD, March, 1978, 39pp.
- 33) BARKER, D.B., FOURNEY, W.L., **Photoelastic Investigation of Fragmentation Mechanisms, Part II — Flaw Initiated Network**, Aug. 1978, 47 pp., Univ. of Maryland, MD
- 34) FOURNEY, W.L., BARKER, D.B., **Effect of Time Delay on Fragmentation in a Jointed Model**, Univ. of Maryland, MD, Aug. 1979, 31pp.
- 35) WINZER, S.R., ANDERSON, D.A., RITTER, A.P., **Rock Fragmentation by Explosives**, First Int. Symposium on Rock Fragmentation by Blasting, Lulea, Sweden, Aug. 22-26, 1983, pp. 225-249
- 36) MARGOLIN, L.G., ADAMS, T.F., **Numerical Simulation of Fracture**, First Int. Symposium on Rock Fragmentation by Blasting, Lulea, Sweden, Aug. 22-26, 1983, pp. 347-360
- 37) ADAMS, T.F., DEMUTH, R.B., MARGOLIN, L.G., NICHOLS, B.D., **Simulation of Rock Blasting with the Shale Code**, First Int. Symposium on Rock Fragmentation by Blasting, Lulea, Sweden, Aug. 22-26, 1983, pp. 361-373
- 38) MCHUGH, S., **Computational Simulations of Dynamically Induced Fracture and Fragmentation**, First Int. Symposium on Rock Fragmentation by Blasting, Lulea, Sweden, Aug. 22-26, 1983, pp. 407-418

- 39) JOHANSSON, C.H., PERSSON, P.A., **Detonics of High Explosives**, Academic Press, London and NY, 1970, 330pp.
- 40) ROSSMANITH, H.P., **Dynamic Fracture in Glass**, Univ. of Maryland, MD, April, 1978, 77pp.
- 41) LANG, L.C., ROACH, R.J., OSOKO, M.N., **Vertical Crater Retreat – An Important New Mining Method**, Canadian Mining J., Sept., 1977
- 42) LIVINGSTON, C.W., **Fundamentals of Rock Failure**, Quarterly of the Colorado School of Mines, Vol. 51, No. 3, July, 1956
- 43) BAUER, A., **Application of the Livingston Theory**, Quarterly of the Colorado School of Mines, Vol. 56, No. 1, Jan., 1961
- 44) BAER, A., HARRIS, G.R., LAND, L., PREZZIOSI, P., SELLECK, D.J., **How IOC Puts Crater Research to Work**, Eng. and Mining J., Sept., 1965, pp. 117-121
- 45) Headquarters, Dept. of the Army, **Employment of Atomic Demolition Munitions (ADM)**, Field Manual, Washington, DC, Aug. 31, 1971, FM5-26
- 46) CHIAPPETTA, R.F., BURCHELL, S.L., REVEY, G., FISHER, S., ATLAS POWDER COMPANY, FIELD TECHNICAL OPERATIONS, Unpublished Internal Data, Cratering Field Experiments at the Avery Coal Co., PA, 1983-1985
- 47) DAY, P.R., **Controlled Blasting to Minimize Overbreak with Big Boreholes Underground**, Proc. 8th Conference on Explosives and Blasting Techniques, Society of Explosives Engineers, New Orleans, Louisiana, 1982, pp. 262-274
- 48) CROSBY, W.A., BAUER, A., **Wall Control Blasting in Open Pit Mines**, Mining Engineering, Feb., 1982, pp. 155-158
- 49) PIT SLOPE Manual, **Perimeter Blasting**, Canmet, Report 77-14, Canada Center for Mineral and Energy Technology, Canada, May, 1977
- 50) KATSABANIS, P., **A Comparative Study of Emulsion and Slurry Explosives**, MSC Thesis, Queen's University, Kingston, Ontario, Canada, Feb., 1983, 149pp.



111



**FACULTAD DE INGENIERIA U.N.A.M.
DIVISION DE EDUCACION CONTINUA**

CURSOS ABIERTOS

**IV. CURSO INTERNACIONAL DE INGENIERIA GEOLOGICA APLICADA A
OBRAS SUPERFICIALES Y SUBTERRANEAS**

CUARTO MODULO:

TECNOLOGIA SOBRE EL USO DE EXPLOSIVOS

Del 22 al 26 de junio de 1992

**ALTERNATIVE VELOCITY LOADING TECHNIQUES AND DETONATIONS
ENVIROMENT**

AUTOR: R. FRANK CHIAPPETTA

EXPOSITOR: ING. RAUL CUELLAR BORJA

JUNIO - 1992

**ALTERNATE VELOCITY
LOADING TECHNIQUES AND DETONATIONS
IN A PRODUCTION ENVIRONMENT**

by

R. Frank Chiappetta

Atlas powder Company
Field Technical Operations
Tamaqua, Pennsylvania, USA

Presented at:

The Second Pennsylvania Blasting Conference
University Park, Pennsylvania, November 14-15, 1985

The Twelfth Annual Kentucky Blasting Conference
Lexington, Kentucky, December 5-6, 1985

First Annual Mine Blasting Safety and Application Seminar
United States Department of Labor
Mine Health and Health Administration
National Mine Health and Safety Administration
National Mine Health and Safety Academy
January 22-23, 1986

ALTERNATE VELOCITY LOADING TECHNIQUES AND DETONATIONS IN A PRODUCTION ENVIRONMENT

by

R. Frank Chiappetta

ABSTRACT

A simple and cost effective technique to increase fragmentation and burden velocities without making major modification to the overall blast design is with ALTERNATE VELOCITY LOADING OR BOOSTERING OF ANFO. The technique requires the placement of a cartridge or slug of explosive, having higher density and detonation velocity than ANFO, every few feet in an ANFO column. The greater the difference in density and detonation velocity of the Alternate Velocity Load to ANFO, the more pronounced are the results. Emulsions were selected as the Alternate Velocity test explosives because they detonate closer to ideal conditions than most other commercial explosives.

The emulsion explosives embedded in the ANFO column did not require additional boosting. Even a low order ANFO detonation, alone, acted as an effective primer on the Alternate Velocity emulsion explosive. It was also determined that ANFO efficiency suffers greatly, when ANFO is loaded in a dewatered hole.

Testing consisted of single and multi-hole production shots in full-scale environments. Analytical methods, testing procedures and a discussion of the breaking processes are described in detail.

TABLE OF CONTENTS

ABSTRACT.....Pg. 0

INTRODUCTION.....Pg. 2

T1-DETONATION.....Pg. 4

T-2 SHOCK/STRESS WAVE PROPAGATION.....Pg. 12

T-3 GAS PRESSURE EXPANSION.....Pg. 17

T-4 MASS MOVEMENT.....Pg. 19

TIME EVENTS T1-T4 COMBINED.....Pg. 25

CHARACTERIZATION OF ALTERNATE VELOCITY WITH
AN EMULSION EXPLOSIVE IN ANFO.....Pg. 30

ALTERNATE VELOCITY FIELD TESTS IN FULL-SCALE
PRODUCTION SHOTS.....Pg. 37

SUMMARY AND RECOMMENDATIONS FOR FIELD USE....Pg. 49

ACKNOWLEDGEMENTS.....Pg. 51

REFERENCES.....Pg. 52

INTRODUCTION

The breaking and heaving processes resulting from single or multi-hole detonations encompass a complex array of phenomena not all of which are completely understood. However, with the advent of newer, more precise and sophisticated instrumentation, a better definition and explanation of what occurs within and around a borehole at close vicinity are now possible. Clarification of such short lived phenomena in and around a borehole environment is invaluable to us in our basic understanding of the breakage process.

The ATLAS POWDER COMPANY in association with other research organizations has invested heavily in researching specific areas of blasting in an attempt to produce more efficient, consistent and cost effective blasting techniques for the end user. One such technique is described in this paper as ALTERNATE VELOCITY LOADING OR ALTERNATE VELOCITY BOOSTERING OF ANFO. The technique consists of placing a cartridge or slug of explosive, with higher density and velocity of detonation than ANFO, every few feet in an ANFO column. In the last few years, the technique has been used in a wide variety of materials stretching from very soft overburdens to the hardest of granites and in hole diameters ranging from 2-1/2 to 12 inches. With a carefully designed blast utilizing the proper amount and distribution of energy, optimum selection of MS delay timing and ALTERNATE VELOCITY LOADING, excellent results can easily be realized in terms of

fragmentation and mass movement of burdens. Thus, ALTERNATE VELOCITY LOADING is equally applicable to overburden casting in stripping operations and to bench blasting operations in quarries.

In order to understand some of the mechanisms responsible for the success of Alternate Velocity Loading, a review of the basic breakage process is essential. There are basically four time frames designated as T1 to T4 in which detonation, breakage and heaving of material occur during and after detonation of a confined charge. The time frames are defined as follows:

- T1 - Detonation
- T2 - Shock or Stress Wave Propagation
- T3 - Gas Pressure Expansion
- T4 - Mass Movement

Although each time frame is treated as a discrete event for conceptual clarity, it should be emphasized that in a typical shot hole or production blast, one event phase can occur simultaneously with another at specific time intervals. Each time frame is first discussed separately and then in a unified explanation and meshing of events in conjunction with some of the more commonly accepted blasting theories.

T1 - DETONATION

Detonation is the beginning phase of the fragmentation process. The ingredients of an explosive consisting of a fuel and oxidizer combination; upon detonation, are immediately converted to high pressure, high-temperature gases. Pressures just behind the detonation front or head are in the order of 9 Kbars to 275 Kbars, while temperatures range from 3000 to 7000 F. The detonation head is referred to here as the primary reaction zone for the fuel and oxidizer mixture.

Detonation pressure is generally expressed as a function of the velocity of detonation and density of the explosives as,

$$P = (2.325 \times 10^{-7}) \times \rho \times VOD$$

Where P = detonation pressure in Kbars

ρ = density in g/cc

VOD = velocity of detonation in ft/sec.

To change detonation pressure from Kbars to lb/in², multiply Kbars by 14,504. Generally, explosives yielding higher detonation pressures are required to fracture materials which are massive, fine grained, hard, tightly bonded and strongly consolidated with heavy burdens. Typical values of detonation pressure for selected explosives are presented in Table 1.

TABLE 1
DETONATION PRESSURES FOR SELECTED EXPLOSIVES

Explosive	Density (g/cc)	VOD (ft/sec)	Detonation Pressure (Kbars*)	Pressure (psi)
ANFO	0.81	12,000	27.00	391,600
POWERMAX 420	1.19	19,000	100.00	1,450,400
HI-PRIME	1.40	20,000	130.00	1,885,500
"G" BOOSTER	1.60	26,000	251.00	3,640,500

*1 Kbar = 14,504 psi

The detonation wave starts at the point of primer initiation in the explosive column and travels at supersonic speeds. Supersonic refers to velocities which are faster than the speed of sound in the explosive. Typical velocities of detonation for commercial explosives range from 8,000 to 26,000 ft/sec. This velocity, sometimes referred to as the steady-state velocity, remains fairly constant for a given explosive, but varies from one explosive to another, depending primarily on the composition, particle size and density of the explosive. To a lesser extent, the steady state velocity is also affected by the degree of confinement and explosive diameter.

Since the velocity of detonation is greater than the velocity of sound in the explosive, the explosive material directly in front of the detonation head is totally unaffected until the

detonation head passes through it. In a typical 30 foot explosive column loaded with an explosive having a characteristic velocity of detonation of 10,000 ft/sec, complete detonation and energy release within the entire column would occur in about 3 milliseconds. For an explosive with a velocity of detonation of 20,000 ft/sec, detonation and energy release would be complete in 1.5 milliseconds. Detonations of this kind are self-sustaining due to the inertia of the explosive itself that provides confinement necessary to maintain conditions for fast chemical reaction rates. (1)

Figure 1 illustrates a typical hole load configuration. Velocity of detonation within the explosive column was measured with the SLIFER system developed at SANDIA NATIONAL LABORATORIES. For a continuous 11 foot column of cartridge ANFO, the velocity of detonation was measured to be 12,200 ft/sec as indicated by the slope of the straight line segment between points (a) and (b) in Figure 1. The straight line is indicative of a consistent explosive composition, constant density and a stable velocity of detonation. As detonation progresses along the column, not only is a shock wave imparted into the surrounding medium adjacent to the borehole wall, but is also imparted into the stemming as indicated by the slope of the straight line segment between points (b) and (c). In this case, the shock wave velocity through the stemming was measured to be 2,900 ft/sec, or approximately 1/4 that of the velocity of detonation.

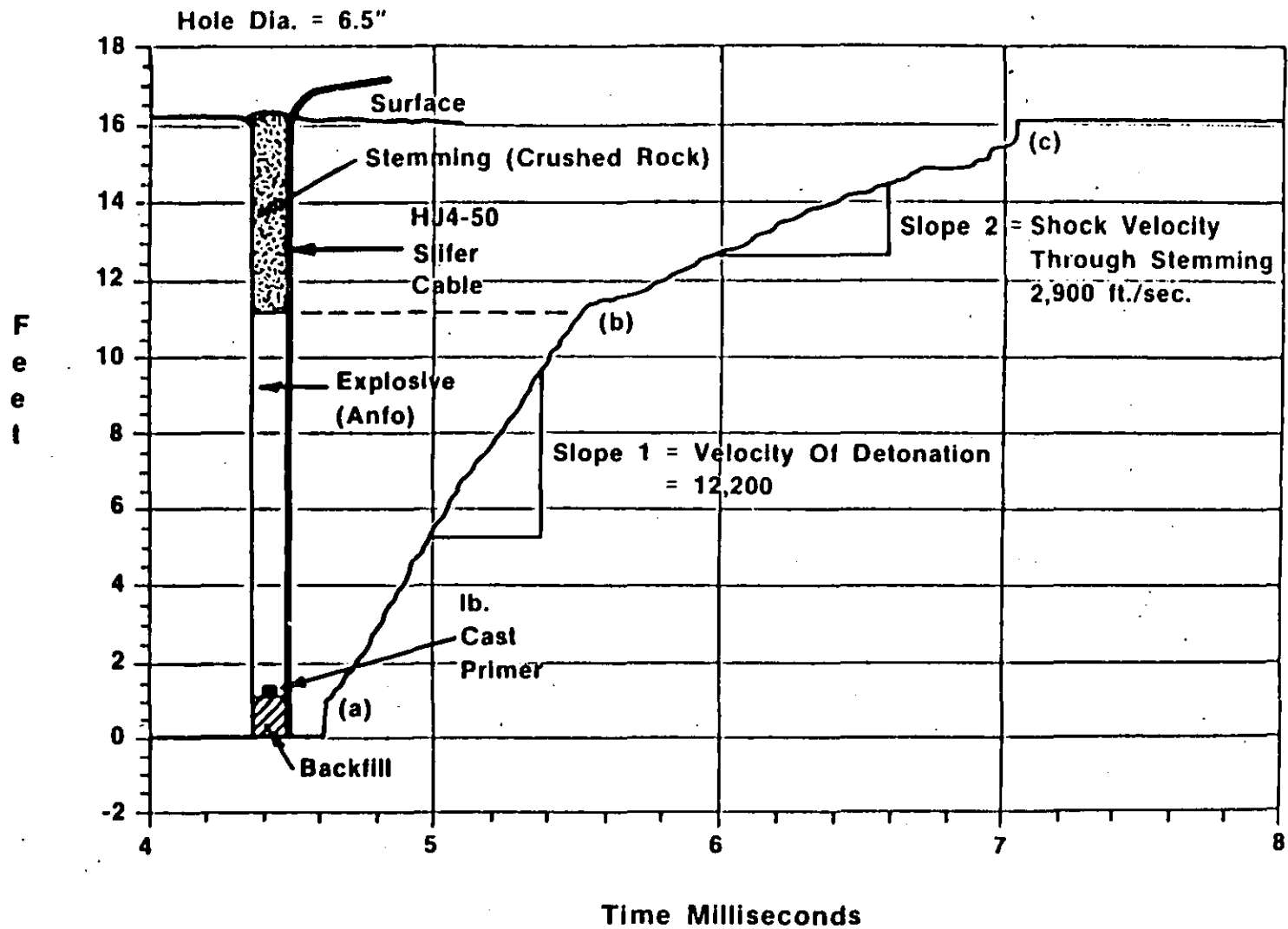


FIGURE 1

VELOCITY OF DETONATION MEASUREMENT USING THE
SLIFER SYSTEM DEVELOPED AT SANDIA NATIONAL
LABORATORIES



- 8

In a stable detonation the detonation wave travels through the column of explosive at a constant rate, (Figure 1). This rate is strictly dependent on the chemical energy released and the density and the diameter of the explosive column. Although stable, this steady-state velocity of detonation is not necessarily the "ideal" or theoretical maximum that is possible for ANFO in a larger diameter hole. If all the energy is liberated before the end of the detonation head, the detonation velocity is ideal. This is diagrammatically illustrated in Figure 2 for high explosives (TNT, RDX, etc.) where the thickness of the reaction zone is relatively small and thin and the detonation front is relatively flat.

The ideal velocity of detonation for any explosive can be calculated from the equilibrium thermodynamics and an appropriate equation of state for a given original density and chemical composition of the expected detonation products. When experimental results closely match with the predicted values, we can also say that the explosive is ideal.

Based on ideal performance calculation using the BKW code, (2), the detonation velocity for ANFO should be 17,700 ft/sec with a 73 Kbar (1,073,000 PSI) detonation pressure. However, experimental results in 3.9" ($\rho = 0.95$ g/cc) and 7.9" ($\rho = 0.90$ g/cc) diameter charges with ANFO gave detonation velocities of 11,400 ft/sec and 13,500 ft/sec, respectively. Finger et al (3) reported detonation velocities for 0.84 g/cc ANFO in the order of 15,400 ft/sec. Measurements made by

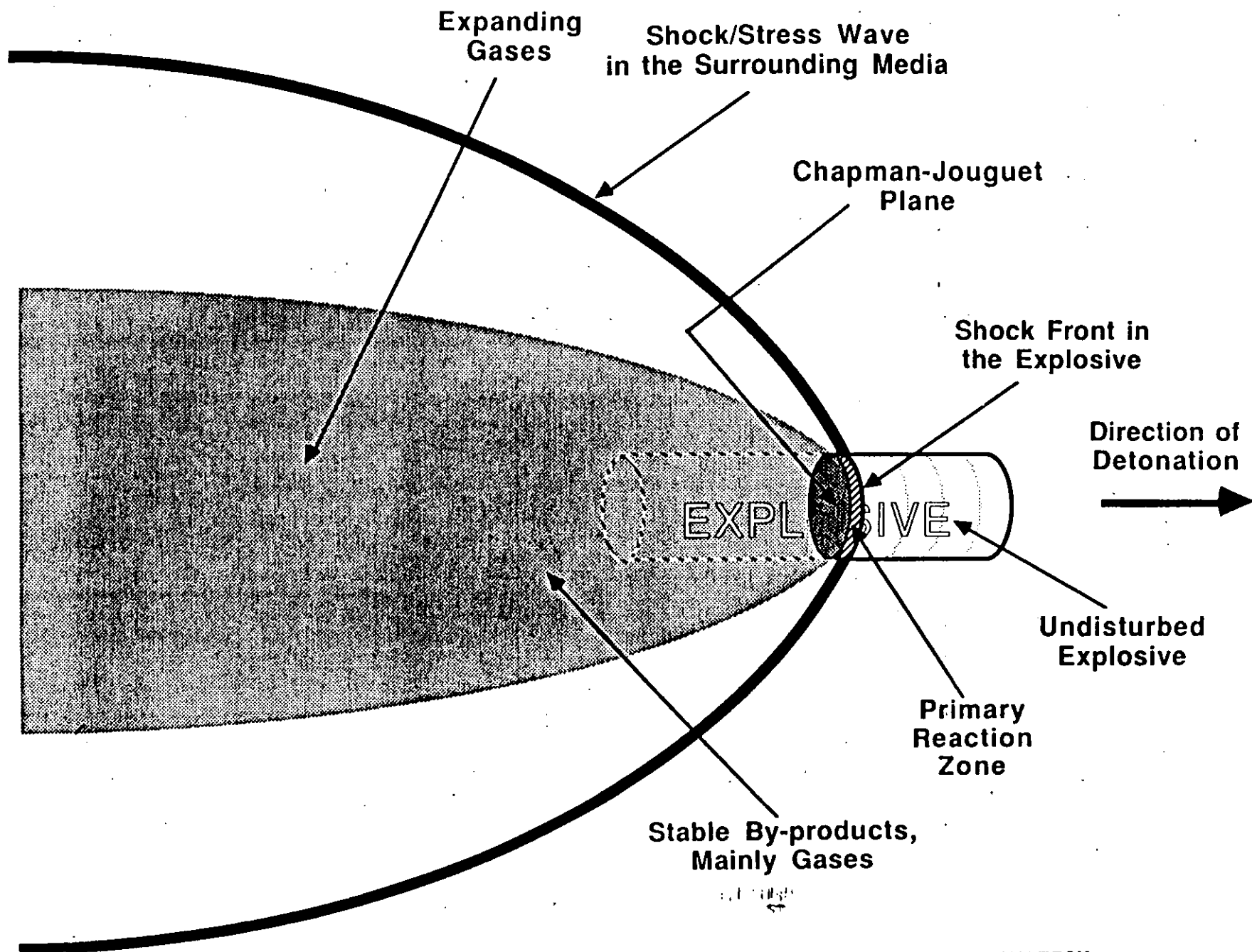


FIGURE 2 - ILLUSTRATION OF AN IDEAL DETONATION

Helm et al (4) also show that detonation velocities in ANFO are well below ideal conditions for large diameter holes up to 11.5" Persson(9) reported detonation velocities very close to the theoretical value of 17,800 ft/sec for 10.5" diameter holes when confined in rock. However, Atlas field studies for measurements in hole diameters up to 12" resulted in detonation velocities, at best, of 15,000 ft/sec. This is still well below our computer calculations of 17,000 - 19,000 ft/sec for ANFO when using different codes and equations of state.

Clearly then, detonation velocities for ANFO in hole diameters less than 17" are less than ideal. When this occurs, the reaction in the detonation head is said to be non-ideal and takes the general (exaggerated) shape as is illustrated in Figure 3. Compared to an ideal reaction zone, the non-ideal reaction zone is not flat, but rounded at the front and somewhat longer. At diameters less than that at which ideal detonation occurs (such as in most production holes) the non-ideal regime holds. Under these conditions, the detonation velocities are less than ideal, and it suggests that an ANFO prill entering the detonation is still not completely reacted by the time the tail end of the detonation has passed (refer to Figure 3). This accounts for the reduced detonation velocity.

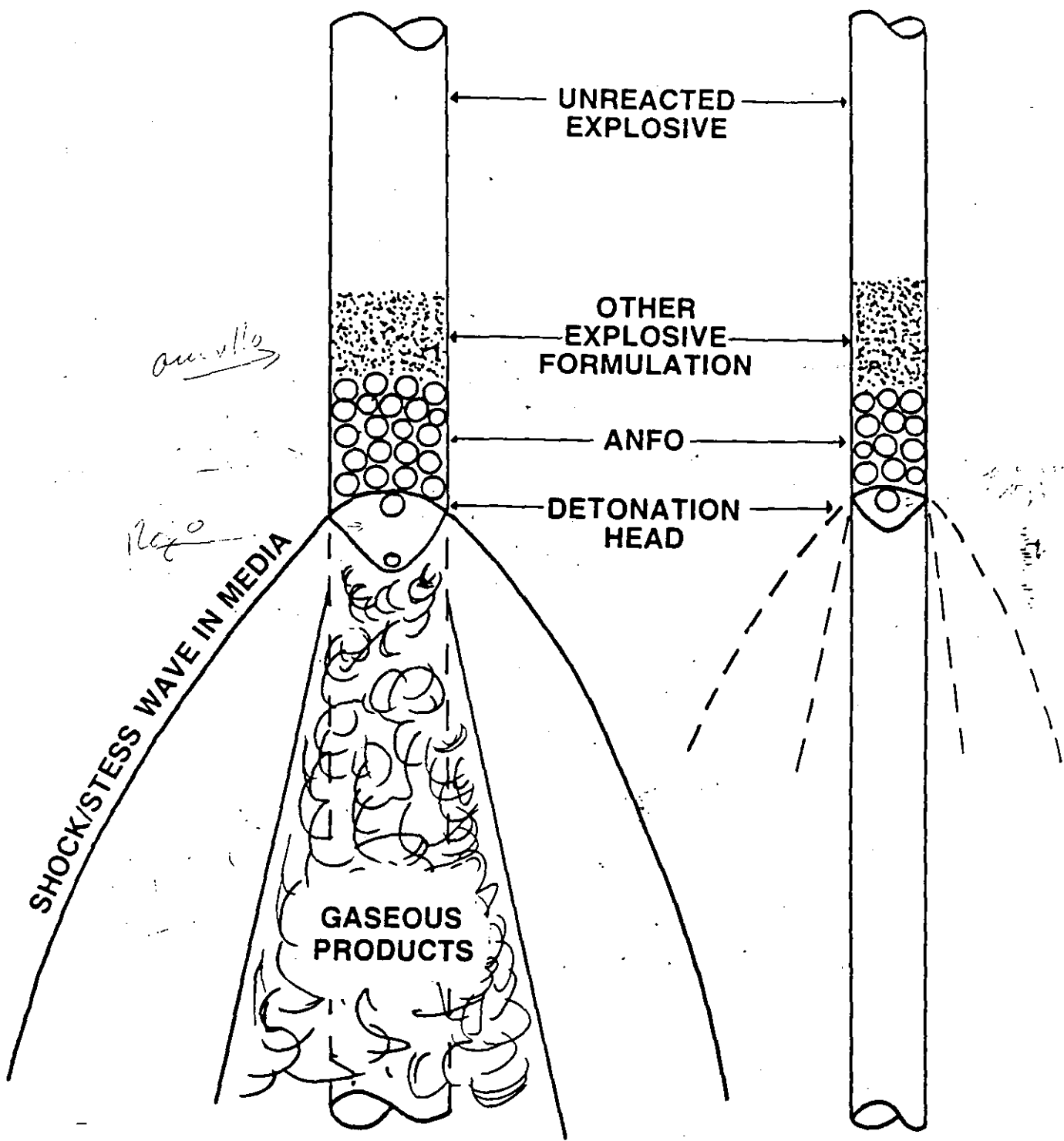


FIGURE 3

ILLUSTRATION OF A NON-IDEAL DETONATION

It also suggests that ANFO not consumed in the primary reaction zone may be reacting outside of the detonation head, that is, just behind the reaction zone at lower temperatures and pressures in the expanding gas zone.

In addition to ANFO, most commercially used explosives are of the non-ideal type. This includes slurries, watergels and emulsions. Performance of slurries and watergels, as in the case of ANFO, is dependent upon charge geometry and confinement. Furthermore, a large fraction of the explosive energy comes from the reaction of the oxidizer and fuel, which are in discrete phases whose dimensions vary. The larger the dimensions of these phases, the larger become the reaction times and the reaction zones. In the case of emulsion explosives, which comprise a better intimate mixture on a smaller scale, actual detonation velocities are very close to ideal. Thus, emulsion explosives allow a more efficient release of energy in the primary reaction zone, and for this reason have been selected as our test explosive as the alternate velocity load.

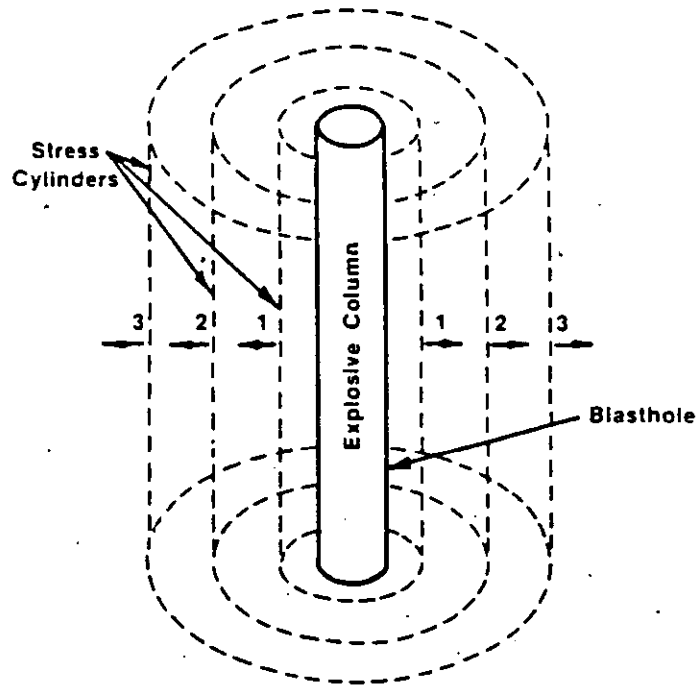
T2 - SHOCK AND STRAIN WAVE PROPAGATION

The second phase, immediately following detonation or in conjunction with the detonation phase of T1, is the shock and strain wave propagations throughout the rock mass. This disturbance or emitted pressure wave(s) emitted into the rock mass results, in part, from the rapidly expanding high-

pressure gas impacting the borehole wall. The geometry of dispersion depends primarily on the shape of the charge. If the charge is shot, with a length to diameter ratio of less than or equal to 6:1, then the disturbance is propagated in the form of an expanding cylinder, (Figure 4). However, in a typical, bottom primed, cylindrical shot hole normally encountered in bench blasting, the strain waves originally formed near the point of initiation are already in progress and propagating into the surrounding medium, while the detonation is still progressing within the explosive column. Thus, close to the shot hole, strain wave propagation is neither perfectly spherical nor cylindrical but more like that shown in Figure 5.

The pressure next to the borehole wall will rise instantaneously to its peak and then rapidly decay exponentially. The quick decay is due to cavity expansion around the borehole and increased gas cooling. Cavity expansion around the borehole can occur through crushing, pulverization, and/or displacement of material and can range anywhere from about one to three holes diameters depending on the medium and explosive used. Generally, extensive compressive, shear and tensile failure occur as a region of pulverized material, since the wave energy is at its maximum near the borehole wall.

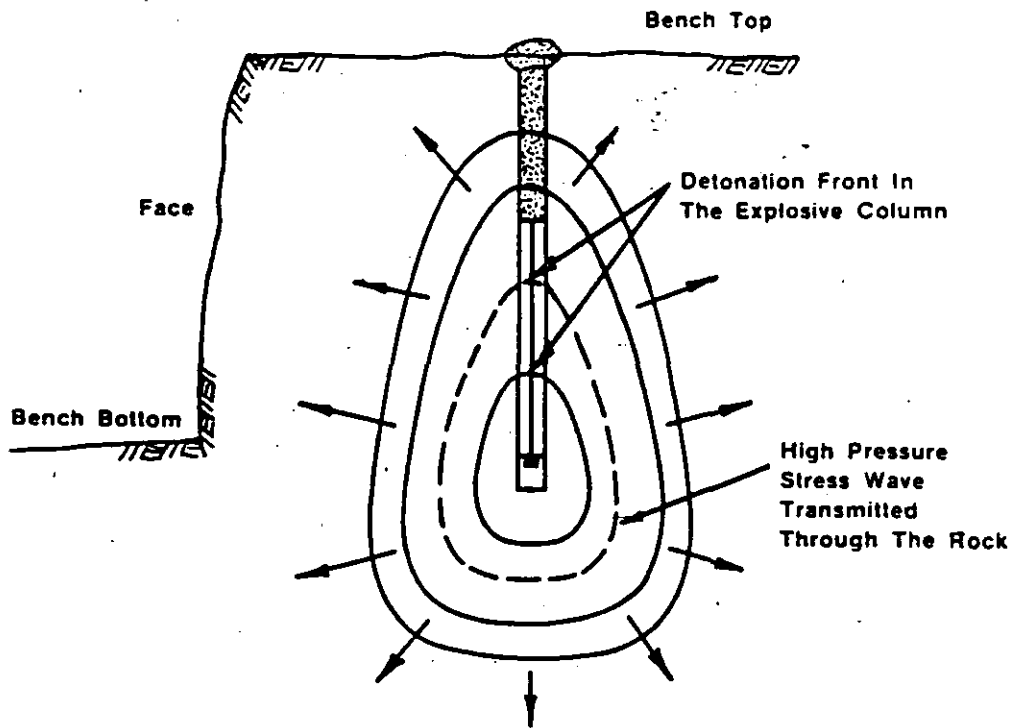
As the strain wave front proceeds outward, it has a tendency to compress the material at the wave front through a volume



1,2,3 Successive Positions Of Stress Wave

THEORETICAL POSITIONS OF THE OUTBOUND DISTURBANCE FROM A COLUMN CHARGE

FIGURE 4



SECTION THROUGH THE FACE DURING DETONATION SHOWING EXPANDING STRESS WAVE FRONT

FIGURE 5

change. At right angles to this compressive front, there exists another component referred to as the tangential or "hoop" stress. The tangential stress, if large enough, can cause tensile failures at right angles to the direction of propagation. The largest tensile failures are expected to occur close to the borehole where the tangential stress is high enough for failure to occur. Both the compressive and tensile components of the wave front decay with distance from the borehole.

When the compressive wave front encounters a discontinuity or interface, some of the energy is transferred across the discontinuity and some is reflected back to its point of origin.(5) For the most part, the partitioning of energy depends on the ratio of the acoustic impedance of the materials on either side of the interface, as illustrated in Figure 6. Acoustic impedance, Z , for any material is defined as:

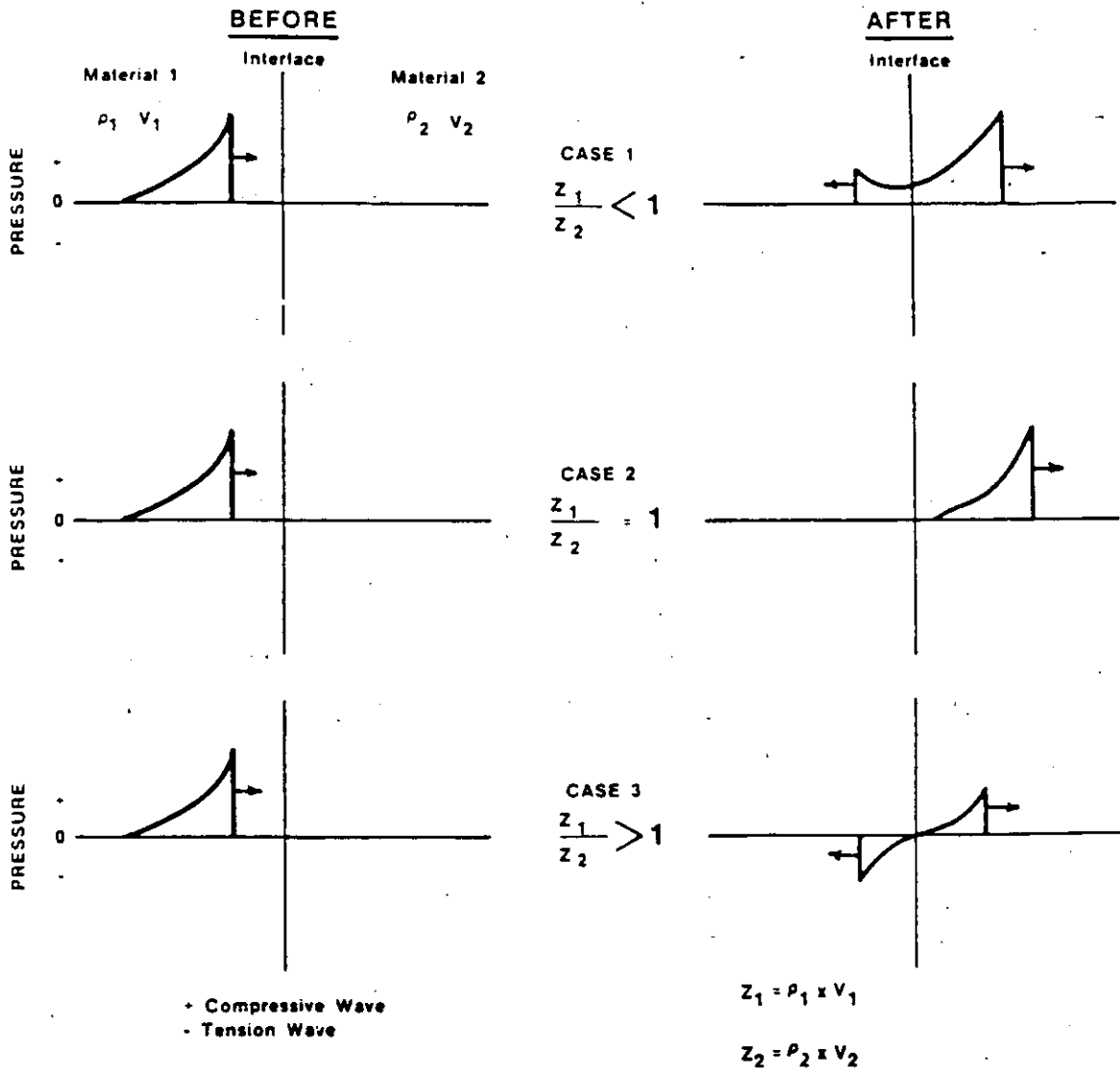
$$Z = \rho \times V$$

Where: Z = acoustic impedance

ρ = density of material

V = sonic velocity of material

In reference to Figure 6, where the ratio of the acoustic impedance of material 1 to material 2 is less than one, some of the wave energy is transferred into material 2 and some reflected back, but both waves remain compressional. When the acoustic impedance ratio is 1, all of the energy is



**INTERACTION OF STRESS WAVES
AT AN INTERFACE
FIGURE 6**

transferred into material 2 and no reflected wave occurs. When the impedance ratio is greater than 1, then some of the energy gets transferred into material 2 as a compressive wave and the remaining energy gets reflected at the interface as a tensile wave. When a compressive wave travelling through rock encounters an interface such as a free face, nearly all of the energy will be reflected back as a tensile wave. If the burden distance between the free face and explosive column is relatively small in contrast to normal burdens for a chosen explosive, then most of the energy is consumed in spalling at the free face.

The interaction of stress waves in the outgoing compressive and reflected tensile modes around discontinuities and flaws within the rock mass is an area of intense research and is considered to be quite important in some of the newer blasting theories. In order to effectively utilize the interaction of shock waves in a production environment, ultra-precise detonators with precisions in the order of a few hundred microseconds about the mean are suggested for the next generation of detonators.

T3 - GAS PRESSURE

During and/or after strain wave propagation, the high pressure, high temperature gases impart a stress field around the blasthole that can expand the original borehole, extend

radial cracks and jet into any discontinuity. It is during this phase where some controversy exists as to the main mechanism of fragmentation. Some believe that the fracture network throughout the rock mass is completed while others believe that the major fracturing process is just beginning. In any case, it is the gases that have jetted into discontinuities and the fracture network that is either fully developed or being developed, which are responsible for the displacement of broken material. Past, current and newer blasting theories are listed as follows:(6)

- 1) Reflection Theory
- 2) Gas Expansion Theory
- 3) Flexural Rupture
- 4) Stress Wave & Gas Expansion Theory
- 5) Combined Theory
- 6) Nuclei or Stress-Wave/Flaw Theory
- 7) Torque Theory
- 8) Cratering Theory

It is not clear as to the exact travel paths that gases take within the rock mass, although it is agreed that they will always take the path of least resistance. This means that gases will first migrate into existing cracks, joints, faults, and discontinuities, in addition to seams of material which exhibit low cohesion or bonding at interfaces. If a discontinuity or seam between the borehole and free face is sufficiently large, the high pressure gases will immediately vent to the atmosphere, rapidly reducing the total confinement pressures, and results in reduced displacement of broken and fragmented material.

The confinement time of gas pressures within a rock mass vary significantly depending on the amount and type of explosive, material type and structure, fracture network, amount and type of stemming, and burden. Studies by Chiappetta et al (7) with the use of high-speed photography in full-scale bench blasts, have shown that gas confinement times before the onset of movement can vary from a few milliseconds to tens of milliseconds. To date, confinement times have been measured to range from 5 to 110 milliseconds for a variety of materials, explosives and burdens. Generally, but not always, confinement times can be decreased by employing higher energy explosives, decreasing the burden, or a combination of both. This applies equally to material at the bench face or at the bench top, as in the case of stemming blowouts or cratering. It is evident that only suitably burdened and well stemmed charges can deliver their full potential of additional gas extension fracturing and mass movement.

T4 - MASS MOVEMENT

Mass movement of materials is the last stage in the breaking process. The majority of fragmentation has already been completed through compressional and tensile stress waves, gas pressurization or a combination of both. However, some degree of fragmentation, although slight, occurs through in-flight collisions and also when the material impacts the

ground. Generally, the higher the bench height, the greater is this type of breakage owing to the increased impact velocities of individual fragments when falling onto the bench floor. Similarly, material ejected from opposite rows of a "V-shot" design upon head-on collisions can result in increased fragmentation. This phenomenon was evidenced and documented with the use of high-speed photography of bench blasts.

Mass burden movement of fragmented material is shown in Figure 7 for a number of typical face conditions encountered in bench blasting operations. Face profiles and velocities are based on the results of high-speed photographic analysis performed at the ATLAS POWDER COMPANY. Where no subdrilling is utilized, (a and b), two types of face movement may be encountered. In Figure 7a the entire length of face burden, directly in front of the explosive column, moves out similar to a plane wave and the face velocity at any point is constant. This behavior is usually encountered where material is very competent, quite brittle, and structured with well defined, largely spaced joints much greater than the spacings or burdens employed in blast designs. When the material is soft, highly fissured, and/or closely jointed as might be found in coal and some sedimentary deposits, face profiles resembling that of flexural rupture are more likely. In this case, the greatest displacement and velocity occur adjacent to the center of the explosive column with the least amount of movement occurring at the toe and crest.

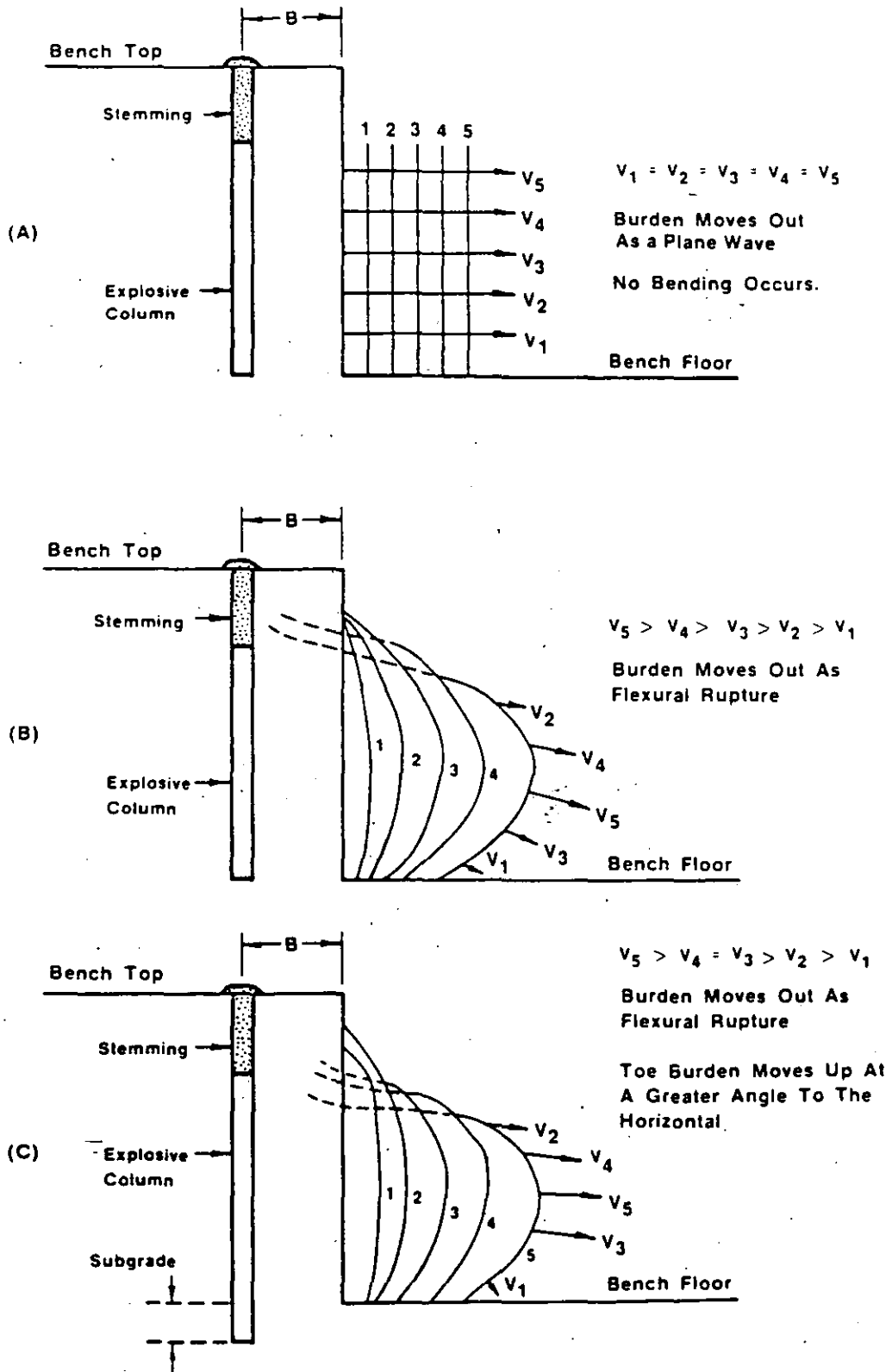


FIGURE 7

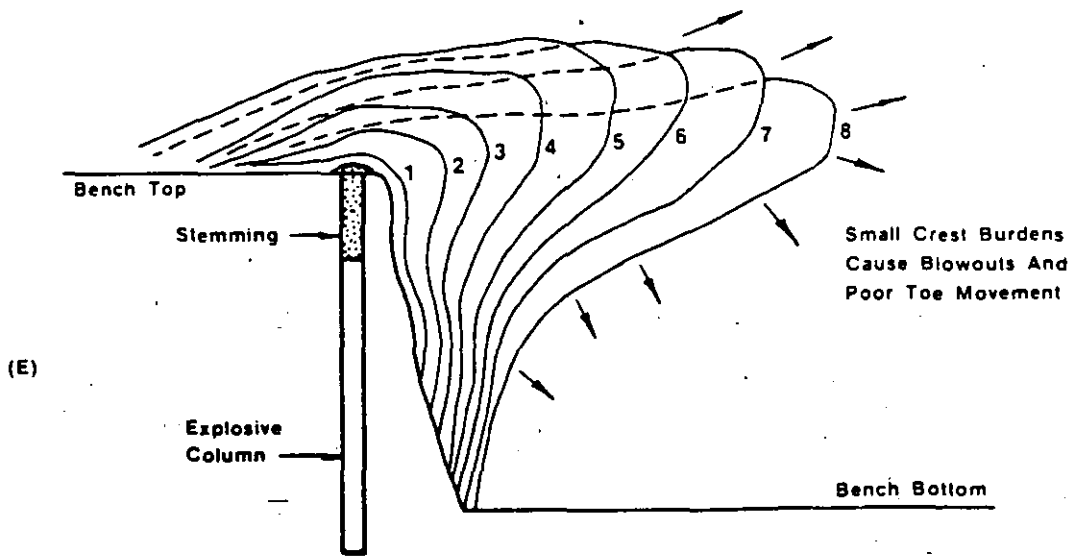
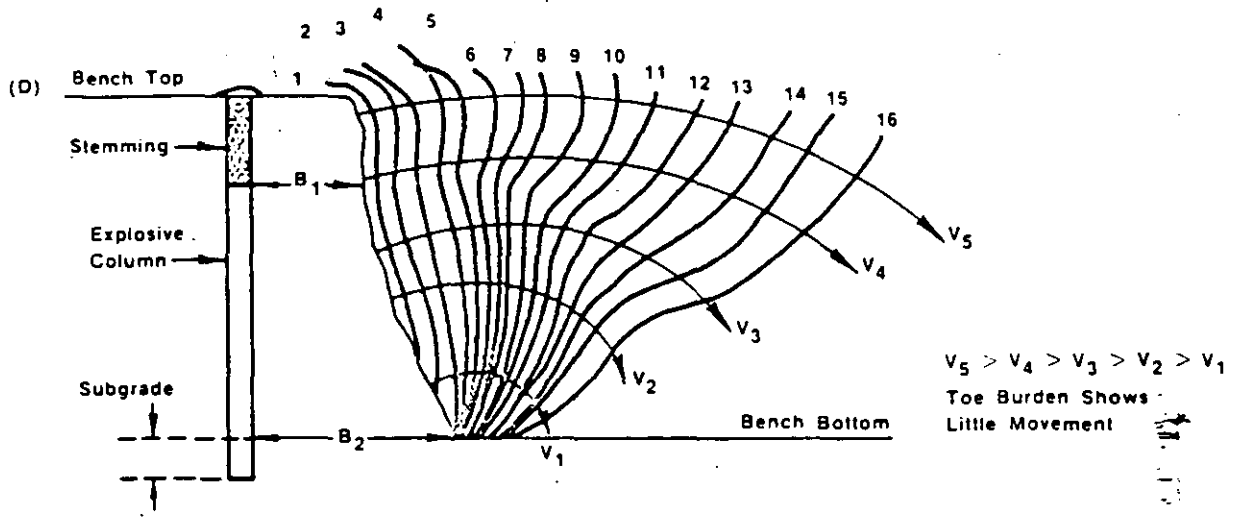


FIGURE 7 (Cont'd)

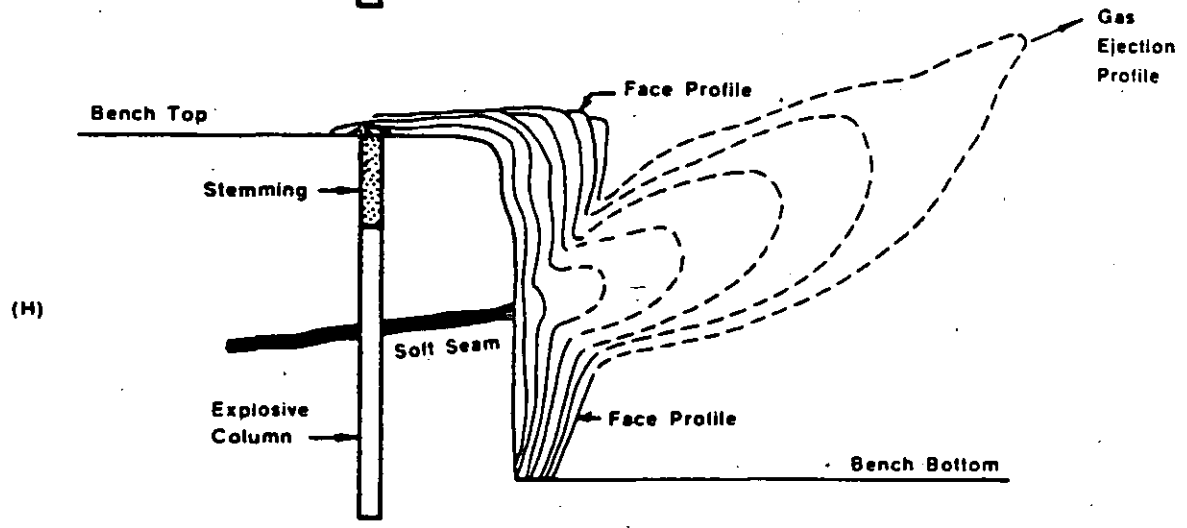
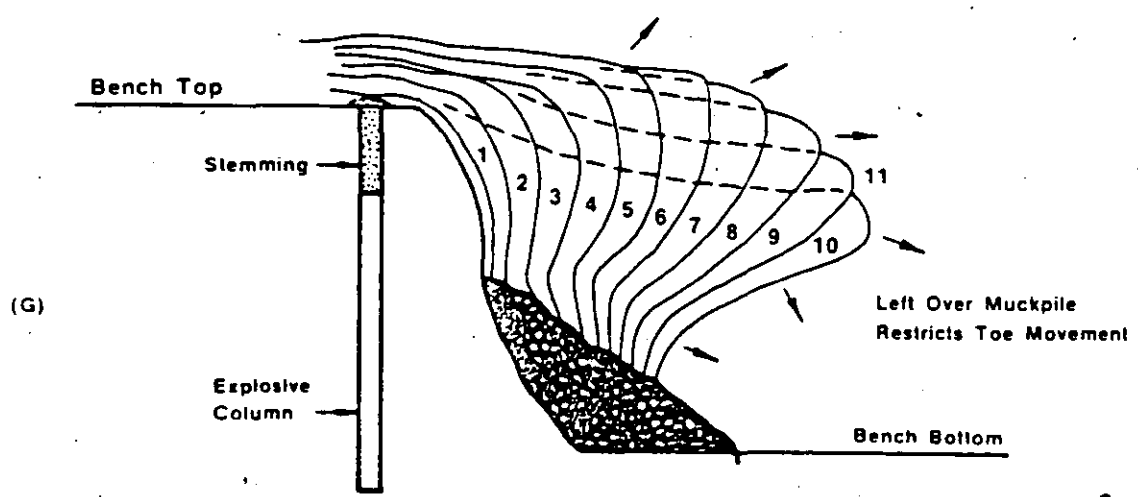
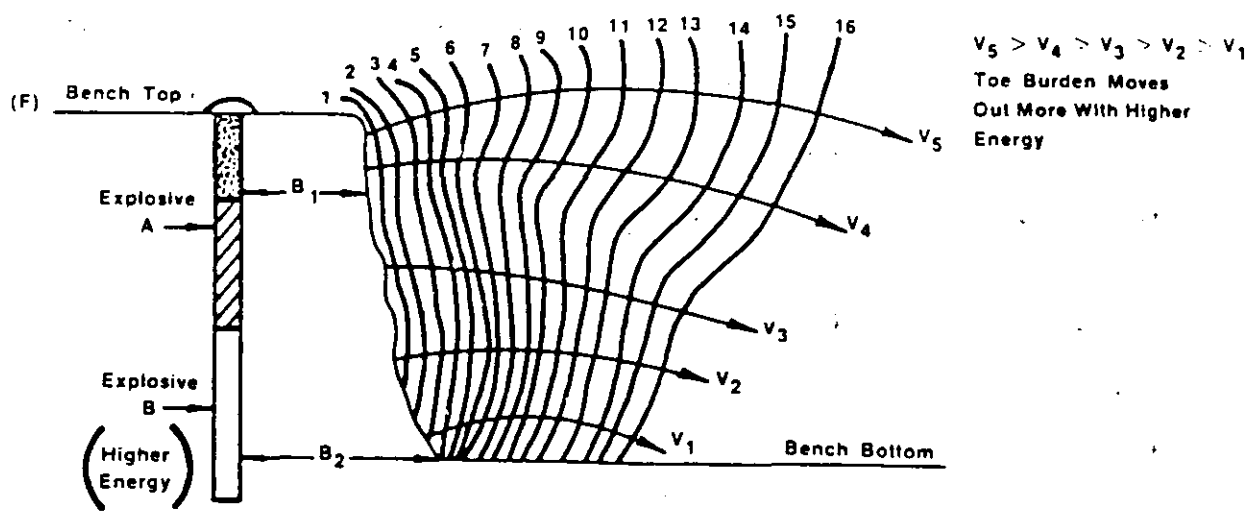


FIGURE 7 (Cont'd)

When identical conditions in Figure 7b are assumed and when subdrilling is employed, face movement results in much the same way except that the toe burden is displaced upwards faster and at a greater angle to the horizontal. (Figure 7c)

The first three cases assumed a relatively straight face between the crest and toe, however, in many bench blasting operations, the condition is more like that illustrated in Figure 7d, where toe burden is considerably greater than the crest burden. The toe burden is too great for the explosive selected, hence, very little movement occurs at the toe while the greatest displacement results in the upper half of the bench.

Three options are available to increase toe movement:

- * Employ angle drilling in an attempt to maintain constant burdens from the crest to the toe
- * Use a higher energy bottom charge in the current vertical drill holes.
- * Decrease the burden with the current drill holes.

In selecting the latter, care should be exercised so as not to decrease the burden to the point of obtaining the condition shown in Figure 7e. The toe burden is now correct for the explosive selected, but the crest burden is substantially reduced. This may bring about many adverse conditions near the crest burden such as flyrock, blowouts and increased airblast complaints. Because confinement pressures are released near the crest (in this case, a path of least resistance relative to the toe burden), restricted toe

movement will result. It is better to use the same burden, but with a high energy bottom charge near the toe. This load configuration as shown in Figure 7 f tends to pressurize more of the burden mass for longer periods without adverse effects, and adequate toe movement generally results.

Where large leftover muckpiles are left against the face, Figure 7g, toe movement will be restricted and increased ground vibration levels are likely. Unless the situation requires a buffer, such as when blasting in the vicinity of mining equipment or to avoid dilution of an ore blast adjacent to a waste muckpile, it should be avoided.

Where seams are encountered in a blast, Figure 7h, tremendous gas ejections with velocities up to 600 ft/sec can occur. When such gas venting occurs, it will adversely affect other parts of the burden to displace adequately and inevitably leads to poor overall blasting results. A stemming deck immediately adjacent to the seam will give better results.

TIME EVENTS T1 - T4 COMBINED

Up to this point, events T1 to T4 have been discussed more or less as separate isolated events. However, in a real blasting environment, more than one event can occur at the same time.

Consider a single vertical hole in a quarry face with the primer located near the bottom of the hole as is illustrated in Figure 8. Assume the explosive used is 40 feet of ANFO with a velocity of detonation equal to 13,000 ft/sec, the material blasted is limestone with a sonic wave velocity of 15,000 ft/sec and a density of 2.3 g/cc. Upon initiation of the primer, it takes only a few microseconds and a distance of 2 to 6 hole diameters up the column to form a full detonation head. When a full detonation head is formed, it travels up the explosive column with a velocity characteristic of the steady-state velocity, (in this case 13,000 ft/sec). It takes approximately 3.0 msec for the 40 foot column of ANFO to be completely detonated.

Within this 3.0 msec, many other things have occurred. Starting at the bottom of the hole and progressing up the column, borehole expansion through crushing of the borehole walls has taken place. This produces compressive stress waves with tangential components emanating from the borehole walls and progressing outward in every direction with a velocity characteristic of the sonic wave velocity of limestone. It takes approximately 1.0 msec for the compressive strain wave to traverse 15 feet of burden to the free face. Behind the strain wave propagation some radial cracks start to develop in the crushed zone region of the borehole with a velocity ranging from 25 to 50% of the P-wave velocity for limestone. If the intensity of the compressive strain pulse is high enough, new crack and/or extensions of pre-existing cracks

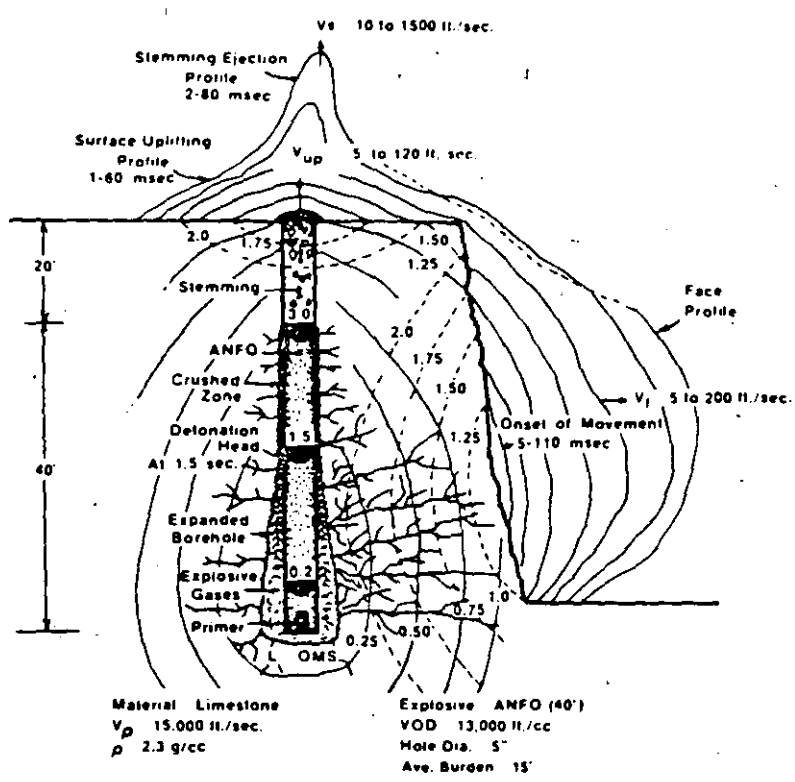


ILLUSTRATION SHOWING THE INTERACTION OF TIME EVENTS T1 TO T4 IN A TYPICAL QUARRY BENCH
FIGURE 8

and flaws can be initiated anywhere between the crushed zone next to the borehole and the free face. The greatest number of cracks are generally found closest to the borehole.

When the compressive wave strikes a free face, it is immediately converted to a tensile strain wave which starts at the free face and travels back through the rock mass towards the borehole. Owing to the new fractures created from the outgoing compressive strain wave, the tensile strain wave will take somewhat longer to travel the same burden distance of 15 feet. If the burden is small enough and the intensity of the reflected strain wave is large enough, then some spalling at the free face or bench top is expected, although no significant mass movement will occur.

At 3 msec after detonation and assumed complete reaction of ANFO, the original high temperature, high pressure gases have reached a new equilibrium due to borehole expansion. Both temperature and pressure have dropped significantly resulting in an energy reduction ranging from 25 to 60% of the theoretical energy originally available. This remaining energy acts on the surrounding "preconditioned" rock mass to displace it in the direction of least resistance. Further fragmentation can occur at this stage from gases entering and extending preexisting cracks or discontinuities. It is at this stage where some blasting theories are contradictory. Some believe that the major fracture network is completed within about 3 msec due to the interaction of stress waves on

the surrounding material, while others believe that the major fracture network is just beginning.

Regardless of which time frame is responsible for the development of a fracture network, mass movement and displacement of material at the bench top or face occurs much later in time due to the confinement of gas pressure within the rock mass. The onset of mass movement depends on the material response in conjunction with the strain and gas pressure stimulus generated from the explosive. For typical stemming and burdens encountered in the field, bench top swelling occurs between 1 to 60 msec, stemming ejections between 2 to 80 msec and bench burdens between 5 to 110 msec. Surface uplifting velocities around the collar region of a hole occur between 5 and 120 ft/sec, stemming ejection between 10 to 1500 ft/sec and burden velocities between 5 to 200 ft/sec. Gas ejection velocities at discontinuities have been recorded as high as 700 ft/sec and often occur in less than 5 msec.

CHARACTERIZATION OF ALTERNATE VELOCITY LOADING
WITH AN EMULSION EXPLOSIVE IN ANFO

It is evident from the discussion so far that the selection of conventional blast design variables can have a pronounced effect on overall results regarding fragmentation and mass movement of burdens. Without making major modifications in the blast design, a simple and cost effective technique to further improve fragmentation and/or increase burden velocities is with Alternate Velocity Loading. Alternate Velocity Loading is achieved by sparingly placing a cartridge or slug of emulsion explosive every few feet in the ANFO column (refer to Figure 9). Field trials conducted in a wide variety of materials have generally resulted in improved fragmentation and increased burden velocities. It appears that when an explosive of higher density and detonation velocity (i.e., emulsion) is embedded within the column of the main charge with a lower density and detonation velocity (i.e., ANFO), improvements in blasting results are the norm. Whether the material exhibits physical and strength properties characteristic of granites, limestones and dolomites, or overburden, unconsolidated type materials, the results are often dramatic and repeatable.

In the course of implementing the Alternate Velocity Technique, a few groups in the industry believed that ANFO did not possess sufficient detonation pressure to act as an effective

primer on the emulsion explosive. They also stipulated that the technique could not be cost effective because each emulsion cartridge or slug required a primer and detonator assembly for it to succeed.

As an investigative approach to address these thoughts, the ATLAS POWDER COMPANY embarked on a joint research program with SANDIA NATIONAL LABORATORIES where over 100 holes were fired under controlled conditions in a field environment. Instrumentation consisted of continuous velocity probes (Slifer System), pressure sensors to measure gas pressure, accelerometers to measure shock in the surrounding rock mass, survey gear to quantify the extent of damage, mounds, craters and multiple high-speed cameras to quantify gross movement and gas venting.

An Alternate Velocity test was performed in a full-scale, 6-1/2" diameter, production hole, with ANFO ($\rho = 0.81$ g/cc) as the main charge, and an Apex grade of cartridge emulsion explosive (5" x 30lb, $\rho = 1.25$ g/cc) as the Alternate Velocity explosive. Borehole depth was approximately 40 feet and each emulsion cartridge was 3' in length. Continuous velocity of detonation measurements were performed by Sandia National Laboratories using the Slifer System for the entire length of the hole. (8) Results are illustrated as displacement versus time plots in Figures 9 and 10.

Explosive loading, starting at the bottom of the hole, consisted of a one pound ATLAS Cast G Booster, followed by a

3 foot cartridge of emulsion, 10 feet of ANFO, a 3 foot cartridge of emulsion, 11 feet of ANFO, a 3 foot cartridge of emulsion, and approximately 10 feet of 1/2" - 1-1/8" of crushed rock for stemming.

Figure 9 illustrates the actual, untouched and unfiltered results obtained from the field, while Figure 10 illustrates a filtered close-up of results in the bottom 20 feet of the borehole. The filtered close-up gives better resolution and allows for more accurate measurement of detonation velocity. Detonation velocity results are presented in Table 2.

TABLE 2
DETONATION VELOCITY RESULTS FOR THE ALTERNATE VELOCITY TEST
(Emulsion and ANFO)

COLUMN POSITION	COLUMN LENGTH (ft)	AVERAGE VELOCITY OF DETONATION (ft/sec)	COLUMN EXPLOSIVE/MATERIAL
A - B	3	20,500	EMULSION
B - C	5	13,000 - 2,045	WET ANFO
C - D	5	2,045	WET ANFO
D - E	3	20,000	EMULSION
E - F	11	12,500	DRY ANFO
F - G	3	9,000 - 16,000	EMULSION ANFO STEMMING
G - H*	10	1,000	STEMMING

* Shock wave velocity through stemming.

FAIRDALE MINE ALT
SLIFER 1S40H

55FT HJ4-50 SLIFER

SAMPLE INT= 2.5 USEC

TEST DAY 15-NOV-84 11:51:40
PLOT DAY 15-NOV-84 12:56:02
DAASY FILTER= 80 KHZ

SLIPLT

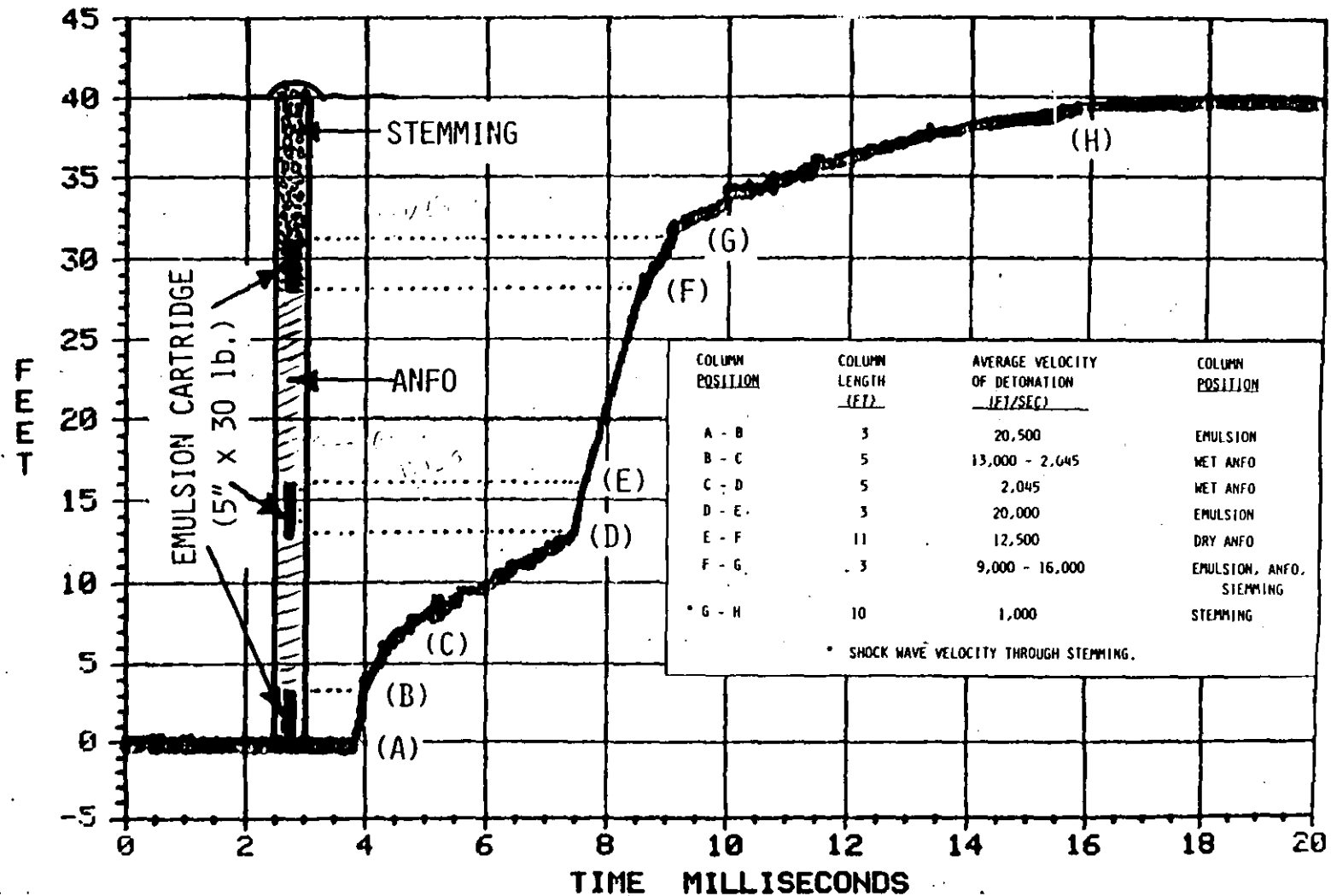


FIGURE 9 DISPLACEMENT vs TIME - Velocity of detonation measurement using the Slifer System developed at SANDIA NATIONAL LABORATORY.
(FAIRDALE QUARRY, Macklin Brothers Stone Company, Fairdale, IL)

FAIRDALE MINE
SLIFER 1S40H

ALT 55FT HJ4-50 SLIFER
SAMPLE INT= 2.5 USEC

TEST DAY 15-NOV-84 11:51:40
PLOT DAY 1-NOV-85 13:43:34
DAASY FILTER= 10 KHZ

SLIPLT

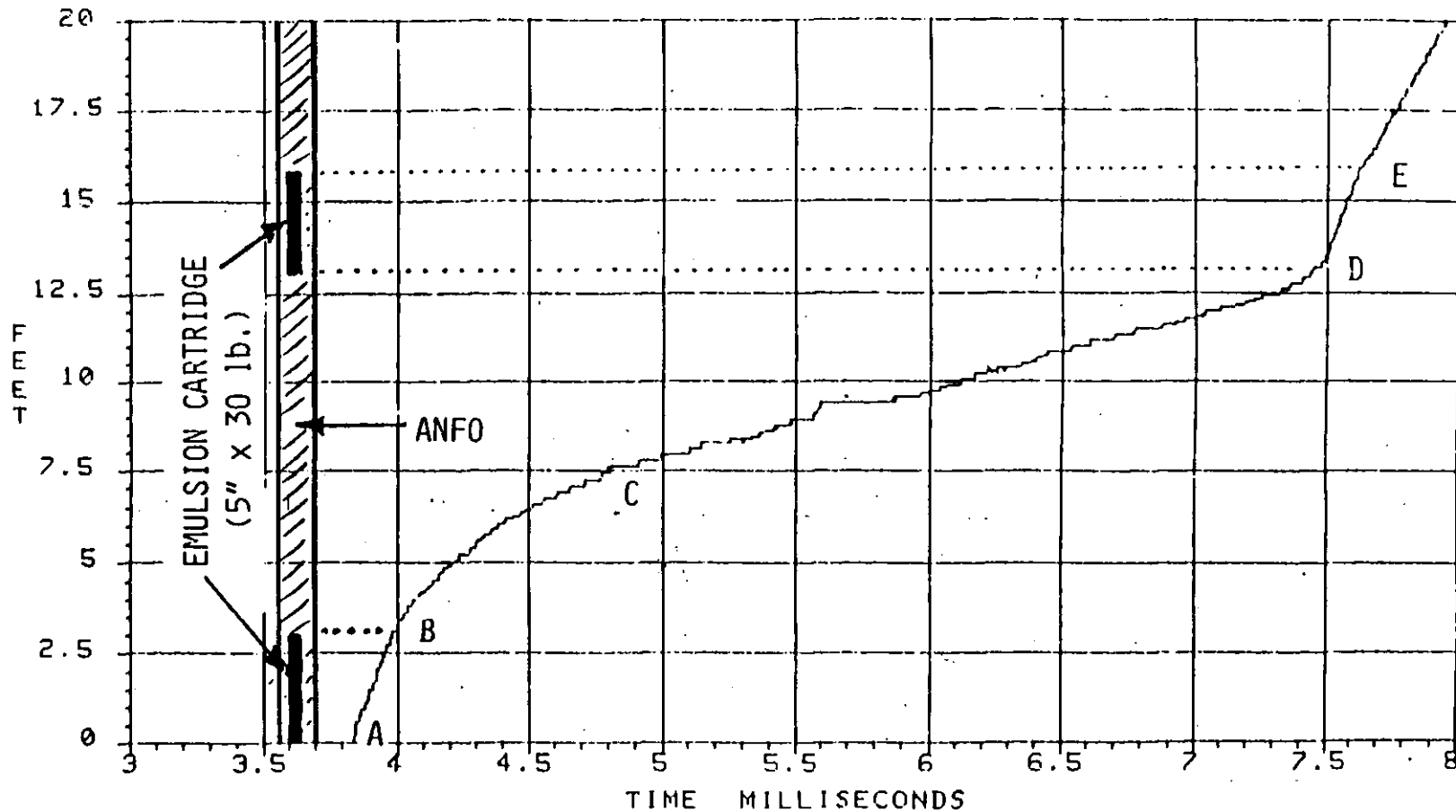


FIGURE 10

FILTERED CLOSE-UP OF FIGURE 9

(FAIRDALE QUARRY, Macklin Brothers Stone Company, Fairdale, IL)

Many important and interesting points are noteworthy in the results. Between points (a) and (b), the velocity of detonation for the 3 foot length of emulsion cartridge is 20,500 ft/sec. Between (b) and (c), the velocity of detonation in ANFO is quickly reduced from 13,000 ft/sec to 2,045 ft/sec and the ANFO detonation at this velocity is sustained until just before point (d) is reached. Just before point (d) is reached, or 6" below the second emulsion cartridge, ANFO is increasing in detonation velocity from 2,045 ft/sec to 4,900 ft/sec. ANFO with a detonation velocity of 4,900 ft/sec and a density of 0.81 g/cc is equivalent to a detonation pressure of approximately 4.5 Kbars. At point (d), the detonation head in ANFO encounters the second emulsion cartridge, which when detonated, at 20,000 ft/sec between points (d) and (e), brings ANFO immediately back up to its normally rated detonation velocity of 12,500 ft/sec. Thus, even a low order ANFO detonation can act as a very effective primer for the emulsion cartridge without additional boosting on the emulsion cartridge.

The decrease in the ANFO detonation velocity between points (b) and (c) is attributed to water trickling into the bottom 12-1/2 feet of the hole from the surrounding rock mass.

The drill hole was drilled one week in advance of testing and it had accumulated approximately 3 feet of water. Prior to testing, the water in the hole was pumped out and it was determined that in one hour, the hole could accumulate about 2" of water in the

bottom. The 2" of water was again pumped out and the hole was backfilled with 6" of crushed rock so that the bottom of the hole would be out of water.

It took approximately one hour from the time of backfilling the hole to firing the shot hole. We feel that there was sufficient wetness and/or tiny amounts of water trickling into the borehole walls for the bottom 12-1/2 feet of the test hole to affect the performance of ANFO. Although the wet ANFO was not purposely planned as part of the test, it does illustrate that even a low order ANFO detonation of 4,900 ft/sec can act as an effective primer on an emulsion. It also illustrates that when water is pumped out of a hole and the hole is loaded with ANFO, ANFO performance can still be drastically affected just by the wetness on the sides of the borehole. Inadequate priming at the bottom of this hole would have probably resulted in a failure.

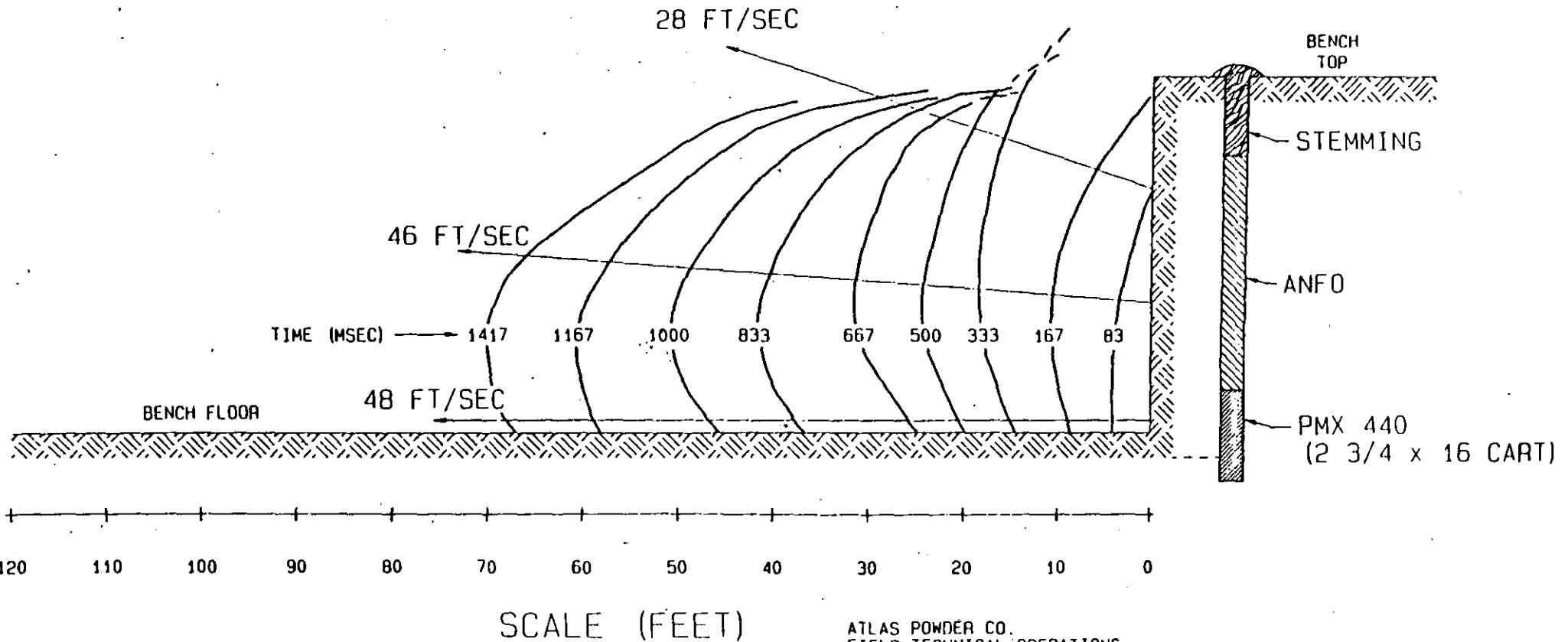
Although ANFO can tolerate up to a 10% water saturation level, it does so at the cost of blasting efficiency. If the center emulsion cartridge was not present, one of two things could have occurred. ANFO may have sustained a low order detonation throughout the remaining column until dry ANFO was reached, or it would have soon failed due to its instability. Between points (e) and (f), the detonation velocity in dry ANFO was 12,500 ft/sec, as expected. Between points (f) and (g), the average velocity of detonation in the top cartridge appeared to fluctuate between 9,000 - 16,000 ft/sec due to the combined effect of emulsion, ANFO and stemming. For optimum results, the top emulsion cartridge should have been placed one to two feet below the stemming column where it would have been completely embedded in the ANFO column. Between points (g) and (h), the average shock wave velocity through stemming was 1,000 - 1,100 ft/sec.

ALTERNATE VELOCITY FIELD TESTS IN FULL-SCALE PRODUCTION SHOTS

A study was conducted in a Southeastern granite quarry to evaluate relative explosive performance in terms of burden velocities for normal and Alternate Velocity Loading Techniques. Four full-scale production shots were made. Three shots were loaded conventionally, using a different type or grade of bottom charge, amounting to seven 2-3/4" x 16" cartridges or nine feet of bottom load and ANFO as a top load. The bottom loads in the conventional shots consisted of Powermax 440 (emulsion), Powermax 460 (emulsion) and a watergel explosive. The fourth shot was made with the same type and amount of bottom charge of Powermax 460 with four additional cartridges of Powermax 460 spaced at 6 foot intervals as the alternate velocity load in the ANFO column. All other blast design variables such as burden, spacing, hole depth, millisecond delay pattern, blasting direction, etc. were kept as constant as was reasonably possible in a production environment. High-speed motion picture photography was used to quantify, evaluate and compare results.

Average face velocities were calculated for three areas of the face; at the toe, 12 feet above the toe, and 24 feet above the toe as illustrated in Figures 11 to 14. Analysis was accomplished by designating the first face profile as occurring at zero time to produce a plot of displacement versus time.

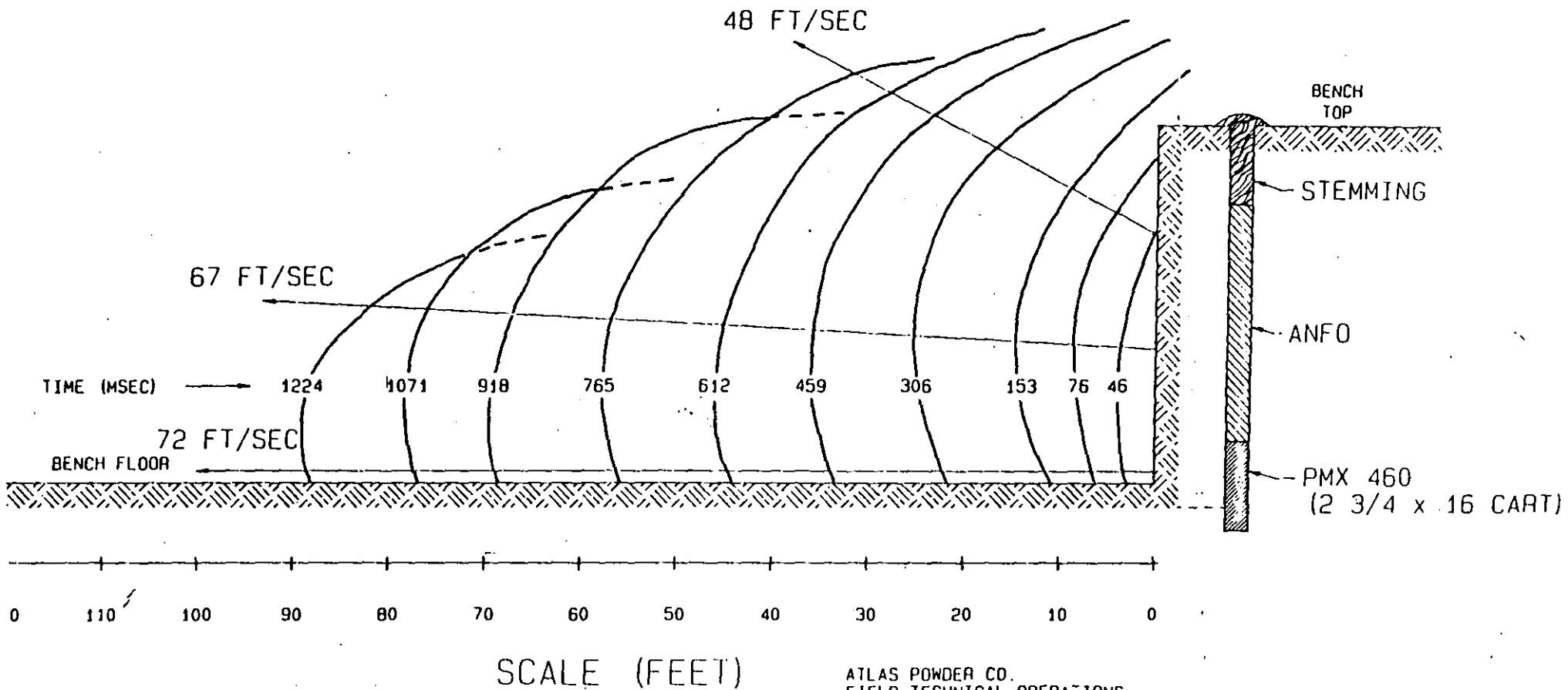
POWERMAX 440 - ANFO



ATLAS POWDER CO.
FIELD TECHNICAL OPERATIONS
TAMAQUA, PA. *SC.*

FIGURE 11

POWERMAX 460 - ANFO



ATLAS POWDER CO.
 FIELD TECHNICAL OPERATIONS
 TAMAQUA, PA. *TC*

FIGURE 12

ALTERNATE VELOCITY LOADING
POWERMAX 460 - ANFO

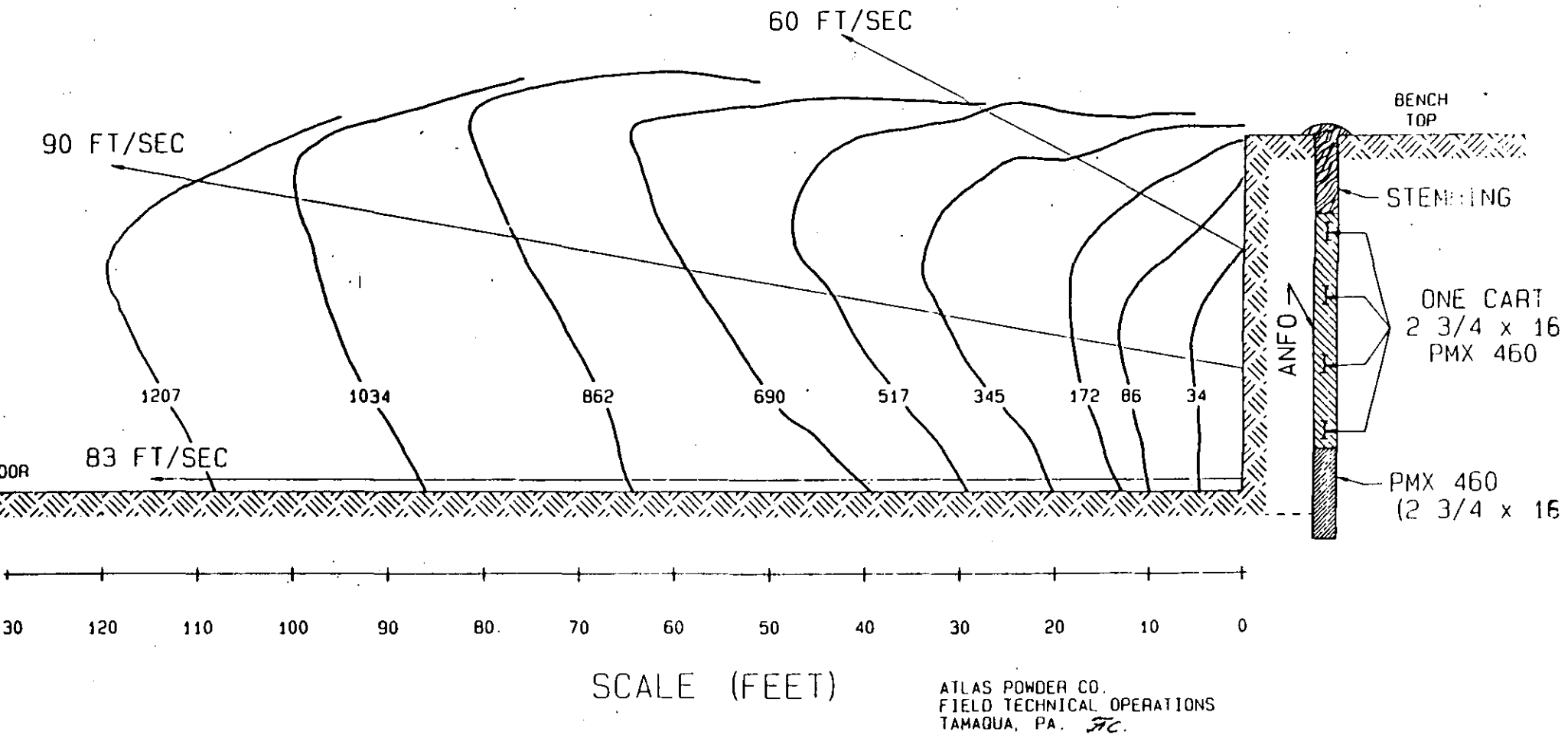
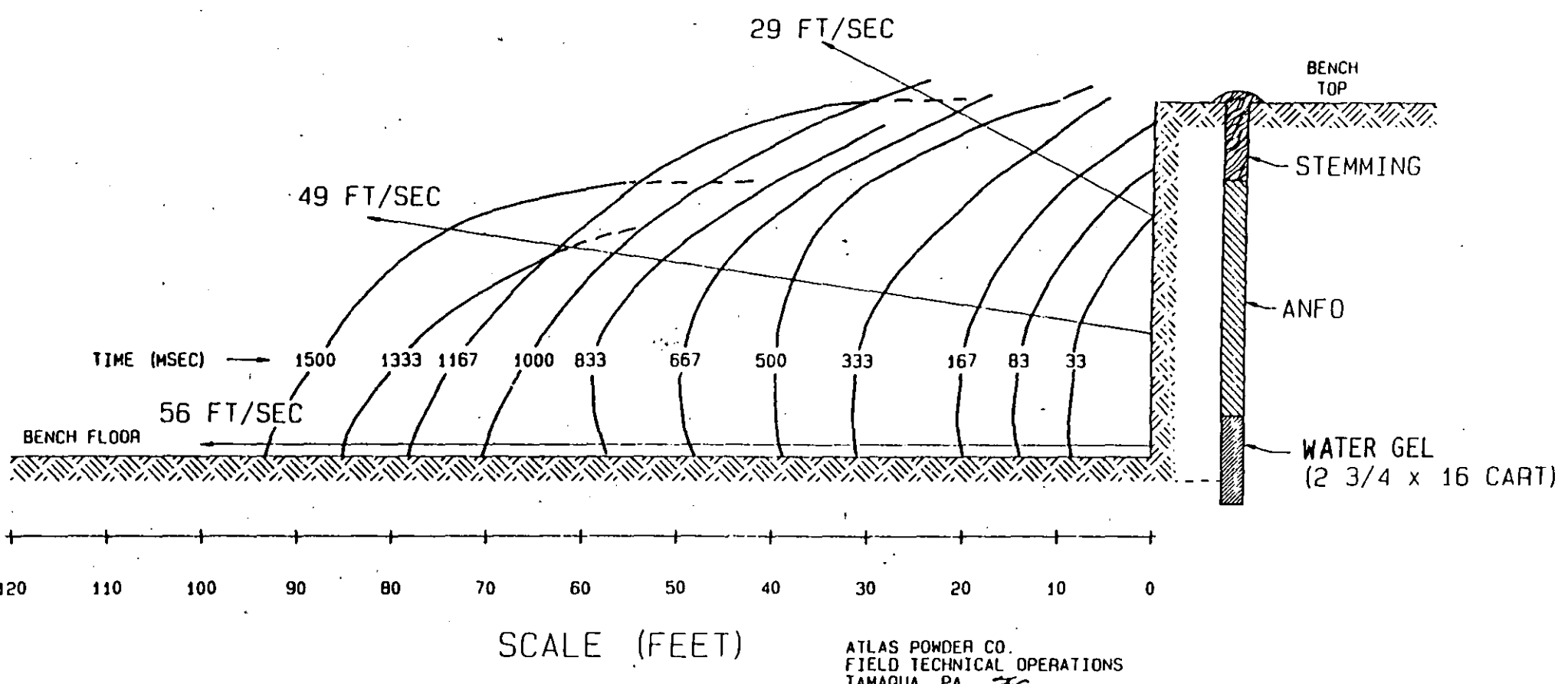


FIGURE 13

WATER GEL - ANFO



ATLAS POWDER CO.
FIELD TECHNICAL OPERATIONS
TAMAQUA, PA. *ETC.*

FIGURE 14

Average burden velocities were calculated using linear regression analysis. Results are summarized in Table 3. Figure 15 illustrates the Table 3 values in graphical form. It is evident that the greatest average burden velocity is achieved with PMX 460 as a bottom load and PMX 460 as alternate velocity boosting of ANFO in the upper load. PMX 460 as a bottom load and straight ANFO as a top load resulted in the second highest burden velocities, followed by the watergel and ANFO, and PMX 440 and ANFO. An error analysis between the last two, (Watergel and ANFO, and PMX 440 and ANFO), revealed that, statistically, the results are equivalent or in other words, there is no significant difference owing to an experimental error of ± 5 ft/sec.

A more detailed analysis has also been performed to compute the instantaneous velocity at any point in the time domain for movement at the toe and 12 feet above the toe. Displacement and time data were fitted to a polynomial equation of degree five with a goodness of fit of no less than 99%. The first derivative of this equation forms a velocity equation, which when plotted, yields the graphs illustrated in Figures 16 and 17 for the instantaneous velocity at the toe and 12 feet above the toe, respectively. Not enough data was available to perform an analysis to the same degree of fit and accuracy for face movement 24 feet above the toe.

TABLE 3

AVERAGE BURDEN VELOCITIES

SHOT NO.	BOTTOM EXPLOSIVE LOAD	TOP EXPLOSIVE LOAD	FACE LOCATION AND VELOCITY (FT/SEC)		
			TOE	12' ABOVE TOE	24' ABOVE TOE
1	POWERMAX 440	ANFO	48	46	28
2	POWERMAX 460	ANFO	72	67	48
3 *	POWERMAX 460	POWERMAX 460 EVERY 6' IN ANFO COLUMN	83	90	60
4	WATERGEL	ANFO	56	49	29

* POWERMAX 460 was used as the Alternate Velocity Explosive

FACE MOVEMENT

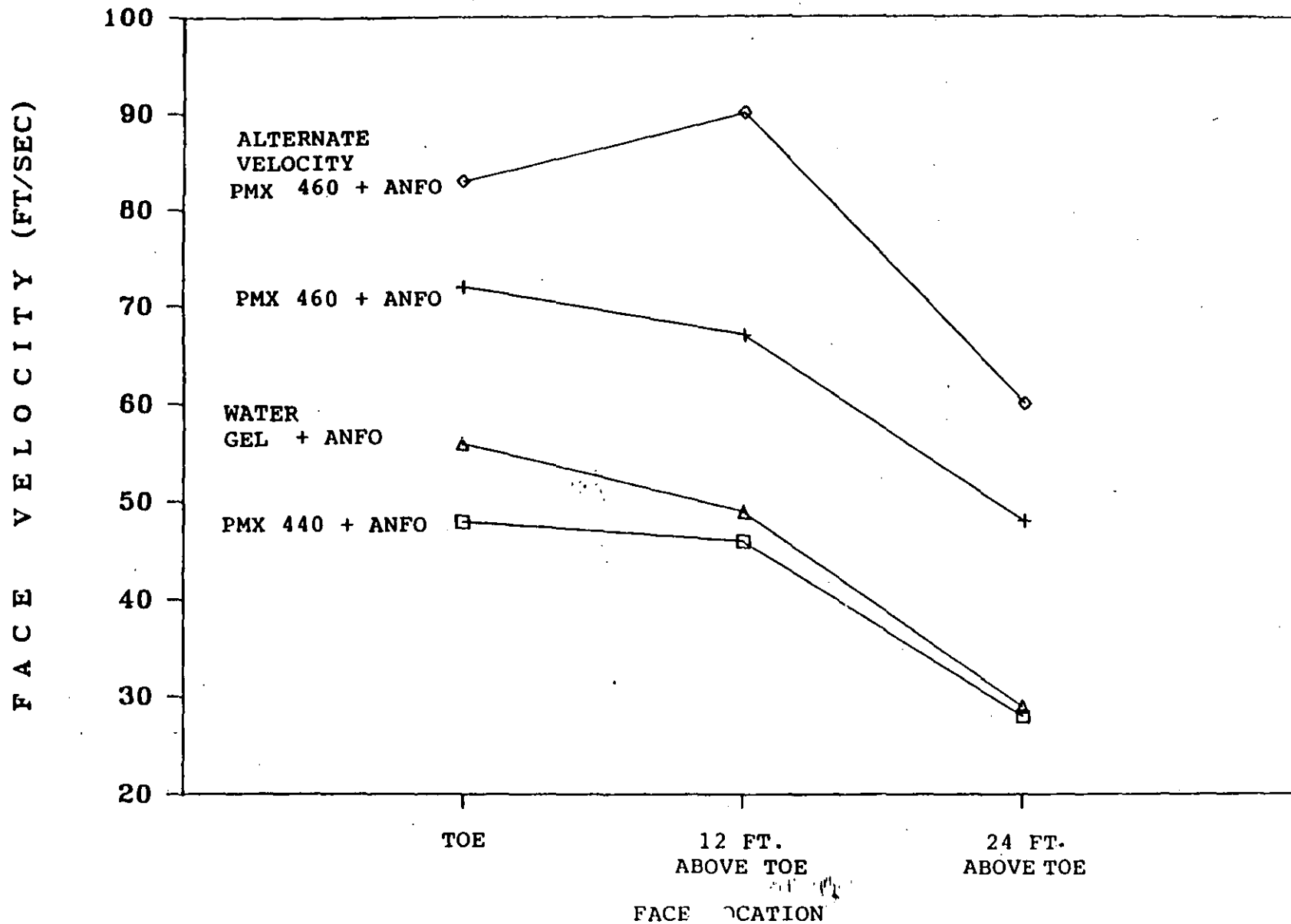


FIGURE 15

FC.

T O E V E L O C I T Y

GRANITE - ATLAS POWDER CO.

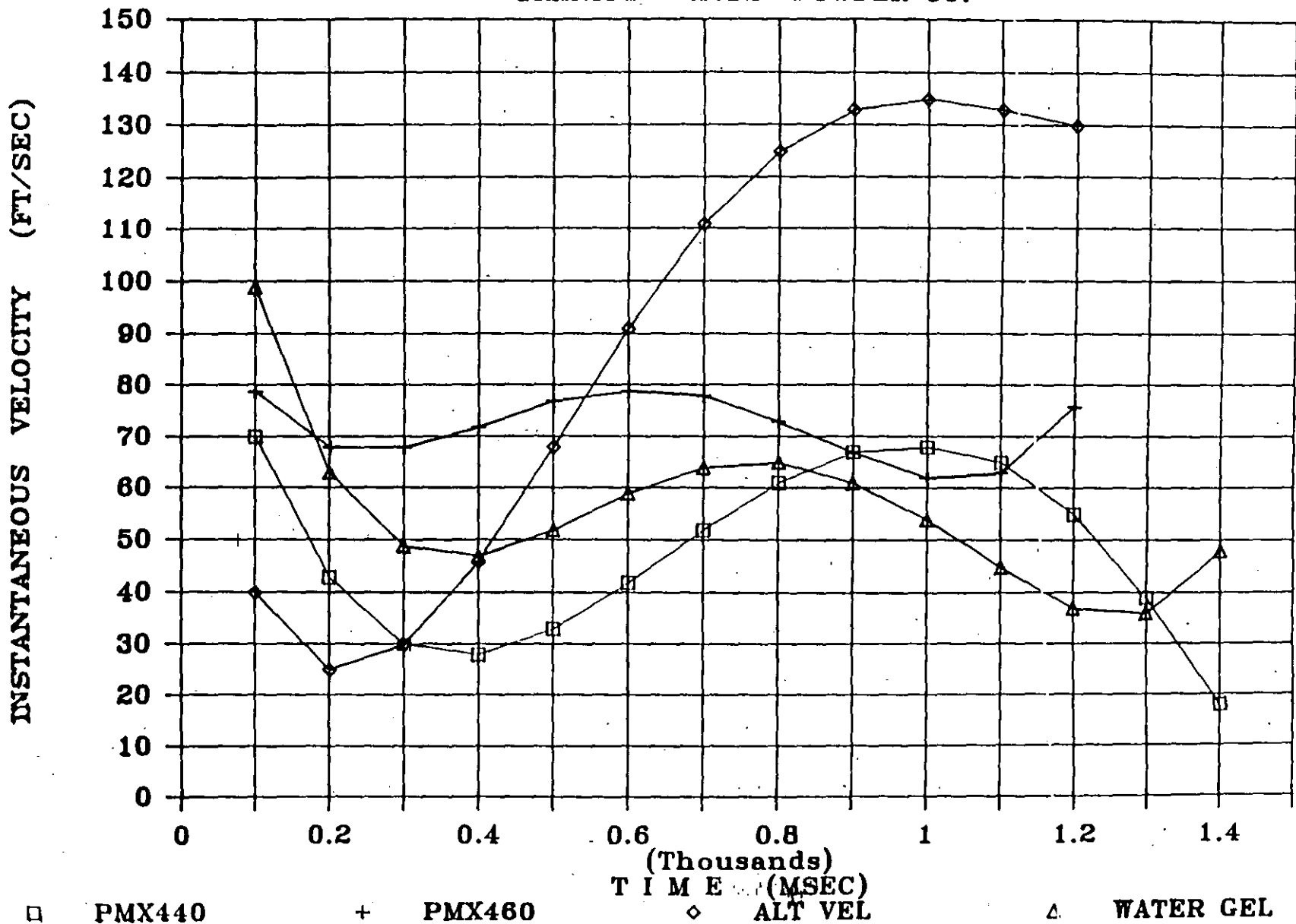


FIGURE 16 INSTANTANEOUS VELOCITY vs TIME FOR TOE MOVEMENT

VELOCITY 12 FT. ABOVE TOE

GRANITE - ATLAS POWDER CO.

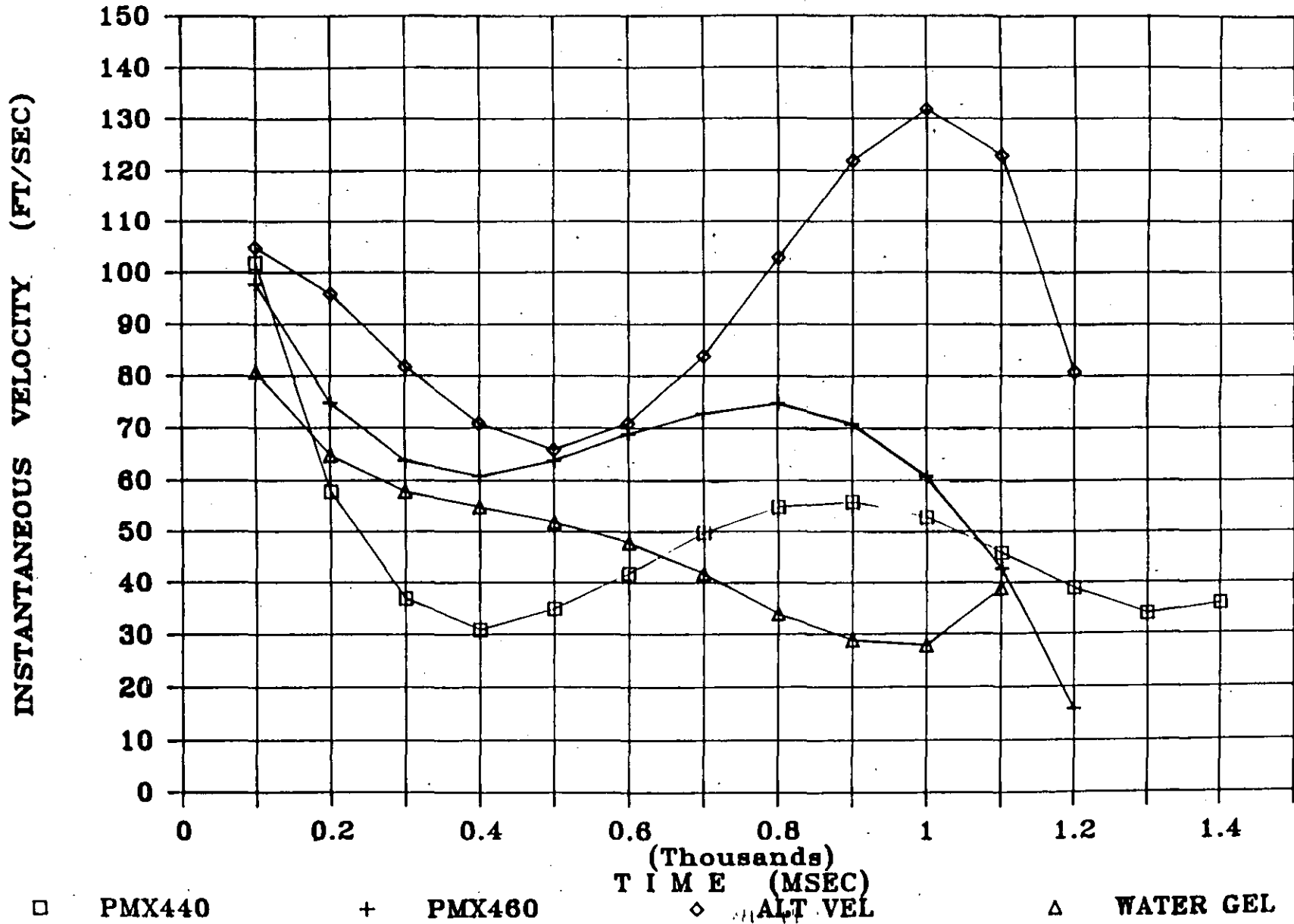


FIGURE 17 INSTANTANEOUS VELOCITY vs TIME FOR BURDEN MOVEMENT
12 FEET ABOVE TOE.

In Figure 16, the PMX 460 bottom load with alternate velocity boosting of ANFO in the upper load generated the most dramatic velocity increase between 200 to 1000 msec into the shot. Beyond 550 msec, velocity for this load configuration exceeded all others. Movement at the toe in this case was attributed to the bottom load and to the bottom third of the upper column. Thus, toe velocity in this case was affected by both bottom and top loads.

If the bottom load is one of much higher energy, it will generate a larger crushed zone and improve fragmentation in that vicinity. It also creates a larger cavity for explosive gases to immediately migrate into and fill the new formed cavity. Gas temperature and pressure drop quickly and it may be for this reason that the initial toe velocity is somewhat less until the alternate velocity boosting temporarily reverses the process by releasing more of the available energy in ANFO as higher temperature, higher pressure gases. This dramatic late increase in gas pressure is evidenced in Figure 16 for the PMX 460 alternate velocity boosting from 200 msec on and is sustained until well over 1000 msec. The key to moving burden material at higher velocities is to sustain these high pressures with appropriate energy and by the timed systematic and controlled release of such energy with precise MS delays.

Instantaneous velocities 12 feet above the toe (Figure 17) are attributed primarily to the upper column load. In this case, the PMX 460 with PMX 460 as alternate velocity boosting in the ANFO column achieved the greatest burden velocity for all times.

It is not definitely clear as to the exact mechanisms and/or processes which actually contribute to increased burden velocities without direct and continuous measurements of temperature and pressure within the borehole. However, based on direct measurement of burden velocities and the fact that it is gas pressure expansion in the borehole and in the surrounding rock mass that is responsible for mass displacement, certain logic can be suggested as follows:

- 1) Since ANFO at best is only 60 - 70% efficient, complete reaction of the ANFO is not occurring as predicted in the detonation head. The addition of alternate velocity boosting may contribute to a more complete reaction of ANFO just behind the detonation head in the partially reacted and expanding gas phase of ANFO.
- 2) The emulsion cartridges used as Alternate Velocity boosting may generate higher temperatures and pressures in their vicinity and thus raise the overall temperature and pressure of the combined emulsion cartridge and ANFO detonation in the new formed cavity. This would tend to pressurize the cavity at higher pressures and possibly for a longer period before the burden responds to mass movement.
- 3) More of the available energy in ANFO is utilized with the technique in production holes less than 17 inches in diameter.

SUMMARY AND RECOMMENDATIONS FOR FIELD USE

Alternate Velocity Boostering of ANFO with emulsion explosives has resulted in the following benefits:

- 1) The technique is simple to employ without major modifications to the overall blast design.
- 2) Improves overall fragmentation, especially in the vicinity of the emulsion cartridge or slug.
- 3) Definitely increases burden velocities and mass movement.
- 4) Increased burden velocities will result in increased cast distances, lower and looser muckpiles and minimal back break and spills.
- 5) A loose muckpile will reduce maintenance costs on excavation equipment through less wear and tear on buckets and tires.
- 6) The technique can be used in any application regardless of material properties or structure where the above mentioned benefits are desirable.
- 7) The Alternate Velocity Emulsion explosive does not require additional priming. ANFO is more than sufficient.
- 8) When ANFO is used in dewatered holes, the alternate velocity emulsion can enhance and increase the detonability of ANFO.
- 9) It appears that the greater the difference in density and detonation velocity of the alternate velocity explosive to ANFO, the more pronounced are the results.
- 10) In essence, the technique allows more of the available energy in ANFO to be converted to useful work. It is cost effective, and a productivity increase should be realized over the short and long terms.

ALTERNATE VELOCITY LOADING RECOMMENDATIONS

HOLE DIAMETER (in)	SPACING FOR CARTRIDGES OR SLUGS OF EMULSION IN ANFO COLUMN (ft)	LENGTH OR AMOUNT OF EXPLOSIVE
2-1/2 to 3-1/2	4 - 6	16 in.
4 to 6-3/4	6 - 8	15 - 30 lb.
7 to 10	8 - 10	30 - 50 lb.
10+	10 - 15	100 lb.

ACKNOWLEDGEMENTS

We wish to express our sincere gratitude to the following organizations and individuals for their assistance, cooperation, and enthusiasm throughout this continuing research effort.

SANDIA NATIONAL LABORATORIES - One of the most professional and dedicated organizations that we have worked with. Reliability in field data acquisition was better than 99% by the field group. A special thanks to P.J. Hommert, R.L. Parrish, D.L. Shirey, R.J. Stanopiewicz, J.E. Uhl, J.S. Kuszmaul, and E.D. Bergeron.

UNITED STATES BUREAU OF MINES - M. Staggs, J. Knopp, and M. Nutting.

MACKLIN BROTHERS STONE COMPANY - R. Macklin

ATLAS POWDER COMPANY - D.G. Borg, C. Postupack, P. Nahan, M.E. Mammele, H.M. Carter, R.E. Barr, C. VanOmmeren, W. Frantz, C. Keefer, W. Schrepple, A.H. Beinlich, V. Bryant, S.L. Burchell, R. Wampler, and C. Stephenson, R.C. Morhard, J. Uzick.

We are also indebted to Ms. Jane Jevit and Joanne Perilli for their assistance in the preparation of this paper.

REFERENCES

- 1) DAVIS, W.C., HIGH EXPLOSIVES, Los Alamos Science, 1983, pp. 48 - 52.
- 2) JOHNSON, J.N., MADER, C.L., and GOLDSTEIN, S., PERFORMANCE PROPERTIES OF COMMERCIAL EXPLOSIVES, Los Alamos National Laboratory, Propellants, Explosives and Pyrotechnics, Vol. 8, pp. 8, 1983; and personal discussion with C.L. MADER, 1985.
- 3) FINGER, M., HELM, F., LEE, E., BOAT, R., CHEUNG, H., WALTON, J., HAYES, B., and PENN, L., CHARACTERIZATION OF COMMERCIAL COMPOSITE EXPLOSIVES, Sixth International Symposium on Detonation, 1976.
- 4) HELM, F., FINGER, M., HAYES, B., LEE, E., CHEUNG, H., WALTON, J., LAWRENCE LIVERMORE LABORATORY REPORT, UCRL - 52042, 1976.
- 5) JOHNSON, Major M.S., EXPLOSIVE EXCAVATION TECHNOLOGY, U.S. Army Engineer Nuclear Cratering Group, Livermore, California, June, 1971, NCG TR No.21, TID-4500
- 6) CHIAPPETTA, F., BLASTING THEORIES, Explosives Technical Handbook, Chapter 11, Atlas Powder Company, Dallas, Texas, 1985, pp. 11-1 to 11-51.
- 7) CHIAPPETTA, F., BAUER, A., DAILEY, P.J., BURCHELL, S.L., THE USE OF HIGH-SPEED MOTION PICTURE PHOTOGRAPHY IN BLAST EVALUATION AND DESIGN, Proceedings, 9th Annual Conference on Explosives and Blasting Techniques, Society of Explosives Engineers, Dallas, Texas, 1983.
- 8) PARRISH, R.L., KUSMAUL, J.S., DEVELOPMENT OF A PREDICTIVE CAPABILITY FOR OIL SHALE RUBBLIZATION: RESULT OF RECENT CRATERING EXPERIMENTS, In Situ Division, Sandia National Laboratories, 17th Oil Shale Symposium, Colorado School of Mines, April, 1984.
- 9) PERSSON, P.A., Swedish Detonic Research Foundation, Unpublished preprint, American Institute of Mechanical Engineering, Preprint No. 75-AO-74, 1975.



**FACULTAD DE INGENIERIA U.N.A.M.
DIVISION DE EDUCACION CONTINUA**

CURSOS ABIERTOS

**IV. CURSO INTERNACIONAL DE INGENIERIA GEOLOGICA APLICADA A
OBRAS SUPERFICIALES Y SUBTERRANEAS**

CUARTO MODULO:

TECNOLOGIA SOBRE EL USO DE EXPLOSIVOS

Del 22 al 26 de junio de 1992

A N E X O

ING. RAUL CUELLAR BORJA

JUNIO - 1992

TIPO DE ROCA

CONSTANTE DE ROCA

DIAMANTE	0.86
CUARZO	0.62
BASALTO	0.62
HORSTENO	0.59
PELDESPATO	0.57
GNEISS	0.54
ESQUISTOS	0.53
MAGNETITA	0.50
GRANITO	0.48
ARENISCA	0.46
DOLOMITA	0.44
• ROCA CALIZA	0.40
PIZAPRA	0.38
LETTA	0.38
CALCITA	0.36
ANTRACITA	0.36
MARMOL	0.36
CARBON BITUMINOSO	0.36
MICA	0.28
YESO	0.24

CONSTANTE DE VOLADURA: (EXPLOSIBILIDAD)

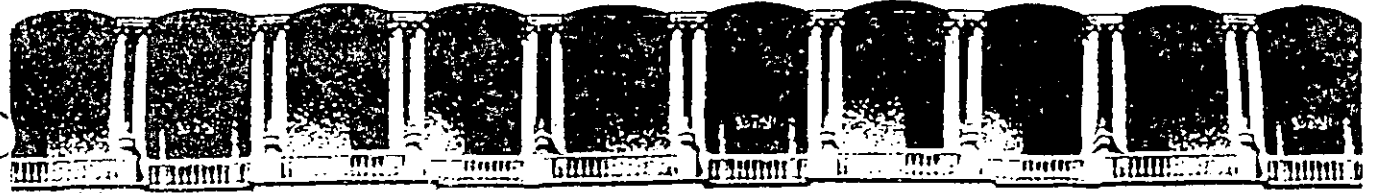
ESTA CONSTANTE TOMA EN CUENTA LA CALIDAD DEL MACIZO ROCOSO.

+ ROCA MUY SOLIDA Y PISURADA	0.60	kg/m ³
+ ROCA MUY SOLIDA	0.55	
+ ROCA NORMAL CON GRIETAS	0.50	
+ ROCA RELATIVAMENTE HOMOGENEA	0.45	
+ ROCA HOMOGENEA	0.40	



INDICE DE DUREZA DE ALGUNOS TIPOS DE ROCA

TIPO DE ROCA	INDICE DE DUREZA
DIAMANTE	10.0
CUARZO	7.0
BASALTO	7.0
HORSTENO	6.5
FELDESPATO	6.2
GNEISES	5.2
ESQUISTOS	5.0
MAGNETITA	4.2
GRANITO <i>LAGUNA VERDE</i>	4.0 <i>6.5</i>
ARENISCAS <i>CARACOL</i>	3.8
DOLOMITAS	3.7
CONGLOMERADO POCO CEMENT.	3.5
CALIZA <i>LA ANGOSTURA</i>	3.3
PIZARRA	3.1
LUTITAS	3.1
CALCITA	3.0
ANTRACITA	3.0
MARMOL	3.0
CARBON BITUMINOSO	2.5
MICA	2.3
YESO	2.0
TALCO	1.0



**FACULTAD DE INGENIERIA U.N.A.M.
DIVISION DE EDUCACION CONTINUA**

CURSOS ABIERTOS

*I CURSO INTERNACIONAL DE INGENIERIA GEOTECNIA APLICADA
A OBRAS*

MODULO IV

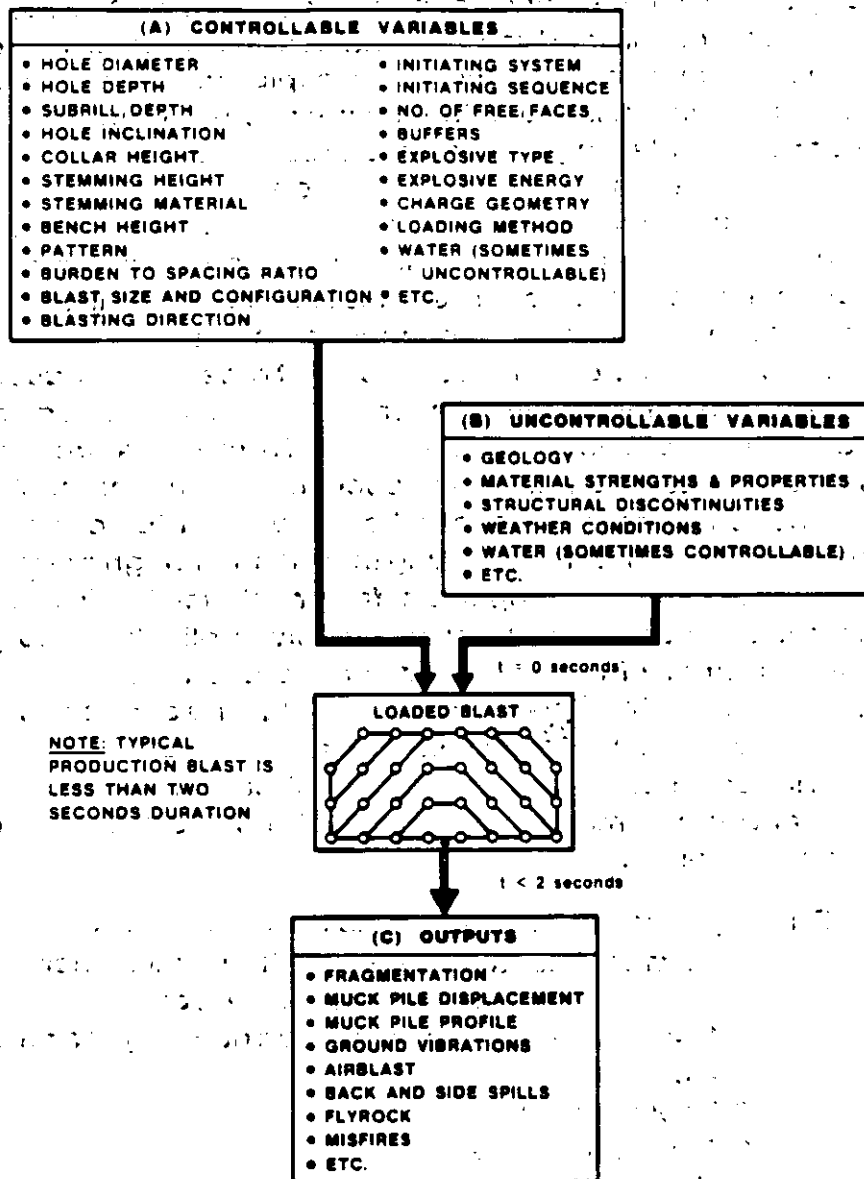
TECNOLOGIA SOBRE EL USO DE EXPLOSIVOS

CHAPTER 11 BLASTING THEORY

R. FRANK CHIAPPETTA

*JUNIO
1992*

variables that are inherent in any blast design to have any practical meaning. Given the diverse nature of field conditions encountered and the overwhelming number of blast design variables to select from, blast results may not always be easily predicted as is outlined in Figure 11-1. Where one theory is successful in one specific environment or application, it may not be as predictive in another.



FIELD MODEL ILLUSTRATING BLAST DESIGN INPUTS AND OUTPUTS

FIGURE 11.1

Often more than one theory is needed to clarify or explain certain results. Parallel this approach to the physicist trying to explain light with only one theory, that is, the wave theory. With the passage of time it became apparent that everything associated with light could not always be adequately explained with this theory alone and hence, another theory, the particle or "packets of energy" theory was developed to explain the phenomena of light in which the first theory failed. With both theories, the physicist could now explain many of the mysteries surrounding light which eventually led to new developments such as the laser. Similarly, in trying to define the mechanisms of rock breakage by explosives, more than one theory or explanation is often needed. In any case, a blasting theory should not only attempt to explain and predict the breaking process, but more importantly, it should suggest and allow new methods and techniques to improve on current blasting practices.

2. TIME EVENTS FOR THE BREAKING PROCESS

There are basically four time frames designated as T1 to T4 in which breakage and displacement of material occur during and after complete detonation of a confined charge.

The time frames are defined as follows:

- T1 — Detonation
- T2 — Shock or Stress Wave Propagation
- T3 — Gas Pressure Expansion
- T4 — Mass Movement

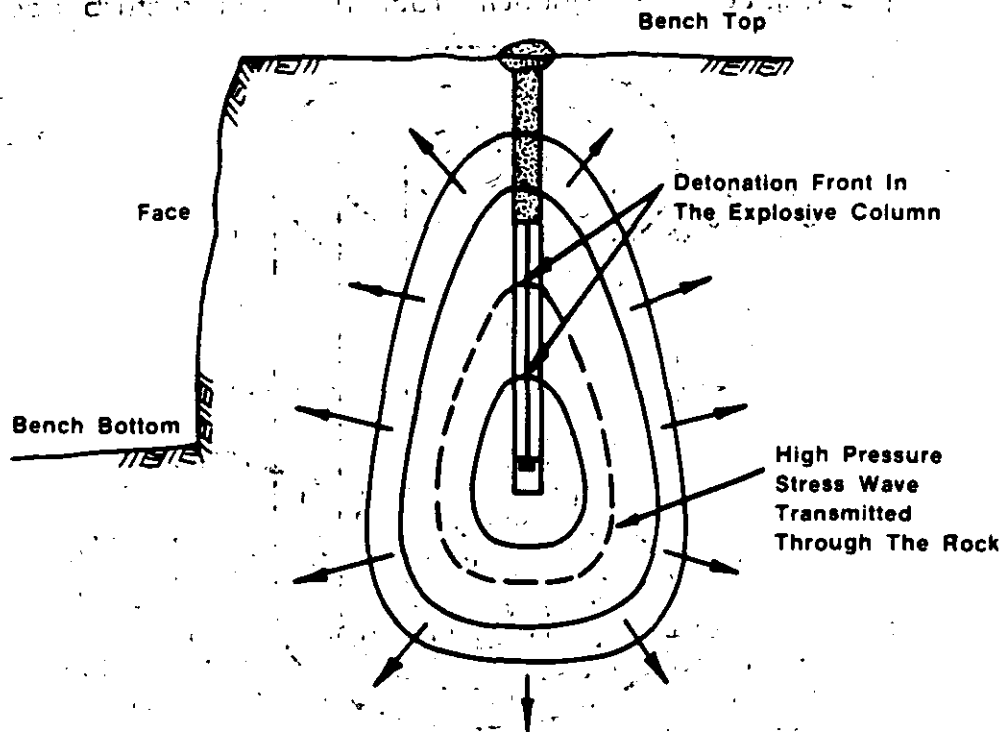
Each time frame is first discussed separately, and then discussed in conjunction with blasting theories for an overall, more detailed explanation and meshing of events. Although these are treated as discrete events, it should be emphasized that in a typical shot hole or production blast, one event phase can occur simultaneously with another at specific time intervals.

a. T1 — DETONATION

Detonation is the beginning phase of the fragmentation process. The ingredients of an explosive consisting of a fuel and oxidizer combination; upon detonation, are immediately converted to high pressure, high temperature gases. Pressures just behind the detonation front are in the order of 9 Kbars to 275 Kbars, while temperatures range from approximately 3000° to 7000°F.⁽²⁾



pressure wave(s) emitted into the rock mass results, in part, from the rapidly expanding high-pressure gas impacting the borehole wall. The geometry of dispersion depends primarily on the shape of the charge. If the charge is shot, with a length to diameter ratio of less than or equal to 6:1, then the disturbance is propagated in the form of an expanding sphere. If the charge is long, with a length to diameter ratio of greater than 6:1, then the disturbance is propagated in the form of an expanding cylinder. (Figure 11-4). However, in a typical, bottom primed, cylindrical shot hole normally encountered in bench blasting, the strain waves originally formed near the point of initiation are already in progress and propagating into the surrounding medium, while the detonation is still progressing within the explosive column. Thus, close to the shot hole, strain wave propagation is neither perfectly spherical nor cylindrical but more like that shown in Figure 11-5.



**SECTION THROUGH THE FACE DURING
 DETONATION SHOWING EXPANDING
 STRESS WAVE FRONT**

FIGURE 11.5

The pressure next to the borehole wall will rise instantaneously to its peak and then rapidly decay exponentially. The quick decay is due to cavity expansion of the borehole and increased gas cooling. Cavity expansion around the borehole can occur through crushing, pulverization, and/or displacement of material and can range anywhere from about one to three hole diameters depending on the medium and explosive used. Generally, extensive compressive, shear and tensile failure occur as a region of pulverized material since the wave energy is at its maximum near the borehole wall.

As the strain wave front proceeds outward, it has a tendency to compress the material at the wave front through a volume change. At right angles to this compressive front, there exists another component referred to as the tangential or "hoop" stress. The tangential stress, if large enough, can cause tensile failures at right angles to the direction of propagation. The largest tensile failures are expected to occur close to the borehole where the tangential stress is high enough for failure to occur. Both the compressive and tensile components of the wave front decay with distance from the borehole.

When the compressive wave front encounters a discontinuity or interface, some of the energy is transferred across the discontinuity and some reflected back to its point of origin.⁽⁴⁾ For the most part, the partitioning of energy depends on the ratio of the acoustic impedance of the materials on either side of the interface, as illustrated in Figure 11.6. Acoustic impedance, Z , for any material is defined as:

$$Z = \rho \times V_p$$

where: Z = acoustic impedance
 ρ = density of material
 V_p = sonic velocity of material

In reference to Figure 11-6, where the ratio of the acoustic impedance of material 1 to material 2 is less than one, some of the wave energy is transferred into material 2 and some reflected back, but both waves remain compressional. When the acoustic impedance ratio is 1, all of the energy is transferred into material 2 and no reflected wave occurs. When the impedance ratio is greater than 1, then some of the energy gets transferred into material 2 as a compressive wave and the remaining energy gets reflected at the interface as a tensile wave. When a compressive wave travelling through rock encounters an interface such as a free face, nearly all of the energy will be reflected back as a tensile wave. If the burden distance between the free face and explosive column is relatively small in



through compressional and tensile stress waves, gas pressurization or a combination of both. However, some degree of fragmentation, although slight, occurs through in-flight collisions and also when the material impacts the ground. Generally, the higher the bench height, the greater is this type of breakage owing to increased impact velocities of individual fragments when falling onto the bench floor. Similarly, material ejected from opposite rows of a "V-shot" design upon head-on collisions can result in increased fragmentation. This phenomenon was evidenced and documented with the use of high-speed photography of bench blasts.

Mass burden movement of fragmented material is shown in Figure 11-7 for a number of typical face conditions encountered in bench blasting operations. Face profiles and velocities are based on the results of high-speed photographic analysis performed at the ATLAS POWDER COMPANY. Where no subdrilling is utilized, (a and b), two types of face movement may be encountered. In 11-7a the entire length of face burden, directly in front of the explosive column, moves out similar to a plane wave and the face velocity at any point is constant. This behavior is usually encountered where material is very competent, quite brittle, and structured with well defined, largely spaced joints, much greater than the spacings or burdens employed in blast designs. When the material is soft, highly fissured, and/or closely jointed as might be found in coal and some sedimentary deposits, face profiles resembling that of flexural rupture is more likely. In this case, the greatest displacement and velocity occur adjacent to the center of the explosive column with the least amount of movement occurring at the toe and crest. When identical conditions in 11-7b are assumed and when subdrilling is employed, face movement results in much the same way except that the toe burden is displaced upwards faster and at a greater angle to the horizontal.

The first three cases assumed a relatively straight face between the crest and toe, however, in many bench blasting operations, the condition is more like that illustrated in Figure 11-7d, where toe burden is considerably greater than the crest burden. The toe burden is too great for the explosive selected, hence, very little movement occurs at the toe while the greatest displacement results in the upper half of the bench.

Three options are available to increase toe movement:

- Employ angle drilling in an attempt to maintain constant burdens from the crest to the toe
- Use a higher energy bottom charge in the current vertical drill holes
- Decrease the burden with the current vertical drill holes

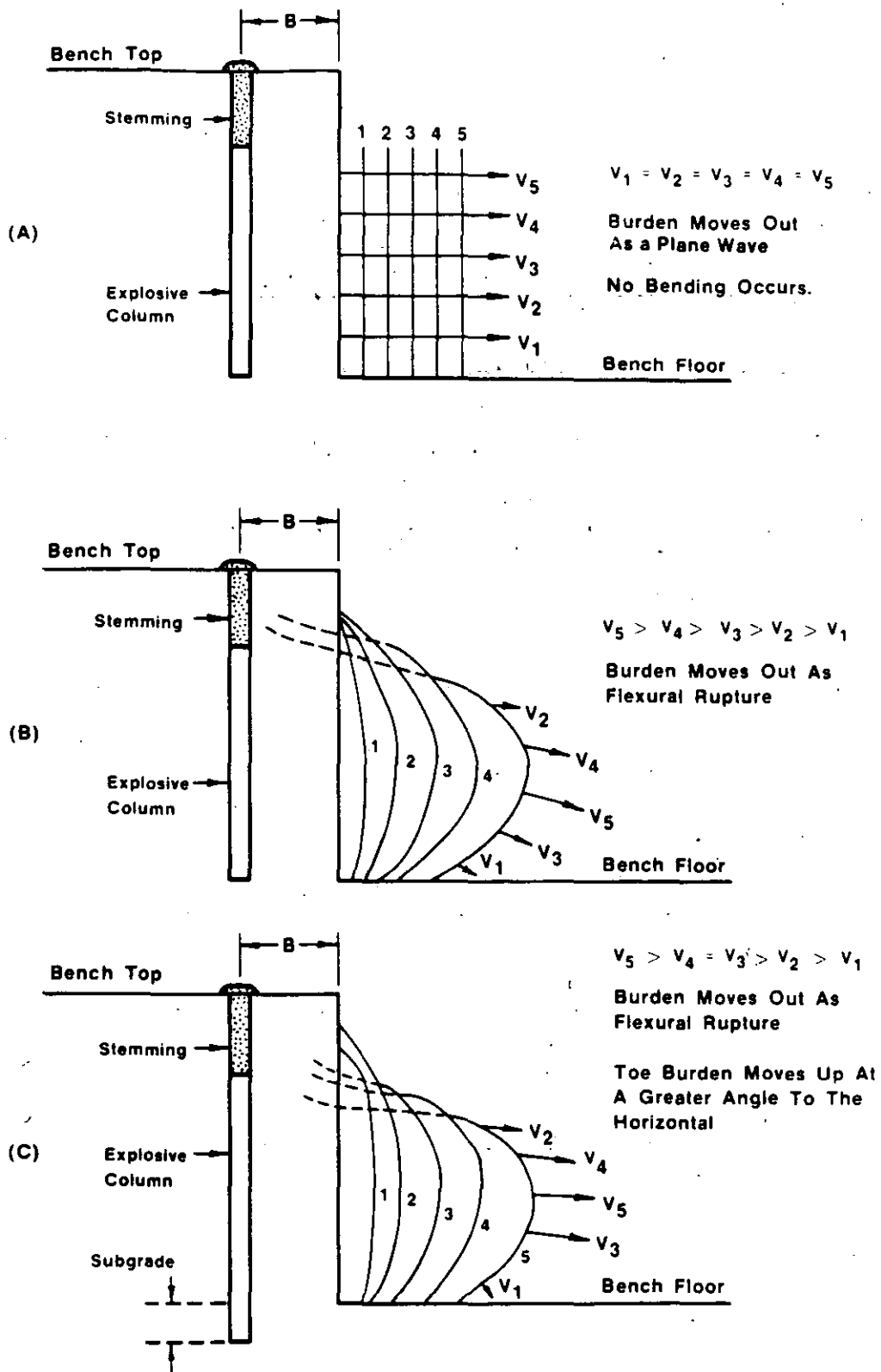


FIGURE 11.7

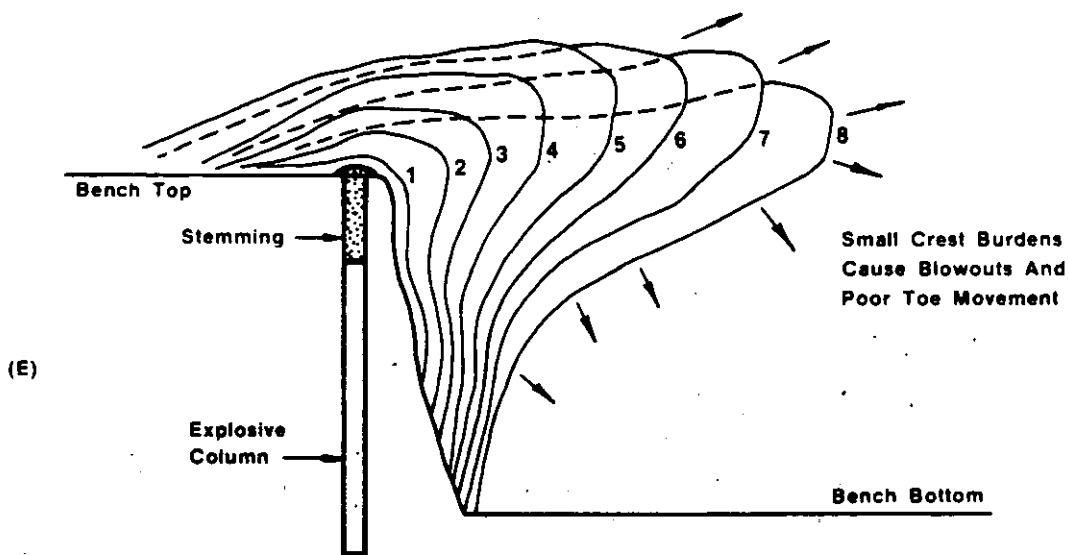
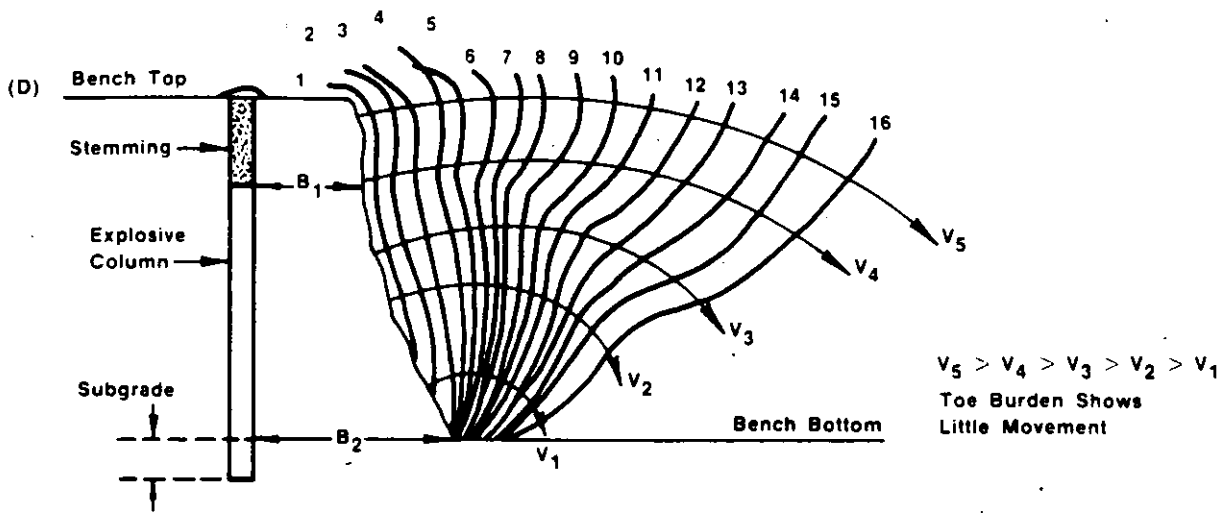


FIGURE 11.7 (Cont'd)

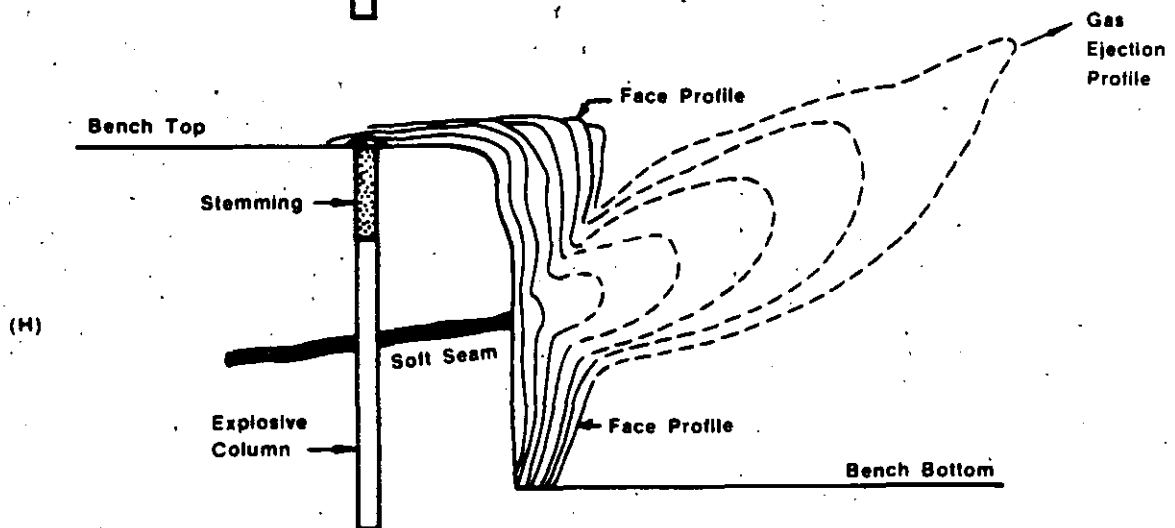
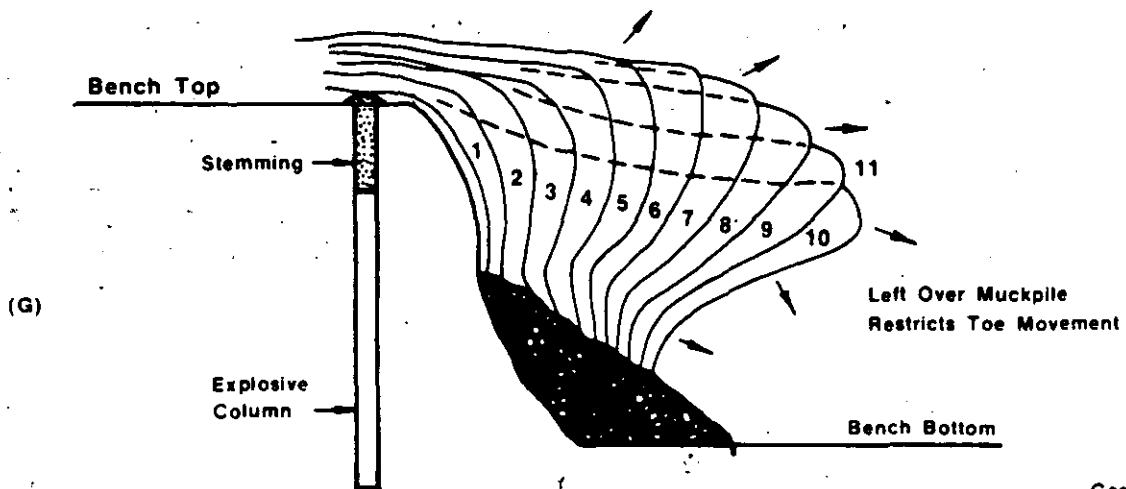
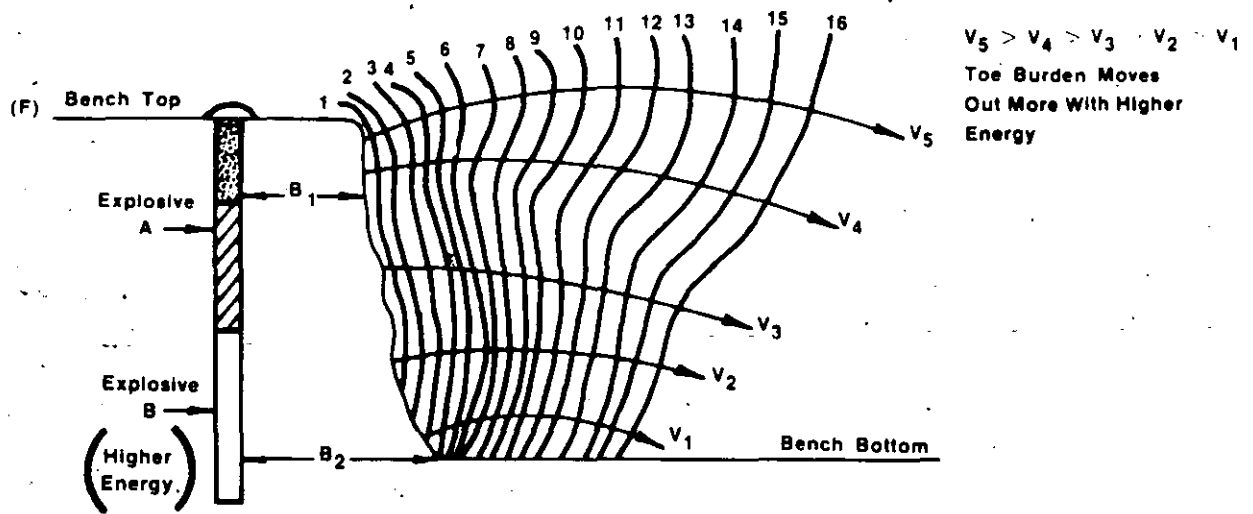


FIGURE 11.7 (Cont'd)

In selecting the latter, care should be exercised so as not to decrease the burden to the point of obtaining the condition shown in Figure 11-7e. The toe burden is now correct for the explosive selected, but the crest burden is substantially reduced. This may bring about many adverse conditions near the crest burden such as flyrock, blowouts, and increased airblast complaints. Because confinement pressures are released near the crest (in this case, a path of least resistance relative to the toe burden), restricted toe movement will result. It is better to use the same burden, but with a higher energy bottom charge near the toe. This load configuration as shown in Figure 11-7f tends to pressurize more of the burden mass for longer periods without adverse effects, and adequate toe movement generally results.

Where large leftover muckpiles are left against the face, Figure 11-7g, toe movement will be restricted and increased ground vibration levels are likely. Unless the situation requires a buffer, such as when blasting in the vicinity of mining equipment or to avoid dilution of an ore blast adjacent to a waste muckpile, it should be avoided.

Where seams are encountered in a blast, Figure 11-7h, tremendous gas ejections with velocities up to 600 ft/sec can occur. When such gas venting occurs, it will adversely affect other parts of the burden to displace adequately and inevitably leads to poor overall blasting results. A stemming deck immediately adjacent to the seam will give better results.

e. TIME EVENTS T1-T4 COMBINED

Up to this point, time events T1 to T4 have been discussed more or less as separate isolated events. However, in a real blasting environment, more than one event can occur at the same time.

Consider a single vertical hole in a quarry face with the primer located near the bottom of the hole as is illustrated in Figure 11-8. Assume the explosive used is 40 feet of ANFO with a velocity of detonation equal to 13,000 ft/sec, the material blasted is limestone with a sonic wave velocity of 15,000 ft/sec and a density of 2.3 g/cc. Upon initiation of the primer, it takes only a few microseconds and a distance of 2 to 6 hole diameters up the column to form a full detonation head. When a full detonation head is formed, it travels up the explosive column with a velocity characteristic of the steady-state velocity, (in this case 13,000 ft/sec). It takes approximately 3.0 ms for the 40 foot column of ANFO to be completely detonated.

Within this 3.0 ms, many other things have occurred. Starting at the bottom of the hole and progressing up the column, borehole



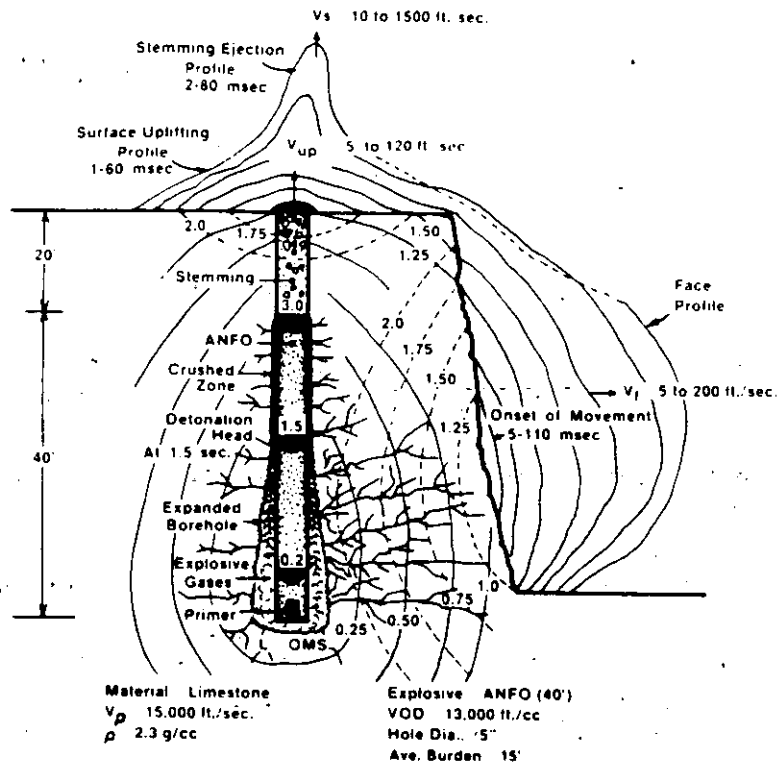


ILLUSTRATION SHOWING THE INTERACTION OF TIME EVENTS T1 TO T4 IN A TYPICAL QUARRY BENCH
FIGURE 11.8

expansion through crushing of the borehole walls has taken place. This produces compressive stress waves with tangential components emanating from the borehole walls and progressing outward in every direction with a velocity characteristic of the sonic wave velocity of limestone. It takes approximately 1.0 msec for the compressive strain wave to transverse 15 feet of burden to the free face. Behind the strain wave propagation some radial cracks start to develop in the crushed zone region of the borehole with a velocity ranging from 25 to 50% of the P-wave velocity for limestone. If the intensity of the compressive strain pulse is high enough, new cracks and/or extensions of pre-existing cracks and flaws can be initiated anywhere between the crushed zone next to the borehole and the free face. The greatest number of cracks are generally found closest to the borehole.

When the compressive wave strikes a free face, it is immediately converted to a tensile strain wave which starts at the free face and travels back through the rock mass towards the borehole. Owing to

the new fractures created from the outgoing compressive strain wave, the tensile strain wave will take somewhat longer to travel the same burden distance of 15 feet. If the burden is small enough and the intensity of the reflected strain wave is large enough, then some spalling at the free face or bench top is expected, although no significant mass movement will occur.

At 3 ms after detonation and complete reaction of ANFO, the original high temperature, high pressure gases have reached a new equilibrium due to borehole expansion. Both temperature and pressure have dropped significantly resulting in an energy reduction ranging from 25 to 60% of the theoretical energy originally available. This remaining energy acts on the surrounding "preconditioned" rock mass to displace it in the direction of least resistance. Further fragmentation can occur at this stage from gases entering and extending preexisting cracks or discontinuities. It is at this stage where some blasting theories are contradictory. Some believe that the major fracture network is completed within about 3 ms due to the interaction of stress waves on the surrounding material, while others believe that the major fracture network is just beginning.

Regardless of which time frame is responsible for the development of a fracture network, mass movement and displacement of material at the bench top or face occurs much later in time due to the confinement of gas pressure within the rock mass. The onset of mass movement depends on the material response in conjunction with the strain and gas pressure stimulus generated from the explosive. For typical stemming and burdens encountered in the field, bench top swelling occurs between 1 to 60 ms, stemming ejections between 2 to 80 ms and bench burdens between 5 to 110 ms. Surface uplifting velocities around the collar region of a hole occur between 5 and 120 ft/sec, stemming ejections between 10 to 1500 ft/sec and burden velocities between 5 to 200 ft/sec. Gas ejection velocities at discontinuities have been recorded as high as 700 ft/sec and often occur in less than 5 ms.

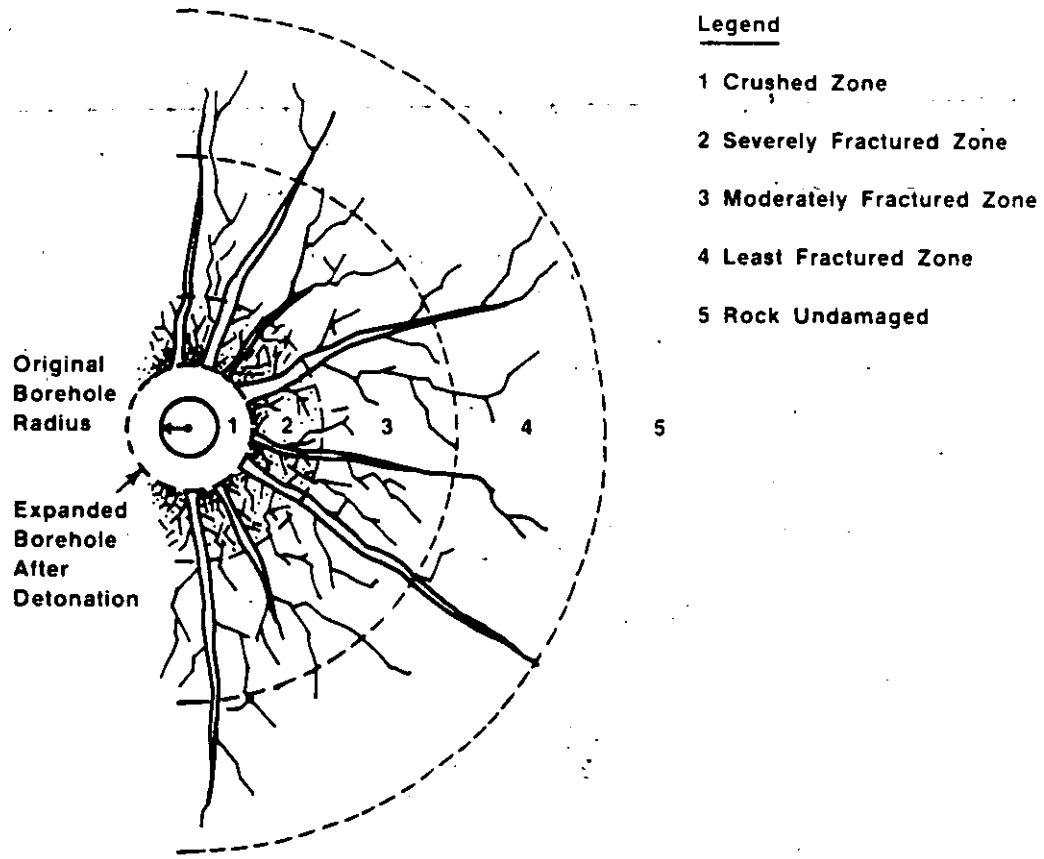
3. RUPTURE RADIUS

The degree of damage and fracturing around a borehole can be characterized by four zones as illustrated in Figure 11-9. In the crushed zone immediately around the borehole, the explosive induced pressures and stresses exceed the dynamic compressive strength of the rock by factors ranging from 40 to 400. These high pressures acting against the borehole wall will crush, pulverize and shatter the surrounding rock mass, causing



intense damage. This zone is also referred to as the hydrodynamic zone in which the elastic rigidity of the rock becomes insignificant. (6)

Next to the crushed zone is a region defined by a severely fractured zone referred to as the non-linear zone. Here fracturing can range from severe crushing through partial fracturing, to plastic deformation. Extension



ZONES OF RUPTURE RADIUS
FIGURE 11.9

of cracks can occur from previously formed cracks by the tangential component (hoop stress) of the shock wave, infiltration of gas pressure and at flaw sites.

In zones 3 and 4 (elastic zones) tensile failures and crack extensions occur in a less intense mode because the stress wave amplitude has attenuated significantly. Much of the original energy from the detonation has been consumed in the form of heat, friction, and fracturing in zones 1 and 2. The peak amplitude of the compressive stress is now much smaller than the compressive strength of the rock so no new fractures are likely in this wave type. However, the tangential stress component of the wave is still substan



tially larger than the tensile strength of the rock. Since the tensile strength of rock is about 1/15 to 1/10 of the compressive strength, the tangential stress of the wave is large enough to cause radial fractures. These new fractures are formed from the extension of cracks in the non-linear zone (zone 2) or from cracks initiated from microfractures and flaws inherent in a typical rock mass.

Once the tangential stress has attenuated below the critical tensile strength of the rock, no further breakage occurs beyond this point as illustrated in zone 5 (Figure 11-9). Once the wave or disturbance passes into and through this zone, the individual particles of the medium will oscillate and vibrate about their rest positions within the elastic limits of the rock and so no permanent damage results. It is this region where seismic waves are carried considerable distances and are responsible for ground vibrations.

Table 11-2 gives an idea of the degree of maximum damage found around the crushed and fractured zones in terms of charge radii for a number of conditions. Results are based on the works of many researchers conducted in a number of different materials with varying explosives. For a given explosive, the rupture radius is greater in soft rock than hard rock. Given the same rock, the rupture radius is greater for higher strength explosives than lower strength ones. Thus, the degree of radial rupture is influenced by the explosive, material properties and structure.

**TABLE 2
DEGREE OF DAMAGE AROUND A
BOREHOLE IN TERMS OF CHARGE RADII**

SOURCE	EXPLOSIVE	EXPLOSIVE AMOUNT	CHARGE SHAPE	MATERIAL OR ROCK TYPE	CRUSHED ZONE IN CHARGE RADII (MAX)	RADIUS OF DAMAGE IN CHARGE RADII (MAX)	COMMENTS
Olsen (7)	C4	0.25 kg	S	Granite	—	18	
		2.00 kg	S	Granite	—	20	
Siskind (8)	60% Dynamite	—	C	Shale	—	45-55	
	ANFO	—	C	Shale	—	15-22	
Cattermole (9)	60% Dynamite	—	C	Tuffaceous Pyroclastic	3.0	20-30	
Colorado (10)	—	—	—	Soft Rock	—	26-29	
School of Mines	—	—	—	Hard Rock	—	20-23	
Derlich (11)	Nuclear (TNT)	—	—	Granite	1.9	4.9	
Alchison (12)	—	3.6 kg (max)	C	Granite	3-4.5	—	
D'Andree (13)	C4	0.00 216 kg to 0.467 kg	S	Granite	2.3	—	
Siskind (14)	ANFO	—	C	Granite	—	14	
Kuttler et al (8)	Underwater Spark Discharge	—	S	Plexiglass & Rock	—	6	Theoretically Calculated
			C	Plexiglass & Rock	—	9	Theoretically Calculated
Yock et al (15)	—	—	—	Granite, Limestone & Concrete	8-12	30-50	
Rorq (16)	Nuclear	—	—	Competent	2.7-3.5	—	Horizontal Fracturing Below Shot Point
					2.0	—	

4. BLASTING THEORIES (Past & Present)

In this section, blasting theories of the past and present are discussed in concept form. Table 11-3 is a list of some of the more common thoughts regarding breakage mechanisms and the researchers responsible for their introduction. This list is by no means complete, but it does illustrate how certain thoughts on blasting theory started with the simple reflection theory after World War II and progressed to the more complex nuclei or stress-wave flaw theory of the present.

Since each theory has inherent strengths and weaknesses, the main concepts of each theory are best explained with a brief description. Blasting theories discussed are:

- a) Reflection Theory (Reflected Stress Waves)
- b) Gas Expansion Theory
- c) Flexural Rupture
- d) Stress Waves & Gas Expansion Theory
- e) Stress Waves, Gas Expansion & Stress-Wave/Flaw Theory
- f) Nuclei or Stress-Wave/Flaw Theory
- g) Torque Theory
- h) Cratering Theory
- i) Cratering Mechanisms

a. REFLECTION THEORY (Reflected Stress Waves) (17, 18, 19, 20)

One of the first attempts to explain, analytically, how rock breaks when a concentrated explosive charge is detonated in a borehole near a free surface was with the reflection theory. The concept was simple, straight forward, and based strictly on the well known fact that rock is always less resistant in tension than in compression. A compressive strain pulse is generated by the detonation of an explosive charge, moves through the rock in all directions with a decaying amplitude, and is reflected only at a free surface. At the free surface, the compressive strain pulse is converted into a tensile strain pulse that progresses back to its point of origin. (See Figure 11-10). Since rock is weakest in tension, it is easily pulled apart by the reflected tensile strain pulse and damage at the face appears in the form of spalling. The high pressure, expanding gases, are not deemed directly responsible for the major degree of fracturing that occurs.

A more detailed explanation follows: Detonation of an explosive charge in rock generates a large quantity of high temperature, high pressure gas in a very short time. Typically, this occurs in a few microseconds for small cylindrical charges and in a few milliseconds



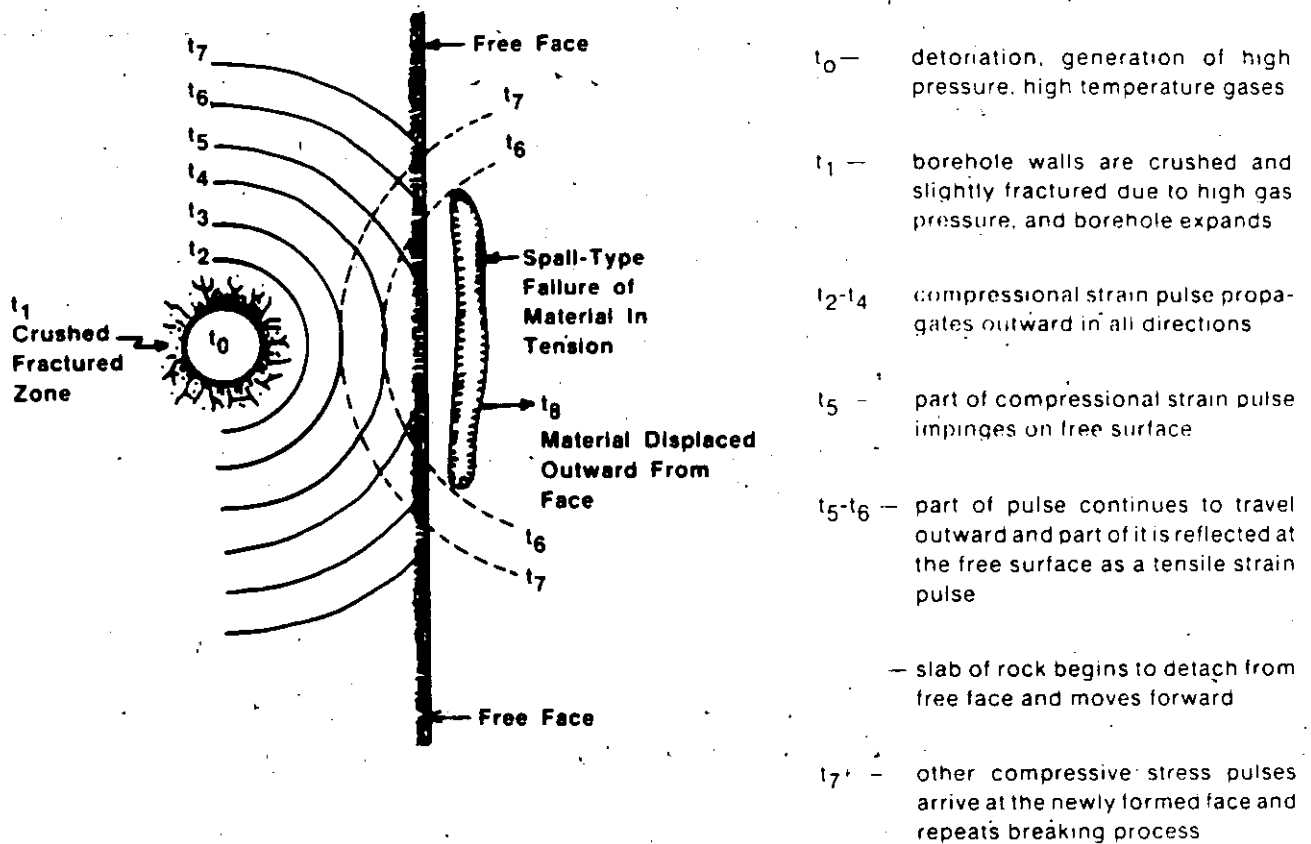
**TABLE 11.3
BLASTING THEORIES AND
THEIR BREAKAGE MECHANISM**

DATE	RESEARCHER(S)	BREAKAGE MECHANISMS				
		TENSILE REFLECTED WAVES	COMPRESSIONAL STRAIN WAVES	GAS PRESSURE	FLEXURAL RUPTURE	NUCLEI STRESS-FLAW
1949	Obert, Duvall (17) (18)	1				
1956	Hind (19)	1				
1957	Duvall, Atchison (20)	1				
1958	Rinehart (21)	1				
1963	Langfors, Kihlstrom (22)		2	1		
1966	Starfield (23)	1				
1970	Porter, Fairhurst (24)		2	1		
1970	Persson, Lunborg, Johansson (25)		1			
1971	Kutter, Fairhurst (6)		1	1		
1971	Field, Ladegarrd - Pederson (26)		1	1		
1972	Johansson, Persson (27)	2		1		
1972	Lang, Faureau (28)	4	2	1		3
1973	Ash (29)			1	1	
1974	Hagan (30) (31)		1			
1978	Barker, Fourney, Dally (32) (33) (34)					1
1983	Winzer, Anderson, Ritter (35)					1
1983	Adams, Margolin (36) (37)					1
1983	McHugh (38)					1

for long cylindrical charges found in normal bench blasting. This gas pressure acting against the borehole wall generates a compressive strain or stress pulse of high amplitude which will crush and/or fracture rock next to the borehole. This stress pulse travels radially outward in all directions from the shot point at speeds equal to or greater than the velocity of sound in the medium. Due to wave divergence and energy absorption by the rock, the pulse amplitude decreases very rapidly. Thus, the extent of the crushed zone immediately next to the borehole is relatively small.

When a longitudinal compressive stress strikes a free surface, two reflected pulses are generated, a tensile and shear pulse. The amount of energy imparted to each depends on the angle of incidence of the compressional stress pulse. Of the two reflected pulses, the tensile one predominates in breaking rock as it moves back into the rock.

The effective transfer of detonation pressure to stress in the rock depends on the impedance match of the explosive to rock. A smaller explosive to rock impedance ratio was shown to provide a more effective transfer of this pressure to stress. The concept of reflection breakage is illustrated in Figure 11-10. The time order of key events are:



**REFLECTION THEORY
TENSILE FRACTURE BY REFLECTION
OF A COMPRESSIVE STRAIN
PULSE AT A FREE SURFACE**

FIGURE 11.10

Slabs broken off closer to the hole are displaced with lower velocities.



b. GAS EXPANSION THEORY (25) (39)

The pressure acting on the walls of an explosive filled hole, upon detonation, will be approximately one-half of the detonation pressure due to expansion of the borehole. This pressure will propagate out from the borehole into the rock as a shock wave. The material between the borehole and the shock front is compressed and flows elastically or plastically, depending on the pressure and strength of the rock. Some radial cracks form next to the borehole wall starting at about two hole radii out and then propagate radially inwards as well as outward. The greatest frequency of radial cracks are next to the borehole, but a few extend farther out. When no free face exists, a small number of these radial cracks become very much larger than the others.

By the time the shock wave reaches the free surface, radial crack lengths formed are less than one quarter of this distance. At this stage the longest of cracks have extended inwards and reached the borehole wall. Gas pressure is now capable of entering these cracks and if the pressure is high enough can reach out towards the crack tips, thus further elongating the cracks. This has the effect of aiding cracks that interact with the returning tensile wave and cause them to reach the free surface. Up to this point, acceleration of the rock mass between the hole and free face has been negligible. Only after the cracks have reached the free surface is the rock accelerated by the remaining gas pressure.

The key point of the gas expansion theory are:

- Radial cracks are initiated not immediately next to the borehole but about two hole radii out and extend inwards toward the hole as well as outwards towards a free face.
- Rock displacement does not occur until pressurized radial cracks extend to the free surface.

c. FLEXURAL RUPTURE (A Gas Expansion Theory) (29)

During detonation of an explosive confined in a borehole, two distinct pressures are formed: one from the detonation itself and the other from the highly heated gases acting on the borehole walls. In



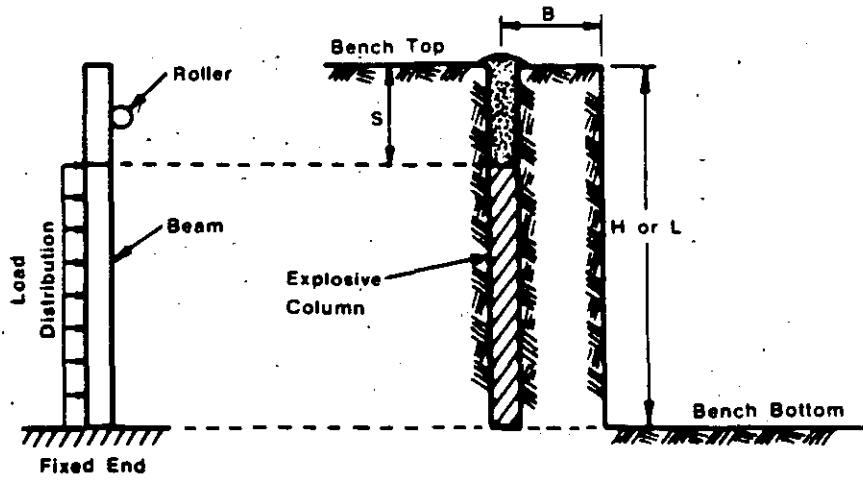
this theory, ninety percent of the total energy to break rock is in the latter. Detonation pressure acts only momentarily against any one part of the borehole's internal surface area, while gas pressure is sustained considerably longer until some form of cavity volume change occurs. Gas pressure, then, is the major component responsible for fragmentation and flexural rupture.

Radial cracks form only in planes parallel with the borehole axis. No cracks develop where the explosive is not in immediate contact, thus most cracks form adjacent to the borehole wall where tangential stresses are produced within the borehole's wall as the cavity is pressurized. Provided strain energies at crack tips are adequate, extension of fractures continue. Breakage by reflection of strain energy at a free face is considered negligible. Gas pressure drives the radially produced cracks through the burden to the free face and displaces rock through bending and in the direction of least resistance generally following naturally occurring planes of weakness. It is during this final stage where the major breakup of intact material takes place.

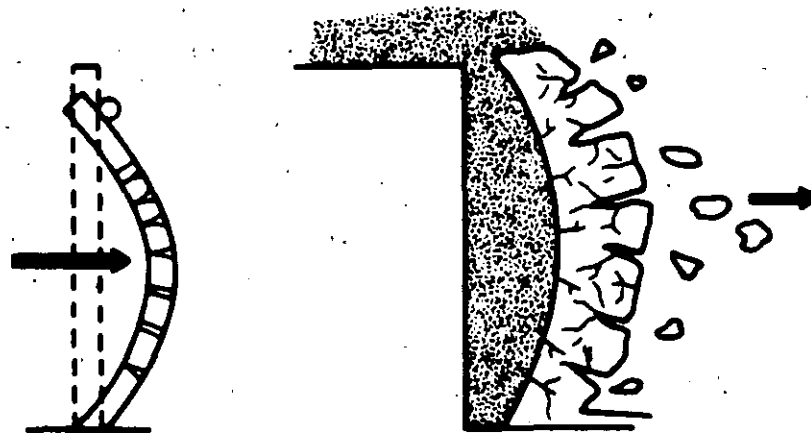
Breaking of rock by flexural rupture is analogous to bending and breaking a beam as illustrated in Figures 11-11 and 11-12. A rectangular beam is used to represent the field configuration of bench height, H , and burden, B , in the form of a modified cantilever beam model. The fixed end of the beam represents toe conditions while a roller, placed directly opposite the center of the stemming column, represents the stemming function. The roller allows the collar region to rotate and move longitudinally but does not allow deflection normal to the borehole axis. Although not shown for clarity of concept, the beam thickness in Figures 11-11, and 11-12 is actually equal to the burden. Borehole pressure is represented as a load distributed along the length of blasthole containing the explosive. Rock weight of the bench segment is considered negligible relative to the load resulting from the borehole gas pressure. Maximum contribution of total rock load acting at floor level is only at a ratio of about 1:100,000 or more compared to gas pressure.

The degree of fragmentation is controlled by the stiffness property of the burden-rock mass. This stiffness depends on existing restraints to movement, rock (Young's modulus), radially-cracked block's geometric shape as defined by its average thickness, width, and length. In terms of blast configuration, burden, spacing, and bench height are the controlling factors for any given rock.





BEAM BENDING MODEL BEFORE DETONATION
FIGURE 11.11



BEAM BENDING MODEL AFTER DETONATION
FIGURE 11.12

To achieve adequate flexural rupture, the burden to length (B/L) ratio becomes critical because stiffness varies with the third power of this ratio. For a given explosive diameter and reflective B value, decreasing the bench height L has the effect of,

- i) stiffening the burden rock
- ii) reduces fragmentation
- iii) inhibits the necessary lateral and upward displacements needed to break collar material and remove toes

Reducing burden for a given bench height has the opposite effect. Doubling the bench height for a given burden, or reducing the burden by one-half for a constant bench height has the effect of reducing the stiffness theoretically some eight times, although in practice a B/L ratio of 1/3 is often adequate.

d. STRESS WAVE AND GAS EXPANSION THEORY (6)

- In 1971, Kutter and Fairhurst combined the concepts of strain wave induced fracturing and gas pressure as the main mechanisms to fragment rock. Their experiments were performed with homogenous plexiglass and rock models.

After detonation, an intense pressure wave is emitted into the rock from the impact of the rapidly expanding high pressure gas. This pressure rises immediately to its peak and can be assumed to be one-half to one-quarter of the detonation pressure. Due to cavity expansion around the borehole and the cooling of the gases, the pressure decays exponentially. In spite of the decay, the pressure is sufficient to exert a quasi-static pressure on the rock boundary for a relatively long time.

The amount of energy in the shock wave is calculated to be only a fraction of the total energy released by the explosive. In granite this was measured to range between 10 to 18 percent while in salt it was only 2 to 4% of the total energy released. The remaining energy is contained in the gas pressure. However, the compressional wave energy is sufficiently high next to the borehole to cause extensive breakage.

A radially fractured zone is the first fracture pattern to develop around the new expanded cavity. Next to develop is a ring of wider spaced radial cracks.



This width of radially fractured zone depends on:

- the tensile strength of the rock
- wave velocity of the rock
- input pressure of the explosive
- detonation velocity of explosive
- extent of energy absorption in the rock mass

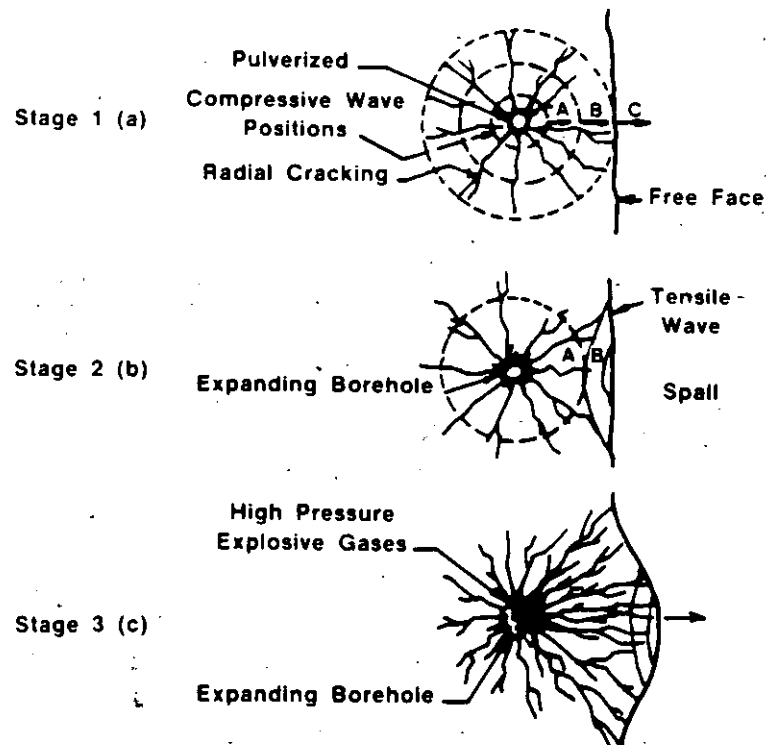
The diameter of the fractured zone was theoretically calculated to be around six hole diameters for a spherical charge and nine hole diameters for a cylindrical charge. It is in this expanded or equivalent cavity that the gas pressure becomes active and not in the original borehole. Thus cracks are pressurized and free to extend toward a free face. The original stress wave functions only to precondition the rock by initiating (in tension) radial cracks at the borehole wall.

The main points of interest of the stress wave and gas expansion theory are:

- Both stress waves and high pressure gases play an important role in fragmenting material. Neither the strain wave or gas pressure alone is responsible for rock fragmentation in blasting.
- Radial cracks originate at the borehole wall.
- Pre-existing cracks would reinitiate under stress, but no new cracks would form in the area occupied by an old crack.
- Presence of a free surface favors extension of gas pressurized radial cracks in that direction.
- In-situ stresses affect the direction in which radial cracks travel.
- For a given borehole size, an increase of explosive charge beyond an optimum amount does not increase the fractured zone, but results only in additional crushing around the cavity.

e. GASEXPANSION, STRESS WAVES, STRESS-WAVE FLAW, AND REFLECTION – (Combined Theory) (28)

Stage 1—On detonation of the explosive the high pressure shatters the rock in an area adjacent to the drill hole. The outgoing shock wave traveling at 9,000 to 17,000 feet per second sets up tangential stresses that create radial cracks which move out from the region of the hole. The first radial cracks develop in one to two milliseconds. (Figure 11-13a)



**FRACTURES OPENED UP AND PROPAGATED BY GAS EXPANSION
PRODUCING AN ISOLATED FRAGMENTED ROCK MASS OR CRATER
FIGURE 11.13**

Stage 2—The pressure associated with the outgoing shock wave of the first stage is positive. If the shock wave reaches a free face it will reflect, but in so doing the pressure falls rapidly to negative values and a tension wave is created. This tension wave travels back into the rock and since this material is less resistant to tension than to compression, primary failure cracks will develop due to the tensile strength of this reflected wave. If these tensile stresses are sufficiently intense they may cause scabbing or spalling at the free face. (Figure 11-13b)

In rock breaking this spalling effect appears to be of secondary importance. It has been calculated that the explosive load must be in the order of 8 times the normal load to cause failure of the rock by reflected shock wave alone.

In the first and second stages, the function of the shock wave energy is to condition the rock by inducing numerous small fractures. In most explosives the shock wave energy theoretically amounts to only 5 to 15% of the total energy of the explosive. This strongly suggests that the shock wave is not directly responsible for any signifi-



cant amount of rock breakage, but it does provide the basic conditioning for the last stage of the breakage process.

Stage 3—In this last stage the actual breakage of rock is a slower action. Under the influence of the exceedingly high pressure of the explosion gases, the primary radial cracks are enlarged rapidly by the combined effect of tensile stress induced by radial compression and by pneumatic wedging. When the mass in front of the borehole yields and moves forward, the high compressive stresses within the rock unload in much the same way as a compressed coil spring being suddenly released. The effect of unloading is to induce high tension stresses within the mass which complete the breakage process started in the second stage. The small fractures and threshold fracture conditions created in the second stage serve as zones of weakness to initiate the major fragmentation reactions. (Figure 11-13c)

f. NUCLEI OR STRESS WAVE—FLAW THEORY (32, 33, 34, 35, 37, 38)

This relatively new theory was formulated at the University of Maryland in the fracture mechanics laboratory. Laboratory tests were conducted in homolite-100 models, both unflawed and flawed, by simulating many of the geologic structures and discontinuities (joints, fractures, bedding planes) typically found in large scale bench blasting. Results showed that stress waves were quite important in the fragmentation process and caused a substantial amount of crack initiation at regions rather remote from the borehole. These regions consisted of small or large flaws, joints, bedding planes, and other discontinuities that acted as a nuclei for crack formation, development or extension. This new stress wave dominated mechanism of fragmentation is referred here as the nuclei theory.

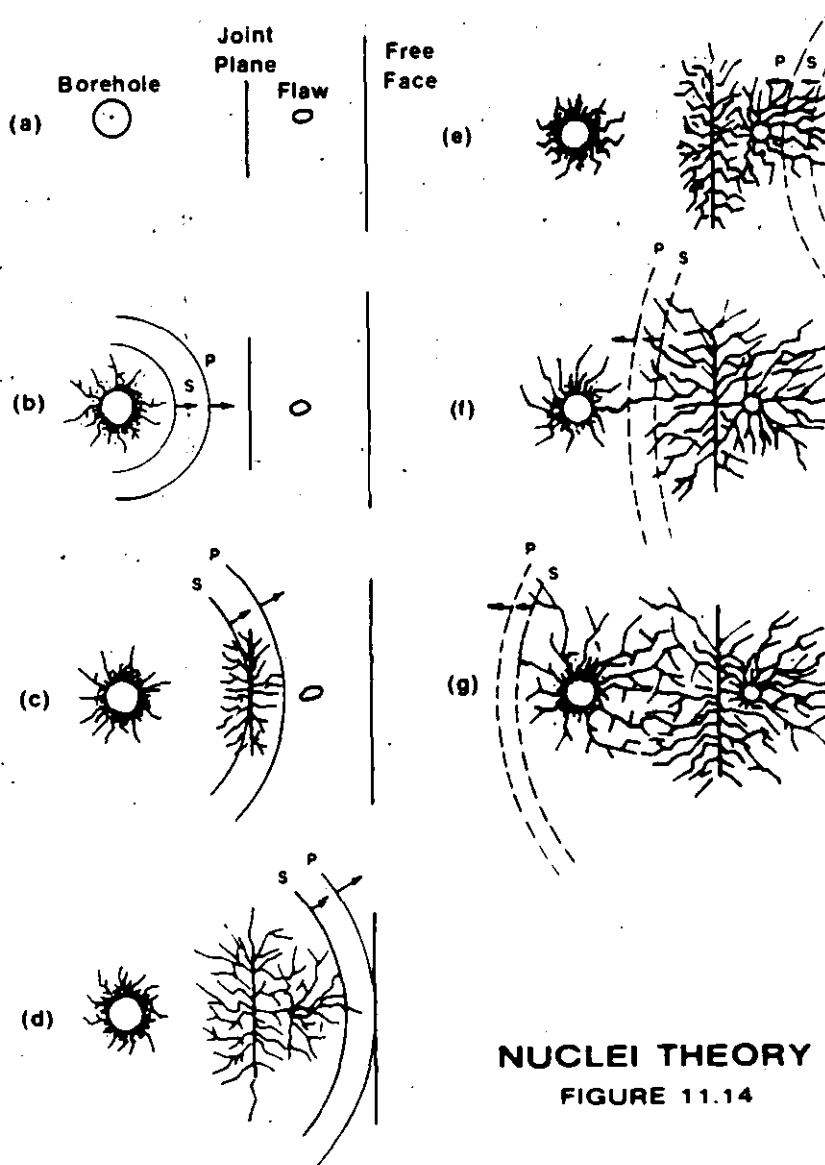
The theory and actual mechanisms of stress wave propagation and interaction in a flawed medium are quite complex. They involve many phases such as: (40)

- detonation and crack nucleation around borehole
- crushed zone extension
- dynamic crack stability
- activation of flaws
- coalescence of wave velocities and strains
- branching of cracks
- interaction of cracks and reflected wave systems
- instability of crack direction
- random progressive failure



In more simple terms, the important points of the theory are explained with the illustration in Figure 11-14. A borehole is located behind a free face with two discontinuities, a joint plane and a small flaw, located between the borehole and free face. Assume all other areas in the medium to be homogeneous and flaw free.

In unflawed material, only 8 to 12 dominant cracks emerge from a dense radial network around the borehole. These dominant cracks can travel significant distances and consequently form large pie shaped segments, that alone are not conducive for good fragmentation. Stress waves continuing away from the fractured zone around the borehole result in no further damage.



In flawed material or sections of the material which contain flaws, fragmentation is quite different. Consider the P and S waves propagating away from the fracture network around the borehole in Figure 11-14b and 11-14c. Refer to Chapter 12—Vibration/AirBlast section for a discussion on Seismic Waves. No fracturing takes place until the flaw (joint plane) is initiated by the P wave tail and the leading front of the S wave. (Figure 11-14c). The remainder of the S wave has sufficient energy to keep the crack from arresting. A similar effect occurs as the P and S waves move past the small flaw between the joint plane and the free face. (Figure 11-14d). It is important to note that cracks are initiated at flaw sites remote from the borehole region by the combined action of the P wave tail and the S wave front. Flaws initiated in the immediate borehole vicinity of these waves have only a small effect. Note also, that the outward directed P and S waves can initiate flaws anywhere independent of the presence of a free surface.

When a P wave encounters a free face (Figure 11-14d and 11-14e), it is reflected and travels back into the medium as a tensile wave to meet the outgoing S wave. At this stage, constructive interference can occur which allows for further crack initiation or extension of cracks previously formed. New wave systems (PP, PS, SP, SS, PP, and S, PS, and S) will also form from the original outgoing wave system upon reflection at a free surface or discontinuity. These new wave systems can also contribute to crack extensions. Figure 11-14f and 11-14g illustrate further crack extensions when all wave systems have been reflected back towards the hole.

The important points of the nuclei or stress-wave flaw theory are:

- the fracture network spreads with the speed of the P and S waves, which initiate fracture around flaws remote from the borehole
- in highly flawed material, fragmentation results from the nucleation of new cracks at flaws and reinitiation of old cracks from the reflected stress wave systems
- gas pressurization does not contribute significantly to the fragmentation process

Computational models incorporating stress wave/flaw interaction as a mechanism of nucleating and extending cracks is growing in popularity. (32-38, 40) Although the models differ in approach and/or details, the main idea is that shock and/or stress waves fragment

material and gas pressure acts to displace the broken material. Stress wave functions not only to initiate fractures at or near the borehole wall, but also initiate fractures throughout the rock mass being blasted.

Recent work in full scale production shots and in large blocks added further insight into this phenomena. (35) Stress wave induced fracturing at flaws and discontinuities removed from the borehole was found to be considerably greater than either spalling or borehole radial tensile failure documented by earlier works. Gas pressurized radial fracturing, in typical bench blasting operation, was found to be only a minor contributor to the overall fragmentation of the rock mass.

Some key points of Winzer's theory and observations are:

- i) new fractures are seen to form at the face at about twice the time it takes for the P wave to traverse the burden distance
- ii) old fractures are the loci of new fractures or are re-initiated themselves early in the event; they continue to be active for several tens of milliseconds after detonation of the explosive
- iii) fragmentation continues in blocks of rock, following detachment from the main rock mass, by trapped stress waves
- iv) the fracture pattern on the free face is well developed prior to the expected time of arrival of radial cracks from the borehole
- v) in blasted faces from production-scale shots, fractures are observed to have initiated at, and propagated from, joint and bedding planes, suggesting the same operating mechanism(s) as those observed in homolite models at the University of Maryland
- vi) gas venting occurs through already open cracks relatively late in the event, indicating that the majority of fractures observed on the free face are not gas pressurized
- vii) in more massive rock stress waves are transmitted with higher velocity and less attenuation, but fewer fractures will form because there are few fracture sites. However, more radial fractures will form in massive rock, while fewer fractures form at a distance from the borehole



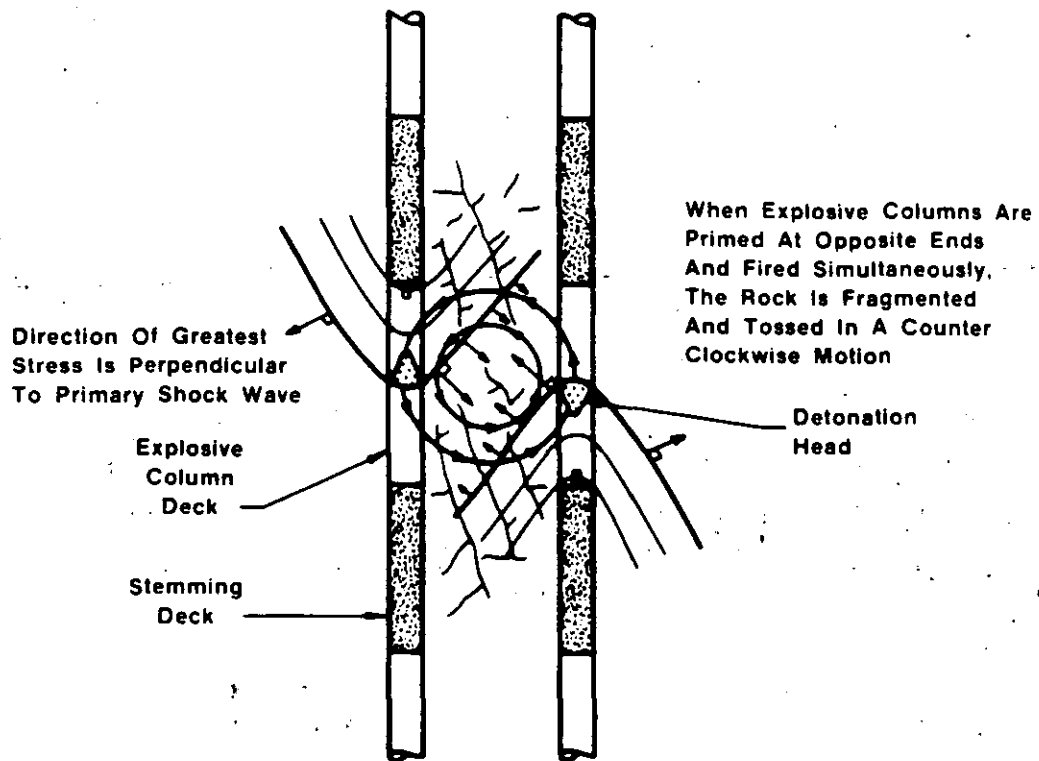
- viii) large fragments will form early in the event, and as they move and fractures open, large segments of the rock mass will be effectively isolated from further stress energy
- ix) in more heavily fractured rock, the stress wave velocity will be lower and attenuation higher, but there are more fractures to serve as initiation sites
- x) the stress wave takes longer to penetrate the mass, and movement of the rock can be expected to be slower as more energy is absorbed by the rock mass
- xi) cracks open more slowly, and smaller masses of rock are isolated early in the event, so that later arriving stress waves can continue to increase crack initiation and propagation

g. TORQUE THEORY

The success of this theory is totally dependent on the absolute, accurate timing of initiators. When two adjacent explosive columns are initiated simultaneously from opposite ends, a compressional shock wave from each column traveling parallel but in opposite directions is formed. (Figure 11-15) The greatest stress is always directed perpendicular to the primary shock front. This stress is also assumed to be greatest near the detonation head in the explosive and diminishes with distance away from the detonation head. An uneven stress distribution is formed between explosive columns when the columns are fired simultaneously and from opposite directions. This action tends to toss the fragmented rock between explosive columns in a counterclockwise motion. Reversing the primers of each explosive column will toss the material in a clockwise motion. This action is precisely what is needed to obtain uniform fragmentation and avoid tight muck piles such as in the case of in-situ retorting. For this theory to work, exact initiators are crucial; nothing less will do, especially when using explosives with very high velocity of detonation.

h. CRATERING THEORY (41-45)

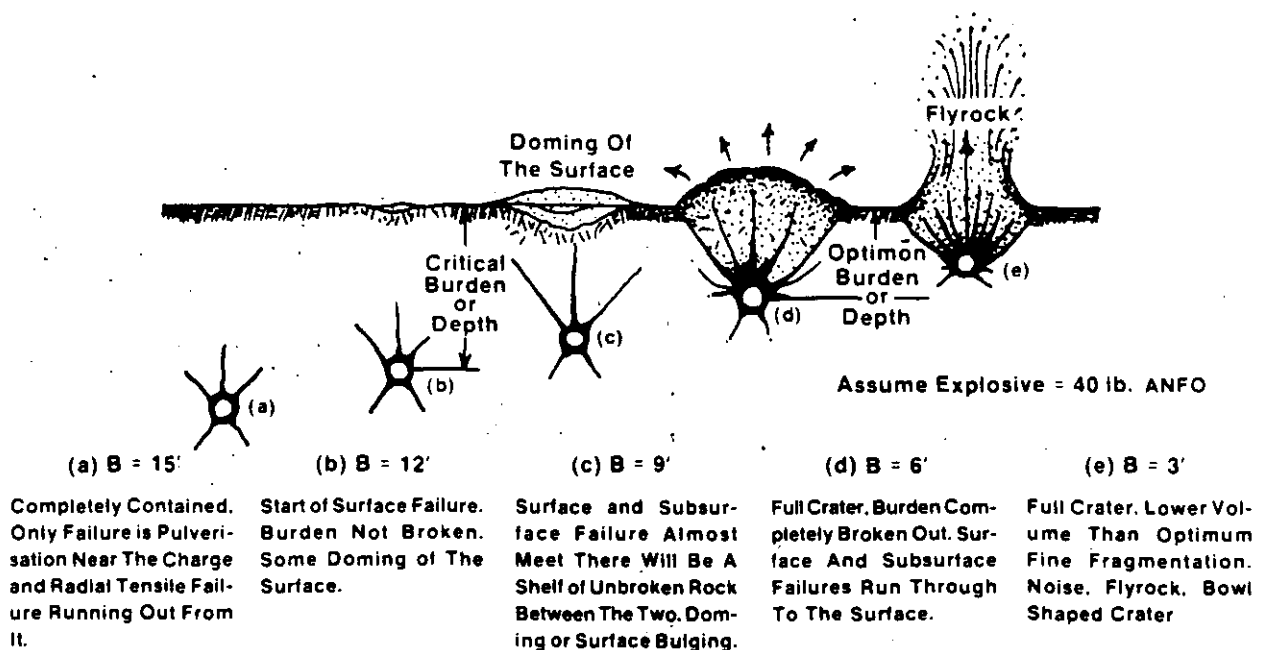
The concept of cratering, its development, and resulting applications were originally proposed by C.W. Livingston and later modified by others such as Lang and Bauer. (41) (43) (44) It involves a spherical charge of length to diameter ratio of less than or equal to 6 to 1, detonated at an empirically determined distance beneath the sur-



**APPLICATION OF NEW BLASTING
THEORY TO IN-SITU RETORTS
BLASTING
FIGURE 11.15**

face to optimize the greatest volume of permanently fragmented material between the charge and free surface. This implies that given a specific explosive and material, there exists a burden distance between the charge and free surface which yields the largest crater (Figure 11-16d). This burden is referred to as the optimum burden or depth. Similarly, there exists another burden distance referred to as the critical distance, which is too far below the surface to result in any crater or expulsion of material at the surface, other than minor radial cracks. This is the point where material at the surface just begins to show evidence of failure, (Figure 11-16b).





SCHEMATIC OF THE EFFECT OF DECREASING THE BURDEN ON CHARGES FIRED IN ROCK
FIGURE 11.16

Livingston determined, experimentally and theoretically, that there was a constant factor between this critical burden distance and the cube root of the weight of explosive and expressed it as:

Strain Energy Equation

$$N = E \times W^{\frac{1}{3}}$$

where:

N = critical distance in feet

W = weight of explosive in pounds

E = proportionality constant or the **strain energy factor** which has no units and is constant for one given explosive - rock combination

If a sufficient number of tests are performed as illustrated in Figure 11-16, then the strain energy factor could be calculated. For example if the critical burden was found to be 12 feet when using 40 pounds of ANFO, then

$$E = \frac{N}{W^{\frac{1}{3}}}$$

$$E = \frac{12}{(40)^{\frac{1}{3}}}$$

$$E = \frac{12}{3.42}$$

$$E = 3.51$$

Strain Energy Factor = 3.51

This strain energy factor, E, will differ if the same explosive is used in a different material or the same material is blasted with a different explosive. When rock gets more brittle, E increases and the optimum crater volume occurs at lower values of depth ratio. In softer material, E decreases and the optimum crater volume occurs at higher values of depth ratio.

The strain energy equation can be written in another form that relates the charge depth from surface to the depth ratio, strain energy and explosive weight as:

Upper Limit of Shock Range

$$d_c = \Delta \times E \times W^{\frac{1}{3}}$$

where:

d_c = distance from surface to the center of gravity of the charge in feet

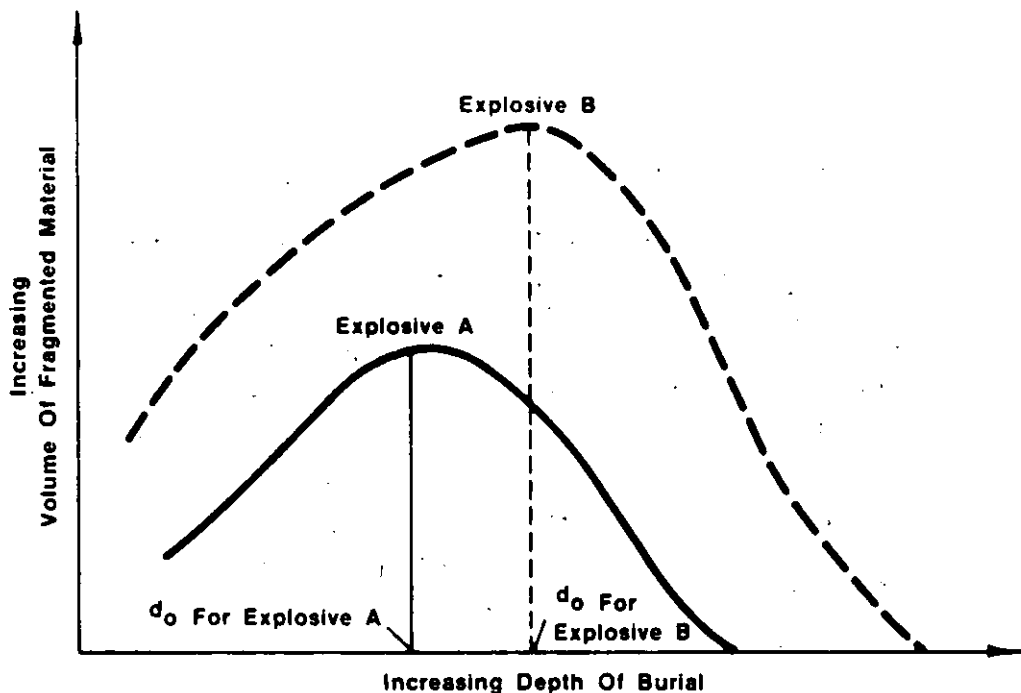
Δ = depth ratio = $\frac{\text{depth of burial}}{\text{critical depth}}$

W = weight of explosive in pounds

If d_c is the optimum burden that yields the greatest volume of fragmented material, then it is referred to as d_o and the optimum depth ratio is referred to as Δ_o .



Crater data can be plotted in a number of different ways. Figure 11-17 illustrates the effect of two explosives, A and B on the amount of fragmented material that each is capable of achieving at different depths of burials. Note that the higher energy explosive always fragments a greater volume of material at the same depth of burial as explosive A, but that the optimum depth of burial differs for each explosive.

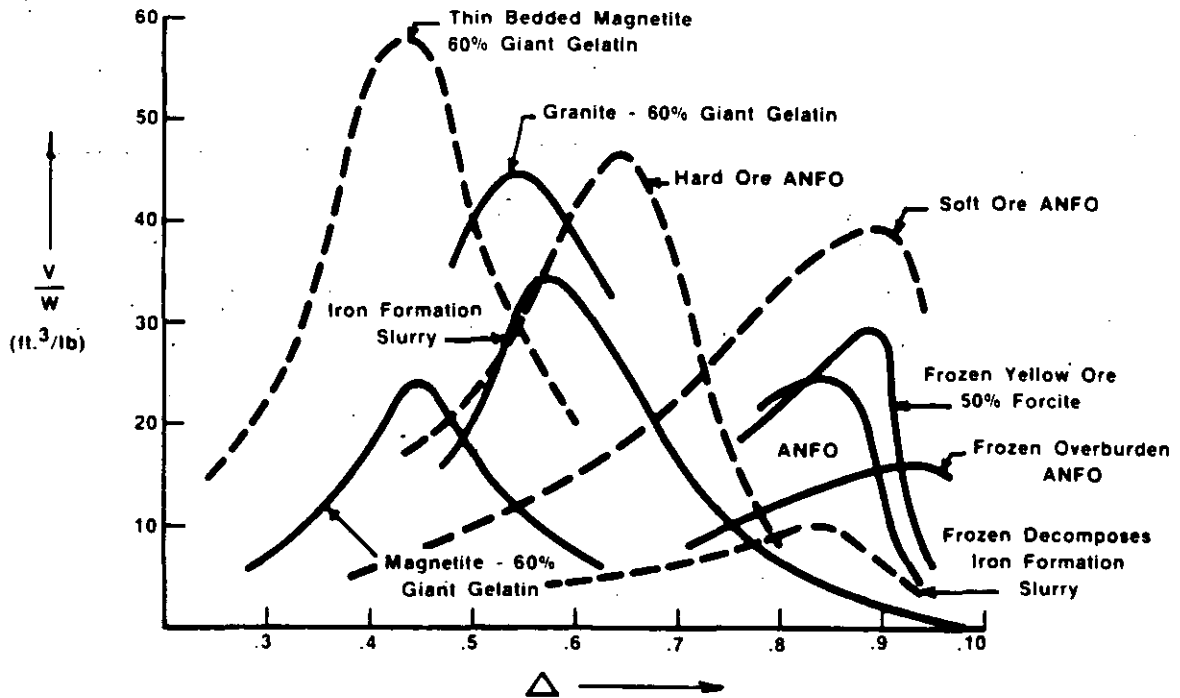


VOLUME OF FRAGMENTED MATERIAL VERSUS DEPTH OF BURIED FOR TWO EXPLOSIVES IN THE SAME MATERIAL

FIGURE 11.17

Another method of representing crater data on a common base is by plotting V/W on the y-axis and the depth ratio on the x-axis as shown in Figure 11-18. (V is the volume of broken material in cubic feet, W is the weight of explosive in pounds, and the depth ratio has been defined as the depth of burial divided by the critical depth. The important thing to note is that the optimum depth ratio, (Δ_0), varies with each explosive-rock combination. The advantage of performing such field experiments is that one would obtain crater data specifically suited to the user environment for a number of different explo-

sives. Although the curves in Figure 11-18 are fitted as smooth curves, one should remember that some scatter of data is always present and it is important to take this into account for crucial applications of cratering.

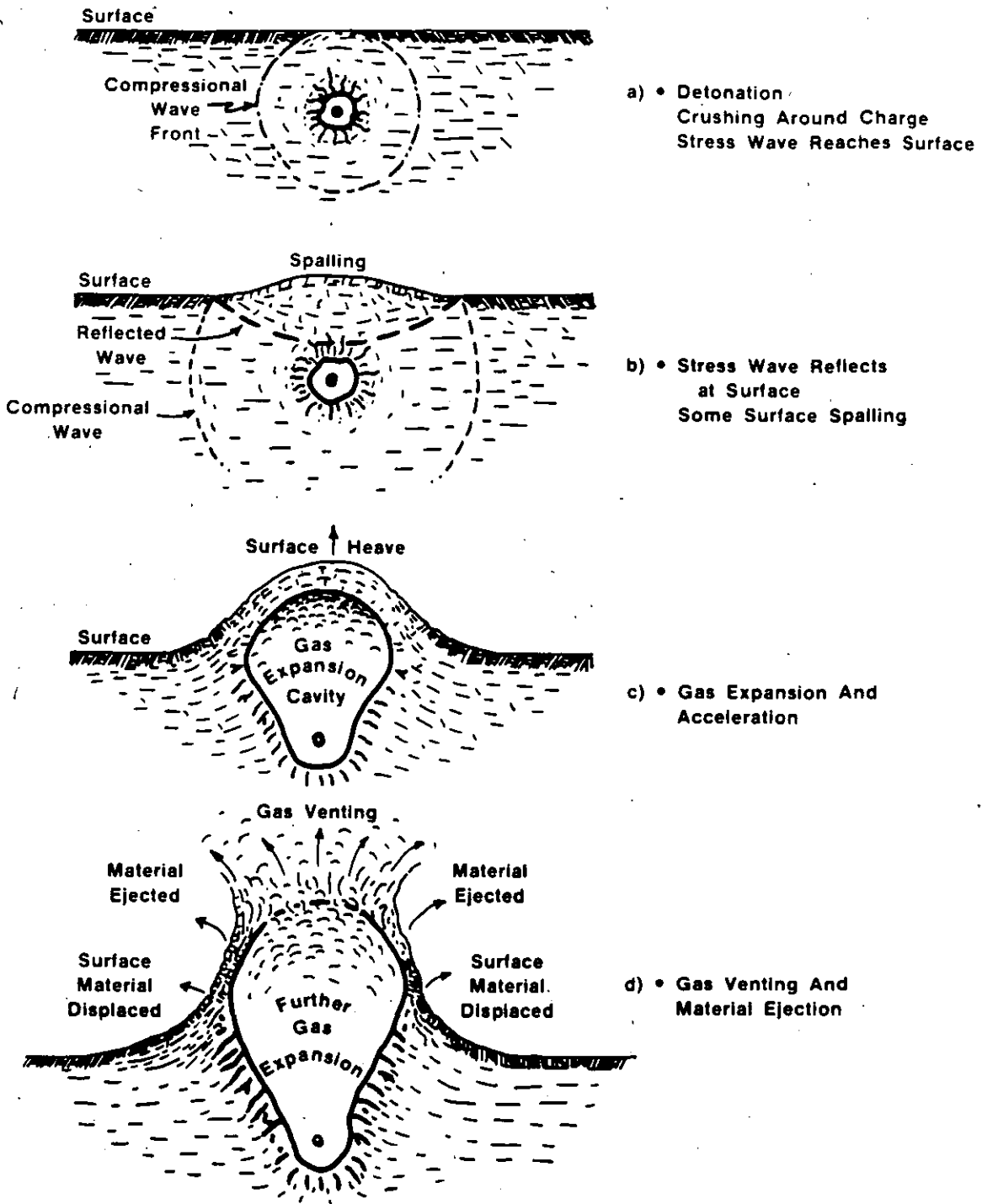


ROCK REMOVED IN CU. FT. PER LB.
OF EXPLOSIVE VS DEPTH RATIO
FIGURE 11.18 (44)

I. CRATERING MECHANISMS (4) (45)

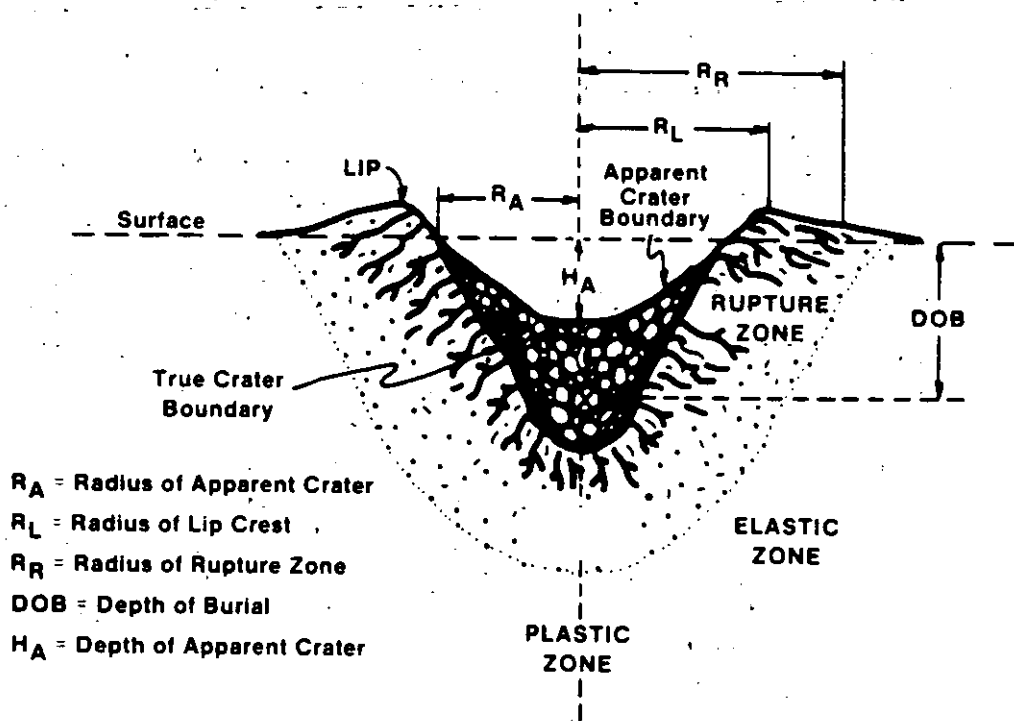
As the high pressure explosive gases expand against the medium immediately surrounding the explosion, a spherical shock wave is generated causing crushing, compaction and plastic deformation. (Figure 11-19a) For commercial explosives the initial shock pressures are on the order of 100 to 200 thousand atmospheres (one atmosphere = 14.7 pounds per square inch). As the shock front moves outward in a spherically diverging shell, the medium behind the shock front is put into radial compression and tangential tension. This results in the formation of radial cracks directed outward from the cavity. The peak pressure in the shock front becomes reduced due to spherical divergence and the expenditure of energy in the medium. For shock pressures above the dynamic crushing strength





CRATERING EVENTS AND MECHANISMS
FIGURE 11.19

of the medium, the material is crushed, heated and physically displaced, forming a cavity. In regions outside this limit the shock wave will produce permanent deformation by plastic flow, until the peak pressure in the shock front has decreased to a value equal to the plastic limit of the medium. This is the boundary between the plastic and elastic zones shown in Figure 11-20.



EMPLOYMENT OF ATOMIC DEMOLITION MUNITIONS
DEPARTMENT OF THE ARMY, WASHINGTON, D.C. AUG. 1971
FIGURE 11.20

When the compressive shock front encounters a free face, it must match the boundary condition that the normal stress or pressure be zero at all times. This results in the generation of negative stress, or rarefaction wave which propagates back into the medium (Figure 11-19b). Thus the medium which was originally under high compression is put into tension by the rarefaction wave. This phenomenon causes the medium to break up and fly upward with a velocity characteristic of the total momentum imparted to it. In a loose soil material, this spalling makes almost every particle fly into the air individually, while in a rock



medium the thickness of the spalled material is generally determined by the presence of pre-existing fracture patterns and zones of weakness. As the distance from surface increases, the peak negative pressure decreases until it no longer exceeds the tensile strength of the medium. The velocity of spalled material also decreases in proportion to the peak pressure. This breakage mechanism is predominant only for charges placed at very shallow depths of burial.

The two mechanisms described so far are short term, lasting only a few milliseconds. The gas acceleration mechanism, however, is a much longer lasting process which imparts motion to the medium around the detonation by the expansion of gases trapped in the explosion-formed cavity. (Figure 11-19c and 11-19d) These gases are produced in the surrounding material by vaporization and chemical changes induced by the heat and pressure of the explosion. Venting occurs because the material is no longer cohesive enough to contain the explosion gases. As the gases are released, fragments assume free ballistic trajectories. At depths of burial at which crater dimensions are maximum, the gases produced will give appreciable acceleration to overlying material during its escape or venting through cracks extending from the cavity to the surface. At shallow depth of burials the spall velocities are so high that the gases are unable to exert any pressure before venting occurs. For very deep explosions the weight of the overburden precludes any significant gas acceleration of the overlying material. Gas acceleration is the dominant mechanism at optimum depth of burial. With a constant weight of explosive, the optimum depth of burial varies with the surrounding material.

At deep depths of burial, the mechanism of overburden collapse (subsidence) becomes dominant. This effect is closely linked to the crushing, compaction and plastic deformation mechanism which produces an underground cavity. At these depths of burial, spall and gas acceleration will not impart sufficient velocity to the overlying material to physically eject it from the crater. Most throwout returns to the crater as fallback material. In a rock medium the bulking action of the rock, when it is disoriented from its original fracture pattern, could produce a volume greater than the underground cavity. This could result in no crater or a mound above the ground rather than a crater.

At even deeper depths of burial, about twice or deeper of that of optimum, another type of subsidence occurs. In this case the spall and gas acceleration has no significant effect on the overlying material. Only an underground cavity is formed. When the pressure in the cavity decreases below overburden pressure, the roof of the cavity begins to collapse. In most media this collapse will continue upward



forming a chimney of collapsed material. In soil, where the density of the material will not significantly change after it has fallen, the volume of the underground cavity will be transmitted to the surface.

Figure 11-21 illustrates surface time profiles after detonation of a 40 pound equivalent charge of ANFO, buried 8.0 feet in an unconsolidated, sedimentary type material. (46) High-speed photography was

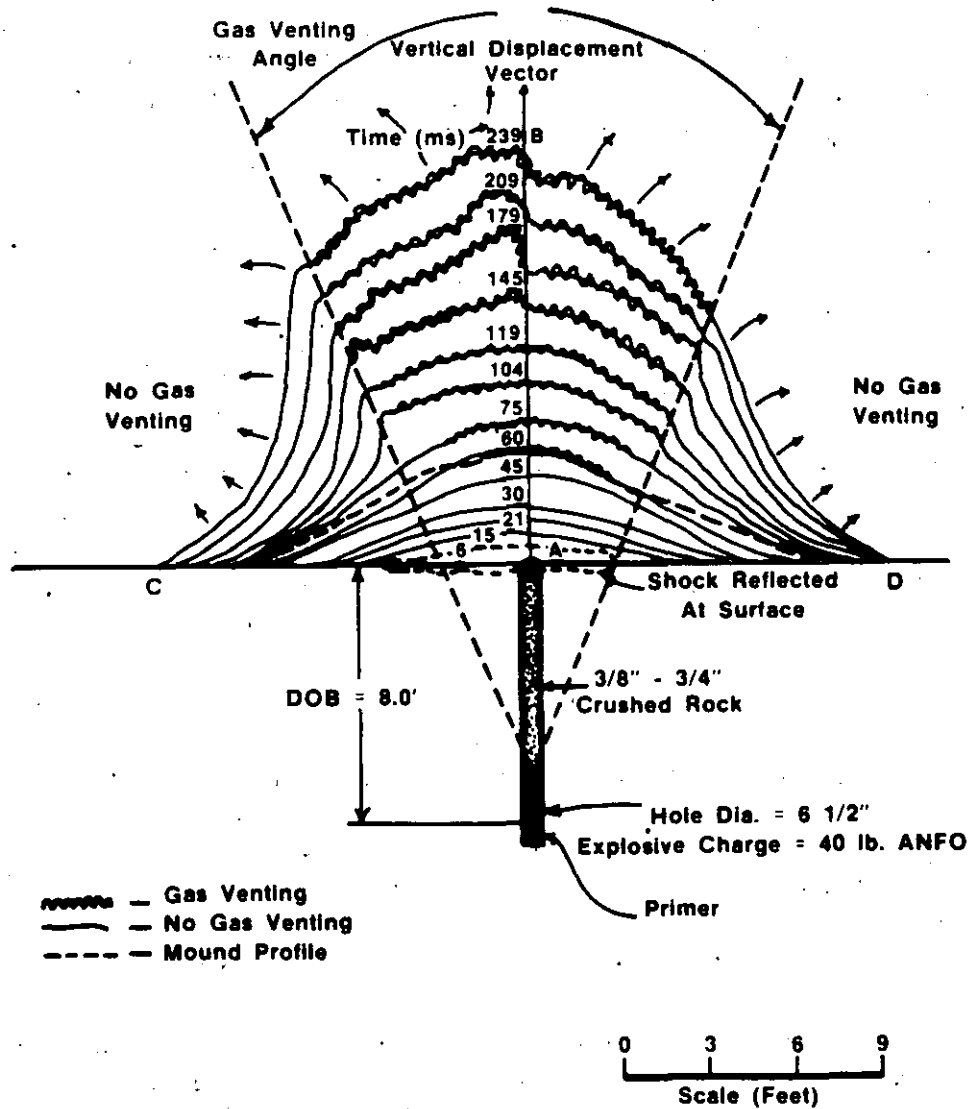
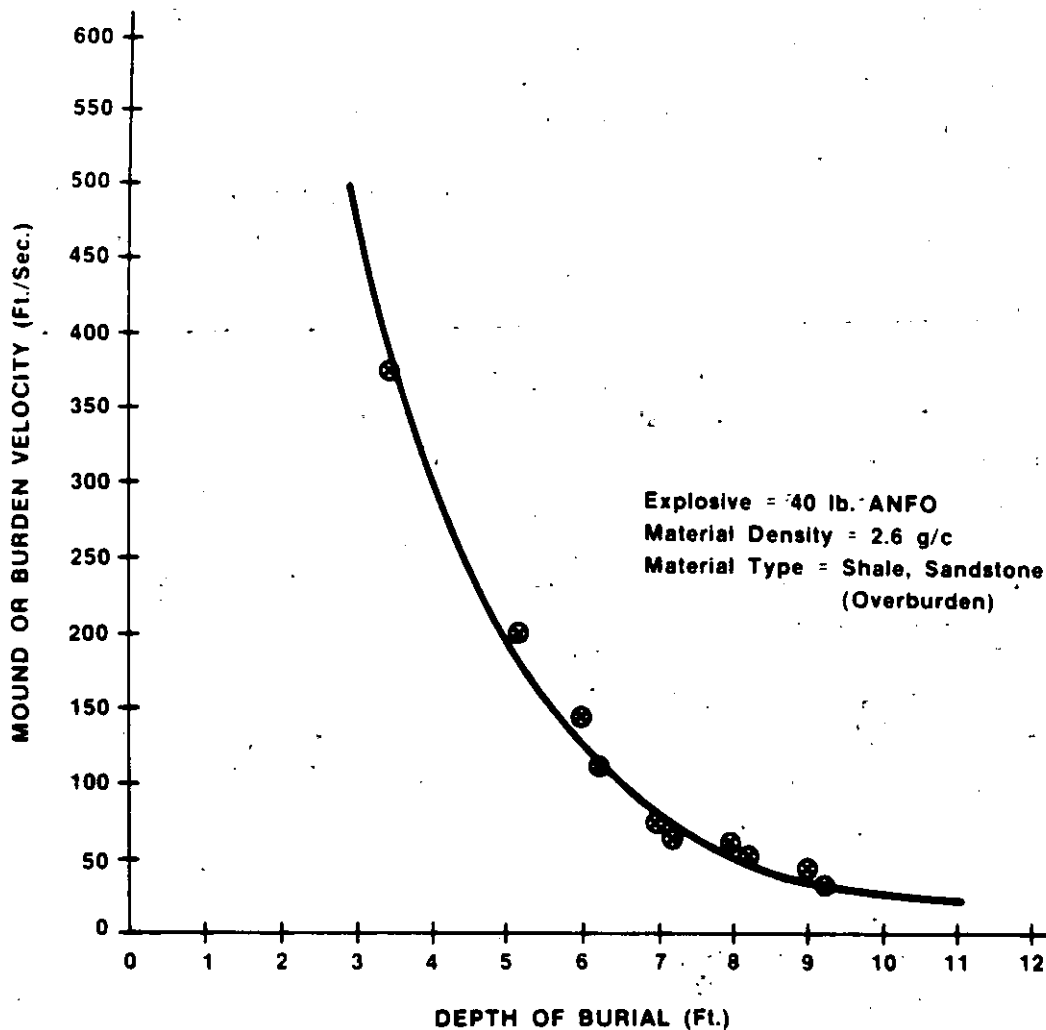


FIGURE 11.21

used to document the effects of shock and gas pressure. The first observation was that of brisance or the reflection of the compressive shock at the surface a few milliseconds after detonation. This is indicated by the dotted eclipse immediately above the charge hole or surface. With sufficient camera coverage and appropriate viewing angles, this shock ring can often be used to estimate, in rough, the degree of crater damage. In this case, sufficient viewing angles were not available and so only part of the total reflected shock could be resolved. Because the charge was placed at a depth significantly greater than the optimum depth of burial, no appreciable spalling occurred. Gas pressure was the dominant mechanism responsible for uplifting and ejecting material radially outward.

As gas expansion occurs around the charge cavity, the material above the charge is compacted and heaved upwards. Between 0 to 45 milliseconds after detonation, the uplifted material is resilient and compacted enough to maintain sufficient cohesion to contain all gases resulting from expansion. At 60 ms gas venting begins to occur directly above the charge and continues to expand in a well defined arc with respect to time. If the gas venting contacts at each end of each time profile are connected with straight lines, the lines will most always point toward the top or the center of the charge. In this case, the gas venting angle was measured to be approximately 45 degrees. The gas venting angle is useful in determining how much of the top part of a cylindrical charge, as found in production holes, actually contributes to gas venting, cratering and/or lost energy through lack of stemming confinement. At either side of the gas venting angle, no gas venting occurs, but material fragments are displaced and/or ejected outwardly. Material fragments are also ejected from within the bounds of the gas venting angle. Owing to a charge depth beyond optimum, the final result is a mound rather than a crater. The mound is indicated by the shaded section underneath the 60 ms time profile.

The initial instantaneous uplifting velocity above the charge is generally high but diminishes to zero when the material has reached its highest displacement. In reference to Figure 11-21, the average initial velocity along the vertical displacement vector up to 45 ms is 68 ft/sec. The average velocity from 60 ms to 239 ms is 54 ft/sec. The difference in velocity is attributed to the effects of gas venting and expansion beyond 60 ms. These velocities are dependent on material type and structure, explosive and depth of burial. In general, the velocity will decrease exponentially with depth for a given explosive and material type as shown in Figure 11-22. (46)



**MOUND OR BURDEN VELOCITY VS. DEPTH OF BURIAL
 FOR 40 POUND CHARGES OF ANFO
 FIGURE 11.22**

5. DECOUPLING

Decoupling is generally used as a control to reduce backbreak to the final planned excavation limit for pit wall slopes in open pit mines, shafts, drifts, ditches, road cuts and mine benches.

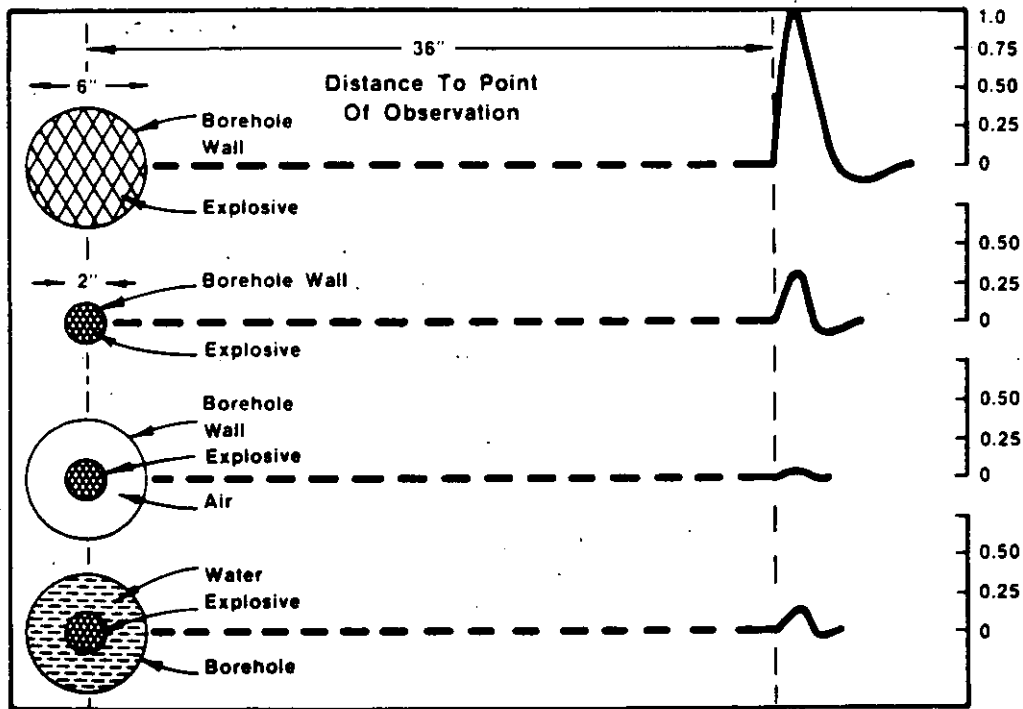
Since the borehole pressure is quite intense for a fully coupled borehole, exceeding many times that of the dynamic compressive strength of the rock, it must be reduced to avoid extensive damage. The three principal modes of rock failure occur by exceeding the dynamic compressive, shear



or tensile strengths. Ideally, the borehole pressure should be somewhere between the compressive and tensile strength of the rock, so as to avoid extensive crushing at the borehole wall, yet provide enough pressure to extend a single predominant crack between any two perimeter holes in the control line of holes.

A good example of decoupling in air and water in relation to fully coupled holes is illustrated in Figure 11-23. (47) The pressure imparted in the rock mass at 36" away for the same explosive is shown for four conditions:

- i) a 6" diameter explosive in a 6" hole
- ii) a 2" diameter explosive in a 2" hole
- iii) a 2" diameter explosive in a 6" hole (air decoupled)
- iv) a 2" diameter explosive in a 6" hole (water decoupled)



**EFFECT OF AIR AND WATER DECOUPLING
VS FULLY COUPLED HOLES
FIGURE 11.23 (47)**

All measured stress levels are compared relative to the 6" diameter explosive in a 6" diameter hole. A number of important points are immediately evident. The greatest stress level was achieved with a fully coupled

explosive in a 6" diameter hole. The next highest stress level was achieved, again, with a fully coupled explosive, even though the hole diameter was reduced three-fold to a 2" diameter. Water decoupling followed next and air decoupling produced the smallest stress level. Thus, an air decoupled charge is the most effective means of reducing borehole pressure and consequently the peak stress level within the rock mass.

A reasonably reliable method of calculating the borehole pressure is with the following formula which takes into account two decoupling ratios. (48) (49) (50)

$$P_b = 1.69 \times 10^{-3} \times \rho \times VOD^2 \times \left[\frac{V_c \times d_e}{d_h} \right]^{2.6}$$

where:

P_b = Borehole pressure in PSI.

ρ = Density of explosive in g/cc

VOD = Velocity of detonation in ft/sec

c = Percentage of explosive column loaded expressed as a decimal

d_e = Explosive diameter (in.)

d_h = Hole diameter (in.)

This formula is best suited for explosives which contain no metallic elements or relatively small amounts, since the addition of energizing metals lowers the detonation velocity of the explosive and hence, the borehole pressure as calculated by this equation. Computer codes such as TIGER and EXPLODE are used to calculate borehole pressures from explosives containing metallic elements.

6. REFERENCES

- 1) CHIAPPETTA, R.F., BORG, D.G., **Increasing Productivity Through Field Control and High-Speed Photography**, First International Symposium on Rock Fragmentation by Blasting, Lulea, Sweden, Aug., 1983, pp. 301-331
- 2) DAVIS, W.C., **High Explosives**, Los Alamos Science, 1983, pp. 48-52



- 3) CHIAPPETTA, R.F., BAUER, A., BURCHELL, S.L., **The Use of High-Speed Motion Picture Photography in Blast Evaluation and Design**, Proceedings 9th Annual Conference on Explosives and Blasting Techniques, Society of Explosives Engineers, 1983
- 4) MAJOR JOHNSON, M.S., **Explosive Excavation Technology**, U.S. Army Engineer Nuclear Cratering Group, Livermore, California, June, 1971, NCG Technical Report No. 21, TID-4500
- 5) ATLAS POWDER COMPANY, Field Technical Operations, Tamaqua, PA, USA, Internal unpublished data, 1981-1985
- 6) KUTTER, H.K., FAIRHURST, C., **On the Fracture Process in Blasting**, Int. J. Rock Mech. Min. Sci., Vol. B, pp. 181-202, Pergaman Press, 1971, Great Britain
- 7) OLSON, J.J., WILLARD, R.J., FOGELSON, D.E., HJELMSTAD, K.E., **Rock Damage from Small Charge Blasting in Granite**, USBM, RI 7751, 1973, 44pp.
- 8) SISKIND, D.E., STECKLEY, R.C., OLSEN, J.J., **Fracturing in the Zone Around a Blasthole**, White Pine, Michigan, USBM, RI 7753, 1973, 20pp.
- 9) CATTERMOLE, J.M., HANSON, W.R., **Geologic Effects of the High Explosives Test in U.S.G.S.**, Tunnel Area, Nevada Test Site, U.S. Geol. Survey, Prof. Paper 382-B, 1962, 29pp.
- 10) Colorado School of Mines, **Underground Explosion Test Program**, Ser. I and Ser. II experiments, December 1948
- 11) DERLICH, S., **Underground Nuclear Explosion Effects in Granite Rock Fracturing**, Proc. Symposium of Engineering with Nuclear Explosives, Las Vegas, Nevada, January, 1970, pp. 508 and 518
- 12) ATCHISON, T.C., TOURNAY, W.E., **Comparative Studies of Explosives in Granite**, USBM RI 5509, 1959, 28pp.
- 13) D'ANDREA, D.V., FISCHER, R.L., HENDRICKSON, A.D., **Crater Scaling in Granite for Small Charges**, USBM RI 7409, 1970, 28pp.
- 14) SISKIND, D.E., FUMANTI, R.R., **Blast Produced Fractures in Lithonia Granite**, USBM RI 7901, 1974, 38pp.



- 15) VOVK, A.A., MIKHALYUK, A.V., BELINSKI, I.V., **Development of Fracture Zones in Rocks during Camouflet Blasting**, translated from FIZLKO-TEKLINICHESKIE PROBLEMY ROZRABOTKI POLEZRYKH ISKI-PAEMYKH, No. 4, pp. 39-45, July-Aug., 1973
- 16) BORG, I.Y., **Extent of Pervasive Fracturing Around Underground Nuclear Explosions**, Int. J. Rock Mech. Mining Science, 10, 11-18, 1973
- 17) OBERT, L., DUVALL, W.I., **A Gauge and Recording Equipment for Measuring Dynamic Strain in Rock**, U.S. Dept. Int., Bureau of Mines, RI 4581, 1949
- 18) OBERT, L., DUVALL, W.I., **Generation and Propagation of Strain Waves in Rock**, USBM RI 4663, 1950
- 19) HINO, U., **Frangmentation of Rock through Blasting**, Q. Colorado School of Mines, 51, 189, 1956
- 20) DUVALL, W.I., ATCHISON, T.C., **Rock Breakage by Explosives**, USBM RI 5356, 1957
- 21) RINEHART, J.S., **Fracturing Under Impulse Loading**, University of MO-Rolla, School of Mines and Met, Bulletin, Tech Ser., 95, 46, 1958
- 22) LANGFORS, U., KIHSTROM, B., **The Modern Technique of Rock Blasting**, John Wiley and Sons, NY, 405pp., 1963
- 23) STARFIELD, A.M., **Strain Wave Energy in Rock Blasting**, Proc. 8th Symposium on Rock Mech., Univ. of Minnesota, 1966
- 24) PORTER, D.D., FAIRHURST, C., **A Study of Crack Propagations Produced by the Sustained Borehole Pressure in Blasting**, Proc. 12th Symposium Rock Mech., Univ. of Missouri, Rolla, 467, 1970
- 25) PERSSON, P.A., LUNDBORG, N., JOHANSSON, C.H., **The Basic Mechanism in Rock Blasting**, Proc. 2nd Congress Int. Society for Rock Mech., Belgrade, 1970
- 26) FIELD, J.E., LADEGAARD-PEDERSON, A., **The Importance of the Reflected Stress Wave in Rock Blasting**, Int. J. Rock. Mech. Min. Sci., 1971



- 27) JOHANSSON, C.H., PERSSON, P.A., **Frangmentation Systems**, Proc. and Papers of Int. Society of Rock Mech., 3rd Congress, Denver, CO, Sept. 1-4, 1974
- 28) LANG, L.C., FAVREAU, R.F., **A Modern Approach to Open Pit Blast Design and Analysis**, CIM Bulletin, pp. 37-44, June, 1974
- 29) ASH, R.L. **The Influence of Geological Discontinuities on Rock Blasting**, PhD. Thesis, Univ. of Minnesota, June, 1973
- 30) HAGEN, T.N., **Rock Breakage by Explosives**, Australian Geomechanics National Symposium on Fragmentation, Adelaide, 1974
- 31) HAGEN, T.N., JUST, G.D., **Rock Breakage by Explosives—Theory, Practice, Optimization**, Proc. 3rd Congress Int. Society for Rock Mechanics, Denver, CO, Sept. 1-4, 1974
- 32) BARKER, D.B., FOURNEY, W.L., DALLY, J.W., **Photoelastic Investigation of Fragmentation Mechanisms, Part I — Borehole Crack Network**, Univ. of Maryland, MD, March, 1978, 39pp.
- 33) BARKER, D.B., FOURNEY, W.L., **Photoelastic Investigation of Fragmentation Mechanisms, Part II — Flaw Initiated Network**, Aug. 1978, 47 pp., Univ. of Maryland, MD
- 34) FOURNEY, W.L., BARKER, D.B., **Effect of Time Delay on Fragmentation in a Jointed Model**, Univ. of Maryland, MD, Aug. 1979, 31pp.
- 35) WINZER, S.R., ANDERSON, D.A., RITTER, A.P., **Rock Fragmentation by Explosives**, First Int. Symposium on Rock Fragmentation by Blasting, Lulea, Sweden, Aug. 22-26, 1983, pp. 225-249
- 36) MARGOLIN, L.G., ADAMS, T.F., **Numerical Simulation of Fracture**, First Int. Symposium on Rock Fragmentation by Blasting, Lulea, Sweden, Aug. 22-26, 1983, pp. 347-360
- 37) ADAMS, T.F., DEMUTH, R.B., MARGOLIN, L.G., NICHOLS, B.D., **Simulation of Rock Blasting with the Shale Code**, First Int. Symposium on Rock Fragmentation by Blasting, Lulea, Sweden, Aug. 22-26, 1983, pp. 361-373
- 38) MCHUGH, S., **Computational Simulations of Dynamically Induced Fracture and Fragmentation**, First Int. Symposium on Rock Fragmentation by Blasting, Lulea, Sweden, Aug. 22-26, 1983, pp. 407-418



- 39) JOHANSSON, C.H., PERSSON, P.A., **Detonics of High Explosives**, Academic Press, London and NY, 1970, 330pp.
- 40) ROSSMANITH, H.P., **Dynamic Fracture in Glass**, Univ. of Maryland, MD, April, 1978, 77pp.
- 41) LANG, L.C., ROACH, R.J., OSOKO, M.N., **Vertical Crater Retreat - An Important New Mining Method**, Canadian Mining J., Sept., 1977
- 42) LIVINGSTON, C.W., **Fundamentals of Rock Failure**, Quarterly of the Colorado School of Mines, Vol. 51, No. 3, July, 1956
- 43) BAUER, A., **Application of the Livingston Theory**, Quarterly of the Colorado School of Mines, Vol. 56, No. 1, Jan., 1961
- 44) BAER, A., HARRIS, G.R., LAND, L., PREZZIOSI, P., SELLECK, D.J., **How IOC Puts Crater Research to Work**, Eng. and Mining J., Sept., 1965, pp. 117-121
- 45) Headquarters, Dept. of the Army, **Employment of Atomic Demolition Munitions (ADM)**, Field Manual, Washington, DC, Aug. 31, 1971, FM5-26
- 46) CHIAPPETTA, R.F., BURCHELL, S.L., REVEY, G., FISHER, S., ATLAS POWDER COMPANY, FIELD TECHNICAL OPERATIONS, Unpublished Internal Data, Cratering Field-Experiments at the Avery Coal Co., PA, 1983-1985
- 47) DAY, P.R., **Controlled Blasting to Minimize Overbreak with Big Boreholes Underground**, Proc. 8th Conference on Explosives and Blasting Techniques, Society of Explosives Engineers, New Orleans, Louisiana, 1982, pp. 262-274
- 48) CROSBY, W.A., BAUER, A., **Wall Control Blasting in Open Pit Mines**, Mining Engineering, Feb., 1982, pp. 155-158
- 49) PIT SLOPE Manual, **Perimeter Blasting**, Canmet, Report 77-14, Canada Center for Mineral and Energy Technology, Canada, May, 1977
- 50) KATSABANIS, P., **A Comparative Study of Emulsion and Slurry Explosives**, MSC Thesis, Queen's University, Kingston, Ontario, Canada, Feb., 1983, 149pp.



7. UNDERGROUND BLASTING



Fig. 7.1 Tunneling.

7.1 Tunneling.

There are two reasons to go underground and excavate:

- to use the excavated space, e.g. for storage, transport etc.
- to use the excavated material, e.g. mining operations.

In both cases tunneling forms an important part of the entire operation. In underground construction it is necessary to gain access to the construction site by

tunneling, but the tunnel can be a purpose in itself e.g. road, water, cable tunnels etc.

In mining operations tunnels are used as adits to the mining site and for preparatory work as well as for internal communication.

Tunnels are driven mainly in horizontal or close to horizontal directions but also inclined, from vertically upwards to vertically downwards. In the following, tunneling, raise shafts and sink shafts will be dealt with in detail while storage in rock caverns and mining will be dealt with more briefly.

Tunneling is the most frequently occurring underground operation which also forms part of the construction of rock chambers etc. and is normally an integral part of mining operations.

The development of tunnel driving techniques has been tremendous during the last few years. The drilling techniques have developed from pneumatic drilling machines to electro-hydraulic drilling jumbos with a very high capacity. The charging of the blastholes can be carried out quickly either manually with plastic pipe charges or mechanically with pneumatic charging equipment.

The development of explosives has moved in the direction of safer products with better fumes characteristics. Modern explosives like Emulite and Dynamex M are well oxygen-balanced with a minimum of noxious fumes.

Initiating systems like NONEL have shortened the charging time and added further safety to the blasting operation due to their insusceptibility to electrical hazards.

The modern drilling equipment has shortened the drilling time, the NONEL system has made connecting of the detonators safer and faster and Emulite, with its excellent fumes characteristics, has shortened the ventilation time.

All the above contribute to a faster work cycle:

- drilling
- charging
- blasting
- ventilation
- scaling
- grouting (if necessary)
- loading and transport
- setting out for the new blast

The shorter work cycle calls for better work planning as well as better precision and accuracy in the different operations of the work cycle.

In the following, the drilling, charging and blasting operations will be dealt with. It is obvious that it is of the utmost importance that the holes should be drilled at the right locations and with the right inclination. The marking of the holes on the rock face as well as collaring and drilling must be carried out accurately.

Langefors in "The modern technique of Rock Blasting", says about drilling precision: "The scattering of the drill holes as a quantitative factor is often disregarded. It is included quite indefinitely in the technical margin together with the rock factor. In discussing blasting as a whole it would be a great advantage if

attention could be paid to the drilling precision in calculating the charges and in constructing the drilling pattern; for the blasting of the cut it is essential."

The main difference between tunnel blasting and bench blasting is that tunnel blasting is done towards one free surface while bench blasting is done towards two or more free surfaces. The rock is thus more constricted in the case of tunneling and a second free face has to be created towards which the rock can break and be thrown away from the surface. This second face is produced by a cut in the tunnel face and can be either a parallel hole cut, a V-cut, a fan-cut or other ways of opening up the tunnel face.

After the cut opening is made, the stoping towards the cut will begin. The stoping can be compared with bench blasting, but it requires a higher specific charge due to higher drilling deviation, desire for good fragmentation, and absence of hole inclination. In addition, overcharge of a tunnelblast does not have the same disastrous effect as in an open air blast, where high precision in calculation is a must.

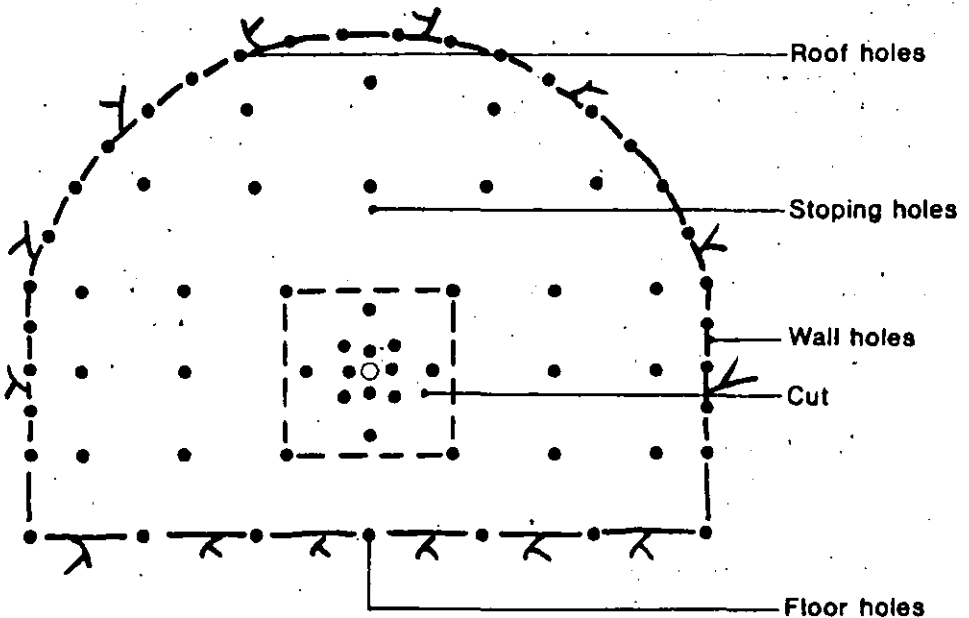


Fig. 7.2 Nomenclature.

In the case of V-cuts and fan cuts, the cut holes will occupy the major part of the width of the tunnel.

The contour holes – roof holes, wall holes and floor holes – have to be angled out of the contour, "look-out", so the tunnel will retain its designed area. The "look-out" should only be big enough to allow space for the drilling equipment for the coming round. As a guide value, the "look-out" should not exceed:

$$10 \text{ cm} + 3 \text{ cm/m hole depth}$$

which keeps the "look-out" to around 20 cm.

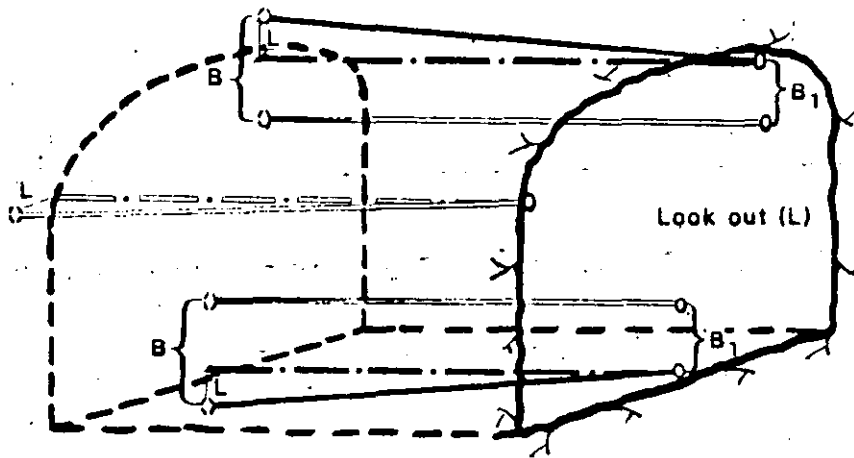


Fig. 7.3 Look-out.

The consumption of explosives in tunnel blasting is higher than in bench blasting. The specific charge is 3 to 10 times higher than that for bench blasting, depending mainly on reasons mentioned above like large drilling scatter, higher fixation of the holes, heave of lower rock upwards to ensure swell and lack of cooperation between adjacent blastholes.

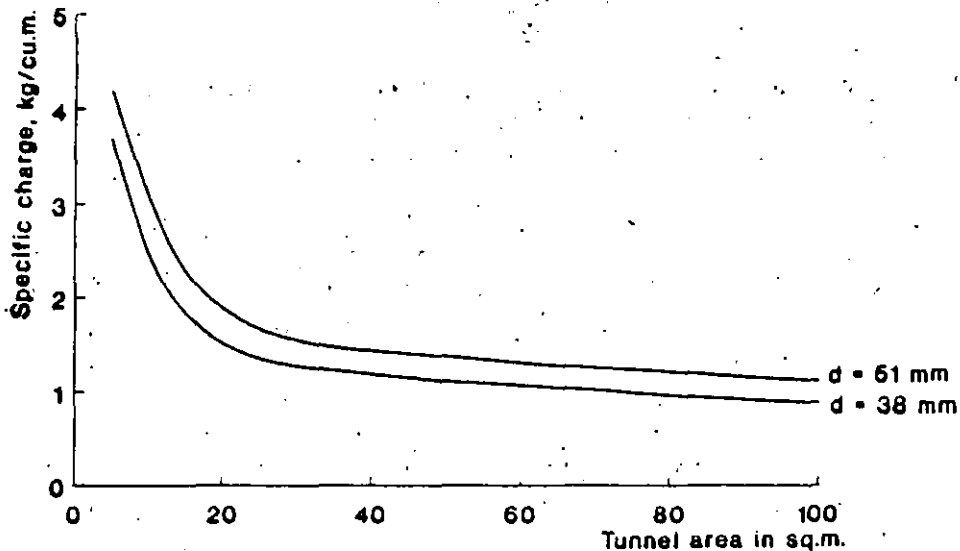


Fig. 7.4 Specific charge for different tunnel areas.

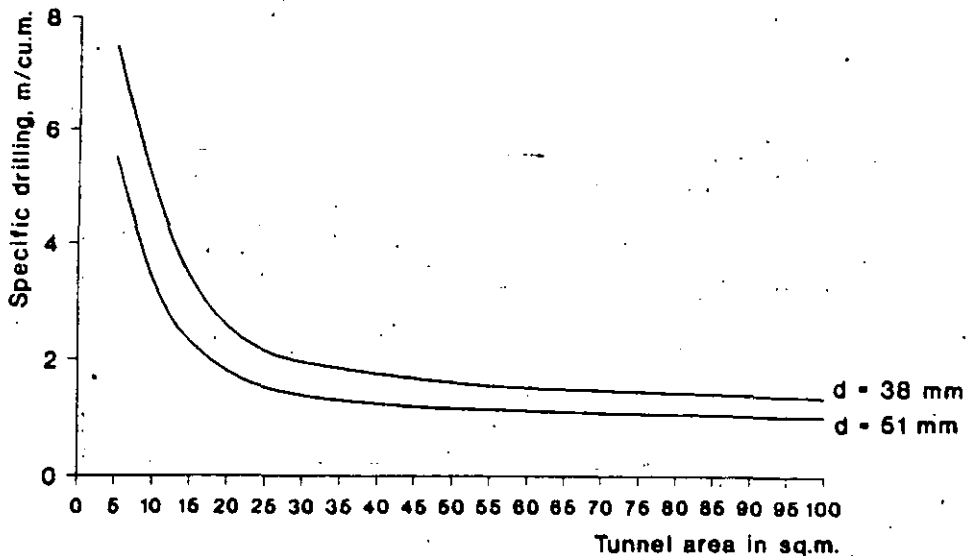


Fig. 7.5 Specific drilling for different tunnel areas.

The consumption of explosives will be greatest in the cut area of the blast. A 1×1 m area around the empty hole/s in a parallel cut will consume approx. 7 kg/cu.m. and the specific charge will decrease with the distance from the cut until it reaches a minimum value of about 0.9 kg/cu.m.

7.1.1 The cut.

The most commonly used cut in tunneling today is the **circular cut** or **large hole cut** as most of the modern drilling equipment is designed for horizontal drilling perpendicular to the rock face. (Other cuts will be dealt with in the end of this chapter.)

All cut holes in the large hole cut are drilled parallel to each other and the blasting is carried out towards an empty large drill hole which acts as an opening. The parallel hole cut is a development of the **burn cut**, where all the holes are parallel and normally of the same diameter. One hole in the middle is given a heavy charge and the four holes around it are left uncharged, in other cases the middle hole is left uncharged and the four holes are charged.

However, the burn cuts generally result in less advance than the large hole cuts. The burn cut will therefore be disregarded and only the **large hole cuts** will be dealt with.

The cut may be placed at any location on the tunnel face, but the location of the cut influences the throw, the explosives' consumption and generally the number of holes in the round.

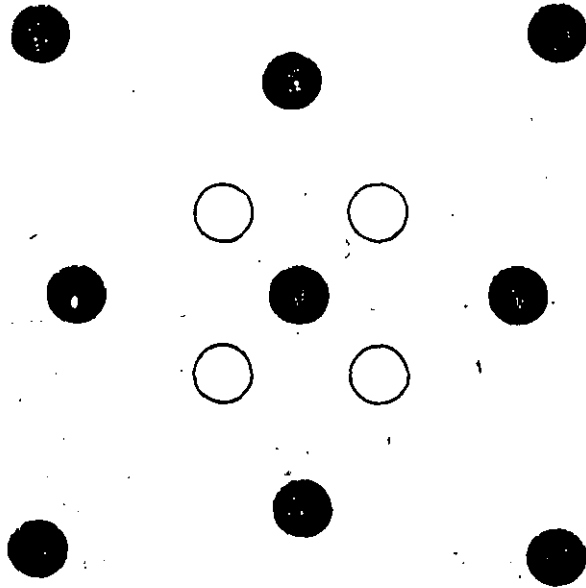


Fig. 7.6 Burn cut.

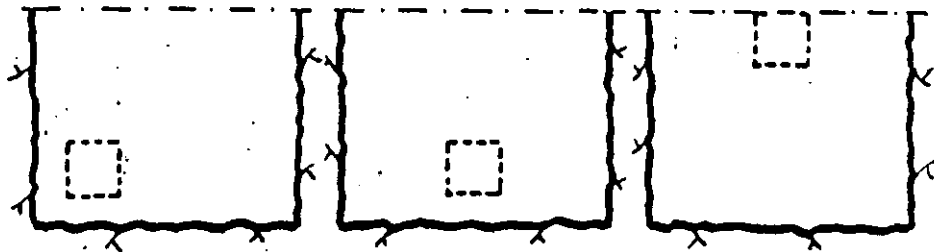


Fig. 7.7 Location of the cut.

If the cut is placed close to a wall, there is a probability of better exploitation of the drilling pattern with less holes in the round. Furthermore, the cut may be placed alternatively on the right or left side thus placing the cut in relatively undisturbed rock. To obtain good forward movement and centering of the muckpile, the cut may be placed approximately in the middle of the cross section and quite low down. This position will give less throw and less explosives' consumption because of more stoping downwards. A high position of the cut gives an extended and easily loaded muckpile, but higher explosives' consumption and normally more drilling due to more upwards stoping.

The normal location of the cut is on the first helper row above the floor. As mentioned before, the large hole cut is the most common cut today. The cut is composed of one or more uncharged large diameter holes which are surrounded by small diameter blastholes with small burdens to the large hole/s. The blastholes are placed in squares around the opening.

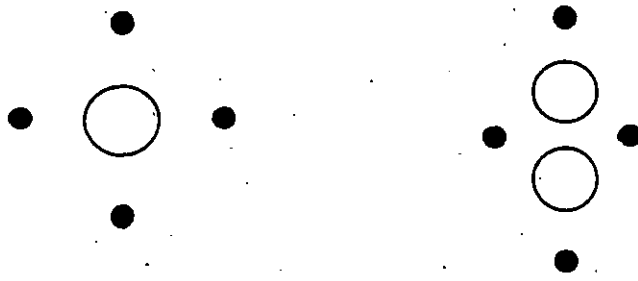


Fig. 7.8 Typical designs of large hole cuts.

The number of squares in the cut is limited by the fact that the burden in the last square must not exceed the burden of the stopping holes for a given charge concentration in the hole.

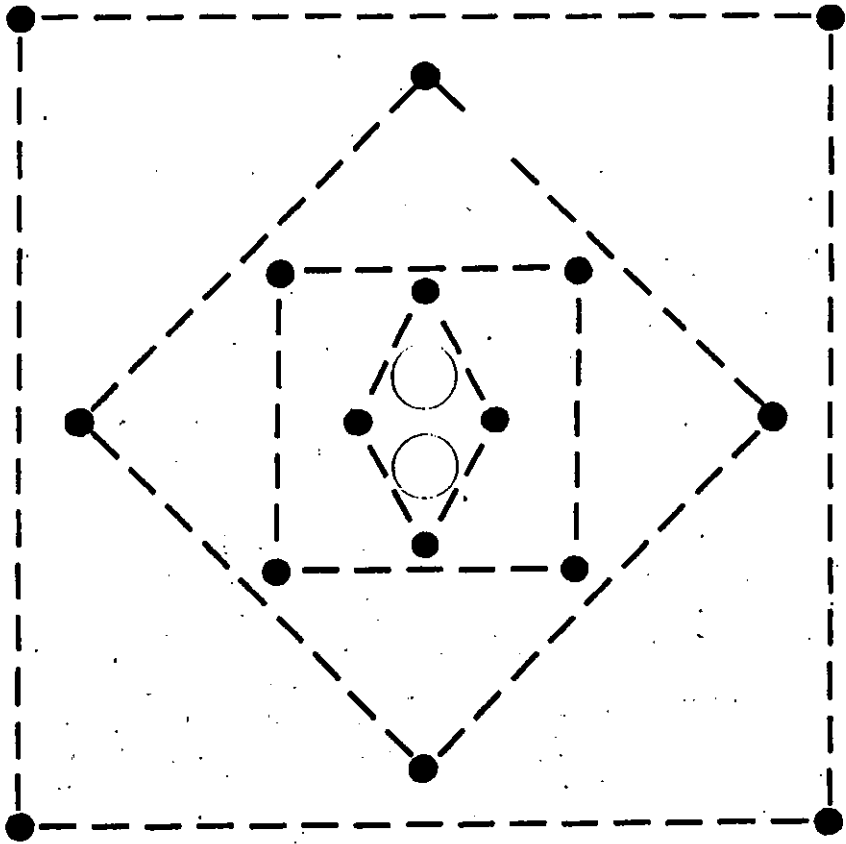


Fig. 7.9 The complete cut.

The cut holes occupy an area of approx. 2 sq. m. (Small tunnel areas, as a matter of fact, consist only of cut holes and contour holes.)

When designing the cut, the following parameters are of importance for a good result:

- the diameter of the large hole
- the burden
- the charge concentration.

In addition, the drilling precision is of the utmost importance, especially for the blast-holes closest to the large hole/s. The slightest deviation can cause the blasthole to meet the large hole or the burden to become excessively big. Too big a burden will only cause breakage or plastic deformation in the cut, resulting in a smaller or greater loss in advance.

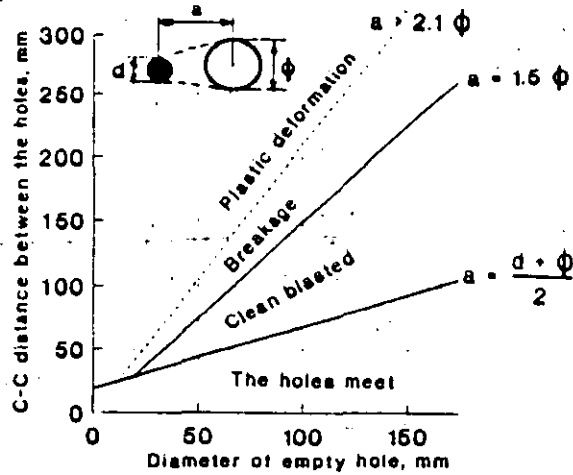


Fig. 7.10 Result when blasting from varying distances towards an empty hole of varying diameter.

(The Modern Technique of Rockblasting)

One of the parameters for good advance of the blasted round is the diameter of the large empty hole. The larger the diameter, the deeper the round may be drilled and a greater advance can be expected.

One of the most common causes of short advance is too small an empty hole in relation to the hole depth.

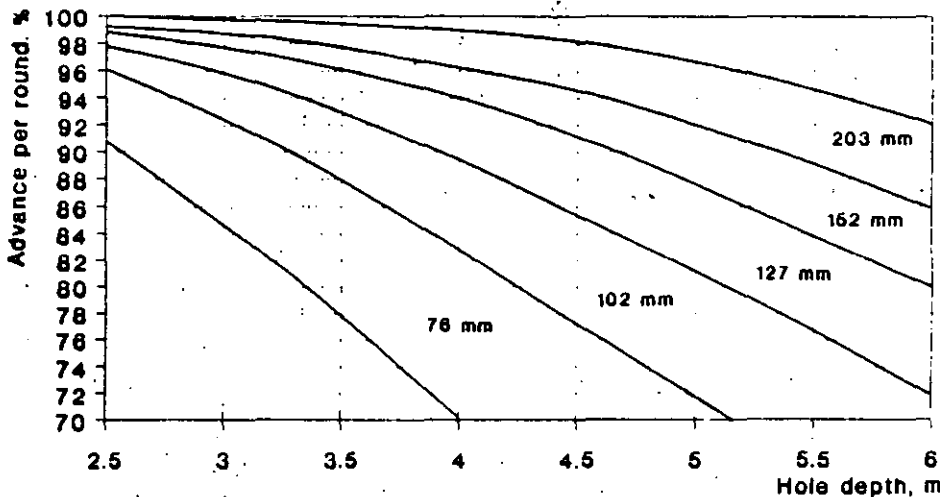


Fig. 7.11 The relation between advance in per cent of the drill depth and different empty hole diameters.

As can be seen from the graph, an advance of approx. 90 % can be expected for a hole depth of 4 m and one empty hole with 102 mm diameter.

If several empty holes are used, a fictitious diameter has to be calculated. The fictitious diameter of the opening may be calculated in accordance with the following formula:

$$D = d\sqrt{n}$$

where D = fictitious empty large hole diameter
 d = diameter of empty large holes
 n = number of holes

In order to calculate the burden in the first square, the diameter of the large hole is used in the case of one large hole and the fictitious diameter in the case of several large holes.

Calculation of the 1st square.

If we look at the graph 7.10 we find that the distance between the blasthole and the large empty hole should not be greater than $1.5 \emptyset$ for the opening to be clean blasted. If the distance is longer, there is merely breakage and when the distance is shorter, there is a great risk that the blasthole and empty hole will meet.

So the position of the blastholes in the 1st square is expressed as:

$$a = 1.5 \emptyset$$

Where a = C-C distance between the large hole and the blasthole
 \emptyset = diameter of the large hole

In the case of several large holes, the relation is expressed as:

$$a = 1.5 D$$

Where a = C-C distance between the center point of the large holes and the blasthole
 D = fictitious diameter

Charging of the holes in the 1st square.

The holes closest to the empty hole/s must be charged carefully. Too low a charge concentration in the hole may not break the rock, while too high a charge concentration may throw the rock against the opposite wall of the large hole with such high a velocity that the broken rock will be recompacted there and not blown out through the large hole. Full advance is then not obtained.

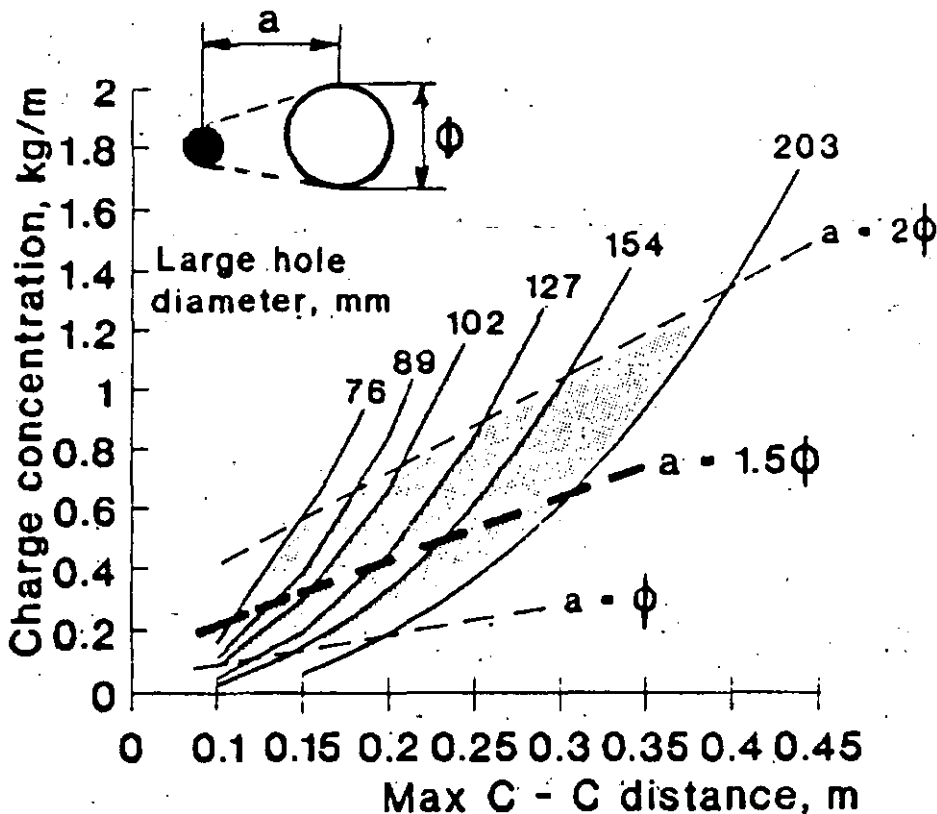


Fig. 7.12 The minimum required charge concentration (kg/m) and maximum C-C distance (m) for different large hole diameters.

The requisite charge concentration for different C-C distances between the large hole and the nearest blasthole/s may be found in graph 7.10 for different large hole diameters. The normal relation for the distance is $a=1.5 \phi$. An increase in the C-C distance between the holes will cause subsequent increment of the charge concentration.

The cut is often somewhat overcharged to compensate for error in drilling which may cause too small an angle of breakage. However, too high a charge concentration may cause recompaction in the cut.

Calculation of the remaining squares of the cut.

The calculation method for the remaining squares of the cut is essentially the same as for the 1st square, with the difference that the breakage is towards a rectangular opening instead of a circular.

As is the case of the 1st square, the angle of breakage must not be too acute as small angles of breakage can only be compensated to a certain extent with higher charge concentration.

Normally the burden (B) for the remaining squares of the cut is equal to the width (W) of the opening. $B=W$.

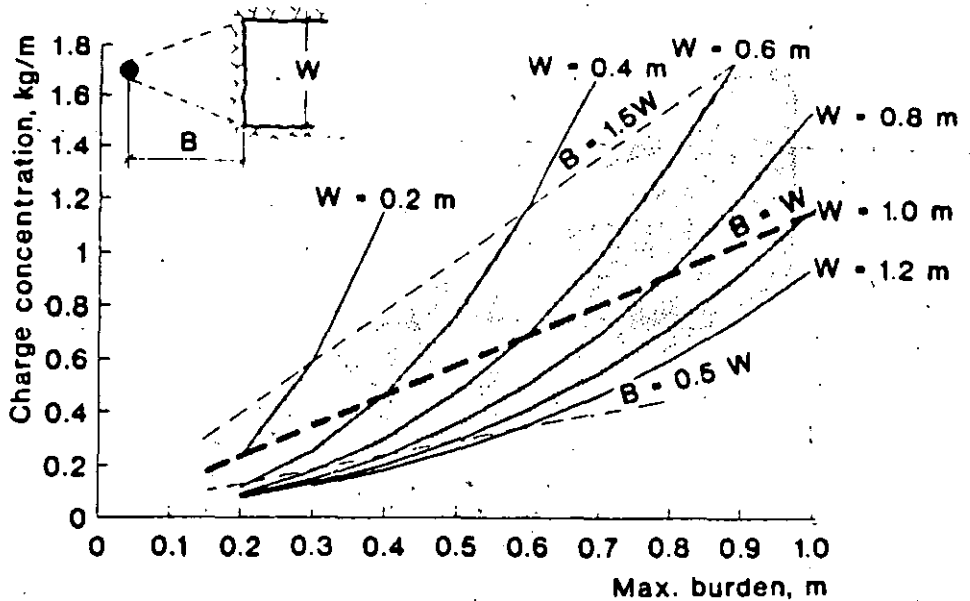


Fig. 7.13 The required minimum charge concentration (kg/m) and maximum burden (m) for different widths of the opening.

The charge concentration obtained in graph 7.12 is that of the column of the hole. In order to break the constricted bottom part, a bottom charge with twice the charge concentration and a height of $1.5 \times B$ should be used. The stemming part of the hole has a length of $0.5 \times B$.

Design of cut.

The following formulae are used for the geometric design of the cut area:

The cut:

1st square:

$$a = 1.5 \varnothing$$

$$W_1 = a\sqrt{2}$$

\varnothing mm =	76	89	102	127	154
--------------------	----	----	-----	-----	-----

a mm =	110	130	150	190	230
--------	-----	-----	-----	-----	-----

W_1 mm =	150	180	210	270	320
------------	-----	-----	-----	-----	-----



2nd square:

$$B_1 = W_1$$

$$C-C = 1.5W_1$$

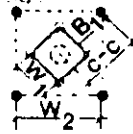
$$W_2 = 1.5W_1\sqrt{2}$$

\varnothing mm =	76	89	102	127	154
--------------------	----	----	-----	-----	-----

W_1 mm =	150	180	210	270	320
------------	-----	-----	-----	-----	-----

C-C =	225	270	310	400	480
-------	-----	-----	-----	-----	-----

W_2 mm =	320	380	440	560	670
------------	-----	-----	-----	-----	-----



3rd square:

$$B_2 = W_2$$

$$C-C = 1.5W_2$$

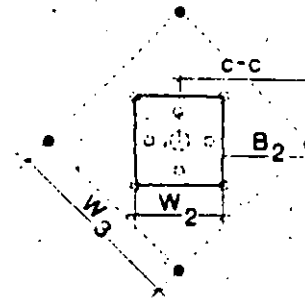
$$W_3 = 1.5W_2\sqrt{2}$$

\varnothing mm =	76	89	102	127	154
--------------------	----	----	-----	-----	-----

W_2 mm =	320	380	440	560	670
------------	-----	-----	-----	-----	-----

C-C =	480	570	660	840	1000
-------	-----	-----	-----	-----	------

W_3 mm =	670	800	930	1180	1400
------------	-----	-----	-----	------	------



4th square:

$$B_3 = W_3$$

$$C-C = 1.5W_3$$

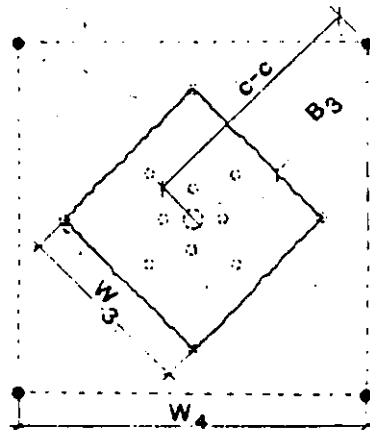
$$W_4 = 1.5W_3\sqrt{2}$$

\varnothing mm =	76	89	102	127
--------------------	----	----	-----	-----

W_3 mm =	670	800	930	1180
------------	-----	-----	-----	------

C-C =	1000	1200	1400	1750
-------	------	------	------	------

W_4 mm =	1400	1700	1980	2400
------------	------	------	------	------



The above distances apply to 38-mm blastholes. If larger blastholes are used which can accommodate more explosives, the values can be adjusted.

However, an increased amount of explosives in the cut holes may not increase the burden to any greater extent.

7.1.2 Stopping.

When the cut holes have been calculated, the rest of the tunnel round may be calculated.

The round is divided into:

- * floor holes
- * wall holes
- * roof holes
- * stopping holes with breakage upwards and horizontally
- * stopping holes with breakage downwards

To calculate burdens (B) and charges for the different parts of the round the following graph (7.14) may be used as a basis.

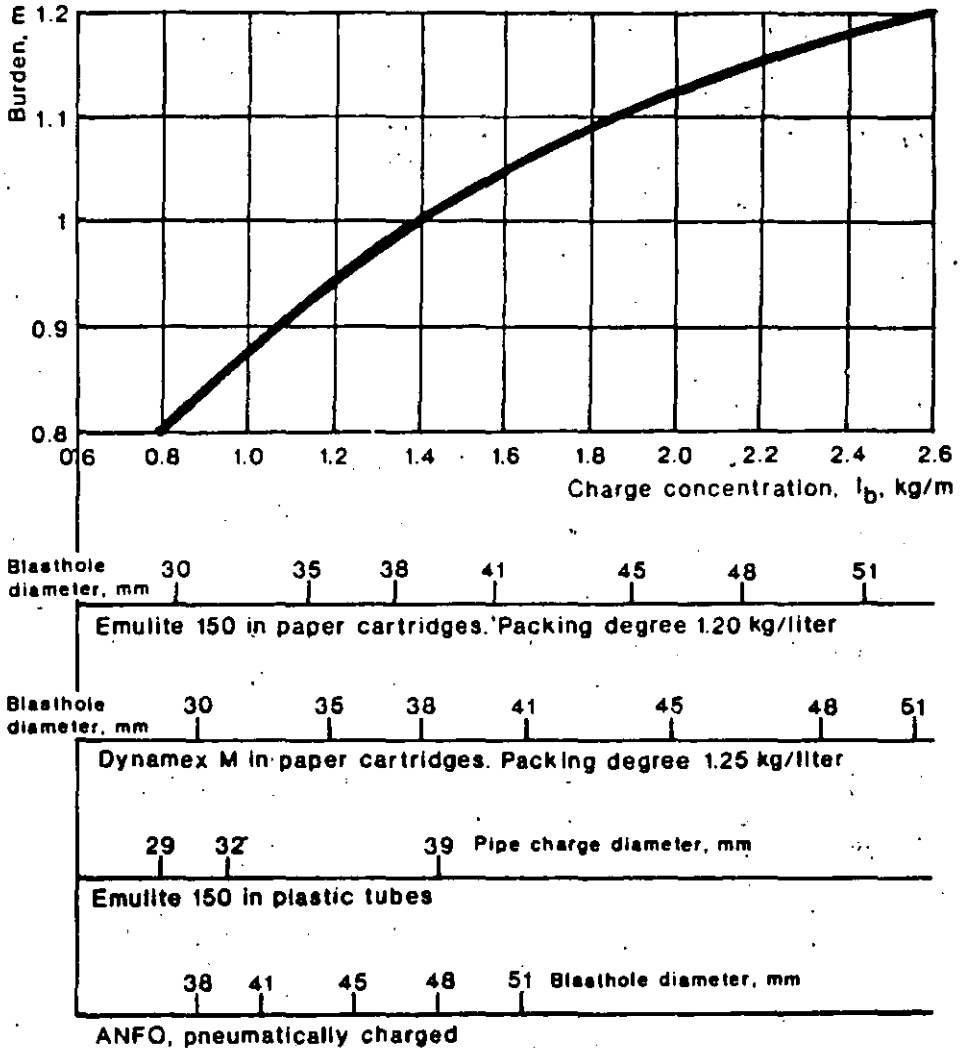


Fig. 7.14 The burden B in relation to the concentration of the bottom charge for different hole diameters and different explosives.

For Emulite 150 in paper cartridges, the uppermost blasthole diameter table is used as input data.

For Emulite 150 and Dynamex M in plastic pipe cartridges, the pipe diameter is used as input data and for ANFO the lowest blasthole diameter table is used as input data.

When the burden (B), the hole depth (H) and the concentration of the bottom charge (l_b) are known, the following table will give the drilling and charging geometry of the round.

Part of the round:	Burden (m)	Spacing (m)	Height bottom charge (m)	Charge concentration		Stemming (m)
				Bottom (kg/m)	Column (kg/m)	
Floor	$1 \times B$	$1.1 \times B$	$1/3 \times H$	l_b	$1.0 \times l_b$	$0.2 \times B$
Wall	$0.9 \times B$	$1.1 \times B$	$1/6 \times H$	l_b	$0.4 \times l_b$	$0.5 \times B$
Roof	$0.9 \times B$	$1.1 \times B$	$1/6 \times H$	l_b	$0.3 \times l_b$	$0.5 \times B$
Stoping:						
Upwards	$1 \times B$	$1.1 \times B$	$1/3 \times H$	l_b	$0.5 \times l_b$	$0.5 \times B$
Horizontal	$1 \times B$	$1.1 \times B$	$1/3 \times H$	l_b	$0.5 \times l_b$	$0.5 \times B$
Downwards	$1 \times B$	$1.2 \times B$	$1/3 \times H$	l_b	$0.5 \times l_b$	$0.5 \times B$

The design of the drilling pattern can now be carried out and the cut located in the cross section in a suitable way.

7.1.3 The contour.

The contour of the tunnel is divided into floor holes, wall holes and roof holes. The burden and spacing for the floor holes are the same as for the stoping holes. However, the floor holes are more heavily charged than the stoping holes to compensate for gravity and for the weight of the rock masses from the rest of the round which lay over them at the instant of detonation.

For the wall and roof holes two variants of contour blasting are used, **normal profile blasting** and **smooth blasting**.

With **normal profile blasting** no particular consideration is given to the appearance and condition of the blasted contour. The same explosives as in the rest of the round are utilized (but with a lesser charge concentration) and the contour holes are widely spaced. The contour of the tunnel becomes rough, irregular and cracked. The **smooth blasting** technique has been developed to obtain a smoother and stronger tunnel profile.

Smooth blasting is carried out by drilling the contour holes rather close to each other and using weaker explosives. (Gurit 17×500 mm and Gurit 11×460 mm have been specially developed for the requirements of smooth blasting.)

Smooth blasting is today a common technique in underground rock excavation as it produces tunnels with a regular profile, requiring substantially less reinforcement than if normal profile blasting is used.

Smooth blasting is dealt with in detail in Chapter 8.4 Smooth blasting, where charging tables for smooth blasting can be found.

7.1.4 The firing pattern.

The firing pattern must be designed so that each hole has free breakage. The angle of breakage is smallest in the cut area where it is around 50° . In the stopping area the firing pattern should be designed so that the angle of breakage does not fall below 90° .

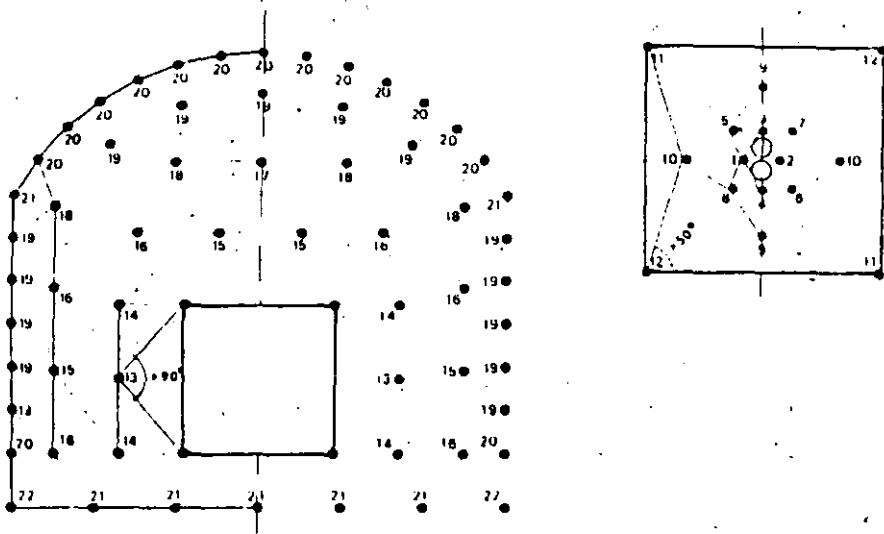


Fig. 7.15 Firing sequence for tunnel in numerical order.

It is important in tunnel blasting to have long enough time delay between the holes. In the cut area, the delay between the holes must be long enough to allow time for breakage and throw of rock through the narrow empty hole. It is proved that the rock moves with a velocity of 40 to 60 meters per second. A cut drilled to 4 m depth would thus require a delay time of 60 to 100 ms to be clean blasted. Normally delay times of 75 to 100 ms are used in the cut.

In the first two squares of the cut only one detonator of each delay should be used. In the following 2 squares two detonators of each delay may be used. In the stopping area, the delay time must be long enough for the movement of the rock. Normally the delay time is 100 to 500 milliseconds.

For the contour holes the scatter in delay between the holes should be as small as possible to obtain a good smooth blasting effect. Therefore, the roof should be blasted with the same interval number, normally the second highest of the series. The walls are also blasted with the same period number but with one delay lower than that of the roof.

Detonators for tunneling can be electric or non-electric.

The electric detonators are manufactured as MS (millisecond) and HS (half-second) delay detonators.

The non-electric detonators are manufactured as deci-second and half-second delay detonators.

Recommended detonators for tunneling:

Electric detonators:

	Interval No.	Delay time
VA/MS	<u>1</u>	25 ms
VA/MS	<u>4</u>	100 ms
VA/MS	<u>7</u>	175 ms
VA/MS	<u>10</u>	250 ms
VA/MS	<u>13</u>	325 ms
VA/MS	<u>16</u>	400 ms
VA/MS	<u>18</u>	450 ms
VA/MS	<u>20</u>	500 ms
VA/HS	2	1.0 sec
VA/HS	3	1.5 sec
VA/HS	4	2.0 sec
VA/HS	5	2.5 sec
VA/HS	6	3.0 sec
VA/HS	7	3.5 sec
VA/HS	8	4.0 sec
VA/HS	9	4.5 sec
VA/HS	10	5.0 sec
VA/HS	11	5.5 sec
VA/HS	12	6.0 sec

The MS and HS series give 19 periods which is sufficient in most cases. The VA/MS and VA/HS detonators may be used in the same round, as the electric characteristics of the VA detonators are the same, independent of the delay times.

Recommended legwire lengths for a 4 m hole depth are 5.0 and 6.0 m.

Non-electric detonators:

	Interval numbers	Delay time	Delay time between intervals
Nonel GT/T	0	25 ms	
Nonel GT/T	1-12	100-1200 ms	100 ms
Nonel GT/T	14, 16		
	18, 20	1400-2000 ms	200 ms
Nonel GT/T	25, 30, 35		
	40, 45, 50		
	55, 60	2500-6000 ms	500 ms

This tunnel series gives 25 different periods and is thus even more versatile than the electric tunnel series.

Recommended tube lengths for bunch blasting with Nonel are 6.0 to 7.8 m.

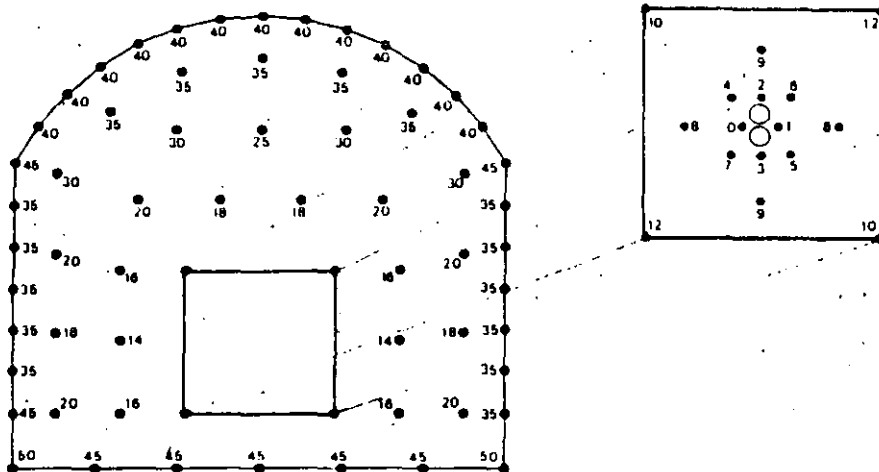


Fig. 7.16 Typical firing pattern for NONEL GTIT.

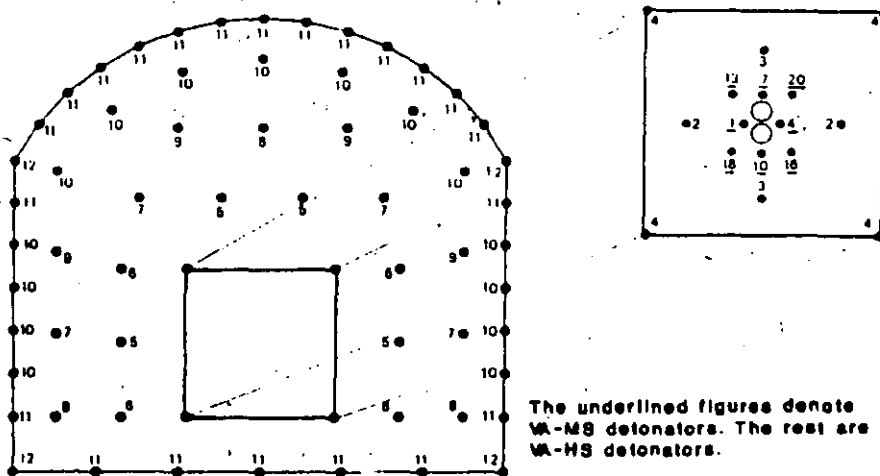


Fig. 7.17 Typical firing pattern for VA/MS and VA/HS detonators.

In the 4th square of the cut, four units of VA/HS interval No. 4 are used. This is made possible by wide range of scatter (± 200 ms) within the interval for HS detonators.

7.1.5 Cuts with angled holes.

The V-cut.

The most common cut with angled holes is the V-cut.

A certain tunnel width is required in order to accommodate the drilling equipment. Furthermore, the advance per round increases with the width and an advance of 45 to 50 % of the tunnel width is achievable.

The angle of the cut must not be too acute and should not be less than 60° . More acute angles require higher charge concentration in the holes.

The cut normally consists of two V:s but in deeper rounds the cut may consist of triple or quadruple V:s.

Each V in the cut should be fired with the same interval number using MS detonators to ensure coordination between the blastholes with regard to breakage. As each V is blasted as an entity one after the other, the delay between the different V:s should be in the order of 50 ms to allow time for displacement and swelling.

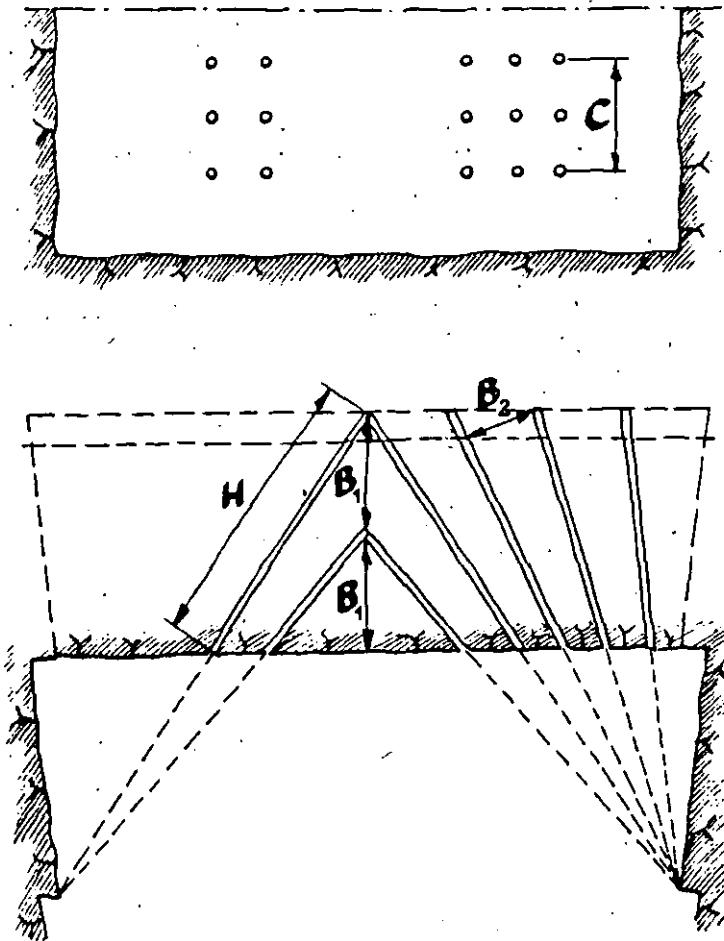


Fig. 7.18 V-cut.

Calculation of the V-cut.

The following graph (7.19) gives the height of the cut (C) and the burdens B_1 and B_2 for the cut.

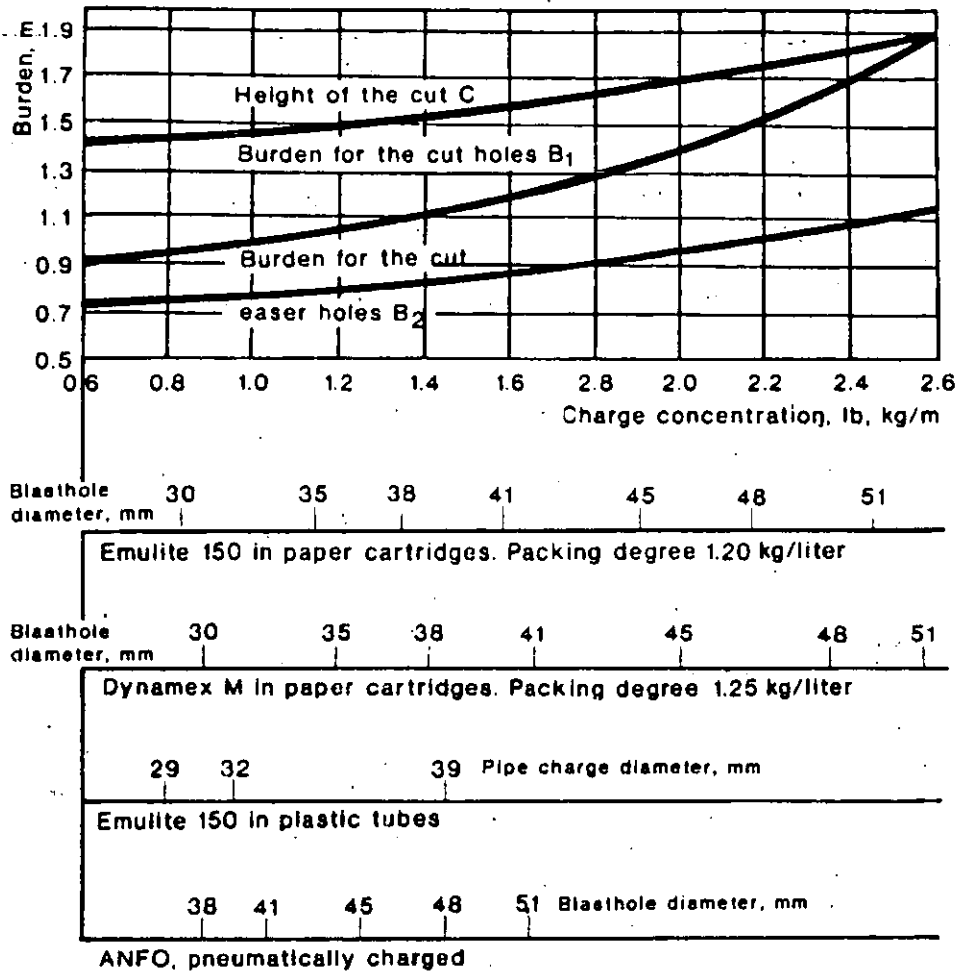


Fig. 7.19 The burdens B_1 , B_2 and the cut height C in relation to the bottom charge for different blasthole diameters and different explosives.

Charging the cut holes.

The charge concentration in the bottom of the cut holes (l_b) can be found in graph 7.19.

The height of the bottom charge (h_b) for all cut holes is:

$$h_b = \frac{1}{3} \times H \quad \text{where } H = \text{hole depth (m)}$$

The concentration of the column charge (l_c) is:

$$l_c = 30 \text{ to } 50 \% \text{ of } l_b$$

The uncharged part (stemming) of the holes in the cut (h_0) is:

$$h_0 = 0.3 \times B_1$$

The uncharged part for the rest of the cut is:

$$h_0 = 0.5 \times B_2$$

For the rest of the round, the method of calculation is the same as that in Chapter 7.1.2 Stoping.

The fan cut.

The fan cut is another example of angled cuts. Like the V-cut, a certain width of tunnel is required to accommodate the drilling equipment to attain acceptable advance per round.

The principle of the fan cut is to make a trench like opening across the tunnel and the charge calculations are similar to those in Chapter 5.6 Opening the bench. Due to the geometrical design of the cut the constriction of the holes is not large, making the cut easy to blast.

The drilling and charging of the holes are similar to that of the cut holes in the V-cut.

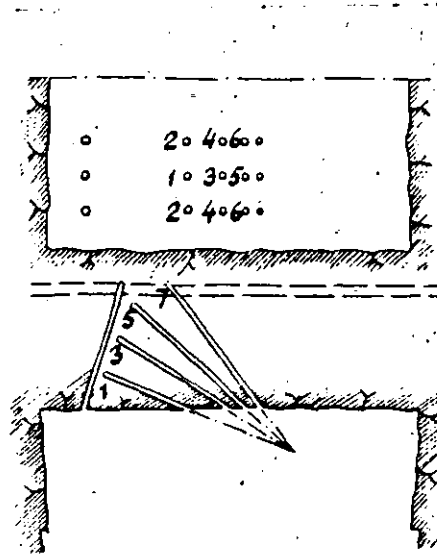


Fig. 7.20 Fan cut.

7.1.6 Example of calculation.

The project is a 1,500 m long road tunnel with a cross section area of 88 sq.m.

A blasthole diameter of 38 mm is chosen as the tunnel contour is to be smooth blasted. A larger blasthole diameter might cause overbreak from the stopping part of the round.

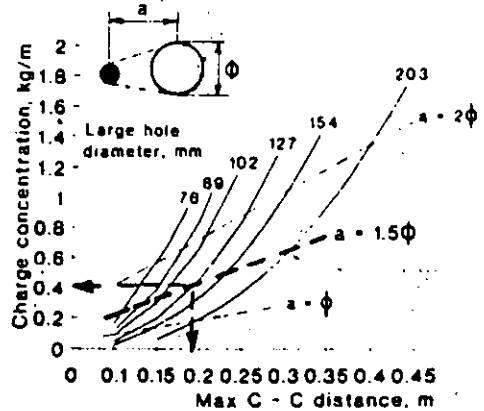
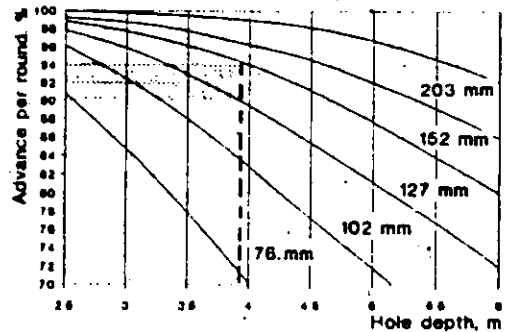
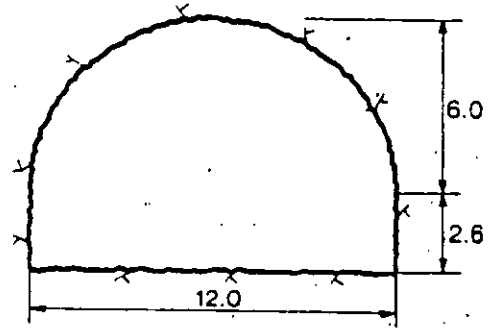
The drilling equipment is an electro hydraulic jumbo with 4.3 m steel length and feed travel of 3.9 m.

The expected advance is 95 % of the blasthole depth.

The explosive is Emulite 150 in 29 and 25 mm cartridges for the cut, stoping and floor. Gurit 17×500 mm in plastic cartridges is used for the contour. Nonel GT/T is used for initiation.

To attain an advance of more than 90 % of the blasthole depth, 3.9 m, a large hole diameter of 127 mm should be chosen.

2×89 mm large holes can be an alternative.



1st square.

The distance from the center of the large hole to the center of the closest blasthole is:

$$a = 1.5 \phi$$

$$a = 1.5 \times 127 = 190 \text{ mm}$$

The width of the 1st square is:

$$W_1 = a\sqrt{2}$$

$$W_1 = 190\sqrt{2} = 270 \text{ mm}$$

The requisite charge concentration for the holes in the 1st square is 0.4 kg/m of Emulite 150. For practical reasons Emulite in 25×200 mm cartridges are used giving a charge concentration of 0.55 kg/m.



An overcharge of this magnitude does not cause any inconvenience.

The uncharged part of the hole is equal to the C-C distance: $h_0 = a$

The charge of the hole is the length of the charge $H - h_0$ times the actual charge concentration.

$$Q = l_c(H - h_0)$$

$$Q = 0.55(3.9 - 0.2)$$

$$Q = 2.0 \text{ kg}$$

Key data for the 1st square:

$$a = 0.19 \text{ m}$$

$$W_1 = 0.27 \text{ m}$$

$$Q = 2.0 \text{ kg}$$

2nd square.

The blasting of the 1st square created an opening of $0.27 \times 0.27 \text{ m}$. The burden in the 2nd square is equal to the width of the opening created.

$$B_1 = W_1$$

$$B_1 = 0.27 \text{ m}$$

$$C-C = 1.5W_1$$

$$C-C = 0.40 \text{ m}$$

$$W_2 = 1.5W_1\sqrt{2}$$

$$W_2 = 0.56 \text{ m}$$

The requisite charge concentration for the holes in the 2nd square is approx. 0.37 kg/m .

Emulite 150 in $25 \times 200 \text{ mm}$ paper cartridges is used making the practical charge concentration 0.55 kg/m .

The uncharged part of the hole is $0.5 \times B$.

$$Q = l_c(H - h_0)$$

$$Q = 0.55(3.9 - 0.15)$$

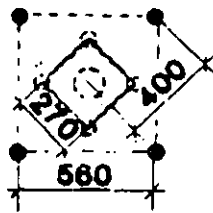
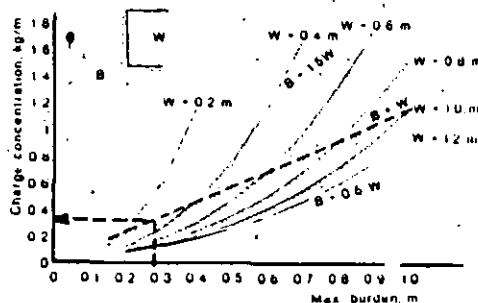
$$Q = 2.0 \text{ kg}$$

Key data for the 2nd square:

$$B = 0.27 \text{ m}$$

$$W_2 = 0.56 \text{ m}$$

$$Q = 2.0 \text{ kg}$$



3rd square.

The opening has now a width $W=0.56$ m. The burden B is equal to W_2 .

$$B_2 = W_2$$

$$B_2 = 0.56 \text{ m}$$

$$C-C = 1.5W_2$$

$$C-C = 0.84 \text{ m}$$

$$W_3 = 1.5W_2\sqrt{2}$$

$$W_3 = 1.18 \text{ m}$$

The requisite charge concentration is approx. 0.65 kg/m. Now the 25×200 mm cartridges do not provide sufficient charge concentration to ensure breakage. A larger dimension of Emulite 150 must be used unless the cartridges are tamped.

Emulite 29×200 mm in paper cartridges give a charge concentration of 0.90 kg/m. The hole will thus be overcharged.

The uncharged part of the hole is $0.5 \times B$.

$$Q = l_c(H-h_0)$$

$$Q = 0.90(3.9-0.3)$$

$$Q = 3.2 \text{ kg}$$

Key data for the 3rd square:

$$B = 0.56 \text{ m}$$

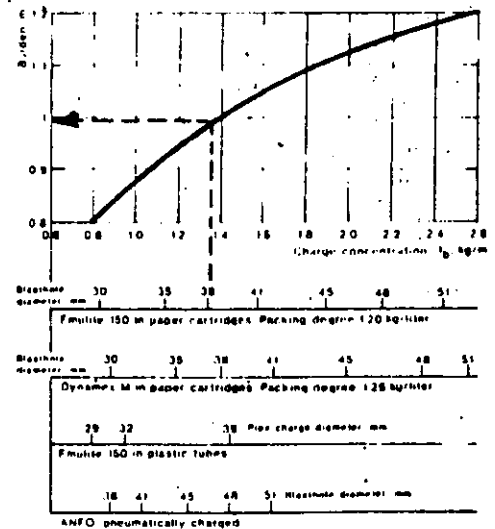
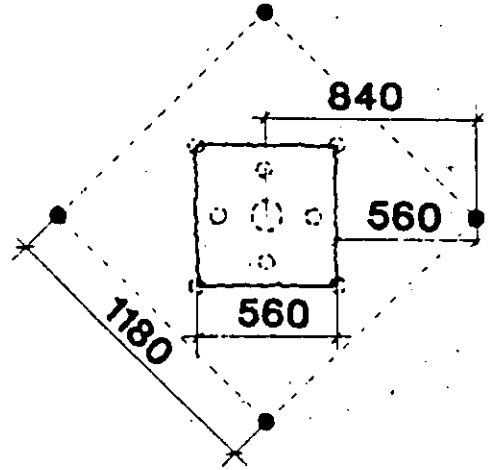
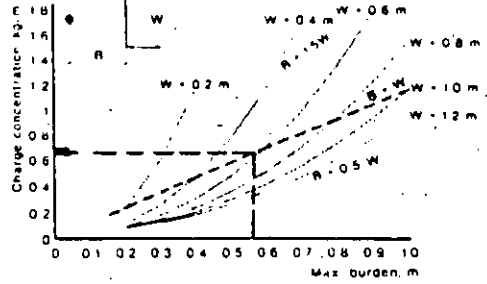
$$W_3 = 1.18 \text{ m}$$

$$Q = 3.2 \text{ kg.}$$

4th square.

The width of the opening is now 1.18 m. If B is chosen equal to W , the burden will be greater than that of the stoping part of the round. Therefore, the burden must be adjusted to that of the stoping part and the charge calculations are made as for stoping holes.

The burden is chosen from the graph 7.14 to 1.0 m.



The charge concentration of the bottom charge is found in the same graph to be 1.35 kg/m.

From the adjoining table the charge of the hole can be calculated,

$$l_b = 1.35 \text{ kg/m}$$

$$h_b = 1/3H$$

$$h_b = 0.33 \times 3.9$$

$$h_b = 1.3 \text{ m}$$

$$Q_b = l_b \times h_b$$

$$Q_b = 1.35 \times 1.3$$

$$Q_b = 1.75 \text{ kg}$$

Part of the round	Burden (m)	Spacing (m)	Height bottom charge (m)	Charge concentration		
				Bottom (kg/m)	Column (kg/m)	Stemming (m)
Floor	1.4-B	1.1-B	1.3-H	l_b	$0.4 \times l_b$	$0.2 \times B$
Wall	0.9-B	1.1-B	1.6-H	l_b	$0.4 \times l_b$	$0.5 \times B$
Roof	0.9-B	1.1-B	1.6-H	l_b	$0.3 \times l_b$	$0.5 \times B$
Sloping						
Upwards	1-B	1.1-B	1.3-H	l_b	$0.5 \times l_b$	$0.5 \times B$
Horizontal	1-B	1.1-B	1.3-H	l_b	$0.5 \times l_b$	$0.5 \times B$
Downwards	1-B	1.2-B	1.3-H	l_b	$0.5 \times l_b$	$0.5 \times B$

In the bottom charge Emulite in paper cartridges with 29 mm diameter is used and tamped well.

The column charge is:

$$l_c = 0.5 \times l_b$$

$$l_c = 0.5 \times 1.35$$

$$l_c = 0.67 \text{ kg/m}$$

The product with dimensions closest to this is Emulite 150, 29×200 mm with an $l_c = 0.90 \text{ kg/m}$

Practical $l_c = 0.90 \text{ kg/m}$

$$h_c = 0.5B$$

$$h_c = 0.5 \times 1.0 = 0.5 \text{ m}$$

$$h_c = H - h_b - h_o$$

$$h_c = 3.9 - 1.3 - 0.5$$

$$h_c = 2.1 \text{ m}$$

$$Q_c = l_c \times h_c$$

$$Q_c = 0.90 \times 2.1$$

$$Q_c = 1.9 \text{ kg}$$

$$Q_{tot} = Q_b + Q_c$$

$$Q_{tot} = 1.75 + 1.9$$

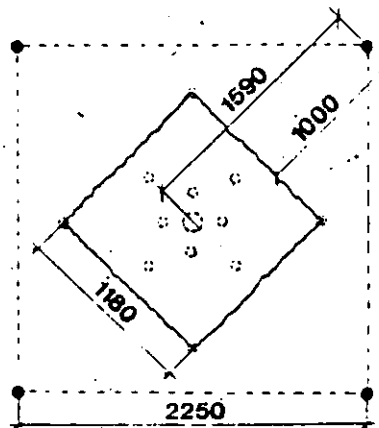
$$Q_{tot} = 3.65 \text{ kg}$$

Key data for the 4th square:

$$B = 1.0 \text{ m}$$

$$W_4 = 2.2 \text{ m}$$

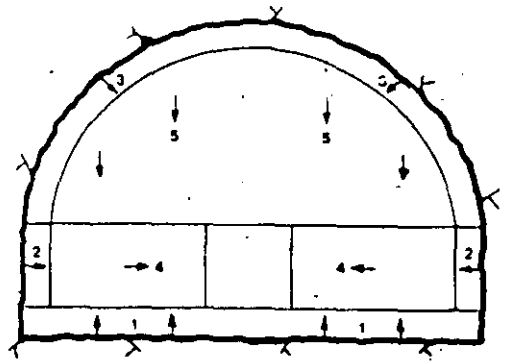
$$Q = 3.65 \text{ kg}$$



After the cut has been designed, the rest of the round is calculated.

This is most simply done in the following order:

1. Floor holes.
2. Wall holes.
3. Roof holes.
4. Stopping, upwards and horizontal.
5. Stopping downwards.



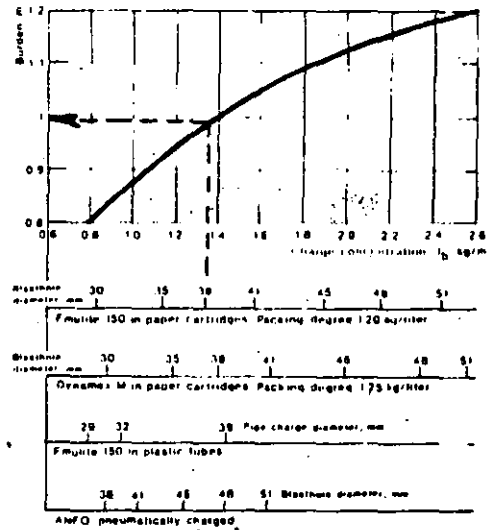
The reason for starting with the perimeter holes is to decide the burdens and spacings for the outer boundaries of the round.

When these calculations are completed the cut and the stoping holes may be located in accordance with the parameters which apply to them.

1. The floor holes.

In the calculation of all perimeter holes, the "look-out" has to be taken into account. As mentioned earlier, the "look-out" should not exceed 10 cm + 3 cm/m of hole depth. In this case the "look-out" should be limited to 20 cm.

The burden is 1.0 m according to the graph and the spacing is $1.1 \times B$. Due to "look-out", the holes above the floor holes are set out 0.8 m above the floor. The spacing is 1.1 m.



Bottom charge:

$$l_b = 1.35 \text{ kg/m}$$

$$h_b = 1/3 \times 3.90 = 1.30 \text{ m}$$

$$Q_b = 1.35 \times 1.3 = 1.75 \text{ kg}$$

Column charge:

$$l_c = l_b = 1.35 \text{ kg/m}$$

$$h_o = 0.2 \times B = 0.2 \text{ m}$$

$$h_c = H - h_b - h_o = 2.4 \text{ m}$$

$$Q_c = 1.35 \times 2.4 = 3.25 \text{ kg}$$

Total charge:

$$Q = 1.75 + 3.25 = 5.0 \text{ kg}$$

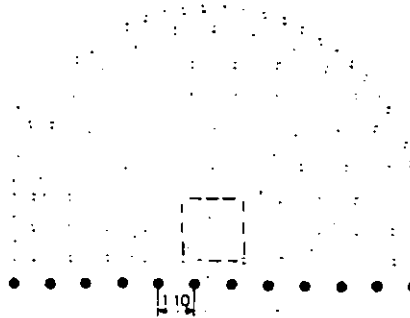
Part of the round	Burden (m)	Spacing (m)	Height bottom charge (m)	Charge concentration		Stomping (m)
				Bottom (kg/m)	Column (kg/m)	
Floor	1-B	1.1-B	1.3-H	l_b	1.0- l_b	0.2-B
Wall	0.9-B	1.1-B	1.6-H	l_b	0.4- l_b	0.5-B
Roof	0.9-B	1.1-B	1.6-H	l_b	0.3- l_b	0.5-B
Stopping Upwards	1-B	1.1-B	1.3-H	l_b	0.5- l_b	0.5-B
Horizontal	1-B	1.1-B	1.3-H	l_b	0.5- l_b	0.5-B
Downwards	1-B	1.2-B	1.3-H	l_b	0.5- l_b	0.5-B

Key data for floor holes:

B = 1.0 m

S = 1.1 m

Q = 5.0 kg.



2. The wall holes.

In this particular case the walls are very low and do not make a good example for the design of the drifting and charging pattern.

The drilling pattern is taken from the smooth blasting table and the burden is chosen to 0.8 m and the spacing to 0.6 m.

The uncharged part of the hole is 0.2 m.

The charge concentration for Gurit 17x500 mm is 0.23 kg/m. The holes will be charged with 7 tube charges and 1 stick of Emulite 150, 25x200 mm in the bottom.

Bottom charge:

$Q_b = 0.11 \text{ kg}$

Column charge:

$Q_c = 7 \times 0.115 = 0.81 \text{ kg}$

Total charge:

$Q = 0.11 + 0.81 = 0.92 \text{ kg}$

The "look-out" has to be considered, so the burden to be set out on the face is $0.8 - 0.2 = 0.6 \text{ m}$.

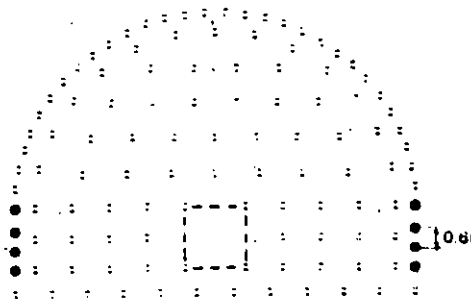
Key data for the wall holes:

B = 0.8 m

S = 0.6 m

Q = 0.92 kg

Perimeter hole diam mm	Charge concentration kg/m	Charge type	Burden m	Spacing m
25 32	0.11	11 mm Gurit	0.3 0.5	0.25 0.35
25 48	0.23	17 mm Gurit	0.7 0.9	0.50 0.70
51 64	0.42	22 mm Gurit	1.0 1.1	0.80 0.90
51 64	0.45	22 mm Emulite	1.1 1.2	0.80 0.90



3. The roof holes.

The conditions for the roof holes are equal to those of the wall holes. The burden is chosen to 0.8 m and the spacing to 0.6 m.

The charge concentration is the same as for the wall holes.

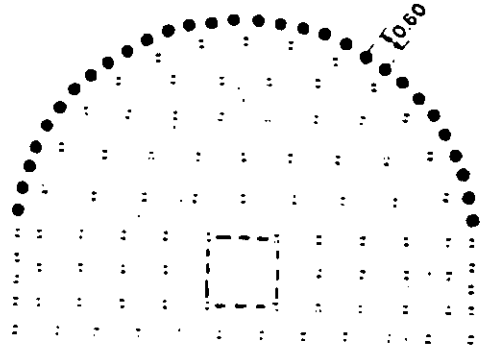
The "look-out" must be considered in this case as well.

Key data for the roof holes:

$$B = 0.8 \text{ m}$$

$$S = 0.6 \text{ m}$$

$$Q = 0.92 \text{ kg.}$$



4. Stopping upwards and horizontally.

The stopping holes are calculated in a similar way to the floor holes, but less explosives are needed. While the floor holes must be charged to compensate for gravity and heavage of broken rock, the stopping holes can normally contain less explosives as the direction of breakage is horizontal or close to horizontal.

Charge: Bottom, tamped Emulite 29 mm, $l_b = 1.35 \text{ kg/m}$.

Charge: Column, Emulite 29 mm in paper cartridges with $l_c = 0.90 \text{ kg/m}$.

The burden B is 1.0 m, according to the graph 7.14.

The spacing S will be 1.1 m according to adjoining table.

Bottom charge:

$$l_b = 1.35 \text{ kg/m}$$

$$h_b = 1/3 \times 3.90 = 1.30 \text{ m}$$

$$Q_b = 1.35 \times 1.3 = 1.75 \text{ kg}$$

Column charge:

$$l_c = 0.90 \text{ kg/m}$$

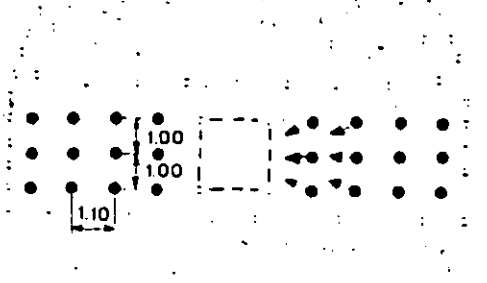
$$h_o = 0.5 \times B = 0.5 \text{ m}$$

$$h_c = H - h_b - h_o = 2.1 \text{ m}$$

$$Q_c = 0.90 \times 2.1 = 1.9 \text{ kg}$$

Total charge:

$$Q = 1.75 + 1.9 = 3.65 \text{ kg}$$



Part of the round	Burden (m)	Spacing (m)	Height bottom charge (m)	Charge concentration		
				Bottom (kg/m)	Column (kg/m)	Stemming (m)
Floor	1 - B	11 - B	13 - H	l_b	$1.0 \cdot l_c$	02 - B
Wall	0.9 - B	11 - B	16 - H	l_b	0.4 - l_c	05 - B
Roof	0.9 - B	11 - B	16 - H	l_b	0.3 - l_c	05 - B
Stopping						
★ Upwards	1 - B	11 - B	13 - H	l_b	0.5 - l_c	05 - B
★ Horizontal	1 - B	11 - B	13 - H	l_b	0.5 - l_c	05 - B
Downwards	1 - B	12 - B	13 - H	l_b	0.5 - l_c	05 - B

Key data for stoping holes upwards and horizontal:

B = 1.0 m

S = 1.1 m

Q = 3.65 kg

Part of the round	Burden (m)	Spacing (m)	Height bottom charge (m)	Charge concentration		Stemming (m)
				Bottom (kg/m)	Column (kg/m)	
Floor	1.1 × B	1.1 × B	1/3 × H	1 ₀	1.0 × 1 ₀	0.2 × B
Wall	0.9 × B	1.1 × B	1/6 × H	1 ₀	0.4 × 1 ₀	0.5 × B
Roof	0.9 × B	1.1 × B	1/6 × H	1 ₀	0.3 × 1 ₀	0.5 × B
Stoping:						
Upwards	1 × B	1.1 × B	1/3 × H	1 ₀	0.5 × 1 ₀	0.5 × B
Horizontal	1 × B	1.1 × B	1/3 × H	1 ₀	0.5 × 1 ₀	0.5 × B
Downwards	1 × B	1.2 × B	1/3 × H	1 ₀	0.5 × 1 ₀	0.5 × B

5. Stoping downwards.

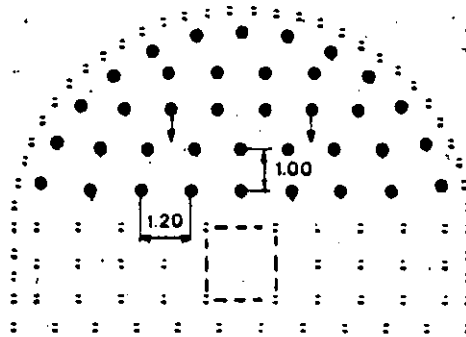
The design of the drilling pattern for stoping downwards is similar to stoping in other directions with the difference that larger spacing may be permitted. The charge of the holes is the same in all stoping.

Key data for stoping holes downwards:

B = 1.0 m

S = 1.2 m

Q = 3.65 kg



SUMMARY

The round consists of 127 blastholes with 38 mm diameter and 1 large hole with 127 mm diameter.

The round is charged as follows:

Part of the round	No. of holes	Kind of explosive	Weight per hole (kg)	Total (kg)
Cut				
1st square	4	Emulite 150, 25 mm	2.0	8.0
2nd square	4	Emulite 150, 25 mm	2.0	8.0
3rd square	4	Emulite 150, 29 mm	3.2	12.8
4th square	4	Emulite 150, 29 mm	3.65	14.6
Floor holes	12	Emulite 150, 29 mm	5.0	60.0
Wall holes	8	Emulite 150, 25 mm	0.11	0.9
		Gurit 17 mm	0.81	6.5
Roof holes	30	Emulite 150, 25 mm	0.11	3.3
		Gurit 17 mm	0.81	24.3
Stoping:				
Upwards	8	Emulite 150, 29 mm	3.65	29.2
Horizontal	16	Emulite 150, 29 mm	3.65	58.4
Downwards	37	Emulite 150, 29 mm	3.65	135.1

Consumption per round: Emulite 150, 25×200 mm	20.1 kg
Emulite 150, 29×200 mm	310.1 kg
Gurit	30.8 kg
Nonel GT/T	127 units

The expected advance per round is over 90 %. It is assumed to be 3.55 m.

Specific charge: $\frac{361.1}{3.55 \times 88.0} = 1.16 \text{ kg/cu.m.}$

Explosives consumption for the whole project:

Number of rounds: $1500/3.55=425$

Consumption of

Emulite 150, 25×200 mm $20.2 \times 425 = \text{approx. 9 tons}$

Emulite 150, 29×200 mm $310.1 \times 425 = \text{approx. 132 tons}$

Gurit $30.8 \times 425 = \text{approx. 13 tons}$

Nonel GT/T $127 \times 425 = \text{approx. 54000 units.}$

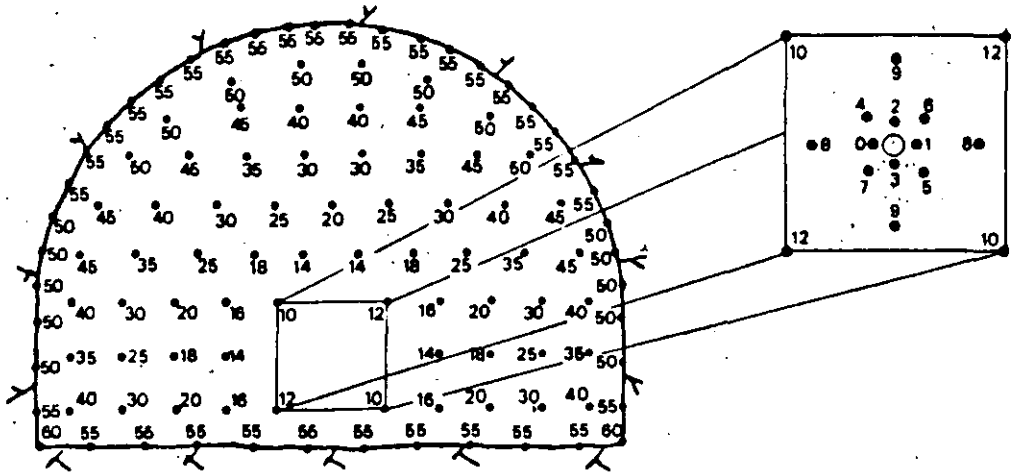


Fig. 7.21 Drilling and firing pattern.

7.2 Shafts.

In mining, shafts form a system of vertically or inclined passageways which are used for transportation of ore, refill, personnel, equipment, air, electricity, ventilation etc.

In underground construction, shafts are driven for the building of penstocks, cable shafts, ventilation and elevator shafts, surge chambers etc. In addition, shafts are driven as "glory holes" for transportation of material which is not accessible by other means than vertical or close to vertical tunnels.

Shafts are either driven downwards, sink shafts, or upwards, raise shafts.

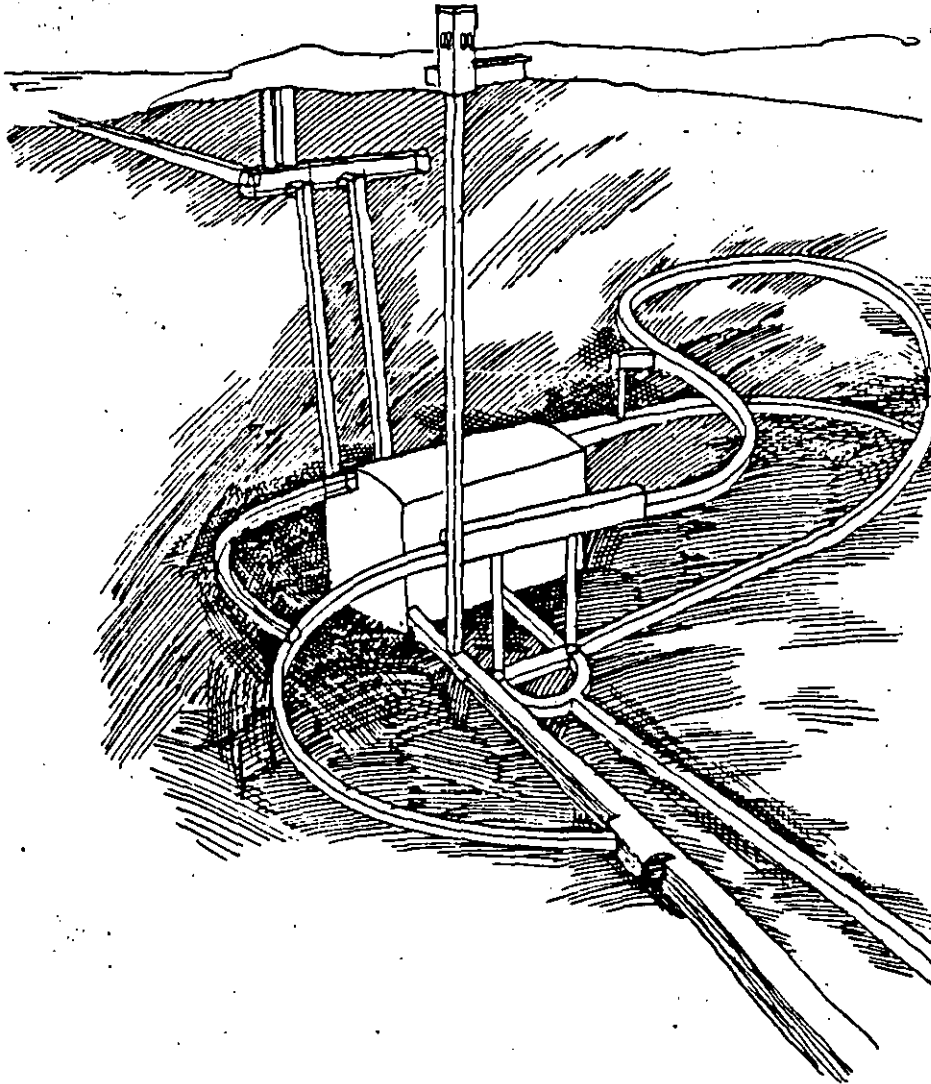


Fig. 7.22 Typical tunnel system in a hydroelectric power plant.

7.2.1 Sink shafts.

Sink shafts are passageways sunk from the surface downwards or underground from one level to a lower one. The majority of the sink shafts are driven vertically.

Shaft sinking is one of the most difficult and risky blasting jobs as the work area is normally wet, narrow and noisy. Furthermore, the drilling and blasting crews are exposed to falling objects.

The advance is slow as the rock has to be removed between each blast with special equipment which has limited digging capacity. The blasted rock must be well fragmented to suit the excavation equipment.

The design of the cross section of the shaft principally depends on the quality of the rock. Nowadays most of the shafts are made with a circular cross section which gives better distribution of the rock pressure, thus decreasing the need for reinforcement, especially in deep shafts.

The most common drilling and blasting methods are benching and blasting with pyramid cut.

The benching method is a fast and efficient method as the time-consuming cleaning of the floor between the blasts can be minimized. It is also easy to keep the shaft free from water as a pump can always be placed in the lower blasted part of the shaft. The drilling and charging pattern is similar to that of smaller surface blastings.

The burden and spacing vary with the hole diameter but the drilling pattern is more closely spaced than for surface blasting due to higher constriction.

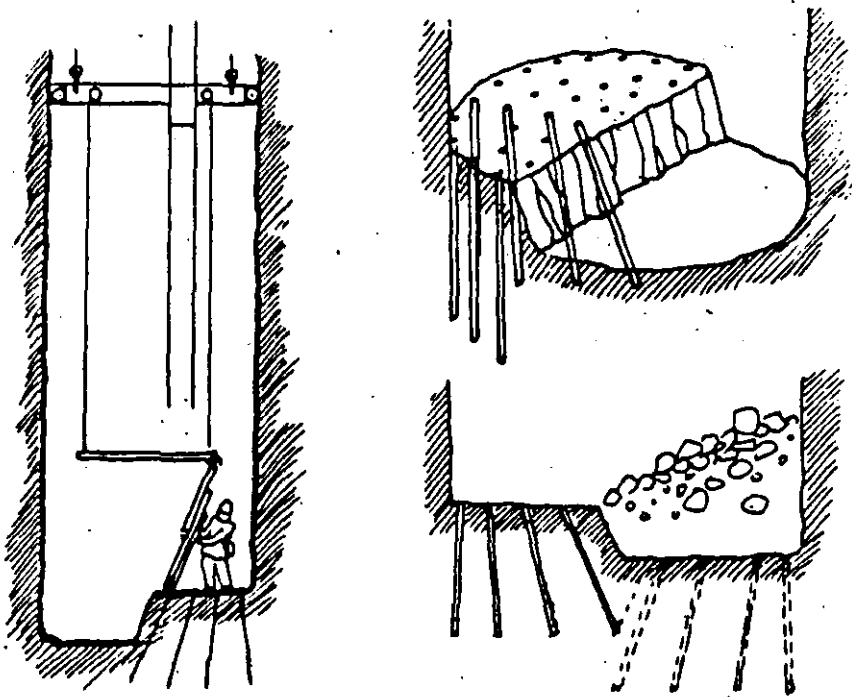


Fig. 7.23 Shaft sinking by benching.

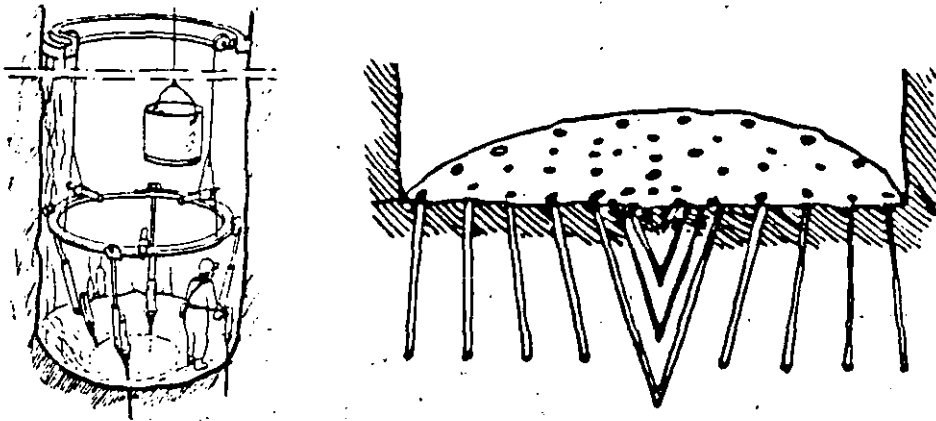


Fig. 7.24 Shaft sinking with pyramid cut.

Shaft sinking with **pyramid cuts** is similar to tunnel blasting with V-cuts. The drilling is done with a "drill-ring" which is composed of a circular I-beam to which the drilling machines are fixed. The "drill-ring" may be fixed to the shaft walls with bolts. Due to the construction of the "drill-ring", the cut will be conical.

The explosives used in shaft sinking must always be water resistant. Even if the ground is dry, the flushing water from the drilling will always stay in the blastholes.

For this reason explosives with excellent water resistance properties are preferred. Emulite 150 and Dynamex M are easily tamped to utilize the hole volume well, thus decreasing the number of holes and the drilling and charging time. The specific charge in shaft sinking is rather high, ranging from 2.0 kg/cu.m. to 4.0 kg/cu.m.

The initiation of the blast may be done with electric detonators or non-electric detonators. As a sink shaft is a small confined area, thunderstorms are a particular hazard as stray currents tend to be transmitted down the shaft on pipes and cables. To avoid problems with evacuation of the blasting crew during a thunderstorm, NONEL detonators should be used.

7.2.2 Raise shafts.

The drifting of raise shafts – shafts which are driven from blasted underground chambers or tunnels, vertically or inclined upwards – is one of the most difficult, most costly and most dangerous undertakings in mining and construction.

As the drifting of raise shafts has increased in the world, new methods have been developed to make the work more mechanized, cheaper and safer.

Raise shafts were drifted in more or less the same way for decades until the 1950's when new types of raise shaft elevators were taken into use.

Various raise shaft drifting methods where blasting is part of the method.

Older methods:

- Timbered shafts
- Open shafts

Modern methods:

- Boliden elevator type Jora
- Alimak Raise Climber
- Longhole drilling

To start with the older methods, the timbered shaft method was the most common method in Sweden until some 40 years ago and is still occasionally used for shorter shafts. The raise shaft is driven vertically and divided into two sections by a timber wall which is extended before each blast. When the round is fired, one section is filled with rock. The blasted rock will then act as a working platform for the next round. In order to maintain the working height at the face some rock has to be excavated after each blast. The second section is used as a ladderway and for transportation of equipment, drill steel, explosives and timber. The ventilation is also placed in this section which is covered during blasting.

Timbered raise shafts have been driven up close to 100 m, but normally the maximum height should not exceed 60 m. The cross section area is usually 4 sq.m. and the advance per round approx. 2.2 m.



Fig. 7.25 Timbered raise shaft.

The timbered shaft method was replaced by open shaft methods when the cost of timber became too high. In one of these methods a working platform of planks is laid on timber which is supported by bolts in the shaft walls. New bolt holes are drilled in the shaft walls when the round is drilled so the platform can be moved upwards as the work proceeds.

Another open shaft method is to use steel tubes instead of timber. The steel tubes are bolted to the shaft walls and the tubes support the platform.

The open shaft methods are rarely used and when used, only for short raises, up to 25 m. From a safety point of view none of the open shaft methods is to be recommended.

The cross section is normally 4 sq.m. and the advance approx. 2.2 m.

The JORA lift method.

Raise shafting using a lift cage hanging on a wire which runs through a large drillhole has been used in Sweden and other countries since the 1940's, but it was not until the 1950's when Boliden AB developed the JORA lift, that the method came into wider use.

A large hole, diameter 110 to 150 mm, is drilled from an upper level in the center of the intended shaft. Through the hole a wire is sunk down to the lower level and a working platform with a lift cage is fastened to it. By a lifting gear the platform is elevated up to the shaft face by remote control from the lift cage.

The drilling and charging are carried out from the platform on the top of the lift cage and some scaling can be done from the cage with the protection of the platform. During the scaling, drilling and charging operations the platform is fixed with bolts to the shaft walls. Before blasting the platform is lowered down and placed on a sledge like vehicle and towed aside.

The wire is lifted up through the large hole before blasting. The large hole is used as cut hole in the blasting of the round. Due to the large size of the cut hole, advances of up to 4 m are obtained. The area is approx. 4 sq.m. and the maximum height is 100 m. In this method it is necessary to have free space above the shaft for the drilling of the large hole and for the placing of the lifting gear.

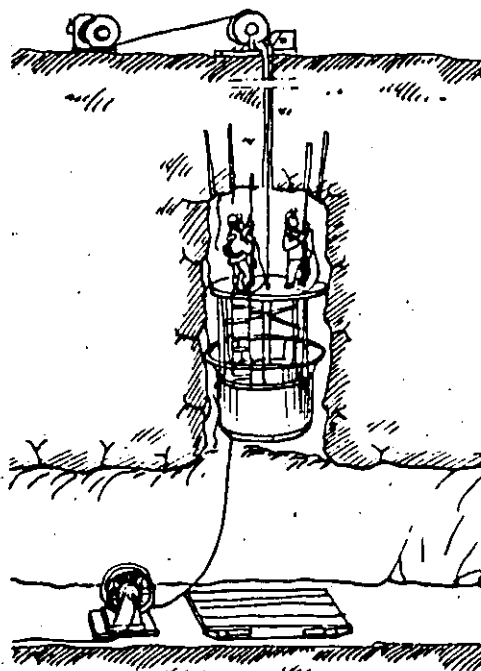


Fig. 7.26 The JORA lift.

The ALIMAK Raise Climber.

The Alimak raise shaft driving method was introduced in 1957 and became the most utilized system in the world because of its flexibility, safety, economy and speed.

The equipment consists of a raise climber with a working platform, which covers practically the entire area of the shaft. Under the platform there is a cage for the transport of personnel, material and equipment. The raise climber is propelled by a rack and pinion system along a special guide rail. The rail system incorporates a tube system for the air and water supply to the drilling equipment. The system also provides air for the blasting with NONEL and to ventilate the raise after the blasting.

The platform is equipped with a protective roof under which the blaster stands during scaling and drilling operations. If the inclination of the raise shaft is 60° or less the scaling may be done gradually during the ascent under the protection of the previously scaled hanging wall.

The Alimak method can be used for vertical as well as inclined shafts. The lower limit of the inclination depends on the angle of repose of the rock.

Unlike other modern methods for raise shafting, the Alimak needs only one point of attack, the lower one. The

upper break-through point may be prepared while the raise is driven.

The lengths which may be driven are only limited by the time which is at the blasting crews' disposal for ascent, scaling, drilling, charging, descent and blasting. For an 8 hour shift, the upper limit should be around 2,000 m. The lengths are also limited by the type of drive. The air-driven raise climber may be used for up to 150 m shaft length, electric drive up to 900 m. For longer shafts diesel-hydraulic driven climbers are used.

The area is normally 4 sq. m., but inclined shafts have been driven full face up to 36 sq. m.

Drilling and charging patterns are the same for all above mentioned raise shafting methods. Normally a raise shaft of 4 sq. m. is driven upwards and then the shaft is stoped to its final area. However, sometimes the shaft is driven "fullface" and as mentioned earlier areas up to 36 sq. m. have been successfully blasted.

The drilling and firing pattern for a raise shaft does not differ from that of a horizontal tunnel of the same size.

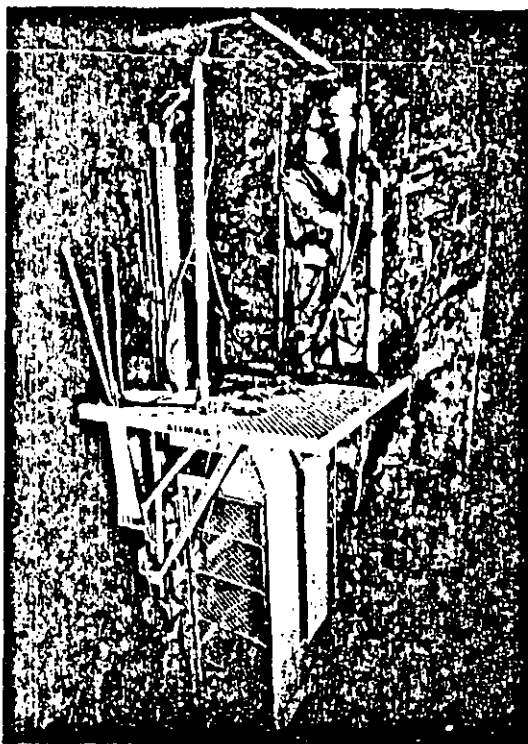


Fig. 7.27 The ALIMAK Raise Climber.

The Alimak work cycle:

Drilling:

The drilling and charging is carried out from the raise climber's platform under a specially designed protective roof. Both air and water to the drilling machines are supplied through tubes in the guide rail sections.

Blasting:

After drilling and charging the round, the raise climber is driven to the bottom and under the roof of the drift. During the blast, the climber is therefore well protected from falling rock.

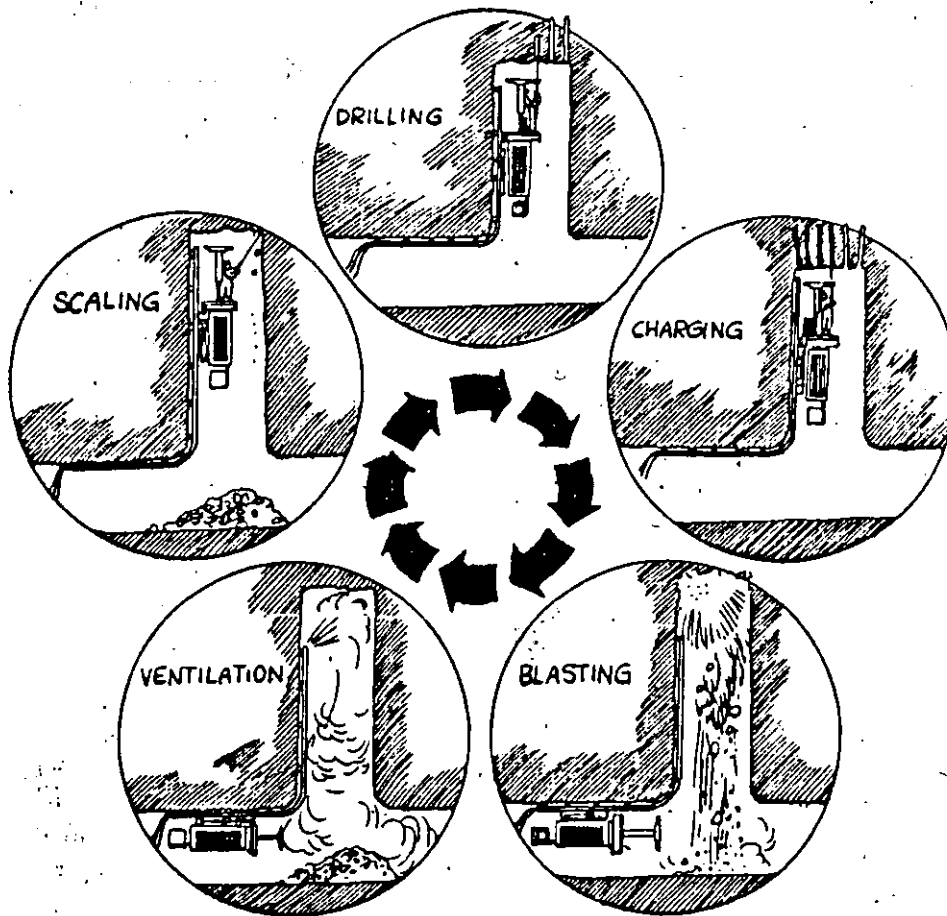


Fig. 7.28 The ALIMAK work cycle.

Ventilation:

After blasting the raise is ventilated and sprayed with water. The top of the guide rail is protected by a header plate which also acts as a water diffuser during the ventilation phase.

Scaling:

Scaling of the roof and walls of the raise is done from under the protective roof which gives the workmen good protection.

Generally large hole cuts are used and the design of the cut varies with the diameter of the large hole. (See 7.1.1 The cut, in Chapter Tunneling.)

The normal hole depth is 2.4 m and the expected advance 2.1 to 2.2 m.

The drilling is done with stopers, which are designed for raise driving, overhead drilling and roof bolting or drilling machines with jack legs.

For the blastholes drill series 11 (34 to 32 mm) is used and the large hole diameter is normally 75 mm.

For the stability of the walls and to avoid overbreak, the walls of the raise are normally smoothblasted. The smooth blasting method is also used if the shaft is to be widened at a later stage in order to avoid excessive scaling and to decrease the risk of rockfall.

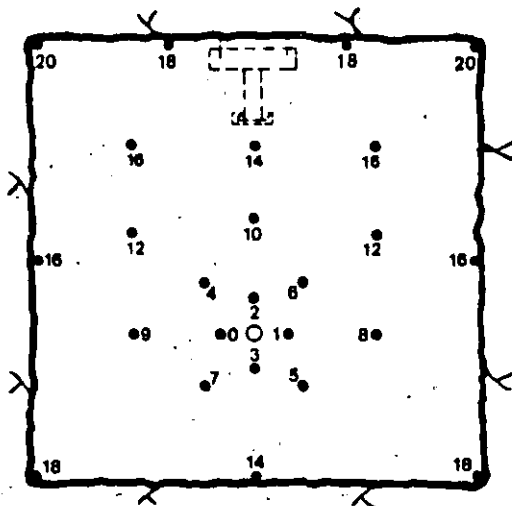


Fig. 7.29 Drilling and firing pattern for 4 sq. m. raise shaft.

A normal pilot shaft has an area of 4 sq.m. Normally one round is drilled and blasted per shift with an advance of 2.2 m. Working 2 shifts per day, the advance should be 4.4 m but taking disturbances in the work cycle into account, the long term advance is approx. 3.5 m/day or 70 to 90 m per month.

Shaft raising by long hole drilling.

In this method, all drilling is done downwards with parallel holes and the whole area is drilled at the same time:

Great precision in drilling and charging is a must and the lack of precision has earlier limited the practical height to 25 to 30 m. Now, with new drillrigs e.g. Atlas Copco Simba, the drilling can be carried out with great precision in any direction from vertical to 50°. With the Simba the deviation can be kept under 0.5 % for holes up to a length of 50 m.

The long hole drilling method is also advantageous from a safety point of view as all drilling and charging work is carried out from a safe location.

Two different cuts are used:

- large hole cut (blasting towards a large hole).
- crater cut (blasting towards the lower free face of the raise).

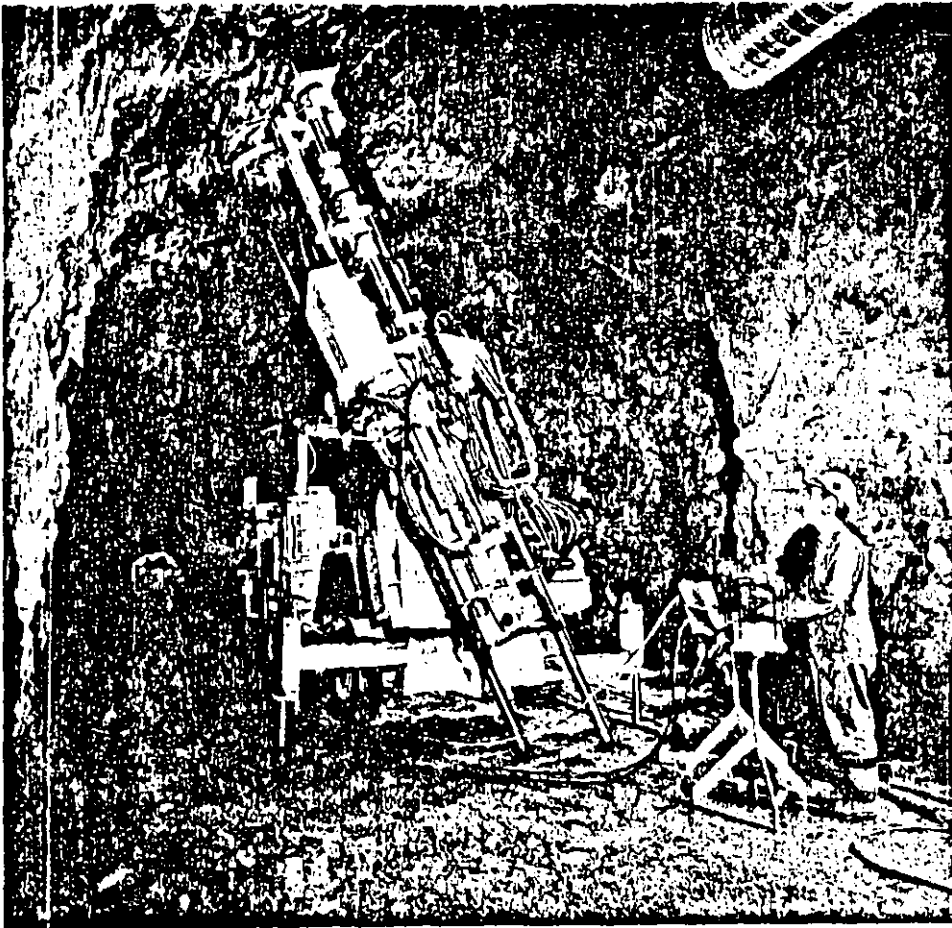
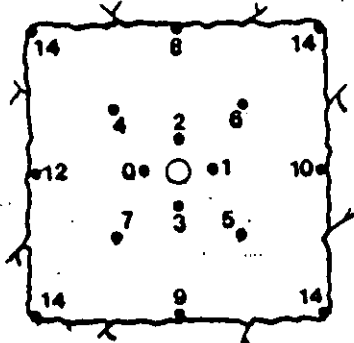


Fig. 7.30 Simba.

The large hole cut came first and is still the most common one. The drill holes in the round have a diameter of 50 to 75 mm and the central large hole is reamed to a diameter of 102 to 203 mm.



Large hole 163 mm
Blastholes 64 mm

Fig. 7.31 Firing sequence for 4 sq.m. raise.

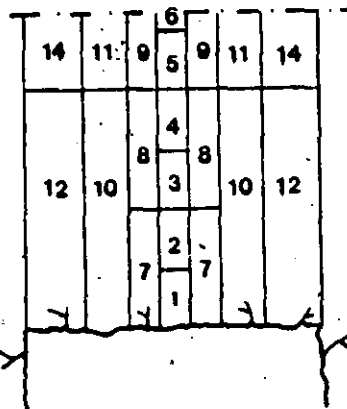


Fig. 7.32 Round sequence for raises with larger cross section.

The design and charging of the cut follow the same principles as described in Chapter 7.11 Tunneling, The cut. The firing sequence depends on the faulty drilling so the hole with the smallest real burden is fired with the lowest period number. It is therefore necessary to map every hole with regard to the faulty drilling.

The charging is done from the upper level. A piece of wood is lowered down on a rope and when the wood passes the lower mouth of the hole the rope is tightened and the piece of wood forms a plug for the lower part of the hole. The charges are lowered to the bottom of the hole. The hole should not be stemmed as the stemming may sinter and block the hole for the subsequent blast. The holes may be relatively overcharged compared with a tunnel cut as the charges are not confined at either end. Furthermore, the blastholes are normally of larger diameter than those used in tunnels. The risk of recompaction of the rock in the cut section can be considered as low even if the holes are considerably overcharged.

Crater blasting.

The blasting of a long hole drilled raise can also be carried out towards the free lower surface of the raise with a crater cut. No large diameter center hole is needed but the blastholes normally have a larger diameter than in the previous method. The crater blasting method is used only for the cut section to open a hole of approx. 1 sq.m., then normal stoping will follow.

The crater cut consists of five holes, one center hole and four edge holes. The center hole is blasted first whereupon the edge holes are blasted one by one with different delays.

Before charging, the holes are plugged with a piece of wood which is lowered down from the upper surface on a rope and secured to the lower rock surface. The hole is then filled with sand to the calculated level of the explosives charge. The charge should have a diameter close to that of the hole.

The charge is then stemmed with water. (Any other stemming may sinter and block the hole, making subsequent blasting operations impossible.)

The requisite charge weight and depth of the charge are calculated from Livingstone's theories as follows:

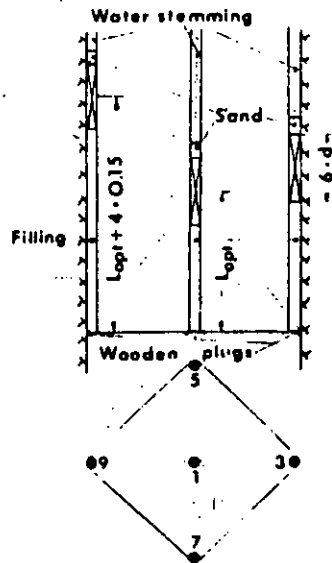


Fig. 7.33 Drilling, charging and firing pattern for crater cut.

1. The length of the charge shall be 6 times the blasthole diameter.

$$l = 6 \times d \quad (\text{mm})$$

2. The optimum depth of the charge is 50 % of the critical depth.

$$L_{\text{opt}} = 0.5 \times L_{\text{crit}} \quad (\text{mm})$$

3. The critical depth depends on the charge weight.

$$L_{\text{crit}} = S \times Q^{1/3} \quad (\text{mm})$$

where S = the strain energy factor approx. 1.5 (depending on the explosive used and the type of rock)

Q = charge weight in kg.

4. The charge weight is then

$$Q = \frac{3 \times d^3 \times \pi \times p}{2} \quad (\text{kg})$$

where p = charging density (1.2 kg/liter for Emulite 150 and 1.35 kg/liter for Dynamex M)

5. The optimum charge depth is then related to charge weight, explosives density, blasthole diameter and strain energy factor as follows:

$$L_{\text{opt}} = 0.5 \times S \times \sqrt[3]{\frac{3 \times \pi \times d}{2} \times d \times 10} \quad (\text{mm})$$

The crater theory is valid only for the center hole. The charge of the edge holes is placed so that the burden is less than the charge depth of the crater hole. The charge depth increases with 10 to 20 cm between each hole.

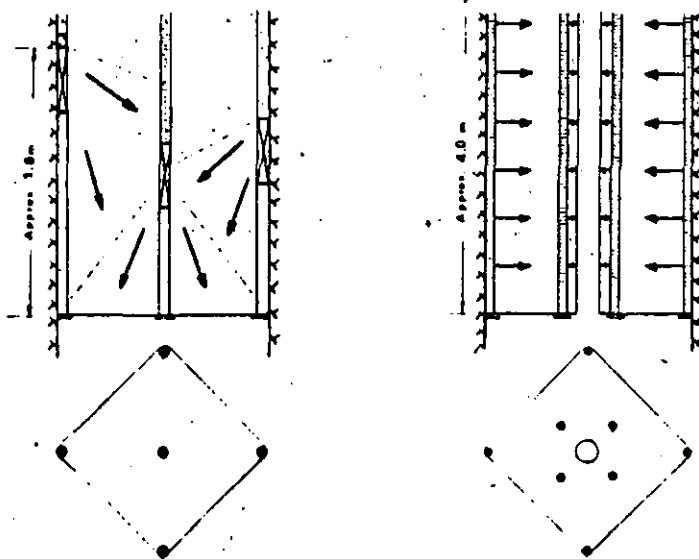


Fig. 7.34 Comparison of crater cut and standard large hole cut.

The advantages with crater cut compared to large hole cut are:

1. Lower cost for drilling and explosives as less holes are drilled in the cut. The same hole diameter is used in all holes.
2. Drilling precision is not as essential as for large hole cuts.
3. Simpler blasting practice with less need for well trained personnel.

The disadvantage with the crater cut method is the relatively short rounds that may be shot each time.

7.3 Underground chambers.

The military defense forces started early to utilize solid rock for construction of fortifications which gave many advantages over surface construction. Solid rock is difficult to penetrate and underground chambers are difficult to discover and easy to guard.

The field of application is huge: Protection for guns, ammunition and soldiers, protection for submarines and smaller warships, storage for material, fuels and foodstuffs and not least as air-raid shelters for civilians.

Oil was initially stored in surface tanks, but after WWII storage in unlined storage chambers has become the most common method. The increased exploitation of sub-surface storage has to a great extent been due to the rapid development of rock blasting techniques. The increased mechanization of the operations has resulted in relatively unchanged construction costs over a number of years, while at the same time the price of land has increased considerably.

Common to all types of underground chambers is that they are well protected from a military point of view. They are well camouflaged and more difficult to damage than surface storage facilities if attacked from the air or overland. They require little land: surface space is only needed for access roads, ventilation etc. From an environmental point of view sub-surface storage is safer, as leakage does not often occur from underground chambers. It is safer than surface storage in case of fire, as the supply of oxygen is often insufficient to allow a bigger fire to develop.

Underground chambers have many fields of application:

- storage for different products
 - cold storage for food, wines, water, oil etc.
- garages, telephone exchanges, swimming pools
- military and civil stores and workshops
- air-raid shelters for people
 - aircrafts
 - warships
 - archives
- storage for lightly contaminated nuclear waste
- storage of nuclear residue
- hydro-electric powerstations

Some of the applications may be combined. In wartime, the space which is normally used for garages, workshops or swimming pools can be utilized as air-raid shelters.

The basis for underground chambers is a qualitative sound rock to build in. Some economic aspects have to be considered. If the chamber is located at too shallow a level, the cost of reinforcing the rock may be high as the quality of the surface rock is normally poorer than rock at deeper levels. However, deep location results in long access roads, which may cause problem both during construction and when the chambers come into use.

From the point of view of rock blasting techniques, the construction of underground chambers does not differ from that of tunnels of the same magnitude. The width of underground chambers cannot be too great due to the inability of the rock to support the roof by its own strength. For oil storage chambers and machine halls for hydro-electric power-plants, widths of 20 to 24 m have been constructed without need for heavy reinforcement. The height of the chambers may be up to 40 m.

Small underground chambers, with a height of less than 8 m are blasted as tunnels. In larger chambers, the operation has to be divided into several stages of drilling and blasting in which different methods are used:

- pilot tunnel with side stoping
- horizontal benching
- vertical benching.

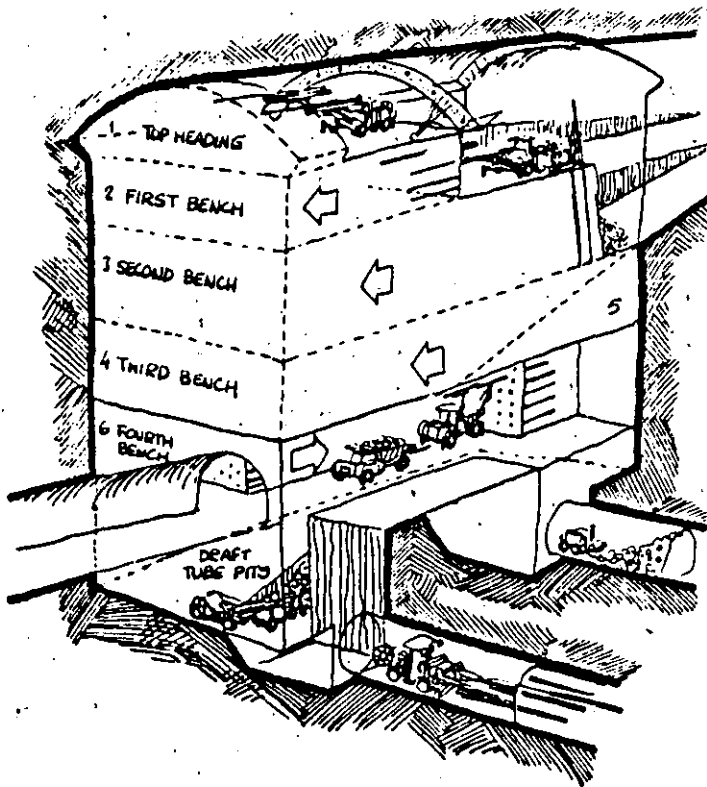


Fig. 7.35 Drifting stages in underground chamber.

The pilot tunnel is drifted at the roof of the chamber to facilitate scaling and reinforcement. The side stoping to full width is then carried out. Scaling and, if necessary, bolting and shotcreting of the roof are done simultaneously to avoid future expensive reinforcement work.

Then blasting is carried out in one or several benches. It is common for the first bench to be a horizontal bench utilizing the drilling equipment for the tunnel. Some rock chambers are also designed in such way that no space is available close to the wall for the boom of the vertical drilling equipment. The disadvantage with horizontal benching is that the height and depth of the round depends on the drilling equipment. The height is normally limited to 8 m and the depth of the round to 4 m. Other limitation on the blast design is that the blasthole diameter can rarely exceed 51 mm.

Excavation of the blasted material must be carried out between each blast. Vertical benching is the dominant method for benching in rock chambers. The advantages with vertical benching is that drilling and excavation may be carried out simultaneously. The bench height may be varied within a wide range and larger blastholes may be used, often with better economy as a consequence. It is also easier to obtain a smoother contour with vertical benches than with horizontal.

The charge calculations for the pilot tunnel, side stoping and horizontal benching are the same as presented in Chapter 7 Tunneling, where the side stoping is calculated as stoping holes with horizontal breakage and the vertical bench as stoping holes with upwards breakage.

The vertical benching is calculated in accordance with Chapter 5 Bench blasting. If excavation is not carried out between the blasts, the specific charge has to be increased in order to compensate for movement of rock from previous rounds. See 5.8 Swelling.

Access tunnels are required for each bench for the transport of rock and equipment.

In certain cases, restrictions due to geological reasons, ground vibrations etc., may affect the execution of the work.

In Fig. 7.36 the roof must be bolted with 8 m long bolts and sprayed with concrete before any side stoping can be done.

The vertical bench is limited to a height of 4 m which makes it feasible to make a raise shaft, "glory hole", for the transport of the blasted rock. The raise shaft is a long hole drilled one, from the upper level and the blasting starts at the lower level. See Chapter 7.2.2.

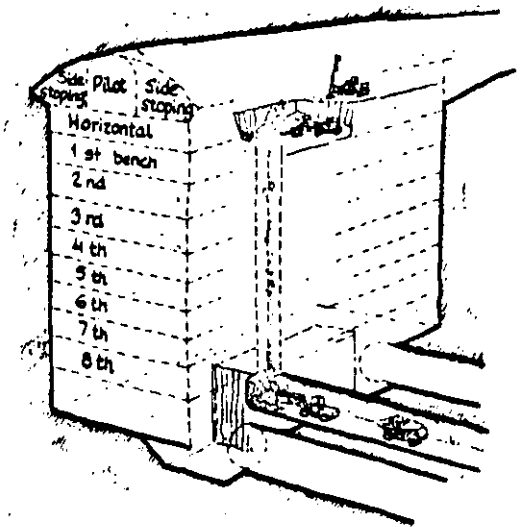


Fig. 7.36 Drifting stages for machine hall in hydro-electric power plant.

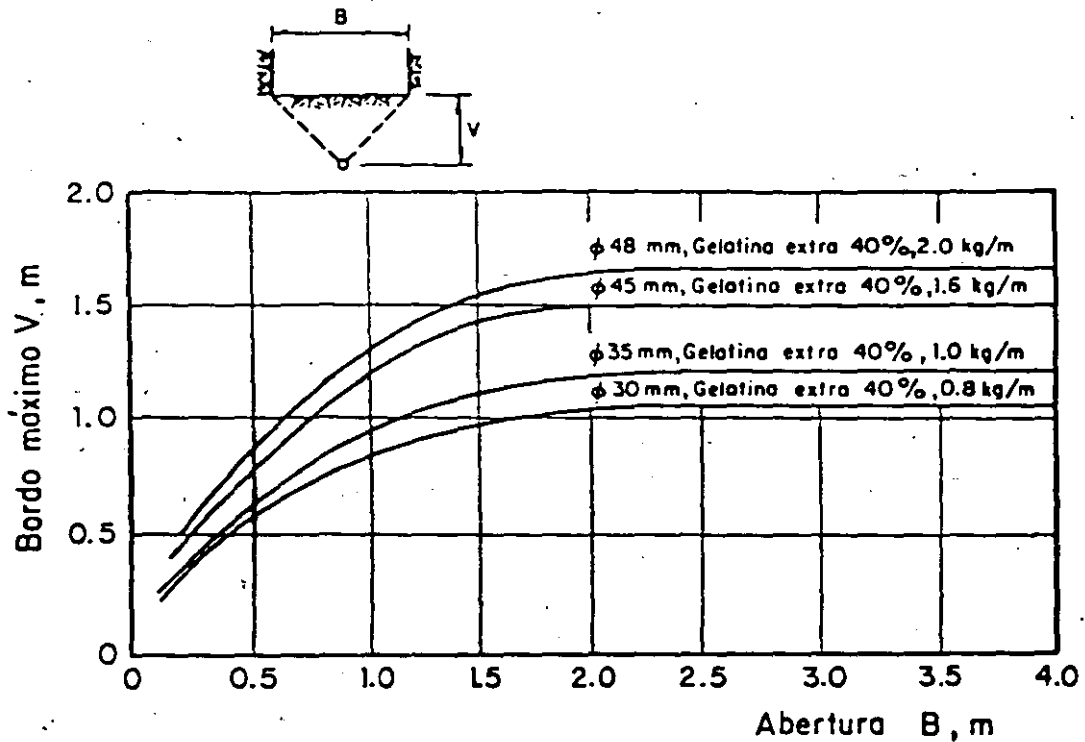


FIG I.34 Relación entre abertura, B , concentración de carga y bordo máximo, V

ciamientos de los barrenos de cada una de las zonas del túnel que se señalan en la fig I.38.

-Barrenos ayudantes con proyección horizontal o hacia arriba

El bordo o distancia entre los barrenos y la cavidad central no debe ser mayor que la mitad de la profundidad del barreno menos veinte centímetros. No deberá tomarse esta condición como base para el cálculo.

El espaciamiento de los barrenos debe ser igual a 1.1 veces el bordo.

tad de la concentración de la carga de fondo. La zona de retaque debe ser igual a la mitad del bordo.

TABLA I.12 Carga específica de fondo

Diámetro de los barrenos, en mm	Carga específica, en kg/m ³
30	1.1
40	1.3
50	1.5

*A ytas Horiz
o arriba*
(D.S. 21.1)

En la tabla I.13 se muestran los espaciamentos calculados de acuerdo con las cargas específicas de fondo necesarias, considerando explosivos de peso volumétrico de 1.3 g/cm³ y el diámetro de barrenos de la tabla I.12.

TABLA I.13 Espaciamentos y bordos en función de los diámetros de los barrenos

Diámetro de barreno, en mm	Area por barreno, en m ²	Bordo, en m	Espaciamento, en m
32	0.91	0.90	1.00
35	1.00	0.95	1.05
38	1.15	1.00	1.15
45	1.44	1.15	1.25
48	1.57	1.20	1.30*
51	1.71	1.25	1.35*

A ytas Horiz

Arriba
(D.S. 21.1)

* Estos espaciamentos son sólo para túneles de gran diámetro; en el caso de áreas menores su magnitud es menor como se muestra en las gráficas de la fig I.34.

Las concentraciones y cargas de fondo y de columna de la tabla I.14 han sido calculadas a partir de las recomendaciones anteriores, en función del diámetro de los barrenos. Estos datos han sido obtenidos de la práctica e incluyen los errores normales de perforación.

28
12
4

B.1

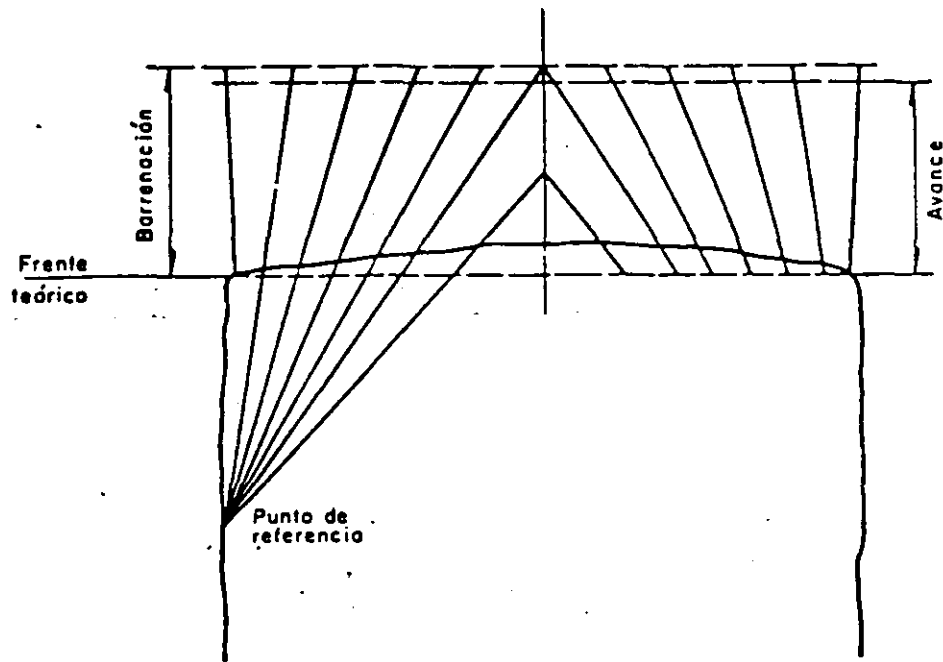
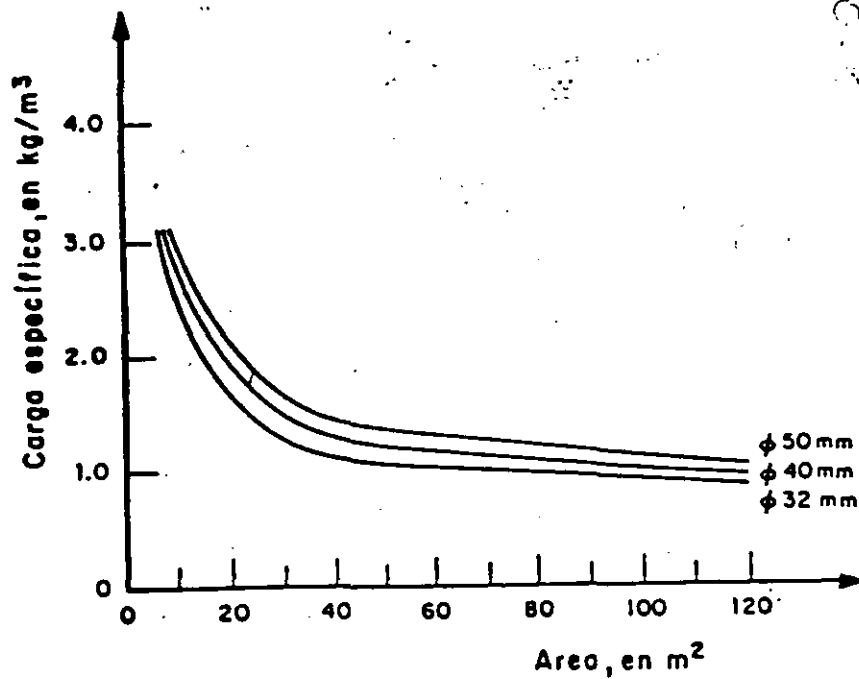


FIG I.35 Distribución en planta de los barrenos de la cuña y los de fuera de la cuña



$Q = 120'' \cdot 14.12 \text{ mm}^2$
 $\Delta = 17.7'' \cdot 47.62 \text{ mm}^2$

FIG I.36 Cargas específicas utilizadas normalmente en túneles

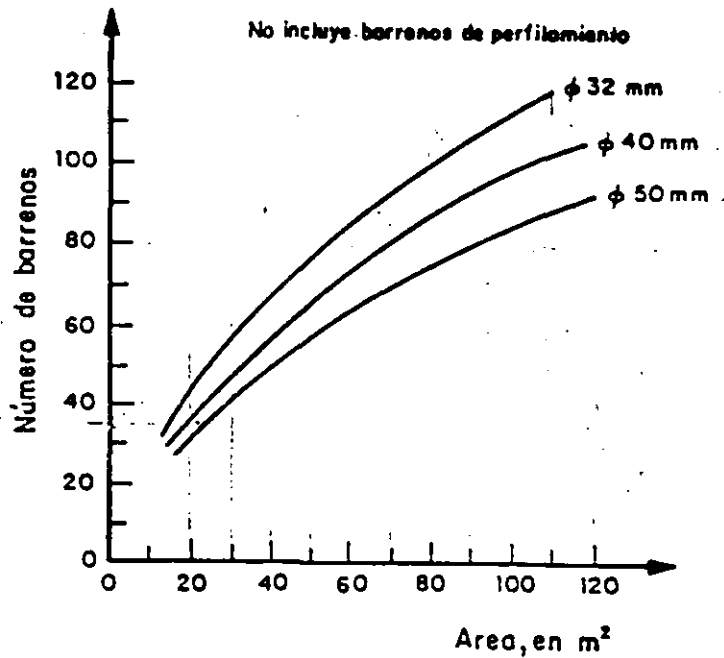


FIG I.37 Número de barrenos en función del área del frente

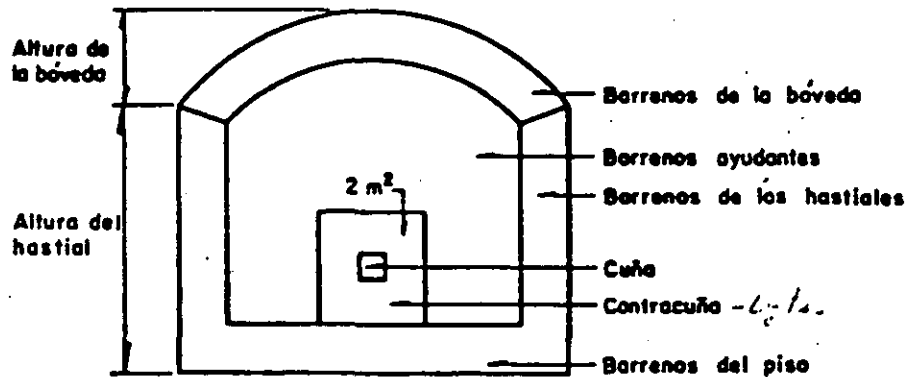


FIG I.38 Zonas de distribución de los barrenos

La carga de fondo ocupa el tercio inferior del barreno con la carga específica de la tabla I.12.

La concentración de la carga de columna en kg/m puede tomarse igual a la mi

The relationship can also be used for the "cut spreader" holes above the holes in the cut, the width of the free surface corresponding to the diameter of the large hole as follows:

$$V = 0.7 \times B$$

The loosening section should be so wide that the stopping holes have the possibility to break out at the right angle which implies $2 \times V_{\text{stopping holes}}$.

The burden for the holes in the cut must not be confused with the centre-to-centre distance normally used. The table below can serve as a guide:

CUT

Large hole diameter	Small hole diameter	Burden	Centre-to-centre distance
mm	mm	mm	mm
57	32	40	85
76	32	53	107
76	45	53	113
2 × 57	32	80	125
2 × 57	45	80	131
2 × 76	32	106	160
2 × 76	45	106	167
100	45	70	143
100	51	70	146
125	51	88	176

In the case of easily blasted rock, the centre-to-centre distance may need to be increased.

CUT

Experience shows that the nearest holes in the cut can be charged as follows:

Drill hole diameter	Charge concentration	Suitable large hole diameter
mm	kg/m	mm
32	0.25 ¹	57 - 2 × 76
35	0.30 ¹	76 - 2 × 76
38	0.36 ¹	76 - 2 × 76
45	0.45	2 × 76 - 125
48	0.55	2 × 76 - 125
51	0.55	2 × 76 - 125

¹ 25 mm Donarit I can normally be used in spite of the fact that it corresponds to a Gelatine Donarit I charge of 0.46 kg/m.

A similar form of cut with double large holes, diameter 76 mm, has been used a great deal:

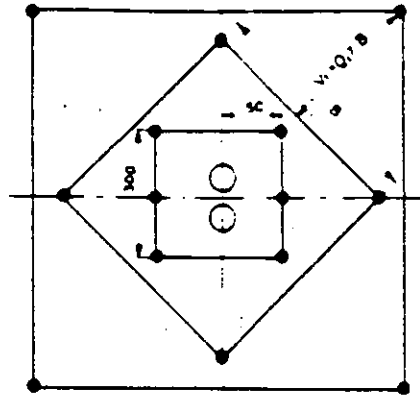


Fig. 9.2.3

The figure also shows the make-up of the "cut spreader" holes outside the cut. The charge in the "cut spreader" holes is large because of the great constriction.

AYTES CUÑA

Burden	Bottom charge	Column charge, kg m with diam., mm			
		32	38	45	48
m	kg				
0.20	0.25	0.30	0.45	0.60	0.75
0.30	0.40	0.30	0.45	0.60	0.75
0.40	0.50	0.35	0.50	0.70	0.80
0.50	0.65	0.50	0.70	1.00	1.15
0.60	0.80	0.50	0.70	1.00	1.15
0.70	0.90	0.50	0.70	1.00	1.15

Uncharged section = $0.5 \times V$.

Loosening holes with burden greater than 0.70 m are charged in the same way as stopping holes with horizontal breakage (see section 9.1 entitled Charge calculations).

Fig. 9.2.4 shows a cut made up of large gauge holes and the cut spreader section for various drill hole diameters. The outermost holes in the cut spreader section can be described as stopping holes but they have been adapted to some extent geometrically so that they fit into the picture more easily.

SALIDA HACIA ABAJO

Drill hole diam.	Depth of hole	Burden	Hole spacing	Bottom charge		Column charge		Uncharged section
				kg	kg m	kg	kg m	
mm	m	m	m	kg	kg m	kg	kg m	m
33	1.6	0.60	0.70	0.60	1.10	0.30	0.40	0.30
32	2.4	0.90	1.10	0.80	1.00	0.55	0.50	0.45
31	3.2	0.85 ¹	1.10	1.00	0.95	0.85	0.50	0.45
38	2.4	0.90 ¹	1.20	1.15	1.44	0.80	0.70	0.50
37	3.2	1.00 ¹	1.20	1.50	1.36	1.15	0.70	0.50
45	3.2	1.15 ¹	1.40	2.25	2.03	1.50	1.00	0.55
48	3.2	1.20 ¹	1.45	2.50	2.30	1.70	1.15	0.60
48	4.0	1.20 ¹	1.45	3.00	2.30	2.45	1.15	0.60
51	3.2	1.25 ¹	1.50	2.70	2.60	1.95	1.30	0.60
51	4.0	1.25 ¹	1.50	3.40	2.60	2.70	1.30	0.60

¹ In tunnels with a cross-sectional area of more than 70 m², the burden and hole spacing can often be increased considerably since the drill holes break much more easily. Blasting then becomes similar to bench blasting.

In most cases the burden can be increased by 10%, so that the hole spacing is also considerably greater.

The spacing of the stopping holes can be increased to larger areas with respect to the cross-sectional area of the tunnel. It can also be said that in many cases where rock is easy to blast, the hole spacing shown in the table may be too close. In practice a lower charge concentration in the bottom section is often attained than that shown in the table. This implies that in the case of easily blasted rock, the hole spacing shown in the table can be used even if the charge concentration is lower.

Calculating the charge in wall holes

Normally the walls and roof of the tunnel are smooth-blasted (see section 9.5 entitled *Smooth blasting*). This calculation concerns cases where no smooth blasting is carried out.

The burden including "look-in" or "look-out" is selected as being $0.9 \times$ the burden for the stopping holes.

$$\text{Hole spacing} = 1.2 \times V.$$

The height of the bottom charge is reduced to $1/6 \times$ depth of hole.

Uncharged section = $0.5 \times$ burden. The concentration of the column charge is reduced to $0.40 \times$ the concentration of the bottom charge.

DE PARED

Example:

Drill hole diam.	Depth of hole	Burden	Hole spacing	Bottom charge		Column charge		Uncharged section
				kg	kg m	kg	kg m	
mm	m	m	m	kg	kg m	kg	kg m	m
33	1.6	0.55	0.65	0.30	1.10	0.45	0.45	0.30
32	2.4	0.80	0.95	0.40	1.00	0.65	0.40	0.40
31	3.2	0.80	0.95	0.50	0.95	0.90	0.40	0.40
38	2.4	0.90	1.10	0.60	1.44	0.85	0.60	0.45
37	3.2	0.90	1.10	0.75	1.36	1.20	0.55	0.45
45	3.2	1.00	1.20	1.10	2.03	1.80	0.80	0.50
48	3.2	1.10	1.30	1.20	2.30	2.00	0.90	0.55
48	4.0	1.10	1.30	1.50	2.30	2.50	0.90	0.55
51	3.2	1.15	1.40	1.40	2.60	2.10	1.00	0.60
51	4.0	1.15	1.40	1.70	2.60	2.70	1.00	0.60

TECHO

Calculating the charge in roof holes

The hole spacing is carried out as for the wall holes. The column charge is reduced to $0.30 \times$ the concentration of the bottom charge.

Drill hole diam.	Depth of hole	Burden	Hole spacing	Bottom charge		Column charge		Uncharged section
				kg	kg/m	kg	kg/m	
mm	m	m	m	kg	kg/m	kg	kg/m	m
31	1.6	0.55	0.65	0.30	1.10	0.35	0.35	0.30
32	2.4	0.80	0.95	0.40	1.00	0.50	0.30	0.40
31	3.2	0.80	0.95	0.50	0.95	0.70	0.30	0.40
38	2.4	0.90	1.10	0.60	1.44	0.70	0.45	0.45
37	3.2	0.90	1.10	0.75	1.36	0.90	0.40	0.45
45	3.2	1.00	1.20	1.10	2.03	1.30	0.60	0.50
48	3.2	1.10	1.30	1.20	2.30	1.45	0.70	0.55
48	4.0	1.10	1.30	1.50	2.30	1.95	0.90	0.55
51	3.2	1.15	1.40	1.40	2.60	1.70	0.80	0.60
51	4.0	1.15	1.40	1.70	2.60	2.25	0.80	0.60

DE PISO

Example:

Drill diam.	Drilling depth	Burden	Hole spacing	Bottom charge		Column charge		Uncharged section
				kg	kg/m	kg	kg/m	
mm	m	m	m	kg	kg/m	kg	kg/m	m
33	1.6	0.60	0.70	0.60	1.10	0.70	0.75	0.10
32	2.4	0.90	1.00	0.80	1.00	1.00	0.70	0.20
31	3.2	0.90	0.95	1.00	0.95	1.30	0.65	0.20
38	2.4	1.00	1.10	1.15	1.44	1.40	1.00	0.20
37	3.2	1.00	1.10	1.50	1.36	1.80	0.95	0.20
45	3.2	1.15	1.25	2.25	2.03	2.60	1.40	0.25
48	3.2	1.20	1.30	2.50	2.30	3.00	1.60	0.25
48	4.0	1.20	1.30	3.00	2.30	4.25	1.60	0.25
51	3.2	1.25	1.35	2.70	2.60	3.20	1.80	0.25
51	4.0	1.25	1.35	3.40	2.60	4.75	1.80	0.25

Calculating the charge in stopping holes with breakage downwards

Since these drill holes require less force for swelling and furthermore are helped by the force of gravity, the specific charge in the bottom section can be reduced to:

Drill hole diameter	Specific charge
mm	kg/m ³
30	1.0
40	1.2
50	1.4

Hole spacing can be increased to $1.2 \times$ burden. Otherwise the calculation is made up in the same way as for the stopping holes described earlier. In the case of tunnels with small cross-section areas, burden and hole spacing are decreased according to the geometrical conditions.

The hole spacing indicated in the table applies on condition that the charge concentration in the bottom section attains the value in the table. If the charging method used results in a lower concentration, then the holes must be more closely spaced so that the required specific charge is attained.

SALIDA HORIZ. Y HACIA ARRIBA

The concentration and strength of the bottom charge and the column charge can be calculated from the relationship mentioned earlier:

Drill hole diam.	Depth of hole	Burden	Hole spacing	Bottom charge		Column charge		Uncharged section
				kg	kg/m	kg	kg/m	
33	1.6	0.60	0.70	0.60	1.10	0.30	0.40	0.20
32	2.4	0.90	1.00	0.80	1.00	0.55	0.50	0.45
31	3.2	0.90	0.95	1.00	0.95	0.85	0.50	0.45
38	2.4	1.00	1.10	1.15	1.44	0.80	0.70	0.50
37	3.2	1.00	1.10	1.50	1.36	1.15	0.70	0.50
45	3.2	1.15	1.25	2.25	2.03	1.50	1.00	0.55
48	3.2	1.20	1.30	2.50	2.30	1.70	1.15	0.60
48	4.0	1.20	1.30	3.00	2.30	2.45	1.15	0.60
51	3.2	1.25	1.35	2.70	2.60	1.95	1.30	0.60
51	4.0	1.25	1.35	3.40	2.60	2.70	1.30	0.60

33-38 mm covers the range for both drill series 11 and 12 and also full-length drill rods with 33 and 38 mm bits respectively.

Burden and hole spacing are those used in practice - faulty drilling is included in the basic calculation for tunnel blasting.

The table shows that faulty drilling and swelling requirements are compensated for by larger bottom charges as hole depth is increased. Full utilization of the largest diameter holes implies large charges per hole which, from the viewpoint of rock technology, is unfavourable.

Calculating the charge in the floor holes

The burden and spacing for the floor holes can be calculated in the same way as for the stoping holes mentioned above. However, it is important for the "look-in" or "look-out" to be included in the burden dimensions. Since "look-out" is included in the burden, the drill holes close to the floor must be collared for burden and "look-out". For example with a burden of 1.00 m and "look-out" of 0.20 m, the holes in the round must be collared $1.00 - 0.20 \text{ m} = 0.80 \text{ m}$ above the floor hole collaring point. The uncharged section is taken to be $0.2 \times$ burden. The column charge concentration is increased to 70% of the bottom charge.

TABLA I.14 Cargas, espaciamentos y bordos en barrenos ayudantes con proyección horizontal o hacia arriba

Taco

Diámetro barreno. mm	Profundi- dad ba- rreno, m	Bordo m	Espacia- miento m	Carga de fondo		Carga de columna		Zona de retaque m
				kg	kg/m	kg	kg/m	
33	1.6	0.60	0.70	0.60	1.10	0.30	0.40	0.30
32	2.4	0.90	1.00	0.80	1.00	0.55	0.50	0.45
31	3.2	0.90	0.95	1.00	0.95	0.85	0.50	0.45
38	2.4	1.00	1.10	1.15	1.44	0.80	0.70	0.50
37	3.2	1.00	1.10	1.50	1.36	1.15	0.70	0.50
→ 45	3.2	1.15	1.25	2.25	2.03	1.50	1.00	0.55
48	3.2	1.20	1.30	2.50	2.30	1.70	1.15	0.60
48	4.0	1.20	1.30	3.00	2.30	2.45	1.15	0.60
51	3.2	1.25	1.35	2.50	2.60	1.95	1.30	0.60
51	4.0	1.25	1.35	3.40	2.60	2.70	1.30	0.60

-Barrenos de piso

El bordo y el espaciamento de estos barrenos debe calcularse del mismo modo que los barrenos ayudantes. Sin embargo, debe considerarse en el bordo una corrección debido al emboquille de preparación para la voladura siguiente. Por ejemplo, con un bordo de 1.00 m y un margen para emboquille de 0.20 m, la segunda fila de barrenos del piso debe estar 0.80 m arriba de la entrada de los barrenos de la primera fila. La zona de retaque debe ser de 0.20 veces el bordo, es decir, mucho menor que en los barrenos ayudantes y la concentración de la carga de columna se fija hasta de un 70 por ciento de la concentración de la carga de fondo.

En la tabla I.15 se presentan las concentraciones de carga de fondo y de columna, el espaciamento, el bordo y la zona de retaque para distintos diámetros de barrenos.

-Barrenos ayudantes con proyección hacia abajo

Debido a la ayuda de la gravedad, estos barrenos requieren una menor carga específica que los anteriores. La carga específica de fondo puede ser la de la tabla I.16.

TABLA I.15 Cargas, espaciamientos y bordos en barrenos de piso

Diámetro barreno mm	Profundi- dad barre- no, m	Bordo m	Espacia- miento m	Carga de fondo		Carga de columna		Zona de retaque m
				kg	kg/m	kg	kg/m	
33	1.6	0.60	0.70	0.60	1.10	0.70	0.75	0.10
32	2.4	0.90	1.00	0.80	1.00	1.00	0.70	0.20
31	3.2	0.90	0.95	1.00	0.95	1.30	0.65	0.20
38	2.4	1.00	1.10	1.15	1.44	1.40	1.00	0.20
37	3.2	1.00	1.10	1.50	1.36	1.80	0.95	0.20
45	3.2	1.15	1.25	2.25	2.03	2.60	1.40	0.25
48	3.2	1.20	1.30	2.50	2.30	3.00	1.60	0.25
48	4.0	1.20	1.30	3.00	2.30	4.25	1.60	0.25
51	3.2	1.25	1.35	2.70	2.60	3.20	1.80	0.25
51	4.0	1.25	1.35	3.40	2.60	4.75	1.80	0.25

TABLA I.16 Carga específica de fondo

Diámetro de los barrenos, en mm	Carga específica, en kg/m ³
30	1.0
40	1.2
50	1.4

El espaciamiento de estos barrenos puede ser de 1.2 veces el bordo. Las de más características son las señaladas para los otros barrenos ayudantes.

En túneles de sección transversal pequeña las cargas deberán aumentarse y el bordo y el espaciamiento disminuirse de acuerdo con las funciones de las gráficas que se presentan en las figs I.34, I.36 y I.37.

En la tabla I.17 se presentan las cargas, bordos y espaciamientos de estos barrenos. Los espaciamientos indicados son aplicables siempre que la con-

B.I

centración de carga en el fondo alcance, asimismo, el valor señalado. Si la concentración de carga resulta menor, el espaciamiento deberá reducirse para obtener la carga específica requerida.

Los valores de espaciamientos y bordos indicados en la tabla I.17 pueden aumentarse, particularmente cuando la roca es fácil de excavar y cuando los túneles tienen un área de más de 70 m². También es frecuente en estos casos utilizar los espaciamientos señalados pero con menores concentraciones de carga.

TABLA I.17 Cargas, espaciamientos y bordos en barrenos ayudantes con proyección hacia abajo

Diámetro barreno, mm	Profundi- dad barre- no, m	Bordo, m	Espacia- miento, m	Carga de fondo		Carga de columna		Zona de retaque, m
				kg	kg/m	kg	kg/m	
33	1.6	0.60	0.70	0.60	1.10	0.30	0.40	0.30
32	2.4	0.90	1.10	0.80	1.00	0.55	0.50	0.45
31	3.2	0.85	1.10	1.00	0.95	0.85	0.50	0.45
38	2.4	1.00	1.20	1.15	1.44	0.80	0.70	0.50
37	3.2	1.00	1.20	1.50	1.36	1.15	0.70	0.50
45	3.2	1.15	1.40	2.25	2.03	1.50	1.25	0.55
48	3.2	1.20	1.45	2.50	2.30	1.70	1.15	0.60
48	4.0	1.20	1.45	3.00	2.30	2.45	1.15	0.60
51	3.2	1.25	1.50	2.70	2.60	1.95	1.30	0.60
51	4.0	1.25	1.50	3.40	2.60	2.70	1.30	0.60

-Barrenos de los hastiales

Las voladuras de los hastiales y de la bóveda corresponden por lo común al tipo de voladuras denominado recorte o poscorte perimetral (inciso 7.2.1.5). En esta sección se tratan los casos que no son voladuras de recorte.

El bordo, considerando el emboquille de preparación para la voladura siguiente, se toma igual a 0.90 veces el bordo de los barrenos ayudantes.

B.I

- H profundidad del barreno, en m
 q carga específica, en kg/m³
 d diámetro del barreno, en mm
 Q_{bk} concentración de la carga de fondo, en kg/m
 Q_{pk} concentración de la carga de columna, en kg/m;
 h_b altura de la carga de fondo, en m
 h_o longitud del retaque, en m
 E Distancia entre barrenos, en m

TABLA I.19 Cargas, espaciamentos y bordos en barrenos de la bóveda

Diámetro barreno mm	Profundidad barreno, m	Bordo m	Espaciamiento m	Carga de fondo		Carga de columna		Zona de retaque m
				kg	kg/m	kg	kg/m	
33	1.6	0.55	0.65	0.30	1.10	0.35	0.35	0.30
32	2.4	0.80	0.95	0.40	1.00	0.50	0.30	0.40
31	3.2	0.80	0.95	0.50	0.95	0.70	0.30	0.40
38	2.4	0.90	1.10	0.60	1.44	0.70	0.45	0.45
37	3.2	0.90	1.10	0.75	1.36	0.90	0.40	0.45
45	3.2	1.00	1.20	1.10	2.03	1.30	0.60	0.50
48	3.2	1.10	1.30	1.20	2.30	1.45	0.80	0.55
48	4.0	1.10	1.30	1.50	2.30	1.95	0.90	0.55
51	3.2	1.15	1.40	1.40	2.60	1.70	0.80	0.60
51	4.0	1.15	1.40	1.70	2.60	2.25	0.80	0.60

-Barrenos ayudantes con proyección horizontal o hacia arriba

d(mm)	q(kg/m ³)
30	1.1
40	1.3
50	1.5
h _b	H/3

$$v_1 \leq \frac{H - 0.40 \text{ m}}{2} \quad (\text{ésta es una condición y no es una base de cálculo}) \quad (I.4)$$

B.I

Acotaciones, en mm

○ Barreno vacío

● Barreno cargado

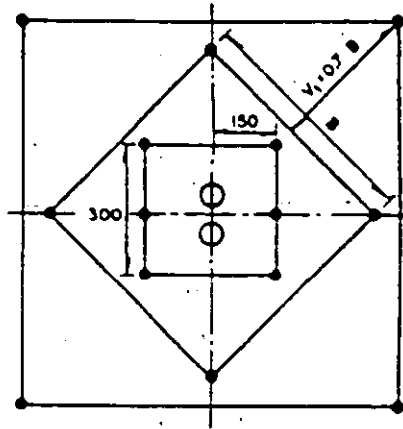


FIG I.39 Cuña de dos barrenos centrales y contracuña

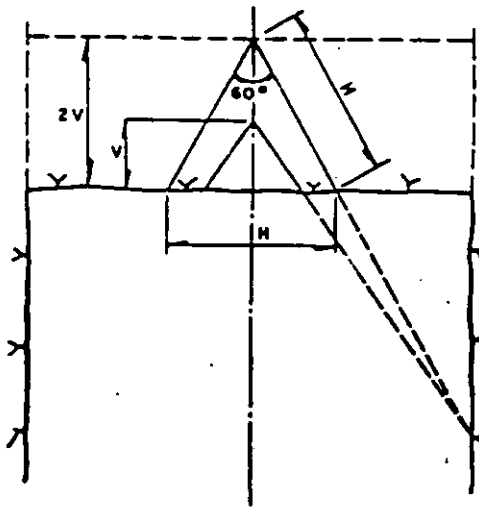


FIG I.40 Cuña en V

tabla I.23 se proporcionan valores que pueden servir de orientación en la determinación de la dimensión y carga de la cuña en V.

En cuñas en V la longitud de la carga de fondo debe ser de cuando menos un tercio de la profundidad del barreno. La carga de columna debe ser igual a la mitad de la carga de fondo. La zona de retaque debe ser un tercio de la dimensión V de la cuña, pero debe ser adaptada al espaciamiento de los barrenos de manera que no haya exceso de carga en la parte de la columna.

TABLA I.21 Cargas asignadas a los barrenos más próximos al central (Cuña)

Diámetro de los barrenos cargados, mm	Carga asignada (kg/m)	Diámetro del barreno central, mm
32	0.25	de 57 a 2 x 76
35	0.30	de 76 a 2 x 76
38	0.36	de 76 a 2 x 76
→ 45	→ 0.45	de 2 x 76 a 125
48	0.55	de 2 x 76 a 125
51	0.55	de 2 x 76 a 125

En la tabla I.22 se presentan valores de cargas que han dado buenos resultados en barrenos de contracuña.

TABLA I.22 Valores empíricos de carga en barrenos de contracuña (Ayudantes)

Bordo o separación entre barrenos m	Carga de fondo kg	Carga de columna en kg/m para diámetros de los barrenos cargados de:			
		32 mm	38 mm	45 mm	48 mm
0.20	0.25	0.30	0.45	0.60	0.75
0.30	0.40	0.30	0.45	0.60	0.75
0.40	0.50	0.35	0.50	0.70	0.80
→ 0.50	0.65	0.50	0.70	1.00	1.15
0.60	0.80	0.50	0.70	1.00	1.15
0.70	0.90	0.50	0.70	1.00	1.15

* Longitud sin carga (taro) = 0.5 V.

d) Cuña en V

En esta sección se proporcionan reglas generales para el cálculo de cargas considerando una cuña de vértice interior de 60°. Si este ángulo es menor la carga debe incrementarse.

La dimensión V de la cuña (fig I.40) es función de la cantidad de explosivos que pueden cargarse en los barrenos con arreglo a su diámetro. En la

Los cartuchos largos de diámetro pequeño de explosivos de baja densidad, permiten una distribución adecuada de la carga a lo largo del barreno. Los cartuchos de 20 cm de longitud se han empleado con éxito en voladuras de poscorte perimetral utilizando espaciadores entre cartuchos para reducir la carga total en kg/m; sin embargo, este procedimiento da como resultado concentraciones de carga relativamente altas en distintos puntos.

7.2.1.6 Precorte

En el precorte los barrenos de contorno se disparan antes de efectuar la voladura propiamente dicha. El precorte produce una grieta entre los barrenos de contorno. Esta grieta evita que las ondas de choque de la voladura principal se transmitan en toda su intensidad hacia la pared terminada y minimiza la profundidad de la fragmentación en la roca. Como los barrenos están muy próximos entre sí, las grietas se forman siguiendo las líneas de barrenos, y los mismos barrenos constituyen el inicio del agrietamiento. Esto significa que la inclusión de barrenos vacíos entre los cargados, puede mejorar los resultados.

En la tabla I.25 se indican algunas cargas y espaciamientos en función del diámetro de los barrenos.

Si no existen limitaciones en las vibraciones del terreno se utiliza el encendido instantáneo; por lo contrario, si es necesario limitar la magnitud de las vibraciones del terreno se utilizan microretardos. La formación de grietas resulta menos eficiente que con la iniciación instantánea, a menos que se reduzca el espacio entre barrenos. Si el tiempo de retardo es muy grande no se logra el precorte.

TABLA I.25 Precorte

Diámetro del barreno mm	Espaciamiento m	Concentración de carga kg/m
25 - 32	0.20 - 0.30	0.08
25 - 32	0.35 - 0.60	0.18
40	0.35 - 0.50	0.18
51	0.40 - 0.50	0.36
64	0.60 - 0.80	0.38

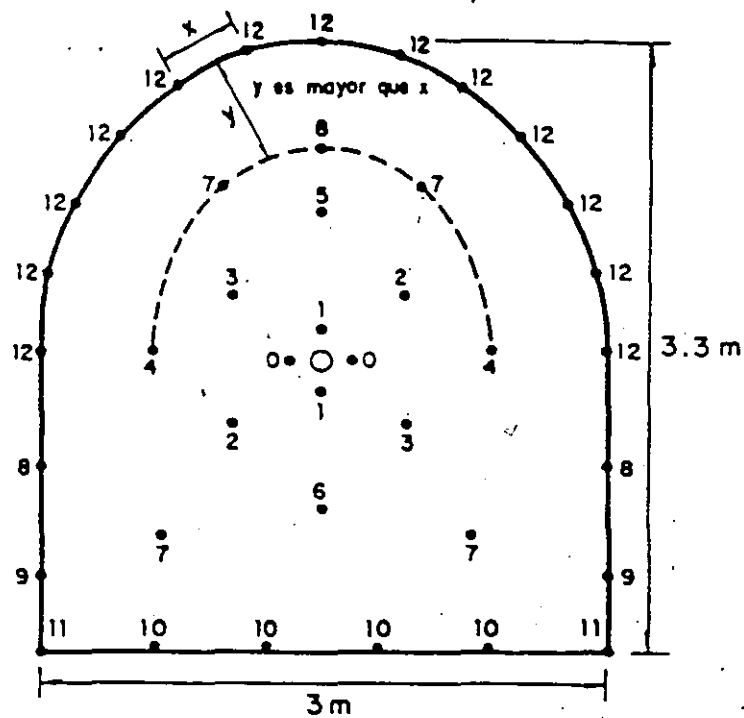


FIG I.41 Distribución típica de retardos en un túnel

que la roca fragmentada ya ha sido desplazada, ofreciéndoles un espacio de alivio suficiente. Este alivio permite una voladura del bordo final con un sacudimiento mínimo.

En la tabla I.24 se proporcionan valores prácticos recomendados de espaciamientos, bordos y concentraciones de carga promedio para dos diámetros de barreno, utilizando explosivos de 1.2 a 1.3 g/cm³ de peso volumétrico.

TABLA I.24 Poscorte perimetral

Diámetro barreno mm	Espaciamiento m	Bordo m	Concentración total de carga en el barreno kg/m
38 - <u>45</u>	<u>0.60</u>	0.90	0.18 - <u>0.38</u>
51	0.75	1.05	0.18 - 0.38

TABLA 8.1

Concentración de la carga (1) en kg/m para cueles cilindricos y máxima distancia cuando se dispara hacia barrenos vacíos con diámetros comprendidos entre $\phi = 2 \cdot 57$ y 200 mm (d representa el diámetro del barreno cargado). La potencia relativa del explosivo es $s = 1,0$.

ϕ mm	50	2 · 57	75	83	100	2 · 75	110	125	150	200
32	0,2	0,3	0,3	0,35	0,4	0,45	0,45	0,5	0,6	0,8
37	0,25	0,35	0,35	0,4	0,45	0,53	0,53	0,6	0,7	0,95
45	0,30	0,42	0,42	0,50	0,55	0,65	0,65	0,7	0,85	1,10
λ mm	90	150	130	145	175	200	190	220	250	330

Hay que señalar, especialmente con barrenos vacíos de pequeños diámetros, lo mucho que hay que aumentar la carga cuando se incrementa la distancia entre centros. Para $\phi = 30$ mm se necesita una carga de 1,0 kg/m para una distancia entre centros de 11 cm y menos de la mitad de la concentración de carga para una distancia de 8 cm. Este es

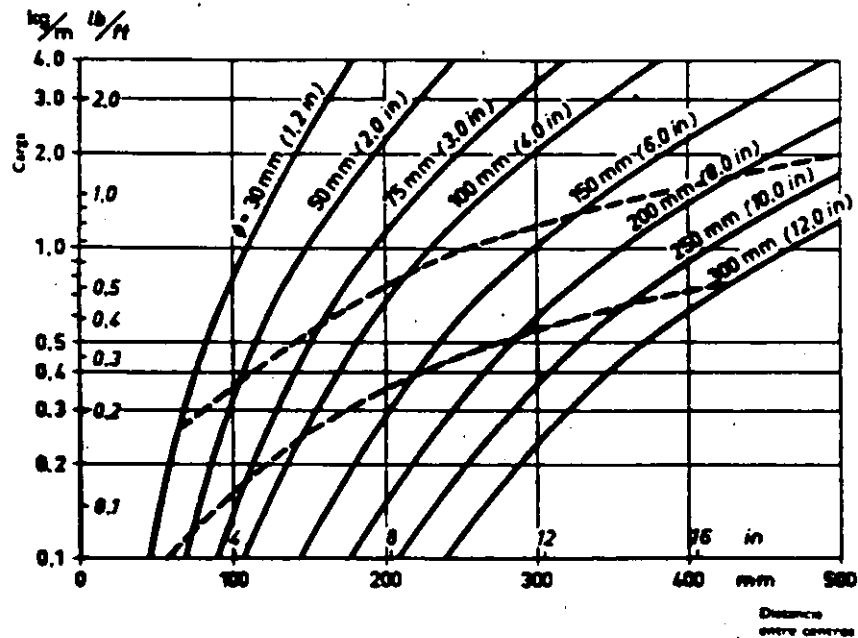


FIG. 8.4

Relación entre la cantidad de carga y la distancia entre los barrenos cuando se dispara hacia un barreno vacío con un diámetro de 30-150 mm ---- corresponde a las líneas de puntos de la figura 8.5. Diámetro de los barrenos cargados = 32 mm.

TABLA 7.2

Concentración de la carga, en kg/m, para diversas piedras (V) y extensión (B) de la cara libre (tabla preliminar).

Piedra max. V m	Concentración de la carga, kg m											Carga limite l. kg m con piedra libre
	B = 0,10 0,3	0,15 0,5	0,20 0,7	0,25 0,8	0,30 1	0,35 1,2	0,40 1,3	0,50 1,7	0,60 2	0,80 2,7	1,4 m 4,7 ft	
	kg m											
0,10	0,12	0,08	0,06									
0,15	0,30	0,18	0,13	0,11	0,09							
0,20	0,60	0,35	0,24	0,20	0,16	0,14	0,12					
0,25	1,0	0,60	0,35	0,30	0,26	0,22	0,18					
0,30	1,3	0,9	0,60	0,50	0,35	0,31	0,26	0,22	0,18			
0,35		1,2	0,9	0,65	0,45	0,40	0,35	0,30	0,25			
0,40		1,6	1,2	0,9	0,7	0,6	0,50	0,40	0,30	0,24		
0,50			2,0	1,6	1,3	1,0	0,7	0,60	0,50	0,36		0,13
0,60				2,2	1,9	1,6	1,3	1,0	0,7	0,52		0,17
0,70					2,5	2,2	1,8	1,3	0,9	0,7		0,25
0,80						3,2	2,4	1,8	1,4	1,0	0,6	0,32
1,00							4,0	3,0	2,4	1,4	0,9	0,5
1,20								4,4	3,8	2,5	1,2	0,7
1,40									5,0	3,6	1,6	0,9
1,60										4,8	2,4	1,1
2,00											3,0	1,9

Las cifras en libras son 2/3 de las cifras para kg m.

en la que los subíndices a y b se refieren a las figuras 7.5 a y b respectivamente. La relación (7.4) se estudiará en el próximo capítulo; la relación (7.5) se da en la tabla 7.2.

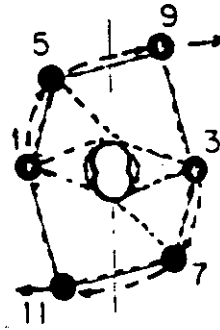
Estas ecuaciones difieren solamente en el valor de la constante, que en las voladuras con una salida circular es un 60% mayor que con una rectangular, debido a la mayor constricción en el primer caso.

Las anteriores relaciones abarcan los datos experimentales actuales, pero las voladuras con una salida rectangular deben estar sujetas a ulteriores consideraciones teóricas. Sin embargo, la parte experimental de la investigación ha alcanzado una etapa que suministra bases para la discusión de algunos de los principales puntos involucrados: la determinación del diámetro óptimo de los barrenos no cargados en las voladuras de cuele paralelo, la construcción de los esquemas de perforación y el cálculo de la carga con miras a la colocación de los taladros y a la dispersión real de la perforación.

Las cargas dadas en la tabla son suficientes para la rotura pero no comprenden necesariamente los valores límites; muchos de los valores

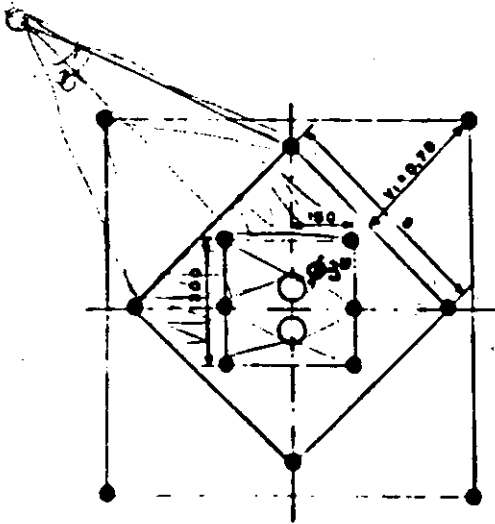


CUÑA "CINCO DE CRUZ"
CON UN BARRENO DE GRAN DIAMETRO



CUÑA COROMANT
(ADECUADA PARA GALERIA PEQUEÑA)

El dispositivo guía se fija a la roca mediante un expansor.



CUÑA DE EXPANSION CON DOS
BARRENOS QUEMADOS DE
GRAN DIAMETRO



CUÑA DE EXPANSION PARA UNO
O DOS BARRENOS QUEMADOS

Avance de 3.9 a 4 m

- No se debe trabajar con diámetros grandes en todo el frente del túnel.

TABLA 8.6

Cueles en doble espiral con diversos diámetros del barreno vacío (ϕ). Datos acordes con la figura 8.10. Las concentraciones de carga l_1 y l_2 se refieren a los barrenos marcados con - y • respectivamente.

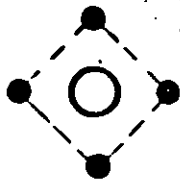
ϕ mm	75	85	100	110	125	150	200
a mm	110	120	130	140	160	190	250
b mm	130	140	160	170	190	230	310
c mm	160	175	195	210	240	290	380
d mm	270	290	325	350	400		
l_1 kg m	0,30	0,35	0,40	0,45	0,5	0,6	0,8
l_2 kg m	0,65	0,75	0,85	0,9	1,1	1,3	1,7

bajar apreciablemente el avance medio. El encendido de los diferentes barrenos del cuele debe efectuarse según la secuencia dada en las figuras 8.10 y 8.11. Respecto a los cueles de doble espiral, Täby y Coromant, el encendido de los barrenos núm. 1 y 2 con detonadores instantáneos puede mejorar los resultados. Estos detonadores instantáneos deben situarse en la boca del barreno. Para evitar el riesgo de decapitación de las otras cargas, los demás detonadores deben colocarse en el fondo de los barrenos. No deberían llevar carga de fondo los 6-8 barrenos más próximos al barreno vacío.

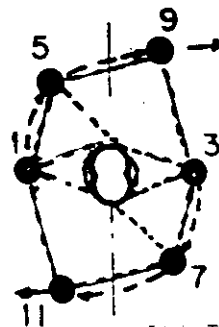
a) Cueles cilíndricos

Cueles en doble espiral (fig. 8.10 a)

El esquema de barrenos en espiral proporciona la abertura más amplia. Sin embargo, cuando se pretendan obtener grandes avances deberá usarse el doble espiral de la figura 8.10 a, adoptando la separación entre barrenos y la concentración de carga de la tabla 8.6. Con el esquema en doble espiral se tiene la ventaja de que pueden iniciarse sucesivamente los barrenos opuestos, con lo que se obtiene una mejor limpieza de la abertura. Además, la seguridad en el avance aumenta, ya que cada sección de la doble espiral puede romper con independencia. Según los datos de avances medios dados en la tabla 8.3, el cuele en doble espiral es definitivamente superior a los demás tipos de cueles, con un avance por lo menos un 20 % mayor que los demás de barrenos paralelos. Una desventaja en la práctica es el hecho de que los dos barrenos más próximos al vacío de 100-110 mm sólo distan 130-140 mm de su centro y en la perforación con estructuras estacionarias y con el equipo actual se precisa una distancia de 160 mm. Esto lleva consigo la necesidad de aumentar el diámetro del barreno vacío hasta 125 mm, con lo que la distancia al centro puede incrementarse hasta 160 mm y, si se desea, aumentar el

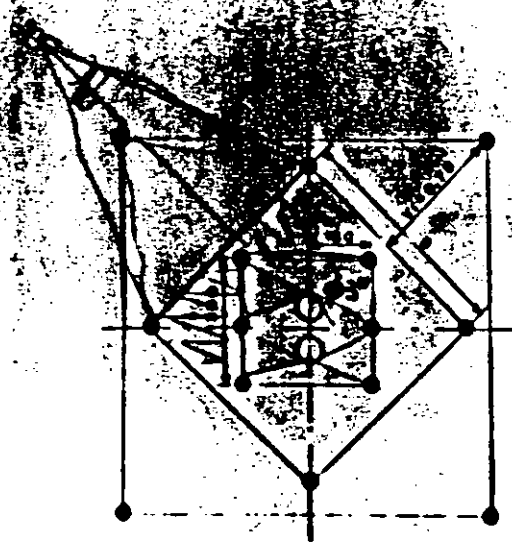


CUÑA "CINCO DE OROS"
CON UN BARRENO DE GRAN DIAMETRO



CUÑA COROMANT
(ADECUADA PARA GALERIA PEQUEÑA)

El dispositivo guía se fija a la roca mediante un expansor.



CUÑA DE EXPANSION CON DOS
BARRENOS QUEMADOS DE
GRAN DIAMETRO



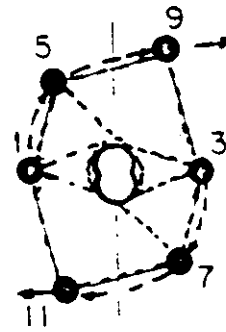
CUÑA DE EXPANSION PARA UNO
O DOS BARRENOS QUEMADOS

Avance de 3.9 a 4 m

- No se debe trabajar con diámetros grandes en todo el frente del túnel.

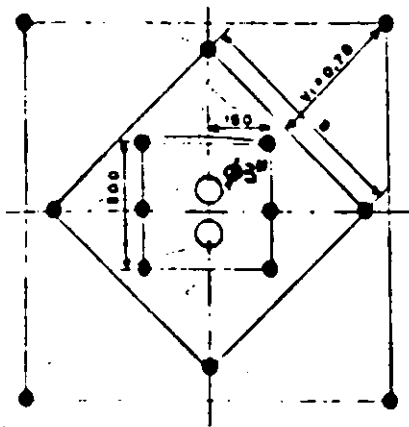


CUNIA "CINCO DE CRUZ"
CON UN BARRENO DE GRAN DIAMETRO



CUNIA COROMANT
(ADECUADA PARA GALERIA PEQUEÑA)

El dispositivo guía se fija a la roca mediante un expansor



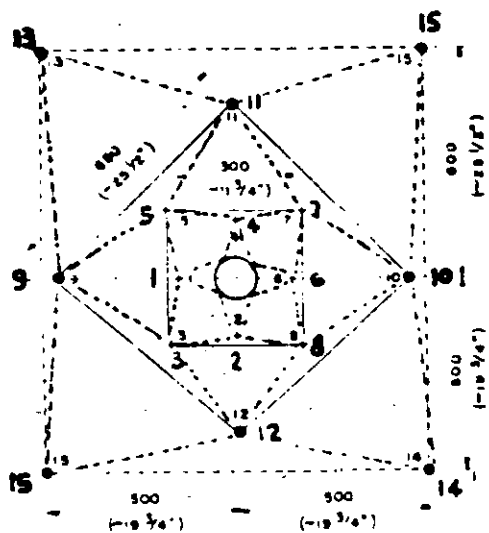
CUNIA DE EXPANSION CON DOS
BARRENOS QUEMADOS DE
GRAN DIAMETRO



CUNIA DE EXPANSION PARA UNO
O DOS BARRENOS QUEMADOS

Avance de 3.9 a 4m

- - No se debe trabajar con diámetros grandes en todo el frente del túnel.



CUNA EN CUATRO SECCIONES CON UN BARRIL DE GRAN DIAMETRO (ES LA CUNA CILINDRICA MAS UTILIZADA)



CUNA FAGERSTA (ADECUADA PARA GALERIA PEQUEÑA)

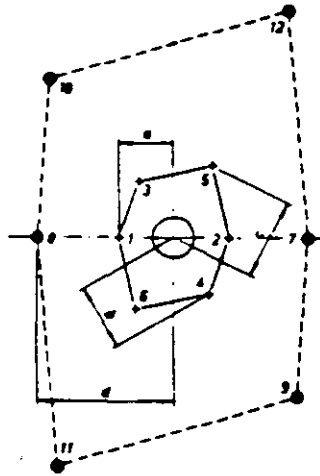


FIG. 8.10 a
Cuele en doble espiral (datos acordes con la tabla 8.6).

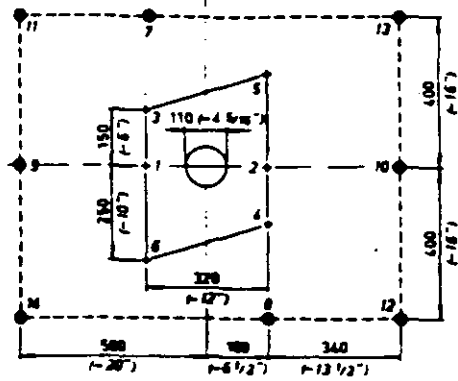


FIG. 8.10 b
Cuele Táby.

avance en un 10 %. Otra alternativa puede ser la de aumentar simplemente la distancia entre estos dos barrenos más próximos a 160 mm, pero se reducirá de esta forma el avance medio un 5-10 %, por lo menos.

Cuele Táby (fig. 8.10 b)

Como puede verse por el esquema de encendido, este es un cuele en doble espiral modificado. En lo referente al avance, es inferior al obtenido con el doble espiral propiamente dicho, según la tabla 8.3, lo

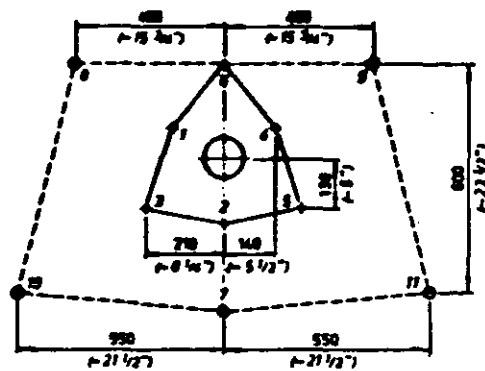
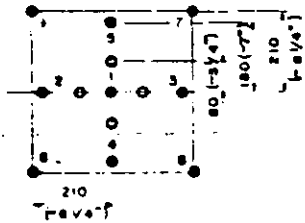


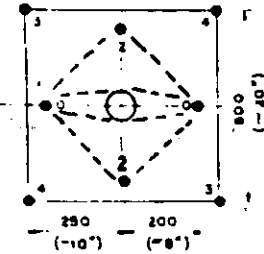
FIG. 8.10 c
Cuele en tres secciones $d = 110$ mm.



CUÑA QUEMADA CON
CUATRO BARRENOS
HUECOS Ø 35 mm
(CUÑA GRONLUND)

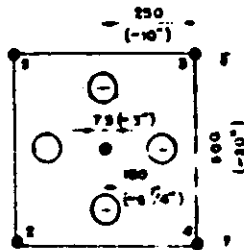
Buena hasta 3.2 m de
profundidad.

- En el barreno central el estopín
esta en la boca del barreno
- En los ayudantes el estopín
esta al fondo.

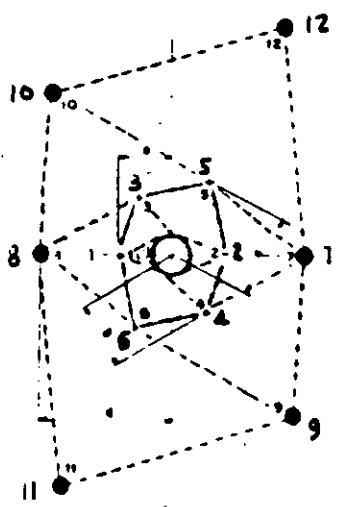


CUÑA QUEMADA MICHIGAN

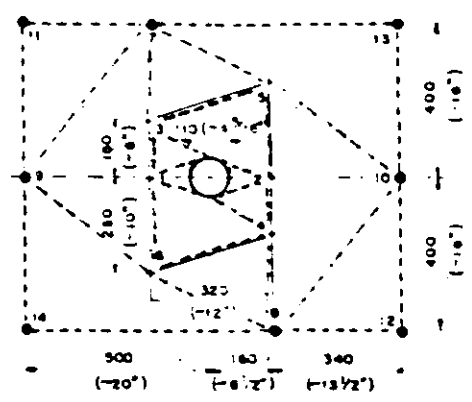
Avance 3.9 m



CUÑA TIPO GATO CON
CUATRO BARRENOS
VACIOS DE DIAMETRO
GRANDE

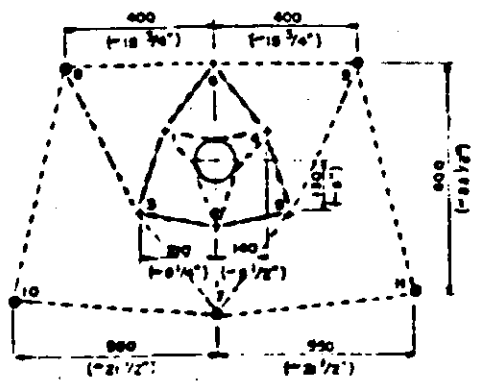


CUÑA EN DOBLE ESPIRAL CON UN BARRENO DE DIAMETRO GRANDE



CUÑA EN DOBLE ESPIRAL MODIFICADO (CUÑA TABY) CON UN BARRENO DE DIAMETRO GRANDE

Más eficiente que la Fagersta



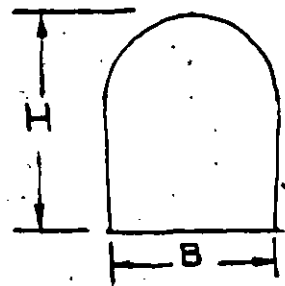
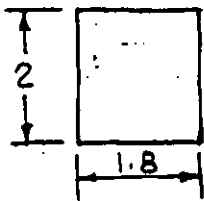
CUÑA DE TRES SECCIONES 25 % MAS EFICIENTE QUE LA TABY

PROCEDIMIENTOS DE EXCAVACION DE CAVIDADES SUBTERRANEAS

Los procedimientos de excavación de cavidades subterráneas dependen de los siguientes factores:

- Calidad del macizo rocoso
- Dimensión de la cavidad
- Filtraciones de agua
- Equipo disponible

A continuación presentaremos algunos de los procedimientos más usuales.

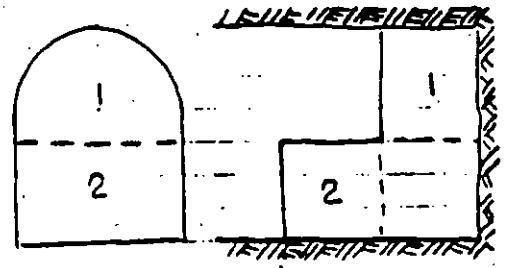
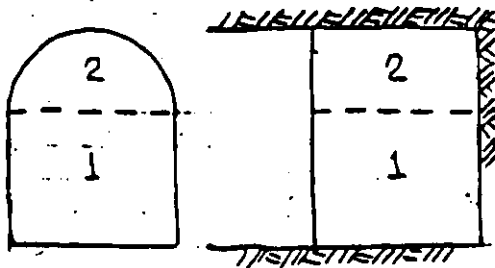


B	H
2.5	3.5 m
6.0	5.0 m
9.0	9.0 m

Sección Portal

SECCION COMPLETA EN ROCA SANA, CON EXPLOSIVOS

- Socavones de exploración
- Galerías de explotación
- Galerías de inyección y drenaje
- Túneles de acceso



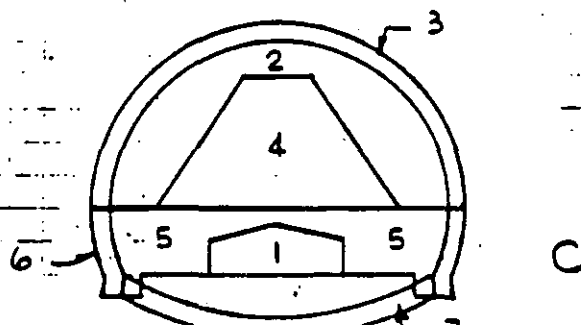
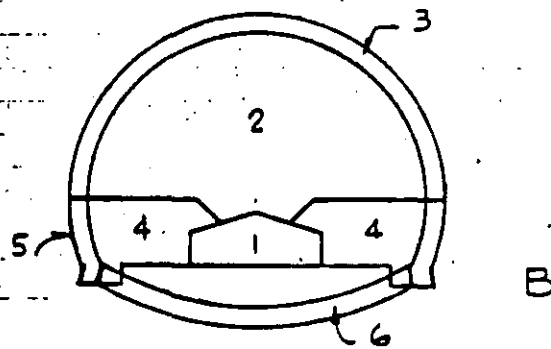
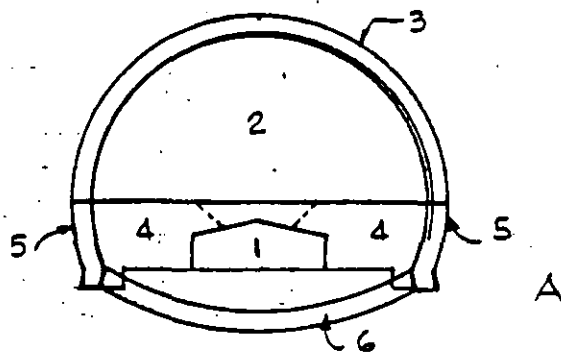
SECCIONES COMBINADAS

- Cuando hay poco techo
- Con perforadora de pierna

Método de túnel piloto sobre el piso del túnel

133

Se utiliza en roca blanda con filtraciones. La galería piloto de avance sirve para drenar el agua de infiltración y tiene área entre 9 y 15 m^2 . En las figuras se indican las tres variantes de este método. La galería piloto puede o no ir ademada con marcos y concreto lanzado.

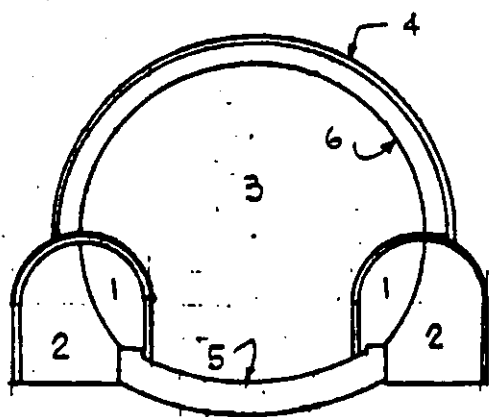


Método de las dos galerías piloto laterales sobre el piso del túnel. Se utiliza en roca blanda.

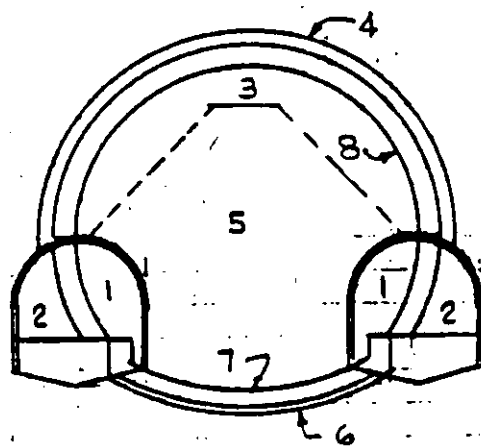
En una primera etapa se excavan los dos túneles piloto los cuales se protegen con marcos metálicos. Se cuelan las guarniciones de piso y arranque de los muros laterales.

En la segunda etapa puede realizarse el resto de la excavación con avances pequeños de 1 ó 2 metros soportando la roca con marcos que se apoyan en los arranques del muro previamente colados.

Cuando la roca no soporta el avance de 1 ó 2 metros, entonces se excava una ranura o corona de 0,75 m a 1 m de longitud que permita la colocación del marco metálico de soporte, continuando con revestimientos de concreto lanzado y finalmente con el núcleo central.



A



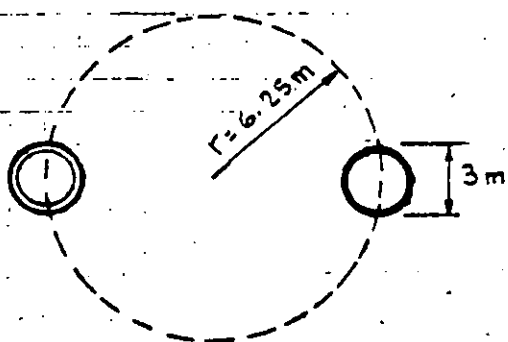
B

Método de soportes laterales piloto. (Japón)

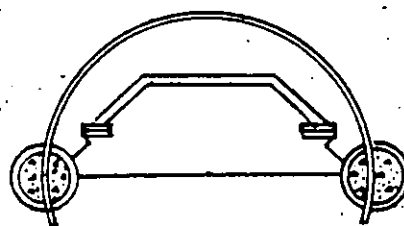
Este método se ha utilizado en túneles por debajo del mar en roca deleznable con fuertes filtraciones (1000 a 1500 lt/seg)

- 1.- Perforación de los dos túneles piloto de 3m de diámetro
- 2.- Colocación del ademe metálico del túnel principal, dentro de las dos galerías piloto. Ademe de tubo de acero.
- 3.- Relleno de concreto de las dos galerías piloto
- 4.- Excavación de la mitad superior
- 5.- Colocación de los marcos metálicos tubulares, los cuales se rellenan con mortero para aumentar su resistencia
- 6.- Excavación de la mitad inferior
- 7.- Colocación de los tornapuntas tubulares inferiores
- 8.- Colado del revestimiento de concreto.

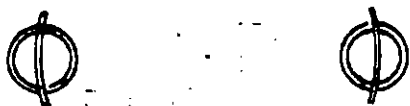
METODO DE SOPORTES LATERALES PILOTO (TUNEL SEIKAN, JAPON)



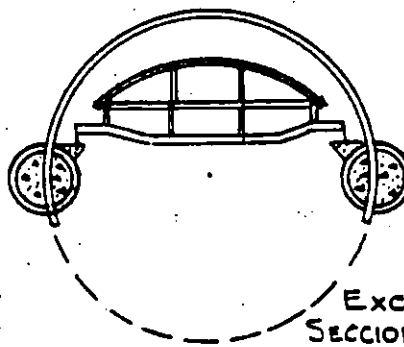
1 PERFORACION TUNELES PILOTO



5 ADEME SECCION SUPERIOR



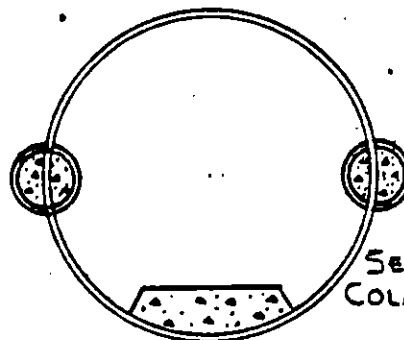
2 COLOCACION ADEME METALICO



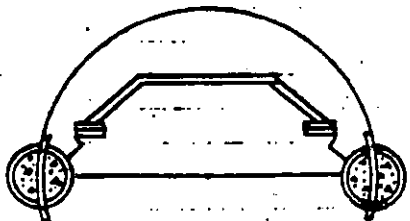
6 EXCAVACION SECCION INFERIOR



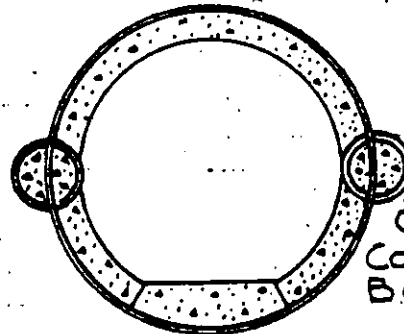
3 CONCRETO TUNELES PILOTO



7 ADEME SECCION INFERIOR COLADO CUBETA



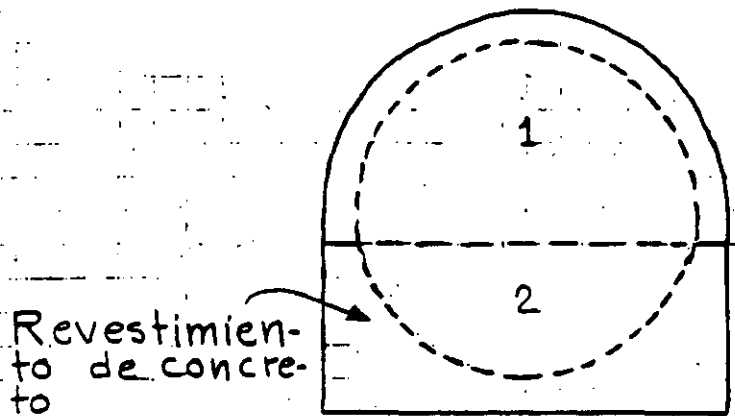
4 EXCAVACION SECCION SUPERIOR



8 COLADO COSTILLAS Y BOVEDA

Método de sección superior y banqueo

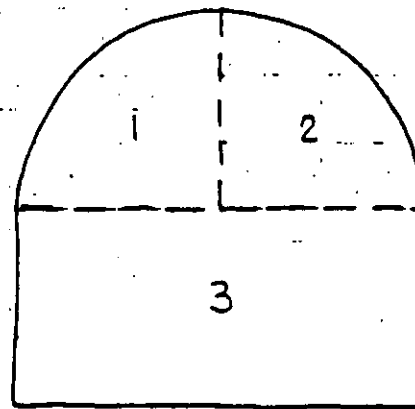
Se utiliza en roca sana.



Sección portal

12 x 12 m

A



Sección portal

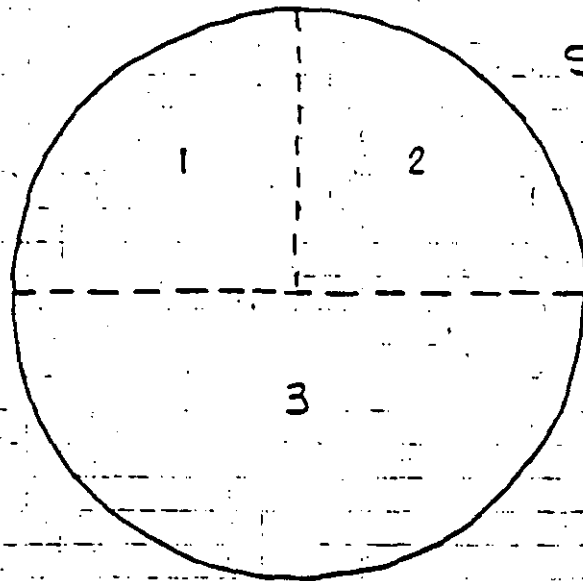
12 x 12 m

B

- Algunas veces la sección superior es necesario excavarla en dos o tres secciones, como en B.
- La mejor geometría se obtiene mediante voladuras de post-corte perimetral (smooth blasting) con barrenación horizontal tanto en la sección superior como en la inferior.

Método de sección superior y banqueo.

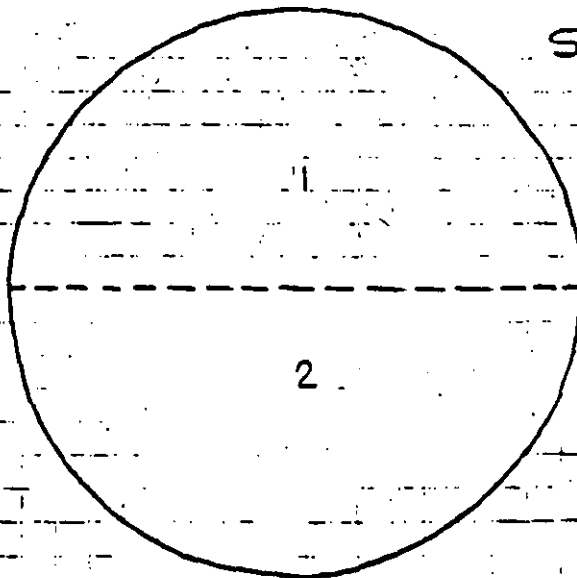
Se utiliza en roca sana.



SECCION CIRCULAR

ϕ 16.5 m

A



SECCION CIRCULAR

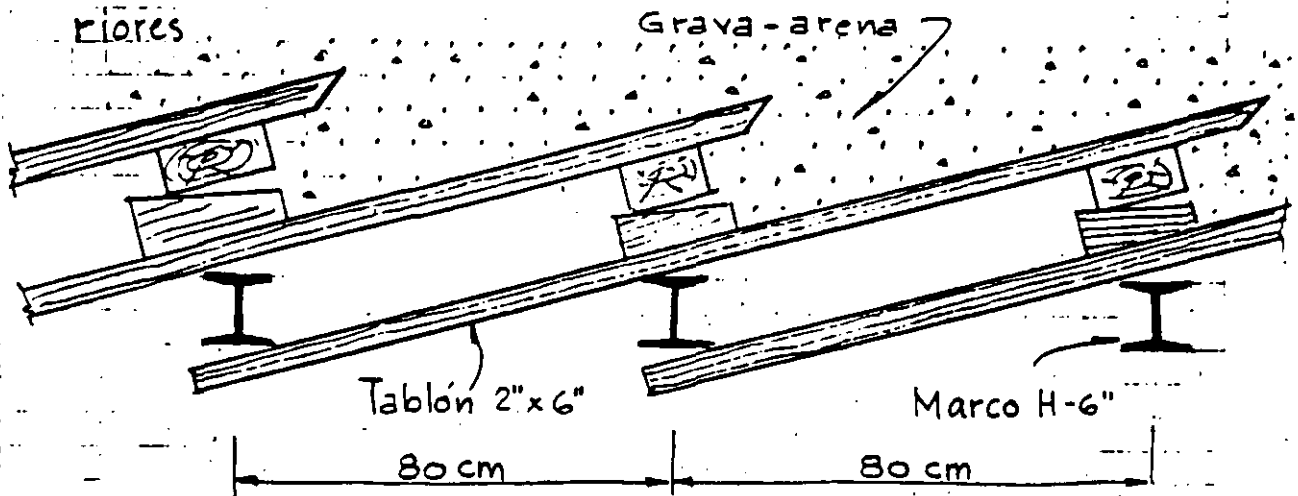
ϕ 16.5 m

B

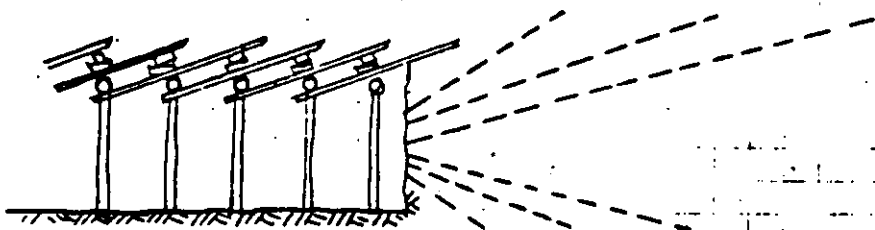
Se deben usar voladuras de post-corte perime-
tral (smooth-blasting)

EXCAVACION CON ESTACAS DE AVANCE AL FRENTE

En suelos medianamente compactos como tepetate (toba sedimentaria de origen volcánico, arenas-limo-arcillosas con poca cementación) o rocas deleznales se requiere de soporte adelante del frente del túnel. En estos casos se hincan cuñas de madera o de metal apoyándose en los marcos anteriores.



ESQUEMA DE SOPORTE



ESTACAS DE AVANCE
MAS AUREOLAS DE INYECCION

TUNELES EN SUELOS BLANDOS

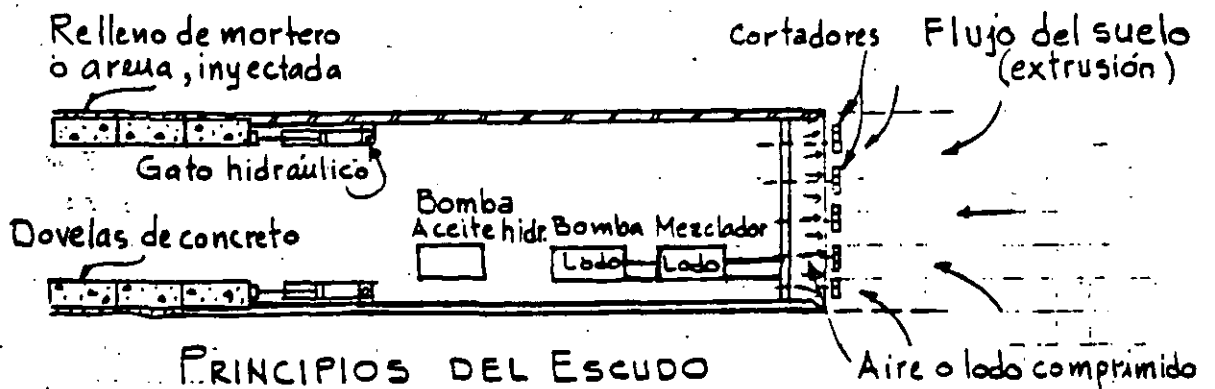
Los procedimientos más usuales son:

- Excavación con escudo
- Cajones hundidos

Los escudos pueden ser abiertos o cerrados según la consistencia del suelo.

Cuando el suelo es muy blando se usan los escudos cerrados con cámara de presión al frente ya sea con aire presurizado o lodo presurizado para evitar la extrusión del suelo hacia el escudo. En algunos casos se ha recurrido a la congelación del suelo para mejorar su consistencia y poderlo excavar.

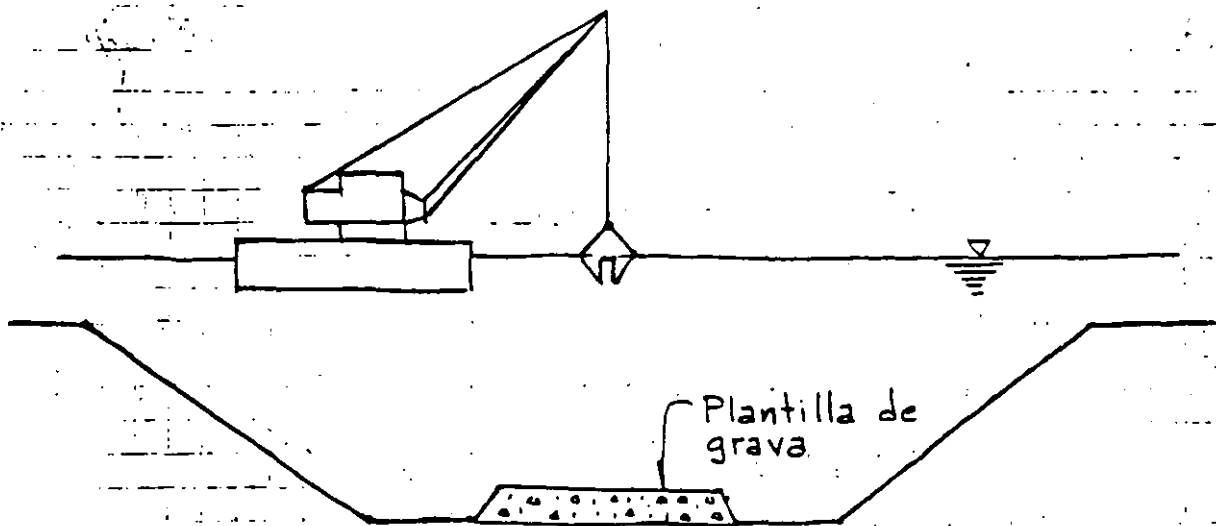
El material excavado se mezcla y se bombea como lodo (slurry) hacia afuera donde se separa el agua de los sólidos para volver a utilizarse.



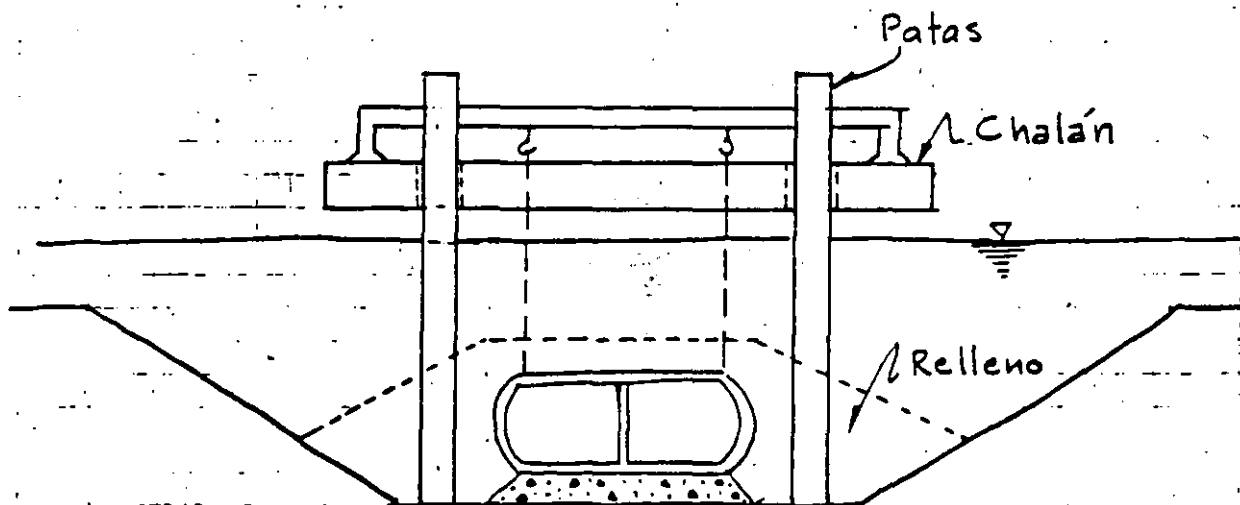
PRINCIPIOS DEL ESCUDO

La excavación del frente puede hacerse a mano o con cortadores

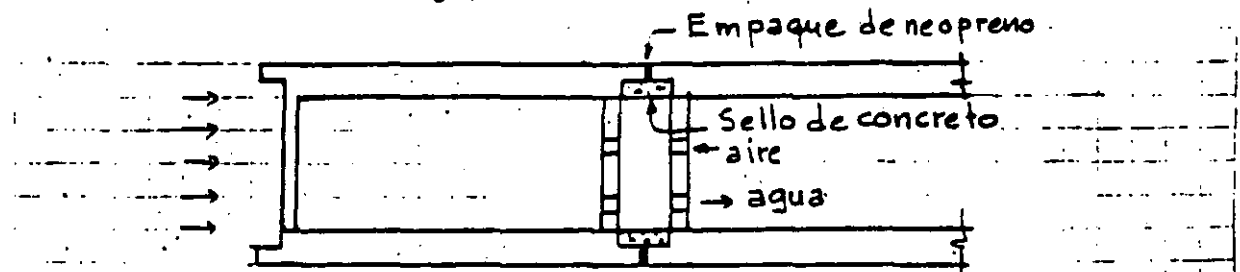
HUNDIMIENTO DE CAJONES



DRAGADO DEL CANAL



HUNDIMIENTO DE LOS CAJONES

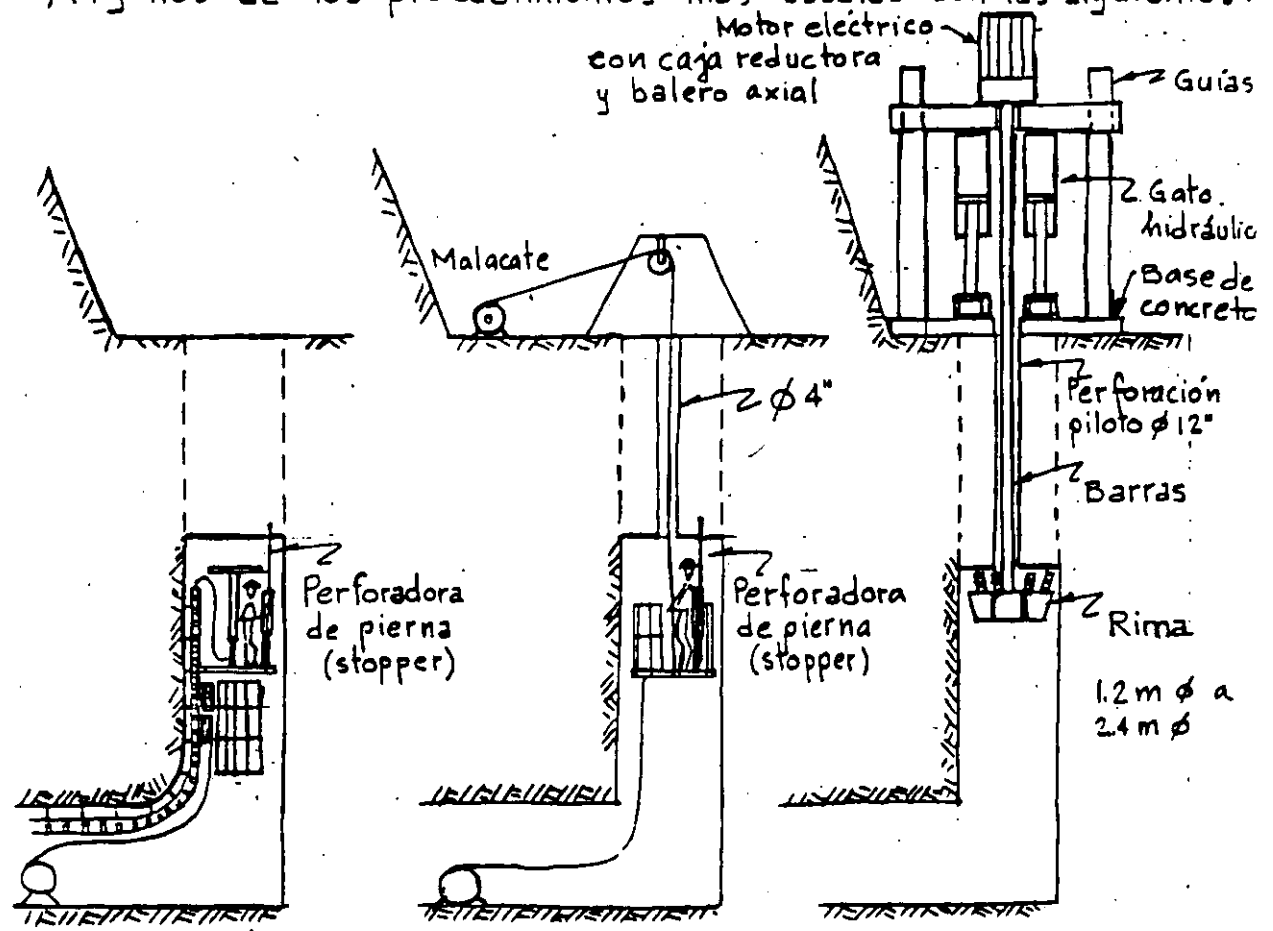


SELLO DE JUNTAS

EXCAVACION DE LUMBRERAS

La excavación de lumbreras depende en buen grado del equipo disponible.

Algunos de los procedimientos más usuales son los siguientes:



JAULA TREPADORA
3.6 a 5.4 m/día

JAULA SUSPENDIDA
3.6 a 5.4 m/día

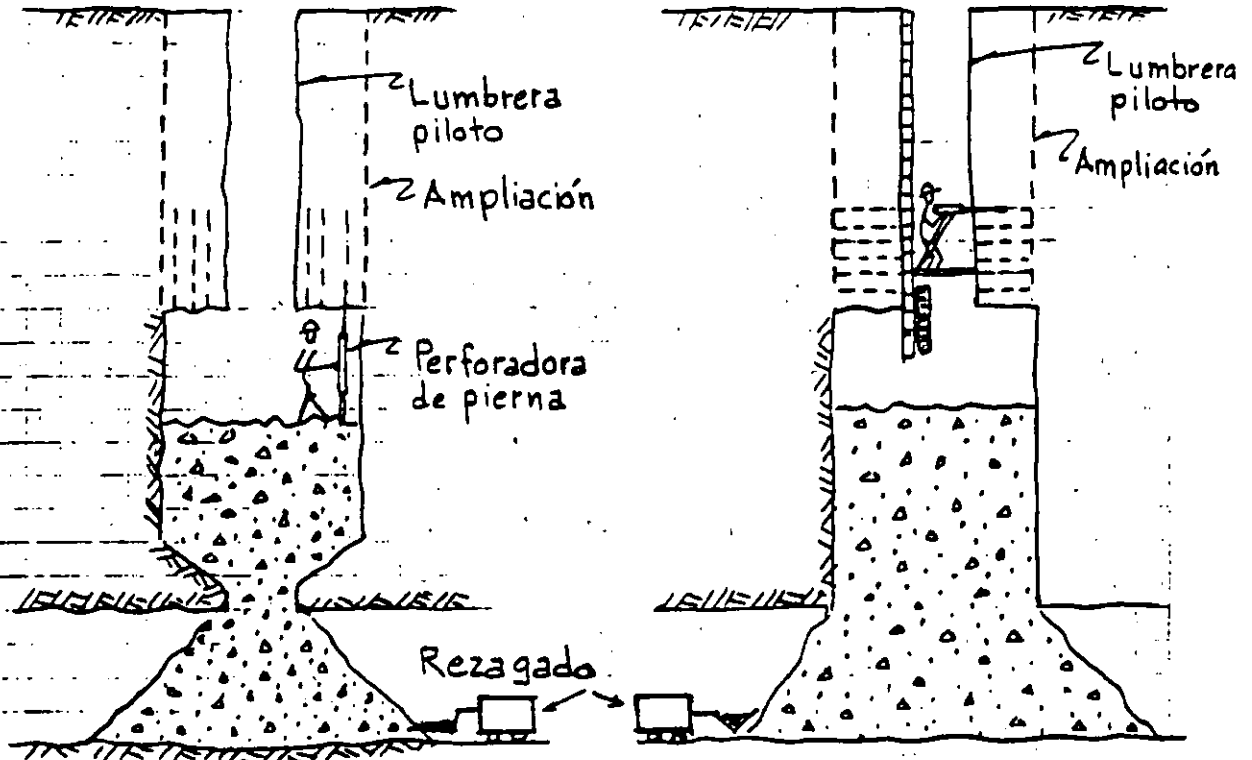
CONTRAPOCERA
16 a 36 m/día

Ventajas de la contrapocera:

- Menor tiempo
- Lumbreras más largas
- Mayor producción

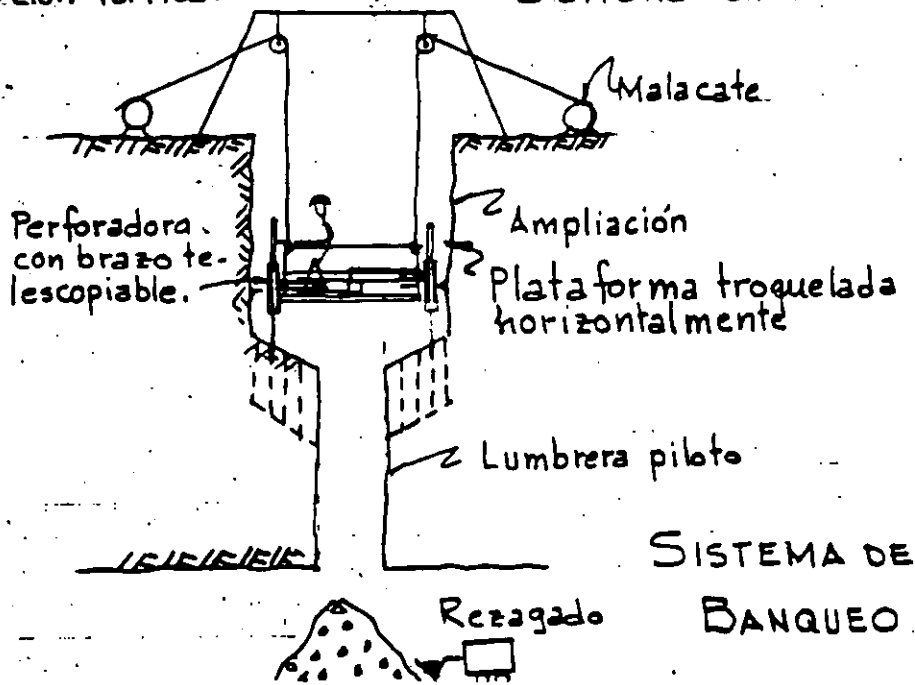
Las jaulas están quedando fuera de uso.

AMPLIACION DE LUMBRERAS



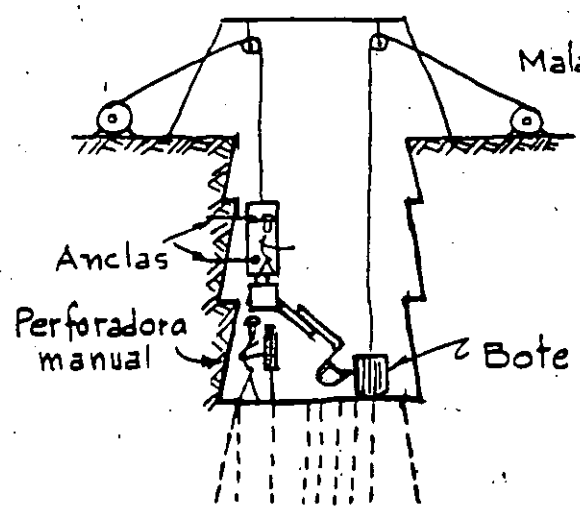
Barrenación vertical

Barrenación horizontal

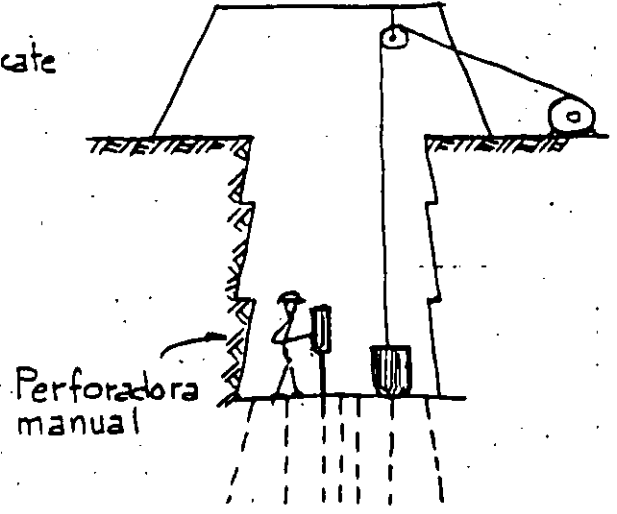


SISTEMA DE BANQUEO

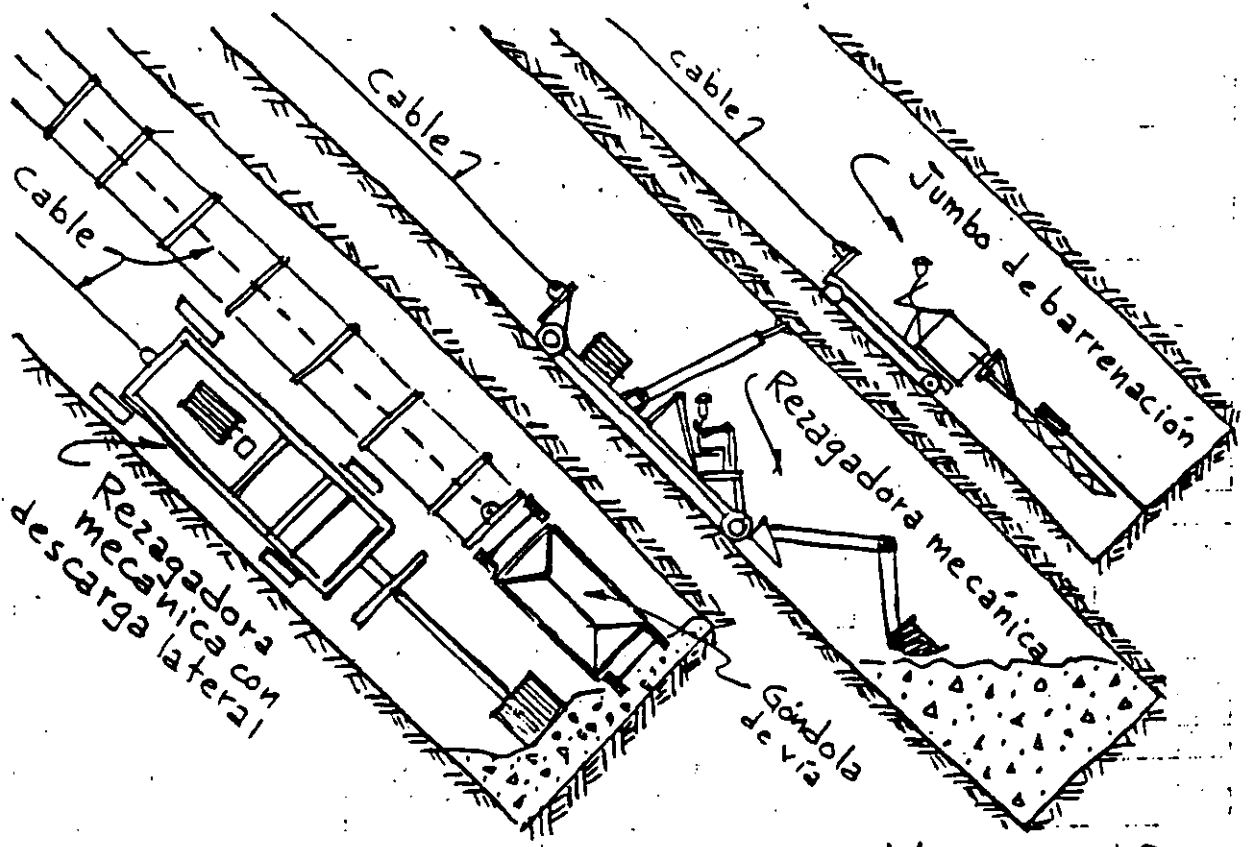
POZOS VERTICALES E INCLINADOS



REZAGADORA MECANICA

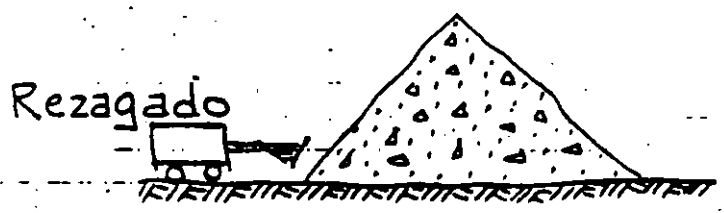
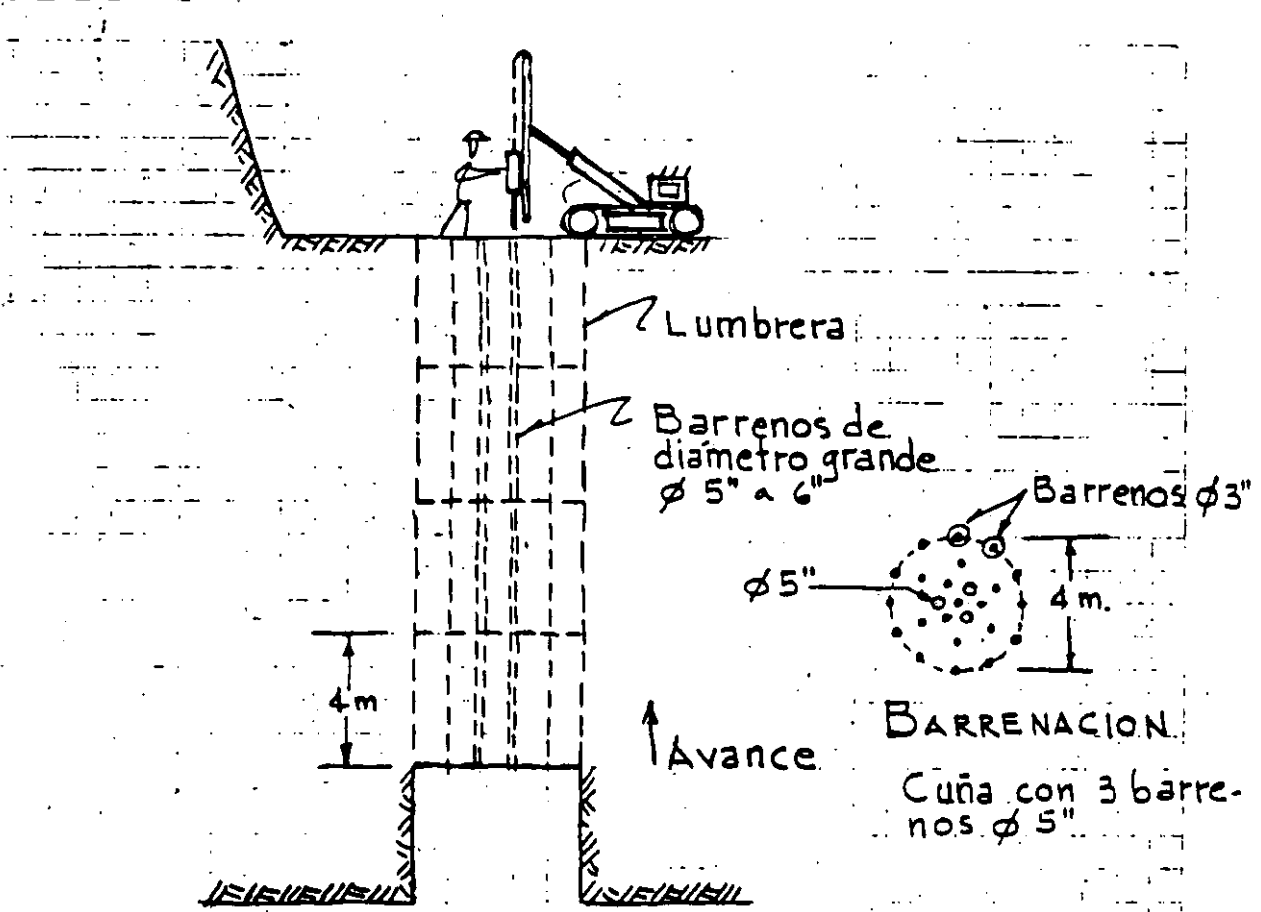


REZAGADO MANUAL



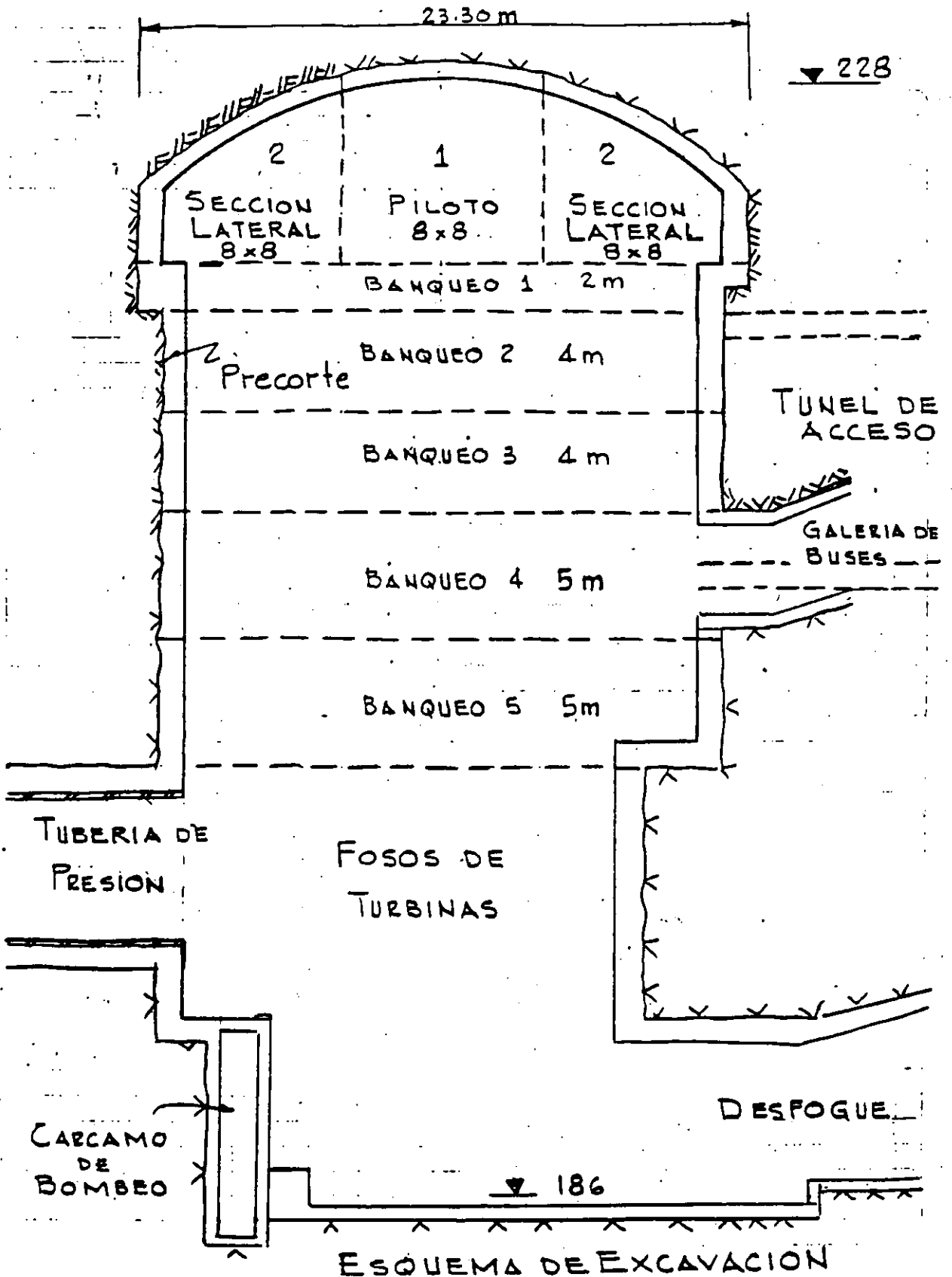
POZO INCLINADO CON EXCAVACION MECANIZADA

LUMBRERAS CON DETONACION HACIA ARRIBA



AVANCE VERTICAL HACIA ARRIBA

EXCAVACION DE CASAS DE MAQUINAS



BOMBEO EN TUNELES .

Las condiciones y características del bombeo de agua en túneles es muy variable.

Dada la importancia que reviste el bombeo para evitar suspensiones de trabajo a causa de inundaciones a continuación presentamos algunos puntos de vista sobre el manejo del agua.

- Tener respaldo de bombas entre 300 y 400 %
- Personal especializado en instalación y mantenimiento.
- Suministro y protección eléctrica adecuado y/o suministro confiable de aire comprimido.
- La bomba debera tener un F.S. = 1.5 para contrarrestar efectos de temperatura y humedad, desgaste y bajas de voltaje. Las pérdidas de carga por fricción son aproximadas al 20%.

BOMBAS USUALES :

Gasto de 2 a 10 lt/seg.
con carga de 15m.

Bombas de turbina y/o de diafragma accionadas por aire comprimido. Sumergibles

Gasto de 2 a 10 lt/seg
con cargas de 50 a 75m

Bombas de pistón, accionadas por bielas acopladas a motor eléctrico. Con pichancho

Gasto de 25 a 100 lt/seg
con cargas de 50 a 75 m

Bombas sumergibles de turbina acopladas a motor eléctrico estanco contra el agua.

Gasto de 100 a 1000 lt/seg.
con cargas de 50 a 100 m

Bombas sumergibles y/o de pozo profundo.

Potencia de una bomba $P = 8QH$, $Q = m^3/seg$, $H = m$, $P = KW$

Si $Q = 80 lt/seg$ y $H = 80 m$; $P = 8 \times 0.08 \times 80 \times 1.2 = 61.44 Kw = 82 HP$
Utilizando un F.S. = 1.5 $P = 125 HP$

VENTILACION EN TUNELES

DURANTE LA CONSTRUCCION

Requerimientos de diseño:

- Calidad del aire fresco: ^{calidad requerida en las áreas de trabajo.}
- Ciclo de trabajo: Número de turnos y horas de ejecución de voladuras.
- Cantidad de aire: Programa de demanda actual y futura, concentración particular de máquinas productoras de gas y polvo.

CALIDAD DEL AIRE

Máximas concentraciones de impurezas del aire permitidas por el Cuerpo Nacional de Trabajo de Salud y Seguridad de Suecia

SUBSTANCIA	CONCENTRACION PROMEDIO (PPM) DURANTE UNA EXPOSICION DE	
	30 min	8 horas
Monóxido de carbono CO	50	25
Dióxido de carbono CO ₂	15 000	5 000
Dióxido de nitrógeno NO ₂	3	2
Oxidos de nitrógeno NO _x No _x = NO · NO ₂	30	20

La contaminación principal del aire proviene de los vehículos diesel y de los explosivos que producen oxidos de carbono y gases nitrosos y cenizas volantes.

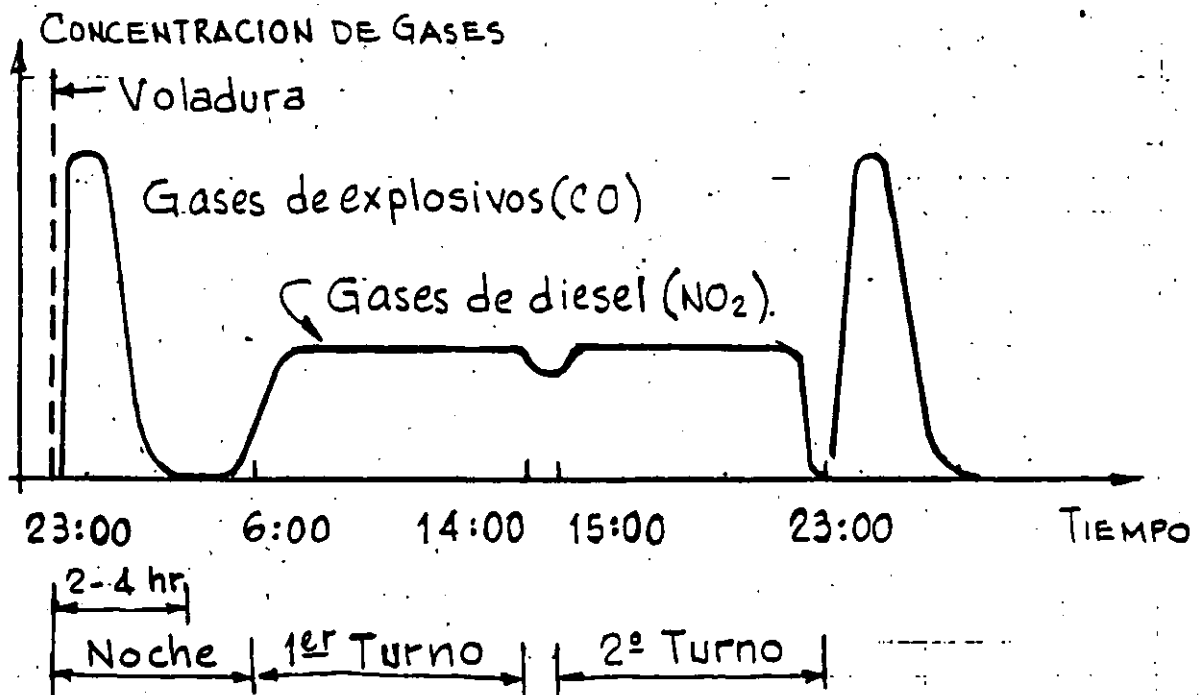
Para el caso de la Mina Kiruna en Suecia, el factor gobernante en el diseño ha sido el bióxido de nitrógeno NO_2 .

Los vehículos diesel deberían estar normalmente equipados con catalizadores y purificadores.

Con el desarrollo futuro de los sistemas de purificación de gases de los vehículos diesel el factor de diseño será el CO_2 .

CICLO DE TRABAJO

A continuación se presenta una gráfica sobre el tipo y concentración de gases medidos en la Mina Kiruna en Suecia durante la operación de dos turnos por día.



CONCENTRACION DE GASES DURANTE EL DIA

Como se sabe los gases de las voladuras caen hasta un nivel aceptable entre 2 y 4 horas después de la voladura,

siempre y cuando la cantidad de aire de ventilación es igual a la capacidad de aire que se utiliza durante el día. Esto significa que durante la noche en la que solo se tienen los gases de los explosivos se requiere una capacidad de ventilación menor.

Se observa claramente la concentración de gases por combustión del diesel al inicio del primer turno.

CANTIDAD DE AIRE

Para determinar la cantidad de aire fresco requerida para estar dentro de los límites permisibles de concentración de gases contaminantes es necesario determinar previamente:

- la cantidad de gases producidos para su limpieza
- la eficiencia del sistema de ventilación que se define como:

$$\frac{C_u}{C_d} = \frac{\text{concentración de impurezas en el aire usado}}{\text{concentración de impurezas en el aire de las áreas de trabajo}}$$

- la calidad del aire abastecido

La cantidad de aire puede determinarse mediante la siguiente expresión, basada en los requerimientos de aire por kilogramo de combustible quemado en un metro cúbico de área de trabajo.

$$Q_e = \frac{P \times 0.27 \times Q_s \times k}{3600}, \text{ m}^3/\text{seg.}$$

en donde:

Q_e = cantidad de aire, $\text{m}^3/\text{seg.}$

P = potencia de máquinas, KW

0.27 = consumo específico, kg/kWh

Q_s = necesidad específica de aire, m^3/kg

recomendación $Q_s = 3000 \text{ m}^3/\text{kg}$ de combustible quemado, según datos de Kiruna.

k = factor de utilización

= 0.15 para operaciones de transporte

= 0.30 para carga y transporte

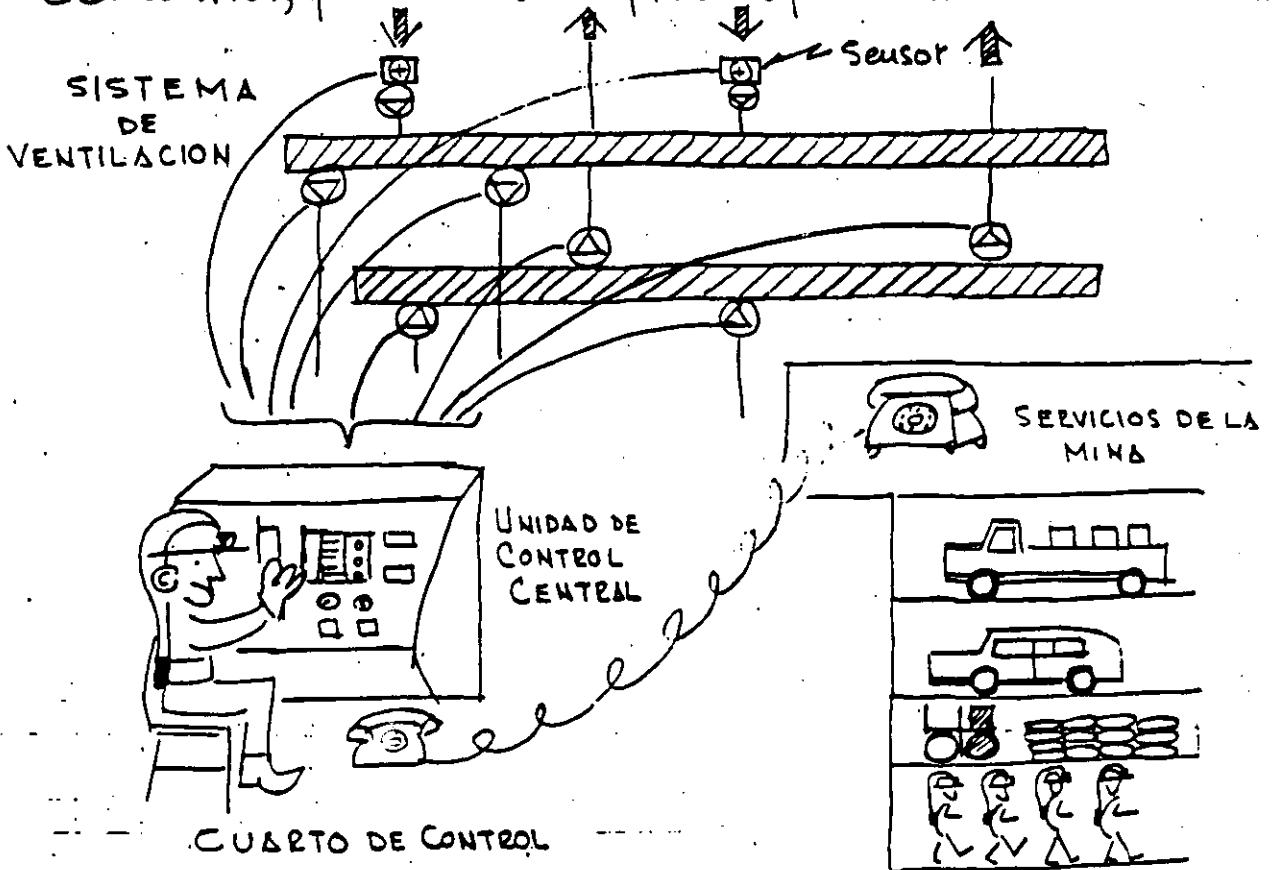
= 0.45 para carga

SISTEMA DE CONTROL

Para estar en mejor posición en el control de la operación del sistema de ventilación fundamentalmente para ahorrar dinero en energía deberá instalarse un sistema de control remoto.

Este sistema está basado sobre una cooperación muy cerrada entre un sistema de señales, un operador y un equipo de mantenimiento.

Si el sistema de ventilación llega a presentarse un defecto por ejemplo: la abertura de una puerta ocasionando fugas, o paro de ventiladores, o temperaturas muy altas, el control unitario manda una señal inmediata al operador del control, quien avisa rápido al personal de mantenimiento.



SELECCION DEL SISTEMA DE VENTILACION

Los arreglos de ventilación pueden hacerse en varias formas. El sistema más adecuado para cada caso dependerá de las condiciones particulares.

INYECCION DE AIRE.. consiste en soplar el aire a través de los ductos hasta los sitios de trabajo y hasta los frentes de excavación. Se obtiene buena ventilación en el frente, teniendo la desventaja que las fugas de aire pueden arrastrar el humo y los gases a todo lo largo del túnel.

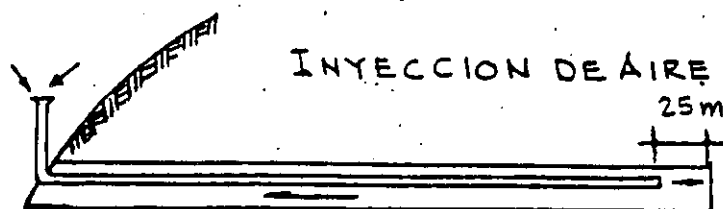
Los ductos de plástico son muy útiles en este caso ya que son fáciles de manejar y ocupan poco espacio.

EXTRACCION FORZADA.. consiste en lanzar los gases, polvo y humo a la atmósfera a través de un ducto metálico que llega hasta el frente. Para obtener una ventilación más eficiente conviene colocar un abanico auxiliar portátil en el piso del túnel junto al frente

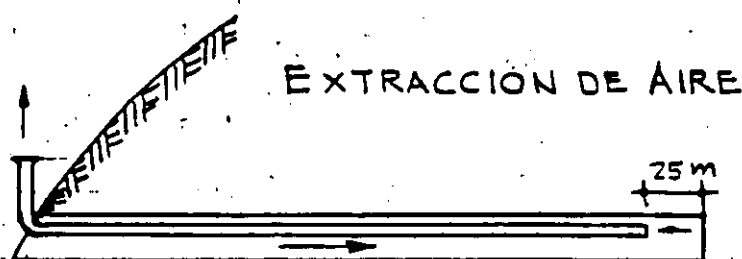
EXTRACCION E INYECCION ALTERNADAS.. da buenos resultados ya que el tiempo de extracción es suficientemente largo para asegurar que todos los gases han salido antes de invertir el sistema con soplado. El sistema implica el uso de ventiladores reversibles y ductos metálicos.

Los ductos deberán estar a 25 m del frente para protegerlos de las voladuras. El ventilador auxiliar será de 30 a 70 % de la capacidad del ventilador principal.

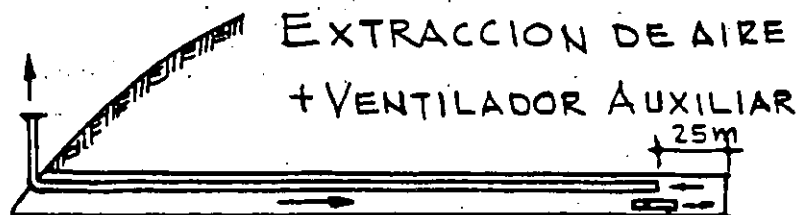
SISTEMAS DE VENTILACION



Simple, se tiene buen control sobre el trayecto del aire. Puede dispersar los gases a lo largo del túnel.



No es muy adecuado. Se tiene pobre ventilación en el frente y en la entrada se produce frío durante el invierno.

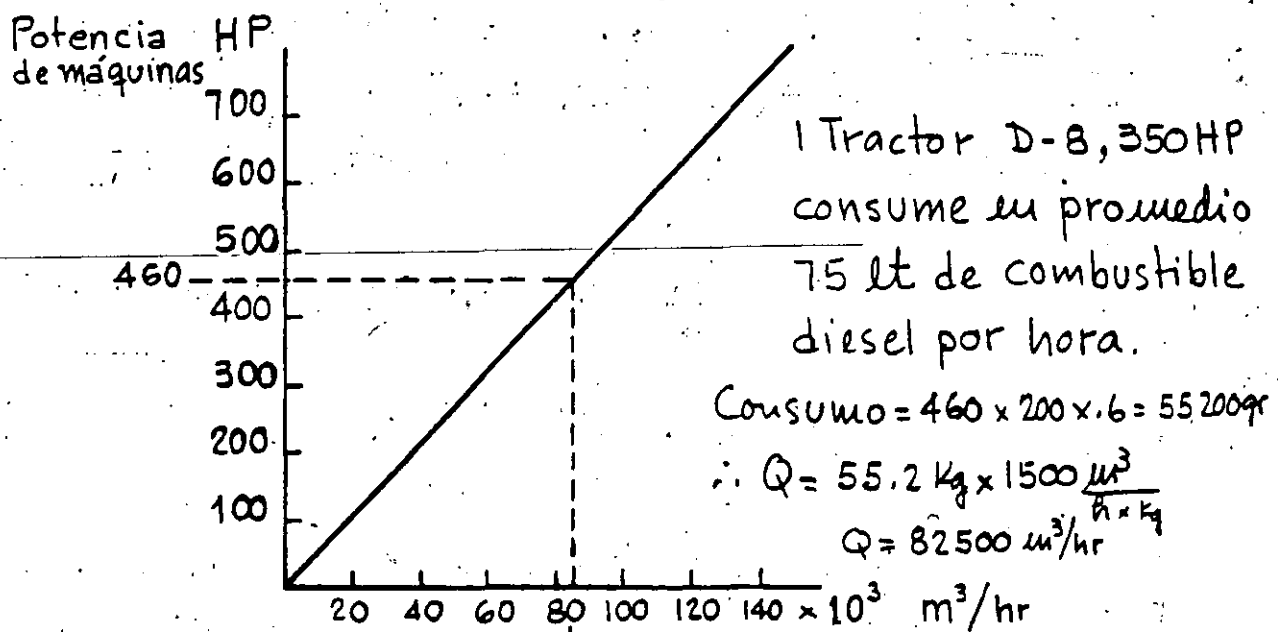


Se obtienen buenos resultados excepto que el enfriamiento en la entrada permanece.

- Los mejores resultados se obtienen inyectando aire durante la barreración y el rezagado con extracción inmediatamente después de la voladura.

CALCULO DEL ABASTECIMIENTO DE AIRE

Según el Cuerpo Nacional Sueco de Protección a los Trabajadores publico en 1969 un método para calcular el abastecimiento de aire de ventilación. Para contrarrestar el efecto de los escapes de gas quemado, deberá abastecerse $1500 \text{ m}^3/\text{hr}$ por Kg de combustible quemado considerando un consumo de diesel de $200 \text{ gr}/\text{HP}/\text{hr}$.



82500 Requerimiento de aire fresco

La gráfica esta basada sobre un promedio de 60% sobre los $200 \text{ g}/\text{HP}/\text{h}$ de consumo de combustible y $1500 \text{ m}^3/\text{hr}$ por kilogramo de combustible quemado.

Ejemplo: Si tenemos 136 HP en cargadores de llantas y 230 HP en tractores y 150 HP en camiones; estos últimos sobre 40' / hora.
 tenemos: Total HP = $136 + 230 + 150 \frac{40}{60} = 460 \text{ HP}$; el aire requerido es: $Q = 82500 \text{ m}^3/\text{h} = 23.7 \text{ m}^3/\text{seg.} = 50000 \text{ p.c.m.}$

VENTILACION DE GASES POR EXPLOSIVOS

Los valores siguientes se utilizan en Suecia para el cálculo general de requerimiento de aire para la ventilación de gases:

$$q = \frac{A}{t} (L + 120) \text{ m}^3/\text{min}$$

en donde:

A = área del túnel m^2

t = periodo de ventilación en minutos.

L = longitud del ducto o del túnel.

q = flujo de aire fresco inyectado.

$$q = 180 \frac{A}{t} \text{ m}^3/\text{min} \text{ para extracción de } \dots$$

$$\text{y } \frac{2}{3} q \text{ m}^3/\text{min} \text{ para el abanico auxiliar}$$

Ejemplo: Para un túnel de 1200 m de largo con 16 m^2 de área con un tiempo de ventilación de 30', se requiere un gasto $q = \frac{16}{30} (1200 + 120)$.

$$\therefore q = 704 \text{ m}^3/\text{min} = 11.7 \text{ m}^3/\text{seg. de aire inyectado}$$

Para extracción de aire: $q = \frac{37}{30} (5000 + 120)$

$$q = 180 \times \frac{16}{30} = 96 \text{ m}^3/\text{min} = 1.6 \text{ m}^3/\text{seg}$$

$$q = 6315 \text{ m}^3/\text{min} = \frac{222841}{110.000}$$

$$+ \text{abanico auxiliar} = \frac{2}{3} \times 1.6 = 1.06 \text{ m}^3/\text{seg}$$

La extracción es aproximadamente 20% de la inyección

$$\text{Extrac } q = 180 \times \frac{37}{30} = 222 \text{ m}^3/\text{min} \times 35 = 7834 \text{ p.c.m.}$$

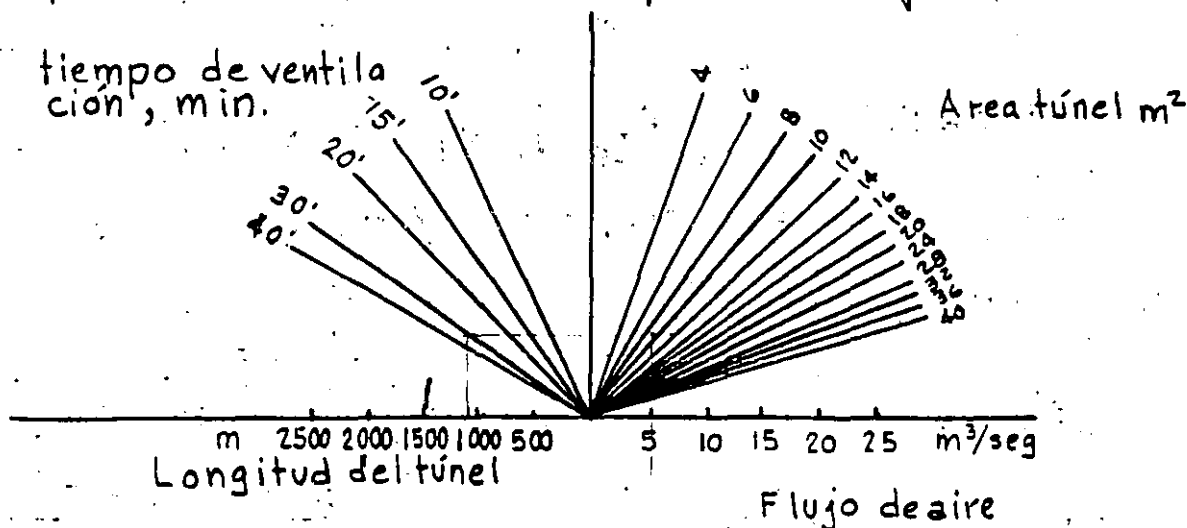
$$= 7 \frac{\text{m}^3}{\text{s}} \times 60 \times 3.29 = 794 \text{ p.c.m.}$$

$$= 27 \frac{\text{m}^3}{\text{min}} \quad Q = 20 \quad V = 15 \text{ m/s}$$

VENTILACION DE GASES POR EXPLOSIVOS EN TUNELES

La expresión $q = \frac{A}{t} (L + 120) \text{ m}^3/\text{min}$, en donde

A = área del túnel en m^2 ; L = longitud del ducto en metros y t = tiempo programado de ventilación se presenta en el nomograma siguiente



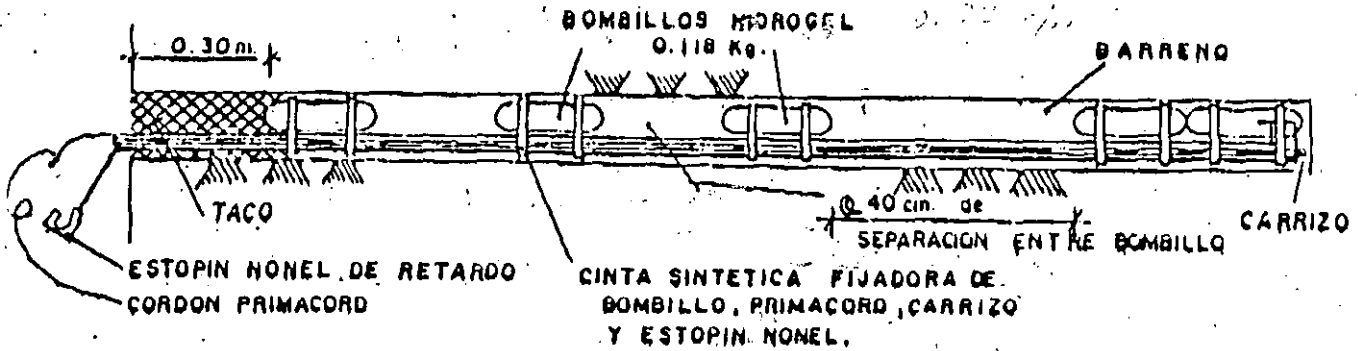
Durante la barrenación el flujo de aire deberá ser por lo menos igual al aire consumido por las perforadoras para alcanzar la disolución del aire aceitoso.

La ventilación prevista para la construcción generalmente es suficiente para el arranque de otras actividades como soldadura, pintura, calentamiento, etc.

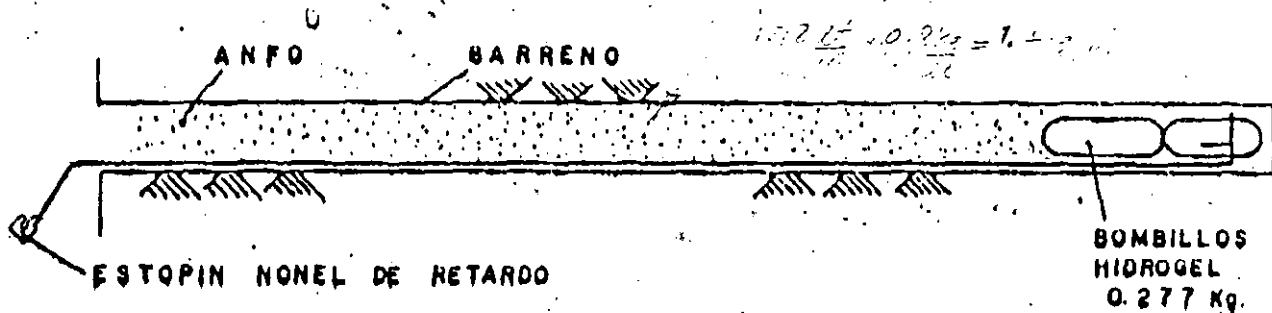
La velocidad del aire fresco debe variar entre 12 y 18 m/seg .

- DETALLE BARRENO DE POSTCORTE

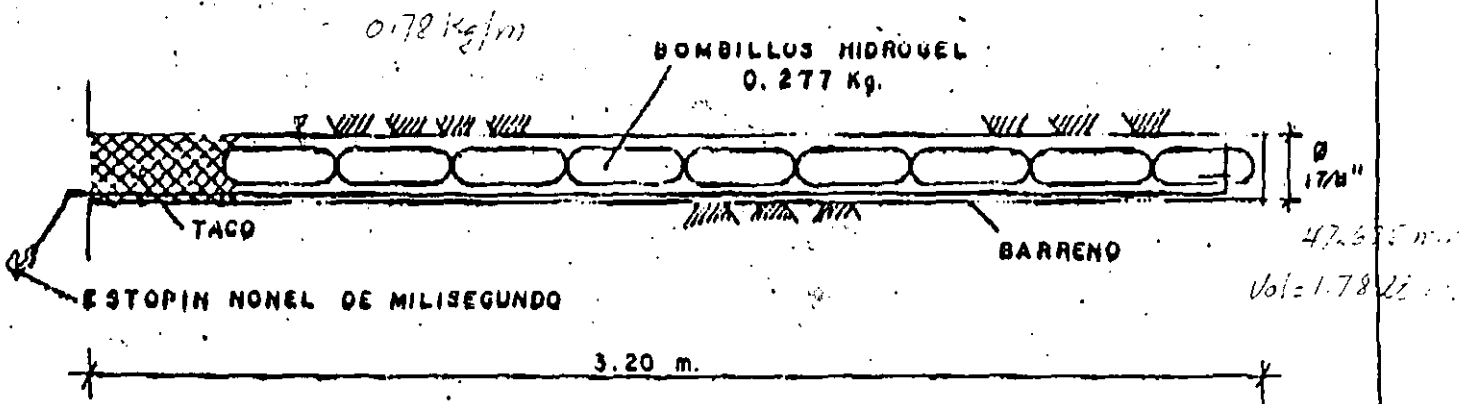
PARA: ING. CUERNA
DE: FIDENCIA



- DETALLE BARRENO DE CUÑA Y TODOS LOS AYUDANTES



- DETALLE BARRENO DE PISO

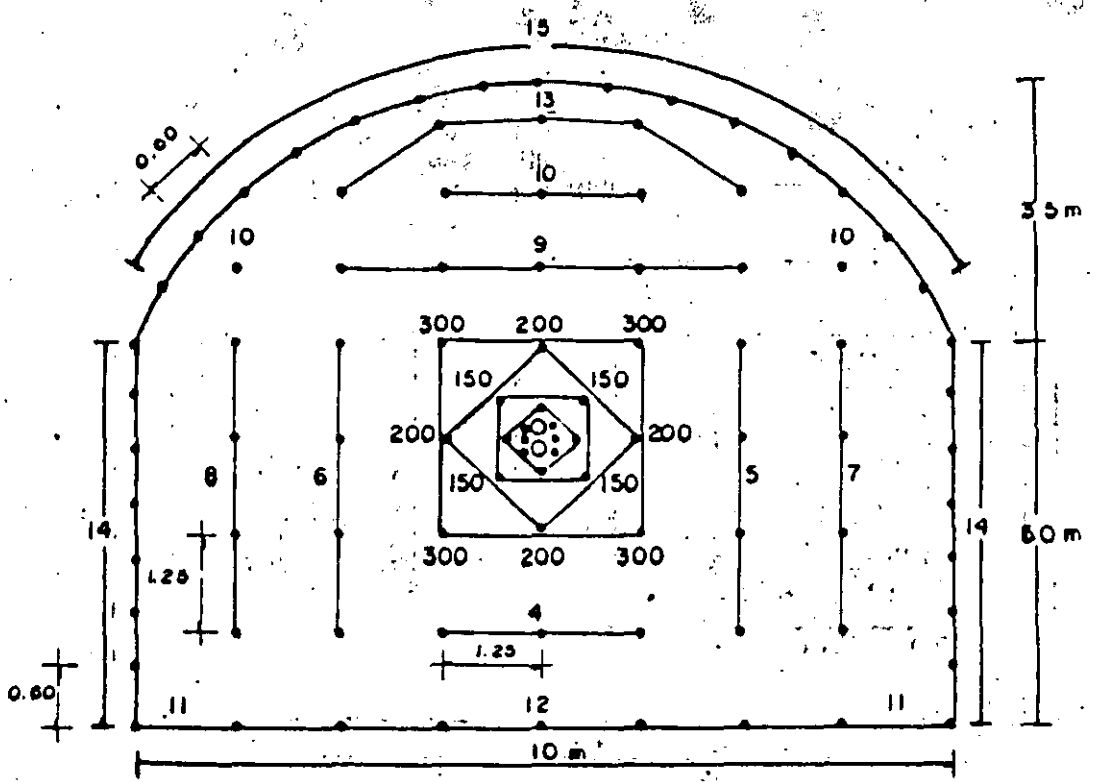


FACTOR DE CARGA = 1.1 Kg/m³

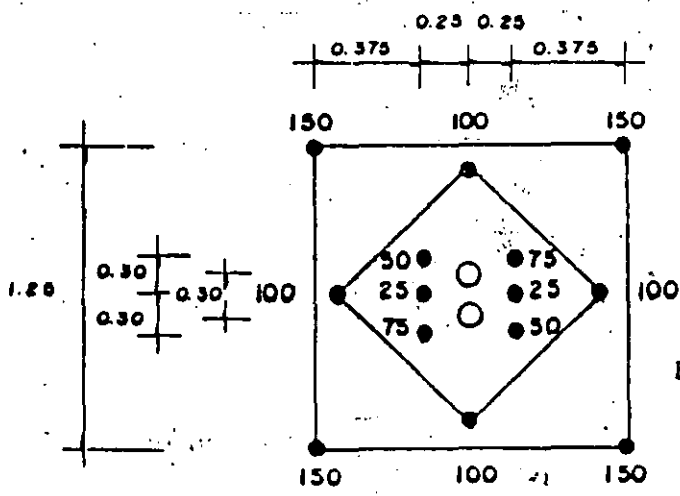
FIG. 4

TUNEL ACCESO A CASA DE MAQUINAS

PLANTILLA DE BARRENACION Y CARGA



Acotaciones en metros



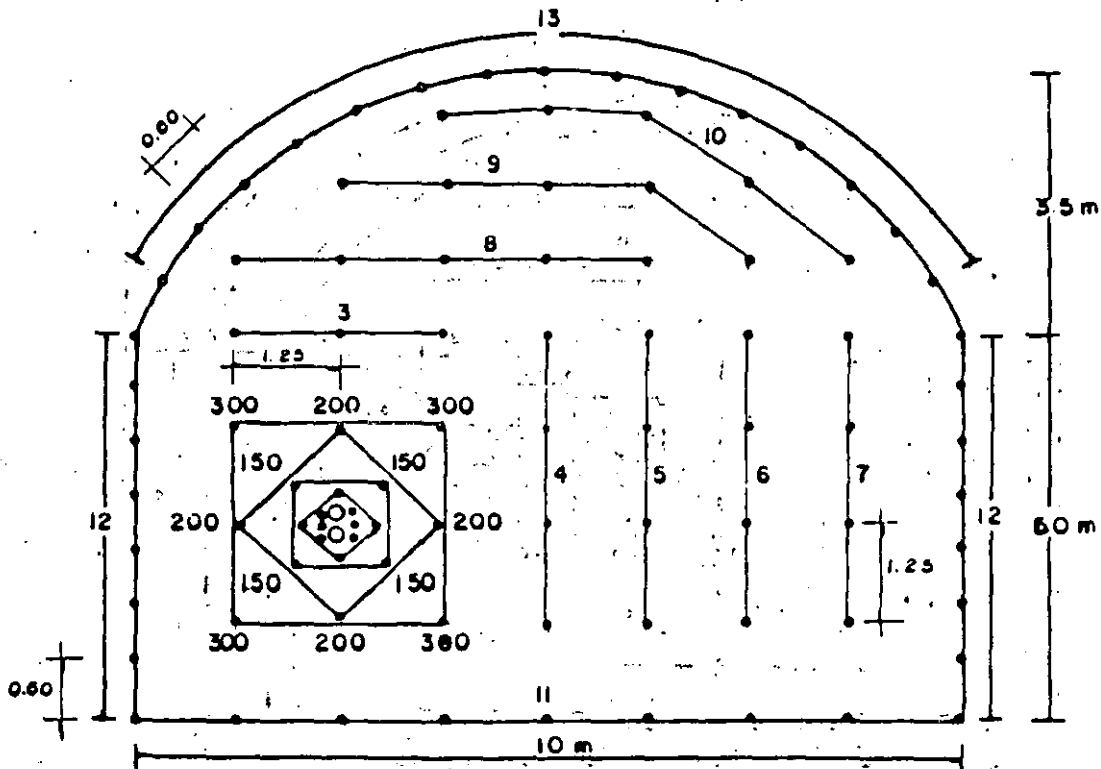
Estopines milisegundos

DETALLE DE CUÑA

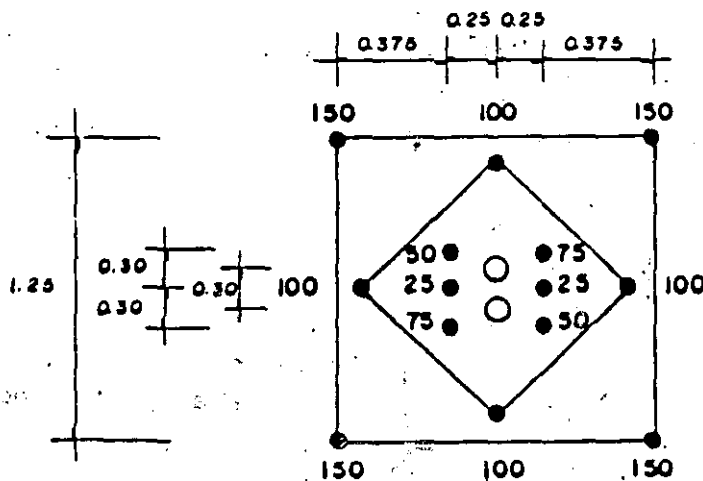
FIG. 7

TUNEL ACCESO A CASA DE MAQUINAS BIFURCACION

PLANTILLA DE BARRENACION Y CARGA



Acotaciones en metros



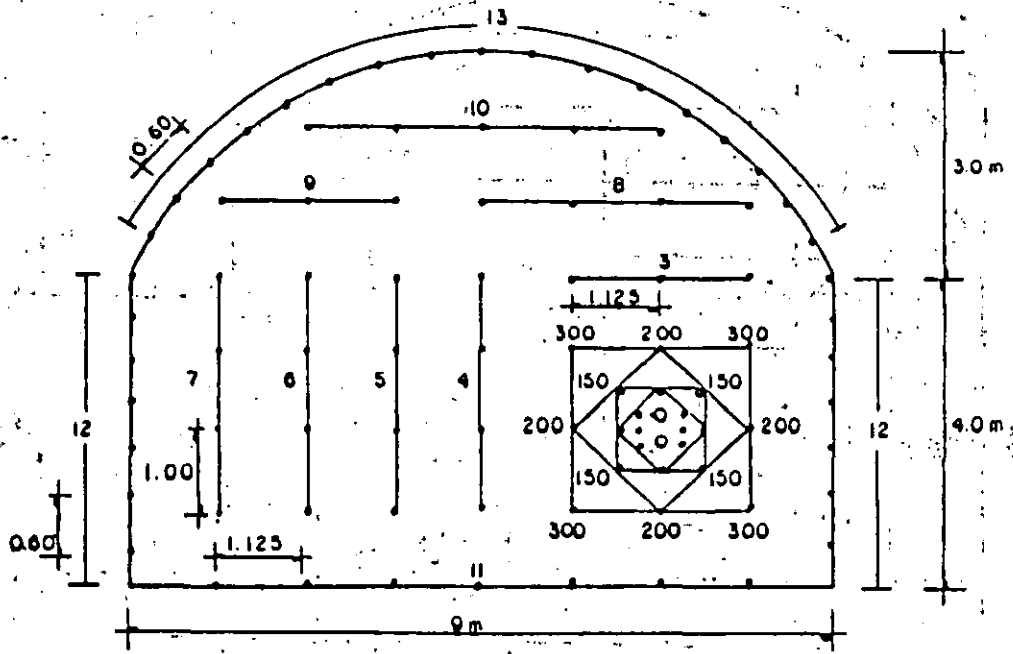
Estopines milisegundos

DETALLE DE CUÑA

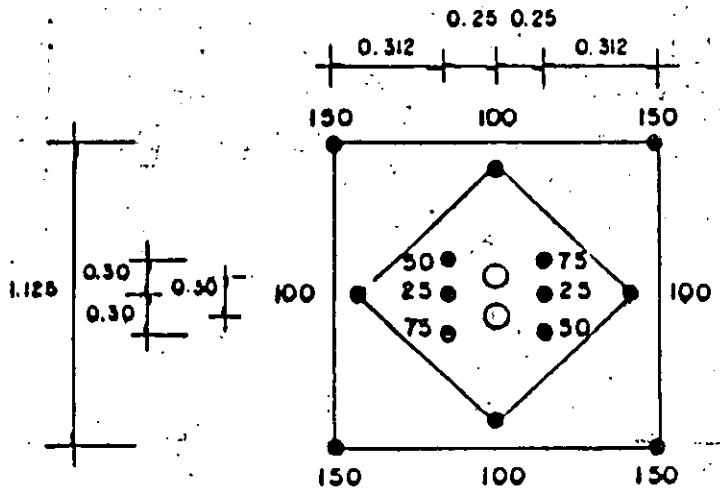
FIG. 8

TUNEL AUXILIAR A TUBERIAS A PRESION BIFURCACION

PLANTILLA DE BARRENACION Y CARGA



Acotaciones en metros



Estopines milisegundos

DETALLE DE CUNA

FIG. 9

FAIRDALE MINE ALT
SLIFER 1S40H

55FT HJ4-50 SLIFER

SAMPLE INT= 2.5 USEC

TEST DAY 15-NOV-84 11:51:49

PLOT DAY 15-NOV-84 12:56:02

DAASY FILTER= 80 KHZ

SLIPLT

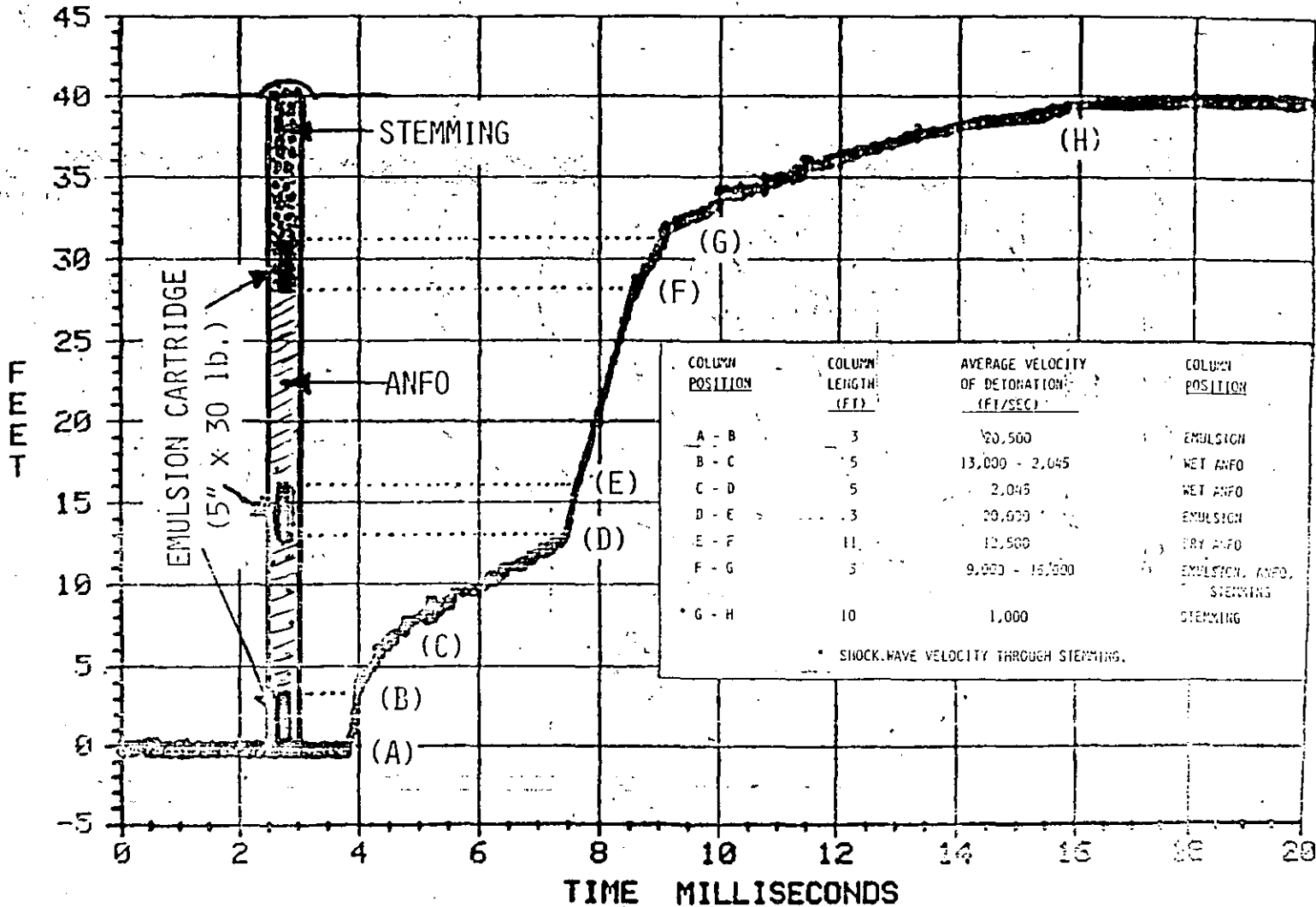


FIGURE 9 DISPLACEMENT vs TIME - Velocity of detonation measurement using the Slifer System developed at SANDIA NATIONAL LABORATORY.
(FAIRDALE QUARRY, M. Lin Brothers Stone Company, Fairdale, IL)

POWERMAX 440 - ANFO

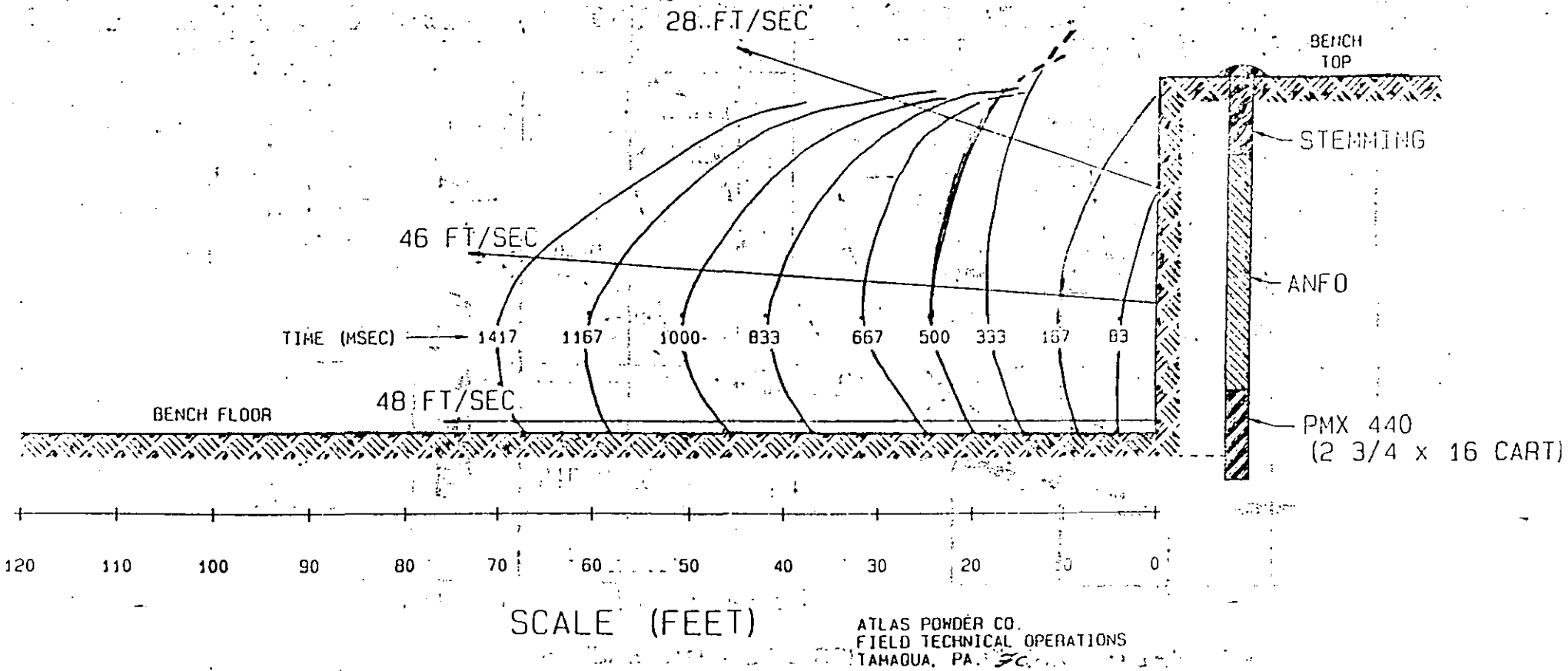
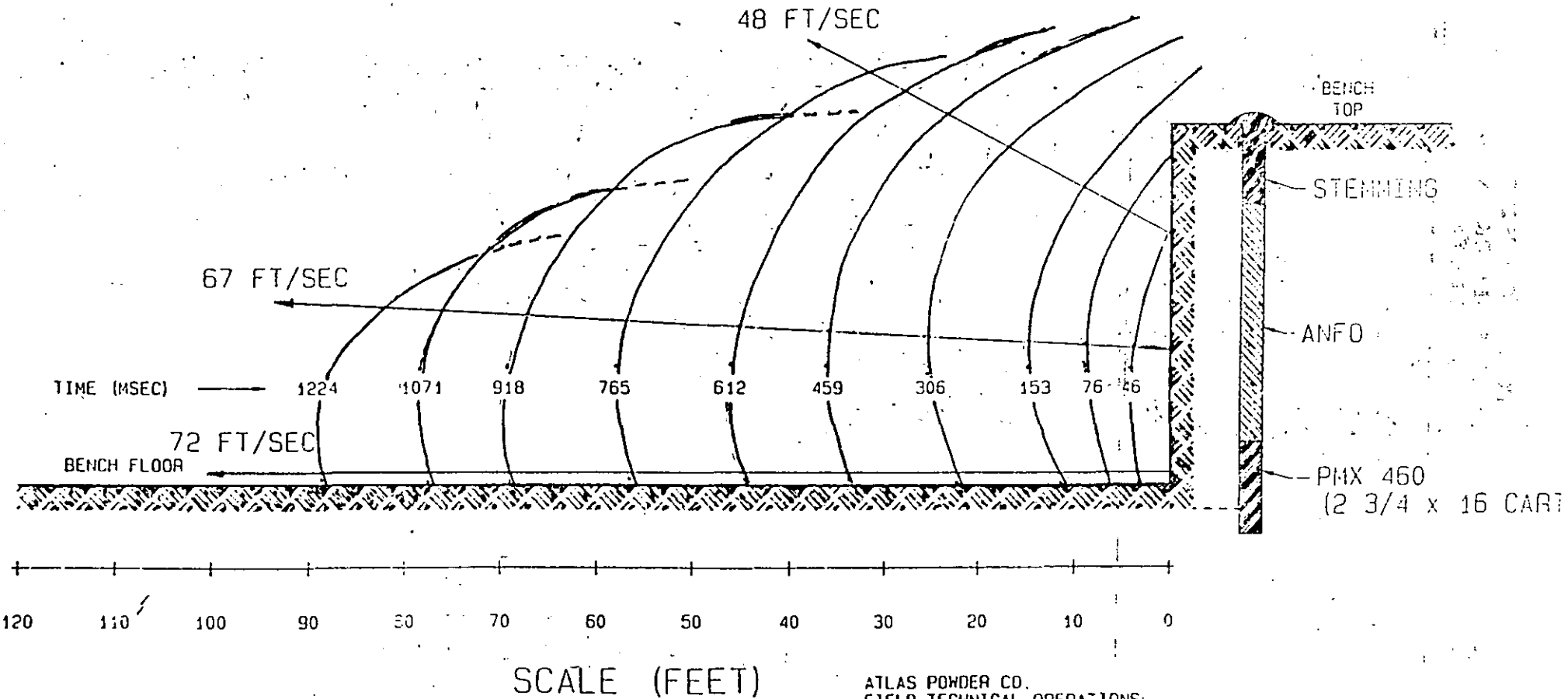


FIGURE 11

ATLAS POWDER CO.
FIELD TECHNICAL OPERATIONS
TAHAQUA, PA.

POWERMAX 460 - ANFO



ATLAS POWDER CO.
FIELD TECHNICAL OPERATIONS
TAMAQUA, PA. *FC.*

FIGURE 2

HOLE
DIAMETER
(in)

SPACING FOR CARTRIDGES OR
SLUGS OF EMULSION IN ANFO
COLUMN (ft)

LENGTH OR
AMOUNT OF
EXPLOSIVE

2-1/2 to 3-1/2

4 - 6

16 in.

4 to 6-3/4

6 - 8

15 - 30 lb.

7 to 10

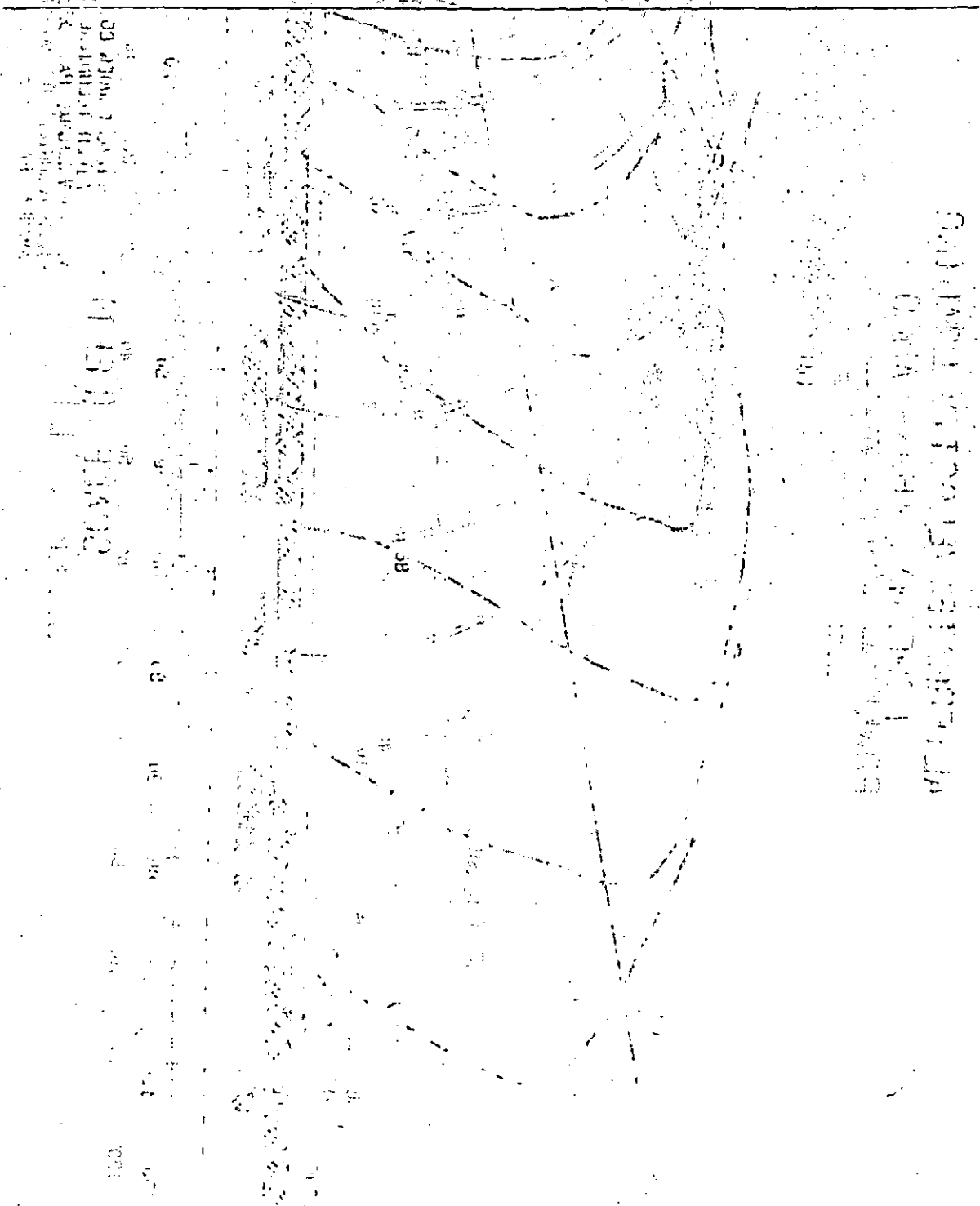
8 - 10

30 - 50 lb.

10+

10 - 15

100 lb.

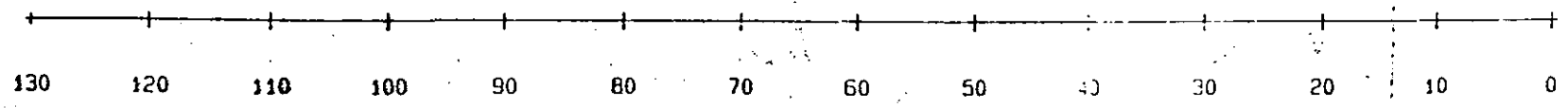
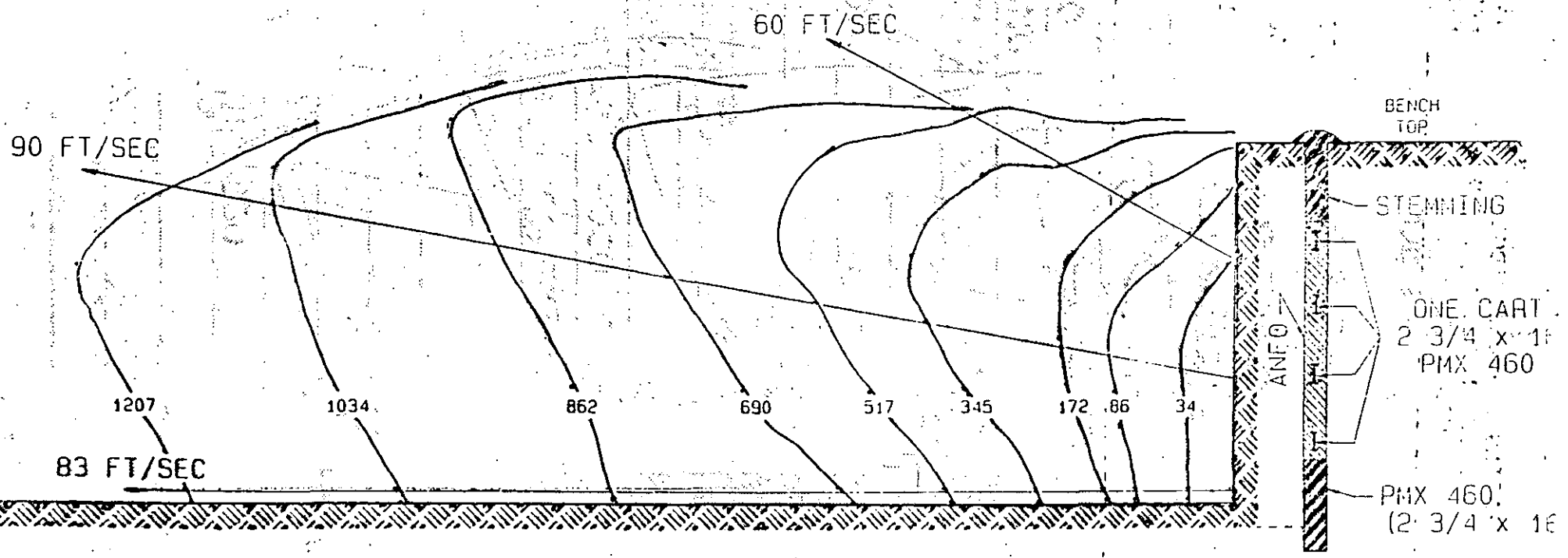


Vertical text on the left side of the diagram, possibly a title or description, oriented vertically.

Vertical text on the right side of the diagram, possibly a title or description, oriented vertically.

ALTERNATE VELOCITY LOADING
 ALTERNATE VELOCITY LOADING
 POWERMAX 460 - ANFO

2/2/21



SCALE (FEET)

ATLAS POWDER CO.
 FIELD TECHNICAL OPERATIONS
 TAMAGUA, PA. *SC*

FIGURE 13